FOODS and raw materials

Volume 10
Issue 2
2022

ISSN 2308-4057 (print)
ISSN 2310-9599 (online)

FRM

food production technology

food production processes and equipment

biotechnology

economics

food hygiene

chemistry and ecology

standardization, certification, quality and safety

automation and informational support of technological processes

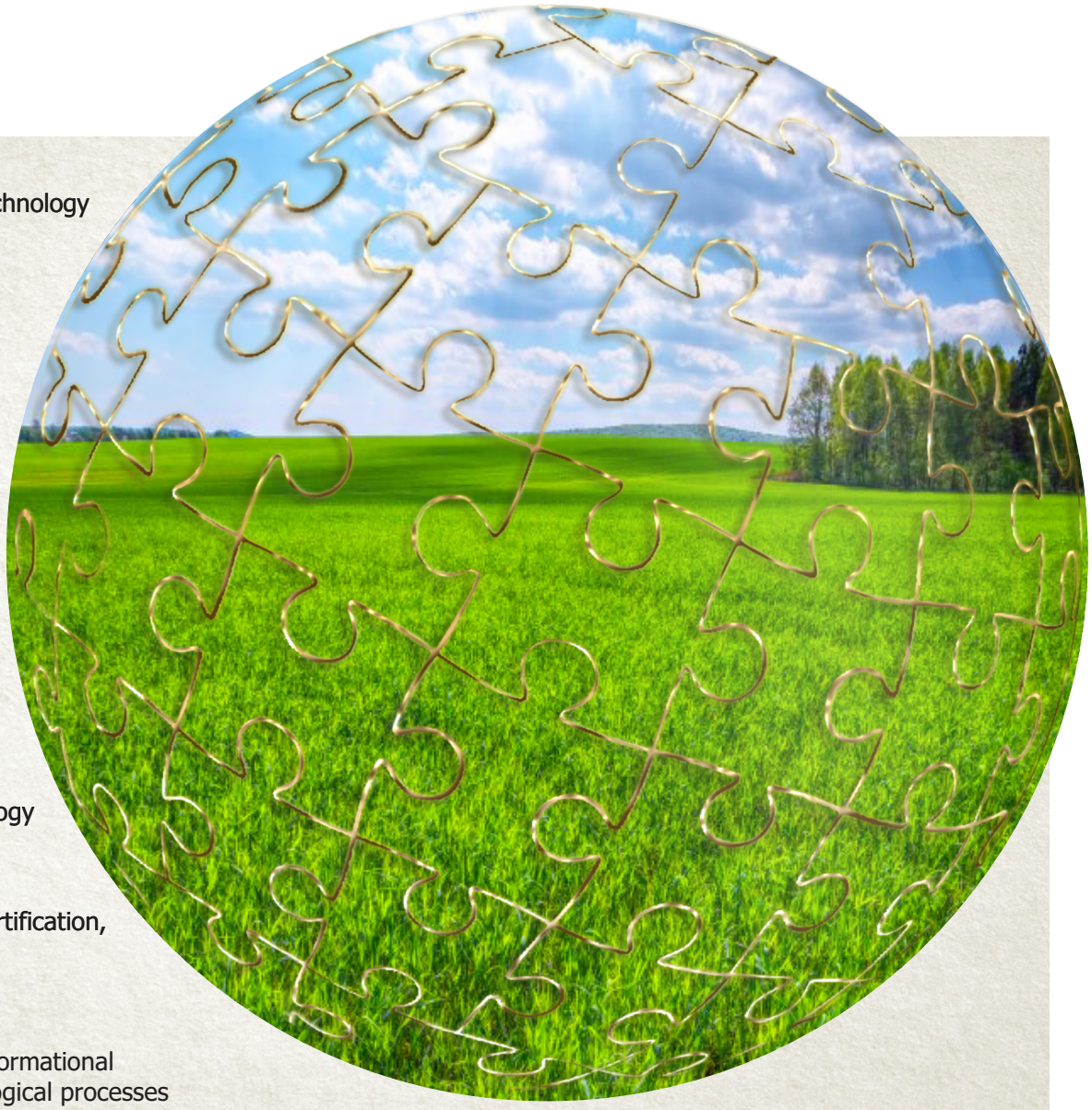

FOODS AND RAW MATERIALS

Kemerovo State University

Vol. 10, no. 2, 2022

ISSN 2308-4057 (Print) ISSN 2310-9599 (Online)

Foods and Raw Materials covers pioneering research in the food industry and related branches. The Journal stimulates scientific communication between academia and manufacturers. The Journal publishes theoretical and empirical research papers to promote new technologies and innovative ideas, bridge the gap between regional, federal, and international scientific publications and educate qualified specialists.

The Journal publishes scientific papers, reports, peer reviews, brief scientific communications, letters to the editor, and related news items.

The Journal is included in the International Data-bases: Emerging Sources Citation Index (Web of Science Core Collection), Scopus, DOAJ, CAS, FSTA, EBSCOhost, ResearchBib, ProQuest, CABI, Agricola, Ulrich's, Google Scholar, OCLC WorldCat, BASE.

Foods and Raw Materials is included in the List of leading Peer-reviewed Scientific Journals recommended by the Higher Attestation Commission of the Russian Ministry of Science and Higher Education of the Russian Federation.

The Journal comes out in print and online. It is published in the English language since 2013 with periodicity of two volumes a year.

All submitted articles are checked for plagiarisms via ithenticate.com and antiplagiat.ru.

The Journal only publishes the manuscripts recom-mended by the reviewers. The Journal uses double-blind review.

Foods and Raw Materials is included in the Russian index of scientific citation (RISC) and registered in the Scientific electronic library eLIBRARY.RU.

Opinions of the authors of the published materials do not always coincide with the editorial viewpoint. Authors are responsible for the content of their research papers.

The Journal is an open access journal. All articles are made freely available to readers immediatly upon publication. Our open access policy is in accordance with the Budapest Open Access Initiative (BOAI) definition.

For submission instructions, subscription and all other information visit this journals online at jfrm.ru/en.

Founder and Publisher: Kemerovo State University (KemSU), 6 Krasnaya Str., Kemerovo, Kemerovo region – Kuzbass 650000, Russia.

Editorial Office: Kemerovo State University, 6 Krasnaya Str., Kemerovo, Kemerovo region – Kuzbass 650000, Russia. Phone: +7(3842)58-81-19. E-mail: fjournal@mail.ru.

Printing Office: Kemerovo State University, 73 Sovetskiy Ave., Kemerovo, Kemerovo region – Kuzbass 650000, Russia.

Publishing editors – Ekaterina V. Dmitrieva, Alena A. Kiryakova; Literary editor – Anastasia Yu. Kurnikova; Computer layout and design – Elena V. Volkova.

Cover image: Kirill A. Gordeenko. Photos credits: contributors

Date of publishing
September 28, 2022

Circulation 500 ex. Open price.
Subscription index: for the unified "Russian Press" catalogue – 40539.

The Federal Service for Supervision of Communications, Information Technology and Mass Media (Media Registration Certificate PI no. FS77-72606 dated April 04, 2018).

16+

Foods and Raw Materials. 2022;10(2)
ISSN 2310-9599 (Print)
ISSN 2308-4057 (Online)

Editorial
Open Access

Available online at https://jfrm.ru/en

Editor's column

Evaluation of scientific activity remains a hot topic in academic communities for at least two reasons. First, novel information technologies and bibliometric databases put scientific indicators into public domain, thus opening achievements of individual researchers, teams, universities, and domestic science to the general public. Second, managers of research and academic organizations have started to use scientific indicators to control the scientific activities of their personnel.

Science is constantly evolving. According to the Institute of World Economy and International Relations (Russian Academy of Sciences), the global research expenditures will double from $1.7 trillion in 2016 to $3.3 trillion in 2035, and the research intensity of the global GDP will grow from 2.2% in 2016 to 2.3% in 2035. Publication activity is traditionally considered to be the main indicator of research work. According to Science and Engineering Indicators, the year of 2016 saw 2.3 million scientific and technical publications. In the same year, China was responsible for 18.6% of total research publications, which made it number one at least by the sheer number of publications, if not by their significance, outside the European Union. Between 2006 and 2016, the USA experienced a rapid decrease in publication activities, which fell from 24.4 to 17.8%. As a result, in 2016 India rose to the third position (4.8%) in terms of the number of publications. In this context, applying scientometric and expert methods to research activities has become a burning issue for the modern scientific community.

Scientometrics uses statistics and mathematics to assess any parameters of scientific activity in the sphere of scientific communication, which makes it a highly promising area of research in the measurement and analysis of scientific publications. At the same time, scientometrics facilitates managerial decisions in the field of science. As a science, scientometrics originated in the second half of the XX century. It was founded by the British information scientist Derek de Solla Price, who is considered to be the herald of scientometrics, and the Soviet scientist Vasily Nalimov, who introduced this term in his monograph, which he published together with Zinaida Mulchenko as early as in 1969. Scientometrics owes many of its breakthroughs to Eugene Garfield, the founder of the Web of Science. Contemporary scientometrics profits from the rapid development of information technologies, colossal information flows, and giant data arrays.

Web of Science and Scopus are the most popular international citation indexes in the world, while the Russian Science Citation Index (RSCI) remains the most influential system of its kind in Russia. International citation indexes are powered by such famous foreign publishers as the EBSCO, Elsevier, Thomson Reuters, Oxford University Press, etc. According to the Scientific Journal Rankings, the TOP 10 countries with the largest number of articles in scientific and technical journals published in 2020 included China (744 042), the USA (624 554), the UK (198 500), India (191 590), Germany (174 524), Italy (127 502), Japan (127 408), Russia (119 195), France (112 838), and Canada (121 111).

Publication activity and citation are measurable signs of scientific communication and a reliable tool of generating new knowledge. Scientometrics sees science as a multifaceted object of financing and investment, where scientific research is a business project. In 2022, the Russian Science Foundation promised to allocate more than 21.5 billion rubles in 2022–2024 to support 1 171 research projects, both new and those registered in 2019. Science is an expensive field of limited financial opportunities. Thus, adequate self-assessment, best practices, and a good development plan are the only survival strategy for any devoted researcher.

In this regard, if a journal has a high scientometric rating, it is officially in high demand by the scientific community. The Thomson Reuters Top 25 Journals by Impact Factor ranges from *The Transactions on Ultrasonics, Ferroelectrics, and Frequency Control* to *The Transactions on Audio Speech and Language Processing*. According to Science Index, the best domestic journals in 2021 were *The Progress in Chemistry* (23 744), *The Resource-Efficient Technologies* (21 698), and *The Progress in Physics* (17 034). In 2021, the highest two-year impact factor belonged to *The Bulletin of the Minin University* (6848), *The Bulletin of St. Petersburg State University of Technology and Design: Industrial Technology* (5020), and *The Economic Issues* (4690). According to the Russian Science Citation Index, Kemerovo State University entered the top 100 scientific organizations in Russia in terms of the quantitative score of publication performance in 2021. We ranked 79 out of 782 universities with the composite score of publication performance of 898,01. We publish *The Foods and Raw Materials* (WOS and Scopus); *Siberian Philological Journal* (WOS and Scopus); *Food Processing: Techniques and Technology* (Scopus), etc.

Scientometrics adjusts to the current digitalization and internetization of global economy, society, and science. Therefore, the external conditions of interaction of science and society, government, economy, and business are as important as the internal ones. Universities that prepare domestic research personnel are extremely important. When scientific organizations and universities develop their own systems for recording publications and evaluating scientific activity, they strive to keep up with the times.

Editor-in-Chief,
Corresponding Member of the Russian Academy of Sciences,
Professor A. Yu. Prosekov

FRM
Foods and Raw Materials. 2022;10(2)
ISSN 2310-9599 (Print)
ISSN 2308-4057 (Online)

Research Article
Open Access

Available online at http://jfrm.ru/en
https://doi.org/10.21603/2308-4057-2022-2-530
https://elibrary.ru/OYYIMN

Genoprotective, antimutagenic, and antioxidant effects of methanolic leaf extract of *Rhamnus alaternus* L. from the Bissa mountains in Algeria

Leila Gadouche[1,2,*], Khayra Zerrouki[2], Azdinia Zidane[2], Adda Ababou[2], Ibtissem Bachir Elazaar[2], Dounya Merabet[2], Wissam Henniche[2], Samah Ikhlef[2]

[1] University of Science and Technology Houari Boumediene, Bab Ezzouar, Algeria
[2] Hassiba Benbouali University of Chlef, Chlef, Algeria

* e-mail: gadoucheleila@gmail.com

Received 13.10.2021; Revised 21.12.2021; Accepted 14.04.2022; Published online 23.06.2022

Abstract:
Rhamnus alaternus L. is a *Rhamnaceae* shrub and a popular traditional medicine in Algeria. The present research objective was to investigate the antioxidant, genotoxic, and antigenotoxic properties of *R. alaternus* methanolic leaf extract.
Antiradical scavenging activity was tested by *α*, *α*-diphenyl-*β*-picrylhydrazyl free radical scavenging and *β*-carotene bleaching method. DNA damage and repair were measured by the *Allium cepa* test with sodium azide as a mutagenic agent. Mitotic index and chromosomal aberrations were calculated by microscopy of meristem roots stained with 2% carmine acetic.
The methanolic extract of *R. alaternus* leaves inhibited the free radical DPPH (IC_{50} = 0.74 ± 0.30 mg/mL) and prevented the oxidation of *β*-carotene (50.71 ± 4.17%). The root phenotyping showed that sodium azide changed their color and shape, decreased their stiffness, and significantly reduced their length. The roots treated with both *R. alaternus* leaf extract and sodium azide demonstrated a better root growth. The roots treated with the methanolic extract were much longer than the control roots ($P < 0.001$). The microscopy images of root meristem treated with the sodium azide mitodepressant agent showed significant chromosomal aberrations, which indicated a disruption of the cell cycle.
The *R. alaternus* leaf extract appeared to have a beneficial effect on cytotoxicity. The antioxidant properties of *R. alaternus* L. makes this plant an excellent genoportector.

Keywords: *Rhamnus alaternus* L., antioxidant activity, *Allium cepa*, chromosomal aberrations, antigenotoxicity, mitotic index

Please cite this article in press as: Gadouche L, Zerrouki K, Zidane A, Ababou A, Bachir Elazaar I, Merabet D, *et al.* Genoprotective, antimutagenic, and antioxidant effects of methanolic leaf extract of *Rhamnus alaternus* L. from the Bissa mountains in Algeria. Foods and Raw Materials. 2022;10(2):196–205. https://doi.org/10.21603/2308-4057-2022-2-530

INTRODUCTION

Radical oxygen species lead to cell damage, which can induce genetic instability responsible for many pathological processes. This damage can be repaired by some natural compounds, e.g. radical scavengers and powerful protective antioxidants [1]. Kitagishi *et al.* proved that medicinal herbs could one day become a promising therapeutic means of cancer therapy [2]. According to Dayani *et al.*, antioxidant, anti-inflammatory, and anti-apoptotic properties of plants and their derivatives make them good radioprotectors against the mutagenic action of X-rays [3].

Phytotherapy relies on medicinal plants and their active compounds. *Rhamnus alaternus* L. (*Rhamnaceae* family), also called *imlilesse* or *safir* in the North of Algeria, is well known for its biological properties [4]. Zeouk and Bakheti reported that a decoction of the aerial part of the *R. alatrenus* leaves and branches has been widely used in traditional medicine to lower blood pressure and treat hepatitis, icterus, musculoskeletal disorders, and gastrointestinal diseases. They also serve as a cataplasm for skin infections [5].

Previous findings proved that *R. alaternus* extracts possess potential antioxidant, cytotoxic antimutagenic, antigenotoxic, and antimicrobial activities [5–8]. In their bibliographic review, Nekkaa *et al.* focused on the phytochemical and pharmacological properties of *R. alaternus* [4]. Its leaf extracts were rich in flavonoids,

tannins, and anthocyanins, which explains their potential antigenotoxic and antimutagenic activity.

Bhouri *et al.* isolated kaempferol 3-O-b-isor-hamninoside and rhamnocitrin 3-O-b-isor-hamninoside from *R. alternus* leaves [9]. These flavonoids are effective free radical scavengers and potent antigenotoxics. However, they can induce apoptosis in human lymphoblastoid cells by the extrinsic apoptotic mechanism including DNA fragmentation, PARP cleavage, and active caspase-3 and caspase-8 [10]. Oligomer flavonoid extract from *R. alaternus* leaves proved to have a good potential for alternative antimelanoma therapies [11].

Although some plant remedies have well-documented protective effects and alleviate many diseases, cytotoxicity studies are very important for developing new drugs. Gadouche *et al.* described the toxic effect of *Aristolochia longa* L. and *Calycotome spinosa* L. on the blood cells and concluded that it should be studied on cancer cells [12]. Natural antioxidants can even protect human organism against the cytotoxic and mutagenic effects of xenobiotics.

In this research, we analyzed the genotoxic and DNA damage protecting activity of *R. alaternus* leaf extract by using the *Allium cepa* assay with azide sodium as a mutagen agent.

STUDY OBJECTS AND METHODS

Plant material. The research featured *Rhamnus alaternus eu-alaternus* L., a subspecies of *Rhamnus alaternus* L. The samples were collected in the Bissa forest located in the north of the Chlef province (Algeria). This species of Algerian flora was identified by Dr. Belhacine, a botanist from the Chlef University [13].

The *R. alaternus* leaves were dried in the dark for 10 days. After that, they were ground into a fine powder and kept in an airtight container, and 10 g of the dry powder was macerated in 100 mL of petroleum ether for 24 h with stirring. The mix was filtered on Whatman No. 1 paper. The maceration included 100 mL of methanol. After filtration, the marc was evaporated in a rotary evaporator at 39°C. The extract obtained was stored at 4°C until use [14].

Quantitative analysis and antioxidant activity. The polyphenols were assayed according to the method developed by Raafat and Samy [15]. The amount of total polyphenols was determined spectrophotometrically using the Folin-Ciocalteu reagent and deduced from a calibration curve established with gallic acid (0–1 mg/mL). The results were expressed in mg of gallic acid equivalent per g of dry matter (mg GAE/g of dry matter). The mix included 250 µL of Folin Ciocalteu's phenol reagent, 50 µL of each concentration prepared from stock solution, and 500 µL of 20% Na_2CO_3 aqueous solution. After vortexing, the solution was adjusted with 5 mL of distilled water. After 30 min of incubation, the absorbance was measured at 765 nm. The same procedure was carried out with the extract obtained from *R. alaternus* leaves.

The flavonoid content was assayed according to the method developed by Hmid *et al.* [16]. After 1 mL of extract was added to 1 mL of 2% aluminum chloride, the absorbance was determined at 430 nm after 10 min of incubation. Quercetin served as calibration curve standard and was established from the concentration of 40 µg/mL of stock solution. Total flavonoids content in the extract was expressed as mg quercetin equivalents per g of sample (mg EQ/g of dry matter).

The DPPH assay followed the method described by Burits and Bucar [17]. The *R. alaternus* extract had the following concentrations: 0.2, 0.4, 1.0, and 2.0 mg/mL. We mixed 50 µL of each concentration with 5 mL of 0.004% DPPH. The absorbance was measured at 517 nm after 30 min of incubation. The results were compared to ascorbic acid, which was used as standard antioxidant and handled under the same conditions. The percentage of inhibition and IC_{50} were calculated according to Sharififar *et al.* [18]. The percentage inhibition was calculated using the following equation:

$$\text{Percentage of inhibition} = \frac{\text{ODcontrol} - \text{ODsample}}{\text{ODcontrol}} \times 100$$

where OD is optical density.

IC_{50} is the concentration of extract required for 50% inhibition of DPPH. It was calculated using a linear regression analysis.

The *β*-carotene-linoleic acid assay was performed according to the method described by Kartal *et al.* [19]. The emulsion included 0.5 mg of *β*-carotene, 1 mL of chloroform, 25 µL of linoleic acid, and 200 mg of tween 40. The chloroform was eliminated in a rotary evaporator under vacuum, and 100 mL of distilled oxygen-saturated water was added to the emulsion. Subsequently, 350 µL of the extract at a concentration of 2 mg/mL was mixed with 2.5 mL of the emulsion. After 48 h of incubation, the absorbance was registered at 490 nm and compared with that obtained with butylohydroxytoluene (BHT), which served as a standard antioxidant and was prepared under the same conditions. The inhibition percentage of bleaching (I, %) was measured for each assay using the following equation:

$$I = \frac{\text{Abcorbance of a sample at 48 h}}{\text{Abcorbance of BHT at 0 h}}$$

***Allium cepa* assay.** The *A. cepa* assay was performed according to Tedesco and Laughinghouse with some modifications [20]. The onion bulbs were kept in a culture medium that included 60 mg/L of $CaSO_4$, 60 mg/L of $MgSO_4$, 96 mg/L of $NaHCO_3$, and 4 mg/L of KCl. They were incubated at 25°C for 72 h until the roots reached 2 cm. Seven onion bulbs were utilized for each treatment as follows:

Sample 1: culture medium + distilled water;
Sample 2: culture medium + sodium azide (50 mg/mL);
Sample 3: culture medium + sodium azide (100 mg/mL);

Sample 4: culture medium + methanolic extract (50 mg/mL);
Sample 5: culture medium + methanolic extract (100 mg/mL);
Sample 6: culture medium + sodium azide (100 mg/mL) + methanolic extract (50 mg/mL);
Sample 7: culture medium + sodium azide (100 mg/mL) + methanolic extract (100 mg/mL).

The effect of the different treatments on the growth (cm) of the *A. cepa* roots was measured at different time intervals: 0, 24, 48, and 72 h. In parallel, the roots were tested for color, shape, and stiffness. After each time interval, the roots were collected for microscopic observation of the meristem cells and stored in 70% ethanol for later use. The roots were fixed in acetic acid and ethanol solution (1:3) for 24 h. After triple rinsing with distilled water, the roots were hydrolyzed with HCl (1N) and incubated in a hot water bath at 60°C for 10 min. After the hydrolysis, the roots were rinsed once again in distilled water and stained with 2% acetic carmine in a hot water bath at 60°C for 10 min. After incubation, the terminal meristem cells of the colored roots were cut with a scalpel under a binocular magnifier. The meristem regions were crushed manually between blade and coverslip to visualize the chromosomes and the different stages of cell division. Meristem cells were counted for each sample and tested for normal or abnormal cell division in search for mutations. The mitotic index and the rate of aberrant cells of each bulb were calculated by the following formula [21]:

$$\text{Mitotic index} = \frac{\text{Number of dividing cells}}{\text{Total number of cells scored}} \times 100$$

$$\%\text{ of observed aberration} = \frac{\text{Number of abberant cells}}{\text{Total number of cells scored}} \times 100$$

Statistical analysis. The experimental data were analyzed using the ExcelSTAT software. The research also included the ANOVA variance analysis, followed by the Tukey's test. The statistically highly significant value was $P < 0.001$.

RESULTS AND DISCUSSION

The total phenol content in *Rhamnus alaternus* L. leaves was 32.6 ± 1.82 mg GAE/g DM, and the total flavonoid content was 27.58 ± 0.01 mg EQ/g DM. The methanolic extract of *R. alaternus* leaves demonstrated a moderate efficiency against free radicals emitted by linoleic acid (50.71 ± 4.17%). Its capacity to beat free radical of DPPH (I% = 80.39 ± 2.33%, IC_{50} = 0.74 ± 0.30 mg/mL) was close to that of ascorbic acid, i.e. 96.80 ± 9.98% with IC_{50} = 0.37 ± 1.10 mg/mL (Table 1).

Plants are excellent indicators of the cytotoxic, cytogenetic, and mutagenic effects of environmental chemicals. They can serve as an alternative for detecting possible genetic damage in cells [22]. Genotoxicity studies were carried out by the *Allium cepa* assay. This method provides a convenient *in vivo* model to evaluate cell cycle alterations induced by mutagens [20].

The *A. cepa* roots treated with distilled water had no morphological change: the growth rate was good, the color was whitish, and the roots were rigid and bulky. However, the roots treated with sodium azide (50 and 100 mg/mL) changed the color and shape of the roots, as well as reduced their rigidity (+very brittle) and growth rate.

The methanolic leaf extract of *R. alaternus* had no negative effect on the morphology. The samples demonstrated good growth, strong rigidity, and whitish color. Their morphology was comparable to the control roots. The roots incubated in both methanolic extract and sodium azide had a phenotype close to the control roots. They were better preserved than the roots treated only with sodium azide. The roots of this sample showed good growth, and the color was comparable to that of the control roots (Fig. 1).

Table 2 shows a highly significant decrease in the growth of the *A. cepa* roots treated with sodium azide at two concentrations (50 and 100 mg/mL) at three time intervals. The data obtained from the sample treated with 50 mg/mL of sodium azide after 48 h was found insignificant ($P < 0.001$).

The roots treated with the methanolic extract of *R. alaternus* leaves showed highly significant growth ($P < 0.001$) after 24 and 48 h. The roots reached 8 cm after 72 h ($P < 0.001$) and were longer than those treated with distilled water (7 cm).

The difference in length for the antigenotoxicity test was highly significant after 48 and 72 h and not significant after 24 h. The roots demonstrated a clearly significant improvement in the diameter after 72 h.

Table 1 Total phenolic content and total flavonoid content of *Rhamnus alaternus* leaves, DPPH inhibition, IC_{50}, and % bleaching of *β*-carotene

Parameter	Leaves of *R. alaternus*	Ascorbic acid	Butylated hydroxytoluene
Polyphenol, mg GAE/g dry matter	32.60 ± 1.82	–	–
Flavonoids, mg QE/g dry matter	27.58 ± 0.01	–	–
DPPH, % (*R. alaternus* extract concentration = 1 mg/mL)	80.39 ± 2.33	96.80 ± 9.98	–
IC_{50}, mg/mL	0.74 ± 0.30	0.37 ± 1.10	–
β-carotene bleaching, % (*R. alaternus* extract concentration = 2 mg/mL)	50.71 ± 4.17	–	98.84 ± 1.69

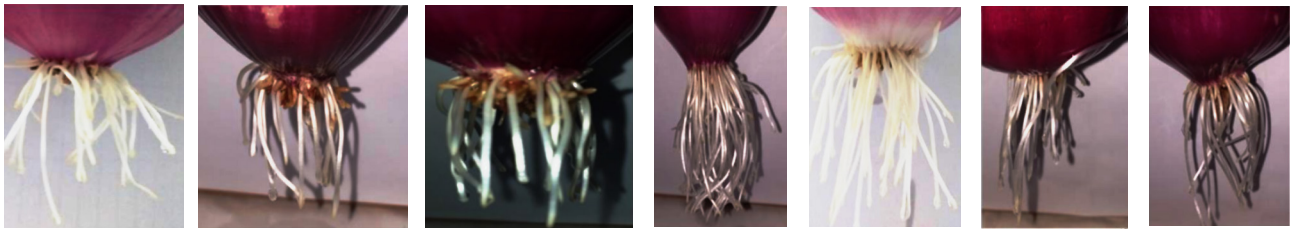

a b c d e f g

Figure 1 Morphological aspects of *Allium cepa* roots: (a) control group; (b) sodium azide (50 mg/mL); (c) sodium azide (100 mg/mL); (d) methanolic extract (50 mg/mL); (e) methanolic extract (100 mg/mL); (f) sodium azide (100 mg/mL) + methanolic extract (50 mg/mL); (g) sodium azide (100 mg/mL) + methanolic extract (100 mg/mL)

Table 2 ΔL – differences in length of the *Allium cepa* roots before and after each treatment, % mitotic index, and chromosomal aberrations

Treatment	Time, h	ΔL, cm	Mitotic index, %	Chromosomal aberrations, %
Control	0	2.66 ± 0.56		
	24	0.57 ± 0.05		
	48	0.84 ± 0.09		
	72	0.70 ± 0.24	69.76 ± 7.01	0
Sodium azide (50 mg/mL)	0	2.36 ± 0.48		
	24	0.50 ± 0.11**		
	48	0.94 ± 0.10		
	72	–0.54 ± 0.31**	34.48 ± 10.50	5.03 ± 1.51**
Sodium azide (100 mg/mL)	0	2.84 ± 0.47		
	24	–1.12 ± 0.18**		
	48	–0.40 ± 0.16**		
	72	–0.03 ± 0.12**	29.25 ± 8.50	7.84 ± 2.41**
Methanolic extract (50 mg/mL)	0	2.93 ± 0.19		
	24	1.09 ± 0.21**		
	48	0.90 ± 0.07**		
	72	0.46 ± 0.15	69.54 ± 14.5	0.43 ± 0.53
Methanolic extract (100 mg/mL)	0	2.80 ± 0.47		
	24	1.87 ± 0.04**		
	48	1.37 ± 0.09**		
	72	1.05 ± 0.02	73.66 ± 9.41	0.29 ± 0.49
Sodium azide (100 mg/mL) + methanolic extract (50 mg/mL)	0	2.71 ± 0.38		
	24	0.11 ± 0.05		
	48	–0.33 ± 0.12**		
	72	0.26 ± 0.18**	51.77 ± 14.44	2.55 ± 1.98
Sodium azide (100 mg/mL) + methanolic extract (100 mg/mL)	0	2.47 ± 0.57		
	24	0.53 ± 0.08		
	48	–0.10 ± 0.07**		
	72	0.13 ± 0.09**	52.34 ± 8.12	3.34 ± 2.82

ΔL is mean difference in length of *Allium cepa* roots before and after treatment

**$P \leq 0.001$

It was 0.26 and 0.13 cm, respectively, for the two extract concentrations.

Microscopy revealed no abnormalities or disturbances in mitotic division: chromosome integrity maintained its high mitotic index (69.76 ± 7.01%), and no chromosomal aberrations were registered (Fig. 2, Table 2).

The microscopy of the roots stained with 2% acetic carmine after treatment with two concentrations of sodium azide revealed several chromosomal anomalies with disruption of all the stages of cell division (Figs. 3 and 4, Table 2). Several cells contained C-mitosis, S-mitosis, chromosomal breaks, bridges, and uneven distribution of chromosomes, which led to disturbed anaphases, metaphases, and telophases. These anomalies were caused by both concentrations of azide; however, they were much more severe at 100 mg/mL of sodium azide.

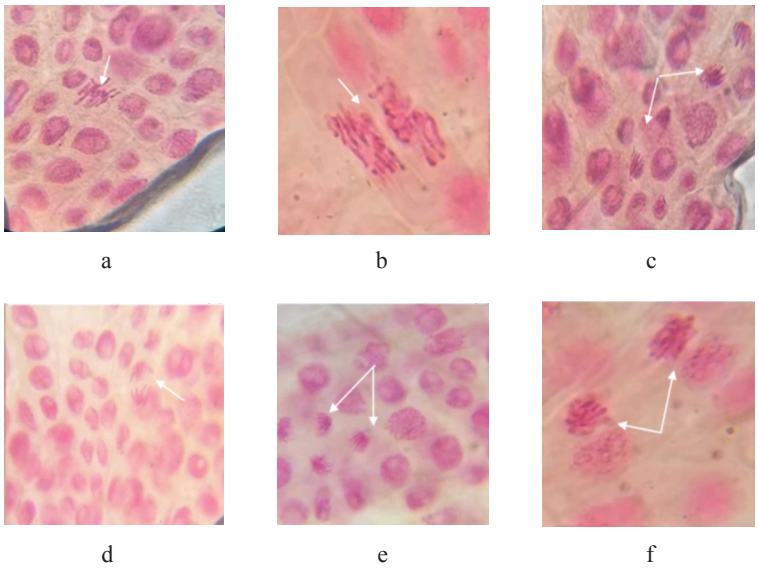

Figure 2 Normal mitotic divisions of *Allium cepa* meristem cells (100×): (a) interphase, prophase, and metaphase; (b) start of anaphase; (c), (e), (f) anaphase; (d) telophase

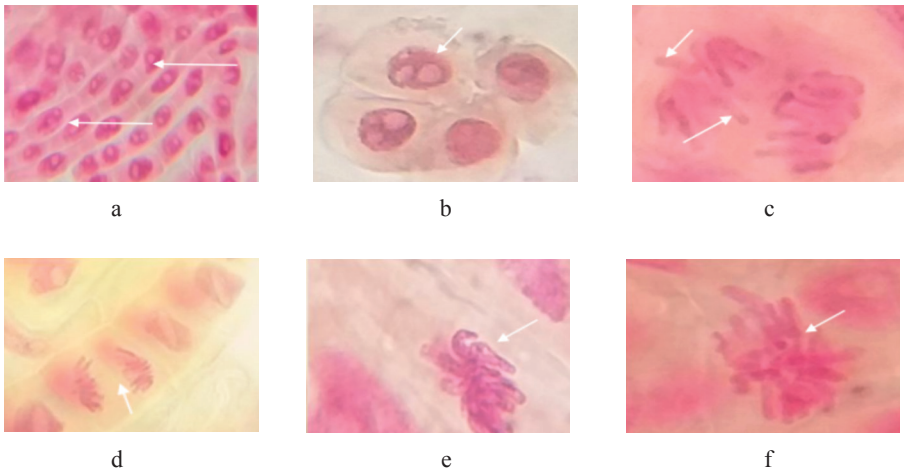

Figure 3 Various anomalies caused by sodium azide at 50 mg/mL (100×): (a) binucleated cell; (b) disturbed telophase; (c) disturbed anaphase; (d) normal anaphase; (e), (f) disturbed metaphase

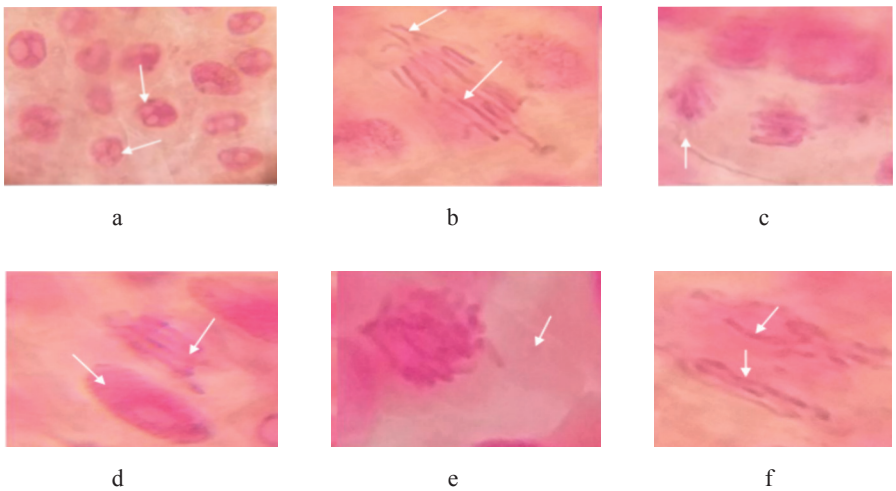

Figure 4 Chromosomes of *Allium cepa* roots treated with 100 mg/mL of sodium azide (100×): (a) binucleated cells; (b) chromosomal break, chromosomal bridge; (c), (e) disrupted (uneven) anaphase; (d) prophase, chromosomal bridge; (f) C-mitosis

Chromosomal aberrations increased together with the concentration of sodium azide. The genotoxic effect was most severe at 100 mg/mL. Both concentrations of sodium azide reduced the mitotic index, which meant that sodium azide blocked cell division. On the other hand, the number of chromosomal aberrations grew together with sodium azide concentration. They were represented mainly by C-mitosis, chromosomal bridges and breaks, and nuclear lesions of binucleate types. Therefore, sodium azide was an aberration inducer (Figs. 3 and 4, Table 2).

Sodium azide produced a cytotoxic effect which led to poor growth and length narrowing. Its mitodepressive effect decreased mitotic activity and increased chromosomic abnormality incidence. Indeed, chemical agents are recognized as factors involved in the structural and numerical modifications of chromosomes. As a result, they cause defects in chromosome segregation, abnormal DNA replication, and DNA breaks. These chromosomal aberrations result from clastogenic and aneugenic effects [23]. This study confirmed the genotoxic effect of sodium azide. According to Al-Qurainy *et al.*, sodium azide is a mutagenic metabolite that damages DNA by substituting one base pair with another [24]. Indeed, the shorter length of *A. cepa* roots treated with sodium azide could be explained by the mitodepressive effect caused by the apoptosis of meristem cells. Other samples demonstrated evolution of the normal length, probably, due to the resumption of mitosis.

Sodium azide induced the development of chromosome bridges in the meristem cells of *A. cepa* roots. According to Neelamkavil and Thoppil, the chromosomal aberrations and nuclear lesions in *A. cepa* root meristems treated with bleaching powder indicated a genotoxic effect, which confirms that sodium azide is genotoxic [25]. The clastogenic effects suggest that bleaching powder caused chromosome and chromatin breaks, which, in return, led to abnormal chromosome number, stickiness, breakage, and reunion of chromosome, as well as to bridges during mitotic division [26, 27].

The mitotic index was higher in the roots treated with two concentrations of the *R. alaternus* extract than in those treated with distilled water. Therefore, the extract induced cell division and, subsequently, produced a genoprotective effect. Moreover, the number of cells in division was high with traces chromosomal aberrations also proven by a marked root length. The samples treated with 50 mg/mL of *R. alaternus* methanolic extract had pycnotic nuclei and chromosomal breaks (Figs. 5 and 6, Table 2). This finding confirms the conclusion made by Ben Ammar *et al.*, who experimented with methanolic, petroleum ether, chloroform, and aqueous extracts of *R. alaternus* leaves and registered no mutagenicity, which means that *R. alaternus* is a promising antimutagenic [28].

The antigentoxic effect showed that the mitotic index was close to that of the control. It had a moderate chromosomal aberration percentage, chromosomal bridges and breaks, and a lower C-mitosis (Figs. 7 and 8, Table 2).

A quantitative analysis of the *R. alaternus* methanolic extract revealed a lot of polyphenols and flavonoids and thus a prominent antioxidant effect. This antioxidant effect might be the cause of the continuous cell division, mitoprotective activity, and a good DNA protection. Perron *et al.* tested 12 polyphenolic compounds, which demonstrated a 100% ability to inhibit DNA damage [29]. The polyphenolic compounds had hydroxyl radicals in their chemical structures, which prevented oxidative DNA damage.

On the other hand, Silva *et al.* showed that flavonoids have special DNA repair mechanisms that enable them to reduce and repair DNA strand breaks induced by oxidative stress [30]. Therefore, polyphenols are effective protectors against oxidative DNA damage.

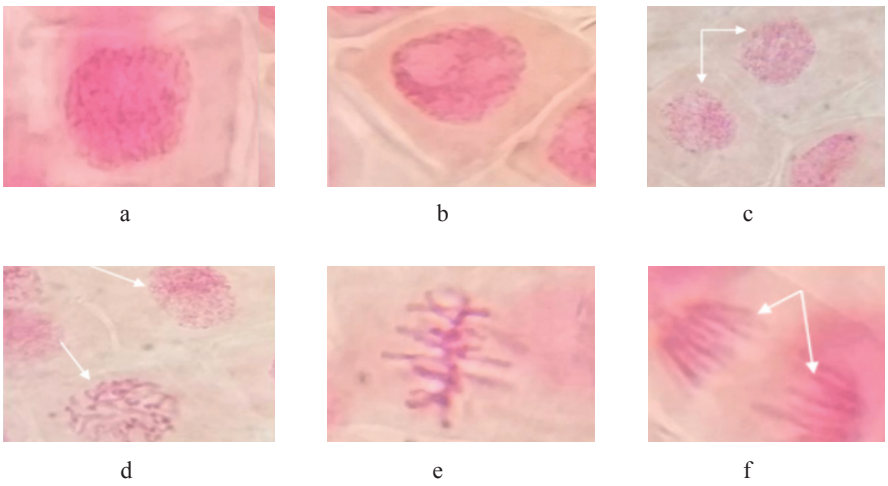

Figure 5 Chromosomes of *Allium cepa* roots treated with 50 mg/mL of *Rhamnus alaternus* leaf extract (100×): (a) prophase; (b) end of interphase; (c) telophase; (d) pycnotic nucleus; (e) metaphase; (f) anaphase

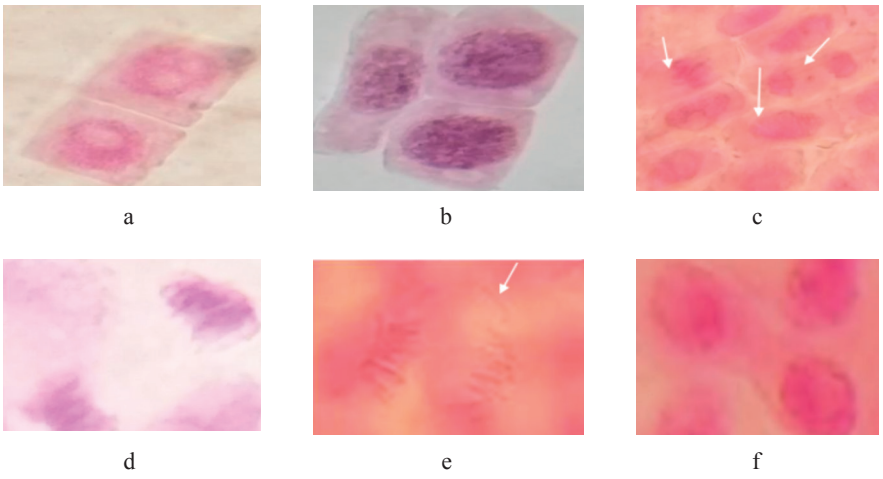

Figure 6 Chromosomes of *Allium cepa* roots treated with 100 mg/mL of *Rhamnus alaternus* leaf extract (100×): (a), (b), (f) telophase/cytodiuresis; (c) anaphase, prophase, and metaphase; (d) anaphase with chromosome breaks; (e) chromosome bridge with an isolated chromosome

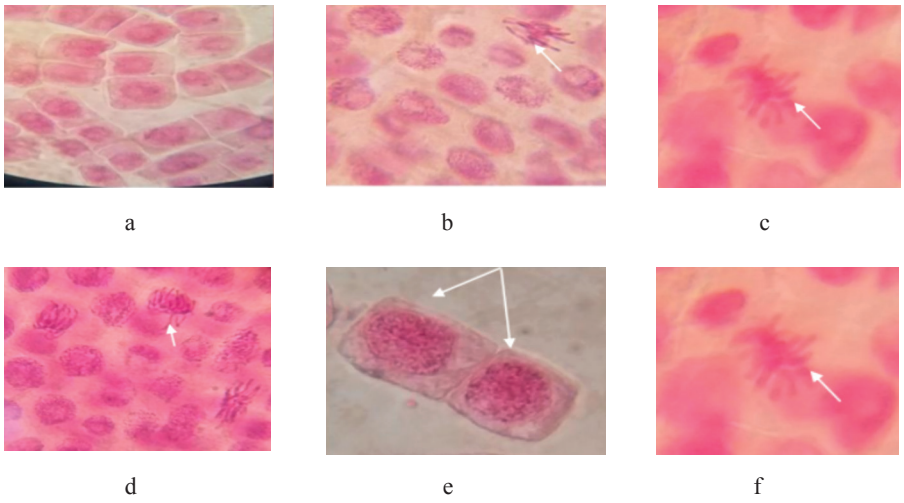

Figure 7 Chromosomes of *Allium cepa* roots treated with 50 mg/mL of methanolic extract and 100 mg/mL of sodium azide (100×): (a) several prophases; (b) several prophases; (c), (f) metaphase; (d) anaphase; (e) telophase start of prophase

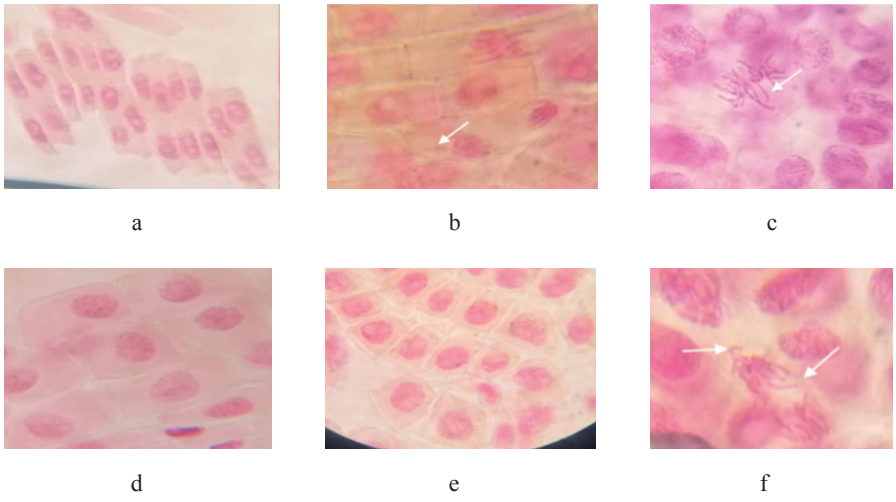

Figure 8 Chromosomes of *Allium cepa* roots treated with 50 mg/mL of methanolic extract and 100 mg/mL of sodium azide (100×): (a) binucleated; (b) metaphase, anaphase; (c) several prophases; (d) prophase; (e) prophase, metaphase, and anaphase.

Polyphenols have a powerful potency to donate electrons or hydrogen atoms, thus hampering oxidative stress, cell damage, and inflammation. They create a defensive obstacle against free radicals and reactive oxygen species. These protective effects might be explained by their antioxidant capacity [31].

Probably, the high content of flavonoids and polyphenols in *R. alaternus* protected the DNA as they opposed to the attack of free radicals emitted by sodium azide. Previous studies attributed the antigenotoxic activity of plant extracts to their numerous phenolic and flavonoid compounds, as well as to their ability to combat oxidative stress. The results imply that the extract managed to protect the genome of

the roots against mutagen because division anomalies were very scarce. These findings confirm those made by Ben Amar *et al.*, who proved that the extract of *R. alaternus* leaves and roots had anti-free-radical, anti-mutagenic, and antiproliferative properties as they trapped mutagenic free radicals [32]. According to Ben Sghaier *et al.*, medicinal plants contain phytochemicals that may have potential chemopreventive activity since they protect DNA from attack of free radicals [33].

CONCLUSION

Medicinal plants contain a lot of secondary metabolites with beneficial therapeutic and pharmacological properties, which deserve extensive research. *Rhamnus alaternus* L. proved to be an effective antioxidant and mitoprotector that can boost the development of pharmacognosy and produce new herbal drugs for the pharmaceutical industry. The genoportective effect of *R. alaternus* leaf extract could be a source of new cancer drugs and protect human genome from the side effects of chemical treatment.

CONTRIBUTION

L. Gadouche conceived and designed the analysis, performed the biological experiments, and wrote the paper. A. Zidane and K. Zerrouki contributed to the data analysis and revised the paper. A. Ababou performed the statistical analysis. I. Bachir Elazaar, D. Merabet, W. Henniche, and S. Ikhlel performed the biological experiments. All the authors revised the manuscript for publication.

CONFLICT OF INTEREST

The authors declare that there was no potential conflict of interests regarding the publication of this article.

REFERENCES

1. Sabahi Z, Soltani F, Moein M. Insight into DNA protection ability of medicinal herbs and potential mechanisms in hydrogen peroxide damages model. Asian Pacific Journal of Tropical Biomedicine. 2018;8(2):120–129. https://doi.org/10.4103/2221-1691.225616
2. Kitagishi Y, Kobayashi M, Matsuda S. Protection against cancer with medicinal herbs via activation of tumor suppressor. Journal of Oncology. 2012;2012. https://doi.org/10.1155/2012/236530
3. Dayani MA, Heidari-Soureshjani S, Salcher J. Radio-protective effects and mechanisms of medicinal plants against X-ray: A systematic review. Journal of Pharmaceutical Research International. 2019;25(1):1–11. https://doi.org/10.9734/JPRI/2018/46764
4. Nekkaa A, Benaissa A, Mutelet F, Canabady-Rochelle L. *Rhamnus alaternus* plant: Extraction of bioactive fractions and evaluation of their pharmacological and phytochemical properties. Antioxidants. 2021;10(2). https://doi.org/10.3390/antiox10020300
5. Zeouk I, Bekhti K. A critical overview of the traditional, phytochemical and pharmacological aspects of *Rhamnus alaternus*: a Mediterranean shrub. Advances in Traditional Medicine. 2020;20:1–11. https://doi.org/10.1007/s13596-019-00388-8
6. Boussahel S, Speciale A, Dahamna S, Amar Y, Bonaccorsi I, Cacciola F, *et al.* Flavonoid profile, antioxidant and cytotoxic activity of different extracts from Algerian *Rhamnus alaternus* L. bark. Pharmacogny Magazine. 2015;11(42):S102–S109. https://doi.org/10.4103/0973-1296.157707
7. Moussi K, Nayak B, Perkins LB, Dahmoune F, Madani K, Chibane M. HPLC-DAD profile of phenolic compounds and antioxidant activity of leaves extract of *Rhamnus alaternus* L. Industrial Crops and Products. 2015;74:858–866. https://doi.org/10.1016/j.indcrop.2015.06.015
8. Ben Ammar R, Kilani S, Bouhlel I, Skandrani I, Naffeti A, Boubaker J, *et al.* Antibacterial and cytotoxic activities of extracts from (Tunisian) *Rhamnus alaternus* (Rhamnaceae). Annals of Microbiology 2007;57(3):453–460. https://doi.org/10.1007/BF03175089
9. Bhouri W, Sghaier MB, Kilani S, Bouhlel I, Dijoux-Franca M-G, Ghedira K, *et al.* Evaluation of antioxidant and antigenotoxic activity of two flavonoids from *Rhamnus alaternus* L. (Rhamnaceae): Kaempferol 3-O-*β*-isorhamninoside and rhamnocitrin 3-O-*β*-isorhamninoside. Food and Chemical Toxicology 2011;49(5):1167–1173. https://doi.org/10.1016/j.fct.2011.02.011

10. Bhouri W, Bouhlel I, Boubaker J, Kilani S, Ghedira K, Ghedira LC. Induction of apoptosis in human lymphoblastoid cells by kaempferol 3-O-β-isorhamninoside and rhamnocitrin 3-O-β-isorhamninoside from *Rhamnus alaternus* L. (Rhamnaceae). Cell Proliferation 2011;44(3):283–290. https://doi.org/10.1111/j.1365-2184.2011.00749.x

11. Chatti IB, Ben Toumia I, Krichen Y, Maatouk M, Ghedira LC, Krifa M. Assessment of *Rhamnus alaternus* leaves extract: Phytochemical characterization and antimelanoma activity. Journal of Medicinal Food. 2021. https://doi.org/10.1089/jmf.2020.0170

12. Gadouche L, Zidane A, Zerrouki K, Azouni K, Bouinoune S. Cytotoxic effect of *Myrtus communis*, *Aristolochia longa*, and *Calycotome spinosa* on human erythrocyte cells. Foods and Raw Materials. 2021;9(2):379–386. https://doi.org/10.21603/2308-4057-2021-2-379-386

13. Quezel P, Santa S. New flora of Algeria and southern desert regions. 2 Vol. Paris: National Centre for Scientific Research; 1963. 1170 p. (In French.).

14. Diallo D, Sanogo R, Yasambou H, Traoré A, Coulibaly K, Maiga A. Study of the chemical compounds of *Ziziphus mauritiana* Lam. (Rhamnaceace) leaves, used traditionally in the treatment of diabetes in Mali. Comptes Rendus Chimie. 2004;7(10–11):1073–1080. (In French.). https://doi.org/10.1016/j.crci.2003.12.035

15. Raafat K, Samy W. Amelioration of diabetes and painful diabetic neuropathy by *Punica granatum* L. extract and its spray dried biopolymeric dispersions. Evidence-Based Complementary and Alternative Medicine. 2014;2014. https://doi.org/10.1155/2014/180495

16. Hmid I, Elothmani D, Hanine H, Oukabli A, Mehinagic E. Comparative study of phenolic compounds and their antioxidant attributes of eighteen pomegranate (*Punica granatum* L.) cultivars grown in Morocco. Arabian Journal of Chemistry. 2013;10:S2675–S2684. https://doi.org/10.1016/j.arabjc.2013.10.011

17. Burits M, Bucar F. Antioxidant activity of *Nigella sativa* essential oil. Phytotherapy Research. 2000;14(5):323–328. https://doi.org/10.1002/1099-1573(200008)14:5<323::AID-PTR621>3.0.CO;2-Q

18. Sharififar F, Mozaffarian V, Moradkhani S. Comparison of antioxidant and free radical scavenging activities of the essential oils from flowers and fruits of *Otostegia persica* Boiss. Pakistan Journal of Biological Sciences. 2007;10(21):3895–3899. https://doi.org/10.3923/pjbs.2007.3895.3899

19. Kartal N, Sokmen M, Tepe B, Daferera D, Polissiou M, Sokmen A. Investigation of the antioxidant properties of *Ferula orientalis* L. using a suitable extraction procedure. Food Chemistry. 2007;100(2):584–589. https://doi.org/10.1016/j.foodchem.2005.09.084

20. Tedesco SB, Laughinghouse IV HD. Bioindicator of genotoxicity: The Allium cepa test. In: Srivastava JK, editor. Environmental contamination. Rijeka: InTech Publisher; 2012. pp. 137–156. https://doi.org/10.5772/31371

21. Yekeen TA, Azeez MA, Akinboro A, Lateef A, Asafa TB, Oladipo IC, *et al.* Safety evaluation of green synthesized *Cola nitida* pod, seed and seed shell extracts-mediated silver nanoparticles (AgNPs) using an *Allium cepa* assay. Journal of Taibah University for Science. 2017;11(6):895–909. https://doi.org/10.1016/j.jtusci.2017.06.005

22. Grant WF. The present status of higher plant assays for the detection of environmental mutagens. Mutation Research Regular Papers. 1994;310(2):175–185. https://doi.org/10.1016/0027-5107(94)90112-0

23. Leme DM, Marin-Morales MA. *Allium cepa* test in environmental monitoring: A review on its application. Mutation Research – Reviews in Mutation Research. 2009;682(1):71–81. https://doi.org/10.1016/j.mrrev.2009.06.002

24. Al-Qurainy F, Al-Hemaid FM, Khan S, Ajmal Ali M, Tarroum M, Ashraf M. Detection of sodium azide-induced mutagenicity in the regenerated shoots of Artemisia annua using internal transcribed spacer (ITS) sequences of nrDNA. Pakistan Journal of Botany. 2011;43(4):2183–2186.

25. Neelamkavil SV, Thoppil JE. Genotoxic assessment of calcium hypochlorite and *Strychnos potatorum* Linn. seeds – Two commonly used water purifying agents. Reviews on Environmental Health. 2015;30(1):19–23. https://doi.org/10.1515/reveh-2014-0066

26. Bhagyanathan NK, Thoppil JE. Genotoxic potential of Cynanchum sarcomedium Meve & Liede coupled with its modulatory action on oxidative-stress–mediated genotoxicity by hydrogen peroxide. Turkish Journal of Biology. 2016;40(1):120–129.

27. Obute GC, Ekeke C, Izuka DC. Genotoxicity assessment of refined petroleum products and popular local soft drink (Zobo) in daily use in Nigeria. Research Journal of Mutagenesis. 2016;6(1):22–30. https://doi.org/10.3923/rjmutag.2016.22.30

28. Ben Ammar R, Kilani S, Abdelwahed A, Hayder N, Mahmoud A, Chibani J, *et al. In vitro* mutagenicity, antimutagenicity and free radical scavenging activity of *Rhamnus alaternus* (Rhamnaceae) extracts. Pakistan Journal of Biological Sciences. 2005;8(3):439–445. https://doi.org/10.3923/pjbs.2005.439.445

29. Perron NR, Hodges JN, Jenkins M, Brumaghim JL. Predicting how polyphenol antioxidants prevent DNA damage by binding to iron. *Inorganic Chemistry.* 2008;47(14):6153–6161. https://doi.org/10.1021/ic7022727

30. Silva JP, Gomes AC, Coutinho OP. Oxidative DNA damage protection and repair by polyphenolic compounds in PC12 cells. European Journal of Pharmacology. 2008;601(1–3):50–60. https://doi.org/10.1016/j.ejphar.2008.10.046

31. Majidinia M, Bishayee A, Yousefi B. Polyphenols: Major regulators of key components of DNA damage response in cancer. DNA Repair. 2019;82. https://doi.org/10.1016/j.dnarep.2019.102679

32. Ben Ammar R, Kilani S, Bouhlel I, Ezzi L, Skandrani I, Boubaker J, *et al.* Antiproliferative, antioxidant, and antimutagenic activities of flavonoid-enriched extracts from (Tunisian) *Rhamnus alaternus* L.: Combination with the phytochemical composition. Drug and Chemical Toxicology. 2008;31(1):61–80. https://doi.org/10.1080/01480540701688725

33. Ben Sghaier M, Bhouri W, Neffati A, Boubaker J, Skandrani I, Bouhlel S, *et al.* Chemical investigation of different crude extracts from *Teucrium ramosissimum* leaves. Correlation with their antigenotoxic and antioxidant properties. Food and Chemical Toxicology. 2011;49(1):191–201. https://doi.org/10.1016/j.fct.2010.10.016

ORCID IDs
Leila Gadouche https://orcid.org/0000-0003-1757-1988
Khayra Zerrouki https://orcid.org/0000-0002-0217-3138
Azdinia Zidane https://orcid.org/0000-0003-1575-5994
Adda Ababou https://orcid.org/0000-0002-2056-0553
Ibtissem Bachir Elazaar https://orcid.org/0000-0002-8637-637X
Dounya Merabet https://orcid.org/0000-0001-6019-444X
Wissam Henniche https://orcid.org/0000-0002-7460-7417
Samah Ikhlef https://orcid.org/0000-0003-1370-9206

Foods and Raw Materials. 2022;10(2)

ISSN 2310-9599 (Online)
ISSN 2308-4057 (Print)

Research Article
Open Access

Available online at http://jfrm.ru/en
https://doi.org/10.21603/2308-4057-2022-2-529
https://elibrary.ru/OVETCV

Digital inventory of agricultural land plots in the Kemerovo Region

Artem O. Rada*, Aleksandr D. Kuznetsov

Kemerovo State University, Kemerovo, Russia

* e-mail: rada.ao@kemsu.ru

Received 21.01.2022; Revised 21.02.2022; Accepted 14.04.2022; Published online 23.06.2022

Abstract:
Cadastral and geodetic land works are expensive, which makes aerial photography extremely valuable for land traceability and inventory. The present research objective was to develop a new digital survey technology for registration of agricultural lands. We assessed the accuracy of the new method and evaluated its decision support options. The study featured the case of the Kemerovo Region – Kuzbass, Russia.

The aerial survey took place in 2021 and involved 17 municipalities of the Kemerovo Region. The software and hardware complex included an unmanned aerial vehicle (UAV) and a module for aerial photography. Photogrammetric, cartometric, and satellite methods were used to define the coordinates of feature points. We developed new software (Sovhoz.avi) to perform the land inventory.

The photogrammetric and cartographic methods proved efficient in determining the feature points and boundaries of land plots. They also appeared accurate enough for land inventory and decision support. The study updated the available land inventory data. About 30% of all land plots were recorded incorrectly; some plots marked as agricultural appeared to belong to the local forest reserves or urban territories. Incorrect data (1.64%) were excluded from the official inventory. The survey covered a total area of 41 000 ha and revealed 1700 illegally used land plots. The updated inventory of unused lands included 3825 new plots (163 400 ha), which can attract prospective investors.

The results can be used by the local authorities to make land management decisions and identify illegal land use.

Keywords: Agricultural land, food, land inventory, unmanned aerial vehicle (UAV), aerial survey, illegal land use

Funding: The research was conducted on the premises of the Research Equipment Sharing Center of Kemerovo State University (KemSU), agreement No. 075-15-2021-694 dated August 5, 2021, between the Ministry of Science and Higher Education of the Russian Federation (Minobrnauka) and Kemerovo State University (contract identifier RF----2296.61321X0032).

Please cite this article in press as: Rada AO, Kuznetsov AD. Digital inventory of agricultural land plots in the Kemerovo Region. Foods and Raw Materials. 2022;10(2):206–215. https://doi.org/10.21603/2308-4057-2022-2-529

INTRODUCTION

The present research featured a new aerial survey software and hardware complex, which included a camera-equipped unmanned aerial vehicle (UAV) and digital twin software tailored for agricultural inventory. The new technology provided a digital account of agricultural lands in the Kemerovo Region aka Kuzbass (West Siberia, Russia). The article introduces an assessment of its accuracy and decision support options.

Food security remains one of the main global issues [1–3]. In fact, famine relief is one of the seventeen Sustainable Development Goals set up by the United Nations [4]. Stable food production and availability presupposes efficiency, land availability being the most important production factor in agriculture [5, 6]. Agricultural land depletion, shortage, and irrational use make it difficult to provide the growing world population with food [7–10]. Therefore, land-use efficiency is an important task of resource-intensive digital precision farming [11–13].

Agricultural land resources are limited. Therefore, their inventory and management require high-quality accurate information about the terrain, its configuration, location, etc. These data help plan agricultural work, calculate potential yields, make decisions on the allocation of machine time, seeds, fertilizers, etc. [14].

Accurate land survey is also vital for crop selection, rotation, and logistics [15]. If an agricultural land plot has a complex terrain and the current crop market conditions are unstable, a high-quality land survey can provide the maximal economic effect [16]. Obviously, agricultural organizations are interested in complete and detailed information about their land.

The poor quality of land data is a relevant agricultural issue in Russia and some other countries [17, 18]. As evidenced in practice, traditional paper maps are mostly inaccurate. They are out of date and fail to chart all the lands in actual agricultural use. For instance, a shrub-overgrown area can still be registered as fit for farming, with crops, seeds, fertilizers, and equipment operation time allocated for its cultivation. Land-use efficiency presupposes official registration, state inventory, and open access, which can prevent mining development of agricultural lands [19, 20]. Land-use efficiency ensures fair taxation, protects the interests of stakeholders, determines the required amount of state support, and assesses the main agricultural indicators. In addition, it enables small farmers and agribusinesses to use land as collateral for a bank loan.

Official state inventories often contain faulty or no data at all, which causes irrational use of agricultural plots and land law violations. Most of these problems result from the high cost of traditional geodetic and cadastral work. Traditional land surveys require a lot of man labor and high transportation costs. As a result, they can be too expensive for most agricultural enterprises [21, 22]. Many agricultural land users are not interested in geodetic investigations of their lands: they prefer to refrain from even one-time cadastral surveys, not to mention regular ones. Digital twins of agricultural areas can solve this problem. Visual data are gathered by UAVs and processed by specialized software.

Aerial surveys and drone-mounted infrared cameras are able to solve a wide range of tasks, e.g. maintaining linear infrastructure facilities, tracking forest fires, monitoring construction and mining operations, counting game population, looking for missing people, developing smart city projects, etc. [23–28]. UAV-based aerial surveys are cheap and require no physical presence on location, thus preventing subjective and objective human errors [29]. Therefore, the new complex increases the accuracy and reduces the cost of agricultural land surveys.

UAVs have become focus of numerous scientific publications on cadastral work and real estate inventory. For instance, Puniach *et al*. wrote about a UAV-based update of cadastral data on territories with frequent landslides [30]. The study covered an area of about 50 ha and involved a DJI S1000 octocopter, which hovered at 145 meters above the ground. A Sony ILCE A7R camera provided an 80% direct overlap and a 60% side overlap. It took 500 images and fixed 33 control points. The data were processed using Agisoft PhotoScan Professional, which determined a landslide with an accuracy of up to 0.5 meters. The research made it possible to update the cadastral database and support the farms affected by landslides. The study demonstrated acceptable accuracy in surveying small agricultural plots. In fact, some studies limit the cadastral capabilities of UAVs to small hard-to-reach areas [31].

Šafář *et al*. studied liDAR laser scanning as a means of updating cadastral records in the Czech Republic [32]. Their research involved a DJI Matrice 600 Pro hexacopter, a LiDAR RIEGL miniVUX-1, and PosPac software. The survey results met the local accuracy requirements. Even a partial use of UAVs in construction monitoring reduced their costs by 18–20%. However, the study, like most publications on this issue, focused on the cadastral registration of capital construction objects, not land plots [33, 34].

Brookman-Amissah *et al*. proved that UAV-based aerial survey determined boundaries of land plots with an accuracy stated by the legislation of Ghana, i.e. up to 3 ft, or 91.5 cm [35]. However, the research involved a lightweight UAV (430 g), which could perform only in the most ideal weather. The research provided no data on heavier commercial-grade UAVs. Thus, the problem of using aerial digital surveys for land inventory is at its initial development stage. It requires new methods for surveys and data processing on larger areas, as well as field tests in real weather conditions.

STUDY OBJECTS AND METHODS

The research featured agricultural land plots located in 17 municipal districts of the Kemerovo Region (West Siberia, Russia). The complex included two unmanned aerial vehicles (UAV): a cantilever high-wing aircraft with a Lun 20 gasoline engine (Spetsialmiy Tekhnologicheskiy Tsentr LLC, St. Petersburg, Russia) and an all-wing drone with a Geoscan 201 electric engine (Geoscan, Saint-Petersburg, Russia). Their maximal takeoff weight was 18.6 and 8.5 kg, respectively. This research employed commercial aircraft-type UAVs, unlike previous studies that featured light helicopter-type drones. In good weather and with no vertical drops, a Lun 20 drone is able to survey an area of 20–55 km^2 per flight, a Geoscan 201 drone – about 9 km^2.

The Lun 20 carried a module for cartographic aerial photography, which included: a turntable to compensate for the wind drift, a Phase iXM-50 aerial camera (Phase One, Denmark), a Javad TRE-3N OEM board for tracking geographic coordinates (Javad GNSS Inc, USA), and a cloud assessment camera. The Geoscan 201 carried a Sony RX1R II digital camera (SONY, Japan) and a Topcon GNSS receiver (Topcon Corporation, Japan). High-precision dual-frequency GNSS receivers Javad Triumph-2 (Javad GNSS Inc, USA) and Trimble R10-2 (Trimble Inc, USA) provided on-ground horizontal and vertical control of geographic coordinates.

The software part of the complex was represented by the Sovhoz.avi, a platform for digital inventory and management of agricultural land. The software was

developed at the Digital Institute of the Kemerovo State University (Kemerovo, Russia). It stores aerial photography data and those obtained from external sources, e.g. official data on the agricultural land plots obtained from federal, regional, and municipal sources. The platform has been accumulating available data on officially registered agricultural land plots since August 2020. The list of sources included:

– Federal Service for State Registration, Cadaster, and Cartography (*Rosreestr*) – digital data on 35 000 sites (2019);
– Ministry of Agriculture and Processing Industry of the Kemerovo Region – digital data from the Unified Federal Information System of Agricultural Lands (2020);
– Committee for State Property Management of the Kemerovo Region – paper documents on 26 000 land plots (2020);
– Municipal Property Management Committees – digital data on 13 000 plots from 17 municipalities of the Kemerovo Region; and
– Municipal Authorities – digital data on 22 000 share lands, federal lands, and plots under registration (2020).

The UAV aerial survey took place in 2021. It aimed at clarifying the available data, forming a unified database of agricultural land management, and identifying illegal land use. The study had several stages. The first stage included an on-ground horizontal and vertical control of geodetic coordinates using GNSS receivers in the RTK mode. After that, the results of aerial photography were linked to geographic coordinates (MSK-42 Zone 1, BSL 1977).

The second stage lasted from May 10 to September 16, 2021. Two teams used the Lun 20 and the Geoscan 201 to perform an aerial survey of agricultural lands. The equipment was checked and programmed a day before the survey, which was carried out on sunny and dry days with a lot of sunlight and moderate or no wind. The obtained nadir images with a pre-set forward and side lap made it possible to construct an orthophotomap and a digital terrain model.

The third stage included data processing for subsequent managerial decisions by the authorities and land users. This stage made it possible to justify the use of photogrammetric and cartometric methods as means of determining the geographical coordinates of land plots.

The present research used standard methods of computer science, probability theory, and mathematical statistics to compare the coordinates obtained by satellite geodetic (GNSS), photogrammetric, and cartometric (orthomosaic) measurements. The procedure followed the requirements of the Order of the Federal Service for State Registration, Cadaster, and Cartography (*Rosreestr*) dated October 23, 2020, No P/0393 "Accuracy and method requirements for determining the feature point coordinates of land plot boundaries and buildings contours".

When it goes about agricultural land plots, the root mean square error (MSE) for determining feature point coordinates cannot exceed 2.5 m, and the pixel projection for aerial photographs should be 35 cm. However, this rule is not applied to private household plots, gardens, garages, and houses. To simulate unfavorable working conditions, the calculations were carried out for points with limited visibility and signal interference. The Agisoft Metashape software (Zhivoy Soft OOO, St. Petersburg, Russia) was used to compare the results of the photogrammetric and cartometric methods. This software in its professional edition determines the geographical coordinates using the photogrammetric method or an orthophotomap.

The MSE for the feature points were calculated by the following formula to compare the survey results obtained by different methods:

$$m = (10 + 1\times10^{-6})\times D \quad (1)$$

where D is the vector length between the feature point and base station point, mm.

The MSE for the location of the feature point of the contour σ, determined by photogrammetric method, was calculated as follows:

$$\sigma = \sqrt{\sigma_o^2 + \sigma_n^2 + \sigma_c^2} \quad (2)$$

where σ_o is the MSE of the orthophotomap; σ_n it the MSE of the base station point; σ_c is the MSE of the control point.

The MSE of the feature point according to the cartometric method was calculated as follows:

$$m = 0.0005\times M \quad (3)$$

The coordinates determined by various methods were tested for accuracy, and the data of the digital land survey were compared. After that, the results were studied for errors, inconsistencies, and violations.

RESULTS AND DISCUSSION

The new software and hardware complex conducted an aerial survey of agricultural land in the Kemerovo Region. The results were used to compare different methods of measuring feature points. In case of the photogrammetric method, the mean square error (MSE) was $\sigma = \sqrt{0.05^{22} + 0.18 + 0.007^2} = 0.053$ m. This MSE did not exceed the regulatory requirements specified above. Tables 1–3 compare three methods as in the case of the Topki municipality. The difference between the feature point coordinates obtained by different methods (Δ) was calculated based on the geodetic inverse.

Table 1 shows that the difference between the results of satellite and photogrammetric methods stayed within 10 cm, as specified in the regulatory requirements. Table 2 compares the data obtained by satellite imagery and cartometrics.

Table 1 Satellite method vs. photogrammetric method

Point	Satellite method		Photogrammetric method		Difference		
	X, m	*Y*, m	*X*, m	*Y*, m	Δ*X*, m	Δ*Y*, m	Δ, m
topki1	1310048.280	617173.700	1310048.295	617173.7108	–0.015	–0.011	0.018
topki2	1310055.216	617162.459	1310055.214	617162.4656	0.002	–0.007	0.007
topki3	1310018.896	617140.355	1310018.896	617140.3557	0.000	–0.001	0.001
topki4	1310011.957	617151.709	1310011.957	617151.705	0.000	0.004	0.004
topki5	1309996.704	617202.782	1309996.709	617202.8057	–0.005	–0.024	0.024
topki6	1309962.871	617182.499	1309962.925	617182.4253	–0.054	0.074	0.092
topki7	1309817.231	617335.634	1309817.226	617335.6422	0.005	–0.008	0.009
topki8	1309857.820	617399.271	1309857.815	617399.2792	0.005	–0.008	0.010
topki9	1309817.909	617376.728	1309817.925	617376.7499	–0.016	–0.022	0.027
topki10	1309819.796	617373.463	1309819.809	617373.4673	–0.013	–0.004	0.014
topki11	1309799.636	617361.148	1309799.637	617361.1525	–0.001	–0.004	0.005
topki12	1309974.076	616743.343	1309974.075	616743.3386	0.001	0.004	0.005
topki13	1309949.763	616775.568	1309949.775	616775.5402	–0.012	0.028	0.030
topki14	1309939.604	616767.828	1309939.621	616767.8154	–0.017	0.013	0.021
topki15	1309963.933	616735.588	1309963.931	616735.5874	0.002	0.001	0.002
topki16	1310339.023	615177.752	1310338.993	615177.7349	0.030	0.017	0.034
topki17	1310344.018	615183.604	1310343.971	615183.5602	0.047	0.044	0.064
topki18	1310349.038	615179.145	1310349.032	615179.1342	0.006	0.011	0.012
topki19	1310344.136	615173.292	1310344.125	615173.2815	0.011	0.010	0.016
topki20	1310320.547	615146.909	1310320.531	615146.8989	0.016	0.010	0.019
topki21	1310288.354	615110.297	1310288.307	615110.3011	0.047	–0.004	0.048
topki22	1310280.513	615117.21	1310280.507	615117.194	0.006	0.016	0.017

Table 2 Satellite method vs. cartometric method

Point	Satellite method		Cartometric method		Difference		
	X, m	*Y*, m	*X*, m	*Y*, m	Δ*X*, m	Δ*Y*, m	Δ, m
topki1	1310048.280	617173.700	1310048.342	617173.7878	–0.062	–0.088	0.107
topki2	1310055.216	617162.459	1310055.244	617162.4891	–0.028	–0.030	0.041
topki3	1310018.896	617140.355	1310018.928	617140.4121	–0.032	–0.057	0.066
topki4	1310011.957	617151.709	1310012.099	617151.6668	–0.142	0.042	0.148
topki5	1309996.704	617202.782	1309996.892	617202.8369	–0.188	–0.055	0.196
topki6	1309962.871	617182.499	1309962.92	617182.4028	–0.049	0.096	0.108
topki7	1309817.231	617335.634	1309817.256	617335.6739	–0.025	–0.040	0.047
topki8	1309857.820	617399.271	1309857.829	617399.3105	–0.009	–0.039	0.040
topki9	1309817.909	617376.728	1309818.126	617376.8517	–0.217	–0.124	0.250
topki10	1309819.796	617373.463	1309819.948	617373.4828	–0.152	–0.020	0.154
topki11	1309799.636	617361.148	1309799.735	617361.2129	–0.099	–0.065	0.118
topki12	1309974.076	616743.343	1309974.117	616743.2482	–0.041	0.095	0.103
topki13	1309949.763	616775.568	1309949.777	616775.6203	–0.014	–0.052	0.054
topki14	1309939.604	616767.828	1309939.546	616767.689	0.058	0.139	0.151
topki15	1309963.933	616735.588	1309964.053	616735.6928	–0.120	–0.105	0.160
topki16	1310339.023	615177.752	1310338.921	615177.6718	0.102	0.080	0.130
topki17	1310344.018	615183.604	1310344.108	615183.3738	–0.090	0.230	0.247
topki18	1310349.038	615179.145	1310348.931	615179.0497	0.107	0.095	0.143
topki19	1310344.136	615173.292	1310344.112	615173.221	0.024	0.071	0.075
topki20	1310320.547	615146.909	1310320.464	615146.8618	0.083	0.047	0.096
topki21	1310288.354	615110.297	1310288.337	615110.2457	0.017	0.051	0.054
topki22	1310280.513	615117.21	1310280.535	615117.2026	–0.022	0.007	0.023

Table 2 demonstrates that the difference between the data obtained by satellite mapping and cartometrics was bigger than in the previous case and reached 25 cm. However, this MSE also stayed within the maximal allowable values. Therefore, the cartometric method proved sufficiently accurate, if compared to the satellite imagery, which served as control. Table 3 compares the data obtained by photogrammetric mapping and cartometrics.

Table 3 Photogrammetric method vs. cartometric method

Point	Photogrammetric method		Cartometric method		Difference		
	X, m	*Y*, m	*X*, m	*Y*, m	Δ*X*, m	Δ*Y*, m	Δ, m
topki1	1310048.29	617173.71	1310048.34	617173.788	–0.047	–0.077	0.090
topki2	1310055.21	617162.47	1310055.24	617162.489	–0.031	–0.023	0.039
topki3	1310018.9	617140.36	1310018.93	617140.412	–0.032	–0.056	0.065
topki4	1310011.96	617151.7	1310012.1	617151.667	–0.142	0.038	0.147
topki5	1309996.71	617202.81	1309996.89	617202.837	–0.183	–0.031	0.186
topki6	1309962.93	617182.43	1309962.92	617182.403	0.005	0.022	0.023
topki7	1309817.23	617335.64	1309817.26	617335.674	–0.029	–0.032	0.043
topki8	1309857.82	617399.28	1309857.83	617399.31	–0.014	–0.031	0.034
topki9	1309817.93	617376.75	1309818.13	617376.852	–0.201	–0.102	0.225
topki10	1309819.81	617373.47	1309819.95	617373.483	–0.139	–0.016	0.140
topki11	1309799.64	617361.15	1309799.73	617361.213	–0.098	–0.060	0.115
topki12	1309974.08	616743.34	1309974.12	616743.248	–0.042	0.090	0.100
topki13	1309949.78	616775.54	1309949.78	616775.62	–0.001	–0.080	0.080
topki14	1309939.62	616767.82	1309939.55	616767.689	0.075	0.126	0.147
topki15	1309963.93	616735.59	1309964.05	616735.693	–0.122	–0.105	0.161
topki16	1310338.99	615177.73	1310338.92	615177.672	0.072	0.063	0.096
topki17	1310343.97	615183.56	1310344.11	615183.374	–0.137	0.186	0.231
topki18	1310349.03	615179.13	1310348.93	615179.05	0.101	0.084	0.132
topki19	1310344.12	615173.28	1310344.11	615173.221	0.012	0.061	0.062
topki20	1310320.53	615146.9	1310320.46	615146.862	0.067	0.037	0.077
topki21	1310288.31	615110.3	1310288.34	615110.246	–0.031	0.055	0.063
topki22	1310280.51	615117.19	1310280.53	615117.203	–0.028	–0.009	0.029

According to Table 3, the results obtained by cartometrics and photogrammetric mapping were very similar, and the MSE stayed within 25 cm. Therefore, a much cheaper aerial survey can replace traditional cadastral and geodetic works, as well as satellite imagery.

The next stage featured the Sovhoz.avi platform, which identified inconsistencies in the available data on agricultural land plots. The analysis involved software and visual control of data using the feature point coordinates of the land plots. The analysis of the data provided by the Federal Service for State Registration, Cadaster, and Cartography showed that the Kemerovo Region has a lot of agricultural land plots with unidentified boundaries. Their area is shrinking, but very slowly.

In 2017, there were 2.44 million ha of land with undetermined boundaries. In 2020, their area decreased by 22%, shrinking to 1.90 million ha. However, the total area of agricultural lands in the Kemerovo Region is about 2.9 million ha. Consequently, 65.5% of all agricultural land has unclear plot boundaries. This situation makes land-use efficiency and business turnover impossible. Moreover, it causes conflicts as it violates the legitimate interests of land users and renders faulty taxation.

The cadastral measuring of all agricultural land boundaries in the region costs 2.7 billion rubles, or 35 million US dollars (January 2022). Land users simply cannot afford it: in 2020, the total value of commercial products produced by agricultural organizations and farms of the Kemerovo Region was about 34.9 billion rubles. Thus, land users would have to spend about 7–10% of their annual revenue on cadastral work. Obviously, they would appreciate much cheaper digital methods.

The Sovhoz.avi software also found some discrepancies in the data obtained from the Committee

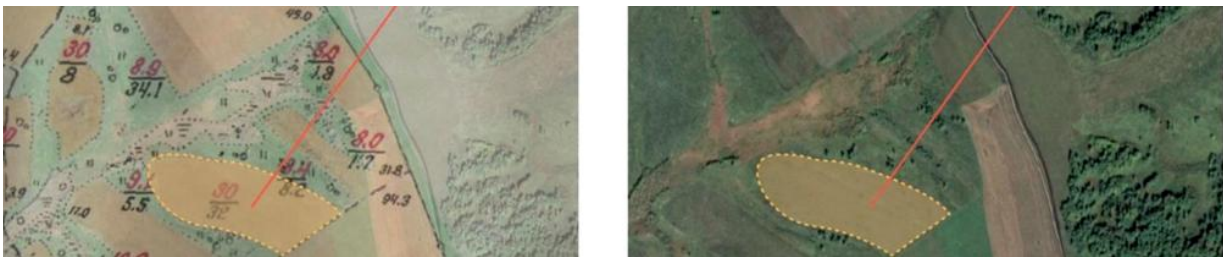

Figure 1 Faulty boundaries revealed by comparing a digitized paper map with the aerial photography data

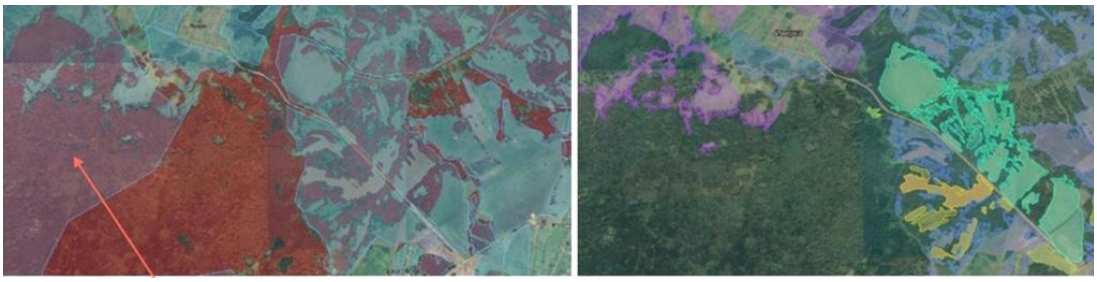

Figure 2 A land plot with a land-use error

Figure 3 An urban land plot misclassified as agricultural

for State Property Management and the Ministry of Agriculture and Processing Industry of the Kemerovo Region. After 1200 paper maps were digitized, 30% of them appeared to be faulty to some extent. Figure 1 illustrates an example of such an error detected after comparing a digitized paper map with the aerial survey data.

According to the paper map provided by the State Property Management Committee, the area of the land plot was about 32 ha. According to the coordinates obtained by the photogrammetric mapping, it was about 16.3 ha. This means that the land owner has to pay almost twice as much land tax while allocating extra resources to cultivate the acres that are not there. The error triggers incorrect agricultural work planning because most indicators, e.g. yield, are initially incorrect. The error occurred as the field partially overgrew with trees and shrubs. A prompt correction will allow the farmer to plan their costs, calculate their yields, and reduce their taxes.

The data on all previously recorded agricultural land plots were subjected to continuous automated control. This measure corrected numerous errors found in the data provided by the authorities. In the Izhmorka municipality, the survey revealed several agricultural plots (5189 ha) on the forest fund lands. The Ministry of Agriculture and Processing Industry of the Kemerovo Region misclassified them as agricultural. Figure 2 is a Sovhoz.avi screenshot which visualizes such an error that affected an area of 2352 ha.

The red arrow on the left slide highlights the area that was classified as agricultural by the Ministry of Agriculture and Manufacturing Industry of the Kemerovo Region. However, the aerial survey on the right slide shows that this area is covered with forest. The data provided by the municipal authorities of the city of Novokuznetsk were subjected to similar control. The Sovhoz.avi platform identified several areas located in the city center and along the main highways that were mistakenly recorded as agricultural (Fig. 3, red circle). As a result, 670 land plots with a total area of 9144.96 ha were removed from the system.

The Sovhoz.avi platform currently contains data on 96 600 agricultural land plots with a total area of 2.4 million ha. After verification, about 0.04 million ha, which is about 1.64% of the total area, were excluded because the data were found unreliable. Since April 30, 2021, the platform has been used by the authorities and local governments of the Kemerovo Region. The users are mostly interested in such options as "view the plots", "check and change boundaries", and "check and change attributes".

In May 2021, Sovhoz.avi was used to monitor the agricultural land use rights. Illegal use of agricultural

Table 4 Number and area of illegally used land plots in the Kemerovo Region

Municipality	May 2021		January 2022		Difference	
	Plots	Area, ha	Plots, number	Area, ha	Plots, number	Area, ha
Belovo	0	0	5	973.11	5	973.11
Guryevsk	4	60.43	8	261.77	4	201.34
Izhmorka	10	345.22	10	345.22	0	0
Kemerovo	6	158.53	5	89.03	–1	–69.50
Krapivino	7	355.29	0	0	–7	–355.29
Leninsk-Kuznetskiy	79	1031.00	27	708.37	–52	–322.63
Mariinsk	8	287.77	29	1112.95	21	825.18
Novokuznetsk	6	161.45	114	2018.35	108	1856.90
Prokopyevsk	13	972.13	95	3871.29	82	2899.16
Promyshlennoe	3	151.95	2	68.82	–1	–83.13
Tisul’	6	51.84	7	1108.50	1	1056.66
Topki	20	345.26	169	3874.49	149	3529.23
Tyazhin	150	11176.53	1037	22136.58	887	10960.05
Chebula	0	0	3	608.88	3	608.88
Yurga	8	418.35	128	2729.34	120	2310.99
Yaya	55	553.75	31	295.88	–24	–257.87
Yashkino	24	907.29	24	907.29	0	0
Total	399	16976.79	1694	41109.87	1295	24133.08

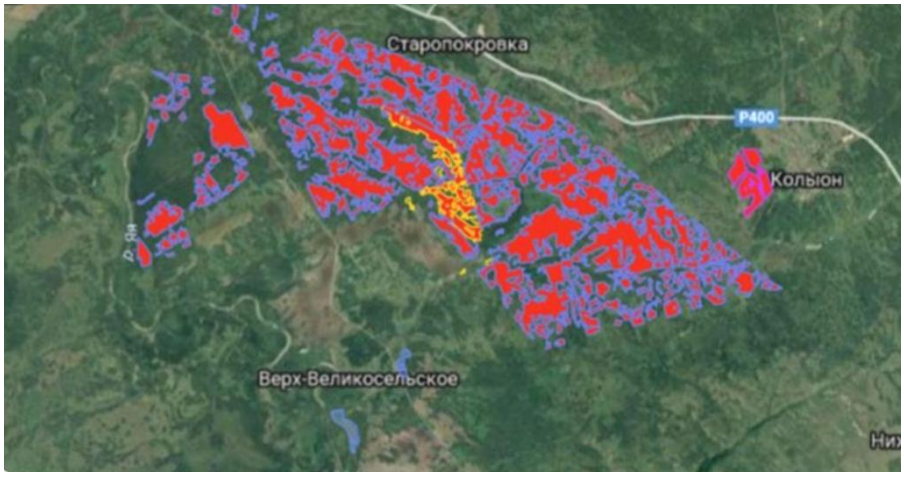

Figure 4 A case of unused land plots with good transport accessibility

land has become a relevant issue in the region as a result of incomplete and conflicting information, as well as a long period of no official control. Agricultural enterprises and individual farmers did not bother to obtain official permission when they decided to develop new plots, thus violating the fiscal interests of the state. In the end, farmers had neither accurate data on the size and configuration of their own lands nor any legal right to use them in transactions. The first stage of the monitoring revealed 688 plots (24 300 ha) with no official registration. While the agricultural profile of these plots was obvious from the aerial survey, the system lacked information about their state registration and permits.

Of the initially identified 688 plots, 488 plots (65.1%, 15 300 ha) proved to be charted correctly. However, 34 plots (7.6%, 1100 ha) had to be inspected by specialists. The inspections revealed that all the plots were used for farming, e.g. animal sheds, barns, etc. The farmers were sent official recommendations to register their land plots. Table 4 illustrates the changes in the number and total area of illegally used land plots in 2021–2022.

Table 4 shows that the scale of illegal agricultural land use differs from municipality to municipality. The Tyazhin municipality is responsible for about 45.4% of the total area and 68.5% of the total number of illegal agricultural land plots. Its disadvantageous location and poor transport accessibility make any control a very complicated task. In some areas, e.g. in the Krapivino municipality, almost all illegal land plots were officially registered in 2021, while in other municipalities they were identified later.

Figure 5 A case of an easy-to-introduce land plot without trees

The Sovhoz.avi software can also identify unused agricultural land plots. Agricultural land-use efficiency is vital for food security and agricultural development. Unused land plots can be offered to businesses that are interested in investing in the local agriculture.

Unused land plots are very different. The Sovhoz.avi platform divided them into those that are easy or hard to introduce into agricultural use. The classification was based on two criteria deduced from the digital inventory data. The first criterion was the location of the plot in relation to settlements and roads. High transportation costs make hard-to-reach areas economically unviable. Therefore, easy-to-introduce areas are located near highways and settlements (Fig. 4), where farmers can hire workers, build warehouses and garages, etc.

The second criterion is vegetation. Unused land plots get overgrown with shrubs and trees. Their uprooting is not cost effective. A field with trees and shrubs is difficult and inefficient to cultivate. Sovhoz.avi can identify trees and shrubs. Figure 5 illustrates another case of an easy-to-introduce land plot in the Novokuznetsk municipality.

Areas with grass and trees are easy to spot (right slide) and measure (left slide, red area). The trees did not prevent Sovhoz.avi from identifying a country road that goes through the overgrown area. The monitoring revealed 3825 unused easy-to-introduce land plots with a total area of 163 400 ha and verified 1682 plots (44%) with a total area of 36 500 ha. These areas can be recorded in a separate inventory to be offered to potential investors.

Hard-to-introduce plots are far from highways and settlements. They are hard to cultivate because of trees and shrubs. Figure 6 gives an example of a hard-to-introduce land plot.

The left slide shows field boundaries (highlighted) charted according to feature point coordinates. The dark green spots are trees and shrubs. The aerial survey (right slide) confirmed that the plot indeed belongs to those hard to introduce into agricultural use. It contains two birch groves, while its southern part is overgrown with shrubs. This plot would be very difficult to return to economic circulation.

The Sovhoz.avi platform revealed 29 140 hard-to-introduce plots with a total area of 447 100 ha. Apparently, hard-to-introduce plots are much more numerous because all convenient plots are already in agribusiness. The platform verified 13 111 plots (44.9%) with a total area of 171 100 ha. These plots may return to economic circulation if the situation in agriculture and food market changes, e.g. prices and food demand continue to rise in 2022.

CONCLUSION

The new aerial survey software and hardware complex, which included a camera-equipped unmanned aerial vehicle and the Sovhoz.avi digital twin software, proved to be an efficient and cheap means of agricultural land inventory. The digital inventory of agricultural land in the Kemerovo Region revealed numerous errors in the available official records. The most common errors included: unidentified boundaries (about 65% of all agricultural plots in the region), distortions of the

Figure 6 A case of a hard-to-introduce land plot with trees

geometric boundaries, and incorrect area calculation. Some plots located in urban areas or forest reserves were misidentified by the authorities as agricultural.

The aerial survey data and the Sovhoz.avi platform can provide local authorities with effective decision-making support. In January 2022, the Kemerovo Region had 1700 illegally used land plots with a total area of about 41 000 ha. The land users were recommended to register their land plots officially. The research also provided a new, updated inventory of unused agricultural land plots, which were divided into those easy or hard to introduce into agricultural use. Easy-to-introduce land plots have a good transport accessibility and no trees or shrubs (3825 plots with a total area of 163 400 ha). They form a promising reserve for the local agricultural development and can be offered to potential investors.

CONTRIBUTION

A.O. Rada supervised the research, set goals and objectives, edited the manuscript, and formulated the conclusions. A.D. Kuznetsov formulated the hypothesis, conducted the research, and wrote the manuscript.

CONFLICT OF INTEREST

The authors declare that there is no conflict of interests regarding the publication of this article.

REFERENCES

1. Cooper M, Müller B, Cafiero C, Bayas JSL, Crespo Cuaresma J, Kharas H. Monitoring and projecting global hunger: Are we on track? Global Food Security. 2021;30. https://doi.org/10.1016/j.gfs.2021.100568
2. Béné C, Bakker D, Chavarro MJ, Even B, Melo J, Sonneveld A. Global assessment of the impacts of COVID-19 on food security. Global Food Security. 2021;31. https://doi.org/10.1016/j.gfs.2021.100575
3. Genkin AS, Mikheev AA. Influence of coronavirus crisis on food industry economy. Foods and Raw Materials. 2020;8(2):204–215. https://doi.org/10.21603/2308-4057-2020-2-204-215
4. Vogliano C, Murray L, Coad J, Wham C, Maelaua J, Kafa R, *et al.* Progress towards SDG 2: Zero hunger in Melanesia – A state of data scoping review. Global Food Security. 2021;29(1). https://doi.org/10.1016/j.gfs.2021.100519
5. Cintina V, Pukite V. Analysis of influencing factors of use of agricultural land. Research for Rural Development. 2018;1:181–187. https://doi.org/10.22616/rrd.24.2018.028
6. Emran S-A, Krupnik TJ, Aravindakshan S, Kumar V, Pittelkow CM. Factors contributing to farm-level productivity and household income generation in coastal Bangladesh's rice-based farming systems. PLoS ONE. 2021;16(9). https://doi.org/10.1371/journal.pone.0256694
7. McLaughlin D, Kinzelbach W. Food security and sustainable resource management. Water Resources Research. 2015;51(7):4966–4985. https://doi.org/10.1002/2015WR017053
8. Fitton N, Alexander P, Arnell N, Bajzelj B, Calvin K, Doelman J, *et al.* The vulnerabilities of agricultural land and food production to future water scarcity. Global Environmental Change. 2019;58. https://doi.org/10.1016/j.gloenvcha.2019.101944
9. Faskhutdinova ER, Osintseva MA, Neverova OA. Prospects of using soil microbiome of mine tips for remediation of anthropogenically disturbed ecosystems. Food Processing: Techniques and Technology. 2021;51(4):883–904. (In Russ.). https://doi.org/10.21603/2074-9414-2021-4-883-904
10. Drozdova MYu, Pozdnyakova AV, Osintseva MA, Burova NV, Minina VI. The microorganism-plant system for remediation of soil exposed to coal mining. Foods and Raw Materials. 2021;9(2):406–418. https://doi.org/10.21603/2308-4057-2021-2-406-418
11. Bolfe ÉL, Jorge LAC, Sanches ID, Júnior AL, da Costa CC, Victoria DC, *et al.* Precision and digital agriculture: Adoption of technologies and perception of Brazilian farmers. Agriculture. 2020;10(12). https://doi.org/10.3390/agriculture10120653
12. Shang L, Heckelei T, Gerullis MK, Börner J, Rasch S. Adoption and diffusion of digital farming technologies – integrating farm-level evidence and system interaction. Agricultural Systems. 2021;190. https://doi.org/10.1016/j.agsy.2021.103074
13. Rada AO, Fedulova EA, Kosinsky PD. New method for efficiency evaluation of digital technologies in agricultural sector. Food Processing: Techniques and Technology. 2019;49(3):495–504. (In Russ.). https://doi.org/10.21603/2074-9414-2019-3-495-504
14. Balafoutis A, Beck B, Fountas S, Vangeyte J, van der Wal TV, Soto I, *et al.* Precision agriculture technologies positively contributing to GHG emissions mitigation, farm productivity and economics. Sustainability. 2017;9(8). https://doi.org/10.3390/su9081339
15. Aune JB, Coulibaly A, Giller KE. Precision farming for increased land and labour productivity in semi-arid West Africa. A review. Agronomy for Sustainable Development. 2017;37(3). https://doi.org/10.1007/s13593-017-0424-z

16. Adenso-Díaz B, Villa G. Crop planning in synchronized crop-demand scenarios: A biobjective optimization formulation. Horticulturae. 2021;7(10). https://doi.org/10.3390/horticulturae7100347

17. Cienciała A, Sobolewska-Mikulska K, Sobura S. Credibility of the cadastral data on land use and the methodology for their verification and update. Land Use Policy. 2021;102. https://doi.org/10.1016/j.landusepol.2020.105204

18. Kocur-Bera K, Frąszczak H. Coherence of cadastral data in land management – a case study of rural areas in Poland. Land. 2021;10(4). https://doi.org/10.3390/land10040399

19. Roić M, Križanović J, Pivac D. An approach to resolve inconsistencies of data in the cadastre. Land. 2021;10(1). https://doi.org/10.3390/land10010070

20. Malashevskyi M, Kuzin N, Palamar A, Malanchuk M. The problems of spatial ordering and taxation of agricultural lands. Geodesy and Cartography. 2017;43(4):166–172. https://doi.org/10.3846/20296991.2017.1412634

21. Lisjak J, Roić M, Tomić H, Mastelić Ivić S. Croatian LADM profile extension for state-owned agricultural land management. Land. 2021;10(2). https://doi.org/10.3390/land10020222

22. García-Morán A, Ulvund S, Unger E-M, Bennett RM. Exploring PPPs in support of fit-for-purpose land administration: A case study from Côte d'Ivoire. Land. 2021;10(9). https://doi.org/10.3390/land10090892

23. Feroz S, Abu Dabous S. UAV-based remote sensing applications for bridge condition assessment. Remote Sensing. 2021;13(9). https://doi.org/10.3390/rs13091809

24. He X, Yang X, Luo Z, Guan T. Application of unmanned aerial vehicle (UAV) thermal infrared remote sensing to identify coal fires in the Huojitu coal mine in Shenmu city, China. Scientific Reports. 2020;10(1). https://doi.org/10.1038/s41598-020-70964-5

25. Tatum MC, Liu J. Unmanned aircraft system applications in construction. Procedia Engineering. 2017;196:167–175. https://doi.org/10.1016/j.proeng.2017.07.187

26. Prosekov A, Kuznetsov A, Rada A, Ivanova S. Methods for monitoring large terrestrial animals in the wild. Forests. 2020;11(8). https://doi.org/10.3390/f11080808

27. Tuśnio N, Wróblewski W. The efficiency of drones usage for safety and rescue operations in an open area: A case from Poland. Sustainability. 2022;14(1). https://doi.org/10.3390/su14010327

28. Mohamed N, Al-Jaroodi J, Jawhar I, Idries A, Mohammed F. Unmanned aerial vehicles applications in future smart cities. Technological Forecasting and Social Change. 2020;153. https://doi.org/10.1016/j.techfore.2018.05.004

29. Montgomery K, Henry JB, Vann MC, Huseth AS, Mitasova H. Measures of canopy structure from low-cost UAS for monitoring crop nutrient status. Drones. 2020;4(3). https://doi.org/10.3390/drones4030036

30. Puniach E, Bieda A, Ćwiąkała P, Kwartnik-Pruc A, Parzych P. Use of unmanned aerial vehicles (UAVs) for updating farmland cadastral data in areas subject to landslides. ISPRS International Journal of Geo-Information. 2018;7(8). https://doi.org/10.3390/ijgi7080331

31. Mantey S, Tagoe ND. Suitability of unmanned aerial vehicles for cadastral surveys. Ghana Mining Journal. 2019;19(1):1–8. https://doi.org/10.4314/gm.v19i1.1

32. Šafář V, Potůčková M, Karas J, Tlustý J, Štefanová E, Jančovič M, *et al.* The use of UAV in cadastral mapping of the Czech Republic. ISPRS International Journal of Geo-Information. 2021;10(6). https://doi.org/10.3390/ijgi10060380

33. Karabin M, Bakuła K, Łuczyński R. Verification of the geometrical representation of buildings in cadastre using UAV photogrammetry. Geomatics and Environmental Engineering. 2021;15(4):81–99. https://doi.org/10.7494/geom.2021.15.4.81

34. Puniach E, Kwartnik-Pruc A. The use of laser scanning and unmanned aerial vehicles in construction surveying in the light of legal regulations in Poland. Journal of Applied Engineering Sciences. 2018;8(2):79–88.

35. Brookman-Amissah M, Mantey S, Kumi-Boateng B, Aikins BE, Masoud AB. Developing a workflow for the use of unmanned aerial vehicles for cadastral mapping in Ghana. Journal of Environment and Earth Science. 2021;11(2):23–31. https://doi.org/10.7176/JEES/11-2-04.

ORCID IDs
Artem O. Rada https://orcid.org/0000-0001-7678-8402
Aleksandr D. Kuznetsov https://orcid.org/0000-0002-1986-3039

Foods and Raw Materials. 2022;10(2)

ISSN 2310-9599 (Online)
ISSN 2308-4057 (Print)

Review Article
Open Access

Available online at http://jfrm.ru/en
https://doi.org/10.21603/2308-4057-2022-2-531
https://elibrary.ru/PETCQR

Ohmic heating application in food processing: Recent achievements and perspectives

Dornoush Jafarpour[1,*], Seyed Mohammad Bagher Hashemi[2]

[1] Islamic Azad University – Fasa Branch, Fasa, Iran
[2] Fasa University, Fasa, Iran

* e-mail: Do.Jafarpour@iau.ac.ir; d.jafarpour84@yahoo.com

Received 30.09.2021; Revised 19.10.2021; Accepted 14.04.2022; Published online 23.06.2022

Abstract:
Food processing is an important operation in the food industry that converts fresh foods into final products with desirable characteristics for consumption and storage. Ohmic heating is an emerging technique for food processing that seems to be a suitable alternative to conventional heat treatment. Recently, there has been a lot of research into ohmic heating applications in processing various foods.

This review highlights the findings of studies conducted in 2018–2022 on the impact of ohmic heating on the physical, chemical, and sensory properties of foodstuffs during processing. We found that this technology provides more reliable process control compared to the traditional technique, namely conventional heating. Although ohmic heating has a positive effect on the quality of foods, its efficiency is limited by certain food components, including acid and fat, that markedly affect the electrochemical attributes of foods.

Therefore, to achieve optimal results, ohmic heating conditions should be set in accordance with the properties of food materials. There is a need for further in-depth studies on the performance of ohmic heating in food processing on a large, rather than a lab scale.

Keywords: Heat treatment, ohmic heating, food processing, novel technology, food quality, alternative method

Please cite this article in press as: Jafarpour D, Hashemi SMB. Ohmic heating application in food processing: Recent achievements and perspectives. Foods and Raw Materials. 2022;10(2):216–226. https://doi.org/10.21603/2308-4057-2022-2-531

INTRODUCTION

Fresh foods have a limited shelf life and spoil very quickly due to a high water content and easy availability of nutrients for microorganisms. Mechanical, physical, chemical, and microbial processes are the main causes of food spoilage. Therefore, processing of foods is very important in order to maintain their health benefits and quality.

Conventional thermal processing is widely used for microbiological safety and food preservation [1]. This technique effectively inactivates pathogens and spoilage microorganisms. However, the application of high temperatures has a negative effect on the food quality, namely color, texture, flavor, as well as nutritional and bioactive compounds [2, 3]. Heat transfer in traditional thermal processing includes three mechanisms, namely convection, conduction, and radiation [4]. The heterogeneous distribution of heat in different parts of food, which occurs because of internal resistance, adds to the negative impact on the food quality.

Therefore, alternative technologies should be used to solve these problems. Ohmic heating, or Joule heating, is an emerging technique for food processing that seems to be a suitable alternative to conventional heat treatment. It generates heat by the passage of alternating current through food and the resistance of food particles to electrical current. In fact, food forms part of an electrical circuit in ohmic heating [5, 6].

Since ohmic heating converts electrical energy to thermal energy, the temperature inside the food rises uniformly and rapidly [7, 8]. As a result, there are fewer sensory changes, less off-flavor, fewer nutritional losses, and less bioactive degradation.

In addition, this new technology ensures the microbiological safety of the final product [9]. Other advantages of ohmic heating include shorter processing time, higher efficiency, and lower maintenance cost. Ohmic heating has a variety of uses in food processing, namely in pasteurization, peeling, blanching, drying, and concentration [4]. Thus, we aimed to review the latest studies on the application of ohmic heating in food processing.

OHMIC HEATING IN THE FOOD INDUSTRY

Ohmic heating application in dairy industry. Ohmic heating technology appeared at the end of the 19th century. Although it was first utilized to pasteurize milk, ohmic heating was not commercialized due to the process control problems, high cost of electricity, and the lack of suitable materials for electrode production. Today, it is applied in dairy processing to produce safe, healthy, and high quality dairy products [10]. Particularly, it is used to pasteurize lactose-free milk since this product has good electrical conductivity. The material of electrodes used in ohmic heating is an important issue in dairy production [11]. Less fouling has been observed in titanium electrodes than in stainless steel electrodes. This phenomenon can be explained by the lower chemical reactivity of titanium compared to stainless steel. Also, milk pasteurized by ohmic heating with titanium electrodes had a safe content of chromium and no iron, while milk pasteurized by ohmic heating with stainless steel electrodes had more iron and chromium [12]. This is an important hygienic aspect for designers of food industry equipment.

The conditions of ohmic heating (variations of frequencies and voltages) are another factor which affects the final product. Costa *et al.* used ohmic heating with different voltages (2, 4, 5, 7, and 9 V/cm at 60 Hz) to process sweet whey and compared the results with conventional heating [9]. The authors reported that a higher electric field intensity resulted in lower luminosity (L^*) and lower color variation (ΔE^*). However, a lower electric field intensity led to better retention of bioactive compounds. This might be due to the relationship between the duration of heat exposure, whey protein denaturation, and the production of bioactive peptides. Besides, the authors recommended the 4 and 5 V ohmic heating for sweet whey, since these conditions ensured suitable sensory and rheological properties with higher bioactive compounds.

In the study of Silva *et al.*, ohmic heating was used for Dulce de leche treatment for the first time [13]. Dulce de leche is a dairy product which is made by evaporation and sugar addition. The authors indicated that the low and intermediate electric field strength gave the product weaker aroma, more bitter taste, and a higher sandiness score. At higher intensity, Dulce de leche was heated for a shorter time, which resulted in a weaker Maillard reaction and fewer Maillard reaction products (such as lactones and furans). Lactones and furans are compounds which affect the aroma and flavor of sterilized products and may also have a negative impact on the quality of Dulce de leche. Furthermore, the ohmic-heated Dulce de leche had a homogeneous accumulation of whey proteins on a smaller scale. This prevented the contact of lactose molecules, as well as inhibited the growth of lactose crystals in size and sandiness in the final product [14].

Ferreira *et al.* processed raspberry-flavored whey beverage under different voltages and frequencies of ohmic heating [15]. The authors reported that certain parameters of this process (10, 100, 1000 Hz at 25 V and 45, 60, 80 V at 60 Hz) had a notable effect on the particle size, rheological properties, and the color of the whey beverage. Overall, ohmic-treated beverages showed higher viscosity than conventionally treated samples. Among ohmic-heated samples, 10 and 1000 Hz exhibited the highest viscosity due to the larger particle size and cell aggregation, while voltage-treated beverages had lower viscosity. In addition, 10 Hz-treated samples exhibited more color changes because of the electrochemical reaction. The authors proposed 10 and 1000 Hz at 25 V as an optimal treatment to achieve the desired color, physical, and rheological attributes.

In another study, Ferreira *et al.* revealed that under extreme conditions of ohmic heating (80 V at 60 Hz and 1000 Hz at 25 V), raspberry-flavored whey beverage had the lowest antioxidant activity, compared to mild and intermediate conditions (45 and 60 V at 60 Hz and 10 and 100 Hz at 25 V) [16]. Furthermore, the ohmic-heated samples showed higher α-glucosidase and α-amylase inhibition in comparison with the conventionally treated beverages. This could be related to the tendency of bioactive compounds in whey proteins to bind to the active sites of enzymes. Reducing the activity of these enzymes can result in lower hydrolysis of disaccharides and polysaccharides, as well as glucose uptake, with blood sugar levels maintained [17].

In a study of whey acerola-flavored beverage, Cappato *et al.* stated that ohmic heating decreased the relaxation period leading to small changes in fatty acid profiles, as well as preserving the nutritional properties of processed drink, compared to conventional heating [18].

Rocha *et al.* examined the quality parameters of Minas Frescal cheese produced from milk pasteurized by using ohmic heating [7]. This technique enhanced protein hydrolysis, resulting in a lower content of protein and a higher content of small peptides, compared to the cheeses made from conventionally treated milk. Cheeses manufactured from milk subjected to ohmic heating at the highest voltage showed the lowest proteolytic activity and the highest protein levels, similarly to the conventional method. Generally, ohmic heating notably decreased the hardness, elasticity, and firmness of the cheeses, yet improving their general acceptability. Low and intermediate electric field intensity (4 and 8 V/cm) increased the production of bioactive compounds and

antioxidant activity. Yet, these voltages altered the fatty acid profile and produced more saturated fatty acids. Therefore, ohmic heating at 8 V/cm was suggested for Minas Frescal cheese due to the shorter period of processing.

It was evidenced that ohmic heating resulted in lower hydroxymethylfurfural production and higher overall acceptability of whey dairy drinks, compared to conventional heating at the same temperatures. This was due to the shorter time to reach the process temperature, uniform heat, and lack of hot spots formation [19]. Thus, ohmic heating could be an innovative method for processing whey dairy drinks with improved sensory properties [20]. Table 1 summarizes recent applications of ohmic heating in food processing.

Ohmic heating application in fruit and vegetable processing. Fresh fruits and vegetables spoil rapidly after harvesting due to their nature (A_w, nutrients, etc.). Thus, it is essential to process and convert them into products which have a longer shelf life [42]. The traditional way is to concentrate fruit juices by conventional heating. However, this method impairs the quality of food due to a low coefficient of heat transfer and a long processing time [4]. An alternative method for concentrating fruit juices is ohmic heating [43].

Fruit juices have high electrical conductivity, which makes them suitable for the ohmic heating technology. Darvishi *et al.* reported that the content of total phenols in ohmic-treated black mulberry juice was 3.0–4.5 times higher than in the samples treated conventionally [3]. The performance of concentration in ohmic heating was by about 38–46% greater than in conventional heating. In addition, the authors stated that as the voltage increased, the process time decreased, resulting in fewer changes in total phenols and pH.

Similarly, high voltages (45 and 50 V) were suggested by Norouzi *et al.* for concentration of sour cherry juice [30]. Although ohmic heating increased the turbidity of sour cherry juice compared to the conventional method, it was still less than the initial turbidity. This might be due to an increase in total phenols with enhanced voltage gradient [44]. The authors also stated that the application of different voltages did not have a significant effect on color changes (ΔE) and color parameters such as *L* (lightness) and *b* (blueness/yellowness).

Minimal alterations in terms of color have also been detected in ohmic-treated sugarcane juice [25, 45]. Fadavi *et al.* evaluated the impact of ohmic heating and conventional heating on tomato juice [4]. They found that ohmic heating caused little changes in the properties of tomato juice (acidity, turbidity, and lycopene) and that these changes would be even less significant in ohmic heating under vacuum.

Conventional and ohmic dewatering of grapefruit and orange pulps were investigated by Stojceska *et al.* [21]. The authors indicated that the moisture content decreased markedly during conventional and ohmic drying, while the amount of vitamin C and pH did not differ significantly.

Another study found that the application of ohmic heating for concentration of orange juice under vacuum significantly reduced the concentration time and led to the production of fruit juice with higher viscosity, better color retention, and less decomposition of vitamin C, compared to processing under atmospheric conditions [46].

Sabanci and Icier added that the changes in the temperature of evaporation during the concentration of orange juice had a notable impact on the time to reach

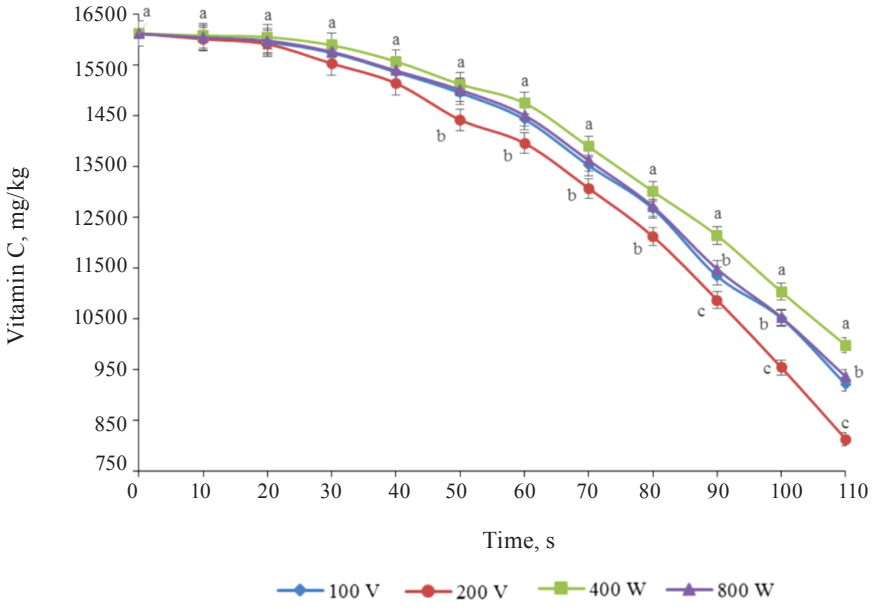

Figure 1 The effects of ohmic and microwave treatments on vitamin C content in cantaloupe juice. With the permission of the publisher, Hashemi *et al.* [22]

Table 1 Ohmic heating applications in food processing

Product	Process purpose	Ohmic heating conditions	Main findings	References
Whey dairy beverages	Thermal processing	6, 9, 12, and 15 V/cm – 500, 1000, 1500, and 2000 Hz	Samples processed by increased voltage gradient and frequencies presented higher overall liking	[20]
Dulce de leche	Thermal processing	0, 2, 4, 6, 8, and 10 V/cm – 60 Hz	Low and intermediate electric field strength resulted in more bitter taste, weaker aroma, and higher sandiness; higher intensity reduced the heating time and weakened the Maillard reaction	[13]
Whey dairy beverage	Thermal processing	6 V/cm – 60 Hz	Ohmic heating led to less hydroxymethylfurfural production and increased overall liking, compared to conventional heating at the same temperatures	[19]
Sweet whey	Thermal processing	2, 4, 5, 7, and 9 V/cm – 60 Hz	Higher electric field intensity resulted in lower luminosity and lower color variation; lower intensity led to better retention of bioactive compounds	[9]
Whey-raspberry flavored beverage	Thermal processing	10, 100, and 1000 Hz – 25 V and 45, 60, and 80 V – 60 Hz	Extreme ohmic heating conditions led to the lowest antioxidant activity, compared to mild and intermediate conditions; ohmic heating-treated samples showed higher α-glucosidase and α-amylase inhibition, as well as higher viscosity, than the conventionally treated beverages; 10 Hz-treated samples exhibited more color changes	[15]
Whey acerola-flavored drink	Pasteurization	45, 60, and 80 V – 60 Hz and 10, 100, and 1000 Hz – 25 V	Ohmic heating led to small changes in fatty acids profiles or preservation of nutritional properties, compared to conventional heating; electric field effects caused small modifications of nutritional aspects, while frequency had a stronger influence on the quality of the product; high frequencies (1000 and 100 Hz) resulted in better bioactive compounds and antioxidant capacity	[18]
Lactose-free milk	Pasteurization	8.25 V/cm – 50 Hz	This product can be subjected to ohmic heating due to its good electrical conductivity; less fouling observed in titanium electrodes than in stainless steel electrodes	[11]
Minas Frescal cheese (MFC)	Pasteurization of milk intended for MFC manufacture	4, 8, and 12 V/cm	Cheeses manufactured from milk subjected to ohmic heating at the highest voltage showed the lowest proteolytic activity and highest protein levels, similar to conventional heating; ohmic heating decreased hardness, elasticity, and firmness, but improved general acceptance of cheeses; production of bioactive compounds and antioxidant activity increased at low and intermediate electric field intensity (4 and 8 V/cm)	[7]
Grapefruit and orange pulps	Drying	30 V/cm	Vitamin C and pH did not differ significantly between ohmic heating and thermal dehydration	[21]
Cantaloupe juice	Pasteurization	100 and 200 V	Higher voltage resulted in a reduced number of pathogens and lower contents of vitamin C, carotene, and phenolic compounds	[22]
Pulque	Pasteurization	60, 80, 100, and 120 V – 60 Hz	Ohmic heating improved the physicochemical and sensory properties, compared to conventional heating	[23]
Tomato juice	Concentration	10.5, 13.2, and 15.8 V/cm – 50 Hz	Ohmic heating caused slight changes in the properties of tomato juice (acidity, turbidity, and lycopene) which were even less pronounced when using vacuum	[4]
Orange juice	Concentration	13 V/cm – 50 Hz	Ohmic heating treatment under vacuum resulted in better retention of vitamin C and fewer color changes, compared to treatment under atmospheric conditions	[24]
Sugarcane juice	Pasteurization	60 Hz	Ohmic heating and ultrasound did not affect phenolic compounds, whose content was similar to fresh juice; only slight color changes were caused by ohmic heating	[25]
Pineapple cubes	Thermal processing	Electrical power was calculated based on the electrical conductivity of pineapple cubes	Lightness and antioxidant properties of the pineapples did not differ significantly between ohmic heating and conventional heating; ohmic heating increased the hardness of the pineapples compared to the conventional method	[26]
	Blanching	25, 30, and 35 V/cm	The highest textural degradation was observed at all electric field strengths at 90 s process time; higher strength (35 V/cm) resulted in a higher drying rate	[27]

Continuation of Table 1

Product	Process purpose	Ohmic heating conditions	Main findings	References
Pear	Assisting in lye peeling	426, 479, 532, 585, and 638 V/m	Ohmic heating enhanced the product yield, efficacy of peeling, as well as the quality of the final product; peel quality was best at much lower concentrations of lye (2% NaOH at 532 V/m and 3% NaOH at 426 and 479 V/m)	[28]
Mulberry juice	Concentration	15, 20, 25, and 30 V/cm – 50 Hz	Ohmic heating provided greater concentration than the conventional method (about 38–46%); higher voltage reduced the process time, resulting in fewer changes in total phenols and pH	[3]
Pekmez	Evaporation	17.5, 20.0, 22.5, and 25.0 V/cm	Energy consumption was higher in conventional heating than ohmic heating for all voltage gradients; energy efficiency increased with higher voltage gradient	[29]
Sour cherry juice	Concentration	8.3, 9.7, 122.0, 11.1, 12.5, and 13.9 V/cm – 50 Hz	Although ohmic heating increased the turbidity of sour cherry juice compared to the conventional method, it was still lower than the initial turbidity; different voltages did not have a significant effect on color parameters such as "*L*" (lightness) and "*b*" (blueness/yellowness)	[30]
Coconut water	Pasteurization	10 and 20 V/cm – 50 Hz	Ohmic heating could completely inactivate peroxidase but not polyphenol oxidase; no pink color found in ohmic heating-treated samples during cold storage, unlike conventionally pasteurized samples	[31]
Short grain rice	Cooking	60 Hz	Ohmic heating adversely affected color parameters (color intensity and lightness), resulting in softer texture compared to the hotplate cooking system	[32]
Noodle	Cooking	10.0, 12.5, 15.0, and 17.5 V/cm – 60 Hz	Temperature come-up time decreased significantly with an increase in electric field; 15 V/cm electric field strength with the holding time of 90 s was suggested as the best treatment in terms of desirable texture and energy efficiency	[33]
Whole and decorticated pearl millet grain	Cooking	60 Hz	Grain pericarp considered the principal factor influencing the cooking process rather than the method of heating; no significant differences observed between conventional open-pan and ohmic heating methods in terms of texture and color	[34]
Pork	Cooking	21 ± 1 V/cm – 60 Hz	Shorter cooking time; such important factors as cooking loss, color, and water holding capacity were not significantly affected, compared to pan cooking	[35]
Vacuum packaged sausage	Post-pasteurization	230 V – 50 Hz	Ohmic heating only slightly changed the texture and color of vacuum packaged sausages, while having no notable impact on pH, water holding capacity, lipid oxidation, or cooking loss	[36]
Beef	Cooking	50 V – 20 kHz	Electrical conductivity is affected by the amount of fat in the muscle tissue; series electric current reduces electrical conductivity, compared to parallel current	[37]
Whole egg	Pasteurization	20 kHz	Ohmic heating improved the hardness and foaming capacity compared to conventional pasteurization and caused slight changes in color; although ohmic heating increased viscosity, its detrimental impact could be reduced by adjusting the process conditions; low temperature pasteurization was proposed due to its low impact on protein denaturation	[38]
Egg white	Pasteurization	20 kHz	Fewer proteins denatured during thermally-induced gelation of egg white protein under ohmic heating	[39]
Starch	Gelation	7 to 27 V/cm – 60 Hz	The stability of starch gels strongly depended on the type of starch and was not affected by the type of heat treatment	[40]
Surimi-canned corn mixed gels	Thermal processing	250 V – 10 kHz	Ohmic heating effectively reduced moisture loss in corn and preserved the texture of corn and surimi gel better than the water-bath heating method	[41]

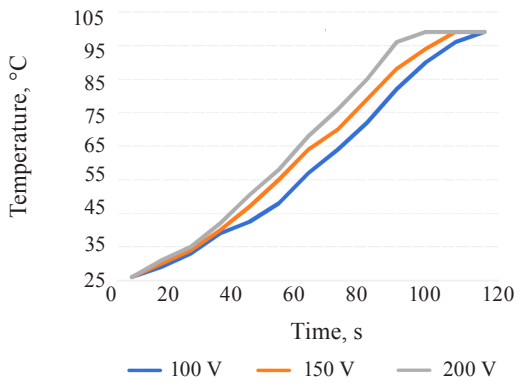

Figure 2 Temperature profile of sour orange juice during ohmic heating for 120 s and three different voltages (100, 150, and 200 V). With the permission of the publisher, Hashemi *et al*. [47]

the target values of total soluble solids, performance, and electrical conductivity [24]. They explained that various values of absolute pressure and, consequently, boiling temperatures applied in ohmic heating affected energy efficiency, according to the second law of thermodynamics. Higher boiling temperature decreased the process time and had a positive effect on energy efficiency.

In some studies, ohmic heating has been used to pasteurize fruit juices. Particularly, Hashemi *et al.* compared the efficiency of ohmic and microwave processes for treatment of cantaloupe juice [22]. They indicated that higher voltage of ohmic heating and microwave power markedly decreased phenolic compounds, vitamin C, and the number of pathogens. In fact, at high voltages compounds are produced that catalyze the decomposition pathways of ascorbic acid in the presence of oxygen due to thermal effects, electrode reactions, and the electrolysis of the solution. Hashemi *et al.* observed the highest degradation of vitamin C in the ohmic treatment at 200 V and the lowest in the microwave treatment at 400 W (Fig. 1) [22].

In another study [47], they found electric current and temperature to be the major variables which affected the pasteurization of sour orange juice. The authors showed that heat transfer in orange juice was accelerated by the application of a higher electric field (Fig. 2).

Alcántara-Zavala *et al.* reported that ohmic heating improved the physicochemical and sensory properties of fermented beverage obtained from the agave plant (known as pulque) [23]. Pulque is an alcoholic beverage with acidic taste. Ohmic heating improved its flavor (alcoholic perception and acidity) and made it more palatable for consumption, compared to conventional heating. Due to its mineral content, pulque showed good electrical conductivity. Its pasteurization with 120 V at 65°C for 5 min was reported as the best treatment.

Rinaldi *et al.* evaluated the physical and chemical impacts of ohmic heating and conventional heating on cubes of pineapple in syrup [26]. They observed insignificant differences in the lightness (L^*) and antioxidant properties between the two methods, while the hardness of the ohmic-treated pineapples was higher than that of those treated conventionally. In addition, Kumar *et al.* observed the highest textural degradation of pineapple cubes at all electric field strengths at 90 s process time [27]. They also found that higher electric field strength resulted in a higher drying rate.

Ohmic heating can be used as an alternative to conventional blanching prior to drying and storage of vegetables and fruits. Kanjanapongkul and Baibua applied ohmic heating to pasteurize coconut water and found that it could completely inactivate peroxidase, but not polyphenol oxidase [31]. In addition, no pink discoloration was reported in the ohmic-heated samples, while the conventionally pasteurized samples featured a pink color during cold storage.

Another application of ohmic heating is in the peeling process. Removing the skin of fruits and vegetables is one of the most common treatments in food processing. The conventional peeling methods (lye, steam, and mechanical method) have several drawbacks, including high peeling losses, high consumption of energy, and environmental issues. Therefore, there is a growing demand for alternative methods [48]. Gupta and Sastry employed ohmic heating to remove the skin of pear [28]. Furthermore, a combination of ohmic heating and CO_2 laser drilling has been used to remove tomato skins [49]. These studies have shown that ohmic heating enhances the product yield, efficacy of peeling, as well as the quality of the final product. However, some parameters should be considered to optimize the peeling process, such as temperature, composition of peeling medium, and electric field strength [28, 50].

Ohmic heating application in grain processing. The boiling of food products, such as rice and noodles, is a time-consuming process. Today, as the people's lifestyles have altered, there is a growing demand for rapid cooking methods and alternatives to traditional methods. Gavahian *et al.* investigated the impact of ohmic heating and traditional cooking on the textural and physical attributes of short grain rice [32]. They reported that although ohmic heating adversely affected the color parameters (color intensity and lightness), it resulted in softer texture in comparison with the hotplate cooking system. In this regard, the corrosion of electrodes and electrochemical reactions have been expressed as factors affecting the color of ohmic-heated foods [32].

Ohmic heating has also been found to markedly reduce the cooking time, fouling, and consumption of energy, compared to the traditional method [51]. Similarly, Jo and Park utilized different electric fields (10.0, 12.5, 15.0, and 17.5 V/cm) for cooking instant noodles [33]. They observed that heat transfer between noodles and soup was expedited at higher electric fields. Therefore, the authors suggested 15 V/cm with the

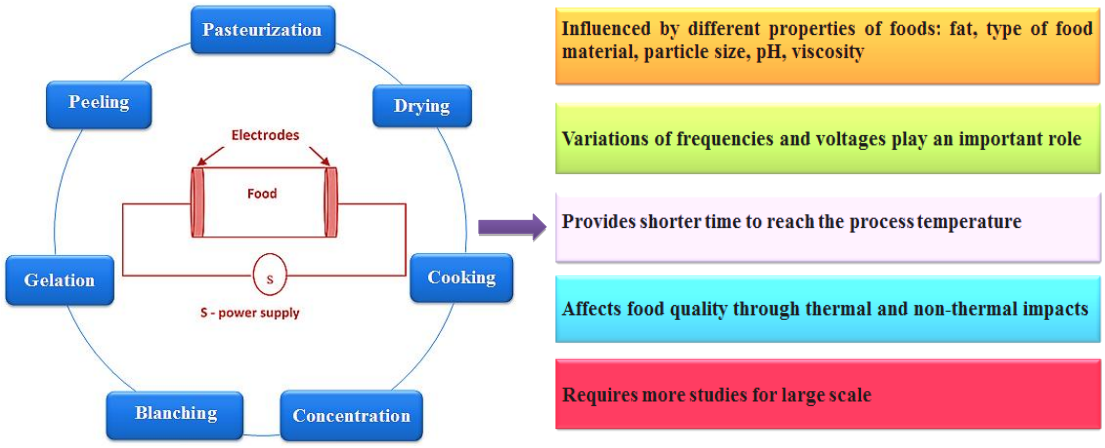

Figure 3 Various applications of ohmic heating in food processing

holding time of 90 s as the best treatment in terms of desirable texture and energy efficiency.

Dias-Martins *et al.* compared the impact of conventional open-pan and ohmic heating on whole and decorticated pearl millet grains [34]. They found the grain pericarp to be the principal factor influencing the cooking process, rather than the method of heating. Regarding pearl millet grain, no significant differences were observed between the two cooking methods in terms of texture and color. However, the ohmic-heated decorticated grains exhibited greater lightness and harder texture, compared to the conventionally cooked grains.

Waziiroh *et al.* examined the basic aspects of using ohmic heating for baking gluten-free bread [52]. They stated that the changes in the physical properties of gluten-free bread during heating depended on the ingredients and their interaction in the dough. They believed that two major factors affected the porosity and viscosity of dough during baking by ohmic heating, namely dough ingredients and their properties (e.g., non-ionic and ionic compounds, particle size, surface hydrophobicity, emulsification ability, etc.) and dough structural properties (foam formation, protein denaturation, and starch gelatinization).

Ohmic heating application in meat industry. It has been investigated that ohmic heating can be used for processing meat and meat products. Several factors affect the electrical conductivity and therefore the efficiency of the ohmic process, including meat structure (type of meat, amount of fat and moisture), lean-to-fat ratio, and electric current direction [35]. Llave *et al.* studied the impact of meat type (Japanese beef and Australian beef) and the direction of electric current (series and parallel) on the electrical conductivity during ohmic cooking [37]. They reported that Japanese meat had lower electrical conductivity than Australian meat due to its higher fat content. Having low electrical conductivity, fat prevents the passage of current by covering lean particles, which reduces the electrical conductivity during ohmic heating, as well as uniform heating. The authors also found that series electric current reduced electrical conductivity, compared to parallel current. Reduction of shrinkage and drip loss were observed in both types of meat during ohmic cooking at 50 V and 20 kHz [37].

Additionally, ohmic heating can be applied to cook pork since it shortens the cooking time without having a significant impact on the water holding capacity, color, and cooking loss, compared to the traditional pan cooking [35]. Similarly, ohmic heating has no significant effect on the properties of scallops (texture, shrinkage, and water release) and reduces the denaturation of actin by shortening the heating time [53].

Inmanee *et al.* investigated the impacts of ohmic heating on *Listeria monocytogenes* contamination and the quality of sausages during post-pasteurization [36]. They showed that the ohmic process effectively inactivated *L. monocytogenes* (≥ 5-log reduction). The authors compared the electrical conductivity of sausage, salt solution, and collagen casing. They found that the collagen casing had a higher electrical conductivity than the sausage and attributed it to the presence of fat, which made up to 20% of the sausage. The salt solution acted as a conductor, with lower conductivity than the sausage and casing.

The study also showed that the ohmic process only slightly changed the texture and color of the vacuum-packaged sausages. At the same time, it had no notable impact on pH, water holding capacity, lipid oxidation, and cooking loss. However, these slight changes in texture and color were not detectable by sensory evaluators. Therefore, ohmic heating has the potential to be applied in the meat and meat products industry with the least impact on their quality.

Other food products. Several studies have investigated the technological attributes of eggs under ohmic heating. Since fresh-laid eggs can be a cause of salmonella infection, manufacturers prefer pasteurized egg for both its safety and ease of handling [54].

Eggs are a rich source of protein and due to their sensitivity to high temperature, great care must be taken during egg pasteurization to prevent proteins denaturation and coagulation. Alamprese *et al.* reported that ohmic heating improved the hardness and foaming capacity of the whole egg, compared to conventional pasteurization, and caused slight changes in its color [38]. The authors stated that although ohmic heating increased viscosity, its detrimental impact could be reduced by adjusting the process conditions. In general, they proved that ohmic treatment could be used as a desirable method for whole egg treatment and proposed low temperature pasteurization due to its low impact on protein denaturation.

Similarly, Llave *et al.* examined color alterations of egg yolk under ohmic treatment and evaluated the correlation between color changes and the degree of protein denaturation [54]. They found that increasing temperatures caused the egg yolk color to gradually turn from plain orange to vivid yellow, while the egg white gradually changed from transparent to cloudy.

In addition, the egg color changes were correlated with the non-denaturation ratio of the second peak temperature. In this regard, Joeres *et al.* indicated that egg white protein did not fully denature during ohmic heating [39]. They believed that this could be related to the oscillatory electric field which partially interfered with the complete denaturation and development of intermolecular beta-sheet structures during thermal gelation of ovalbumin. Also, according to the results of scanning electron microscopy, the ohmic-heated gels had a more open and porous network structure, compared to conventional treatment which exhibited denser gels.

In another study, da Silva *et al.* investigated the impact of ohmic heating on the rheological attributes and stability of gels produced from starch [40]. Particularly, they examined the effect of starch source (cassava and maize) and type of treatment. They found that the stability of starch gels strongly depended on the type of starch and was not affected by the type of heat treatment. The researchers revealed that ohmic heating had several advantages over conventional heating. In particular, it reduced energy and water consumption, as well as wastewater production, and did not affect the properties of the final product.

In a study by Jung *et al.*, ohmic heating was used to process surimi-corn mixture [41]. The authors reported that this technique effectively reduced the amount of moisture loss in corn and preserved the texture of corn and surimi gel better than the water-bath heating method.

Limitations and advantages. Ohmic heating has revealed its potential for processing various foods in industrial applications. Apart from heat treatment, it can also be used as an assisted treatment for other processes like peeling, concentration, and drying (Fig. 3). Although recent studies have indicated that ohmic heating can improve the physical and chemical properties of foods, compared to conventional heating, there are some limitations regarding its application. Operator safety, high capital cost, and corrosion of electrodes are major concerns of food manufacturers to commercialize this novel technology.

Studies have shown that ohmic-treated foods have better texture, better aroma, lower color variation, higher bioactive compounds, and better sensory properties, compared to conventionally treated foods [3, 7, 9, 13, 16, 18, 20, 23, 26, 30, 33, 36, 49]. However, for some foods, there are no significant differences between the two methods in terms of quality [21, 26, 40].

In contrast, some studies have revealed that ohmic heating can adversely affect some physical properties of food such as color [32]. Electrode corrosion and some electrochemical reactions are among its limitations that can affect the food quality. Besides, ohmic heating is not a suitable method for processing foods with a high fat content since fat has low electrical conductivity. Therefore, the ohmic process conditions must be optimized according to the food properties in order to achieve the best result.

Other advantages of ohmic heating are a shorter time to reach the process temperature, lower consumption of energy, uniform distribution of heat, and a shorter total heating period [7, 10, 29, 40, 43]. Although this novel technology has some limitations and drawbacks, its advantages make it a suitable alternative to the traditional heating process.

CONCLUSION

Ohmic heating follows the Joule law to heat foods quickly and evenly, effectively and volumetrically. This method is markedly influenced by different properties of foods, including the amount of fat, type of food material, particle size, pH, viscosity, the content of charged ions, etc. In addition, variations of frequencies and voltages also play an important role in the performance of ohmic heating during food processing. Our review concludes that the processing of food materials by ohmic heating can be carried out in a shorter time, compared to conventional heating. In addition, the quality of foods can be effectively affected by ohmic treatment through both thermal and non-thermal impacts. While its thermal impacts on the food quality have been extensively studied, there is limited information on the non-thermal impacts of this technology on various food properties, such as texture, color, taste, etc. Therefore, a more detailed study is needed to fully realize the thermal and non-thermal impacts of ohmic heating for different foods and under various operating conditions. The ohmic process has many benefits for food industry, including process energy and time savings. Furthermore, this technology provides more reliable process control, compared to the traditional technique. These benefits suggest that ohmic heating can be a superior alternative

procedure for food processing in comparison with the traditional method. However, most studies have been performed on a lab-scale and very few on a pilot plant-scale. Therefore, more research is needed into ohmic heating application on a large-scale to evaluate the potential technical problems and economic issues.

CONTRIBUTION

The authors were equally involved in writing the manuscript and are equally responsible for plagiarism.

CONFLICT OF INTEREST

The authors have declared no conflict of interest.

REFERENCES

1. Gavahian M, Chu Y-H, Farahnaky A. Effects of ohmic and microwave cooking on textural softening and physical properties of rice. Journal of Food Engineering. 2019;243:114–124. https://doi.org/10.1016/j.jfoodeng.2018.09.010
2. Hashemi SMB, Roohi R. Ohmic heating of blended citrus juice: Numerical modeling of process and bacterial inactivation kinetics. Innovative Food Science and Emerging Technologies. 2019;52:313–324. https://doi.org/10.1016/j.ifset.2019.01.012
3. Darvishi H, Salami P, Fadavi A, Saba MK. Processing kinetics, quality and thermodynamic evaluation of mulberry juice concentration process using Ohmic heating. Food and Bioproducts Processing. 2020;123:102–110. https://doi.org/10.1016/j.fbp.2020.06.003
4. Fadavi A, Yousefi S, Darvishi H, Mirsaeedghazi H. Comparative study of ohmic vacuum, ohmic, and conventional-vacuum heating methods on the quality of tomato concentrate. Innovative Food Science and Emerging Technologies. 2018;47:225–230. https://doi.org/10.1016/j.ifset.2018.03.004
5. Müller WA, Ferreira Marczak LD, Sarkis JR. Microbial inactivation by ohmic heating: Literature review and influence of different process variables. Trends in Food Science and Technology. 2020;99:650–659. https://doi.org/10.1016/j.tifs.2020.03.021
6. Wu S, Yang N, Jin Y, Li D, Xu Y, Xu X, *et al.* Development of an innovative induction heating technique for the treatment of liquid food: Principle, experimental validation and application. Journal of Food Engineering. 2020;271. https://doi.org/10.1016/j.jfoodeng.2019.109780
7. Rocha RS, Silva R, Guimarães JT, Balthazar CF, Pimentel TC, Neto RPC, *et al.* Possibilities for using ohmic heating in Minas Frescal cheese production. Food Research International. 2020;131. https://doi.org/10.1016/j.foodres.2020.109027
8. Leong SY, Oey I. Application of novel thermal technology in foods processing. Foods. 2022;11(1). https://doi.org/10.3390/foods11010125
9. Costa NR, Cappato LP, Pereira MVS, Pires RPS, Moraes J, Esmerino EA, *et al.* Ohmic Heating: A potential technology for sweet whey processing. Food Research International. 2018;106:771–779. https://doi.org/10.1016/j.foodres.2018.01.046
10. Pereira RN, Teixeira JA, Vicente AA, Cappato LP, da Silva Ferreira MV, da Silva Rocha R, *et al.* Ohmic heating for the dairy industry: a potential technology to develop probiotic dairy foods in association with modifications of whey protein structure. Current Opinion in Food Science. 2018;22:95–101. https://doi.org/10.1016/j.cofs.2018.01.014
11. Suebsiri N, Kokilakanistha P, Laojaruwat T, Tumpanuvat T, Jittanit W. The pasteurization of milk applying ohmic heating in comparison with conventional method and the quality attributes of lactose-free milk. Phranakhon Rajabhat Research Journal: Science and Technology. 2019;14(1):25–35.
12. Tian X, Yu Q, Wu W, Dai R. Inactivation of microorganisms in foods by ohmic heating: A review. Journal of Food Protection. 2018;81(7):1093–1107. https://doi.org/10.4315/0362-028X.JFP-17-343
13. Silva R, Rocha RS, Guimarães JT, Balthazar CF, Scudino H, Ramos GLPA, *et al.* Dulce de leche submitted to ohmic heating treatment: Consumer sensory profile using preferred attribute elicitation (PAE) and temporal check-all-that-apply (TCATA). Food Research International. 2020;134. https://doi.org/10.1016/j.foodres.2020.109217
14. Rodrigues RM, Fasolin LH, Avelar Z, Petersen SB, Vicente AA, Pereira RN. Effects of moderate electric fields on cold-set gelation of whey proteins – From molecular interactions to functional properties. Food Hydrocolloids. 2020;101. https://doi.org/10.1016/j.foodhyd.2019.105505
15. Ferreira MVS, Cappato LP, Silva R, Rocha RS, Neto RPC, Tavares MIB, *et al.* Processing raspberry-flavored whey drink using ohmic heating: Physical, thermal and microstructural considerations. Food Research International. 2019;123:20–26. https://doi.org/10.1016/j.foodres.2019.04.045
16. Ferreira MVS, Cappato LP, Silva R, Rocha RS, Guimarães JT, Balthazar CF, *et al.* Ohmic heating for processing of whey-raspberry flavored beverage. Food Chemistry. 2019;297. https://doi.org/10.1016/j.foodchem.2019.125018

17. Martinez-Gonzalez AI, Díaz-Sánchez ÁG, de la Rosa LA, Bustos-Jaimes I, Alvarez-Parrilla E. Inhibition of α-amylase by flavonoids: Structure activity relationship (SAR). Spectrochimica Acta – Part A: Molecular and Biomolecular Spectroscopy. 2019;206:437–447. https://doi.org/10.1016/j.saa.2018.08.057
18. Cappato LP, Ferreira MVS, Moraes J, Pires RPS, Rocha RS, Silva R, *et al.* Whey acerola-flavoured drink submitted Ohmic Heating: Bioactive compounds, antioxidant capacity, thermal behavior, water mobility, fatty acid profile and volatile compounds. Food Chemistry. 2018;263:81–88. https://doi.org/10.1016/j.foodchem.2018.04.115
19. Pereira MO, Guimarães GT, Ramos GLPA, do Prado-Silvac L, Nascimento JS, Sant'Ana AS, *et al.* Inactivation kinetics of *Listeria monocytogenes* in whey dairy beverage processed with ohmic heating. LWT. 2020;127. https://doi.org/10.1016/j.lwt.2020.109420
20. Coimbra LO, Vidal VAS, Silva R, Rocha RS, Guimarães JT, Balthazar CF, *et al.* Are ohmic heating-treated whey dairy beverages an innovation? Insights of the Q methodology. LWT. 2020;134. https://doi.org/10.1016/j.lwt.2020.110052
21. Stojceska V, Atuonwu J, Tassou SA. Ohmic and conventional drying of citrus products: energy efficiency, greenhouse gas emissions and nutritional properties. Energy Procedia. 2019;161:165–173. https://doi.org/10.1016/j.egypro.2019.02.076
22. Hashemi SMB, Gholamhosseinpour A, Niakousari M. Application of microwave and ohmic heating for pasteurization of cantaloupe juice: microbial inactivation and chemical properties. Journal of the Science of Food and Agriculture. 2019;99(9):4276–4286. https://doi.org/10.1002/jsfa.9660
23. Alcántara-Zavala AE, Figueroa-Cárdenas JD, Morales-Sánchez E, Aldrete-Tapia JA, Arvizu-Medrano SM, Martínez-Flores HE. Application of ohmic heating to extend shelf life and retain the physicochemical, microbiological, and sensory properties of *pulque*. Food and Bioproducts Processing. 2019;118:139–148. https://doi.org/10.1016/j.fbp.2019.09.007
24. Sabanci S, Icier F, Evaluation of an ohmic assisted vacuum evaporation process for orange juice pulp. Food and Bioproducts Processing. 2022;131:156–163. https://doi.org/10.1016/j.fbp.2021.09.009
25. Rodrigues NP, Brochier B, de Medeiros JK, Marczak LDF, Mercali GD. Phenolic profile of sugarcane juice: Effects of harvest season and processing by ohmic heating and ultrasound. Food Chemistry. 2021;347. https://doi.org/10.1016/j.foodchem.2021.129058
26. Rinaldi M, Littardi P, Ganino T, Aldini A, Rodolf M, Barbanti D, *et al.* Comparison of physical, microstructural, antioxidant and enzymatic properties of pineapple cubes treated with conventional heating, ohmic heating and high-pressure processing. LWT. 2020;134. https://doi.org/10.1016/j.lwt.2020.110207
27. Kumar A, Begum A, Hoque M, Hussain S, Srivastava B. Textural degradation, drying and rehydration behaviour of ohmically treated pineapple cubes. LWT. 2021;142. https://doi.org/10.1016/j.lwt.2021.110988
28. Gupta S, Sastry SK. Ohmic heating assisted lye peeling of pears. Journal of Food Science. 2018;83(5):1292–1298. https://doi.org/10.1111/1750-3841.14116
29. Tunç MT, Akdoğan A, Baltacı C, Kaya Z, Odabaş HI. Production of grape pekmez by Ohmic heating-assisted vacuum evaporation. Food Science and Technology International. 2022;28(1):72–84. https://doi.org/10.1177/1082013221991616
30. Norouzi S, Fadavi A, Darvishi H. The ohmic and conventional heating methods in concentration of sour cherry juice: Quality and engineering factors. Journal of Food Engineering. 2021;291. https://doi.org/10.1016/j.jfoodeng.2020.110242
31. Kanjanapongkul K, Baibua V. Effects of ohmic pasteurization of coconut water on polyphenol oxidase and peroxidase inactivation and pink discoloration prevention. Journal of Food Engineering. 2021;292. https://doi.org/10.1016/j.jfoodeng.2020.110268
32. Gavahian M, Tiwari BK, Chu Y-H, Ting Y-W, Farahnaky A. Food texture as affected by ohmic heating: Mechanisms involved, recent findings, benefits, and limitations. Trends in Food Science and Technology. 2019;86:328–339. https://doi.org/10.1016/j.tifs.2019.02.022
33. Jo YJ, Park SH. Evaluation of energy efficacy and texture of ohmically cooked noodles. Journal of Food Engineering. 2019;248:71–79. https://doi.org/10.1016/j.jfoodeng.2019.01.002
34. Dias-Martins AM, Cappato LP, da Costa Mattos M, Rodrigues FN, Pacheco S, Carvalho CWP. Impacts of ohmic heating on decorticated and whole pearl millet grains compared to open-pan cooking. Journal of Cereal Science. 2019;85:120–129. https://doi.org/10.1016/j.jcs.2018.11.007
35. Ángel-Rendón SV, Filomena-Ambrosio A, Cordon-Díaz S, Benítez-Sastoque ER, Sotelo-Díaz LI. Ohmic cooking: Application of a novel technology in pork and influences on water holding capacity, cooking loss and colour. International Journal of Gastronomy and Food Science. 2019;17. https://doi.org/10.1016/j.ijgfs.2019.100164

36. Inmanee P, Kamonpatana P, Pirak T. Ohmic heating effects on *Listeria monocytogenes* inactivation, and chemical, physical, and sensory characteristic alterations for vacuum packaged sausage during post pasteurization. LWT. 2019;108:183–189. https://doi.org/10.1016/j.lwt.2019.03.027
37. Llave Y, Udo T, Fukuoka M, Sakai N. Ohmic heating of beef at 20 kHz and analysis of electrical conductivity at low and high frequencies. Journal of Food Engineering. 2018;228:91–101. https://doi.org/10.1016/j.jfoodeng.2018.02.019
38. Alampresea C, Cigarinib M, Brutti A. Effects of ohmic heating on technological properties of whole egg. Innovative Food Science and Emerging Technologies. 2019;58. https://doi.org/10.1016/j.ifset.2019.102244
39. Joeres E, Schölzel H, Drusch S, Töpfl S, Heinz V, Terjung N. Ohmic vs. conventional heating: Influence of moderate electric fields on properties of egg white protein gels. Food Hydrocolloids. 2022;127. https://doi.org/10.1016/j.foodhyd.2022.107519
40. da Silva AM, Scherer LG, Daudt RM, Spada JC, Cardozo NSM, Marczak LDF. Effects of starch source and treatment type – Conventional and ohmic heating – On stability and rheological properties of gels. LWT. 2019;109:7–12. https://doi.org/10.1016/j.lwt.2019.04.006
41. Jung H, Moon JH, Park JW, Yoon WB. Texture of surimi-canned corn mixed gels with conventional water bath cooking and ohmic heating. Food Bioscience. 2020;35. https://doi.org/10.1016/j.fbio.2020.100580
42. Bhattacharjee C, Saxena VK, Dutta S. Novel thermal and non-thermal processing of watermelon juice. Trends in Food Science and Technology. 2019;93:234–243. https://doi.org/10.1016/j.tifs.2019.09.015
43. Fadavi A, Salari S. Ohmic heating of lemon and grapefruit juices under vacuum pressure – comparison of electrical conductivity and heating rate. Journal of Food Science. 2019;84(10):2868–2875. https://doi.org/10.1111/1750-3841.14802
44. Sabancı S, Icier F. Effects of vacuum ohmic evaporation on some quality properties of sour cherry juice concentrates. International Journal of Food Engineering. 2019;15(9). https://doi.org/10.1515/ijfe-2019-0055
45. Brochier B, Mercali GD, Marczak LDF. Effect of ohmic heating parameters on peroxidase inactivation, phenolic compounds degradation and color changes of sugarcane juice. Food and Bioproducts Processing. 2018;111:62–71. https://doi.org/10.1016/j.fbp.2018.07.003
46. Hwang JH, Jung AH, Park SH. Efficacy of Ohmic Vacuum Concentration for orange juice concentrates and their physicochemical properties under different voltage gradients. LWT. 2022;154. https://doi.org/10.1016/j.lwt.2021.112750
47. Hashemi SMB, Mahmoudi MR, Roohi R, Torres I, Saraiva JA. Statistical modeling of the inactivation of spoilage microorganisms during ohmic heating of sour orange juice. LWT. 2019;111:821–828. https://doi.org/10.1016/j.lwt.2019.04.077
48. Gavahian M, Sastry SK. Ohmic-assisted peeling of fruits: Understanding the mechanisms involved, effective parameters, and prospective applications in the food industry. Trends in Food Science and Technology. 2020;106:345–354. https://doi.org/10.1016/j.tifs.2020.10.027
49. Silva-Vera W, Avendano-Munoz N, Nunez H, Ramírez C, Almonacid S, Simpson R. CO_2 laser drilling coupled with moderate electric fields for enhancement of the mass transfer phenomenon in a tomato (*Lycopersicon esculentum*) peeling process. Journal of Food Engineering. 2020;276. https://doi.org/10.1016/j.jfoodeng.2019.109870
50. Sawant SR, Pandey JP, Singh A, Prakash O. Performance and evaluation of ohmic heating assisted lye and salt concentration on peeling quality of tomato. International Journal of Current Microbiology and Applied Sciences. 2018;7(9):3515–3524. https://doi.org/10.20546/ijcmas.2018.709.436
51. Zhu F. Modifications of starch by electric field based techniques. Trends in Food Science and Technology. 2018;75:158–169. https://doi.org/10.1016/j.tifs.2018.03.011
52. Waziiroh E, Schoenlechner R, Jaeger H, Brusadelli G, Bender D. Understanding gluten-free bread ingredients during ohmic heating: function, effect and potential application for breadmaking. European Food Research and Technology. 2022;248(4):1021–1034. https://doi.org/10.1007/s00217-021-03942-4
53. Llave Y, Morinaga K, Fukuoka M, Sakai N. Characterization of ohmic heating and sous-vide treatment of scallops: Analysis of electrical conductivity and the effect of thermal protein denaturation on quality attribute changes. Innovative Food Science and Emerging Technologies. 2018;50:112–123. https://doi.org/10.1016/j.ifset.2018.09.007
54. Llave Y, Fukuda S, Fukuoka M, Shibata-Ishiwatari N, Sakai N. Analysis of color changes in chicken egg yolks and whites based on degree of thermal protein denaturation during ohmic heating and water bath treatment. Journal of Food Engineering. 2018;222:151–161. https://doi.org/10.1016/j.jfoodeng.2017.11.024

ORCID IDs
Dornoush Jafarpour https://orcid.org/0000-0002-7895-4862

Foods and Raw Materials. 2022;10(2)

ISSN 2310-9599 (Print)
ISSN 2308-4057 (Online)

Research Article
Open Access

Available online at http://jfrm.ru/en
https://doi.org/10.21603/2308-4057-2022-2-532
https://elibrary.ru/QJVODX

Formulating anti-diabetic nutraceutical tablets based on edible plants from Tripura, India

Bikash Debnath, Kuntal Manna*

Tripura University (A Central University), Suryamaninagar, India

* e-mail: k_manna2002@yahoo.com

Received 29.10.2021; Revised 17.01.2022; Accepted 05.05.2022; Published online 23.06.2022

Abstract:
Nutraceuticals are food-based drugs that are used as dietary supplements to minimize chronic diseases. Diabetes is one of the most common chronic diseases all over the world. Recently, herbal nutraceuticals have taken a promising role in treating diabetes. We aimed to develop herbal nutraceutical tablets and evaluate its anti-diabetic activity using ob/ob mice. Five plant species were collected by field survey methods based on oral interviews with traditional healers of Tripura. The wet granulation method was applied to formulate the herbal nutraceutical tablet. Water- and fat-soluble vitamins were determined by reversed-phase high-performance liquid chromatography. Trace elements were analyzed by atomic absorption spectrophotometry. To evaluate the anti-diabetic activity of the herbal tablets, we determined serum hemoglobin, glycosylated serum protein, and oral glucose tolerance.

The newly formulated herbal nutraceutical tablets provided the optimal energy level. It contained sufficient amounts of essential minerals, such as iron (74.6 ± 2.7 mg/g), sodium (4.4 ± 0.4 mg/g), potassium (5.3 ± 0.7 mg/g), calcium (163.1 ± 2.2 mg/g), magnesium (39.2 ± 1.7 mg/g), and phosphorus (14.6 ± 2.1 mg/g). We also found optimal quantities of water-soluble vitamins, such as vitamin C (27.2 ± 4.3 mg/g), vitamin B_1 (0.6 ± 0 mg/g), vitamin B_3 (0.6 ± 0.2 mg/g), vitamin B_6 (1.1 ± 0.2 mg/g), vitamin B_{12} (0.6 ± 0.2 μg/g), and folic acid (82.6 ± 7.6 μg/g), as well as fat-soluble vitamins, such as vitamin A (287.4 ± 6.3 μg/g), vitamin D_3 (2.6 ± 0.6 μg/g), and vitamin E (0.7 ± 0 ng/g). Finally, the herbal nutraceutical tablet (200 mg/kg) significantly improved the anti-hyperglycemic effect on ob/ob mice (type 2 diabetes), compared to the standard drug, metformin (200 mg/kg).

The results suggest that the newly formulated herbal tablet may be recommended as an anti-diabetic nutraceutical drug.

Keywords: Edible medicinal plant, herbal nutraceutical, tablet dosage, anti-diabetic activity, dietary supplement

Funding: The authors are grateful to the Indian Council of Medical Research (ICMR) (No. 3/1/2/125/2019-Nut) and the All-India Council for Technical Education (AICTE) (No. 8-114/RIFD/RPS-NER/Policy-1/2018-19) for providing financial support.

Please cite this article in press as: Debnath B, Manna K. Formulating anti-diabetic nutraceutical tablets based on edible plants from Tripura, India. Foods and Raw Materials. 2022;10(2):227–234. https://doi.org/10.21603/2308-4057-2022-2-532

INTRODUCTION

Modern lifestyle involves changes in essential food habits [1]. Due to improper diet, people suffer from various kinds of chronic diseases. Obesity, heart disease, and diabetes are among current global issues [2]. Nutraceuticals are food-based drugs which minimize diet-related illnesses. The word "nutraceutical" comes from "nutrition" and "pharmaceutical" [3]. Any pharmaceutical product manufactured from food sources has fundamental nutritional values and minimizes various chronic diseases [4].

Recently, nutraceuticals have gained extensive attention due to their better pharmacological functions with fewer side effects. In 2017, 77% of Americans used nutraceuticals, and their number was rising daily [5]. Nutraceuticals are classified as dietary fiber, probiotics, prebiotics, polyunsaturated fatty acids, antioxidant, vitamins, polyphenols, and spices [6]. Herbal nutraceuticals are prepared from plants, fungi, algae, or their combinations. Various forms of herbal nutraceuticals (powder, tablets, capsules, liquid, etc.) are currently available in the market [7].

About 2500 years ago, Hippocrates wrote, "Let food be thy medicine and medicine be thy food." This quotation is undoubtedly the principle of today [6]. The nutraceutical industry has great potential in some Asian

countries, such as China, Japan, India, South Korea, Thailand, Singapore, and Taiwan. With rich natural resources, skilled human resources, and excellent R&D facilities, these Asian countries are expected to lead the production of herbal nutraceuticals [8, 9].

Tripura is India's state located in the northeastern part of the subcontinent between 22°7' and 24°2' north latitudes and 91°0' and 92°0' east longitudes. Its highest temperature is 35.60°C, and yearly rainfall is 2000 mm. These excellent climatic conditions make Tripura a favorable place for various edible medicinal plants, or plants with nutritional benefits and bioactive compounds for the human body [10, 11].

According to literature, the forest of Tripura is a good source of edible medicinal plants with anti-diabetic properties [12]. Diabetes is a big issue in the Indian health care system. Type 2 diabetes is the most common in adults with uncontrolled diet. Every year, nearly 1 million Indians die due to diabetes. This chronic disease afflicts 2.8% of the global population [13]. Treatment with herbal medicine improves insulin secretion and reduces intestinal glucose absorption in diabetics [14].

This study aimed to formulate herbal nutraceutical tablets from selected edible medicinal plants of Tripura, India, and evaluate its anti-diabetic activity using ob/ob mice (type 2 diabetes model).

STUDY OBJECTS AND METHODS

Ethnomedicinal data collection. Ethnomedicinal data about five edible plant parts (*Musa paradisiaca* fruit, *Musa paradisiaca* stem, *Cmorphophallus paeoniifolius* corn, *Artocarpus heterophyllus* seed, and *Colocasia esculenta* leaf) were collected from oral interviews with traditional healers from three ethnic communities (Tripuri, Reang, and Jamatia) of Tripura. All the interviewees were adults aged over forty [15]. The scientific names of the collected plant specimens were identified with the help of a plant taxonomist and the book, "The Flora of Tripura State" [16].

Processing of plant materials. After identification, we selected plant parts with medicinal properties, washed them thoroughly with distilled water, and then properly air-dried them. The dried samples were ground to fine powder. The powder material was packed in a sealed container and preserved at room temperature for further experiments [17].

Experimental animals. In our experiments, we used laboratory mice as model organisms. Adult Swiss albino mice (18–25 g) of both sexes were used for acute toxicity tests. Male ob/ob mice (type 2 diabetes mice weighing 50–55 g, aged 12 weeks) and male C56BL6 mice (normal mice weighing 28–32 g, aged 12 weeks) were used for an anti-diabetic activity test. The temperature (20°C) and humidity (53%) of the animal house were controlled and maintained throughout the 12/12 h light/dark cycle. Food and water were available except during the fasting period. The care and handling of the animals were in line with the regulations of the National Institutes of Health. The Institutional Ethics Committee (No. 1667/GO/a/12/CPCSEA) approved the study protocol [18].

Acute toxicity test. Acute toxicity tests of five different plant powder samples were measured by the method described by Ali *et al.* with some modification [19]. The Swiss albino mice (18–25 g) of both sexes were divided into two groups, the control group and the experimental group, ten animals in each. The control group received only distilled water, whereas the experimental group received different doses (5, 50, 300, 800, 1200, and 2000 mg/kg body weight) of the powder sample orally. The mice were then kept under observation up to 72 h for mortality or symptoms of toxicity [19].

Formulation of herbal tablet. We used the wet granulation method to prepare novel herbal anti-diabetic nutraceutical tablets. Equal amounts of previously prepared plant materials (*M. paradisiaca* fruit, *M. paradisiaca* stem, *C. paeoniifolius* corn, *A. heterophyllus* seed, and *C. esculenta* leaf) were placed in a rapid mixture granulator, with a 10% starch solution added dropwise into the binder. The damp masses were screened through a sieve #10 and then dried. The dried granules were screened through a sieve #20 and stored in a desiccator until they were ready for tablet compression. The prepared granules were compressed in a single punch tablet press machine (Manesty Type F3, Liver Poole, England) with a punch diameter of 0.75 cm and a compression pressure of 933 Pa (N/m^2). The die volume matched the tablets' weight to confirm that 600 mg was obtained [20].

Evaluation of granules. Tablet granules were evaluated by Wadher *et al.* methods with some modification. Particularly, we determined their bulk density, tapped density, Hausner quotient, Carr's compressibility index, flow rate, and angle of repose [21].

Evaluation of herbal tablets. Weight variation, thickness, hardness, friability, and *in vitro* disintegration time were determined by Wadher *et al.* methods with some modification [21].

Total moisture, total carbohydrate, complete protein, total fat, total ash, and total caloric value of the herbal tablets were determined by Debnath *et al.* method with some modification [17]. Total dietary fiber was measured by Ozoliņa *et al.* method with some modification [22].

Concentrations of minerals were determined by an atomic absorption spectrophotometer. Debnath *et al.* method with some modification was applied to measure the content of minerals in the tablets [17].

Vitamins, namely C, B_1, B_3, B_6, and folic acid were determined by Antakli *et al.* method with some modification, using the RP-HPLC system [23].

Instrumental conditions:

Column: C18 BDS (10 cm×4.6 mm; 3 μm);

Mobile phase: A = Hexane-1-sulfonic acid sodium (5.84 mM):acetonitrile (95:5) with 0.1% triethylamine as solvent at pH 2.5; B = 5.84 mM of hexane-1-sulfonic

Table 1 Ethnomedicinal use report on edible medicinal plant parts selected

Botanical name and family	Local name	Plants parts	Ethnomedicinal use
Musa paradisiaca (*Musaceae*)	Kola	Unripe fruit	Diabetes, hypertension, ulcers, diarrhea
Musa paradisiaca (*Musaceae*)	Kola	Stem	Diabetes, high blood pressure, high acidity
Cmorphophallus paeoniifolius (*Araceae*)	Batama	Corn	Helminths, liver disease, digestive and gastric disorders, diabetes
Artocarpus heterophyllus (*Moraceae*)	Kathal	Seed	Ulcers, constipation, diarrhea; excessive accumulation of fluid in tissues
Colocasia esculenta (*Araceae*)	Kocho	Leaf	Diabetes, microbial infection, liver disease

acid sodium:acetonitrile (50:50) with 0.1% triethylamine as solvent at pH 2.5, pH = 3.54;

Flow rate: 1.6 mL/min;

Injected volume: 20 µL;

Absorbance recorded: Vitamins C and B_1 = 246 nm, vitamin B_3 = 260 nm, vitamin B_6 = 290 nm, vitamin B_9 = = 282 nm.

Determination of fat-soluble vitamins. Vitamins A, D_3, and E were determined by using the reversed-phase high-performance liquid chromatography as reported by Xue *et al.* with some modification [24].

Instrumental conditions:

Column: dC18 (particle diameter 5 µm, 150× 4.6 mm i.d.);

Mobile phase: methanol:water = 98:2;

Flow rate: 1.00 mL/min;

Injected volume: 10 µL;

Absorbance recorded: vitamin E = 230 nm, vitamins A and D_3 = 265nm.

Anti-diabetic activity.

Experimental design. The animals were randomly divided into four groups of six animals for test purposes, namely: a normal group (completely healthy mice) treated with 0.5% sodium carboxymethyl cellulose; a vehicle control group (ob/ob mice) treated with 0.5% sodium carboxymethyl cellulose; a positive control group treated with 200 mg/kg of metformin via gavage; and an experimental group treated with 200 mg/kg herbal nutraceutical tablet via gavage. The experiment lasted four weeks. At the end of the experiment, all the animal groups fasted overnight, and blood samples were collected from the tail vein. Before blood collection, the animals were given pentobarbital as an anesthetic agent [18].

Determination of serum hemoglobin and glycosylated serum protein. Hemoglobin (HbA1c) and glycosylated serum protein were measured by respective kits (Merck Millipore, Germany) according to the manufacturer's instruction [18].

Oral glucose tolerance test. After four weeks of treatment with herbal nutraceutical tablets, the animals were made to fast overnight, and glucose solution (2 g/kg of body weight) was administered orally. After that, their blood samples were collected every 30 min (0, 30, 60, 90, and 120 min). The blood glucose was measured by a glucose meter (i-QARE DS-W®) [18].

Statistical analysis. For the analysis of granules, herbal tablets, proximate compositions, minerals, and vitamins, the data were expressed as mean ± SDs. For the evaluation of anti-diabetic activity in ob/ob mice, the data were expressed as mean ± S.E.M. One-way ANOVA was used to determine significant differences among groups, after which the modified Student's t-test with the Bonferroni correction was applied to compare individual groups. All statistical analyses were performed with SPSS 17.0 software. $P < 0.05$ was considered statistically significant.

RESULTS AND DISCUSSION

Ethnomedicinal study. The field survey showed that the five edible medicinal plants were applied by the healers of Tripura to cure different diseases (Table 1). Ethnomedicinal studies play a vital role in finding medicinal plants that can be used to produce novel crude drugs. They also verify the protection of cultural heritage [11]. The data that we collected from the informants of healers clearly proved that the plants we had selected were of medicinal importance.

Acute toxicity test. Our results indicated no changes of behaviour or mortality caused by the plant samples at the highest dose of 2000 mg/kg b.wt. This meant that this dose had no lethal or toxic effect. Toxicity assessment is one of the crucial steps prior to human uses of any pharmaceuticals or food ingredients. Acute toxicity studies determine adverse effects of any active compound after oral ingestion of a single or multiple doses [19]. We found that the five plant samples under study had no toxic effect.

Evaluation of granules. All the physical parameters of the herbal granules under study were found to be satisfactory (Table 2). The Carr's compressibility index indicates the strength of the powder/granules, while the Hausner ratio determines the powder/granules' inter-particulate friction. Both parameters are used to analyze the powder/granules' flow rate. The Carr's compressibility index of less than 10 or the Hausner ratio of less than 1.11 indicate an "excellent" flow rate, while the Carr compressibility index higher than 38 or the Hausner ratio higher than 1.60 indicate a "very poor" flow rate. Both parameters depend on the bulk density and the tap density of the powder/granules [25]. The angle of repose is another parameter used to evaluate the powder/granules' flow rate. Its value of less than

Table 2 Physical parameters of herbal granules

Physical parameters	Herbal granules prepared with 10% starch solution
Bulk density, g/mL	0.46 ± 0.01
Tapped density, g/mL	0.48 ± 0.01
Hausner quotient	1.07 ± 0.01
Carr's compressibility, %	6.72 ± 0.53
Angle of repose, °	32.29 ± 0.99
Flow rate, g/sec	6.67 ± 0.57

*The values represent mean ± SD for three samples

Table 3 Physical parameters of herbal nutraceutical tablets prepared with 10% starch solution

Physical parameters	Value
Uniformity of weight, mg	610.50 ± 1.70
Uniformity of thickness, mm	3.78 ± 0.041
Hardness, kg/cm^2	3.88 ± 0.078
Friability, %	0.65 ± 0.020
Disintegration time, s	295.33 ± 1.52

*The values represent mean ± SD for three samples

Table 4 Proximate composition of herbal nutraceutical tables

Proximate composition	Total amount, %
Moisture	62.44 ± 2.11
Carbohydrates	1.88 ± 0.52
Protein	0.95 ± 0.65
Fat	0.43 ± 0.53
Ash	1.78 ± 0.53
Dietary fiber	1.66 ± 0.67
Calories, kcal	15.19

*The values represent mean ± SD for three samples

Table 5 Mineral profile of herbal nutraceutical tablets

Minerals	Total amount, mg/g
Iron	74.6 ± 2.7
Sodium	4.4 ± 0.4
Potassium	5.3 ± 0.7
Calcium	163.1 ± 2.2
Magnesium	39.2 ± 1.7
Phosphorus	14.6 ± 2.1

*The values represent mean ± SD for three samples

Table 6 Profiles of water - soluble and fat-soluble vitamins in herbal nutraceutical tablets

Vitamin	Total amount
C (ascorbic acid), mg/g	27.2 ± 4.3
Vitamin B_1 (thiamin), mg/g	0.6 ± 0.0
Vitamin B_3 (niacin), mg/g	0.6 ± 0.2
Vitamin B_6 (pyridoxine), mg/g	1.1 ± 0.2
Vitamin B_{12} (cobalamin), µg/g	0.6 ± 0.2
Vitamin B_9 (folic acid), µg/g	82.6 ± 7.6
Vitamin A (retinol), µg/g	287.4 ± 6.3
Vitamin D_3 (cholecalciferol), µg/g	2.6 ± 0.6
Vitamin E (tocopherol), ng/g	0.7 ± 0.0

*The values represent mean ± SD for three samples

30° indicates an "excellent" flow rate, while the value greater than 56° indicates a "very poor" flow rate [26]. Our results showed an excellent flow rate in the granules prepared with a 10% starch solution (Table 2).

Evaluation of herbal tablets. All the physical parameters of the herbal tablets under study were found to be satisfactory (Table 3). The weight variation test is employed to ensure that each tablet/capsule in the batch contains the same amount of drug ingredients. Checking a tablet's thickness is necessity for packaging since very thick tablets are not suitable for packaging. A tablet's friability and hardness tests are closely related to each other. They determine the physical strength of a tablet. Disintegration refers to the mechanical breakup of a compressed tablet into small granules at a specific time point. The disintegration test provides critical safety data on the drug's bioavailability in the body [27, 28].

In our experiments, 20 tablets were used to check the average uniformity of weight and 10 tablets to check the average uniformity of thickness and hardness. For the friability and disintegration tests, the samples were prepared in triplicate. According to the results (Table 3), the physical parameters of our newly formulated tablets were within the limits established by the United States Pharmacopoeia.

Determination of proximate composition. The proximate composition of the herbal nutraceutical tablets is represented in Table 4. The moisture content is an essential parameter because high moisture affects the physical stability of food products. Their shelf life also depends on the total moisture content [29]. As we can see in Table 4, our newly formulated herbal tablets had a low moisture content (62.44 ± 2.11 %), indicating high physical stability.

Carbohydrates, proteins, and fats hold a special place in human nutrition. The human body requires them in relatively large amounts for normal functioning. These three macronutrients provide energy (measured in calories) in the human body [30]. Our newly formulated herbal nutraceutical tablet contained optimal amounts of carbohydrates (1.88 ± 0.52 %), proteins (0.95 ± 0.65 %), and fats (0.43 ± 0.53 %), as well as provided a good amount of energy (15.19 kcal).

So, the herbal nutraceutical tablets developed may be recommended to people with unbalanced energy levels. Dietary fiber is a complex mixture of polysaccharides. Diets with a high content of fiber alleviate constipation [31]. Our herbal nutraceutical tablet contained a good amount of dietary fiber (1.66 ± 0.67%), so it may be used to reduce constipation.

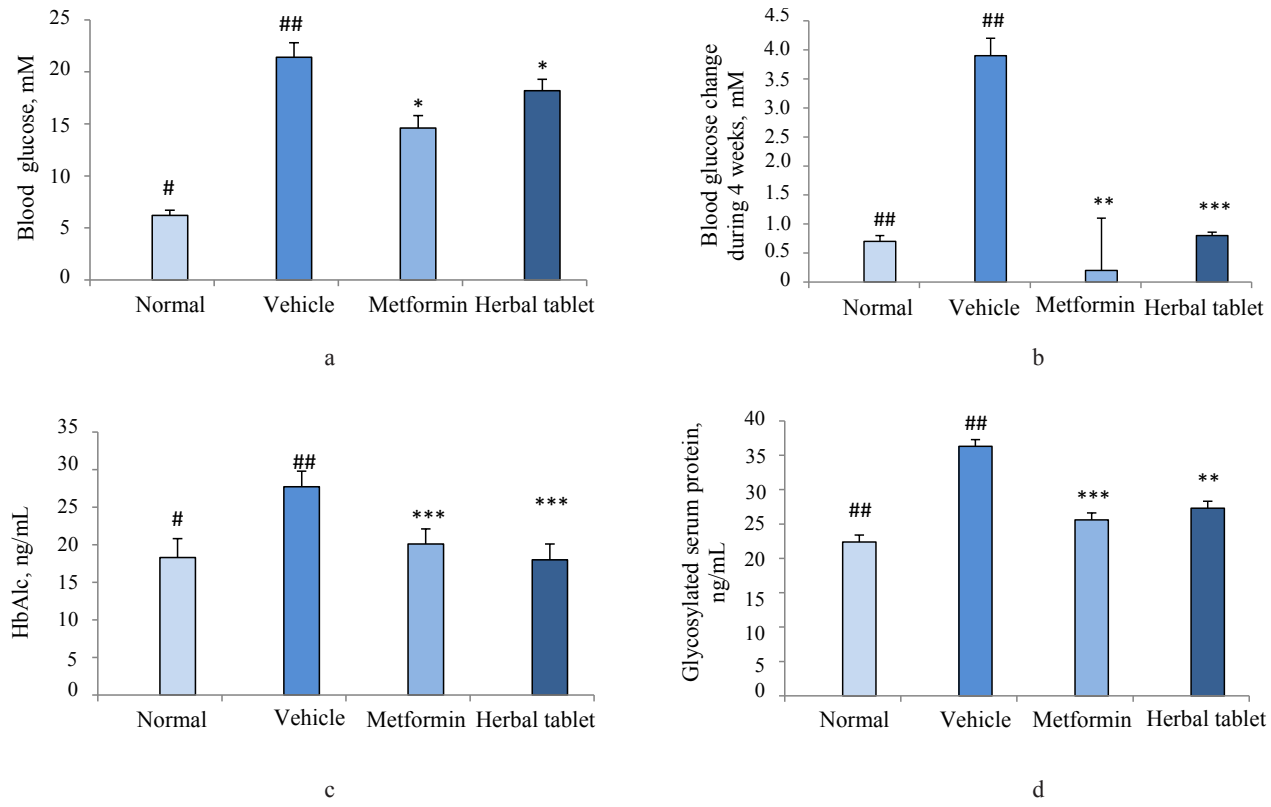

Figure 1 Carbohydrate metabolism parameters of ob/ob mice treated with sodium carboxymethyl cellulose (normal group), sodium carboxymethyl cellulose (vehicle control group), metformin (positive control group), and herbal nutraceutical tablet (experimental group). Each group contained six animals

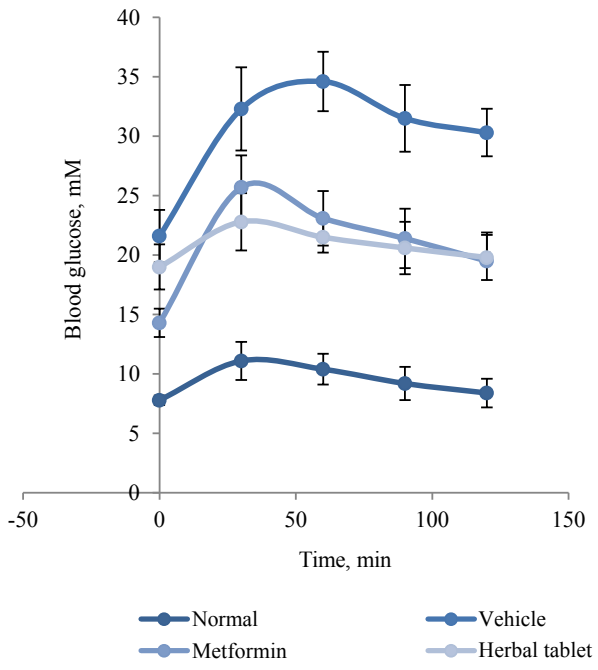

Figure 2 Change of blood glucose with time in ob/ob mice treated with sodium carboxymethyl cellulose (normal group), sodium carboxymethyl cellulose (vehicle control group), metformin (positive control group), and herbal nutraceutical tablet (experimental group). Each group contained six animals

Minerals determination. Iron is an essential microelement for producing blood. Anemia is the most common disease caused by iron deficiency. Every year, approximately 30% of patients suffer from anemia globally, particularly 51% in India [32]. Our herbal nutraceutical tablet had a significant amount of iron (74.6 ± 2.7 mg/g), so it may alleviate the effects of iron deficiency (Table 5). Dietary potassium and sodium are two electrolytes that play a vital role in regulating fluid and blood volume [33]. The tablets developed contained a fair amount of sodium (4.4 ± 0.4 mg/g) and potassium (5.3 ± 0.7 mg/g), so it may be used to regulate the body's fluid and blood volume. Calcium, phosphorus, and magnesium are three crucial micronutrients for healthy bone and teeth formation, as well as metabolic functions [34]. Our herbal nutraceutical tablets contained a considerable amount of these minerals, namely 163.1 ± 2.2, 14.6 ± 2.1, and 39.2 ± 1.7 mg/g, respectively. Therefore, the newly developed herbal tablets can help bone formation and improve metabolic functions in the human body.

Determination of vitamins. We determined the values of water-soluble (C, B_1, B_3, B_6, B_{12}, and folic acid) and fat-soluble vitamins (A, D_3, and E) in our herbal nutraceutical tablets (Table 6). We found rich amounts of vitamin C (27.2 ± 4.3 mg/g) and vitamin A (287.4 ± 6.3 µg/g). Vitamin C is a water-soluble vitamin

that works as an antioxidant and improves the immune function of the human body [35]. Vitamins B_1, B_3, B_6, and B_9 are essential for maintaining the nervous system, digestion, protein metabolism, red blood cells, and skin health. Vitamins A, D_3, and E are common fat-soluble vitamins that support such body functions as vision, hair growth, bone maintenance, immune system regulation, oxidative stress prevention, etc. [36]. Our herbal nutraceutical tablets contained fair amounts of vitamins D_3, E, and B group (Table 6). Therefore, they may be used to treat diseases caused by their deficiency.

Anti-diabetic activity. The treatment of ob/ob mice with our herbal nutraceutical tablets (200 mg/kg body weight) significantly decreased their fasting blood glucose, serum hemoglobin, and glycosylated serum protein (Fig. 1). The effectiveness of the herbal tablet was comparable to that of metformin, a standard drug (200 mg/kg body weight).

A fasting blood glucose test, which is generally called a fasting plasma glucose test, measures the amount of glucose in the blood and determines the patient's risk of prediabetes or diabetes [37]. Our newly formulated herbal tablet (200 mg/kg) reduced the fasting blood glucose level (Fig. 1a and 1b). Serum hemoglobin and glycosylated serum protein are important indicators for the long-term glycemic control [38]. Our experiment showed that the herbal tablet (200 mg/kg) reduced their levels, compared to metformin (200 mg/kg) (Fig. 1c and 1d).

An oral glucose tolerance test determines the body's response to glucose. This test can be used to detect type 2 diabetes [39]. The oral administration of the herbal tablet to ob/ob mice significantly reduced their blood glucose level (Fig. 2). Therefore, this tablet may be used as an anti-diabetic drug.

We also found that the herbal nutraceutical tablet (200 mg/kg) significantly enhanced oral glucose tolerance (Fig. 2). This means that this tablet can be used to alleviate type 2 diabetes mellitus through progressing insulin sensitivity.

CONCLUSION

Our study showed that the newly formulated herbal tablet contained optimal amounts of macro- and micronutrients, water, and fat-soluble vitamins. The tablet also provided significantly higher hypoglycemic activity compared to the standard drug, metformin. The results suggested that the herbal tablets developed may be recommended as an anti-diabetic herbal remedy.

CONTRIBUTION

The authors were equally involved in writing the manuscript and are equally responsible for plagiarism.

CONFLICT OF INTEREST

The authors have declared no conflict of interest in relation to this manuscript.

REFERENCES

1. Farhud DD. Impact of lifestyle on health. Iranian Journal of Public Health. 2015;44(11):1442–1444.
2. Afshin A, Sur PJ, Fay KA, Cornaby L, Ferrara G, Salama JS, *et al.* Health effects of dietary risks in 195 countries, 1990–2017: a systematic analysis for the Global Burden of Disease Study 2017. The Lancet. 2019;393(10184):1958–1972. https://doi.org/10.1016/S0140-6736(19)30041-8
3. Cencic A, Chingwaru W. The role of functional foods, nutraceuticals, and food supplements in intestinal health. Nutrients. 2010;2(6):611–625. https://doi.org/10.3390/nu2060611
4. Schulze MB, Martínez-González MA, Fung TT, Lichtenstein AH, Forouhi NG. Food based dietary patterns and chronic disease prevention. BMJ. 2018;361. https://doi.org/10.1136/bmj.k2396
5. Kunnumakkara AB, Bordoloi D, Padmavathi G, Monisha J, Roy NK, Prasad S, *et al.* Curcumin, the golden nutraceutical: multitargeting for multiple chronic diseases. British Journal of Pharmacology. 2017;174(11):1325–1348. https://doi.org/10.1111/bph.13621
6. Das L, Bhaumik E, Raychaudhuri U, Chakraborty R. Role of nutraceuticals in human health. Journal of Food Science and Technology. 2012;49(2):173–183. https://doi.org/10.1007/s13197-011-0269-4
7. Chauhan B, Kumar G, Kalam N, Ansari SH. Current concepts and prospects of herbal nutraceutical: A review. Journal of Advanced Pharmaceutical Technology and Research. 2013;4(1):4–8. https://doi.org/10.4103/2231-4040.107494
8. Banerjee S. Dietary supplements market in India is rapidly growing – An overview. IMS Management Journal. 2018;10(1).
9. Potential for functional foods in the Indian market [Internet]. [cited 2021 Sep 22]. Available from: https://www.figlobal.com/india/en/visit/news-and-updates/potential-functional-foods-indian-market.html
10. Debnath B, Uddin J, Patari P, Das M, Maiti D, Manna K. Estimation of alkaloids and phenolics of five edible cucurbitaceous plants and their antibacterial activity. International Journal of Pharmacy and Pharmaceutical Sciences. 2015;7(12):223–227.

11. Sofowora A, Ogunbodede E, Onayade A. The role and place of medicinal plants in the strategies for disease prevention. African Journal of Traditional, Complementary, and Alternative Medicines. 2013;10(5):210–229. https://doi.org/10.4314/ajtcam.v10i5.2
12. Choudhury R, Datta Choudhury M, De B, Paul SB. Importance of certain tribal edible plants of Tripura. Indian Journal of Traditional Knowledge. 2010;9(2):300–302.
13. Gheith O, Farouk N, Nampoory N, Halim MA, Al-Otaibi T. Diabetic kidney disease: world wide difference of prevalence and risk factors. Journal of Nephropharmacology. 2015;5(1):49–56.
14. Choudhury H, Pandey M, Hua CK, Mun CS, Jing JK, Kong L, *et al.* An update on natural compounds in the remedy of diabetes mellitus: A systematic review. Journal of Traditional and Complementary Medicine. 2018;8(3):361–376. https://doi.org/10.1016/j.jtcme.2017.08.012
15. Emmanuel MM, Didier DS. Traditional knowledge on medicinal plants use by ethnic communities in Douala, Cameroon. European Journal of Medicinal Plants. 2012;2(2):159–176. https://doi.org/10.9734/EJMP/2012/878
16. Deb DB. The Flora of Tripura State. Vol. 1 and 2. New Delhi: Today and Tomorrow's Printers and Publishers; 1981, 1983.
17. Debnath B, Manna K. Phytochemicals and nutrient profiles, anti-oxidant activity study of three edible parts (flower, fruit and stem) of Musa paradisiaca. Current Biotechnology. 2019;8(1):32–41. https://doi.org/10.2174/2211550108666190315161848
18. Zhang X, Jin Y, Wu Y, Zhang C, Jin D, Zheng Q, *et al.* Anti-hyperglycemic and anti-hyperlipidemia effects of the alkaloid-rich extract from barks of *Litsea glutinosa* in ob/ob mice. Scientific Reports. 2018;8(1). https://doi.org/10.1038/s41598-018-30823-w
19. Ali K, Ashraf A, Biswas NN. Analgesic, anti-inflammatory and anti-diarrheal activities of ethanolic leaf extract of *Typhonium trilobatum* L. Schott. Asian Pacific Journal of Tropical Biomedicine. 2012;2(9):722–726. https://doi.org/10.1016/S2221-1691(12)60217-2
20. Chandira M, Jayakar B. Formulation and evaluation of herbal tablets containing *Ipomoea digitata* Linn. extract. International Journal of Pharmaceutical Sciences Review and Research. 2010;3(1):101–110.
21. Wadher K, Kakde R, Umekar M. Formulation and evaluation of a sustained-release tablets of metformin hydrochloride using hydrophilic synthetic and hydrophobic natural polymers. Indian Journal of Pharmaceutical Sciences. 2011;73(2):208–215. https://doi.org/10.4103/0250-474X.91579
22. Ozoliņa V, Grāmatiņa I, Kunkulberga D. Methodology of dietary fibre determination in grain products. Research for Rural Development. 2009;115–119.
23. Antakli S, Sarkees N, Sarraf T. Determination of water soluble vitamins B_1, B_2, B_3, B_6, B_9, B_{12} and C on a C_{18} column with particle size 3 µM in some manufactured food products by HPLC with UVDAD/FLD detection. International Journal of Pharmacy and Pharmaceutical Sciences. 2015;7(6):219–224.
24. Xue X, You J, He P. Simultaneous determination of five fat-soluble vitamins in feed by high-performance liquid chromatography following solid-phase extraction. Journal of Chromatographic Science. 2008;46(4):345–350. https://doi.org/10.1093/chromsci/46.4.345
25. Shah RB, Tawakkul MA, Khan MA. Comparative evaluation of flow for pharmaceutical powders and granules. AAPS PharmSciTech. 2008;9(1):250–258. https://doi.org/10.1208/s12249-008-9046-8
26. Thapa P, Choi DH, Kim MS, Jeong SH. Effects of granulation process variables on the physical properties of dosage forms by combination of experimental design and principal component analysis. Asian Journal of Pharmaceutical Sciences. 2019;14(3):287–304. https://doi.org/10.1016/j.ajps.2018.08.006
27. Shabana M. A review on the quality control analysis of oral dosage form: tablets. Research and Reviews: Journal of Pharmacy and Pharmaceutical Sciences. 2016;5(2):108–114.
28. Zaid AN, Al-Ramahi RJ, Ghoush AA, Qaddumi A, Zaaror YA. Weight and content uniformity of lorazepam half-tablets: A study of correlation of a low drug content product. Saudi Pharmaceutical Journal. 2013;21(1):71–75. https://doi.org/10.1016/j.jsps.2011.12.009
29. Mathlouthi M. Water content, water activity, water structure and the stability of foodstuffs. Food Control. 2001;12(7):409–417. https://doi.org/10.1016/S0956-7135(01)00032-9
30. Manna K, Debnath B. Phytochemicals, nutritional properties and anti-oxidant activity in young shoots of *Melocanna baccifera*, a traditional vegetable of Northeast India. Journal of Food, Agriculture and Environment. 2020;18(1):59–65.
31. Dhingra D, Michael M, Rajput H, Patil RT. Dietary fibre in foods: a review. Journal of Food Science and Technology. 2012;49(3):255–266. https://doi.org/10.1007/s13197-011-0365-5
32. Abbaspour N, Hurrell R, Kelishadi R. Review on iron and its importance for human health. Journal of Research in Medical Sciences. 2014;19(2):164–174.

33. Pohl HR, Wheeler JS, Murray HE. Sodium and potassium in health and disease. In: Sigel A, Sigel H, Sigel RKO, editors. Interrelations between essential metal ions and human diseases. Dordrecht: Springer; 2013. pp. 29–47. https://doi.org/10.1007/978-94-007-7500-8_2

34. Al-Fartusie FS, Mohssan SN. Essential trace elements and their vital roles in human body. Indian Journal of Advances in Chemical Science. 2017;5(3):127–136.

35. Sami R, Li Y, Qi B, Wang S, Zhang Q, Han F, *et al.* HPLC analysis of water-soluble vitamins (B2, B3, B6, B12, and C) and fat- soluble vitamins (E, K, D, A, and *β*-carotene) of okra (*Abelmoschus esculentus*). Journal of Chemistry. 2014;2014. https://doi.org/10.1155/2014/831357

36. Albahrani AA, Greaves RF. Fat-soluble vitamins: clinical indications and current challenges for chromatographic measurement. Clinical Biochememist Reviews. 2016;37(1):27–47.

37. Perry RC, Shankar RR, Fineberg N, McGill J, Baron AD. HbA_{1c} measurement improves the detection of type 2 diabetes in high-risk individuals with nondiagnostic levels of fasting plasma glucose: The Early Diabetes Intervention Program (EDIP). Diabetes Care. 2001;24(3):465–471. https://doi.org/10.2337/diacare.24.3.465

38. Suo M, Wen D, Wang W, Zhang T. Comparative study on hemoglobin A1c, glycated albumin and glycosylated serum protein in aplastic anemia patients with Type 2 diabetes mellitus. Bioscience Reports. 2020;40(5). https://doi.org/10.1042/BSR20192300

39. Srivastava AK, Mukerjee A, Tripathi A. Antidiabetic and antihyperlipidemic activities of *Cucumis melo* var. *momordica* fruit extract on experimental animals. Future Journal of Pharmaceutical Sciences. 2020;6. https://doi.org/10.1186/s43094-020-00116-z

ORCID IDs
Bikash Debnath https://orcid.org/0000-0001-9698-0012
Kuntal Manna https://orcid.org/0000-0001-5327-365X

Foods and Raw Materials. 2022;10(2)

ISSN 2310-9599 (Online)
ISSN 2308-4057 (Print)

Review Article
Open Access

Available online at http://jfrm.ru/en
https://doi.org/10.21603/2308-4057-2022-2-533
https://elibrary.ru/QXKSOO

Effects of spray-drying parameters on physicochemical properties of powdered fruits

Liew Phing Pui*, Lejaniya Abdul Kalam Saleena

UCSI University, Kuala Lumpur, Malaysia

* e-mail: puilp@ucsiuniversity.edu.my

Received 21.01.2022; Revised 21.02.2022; Accepted 14.04.2022; Published online 23.06.2022

Abstract:
This review features different powdered fruits with optimal storage stability and physiochemical parameters. Spray-drying parameters, such as temperatures and flow rate, can affect the physical properties of powders. Carrier agents provide powders with various favorable qualities, e.g. good flow rate. Commercial spray-drying of fruit juice knows different carrier agents.
The review involved scientific and methodological publications, conference papers, patents, regulatory papers, and Internet resources. They were subjected to grouping, categorization, comparative analysis, and consolidation.
Inlet temperature, maltodextrin concentration, and air flow rate of spray-drying increased the powder yield but decreased the moisture content. Inlet temperature, maltodextrin concentration, and feed flow rate affected the solubility. Effects of atomization rate, air flow rate and free flow rate were assessed in terms of yield, moisture content, hygroscopicity, and solubility.
The article introduces the fundamentals of spray-drying and describes the effect of each spray-drying parameter on the powder quality. The list of parameters included inlet air temperature, atomization rate, air flow, and feed flow rate. We also evaluated the impacts of various carrier agents on the powder quality. The article contributed to a better understanding of how variable parameters affect the quality of food powders. The results provide the food industry with better choice options to adopt certain parameters for specific production needs.

Keywords: Temperature, atomization rate, flow rate, maltodextrin, powder properties

Please cite this article in press as: Pui LP, Saleena LAK. Effects of spray-drying parameters on physicochemical properties of powdered fruits. Foods and Raw Materials. 2022;10(2):235–251. https://doi.org/10.21603/2308-4057-2022-2-533

INTRODUCTION

Dehydration of food allows extending its shelf life by reducing the chemical and microbial activities [1]. Drying reduces the moisture content of powder, which guarantees a long and safe storage [2]. High-water content makes fruit juices highly perishable products with high transportation costs. In this regard, powdered fruit juices are an attractive option for the food business: they are stable, space-effective, and easy to transport [3]. Atomization, droplet-hot air interaction, and moisture evaporation are the three essential processes of spray-drying [4].

Fruits usually undergo such procedures as open sun-drying, hot air drying, solar drying, microwave-drying, freeze-drying, and spray-drying. However, these methods have some disadvantages. For example, hot air drying is time-consuming, and freeze-drying is rather expensive [5, 6]. Spray-drying is a highly suitable process for heat-sensitive products producing powders with good quality [7–9]. Spray-dried powders have good dispersion characteristics and are easy to incorporate into food products [10]. Some resent studies introduced spray-dried powders from cempedak jackfruit and kuini mango [11–13].

Spray-drying is an effective means of making inhalable powders [3]. The list of physicochemical parameters that affect powders during spray-drying includes such process factors as viscosity, particle size, liquid feed flow rate, temperature and pressure of the drying air, the kind of atomizer, etc. As a result, optimizing the drying process is critical for obtaining goods with improved sensory and nutritional properties, as well as for increasing process yield. Studies that feature surface characteristics of powder particles can provide better knowledge of the production process and optimize the powder composition [4].

Effective spray-drying requires a careful selection of operating conditions. For particles ≤ 2 μm, spray-drying has a poor cyclone collection efficiency. A common spray-dryer has an average output of 20–50%, but a new high-performance cyclone developed by the Swiss company BÜCHI increased it to ≥ 70%. Another significant problem with spray-drying is the lack of control over the mean droplet size. As a result, droplets come in a wide range of sizes, and pneumatic nozzles can cause clogging. Ultrasonic nozzles produce more consistent droplets and more uniform size distribution of the powder [7, 8].

Some difficulties, such as stickiness, hygroscopicity, and solubility, can be overcome by introducing the carrier agents before atomization. Biopolymers and gums are the most popular carrier agents. These compounds are typically associated with microencapsulation. They can minimize powder hygroscopicity, protect delicate food components from unfavorable ambient circumstances, reduce food component volatility and reactivity, and improve the appearance of the finished product [10].

Fruit storage provides their off-season supply. However, some fruits tend to rot during storage and lose their nutritional content. The benefits of a dried extract over traditional liquid forms include cheaper storage costs, increased concentration, and active component stability. Spray-drying can produce powders with precise quality criteria in a continuous process [14]. It is a one-stage technology that turns liquid meals or suspensions into powder form. Spray-drying is also used in pharmacy for tablet coating. Spray-drying has three primary steps: atomizing the liquid feed, creating and drying the droplets, and droplet motion.

Problem statement. Spray-dried fruit juice powders have high sugar solids content and usually assume amorphous state [14]. Some recent studies describe the advances in the spray-drying of sugar-rich foods, including fruit juices, pulp, and honey with or without carriers [15]. Products with low molecular weight sugars, e.g. fructose, sucrose, and glucose, have a very low glass transition temperature. Sucrose, glucose, and fructose have the glass transition temperature of 62, 32, and –5°C, respectively. They reduce the glass transition temperature of sugar-rich foods, which are prone to caking during storage [16]. The hygroscopic and thermoplastic nature of dried materials, such as fruit juice powders, are known to cause adhesion to dryer walls, reduce the drying yield, increase stickiness, and decrease solubility [17]. These sugars are very hygroscopic, which increases their stickiness and tendency to agglomeration [18].

Organic lactic, malic, tartaric, and citric acids also make spray-drying difficult. When tartaric, citric, and malic acids were applied at concentrations of ≥ 10% dry matter, they reduced the powder recovery. As a result, spray-drying of fruits with high acid content required more maltodextrin [19]. Spray-drying below +20°C of glass transition temperature helped avoid stickiness but was not economically feasible [20]. Spray-dried blood fruit powder was found to have high solubility and good retention of resveratrol content [21]. This work features the effect of different spray-drying parameters, e.g. temperature, flow rate, flow rate, and carrier concentration, on food powders.

STUDY OBJECTS AND METHODS

The study was carried out at UCSI University in Malaysia's Faculty of Applied Sciences, Department of Food Science and Nutrition. It featured scientific and methodological literature, publications in scientific journals, conference papers, patents, regulatory papers, and Internet resources. The data were grouped, categorized, compared, and consolidated. Because 1995 was the year that the topic of spray-drying was first highlighted, the review includes high-quality peer-reviewed English-language papers published between 1995 and 2021. Most publications were Scopus indexed. The conference papers were chosen based on their citation quantity and keywords. The review did not include books and non-academic resources.

RESULTS AND DISCUSSION

Basic principles of spray-drying. Spray-drying involves five major stages [22, 23]:

1) Concentration. The feed is concentrated before being pumped into the spray-dryer;

2) Atomization. The fluid products are dispersed into fine droplets and pumped into the drying chamber via an atomizer;

3) Droplet-air contact. The atomized feed comes in contact with the hot gas. Water evaporates, leaving a dry product. The contact time between spray-droplets and the hot air is very short, which provides an efficient drying process of heat sensitive materials without thermal decomposition;

4) Droplet drying. It occurs in two sub-stages. The first sub-stage happens at a relatively constant rate. During this sub-stage, the surface of the droplets is quickly moisturized by the water trapped inside the droplets. The second sub-stage happens when the surface of the droplets runs out of moisture. This sub-stage yields a dried product;

5) Separation. The dried powder passes through the cyclone and is then collected in the collection vessel. The air is exhausted from the top of the cyclone and passes through the bag filter.

Main properties of spray-dried powders. Primary powder properties include hygroscopicity, moisture content, solubility, particle density, particle size distribution, appearance, color bulk density, particle morphology, and surface composition [24]. In addition to moisture content, some important characteristics of spray-dried powders also include particle porosity, size, and rehydration [20]. As a result, scientific publications concentrate mostly on the effect of feed qualities and drying conditions on the physical properties of powder,

although the results are sometimes confusing [25]. The spray-dried powders are analyzed in a few common tests (Table 1).

The powder yield depends on the kind of fruit and the carrier agent. For example, orange juice powder has a big range of yield, from 25 to 85% [49]. However, acai juice powder yield was reported as 48.49% [26]. The moisture content is one of the main characteristics of powder which affects mainly solubility and bulk density [24]. Moisture content of spray-dried tomato powder was reported as 3.11–9.30%, whereas watermelon juice powder obtained by the same method had 1.47–2.48% moisture content [50, 51].

Fruit juice powder has a high hygroscopic feed and thermoplastic nature. As a result, it sticks to the dryer walls, which is one of the major problems in spray-drying [52]. The other reason might be its low melting point temperature, high water solubility, and low glass transition temperature [53]. Stickiness normally occurs if particles are not dry enough when they come in contact with one another or with the drying wall and thus stick to the drying chamber [19]. Stickiness causes operational issues and lowers the yield [16, 14].

Reported hygroscopicity of 12.48–15.79 for acai powder, while Rodrigues-Hernandez *et al.* stated 36.32–48.93 for cactus pear juice powder [26, 54]. According to Fitzpatrick *et al.*, particle size and particle distribution eventually have significant impact on the powder flowability, handling, and processing [43, 55].

Solubility is another important property of powders [49, 50]. It can be affected by compressed air flow rates, carrier agents, and low feed rates [24]. The water solubility index increased when maltodextrin reached 96% [56]. According to Mahendran, 30% of maltodextrin produced a guava powder with 95% solubility, whereas 60% of maltodextrin added to guava juice decreased the solubility to 86% [38]. Bulk density is an important powder property as it determines the size of containers, which eventually affect the handling and transportation costs.

Consumers prefer it when the powder is reconstituted well and can be instantly dissolved in water [20, 57]. Mango powder showed a good reconstitution property: it completely dissolved in warm water at 40°C with no suspended particles in the solution [52]. Reconstituted pineapple powder was found to have a lower lightness but a higher redness and yellowness, probably, as a result of the non-enzymatic browning reaction that occurred during spray-drying [58].

Youssefi *et al.* measured the color change in the pear cactus juice powder and its reconstituted solution. The slight changes in the color (ΔE) ranged from 6.7 to 9.8 [17]. L^* was affected neither by the drying conditions nor by the color change, only by the maltodextrin concentration. The L^* values of the reconstituted samples (13.00–16.00) were similar to those of the untreated juice (13.02), which meant that the spray-drying process did not darken the finished product.

Factors affecting the properties of spray-dried powder. Table 2 shows the production of different fruit powders obtained by spray-drying. Spray-drying parameters are important and must be controlled as they affect the quality and quantity of powder. Some parameters of spray-drying include inlet and outlet temperature, air flow rate, feed flow rate, atomizer, carrier agents, and concentration. Different parameters affect such powder properties as bulk density, solubility, hygroscopicity, particle size, flowability, and glass transition temperature [50].

Inlet air temperature and outlet temperature. Table 2 demonstrates the effects of inlet air temperature on the physicochemical properties of spray-dried fruit powders. Such powder properties as moisture content, bulk density, particle size, hygroscopicity, and morphology are all affected by the initial settings of inlet air temperature [61]. Inlet air temperature proved a more important factor than maltodextrin content, judging by bulk density, caking, and water solubility index [62].

Inlet air temperature can range from as low as 80°C for red beet to as high as 205°C in for pear cactus [54, 63]. However, the normal range for spray-drying is 110–160°C [50, 64]. Nevertheless, Phisut reported that the inlet air temperature of 150–220°C is commonly used for food spray-drying [61]. Some recent studies of spray-drying of guava, pineapple, and bael powder revealed the inlet air temperature of 148, 160, and 166°C, respectively [65–67].

Quek *et al.* found that the moisture content of spray-dried powder decreased as inlet air temperature and outlet temperature grew higher [51]. The outlet temperature should be the same to maintain the product quality. For every 2–3°C increase in the inlet air temperature, the outlet air temperature is usually increased by 1°C. According to [49, 51, 68], a higher inlet air temperature reduced the residual moisture content. When the inlet air temperature was increased, the moisture content fell down because the heat transfer happened at a faster rate between the product and the drying air [61].

The inlet air temperature can also affect the hygroscopicity of powder [61]. Similarly, powders produced at higher inlet air temperatures were more hygroscopic [24, 26]. Higher inlet air temperatures lowered the moisture content in the powder, causing the powder to absorb moisture from the environment [61]. Inlet air temperature can also affect bulk density. In particular, increasing the inlet air temperature caused the bulk density to drop [49]. For instance, the bulk density of acai juice powder decreased as the inlet air temperature increased [26].

When temperature increased during spray-drying, case-hardening appeared at the outer layer of atomized powder [61]. Particle size was reported to increase together with temperature. Higher drying temperatures resulted in faster drying rates, triggering an early structural formation and preventing the particles

Table 1 Spray-drying conditions in fruit powder production

Powder	Initial sample	Total solids	Inlet temperature, °C	Outlet temperature, °C	Aspirator rate/air velocity	Feed rate	Atomization rate/ compressor pressure	Analysis	References
Acai	Pulp	–	138–202	82–114	73 m^3/h, 0.06 MPa	5–25 g/min	–	Process yield, moisture content, hygroscopicity, anthocyanin retention, outlet temperature	[26]
Amla	Juice	–	120–200	81–119	75 m^3/h	13–15 mL/min	0.12 mPa	Moisture content, hygroscopicity, bulk density, water solubility index, surface morphology, DPPH, total phenolic content	[27]
Andes berry	Juice	9°B	12	70	10 m^3/h	485 mL/h	4 bar	Particle morphology, size, thermal analysis, volatile compounds, anthocyanin activity	[28]
Bayberry	Juice	11°B	150	80	100% (35 m^3/h)	–	439 L/h	Product recovery, moisture content, water activity, glass transition temperature, surface composition	[29]
Ber	Juice	–	170–210	–	40–80 m^3/h	1 L/h 9–21%	–	Color, bulk density, hygroscopicity, packed density, outlet temperature	[30]
Black currant	Extract	Final 35°B	150, 160, 180, 205	70, 70, 85, 100	–	–	–	Total polyphenol, antioxidant activity	[31]
Black mulberry	Juice	–	110–150	–	800 L/h	150 mL/h	4.65 bar	Yield, moisture content, bulk density, solubility, surface morphology, glass transition temperature, particle size	[32]
Blackberry	Pulp	–	140–180	99–115	35 m^3/h	0.49 kg/h	0.36 m^3 air flow	Moisture content, hygroscopicity, anthocyanin content, color, surface morphology, particle size	[33]
Blueberry	Extract	30% total solids	160	70	–	–	23 000 rpm	Particle size, true density, water-binding capacity, anthocyanin content	[34]

Continuation of Table 1

Powder	Initial sample	Total solids	Inlet temperature, °C	Outlet temperature, °C	Aspirator rate/air velocity	Feed rate	Atomization rate/ compressor pressure	Analysis	References
Cantaloupe	Juice	–	170–190	75–77	–	–	–	Moisture content, water activity, vitamin C, β-carotene content, dissolution, surface morphology	[35]
Elderberry	Juice	10–13°B	70–120	–	–	180 & 300 mL/hr	–	Total phenolic content, color	[36]
Gac	Aril	–	120–200	83–125	56 m^3/h	12–14 mL/min	0.06 mPa	Moisture content, water activity, bulk density, antioxidant activity, color total carotenoid, water solubility index	[37]
Guava	Concentrate	10.5°B	160	80	–	–	40 000 rpm	Moisture content, pH, titratable acidity, total sugars, vitamin C, total soluble solids	[38]
	Slurry	–	170–185	80–85	4 kg/m^2	18–20 rpm	–	Moisture content, solubility, dispersibility, vitamin C	[39]
Indian gooseberry	Juice	19%	120/160	80	–	1.2 mL/min	2.4×10^2 kPa	Moisture content, water activity, vitamin C, dissolution	[40]
Lime	Juice	9.5	140–170	–	–	1.75 g/min	5 bar	Powder recovery, bulk density, surface morphology color	[41]
Orange	Juice	56–57%	160	65	–	–	–	Color, moisture content, titratable acidity, water activity, particle size, bulk density, glass transition temperature	[42]
Pitaya	Juice	50%	145–175	–	–	400 L/h	4.5 bar	Moisture content, water activity, color, true density, bulk density, tap density, Carr Index, Hausner ratio, glass transition temperature, particle size, surface morphology, betacyanin content	[43]
Pomegranate	Juice	20–44°B	110–140	–	0.53 m^3/min	7 mL/min	–	Moisture content, hygroscopicity, anthocyanin content, color, solubility, bulk density, yield, total phenolic content, antioxidant activity	[44]

Continuation of Table 1

Powder	Initial sample	Total solids	Inlet temperature, °C	Outlet temperature, °C	Aspirator rate/air velocity	Feed rate	Atomization rate/compressor pressure	Analysis	References
Red beet	Concentrate	20%	150, 165, 180, 195, 210	87–115	56 m^3/h	390–560 g/h	–	Moisture content, hygroscopicity, drying ratio, drying rate, productivity, bulk density, color, Tg, betayanin content	[45]
Red pitaya peel	Puree	–	155–175	75–85	900 m^3/min	–	15 000 rpm	Color, hygroscopicity, moisture content, solubility, water activity, betacyanin retention	[46]
Satureja Montana L.	Extract	–	135–140	60–70	–	–	20 000–21 000 rpm	Yield, moisture content, bulk density, hygroscopicity, water solubility index, total phenolic content, total flavonoid, sensory evaluation	[47]
Sea buckthorn	Juice	–	148.79–191.21	65–9	2.1 kg/cm^3	30 rpm	50 Hg	Moisture content, dispersibility, vitamin C, overall color change	[48]

The table is based on the findings of this study

from shrinking during drying [69]. A higher inlet air temperature produced powder with larger particles and greater swelling [70]. A lower inlet air temperature resulted in shrunk and smaller particles.

The moisture content in the powder was reported to improve solubility: the solubility of spray-dried raisin extracts and tomato concentrates increased together with the moisture content [18, 24, 50, 51]. The solubility of spray-dried roselle and tomato powder decreased as the drying temperature fell [24, 71]. A larger spray-dryer affected the beetroot powder color changes, namely increased the *a** value and decreased the *b** value [72].

Quek *et al.* focused on the color of spray-dried watermelon powder [51]. When the inlet air temperature increased, the *b** value increased. However, the *a** values increased at 145–165°C and started to decrease at 175°C. The lightness of the powders decreased when the temperature grew higher. At a higher inlet air temperature, the color of the powders turned darker. Red color decreased when the inlet air temperature rose [51]. The stability of heat sensitive pigment depended on the inlet air temperature. The lycopene content in watermelon juice powder decreased at a higher inlet air temperature, which was in agreement with another publication on tomato pulp [50]. The reduction of lycopene content was likely due to thermal degradation and oxidation. On the other hand, Tonon *et al.* also reported that the inlet air temperature affected the anthocyanin content in acai juice powder [68]. A higher inlet air temperature also decreased the amount of pigments in powder [61].

Atomization rate and air flow rate. Tables 3 and 4 illustrate the effects of atomization rate and air flow rate, respectively. As for atomization rate, spray-drying uses different ranges of speed. Atomization rate had a positive effect on sirih powder yield [73]. Amla and

Table 2 Effects of inlet air temperature on physicochemical properties of spray-dried fruit powders

Powder	Inlet air temperature, °C	Yield/ recovery, %	Moisture content	Water activity	Hygroscopicity	Density	Porosity	Particle size	Caking	Solubility	Color	Pigment	Antioxidant activity	Vitamin C	References
Acai	138–202	+ve	–ve	–	+ve	–	–	+ve	–	–	–	–ve	–	–	[26]
Acerola pomace	170–200	–	–ve	–	–ve	–	–	–	–ve	+ve	–	–	–	–	[59]
Amla	100–200	–	–ve	–	–ve	–ve	–	–	–	NS	*L**+ve	–	–ve	–	[27]
Ber	170–210	–	–	–	+ve	–ve	–	–	–	–	–	–	–	–	[30]
Black mulberry	110–150	+ve	–ve	–	–	–ve	–	–	–	+ve	–	–	–	–	[32]
Blackberry	140–180	–	–ve	–	–ve	–	–	NS	–	–	*L**+ve	–ve	–	–	[33]
Cantaloupe	170–190	–	–ve	–	–	–	–	–	–	–	*L**–ve *a**+ve *b** NS	–	–	–	[35]
Gac	120–200	–	–ve	–ve	–	–ve	–	–	–	–	*L** NS TC NS	–ve	–ve	–	[37]
Guava	170–185	–	–ve	–	–	–	–	–	–	+ve	–	–	–	+ve	[39]
Jujube	140–160	–	NS	–	+ve	–	–	–	–	–	*L**–ve TC +ve	–	–	+ve	[60]
Lime	140–170	+ve	NS	–	+ve	–	–	–	–	–	–	–	–	–	[41]
Orange juice	110–170	–	–ve	–	NS	–	NS	–	–	–	–	–	–	–	[49]
Pitaya	145–175	–	–ve	–	–	–	–	–	–	–	LNS	NS	–	–	[43]
Pomegranate	110–150	NS	–ve	–	NS	+ve	–	–	–	+ve	TC +ve *a**–ve	–ve	+ve	–	[44]
Red pittaya peel	155–175	–	–ve	–ve	–ve	–	–	–	–	+ve	*L** +ve *a**–ve	–ve	–	–	[46]
Watermelon	145–175	–	–ve	NS	–	–ve	–	–ve	CI NS HR NS	+ve	*L**–ve *a** NS *b**+ve	–ve	–	–	[51]

+ve – positive effect; –ve – negative effect; NS – no significant effect; – – not reported

orange powder with greater moisture content resulted from an increase in atomization rate [27, 49]. However, Tee *et al.* stated that raising the atomization rate by 80–100% produced sirih powder with low moisture content and low hygroscopicity [73].

As for the air flow rate, Fazeli *et al.* and Goula and Adamopoulos applied air flow rate of 400–800 and 500–800 L/h, respectively, to produce black mulberry and tomato powders [32, 74]. Fazeli *et al.* reported that the powder yield increased with faster air flow rate, producing a powder of lower moisture content and higher solubility [32]. Greater air flow rates reduced the moisture content and increased the density [32, 74]. However, as the air flow rate increased, the solubility of black mulberry fell down while that of tomato increased [32, 74].

Feed solid content and flow rate. Table 5 summarizes the effects of feed flow rate on the physicochemical properties of spray-dried powdered fruits. Most of the initial sample used for spray-drying were in the form of juice [36, 51, 76]. Two types of value were reported for Brix sample solids. Moßhammer *et al.*, used pear cactus juice with 65% of total solids while Roustapour *et al.* reported lime juice with 12% total solids as spray-drying feed [75, 76]. The Brix value also depended on the fruit. For instance, bayberry juice spray-dried into powder had Brix of 7–17°, whereas for pomegranate juice it was 20–44° [65].

Different rates of spray-drying feed have also become subjects of scientific research. Elderberry juice was spray-dried into powder at the feed rate of 180 and 300 mL/h [36]. However, Ferrari *et al.* spray-dried blackberry pulp at the feed rate of 0.49 kg/h [33]. Bazaria and Kumar utilized feed flow rate of 400 mL/h to obtain high-quality spray-dried powdered beetroot [78]. Ribeiro *et al.* used different levels of intake temperature (110, 140, and 170°C), feed flow (0.36, 0.60, and 0.84 L/h), maltodextrin quantity (14–26%), and maltodextrin dextrose equivalent (DE) as independent variables (5, 10, and 15 DE) [79].

Table 3 Effects of atomization rate on physicochemical properties of spray-dried powders

Powder	Atomization rate	Yield/recovery, %	Moisture content	Hygroscopicity	Density	Particle size	Solubility	References
Amla	30–50	–	+ve	NS	NS	–	NS	[27]
Sirih	80–100%	+ve	–ve	–ve	–	–ve	–	[73]
Orange	10 000–25 000 rpm	–	+ve	–	NS	NS	–	[49]

+ve – positive effect; –ve – negative effect; NS – no significant effect; – – not reported

Table 4 Effects of air flow rate on physicochemical properties of spray-dried powders

Powder	Air flow rate	Yield/recovery, %	Moisture content	Density	Solubility	References
Black mulberry	400–800 L/h	+ve	–ve	+ve	–ve	[32]
Lime	47.1–57.8 m^3/h	+ve	NS	NS	–	[41]
Tomato	500–800 L/h	–	–ve	+ve	+ve	[74]

+ve – positive effect; –ve – negative effect; NS – no significant effect; – – not reported

Table 5 Effects of feed flow rate on physicochemical properties of spray-dried fruit powders

Powder	Feed flow rate	Yield/ recovery, %	Moisture content	Water activity	Hygro-scopicity	Density	Particle size	Solu-bility	Color	Pigment content/ retention	References
Acai	5–25 g/min	–ve	+ve		NS	–	–	–	–	–	[26]
Jujube	3–5 m^3/h	–	+ve		–ve	–	–	–	L^*–ve TC +ve	–	[60]
Orange	150–450	–	–ve		–	NS	NS	–	–	–	[49]
Water-melon and carrot	2–5 mL/min	–	+ve		–	–	–	+ve	–	–ve	[77]

+ve – positive effect; –ve – negative effect; NS – no significant effect; – – not reported

Tonon *et al.* observed that high feed flow rates resulted in a lower yield [26]. This correlation was related to the slow heat and mass transfer. Higher feed flow rates triggered wall deposit, which reduced the yield [80]. Feed flow rate also had an adverse effect on the powder moisture content [77]. High feed flow rate shortened the time of contact between the feed and the drying air, thus decreasing the effectiveness of the heat transfer. An increment in feed flow rate also affected the evaporating intensity, which lowered the inlet air temperature and increased the water content in the powder [81]. Chen *et al.* reported that higher feed flow rate resulted in low-hygroscopicity jujube powder [60]. In addition, higher feed flow rates increased the particle size [80]. Higher feed flow rates increased the solubility of fermented carrot-and -watermelon juice powder [82].

Type and concentration of carrier agents. Selecting the best drying aids is one of the most important steps in spray-drying of fruits and vegetables. Drying aids, or wall materials, or carriers, are mostly used to increase the glass transition temperature of the feed. They can improve the recovery by decreasing the stickiness which causes the product to stick together or to the drying chamber [16]. An ideal spray-drying carrier has a high solubility, bland taste, and good emulsifying and drying properties. Its limited solution viscosity is at 35–45% solids content; it is nonhygroscopic, nonreactive, and cheap [83]. Maltodextrin, alginate, Arabic gum, modified starch, inulin, and their combinations served as carriers for spray-drying of carotenoid-rich goldenberry (*Physalis peruviana* L.) juice, while cellobiose was used as control [84].

Table 6 demonstrates different carrier agents in fruit powder production, the most common carrier agents being maltodextrin and Arabic gum. Arabic gum had a high glass transition temperature and proved efficient in flavor retention [85]. Arabic gum is expensive because its supply from Middle East and Africa is as unpredictable as its quality. Maltodextrin is not only neutral in color and taste but also relatively cheap, which makes is the most common carriern commercial spray-drying [7, 16]. Maltodextrin consists of β-D-glucose units that are linked by glycosidic bonds (1→4), with dextrose equivalency (DE) that indicates its reducing capacity [86]. Lee *et al.* studied the use of additives as carriers in spray-drying, as well as the impact on such physicochemical parameters as hygroscopicity, flavor retention, and color indexing [87].

Table 6 Applications of different carrier agents in spray-drying of fruit powders

Powder	Initial sample	Carrier agent	Concentrations/ percentage	Analyses	References
Acai	Pulp	Matodextrin (DE 20) & Arabic gum	6%	Process yield, moisture content, hygroscopicity, anthocyanin retention, outlet temperature	[8]
Amla	Juice	Maltodextrin	3–9% (w/v) juice	Moisture content, hygroscopicity, bulk density, water solubility index, surface morphology, DPPH, total phenolic content	[38]
Bayberry	Juice	Maltodextrin (DE 12 & 19)	1:1 (fruit juice)	Moisture content, color	[64]
		Maltodextrin DE 10	10–50%	Product recovery, moisture content, water activity, glass transition temperature, surface composition	[29]
Black mulberry	Juice	Maltodextrin DE 6, 9, 20	8–16%	Yield, solubility, bulk density, moisture content	[32]
Blackberry	Pulp	Maltodextrin (DE 20)	5–25%	Moisture content, hygroscopicity, anthocyanin content, color, surface morphology, particle size	[33]
Blackcurrant	Extract	Maltodextrin (DE 11, 18, and 21)	Total °B 35	Total polyphenol and antioxidant activity	[31]
Blueberry	Extract	Maltodextrin (DE 18.5)	Total solids 30% (blueberry solids 20%)	Particle size, true density, water-binding capacity, anthocyanin content	[34]
Cantaloupe	Juice	Maltodextrin (DE 9–13)	10%	Moisture content, water activity, vitamin C, carotene content, dissolution, surface morphology	[35]
Elderberry	Juice	Acacia gum & maltodextrin (DE 4–7)	5:1–5:4; 1:1 (juice)	Total phenolic content, color	[36]
Gac	Fruit aril	Maltodextrin DE 12	10–30%	Moisture content, water activity, pH, color, water solubility index, bulk density, carotenoid, antioxidant	[37]
Gooseberry	Juice	Maltodextrin	19% TSS	Moisture content, water activity, vitamin C, dissolution time	[40]
Guava	Juice	Maltodextrin 500 RM1249	7–12%	Moisture content, solubility, dispersibility, vitamin C	[39]
Jucara	Pulp	Arabic gum, Maltodextrin, Gelatin	Arabic gum and Maltodextrin (5–55%), Gelatin (5–15%)	Anthocyanin content, moisture content, water activity, hygroscopicity, solubility, total color change, bulk density	[88]
Lime	Juice	Maltodextrin (DE 5)	10–30%	Moisture content	[76]
Mango	Juice	Maltodextrin, arabic gum, starch wax, crystalline cellulose		Surface morphology, stickiness, solubility, powder diffraction	[14]
Orange	Concentrate	Maltodextrin (DE 6-21)	–	Glass transition temperature, residue formation	[74]
	Juice	Maltodextrin and liquid glucose	–	Particle size, wettability time, insoluble solids, bulk density, moisture content	[49]
Pineapple	Juice	Maltodextrin (DE 10)	10–12.5%	Moisture content, color, bulk density, solubility	[7]
Pitaya	Juice	Maltodextrin	20 and 30%	Moisture content, water activity, color, true density, bulk density, tap density, Carr's Index, Hausner ratio, glass transition temperature, particle size, surface morphology, betacyanin content	[43]

Continuation of Table 6

Powder	Initial sample	Carrier agent	Concentrations/ percentage	Analyses	References
Pitaya	Juice	Maltodextrin DE 10	8–22% w/w	Color, hygroscopicity, moisture content, water activity, solubility, betacyanin content	[46]
Pomegranate	Juice	Maltodextrin, arabic gum, starch wax	8 and 12%	Yield, solubility, color, total anthocyanin, antioxidant	[17]
Seabuckthorn fruit	Juice	Maltodextrin DE 20	20–49 g in 100 mL	Moisture content, solubility, dispersibility, vitamin C, overall color difference	[48]
Strawberry	Juice	Maltodextrin	10–30%	Vitamin C loss, solubility, anti-caking, sensory	[89]
Watermelon	Juice	Maltodextrin (DE 9–12)	3 and 5%	Moisture content, water activity, dissolution, color, carotene content, sugar	[51]

Table 7 Effects of maltodextrin concentration on physicochemical properties of spray-dried powder

Powder	Maltodextrin concentrations, %	Yield/ recovery, %	Moisture content	Water activity	Hygroscopicity	Density	Particle size	Caking	Solubility	Color	Pigment content/ retention	Antioxidant activity	Vitamin C	References
Acai	10–30	–	NS	–	+ve	–	+ve	–	–	–	–	–	–	[26]
Amla	3–9	–	–ve	–	–ve	NS	–	–	NS	L^*+ve	–	–ve	–	[27]
Black mulberry	8–16	+ve	–ve	–	–	–ve	–	–	+ve	TC–	–	–	–	[32]
Blackberry	5–25	–	–ve	–	–ve	–	–	–			–ve	–	–	[33]
Guava	5.95–13.03	–	+ve	–ve	–	–	–	–	+ve	–	–	–	–ve	[39]
Pineapple		–	–	–	–	–ve BD	–	–	–ve	NS	–	–	–	[7]
Pitaya	20 30	–	–ve	NS		+ve	–	NS		L^*+ve	–ve	–	–	[43]
Pomegranate	44.1–59.1	+ve	–ve	–	–ve	+ve BD	–	–	+ve	TC+ve a^*_{RP} –ve	+ve	–	–	[44]
Red pittaya	8–22	–	+ve	+ve	+ve	–	–	–	+ve	L^*–ve a^*–ve	–ve	–	–	[46]

BD – bulk density; TC – total color changes, +ve – positive effect; –ve – negative effect; NS – no significant effect; – – not reported

Maltodextrin has been used to spray-dry sticky products, e.g. orange, tamarind, blackcurrant, raspberry, and apricot juice, honey, mango pulp, raisin juice, lime juice, watermelon pulp, and sweet potato puree because it facilitates the drying process [25]. The percentage of carrier agents incorporated ranges from 3% for watermelon juice powder to 40–64% for pomegranate juice powder [44, 51]. The concentration of maltodextrin was 15, 20, and 25%, respectively, in the production of spray-dried cempedak, papaya, and terung asam powder [90–92]. However, Henao-Ardila *et al.* reported 22.62% maltodextrin concentration as optimal for spray-drying of feijoa pulp, while Dantas *et al.* used 23% of malto-dextrin to produce powdered avocado drink [93, 94]. The flowability, color, antioxidant activity, and phenol content of barberry powder were optimal at 13% (w/w) of maltodextrin [95].

Table 7 shows the effects of maltodextrin concentration on the physicochemical properties of spray-dried powder. Maltodextrin reduced the moisture content, which might be explained by the increment in feed solids and the low amount of free water [38, 50, 51, 96]. With the use of it, the yield was 18–35% but there was more deposit on chamber wall [49]. Maltodextrin increased the yield up to 18–35% but the deposit on the chamber wall reached 65–82% [49]. Yet the concentration of maltodextrin is important in controlling the quality of the powder. For instance, a higher amount of maltodextrin dextrose equivalent made it possible to obtain low-hygroscopicity liquorice [97]. Leyva-Porras *et al.* investigated the effect of spray-drying

Table 8 Applications of Response Surface Methodology (RSM) in spray-drying of fruits

Powder	Starting material	Independent variables	Response variables	Optimization	Design	Software	References
Acai	Juice	Inlet air temperature, feed flow rate, maltodextrin concentration	Process yield, moisture content, hygroscopicity, anthocyanin retention, outlet temperature	RSM	Rotatable central composite design	Statistica 5.5	[26]
Acerola	Juice	Inlet air temperature, Drying aid/acerola, percent replace of maltodextrin by crystalline cellulose	Moisture content, hygroscopicity, water solublity, flowability	RSM	Central composite design (CCD)	Minitab 15	[59]
Black-berry	Pulp	inlet air temperature, maltodextrin concentration	Moisture content, anthocyanin retention, hygroscopicity, particle size, color parameters	RSM	Central composite rotatable design	Statistica 8.0	[33]
Cashew apple	Juice	Drying aid/juice, percent replace of maltodextrin by crystalline cellulose	Ascorbic acid retention, hygroscopicity, flowability, water solubility	RSM	RSM with 11 runs	Minitab 15	[85]
Guava	Slurry	Inlet air temperature, maltodextrin concentration	solubility, moisture content, dispersibility, vitamin C	RSM	CCRD	–	[39]
Jujube	Juice	Inlet air temperature, maltodextrin concentration, feed flow rate	Moisture content, vitamin C, color, hygroscopicity	RSM	Box Behnken	–	[60]
Orange	Juice	Inlet air temperature, atomization rate, flow rate	Particle size, wettability time, insoluble solids, bulk density, moisture content	Full factorial design	Complete random design	–	[49]
Pine-apple	Juice	Atomization rate, maltodextrin concentration	Apparent and true density, color, moisture content, solubility	Complete factorial design	3 repetition at center point	–	[7]
Pome-granate	Juice	Inlet air temperature, maltodextrin concentration, feed/mix concentration	Moisture content, hygroscopicity, anthocyanin content, color, solubility, bulk density, yield, total phenolic content, antioxidant activity	RSM	CCD	Design expert 6.0	[44]
Red pitaya peel	Puree	Inlet air temperature, outlet temperature, maltodextrin concentration	Color, hygroscopicity, moisture content, water activity, solubility, betacyanin content	RSM	CCD	–	[46]

settings on the microencapsulation of bioactive components and the physicochemical qualities of strawberry juice with maltodextrin as a transporting agent [98].

Reduction in maltodextrin generally improved the solubility [7]. Similar observation was reported by Moreirra *et al.*, who used a drying assistance ratio of cashew apple juice dry weight (5:1) and cashew tree gum substituting maltodextrin in 50% of spray-drying of cashew apple juice generated with high solubility (> 90%) [59]. The solubility of spray-dried mango powder decreased as the cellulose concentration grew. At 9% of cellulose, the solubility values of mango powder were 72, 71, and 31% using maltodextrin, arabic gum, and waxy starch, respectively [14]. Quek *et al.* studied watermelon powder production and discovered that adding maltodextrin in greater quantities than 10% led to color loss [51]. These results confirmed those obtained by Farimin and Nordin, who studied roselle-and-pineapple powder [96]. Papadakis *et al.* reported that the exact color of each powder depended on the ratio of raisin juice solids:maltodextrin solids [18].

Optimization of spray-drying process. Response surface methodology is applied to determine the optimum condition of spray-drying because this procedure is comprehensive, simple, and highly efficient [82, 99]. The central composite design builds a quadratic model for the response variable without a complete three level factorial experiment. Only by optimizing the spray-drying process, food producers can obtain better powder properties and yield [26].

Table 8 summarizes the use of response surface methodology as optimization for spray-drying of fruit powder. The main independent variables are

inlet air temperature, maltodextrin concentration, and feed or flow rate [20, 26, 100]. Moisture content and water solubility are the most important properties of food powder [19]. However, yield and hygroscopicity proved to be the common response variables [26, 59]. Consequently, optimization of the amount of carrier is an important step in making a commercial product [16]. Li *et al.* applied the Box-Behken method to obtain the optimal condition of 142.8°C, 23.7% core material, and 11.7% feed solid in spray-drying of plum [101]. Pandey *et al.* reported the inlet temperature of 166.64°C and 9.26% maltodextrin concentration as optimal conditions for fruit slurry spray-drying process [102].

CONCLUSION

This review covered the basic principles of spray-drying while determining the effects of each spray-drying parameter on powder properties. These parameters included inlet air temperature, atomization rate, air flow rate, and feed flow rate. The article also summarized the effects of different carrier agents on the powder. Inlet temperature of spray-dryer and carrier concentration were found to increase the product yield and solubility, as well as to decrease the moisture content, pigment, and antioxidant content.

However, inlet temperature proved to be the main factor that affected the powder density. On the other hand, atomization rate had little effect on powder properties. Certain powder properties depended on the type of fruit and the range of parameters applied. The review showed that the impact of additives and encapsulation on the physicochemical parameters of fruit extract powder is critical. Changing the spray-dryer settings can solve the technical obstacles in spray-drying of fruit extracts. In addition, spray drying is a newer and cheaper method of turning fruit extracts into powder.

CONTRIBUTION

Liew Phing Pui gathered data, donated data and analysis tools, conducted the study, wrote the manuscript, and submitted it. Abdul Kalam Saleena Lejaniya was in charge of data collection and data contribution, formatted the manuscript and proofread the article.

CONFLICT OF INTEREST

The authors note that they have no known conflicting financial or personal interests that might have impacted the findings of this study.

REFERENCES

1. Fellows P. Dehydration. In: Fellows P, editor. Food Processing Technology: Principles and Practice. 2nd ed. Cambridge: Woodhead Publishing Limited, 2000. pp. 311–340.
2. Doymaz I, Kocayigit F. Drying and rehydration behaviours of convection drying of green peas. Drying Technology. 2011;29(11):1273–1282. https://doi.org/10.1080/07373937.2011.591713
3. Souza M, Mesquita A, Souza P, Borges G, Silva T, Converti A, *et al.* New functional non-dairy mixed tropical fruit juice microencapsulated by spray drying: Physicochemical characterization, bioaccessibility, genetic identification and stability. LWT. 2021;152. https://doi.org/10.1016/j.lwt.2021.112271
4. Muzaffar K, Nayik GA, Kumar P. Production of fruit juice powders by spray drying technology. International Journal of Advance Research in Science and Engineering. 2018;7(3):59–67.
5. Wang W, Zhou W. Characterization of spray-dried soy sauce powders using maltodextrin as carrier. Journal of Food Engineering. 2012;109(3):399–405. https://doi.org/10.1016/j.jfoodeng.2011.11.012
6. Perez NE, Schmalko ME. Convective drying of pumpkin: Influence of pretreatment and drying temperature. Journal of Food Process Engineering. 2009;32(1):88–103. https://doi.org/10.1111/j.1745-4530.2007.00200.x
7. Abadio FDB, Domingues AM, Borges SV, Oliveira VM. Physical properties of powdered pineapple (*Ananas comosus*) juice – Effect of malt dextrin concentration and atomization speed. Journal of Food Engineering. 2004;64(3):285–287. https://doi.org/10.1016/j.jfoodeng.2003.10.010
8. Tonon RV, Brabet C, Pallet D, Brat P, Hubinger MD. Physicochemical and morphological characterisation of açai (*Euterpe oleraceae* Mart.) powder produced with different carrier agents. International Journal of Food Science and Technology. 2009;44(10):1950–1958. https://doi.org/10.1111/j.1365-2621.2009.02012.x
9. Chew S-C, Tan C-H, Pui L-P, Chong P-N, Gunasekaran B, Lin NK. Encapsulation technologies: A tool for functional foods development. International Journal of Innovative Technology and Exploring Engineering. 2019;8(5S):154–160.
10. Masters K. Spray drying handbook. Harlow: Longman Scientific and Technical; 1991. 725 p.
11. Pui LP, Karim R, Yusof YA, Wong CW, Ghazali HM. Optimization of spray-drying parameters for the production of "Cempedak" (*Artocarpus integer*) fruit powder. Journal of Food Measurement and Characterization. 2020;14(6):3238–3249. https://doi.org/10.1007/s11694-020-00565-3

12. Gopinathan M, Yusof YA, Pui LP. Effects of different drying methods on the physicochemical and antioxidant content of "cempedak" (*Artocarpus integer* L.) powder. Journal of Food Processing and Preservation. 2020;44(12). https://doi.org/10.1111/jfpp.14966
13. Loo YY, Pui LP. Storage stability of kuini powder in two packaging aluminum laminated polyethylene and polyethylene terephthalate. Malaysian Journal of Analytical Sciences. 2020;24(5):657–669.
14. Cano-Chauca M, Stringheta PC, Ramos AM, Cal-Vidal J. Effect of the carriers on the microstructure of mango powder obtained by spray drying and its functional characterization. Innovative Food Science and Emerging Technologies. 2005;6(4):420–428. https://doi.org/10.1016/j.ifset.2005.05.003
15. Sobulska M, Zbicinski I. Advances in spray drying of sugar-rich products. Drying Technology. 2021;39(12):1774–1799. https://doi.org/10.1080/07373937.2020.1832513
16. Bhandari BR, Dutta N, Howes T. Problems associated with spray drying of sugar-rich food. Drying Technology. 1997;15(2):671–684. https://doi.org/10.1080/07373939708917253
17. Youssefi S, Ehmam-Djomeh Z, Mousavi MS. Comparison of Artificial Neural Network (ANN) and Response Surface Methodology (RSM) in the prediction of quality parameters of spray-dried pomegranate juice. Drying Technology. 2009;27(7):910–917. https://doi.org/10.1080/07373930902988247
18. Papadakis SE, Gardeli C, Tzia C. Raisin extract powder: Production, physical and sensory properties. Proceedings of the 11th international drying symposium IDS'98; 1998; Halkidiki. Halkidiki: Ziti Editions; 1998. p. 1207–1213.
19. Bhandari BR, Snoussi A, Dumoulin ED, Lebert A. Spray drying of concentrated fruit juices. Drying Technology. 1993;11(5):1081–1092. https://doi.org/10.1080/07373939308916884
20. Grabowski JA, Truong V-D, Daubert CR. Spray-drying of amylase hydrolyzed sweetpotato puree and physicochemical properties of powder. Journal of Food Science. 2006;71(5):E209–E217. https://doi.org/10.1111/j.1750-3841.2006.00036.x
21. Sasikumar R, Das M, Deka SC. Process optimization for the production of blood fruit powder by spray drying technique and its quality evaluation. Journal of Food Science and Technology. 2020;57(6):2269–2282. https://doi.org/10.1007/s13197-020-04264-1
22. Parihari A. Performance study of spray dryer using various salt solutions. Masters thesis. Rourkela: National Institute of Technology; 2009. 132 p.
23. Patel RP, Patel MP, Suthar AM. Spray drying tech nology: An overview. Indian Journal of Science Technology. 2009;2(10):44–47.
24. Goula AM, Adamopoulos KG. Spray drying of tomato pulp: Effect of feed concentration. Drying Technology. 2004;22(10):2309–2330. https://doi.org/10.1081/DRT-200040007
25. Goula AM, Adamopoulos KG. Effect of maltodextrin addition during spray drying of tomato pulp in dehumidified air: I. Drying kinetics and product recovery. Drying Technology. 2008;26(1):714–725. https://doi.org/10.1080/07373930802046369
26. Tonon RV, Brabet C, Hubinger MD. Influence of process conditions on the physicochemical properties of acai (*Euterpe oleraceae* Mart.) powder produced by spray drying. Journal of Food Engineering. 2008;88(3):411–418. https://doi.org/10.1016/j.jfoodeng.2008.02.029
27. Mishra P, Mishra S, Mahanta CL. Effect of maltodextrin concentration and inlet temperature during spray drying on physicochemical and antioxidant properties of amla (*Emblica officinalis*) juice powder. Food Bioproducts and Processing. 2014;92(3):252–258. https://doi.org/10.1016/j.fbp.2013.08.003
28. Villacrez JL, Carriazo JG, Osorio C. Microencapsulation of Andes berry (*Rubus glaucus* Benth.) aqueous extract by spray drying. Food and Bioprocess Technology. 2014;7(5):1445–1456. https://doi.org/10.1007/s11947-013-1172-y
29. Fang Z, Bhandari B. Effect of spray drying and storage on the stability of bayberry polyphenols. Food Chemistry. 2011;129(3):1139–1147. https://doi.org/10.1016/j.foodchem.2011.05.093
30. Singh A, Kumar S, Sharma HK. Effect of enzymatic hydrolysis on the juice yield from bael fruit (*Aegle marmelos* Correa) pulp. American Journal of Food Technology. 2012;7(2):62–72. https://doi.org/10.3923/ajft.2012.62.72
31. Bakowska-Barczak AM, Kolodziejczyk PP. Black currant polyphenols: Their storage stability and microencapsulation. Industrial Crops and Products. 2011;34(2):1301–1309. https://doi.org/10.1016/j.indcrop.2010.10.002
32. Fazeli M, Emam-Djomeh Z, Kalbasi Ashtari A, Omid M. Effect of spray drying conditions and feed composition on the physical properties of black mulberry juice powder. Food and Bioproducts Processing. 2012;90(4):667–675. https://doi.org/10.1016/j.fbp.2012.04.006
33. Ferrari CC, Germer SPM, de Aguirre JM. Effects of spray-drying conditions on the physicochemical properties of blackberry powder. Drying Technology. 2012;30(2):154–163. https://doi.org/10.1080/07373937.2011.628429

34. Berg S, Bretz M, Hubbermann EM, Schwarz K. Influence of different pectins on powder characteristics of microencapsulated anthocyanins and their impact on drug retention of shellac coated granulate. Journal of Food Engineering. 2012;108(1):158–165. https://doi.org/10.1016/j.jfoodeng.2011.06.035

35. Solval KM, Sundarajan S, Alfaro L, Sathivel S. Development of cantaloupe (*Cucumis melo*) juice powders using spray drying technology. LWT – Food Science and Technology. 2012;46(1):287–293. https://doi.org/10.1016/j.lwt.2011.09.017

36. Murugesan R, Orsat V. Spray drying of elderberry (*Sambucus nigra* L.) juice to maintain its phenolic content. Drying Technology. 2011;29(14):1729–1740. https://doi.org/10.1080/07373937.2011.602485

37. Kha TC, Nguyen MH, Roach PD. Effects of spray drying conditions on the physicochemical and antioxidant properties of the Gac (*Momordica cochinchinensis*) fruit aril powder. Journal of Food Engineering. 2010;98(3):385–392. https://doi.org/10.1016/j.jfoodeng.2010.01.016

38. Mahendran T. Physico-chemical properties and sensory characteristics of dehydrated guava concentrate: Effect of drying method and maltodextrin concentration. Tropical Agricultural Research and Extension. 2010;13(2):49–54. https://doi.org/10.4038/tare.v13i2.3138

39. Patil V, Chauhan AK, Singh RP. Optimization of the spray-drying process for developing guava powder using response surface methodology. Powder Technology. 2014;253:230–236. https://doi.org/10.1016/j.powtec.2013.11.033

40. Thankitsunthorn C, Laohaprasit N, Srzednicki G. Effects of drying temperature on quality of dried Indian gooseberry powder. International Food Research Journal. 2009;16(3):335–361.

41. Zareifard MR, Niakousari M, Shokrollahi Z, Javadian S. A feasibility study on the drying of lime juice: The relationship between the key operating parameters of a small laboratory spray dryer and product quality. Food and Bioprocess Technology. 2012;5(5):1896–1906. https://doi.org/10.1007/s11947-011-0689-1

42. Shrestha AK, Ua-Arak T, Adhikari BP, Howes T, Bhandari BR. Glass transition behavior of spray dried orange juice powder measured by differential scanning calorimetry (DSC) and thermal mechanical compression test (TMCT). International Journal of Food Properties. 2007;10(3):661–673. https://doi.org/10.1080/10942910601109218

43. Tze NL, Han CP, Yusof YA, Ling CN, Talib RA, Taip FS, *et al.* Physicochemical and nutritional properties of spray-dried pitaya fruit powder as natural colorant. Food Science and Biotechnology. 2012;21(3):675–682. https://doi.org/10.1007/s10068-012-0088-z

44. Horuz E, Altan A, Maskan M. Spray drying and process optimization of unclarified pomegranate (*Punica granatum*) juice. Drying Technology. 2012;30(7):787–798. https://doi.org/10.1080/07373937.2012.663434

45. Cai YZ, Corke H. Production and properties of spray-dried Amaranthus betacyanin pigments. Journal of Food Science. 2000;65(7):1248–1252. https://doi.org/10.1111/j.1365-2621.2000.tb10273.x

46. Bakar J, Ee SC, Muhammad K, Hashim DM, Adzahan N. Spray-drying optimization for red pitaya peel (*Hylocereus polyrhizus*). Food and Bioprocess Technology. 2013;6(5):1332–1342. https://doi.org/10.1007/s11947-012-0842-5

47. Vidović SS, Vladić JZ, Vaštag ZG, Zeković ZP, Popović LM. Maltodextrin as a carrier of health benefit compounds in *Satureja montana* dry powder obtained by spray drying technique. Powder Technology. 2014;258:209–215. https://doi.org/10.1016/j.powtec.2014.03.038

48. Selvamuthukumaran M, Khanum F. Optimization of spray drying process for developing seabuckthorn fruit juice powder using response surface methodology. Journal of Food Science and Technology. 2014;51(12):3731–3739. https://doi.org/10.1007/s13197-012-0901-y

49. Chengini GR, Ghabadian B. Effect of spray-drying conditions on physical properties of orange juice powder. Drying Technology. 2005;23(3):657–668. https://doi.org/10.1081/DRT-200054161

50. Goula AM, Adamopoulos KG. Spray drying of tomato pulp- in dehumidified air: II. The effect on powder properties. Journal of Food Engineering. 2005;66(1):35–42. https://doi.org/10.1016/j.jfoodeng.2004.02.031

51. Quek SY, Chok NK, Swedlund P. The physicochemical properties of spray-dried watermelon powders. Chemical Engineering and Processing: Process Intensification. 2007;46(5):386–392. https://doi.org/10.1016/j.cep.2006.06.020

52. Mani S, Jaya S, Das H. Sticky issues on spray drying of fruit juices [Internet]. [cited 2021 Nov 20]. Available from: https://www.engr.usask.ca/societies/asae-csae/papers/asaepapermbsk02-201.pdf

53. Adhikari B, Howes T, Bhandari BR, Troung V. Effect of addition of maltodextrin on drying kinetics and stickiness of sugar and acid-rich foods during convective drying: experiments and modelling. Journal of Food Engineering. 2004;62(1):53–68. https://doi.org/10.1016/S0260-8774(03)00171-7

54. Rodríguez-Hernández GR, González-García R, Grajales-Lagunes A, Ruiz-Cabrera MA, Abud-Archila M. Spray-drying of cactus pear juice (*Opuntia streptacantha*): Effect on the physicochemical properties of powder and reconstituted product. Drying Technology. 2005;23(4):955–973. https://doi.org/10.1080/DRT-200054251

55. Fitzpatrick JJ, Hodnett M, Twomey M, Cerqueira PSM, O'Flynn J, Roos YH. Glass transition and the flowability and caking of powders containing amorphous lactose. Powder Technology. 2007;178(2):119–128. https://doi.org/10.1016/j.powtec.2007.04.017

56. Phoungchandang S, Sertwasana A. Spray-drying of ginger juice and physicochemical properties of ginger powders. ScienceAsia. 2010;36(1):40–45.

57. Chen XD, Patel KC. Manufacturing better quality food powders from spray drying and subsequent treatments. Drying Technology. 2008;26(11):1313–1318. https://doi.org/10.1080/07373930802330904

58. Jittanit W, Niti-Att D, Techanuntachaikul O. Study of spray drying of pineapple juice using maltodextrin as an adjunct. Chiang Mai Journal of Science. 2010;37(3):498–506.

59. Moreira GEG, Maia Costa MG, de Souza ACR, de Brito ES, de Medeiros MFD, de Azeredo HMC. Physical properties of spray dried acerola extract as affected by temperature and drying aids. LWT – Food Science and Technology. 2009;42(2):641–645. https://doi.org/10.1016/j.lwt.2008.07.008

60. Chen Q, Bi J, Zhou Y, Liu X, Wu X, Chen R. Multi-objective optimization of spray drying of jujube (*Zizyphus jujuba* Miller) powder using response surface methodology. Food and Bioprocess Technology. 2014;7(6):1807–1818. https://doi.org/10.1007/s11947-013-1171-z

61. Phisut N. Spray drying technique of fruit juice powder: Some factors influencing the properties of product. International Food Research Journal. 2012;19(4):1297–1306.

62. Pui LP, Karim R, Yusof YA, Wong CW, Ghazali HM. Effects of inlet temperature and carrier concentration on spray-dried "cempedak" (*Artocarpus integer*) fruit powder and its reconstitution properties. Acta Scientiarum Polonorum, Technologia Alimentaria. 2021;20(2):135–148. https://doi.org/10.17306/J.AFS.0801

63. Obón JM, Castellar MR, Alacid M, Fernandez-Lopez JA. Production of a red–purple food colorant from *Opuntia stricta* fruits by spray drying and its application in food model systems. Journal of Food Engineering. 2009;90(4):471–479. https://doi.org/10.1016/j.jfoodeng.2008.07.013

64. Gong Z, Zhang M, Mujumdar A, Sun J. Spray drying and agglomeration of instant bayberry powder. Drying Technology 2008;26(1):116–121. https://doi.org/10.1080/07373930701781751

65. Aragüez-Fortes Y, Robaina-Morales LM, Pino JA. Optimization of the spray-drying parameters for developing guava powder. Journal of Food Process Engineering. 2019;42(6). https://doi.org/10.1111/jfpe.13230

66. Wong CW, Pui LP, Ng JML. Production of spray-dried Sarawak pineapple (Ananas comosus) powder from enzyme liquefied puree. International Food Research Journal. 2015;22(4):1631–1636.

67. Saha A, Jindal N. Process optimization for the preparation of bael (Aegle marmelos correa) fruit powder by spray drying. International Journal of Food Science and Nutrition. 2018;3(4):44–51.

68. Tonon RV, Freitas SS, Hubinger MD. Spray drying of açai (*Euterpe oleraceae* Mart.) juice: Effect of inlet air temperature and type of carrier agent. Journal of Food Processing and Preservation. 2011;35(5):691–700. https://doi.org/10.1111/j.1745-4549.2011.00518.x

69. Reineccius GA. The spray drying of food flavors. Drying Technology. 2004;22(6):1289–1324. https://doi.org/10.1081/DRT-120038731

70. Nijdam JJ, Langrish TAG. The effect of surface composition on the functional properties of milk powders. Journal of Food Engineering. 2006;77(4):919–925. https://doi.org/10.1016/j.jfoodeng.2005.08.020

71. Al-Kahtani HA, Hassan BH. Spray drying of roselle (*Hibiscus sabdarifa* L.) extract. Journal of Food Science. 1990;55(4):1073–1076. https://doi.org/10.1111/j.1365-2621.1990.tb01601.x

72. Gawałek, J. Effect of spray dryer scale size on the properties of dried beetroot juice. Molecules. 2021;26(1). https://doi.org/10.3390/molecules26216700

73. Tee LH, Luqman Chuah A, Pin KY, Abdull Rashih A, Yusof YA. Optimization of spray drying process parameters of Piper betle L. (Sirih) leaves extract coated with maltodextrin. Journal of Chemical and Pharmaceutical Research. 2012;4(3):1833–1841.

74. Goula AM, Adamopoulos KG. A new technique for spray drying orange juice concentrate. Innovative Food Science and Emerging Technologies. 2010;11(2):342–351. https://doi.org/10.1016/j.ifset.2009.12.001

75. Moβhammer MR, Stintzing FC, Carle R. Evaluation of different methods for the production of juice concentrates and fruit powders from cactus pear. Innovative Food Science and Emerging Technologies. 2006;7(4):275–287. https://doi.org/10.1016/j.ifset.2006.04.003

76. Roustapour OR, Hosseinalipour M, Ghobadian B. An experimental investigation of lime juice drying in a pilot plant spray dryer. Drying Technology. 2006;24(2):181–188. https://doi.org/10.1080/07373930600559035

77. Mestry AP, Mujumdar AS, Thorat BN. Optimization of spray drying of an innovative functional food: Fermented mixed juice of carrot and watermelon. Drying Technology. 2011;29(10):1121–1131. https://doi.org/10.1080/07373937.2011.566968

78. Bazaria B, Kumar P. Optimization of spray drying parameters for beetroot juice powder using response surface methodology (RSM). Journal of the Saudi Society of Agricultural Sciences. 2018;17(4):408–415. https://doi.org/10.1016/j.jssas.2016.09.007

79. Ribeiro CMCM, Magliano LCSA, de Costa MMA, Bezerra TKA, da Silva FLH, Maciel MIS. Optimization of the spray drying process conditions for acerola and seriguela juice mix. Food Science and Technology. 2019;39:48–55. https://doi.org/10.1590/fst.36217

80. Chegini GR, Ghobadian B. Spray dryer parameters for fruit juice drying. World Journal of Agricultural Research. 2007;3(2):230–236.

81. Janiszewska E, Witrowa-Rajchert D. Effect of spray drying parameters on rosemary aroma microencapsulation. Polish Journal of Food and Nutrition Science. 2007;57(3):41–43.

82. Myers RH, Montgomery DC, Anderson-Cook CM. Response surface methodology: Process and product optimization using designed experiments, 3rd edition. New York: Wiley; 2009. 704 p.

83. Murua-Pagola B, Beristain-Guevara CI, Martinez-Bustos F. Preparation of starch derivatives using reactive extrusion and evaluation of modified starches as shell materials for encapsulation of flavoring agents by spray drying. Journal of Food Engineering. 2009;91(3):380–386. https://doi.org/10.1016/j.jfoodeng.2008.09.035

84. Etzbach L, Meinert M, Faber T, Klein C, Schieber A, Weber F. Effects of carrier agents on powder properties, stability of carotenoids, and encapsulation efficiency of goldenberry (*Physalis peruviana* L.) powder produced by co-current spray drying. Current Research in Food Science. 2020;3;73–81. https://doi.org/10.1016/j.crfs.2020.03.002

85. de Oliveira MA, Maia GA, de Figueirado RW, de Souza ACR, de Brito ES, de Azeredo HMC. Addition of cashew tree gum to maltodextrin-based carriers for spray drying of cashew apple juice. International Journal of Food Science and Technology. 2009;44(3):641–645. https://doi.org/10.1111/j.1365-2621.2008.01888.x

86. BeMiller JN, Whistler RL. Carbohydrates. In: Fennema OR, editor. Food chemistry. New York: Marcel Dekker; 1996. pp. 157–223.

87. Lee JKM, Taip FS, Abdullah HZ. Effectiveness of additives in spray drying performance: a review. Food Research. 2018;2(6):486–499. https://doi.org/10.26656/fr.2017.2(6).134

88. Bicudo MOP, Jó J, de Oliveira GA, Chaimsohn FP, Sierakowski MR, de Freitas RA, *et al.* Microencapsulation of Juçara (Euterpe edulis M.) pulp by spray-drying using different carriers and drying temperatures. Drying Technology. 2015;33(2):153–161. https://doi.org/10.1080/07373937.2014.937872

89. Krishnan JR. Development of spray dried strawberry juice powder. Pahang: University Malaysia Pahang; 2008.

90. Pui LP, Karim R, Yusof YA, Wong CW, Ghazali HM. Anti-caking agent effects on the properties of spray-dried "cempedak" fruit powder. Pertanika Journal of Tropical Agricultural Science. 2020;43(4):621–635. https://doi.org/10.47836/pjtas.43.4.15

91. Chang LS, Tan YL, Pui LP. Production of spray-dried enzyme-liquefied papaya (*Carica papaya* L.) powder. Brazilian Journal of Food Technology. 2020;23. https://doi.org/10.1590/1981-6723.18119

92. Chang LS, Eau Yong SM, Pui LP. Production of spray-dried "Terung Asam" (*Solanum lasiocarpum* Dunal) powder. Walailak Journal of Science and Technology. 2020;18(1). https://doi.org/10.48048/wjst.2021.6922

93. Henao-Ardila A, Quintanilla-Carvajal MX, Moreno FL. Combination of freeze concentration and spray drying for the production of feijoa (*Acca sellowiana* b.) pulp powder. Powder Technology. 2019;344:190–198. https://doi.org/10.1016/j.powtec.2018.12.015

94. Dantas D, Pasquali MA, Cavalcanti-Mata M, Duarte ME, Lisboa HM. Influence of spray drying conditions on the properties of avocado powder drink. Food Chemistry. 2018;266:284–291. https://doi.org/10.1016/j.foodchem.2018.06.016

95. Naji-Tabasi S, Emadzadeh B, Shahidi-Noghabi M, Abbaspour M, Akbari E. Physico-chemical and antioxidant properties of barberry juice powder and its effervescent tablets. Chemical and Biological Technologies in Agriculture. 2021;8(1). https://doi.org/10.1186/s40538-021-00220-z

96. Farimin AOA, Nordin E. Physical properties of powdered roselle-pineapple juice – effects of maltodextrin. Thesis of the National Conference on Postgraduate Research (NCON-PGR); 2009; Pahang. Pahang: University Malaysia Pahang; 2009. pp. 90–97.

97. Karaaslan İ, Dalgıç AC. Spray drying of liquorice (Glycyrrhiza glabra) extract. Journal of Food Science and Technology. 2014;51(11):3014–3025. https://doi.org/10.1007/s13197-012-0847-0

98. Leyva-Porras C, Saavedra-Leos MZ, López-Martinez LA, Espinosa-Solis V, Terán-Figueroa Y, Toxqui-Terán A, *et al.* Strawberry juice powders: Effect of spray-drying conditions on the microencapsulation of bioactive components and physicochemical properties. Molecules. 2021;26(18). https://doi.org/10.3390/molecules26185466

99. Pua CK, Hamid NSA, Rusul G, Rahman RA. Production of drum-dried jackfruit (*Artocarpus heterophyllus*) powder with different concentration of soy lecithin and gum Arabic. Journal of Food Engineering. 2007;78(2):630–636. https://doi.org/10.1016/j.jfoodeng.2005.10.041

100. Andrade I, Flores H. Optimization of spray drying of roselle extract (Hibiscus sabdariffa L.). Proceedings of the 14th International Drying Symposium; 2004; São Paulo. São Paulo; 2004. pp. 597–604.

101. Li Y, Tang B, Chen J, Lai P. Microencapsulation of plum (*Prunus salicina* Lindl.) phenolics by spray Drying Technology and storage stability. Food Science and Technology. 2018;38(3):530–536. https://doi.org/10.1590/1678-457x.09817

102. Pandey S, Poonia A, Rai S. Optimization of spray drying conditions for the production of quality ber (*Zizyphus mauritiana* Lamk.) fruit powder. Nutrition and Food Science. 2019;49(6):1088–1098. https://doi.org/10.1108/NFS-12-2018-0339

ORCID IDs
Liew Phing Pui https://orcid.org/0000-0001-5305-4334
Abdul Kalam Saleena Lejaniya https://orcid.org/0000-0001-7852-8073

Foods and Raw Materials. 2022;10(2)

ISSN 2310-9599 (Online)
ISSN 2308-4057 (Print)

Review Article
Open Access

Available online at http://jfrm.ru/en
https://doi.org/10.21603/2308-4057-2022-2-534
https://elibrary.ru/SBBKFV

Effect of gelatin drying methods on its amphiphilicity

Roman A. Voroshilin[1,*], Marina G. Kurbanova[1], Elena V. Ostapova[1], Eduard M. Makhambetov[1], Andrey N. Petrov[2,3], Mohammed El Amine Khelef [3]

[1] Kemerovo State University, Kemerovo, Russia
[2] All-Russian Scientific Dairy Research Institute, Moscow, Russia
[3] Moscow State University of Food Production, Moscow, Russia

* e-mail: rom.vr.22@mail.ru

Received 17.05.2022; Revised 06.06.2022; Accepted 05.07.2022; Published online 23.09.2022

Abstract:
Gelatin is a natural amphiphilic biopolymer that is widely used in food products, pharmaceuticals, and cosmetics. We studied the effect of spray and freeze drying on the solubility and amphiphilicity of gelatin samples.
The control sample was a commercially produced edible gelatin. The experimental samples were spray- and freeze-dried gelatins obtained by enzymatic-acid hydrolysis of cattle bone. Amino acid sequences were determined by matrix-activated laser desorption/ionization. Solubility was assessed visually. Bloom strength of the gelatin gels was measured by a texture analyzer. The ProtScale online service was used to predict the amphiphilic topology of gelatin proteins. Molecular weight distribution of proteins was carried out by electrophoresis in polyacrylamide gel in the presence of sodium dodecyl sulfate.
Spray drying reduced protein degradation and retained more α-chains, while freeze drying increased gelatin's hydrophobicity and decreased its solubility. The predicted topology of protein hydrophobicity based on the amino acid sequences was in line with our results on solubility. The freeze-dried gelatin had a 18% larger amount of low-molecular weight peptides, compared to the control and the spray-dried samples. This was probably caused by the cleavage of peptides during the drying process. Thus, freeze drying can lead to maximum degradation of gelatin components, which may be associated with a longer heat treatment, compared to spray drying.
Thus, spray drying is more suitable for gelatin, since this method improves the stability of its outer and inner structure, ensuring high hydrophilic properties.

Keywords: Drying, gelatin, protein, amino acid sequence, hydrophilicity, hydrophobicity, solubility

Funding: The study was funded by a grant from the President of the Russian Federation for state support of young candidates of sciences (MK-4035.2022.4).

Please cite this article in press as: Voroshilin RA, Kurbanova MG, Ostapova EV, Makhambetov EM, Petrov AN, Khelef MEA. Effect of gelatin drying methods on its amphiphilicity. Foods and Raw Materials. 2022;10(2):252–261. https://doi.org/10.21603/2308-4057-2022-2-534

INTRODUCTION

Gelatin is a protein substance that contains all essential amino acids except tryptophan. It is formed by cross-links between various polypeptide chains that developed after the destruction of the fibrous structure of collagen pre-treated with acid, alkaline, or enzymes. This protein-based hydrocolloid has a wide range of applications in various industries due to its unique structural stability, nutritional properties, and other physicochemical characteristics [1]. Particularly, hydrogels and modified gelatin-based composites are widely used in the food industry, biomedicine, pharmaceuticals, and cosmetology. Gelatin is also used in the production of food packaging materials due to its biocompatibility, biodegradability, non-immunogenicity, and ability to stimulate cell adhesion and proliferation. It can absorb 5–10 times as much water as its weight and is the main ingredient in hard and soft capsules for pharmaceuticals [2–6].

There is a high demand for gelatin in the modern market of food products and components, as well as in the pharmaceutical, medical, and cosmetic markets,

with an annual average of 326 000 tons produced worldwide. According to Grand View Research, the global gelatin market was worth $2.91 billion in 2020. It is estimated to grow by 8% per year and reach about $5 billion by 2025. Russia seeks to produce food gelatin domestically and therefore needs effective technological and biotechnological solutions [7–10]. Current research focuses on optimizing gelatin production technologies and searching for new sources of raw materials to replace the traditional ones (pig skins, bovine skins, and cattle bones).

Today, gelatin is still produced with the technologies developed several decades ago. The process contains the following stages: pre-treatment of raw materials, extraction of gelatin, processing of gelatin broths, gelatinization, and drying. The efficiency of collagen-to-gelatin conversion depends on extraction conditions (temperature, time, and pH), concentration, the quality of raw materials, and their pre-treatment methods.

Using chemical solvents for gelatin extraction can result in a higher gelatin yield along with more low-molecular-weight protein fragments that will affect the gel's strength and melting point. However, industrial production parameters are not always optimal, leading to a low gelatin yield. Therefore, we need to search for alternative solutions to optimize the process.

Drying is an important process to obtain gelatin with improved functional properties. These properties basically depend on the type of raw materials, pre-treatment methods, drying and extraction conditions, as well as the spatial structure of protein molecules and their state. Drying causes physicochemical changes in the structure and functions of proteins. For example, heating, which is part of the drying process, can break covalent and non-covalent bonds leading to changes in the protein structure. If significant, these changes can greatly affect gelatin's functional properties such as solubility, gelation, foaming, emulsification, as well as fat and water absorption. The extent of these changes is mainly determined by the drying methods and conditions [11–15].

Drying methods used in the production of protein ingredients (including gelatin) are convection drying, infrared drying, spray drying, and freeze drying.

Convection is the most common method of food drying. In convection drying, a stream of heated air is directed at a wet sample. The air here is both a heating agent and a dehydrator, since it carries away moisture vapor from the dryer. As a result of this lengthy process and elevated temperatures, the final product loses a significant amount of micronutrients and bioactive compounds. Although this method is simple to use, convection dryers have low productivity which can lead to uneven drying [16, 17].

Infrared heating with microwaves is a new method of heat treatment (drying) that extends shelf life, reduces drying time, and preserves food quality. The microwaves transfer water to the surface where it quickly evaporates under the influence of infrared radiation, which reduces the drying time [18, 19].

Spray drying is widely used in the food industry due to its simplicity and short drying time. This method allows for a good quality powdered product. However, spray drying causes particles to greatly shrink and become denser [20, 21].

Freeze drying is a process of removing water from a product by freezing it and then converting ice into steam. This process consists of three main stages: freezing, primary drying, and secondary drying. Freezing creates a solid matrix suitable for drying. Primary drying removes ice by sublimation, when the pressure in the system is reduced but the temperature remains the same. Secondary drying removes bound water reducing it to residual moisture.

Several studies indicate that protein denaturation during the formation of ice crystals can significantly change the protein structure. Therefore, when optimizing the freezing process, we should take into account the ice surface area, since it can contribute to protein denaturation caused by freezing [22–24].

In spray drying, evaporated material is sprayed through the nozzles of a conical-cylindrical apparatus (spray dryer) to obtain a product in the form of a powder or granules. This method is used to dry solutions or suspensions. Spray-dried products include powdered milk, food and fodder yeast, and egg powder. According to some studies, spray drying can effectively eliminate many of the shortcomings of protein and bioactive peptides, such as low bioavailability, high hygroscopicity, physical and chemical instability, as well as strong bitterness during and after storage [13]. It is also claimed that this method can improve gelatin's functional properties, compared to freeze or vacuum drying [25]. Assumingly, various drying methods affect the solubility and amphiphilicity of gelatin as a high-protein product, thereby changing its functional properties [26].

We studied the effect of spray and freeze drying on the solubility and amphiphilicity (hydrophobicity and hydrophilicity) of gelatin which we obtained in the previous study by enzymatic acid hydrolysis [7].

STUDY OBJECTS AND METHODS

The control sample was a commercially produced edible gelatin. The experimental samples were spray- and freeze-dried gelatins obtained by enzymatic-acid hydrolysis of cattle bone. For this, 3 kg of defatted beef bones was crushed to particles of 3.0 ± 0.5 mm in a laboratory chain grinder. The bones were obtained from a farm in Kuzbass (Russia). The crushed bones were placed in a solution of hydrochloric acid (1M HCl) which contained pepsin with an enzymatic activity of 300 000 units. The hydrolysis was carried out at 27 ± 2°C for 60 to 240 min, with a pH of 1.5–2.0. MS-01 magnetic stirrers (ELMI) were used throughout the experiment to stir the bone material at 100 rpm and 27 ± 2°C to ensure its uniform treatment with the

solution. The hydrolyzed material was centrifuged in a high-speed Avanti J-26S centrifuge (Beckman) to separate the mineral sediment from ossein. Then, the resulting ossein was washed with demineralized water and subjected to gelatin extraction. A detailed scheme of hydrolysis and gelatin extraction is described in our previous work [7].

Next, the gelatin broths were dried by the spray- and freeze-drying methods. The spray-dried gelatin was obtained in a B-290 Mini Spray Dryer (Buchi, Sweden) at 95°C and a rate of 3.0–3.2 mL/min. The freeze-dried gelatin was obtained in an INEY-6M freeze-drier. For this, gelatin broth was poured onto pallets in 1-cm layers and placed in the drying chambers. The chambers were closed with lids and the refrigerator was turned on. The unit entered the freezing mode within 15 min and when the evaporator temperature reached –35°C, the vacuum pump turned on to start the drying mode. The freeze-dried gelatin was then ground in an NS-2000 automatic laboratory mill.

The amino acid sequence of gelatin proteins, which is represented by a single letter code, was determined by matrix-activated laser desorption/ionization on a MALDI Biotyper (Bruker). Amino acid residues, isoelectric point, aliphatic index, molar absorption coefficient, as well as the surface area of the peptides, were determined by the *in silico* bioinformatic methods on the PepDraw online server. The gelatin samples' solubility was evaluated visually. For this, 500 mg of gelatin was mixed with 50 mL of distilled water and stirred actively (200 rpm) with MS-01 magnetic stirrers (ELMI). Dissolution was monitored at water temperatures of 25 and 50°C.

The Bloom strength of gelatin gels was determined on a ST-2 Strukturometr texture analyzer with a Bloom indenter. For this, 7.5 g of gelatin was placed in a glass of cold water (105 mL) and kept at 22°C max for 180 min. Next, the swollen gelatin was heated to 60°C in a water bath and stirred for 15 min until complete dissolution. The solution (6.67% concentration) was poured into a calibrated beaker and kept at 10.0 ± 0.1°C for 17 h. The prepared samples were then placed on the analyzer's table under the Bloom indenter for the study. The arithmetic mean of two determinations was taken as the final result.

The ProtScale online service was used to predict the topology of the hydrophobicity and hydrophilicity of gelatin proteins. In particular, this service allows us to compute and represent (in the form of a two-dimensional graph) the profile produced by any amino acid scale for a selected protein. The amino acid scale is defined by a numerical value assigned to each type of amino acid. ProtScale uses the Kyte and Doolittle scale that assigns individual values to 20 amino acids, namely *Ala*: 1.800, *Arg*: –4.500, *Asn*: –3.500, *Asp*: –3.500, *Cys*: 2.500, *Gln*: –3.500, *Glu*: –3.500, *Gly*: –0.400, *His*: –3.200, *Ile*: 4.500, *Leu*: 3.800, *Lys*: –3.900, *Met*: 1.900, *Phe*: 2.800, *Pro*: –1.600, *Ser*: –0.800, *Thr*: –0.700, *Trp*: –0.900, *Tyr*: –1.300, and *Val*: 4.200, –3.500, –3.500, –0.490.

The molecular weight distribution of proteins was carried out by polyacrylamide gel electrophoresis in the presence of an anionic detergent, sodium dodecyl sulfate (SDS-Na). For this, the dried gelatin samples were dissolved in deionized water at 60°C to create a 0.2% solution. The solution was then mixed with a loading buffer containing 5 μL of dithiothreitol (DTT) and subjected to heat denaturation in boiling water for 5 min. After that, 15-μL samples were loaded into polyacrylamide gels containing 6% of separating gel and 5% of stacking gel to perform electrophoresis. Then, the gels were stained with 0.1% Coomassie Blue R-250 in 25% isopropanol and 10% acetic acid for 2 h, followed by decoloring with 5% alcohol and 10% acetic acid. Next, 2-D gels were detected using the Gel Doc XR Plus Bio-RAD system.

RESULTS AND DISCUSSION

First, we spray- and freeze-dried the experimental samples of gelatin obtained by enzymatic acid hydrolysis. Next, we determined the amino acid sequence of all the dried gelatins (Table 1).

The proteins of the control, spray-dried, and freeze-dried samples are represented by peptide sequences of 85, 93, and 95 amino acids, respectively (Table 1).

These sequences allowed us to determine the amino acid composition (% or g/100 g of total amino acids) of the control and experimental samples. This is a critical indicator of gelatin quality largely depending on raw materials. Glycine and proline are the most important amino acids in gelatin. Collagen consists of three

Table 1 Amino acid sequences of gelatin samples (one-letter coding)*

Control	Experimental samples	
	Spray-dried gelatin	Freeze-dried gelatin
GGPAAGGPAYGGPILILAPAILA	SHILEILDVILDHILILDMILSHESHP	PILEVILEILESHILEMILHILMILS
PYILAAILADNPAANPAYNPILP	YCGDDGGYGPYPDDPGYDDGYH	HPSHPEEPEEEMPEMPPRPPRVR
NAAPNAYPNILPQGAPQGYSEA	EHPILMEMPPYQCCGQNYYNCDD	PVREPEHPHPILMPMPRPREYPY
ASEAYSEILTNAATNAYPATN	ENNPQQRRSVYAEVPYQCCVPGG	ESGQSQYNADEGNNPPPQQRS

*A – alanine; C – cysteine; D – aspartic acid; E – glutamic acid; F – phenylalanine; G – glycine; H – histidine; I – isoleucine; K – lysine; L – leucine; M – methionine; N – asparagine; P – proline; Q – glutamine; R – arginine; S – serine; T – threonine; V – valine; W – tryptophan; Y – tyrosine

identical or different polypeptide chains with a repeating pattern $(Gly\text{-}XY)_n$ (X and Y stand for any amino acid) and a high content of imino acids with a triple helical structure due to hydrogen bonds [27–29].

The composition and content of amino acids, especially imino acids, in gelatin have a significant impact on its structure and functional properties. In particular, the gel's supercoil structure is stabilized by both the hydrogen bonds forming between amino acid residues and the pyrrolidine rings of imino acids. A higher content of imino acids ensures a higher gel modulus, gelling temperature, and melting point [30].

The amino acid composition (% or g/100 g of total amino acids) of the control and experimental gelatin samples are presented in Table 2.

We found that the samples varied mostly in the content of alanine, accounting for 25.840% in the control sample and only 1% in the experimental samples.

None of the samples contained phenylalanine, lysine, or tryptophan. According to literature, the absence of tryptophan is what makes gelatin different from other hydrocolloids of animal origin. This amino acid is mainly present in membrane proteins and has aromatic residues in its structure.

Histidine, arginine, and threonine were not detected in the control sample.

Using the PepDraw online server, we determined the mass of amino acid residues defined as a sum of monoisotopic masses of all amino acid residues in the peptide. We also calculated the isoelectric point represented by a pH value at which the total charge of the peptide equals zero. This calculation shows the partial charge of the peptide at various pH values, starting from 0. Then, we determined the aliphatic index of the protein defined as a relative volume of aliphatic side chains (alanine, valine, isoleucine, and leucine). It can be considered a positive factor in increasing thermal stability of globular proteins.

The mass of amino acid residues in the control, spray-dried, and freeze-dried samples amounted to 13 173.86, 10 830.72, and 11 156.79, respectively.

The aliphatic index values in the control, spray-dried, and freeze-dried samples were 95.96, 87.53, and 70.74, respectively.

The isoelectric points in the control, spray-dried, and freeze-dried samples were 5.97, 4.89, and 5.96, respectively.

The molar absorption coefficients in the control, spray-dried, and freeze-dried samples were 8960.00, 12 800.00, and 3840.00 $M^{-1} \cdot cm^{-1}$, respectively.

The surface area values in the control, spray-dried, and freeze-dried samples were 21 223.00, 23 040.00, and 18 407.00, respectively.

We concluded that the control and the spray-dried samples had more thermostable proteins, since their aliphatic indexes (87 and 96, respectively) were higher than those of the freeze-dried sample (70). The samples' isoelectric points indicated a slightly acidic reaction, therefore their protein molecules were neutral at a pH value of 4.89 to 5.97.

Solubility is an important property of gelatin in food systems. In cold water, gelatin hydrates and swells, and at temperatures above 40°C, it forms a colloidal solution (sol). The solubility index depends on the method

Table 2 Amino acid contents in the control and experimental gelatin samples

Amino acid	Content of total amino acids, % or g/100 g		
	Control	Spray-dried gelatin	Freeze-dried gelatin
A – alanine	25.840	1.050	1.080
C – cysteine	ND	6.320	ND
D – aspartic acid	1.120	11.580	1.080
E – glutamic acid	3.370	6.320	16.130
F – phenylalanine	ND	ND	ND
G – glycine	8.990	9.470	2.150
H – histidine	ND	6.320	6.450
I – isoleucine	8.990	7.370	8.600
K – lysine	ND	ND	ND
L – leucine	8.990	7.370	8.600
M – methionine	ND	3.160	6.450
N – asparagine	10.110	4.210	3.230
P – proline	15.730	10.530	21.510
Q – glutamine	2.250	5.260	4.300
R – arginine	ND	2.110	7.530
S – serine	3.370	4.210	6.450
T – threonine	3.37	ND	ND
V – valine	ND	4.21	3.23
W – tryptophan	ND	ND	ND
Y – tyrosine	7.87	10.53	3.23

ND – not detected

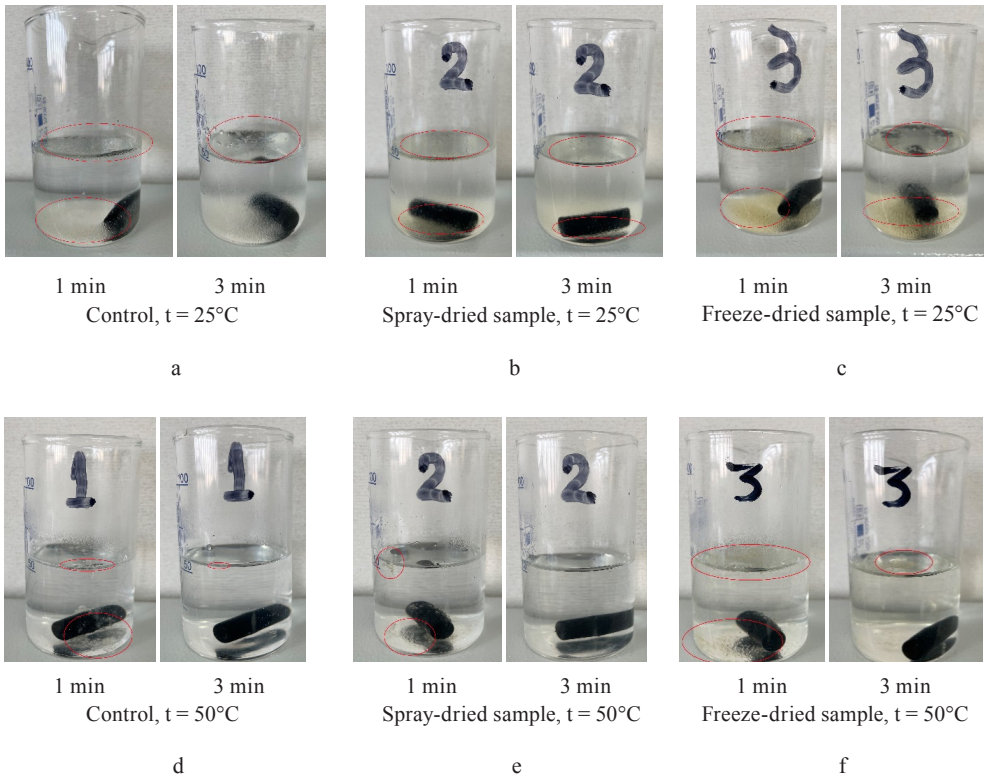

Figure 1 Dissolution of gelatin samples at 25 and 50°C for 1–3 min

of gelatin production. New methods are currently being developed to obtain water-soluble gelatin at temperatures below 40°C. Such gelatin usually has an amorphous powdery form.

Next, we visually assessed the degree of solubility of the gelatin samples at water temperatures of 25 and 50°C (Fig. 1).

As we can see, the control and the spray-dried samples showed higher protein solubility at 25 and 50°C than the freeze-dried sample. According to Fig. 1c and f, gelatin particles did not dissolve after 1 min of mixing at different temperatures, settling on the bottom and on the surface. After 3 min of mixing at 25 or 50°C, the freeze-dried sample still did not dissolve completely, its particles settling on the water surface (Fig. 1f). This could be due to the sample's mechanical grinding in a laboratory mill at the final stage of freeze-drying, which resulted in larger particles than those in the spray-dried gelatin and affected its solubility. We can also assume that spray drying exposes protein molecules to less thermal stress than freeze drying, which causes the highest degree of thermal and dehydration stress.

Next, we evaluated the Bloom strength of the gelatin gels (Fig. 2).

The Bloom value is an important parameter of gelatin's physical and mechanical properties used in food production. It is also used as a criterion in gelatin classifications.

The gel strength index depends on the protein content and the molecular weight of peptides formed in gelatin. In our study, this index was quite high in the control and spray-dried samples, amounting to 229.0 ± 0.5 and 224.0 ± 0.5 Bloom, respectively. The freeze-dried sample's index (186.0 ± 0.5 Bloom) was by 17 and 19% lower than for the control and spray-dried samples. Assumingly, the proteins of the freeze-dried gelatin had a lower molecular weight, which worsened its structural and mechanical properties. We can also assume that this sample might have more low-molecular weight (below 20 kDa) peptides.

Next, we determined the degree of protein hydrophilicity and hydrophobicity based on the amino acid sequences. Using the ProtScale online service (the Kyte and Doolittle scale), we predicted the topology of protein hydrophobicity and hydrophilicity for the control and experimental gelatin samples (Fig. 3).

On the Kyte and Doolittle scale, the peaks above 0 refer to hydrophobicity and those below 0 refer to hydrophilicity. As we can see in Fig. 3a, the control sample had higher hydrophilic properties since its peaks along the X axis ranged from 3 to 21, with a peptide sequence of PAAGGPAY GGPILILAPA I. Most of its peaks were for alanine, proline, isoleucine, and glycine. These amino acids had hydrophobic properties and 1 to 4 uncharged side radicals at pH = 6–7. In general, these peaks characterized a sequence of amino acids with hydrophobic properties.

The region from 22 to 53 had a sequence of LAPYILAAI LADNPAANPA YNPILPNAAP NAY,

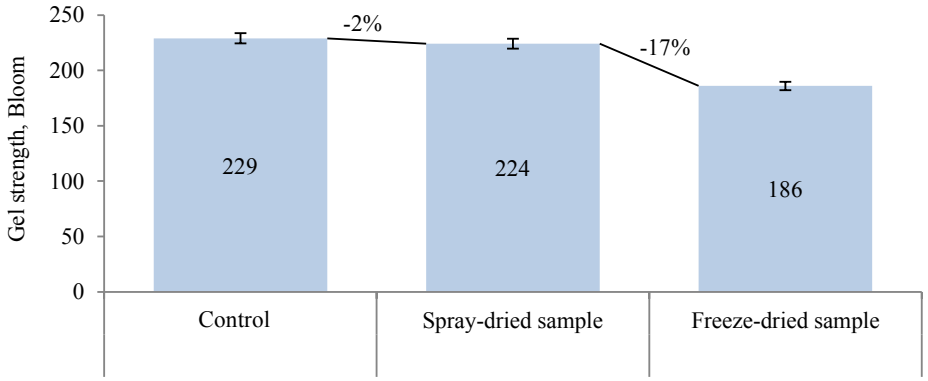

Figure 2 Bloom strength of gelatin gels

whereas the region from 56 to 85 was represented by PQGAPQGYSEAAS EAYSEILTNA ATNAY. Thus, 21 out of 85 amino acids had hydrophobic properties. According to Fig. 3a (control), leucine had maximum hydrophobicity of 2.585 units at point 17 and aspargin had highest hydrophilicity of –2.678 at 89.

The profile of the spray-dried sample is shown in Fig. 3b. As we can see, the peptide region from 5 to 21 represented by AGGPAY GGPILILAPA I and the region from 55 to 57 with a NIL sequence had hydrophobic properties. Most of the peaks were located above 0 and were represented by alanine, isoleucine, and proline. These amino acids had hydrophobic properties and 1 to 3 uncharged side radicals. Leucine (18) had a maximum hydrophobicity value of 2.500 units, while glutamine (77) had a maximum hydrophilicity value of –3.511. Thus, 20 out of 91 amino acids had hydrophobic properties.

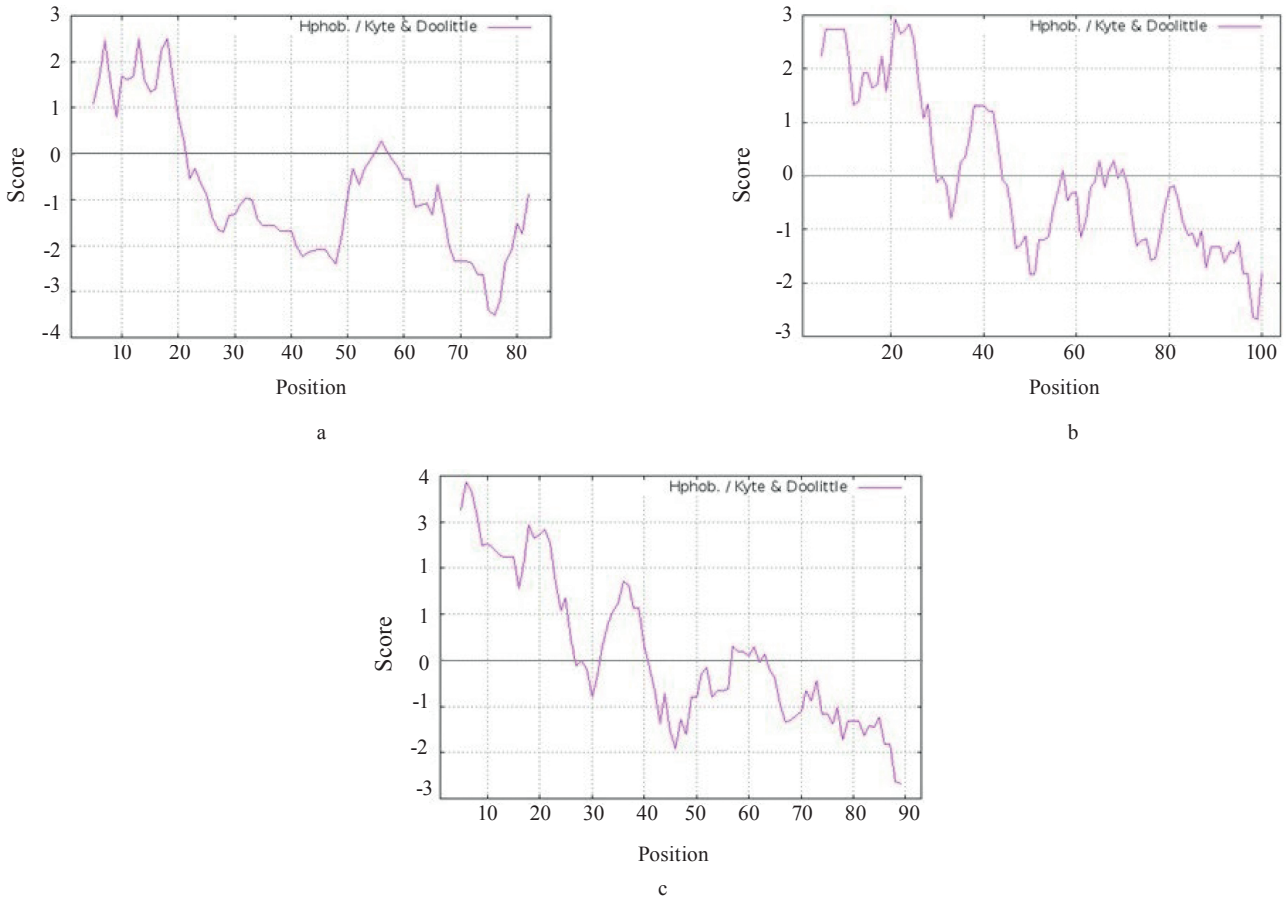

Figure 3 Predicted topology of protein hydrophobicity and hydrophilicity in the control and experimental gelatins (a – control; b – spray-dried sample; c – freeze-dried sample)

The profile of the freeze-dried sample is shown in Fig. 3c. As can be seen, the peptide region from 5 to 26 was represented by a sequence of VILEIL ESHILEMILH ILMILS, the region from 32 to 39 had a sequence of EEPEEEMP, and the one from 57 to 61 was represented by PHPI. Glutamic acid, isoleucine, and leucine had most peaks in the hydrophobicity area. They also had from 4 to 7 uncharged side radicals at pH = 6–7. Isoleucine (6) had maximum hydrophobicity of 3.856 units, while glutamine (76) had maximum hydrophilicity of –5.504 units. Thus, 36 out of 93 amino acids had hydrophobic properties. Our results were consistent with literature on the amphiphilic (hydrophobic and hydrophilic) properties of these amino acids [31–38].

The hydrophobicity values based on the amino acid sequences of the gelatin samples confirmed our data on their solubility. In particular, they proved that the method of drying affects the gelatin's structural and mechanical properties, as well as its physicochemical parameters. Spray drying can improve the proteins' functional properties compared to freeze drying. Therefore, we can conclude that different drying methods affect the solubility and amphiphilicity properties of gelatin, thereby changing its functional properties.

Finally, we analyzed the molecular weight distribution of proteins by polyacrylamide gel electrophoresis in the presence of an anionic detergent, sodium dodecyl sulfate (Fig. 4, Table 3).

According to the results, the control sample's protein fractions were more evenly distributed by molecular weight compared to the experimental samples. Its fractions between 50 and 100 kDa accounted for 72.6% and those below 20 kDa amounted to 6.1138% of the total content. The spray-dried sample showed a somewhat different molecular weight distribution. Its protein fractions between 40 to 100 kDa made up 73.8%, while those below 20 kDa accounted for 5.026315%. The freeze-dried sample had a completely different distribution of protein fractions. Most peptides were found at the level of 40 kDa (42.83855%). Yet, this sample had 30.214499% of proteins with a molecular weight below 20 kDa, which was by 20.23% more than in the control and by 16.64% more than in the spray-dried gelatin. This increase in low-molecular weight peptides by an average of 18% was most likely caused by the cleavage of peptides during freeze drying.

Our results showed that the degree of degradation of gelatin components can depend on the method of drying gelatin broths. Freeze drying can lead to maximum degradation, which may be associated with long heat treatment (5 h). This time is much longer compared to spray drying, although the process of freeze drying takes place at a lower temperature (60°C). Also, temperatures below 0°C cause gelation followed by freezing, which can also lead to structural changes in gelatin. In addition, a faster process of spray drying can slow down the degradation of gelatin proteins.

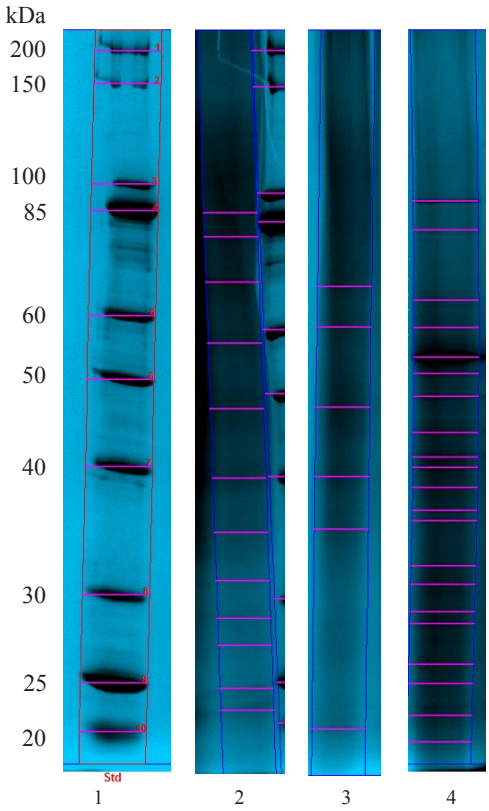

Figure 4 Electropherogram of the molecular weight distribution of gelatin samples (1 – marker; 2 – control, 3 – spray-dried sample, 4 – freeze-dried sample)

These results were consistent with those for gelatin solubility (Fig. 2). Therefore, spray drying is more suitable for maintaining the structure of gelatin and its functional properties.

CONCLUSION

We studied the effect of spray and freeze drying of gelatin broths on the solubility and amphiphilicity of gelatin. The results showed that spray drying can reduce the breakdown of gelatin proteins and retain more α-chains, while freeze drying increases the hydrophobicity of gelatin and decreases its solubility. The predicted topology of protein hydrophobicity, which was based on the amino acid sequences of the gelatin samples, confirmed the results on solubility. Particularly, the freeze-dried gelatin had 36 amino acids with hydrophobic properties out of 93, compared to 21 out of 85 in the control and 20 out of 91 in the spray-dried sample.

We found that the freeze-dried sample had by 18% more low-molecular weight peptides (below 20 kDa) compared to the control and the spray-dried samples. This was most likely caused by the cleavage of peptides during the drying process. Freeze drying can lead to maximum degradation of gelatin components due to long heat treatment. Temperatures below 0°C cause gelation followed by freezing, which can also cause

Table 3 Molecular weight distribution of gelatin samples

Molecular weight, kDa	Molecular weight distribution, %		
	Control	Spray-dried sample	Freeze-dried sample
200	1.316515	3.878759	6.386503
150	3.101737	5.118362	1.334564
100	19.4574	17.810301	1.301436
85	17.85029	13.035829	1.367691
60	14.53681	8.429303	42.83855
50	20.790700	21.727447	3.170772
40	10.111660	12.89394	3.459454
30	0.220568	6.732710	3.530442
25	2.909430	1.157420	3.452356
20	3.591122	4.189303	2.974374
Below 20	6.113800	5.026315	30.214499

structural changes in gelatin. By contrast, a faster spray drying process can, to a certain extent, slow down the degradation of gelatin proteins.

Thus, spray drying is more suitable for gelatin drying, since this method improves the stability of gelatin's outer and inner structure, which was confirmed by high hydrophilicity values of the spray-dried sample. Further research could search for optimal parameters and modes of spray drying for gelatin broths.

CONTRIBUTION

The authors were equally involved in writing the manuscript and are equally responsible for plagiarism.

CONFLICT OF INTEREST

The authors declare that there is no conflict of interest regarding the publication of this article.

REFERENCES

1. Nikitin IA, Nikitina MA, Allilueva NM, Krivosheev AYu. Comprehensive assessment of fruit jelly with an improved carbohydrate profile based on unconventional plant raw materials. Foods and Raw Materials. 2019;7(1):26–34. https://doi.org/10.21603/2308-4057-2019-1-26-34
2. Shatabayeva EO, Mun GA, Shaikhutdinov YM, Khutoryanskiy VV. Gelatin: sources, preparation and application in food and biomedicine. Chemical Bulletin of Kazakh National University. 2020;98(3):28–46. (In Russ.). https://doi.org/https://doi.org/10.15328/cb1112
3. Wang Y, Shi B. Concentration of gelatin solution with polyethersulfone ultrafiltration membranes. Food and Bioproducts Processing. 2011;89(3):163–169. https://doi.org/10.1016/j.fbp.2010.06.004
4. Yang C, Xu L, Zhou Y, Zhang X, Huang X, Wang M, *et al.* A green fabrication approach of gelatin/CM-chitosan hybrid hydrogel for wound healing. Carbohydrate Polymers. 2010;82(4):1297–1305. https://doi.org/10.1016/j.carbpol.2010.07.013
5. Rigueto CVT, Nazari MT, Massuda LA, Ostwald BEP, Piccin JS, Dettmer A. Production and environmental applications of gelatin-based composite adsorbents for contaminants removal: a review. Environmental Chemistry Letters. 2021;19(3):2465–2486. https://doi.org/10.1007/s10311-021-01184-0
6. Baziwane D, He Q. Gelatin: The paramount food additive. Food Reviews International. 2003;19(4):423–435. https://doi.org/10.1081/FRI-120025483
7. Voroshilin RA. Technology of enzymatic-acid hydrolysis of bone raw material in production of gelatine. Theory and Practice of Meat Processing. 2021;6(3):279–284. https://doi.org/10.21323/2414-438X-2021-6-3-279-284
8. Mekhedkin AA. Structure of the gelatin market in the Russian Federation. Agricultural Risk Management. 2020;37(3):63–69. (In Russ.).
9. Prosekov AYu, Kurbanova MG, Gurinovich GV, Voroshilin RA, Patshina MV. Review and analysis of the market of raw materials for the production of food gelatin in the territory of the Siberian Federal District. Technology and Merchandising of the Innovative Foodstuff. 2021;67(2):96–101. (In Russ.).
10. Babich O, Sukhikh S, Pungin A, Ivanova S, Asyakina L, Prosekov A. Modern trends in the in vitro production and use of callus, suspension cells and root cultures of medicinal plants. Molecules. 2020;25(24). https://doi.org/10.3390/molecules25245805

11. Voroshilin RA. Rheological characteristics of gelatin obtained by biocatalytic and ultrafiltration methods. XXI Century: Resumes of the Past and Challenges of the Present Plus. 2021;10(3):117–120. (In Russ.). https://doi.org/10.46548/21vek-2021-1055-0022
12. Aksun Tümerkan ET, Cansu Ü, Boran G, Regenstein JM, Özoğul F. Physiochemical and functional properties of gelatin obtained from tuna, frog and chicken skins. Food Chemistry. 2019;287:273–279. https://doi.org/10.1016/j.foodchem.2019.02.088
13. Rasli HI, Sarbon NM. Effects of different drying method on the rheological, functional and structural properties of chicken skin gelatin as compared to bovine gelatin. International Food Research Journal. 2015;22(2):584–592.
14. Sarabandi K, Gharehbeglou P, Jafari SM. Spray-drying encapsulation of protein hydrolysates and bioactive peptides: Opportunities and challenges. Drying Technology. 2020;38(5–6):577–595. https://doi.org/10.1080/07373937.2019.1689399
15. Shalunov AV, Khmelev VN, Terentiev SA, Nesterov VA, Golykh RN. Ultrasonic dehydration of food products with moisture removal without phase transition. Food Processing: Techniques and Technology. 2021;51(2):363–373. (In Russ.). https://doi.org/10.21603/2074-9414-2021-2-363-373
16. Politowicz J, Lech K, Sánchez-Rodríguez L, Figiel A, Szumny A, Grubor M, *et al.* Volatile composition and sensory profile of oyster mushroom as affected by drying method. Drying Technology. 2018;36(6):685–696. https://doi.org/10.1080/07373937.2016.1274903
17. Senadeera W, Adiletta G, Önal B, Di Matteo M, Russo P. Influence of different hot air drying temperatures on drying kinetics, shrinkage, and colour of persimmon slices. Foods. 2020;9(1). https://doi.org/10.3390/foods9010101
18. Heydari MM, Kauldhar BS, Meda V. Kinetics of a thin-layer microwave-assisted infrared drying of lentil seeds. Legume Science 2020;2(2). https://doi.org/10.1002/leg3.31
19. Buyanova IV, Altukhov IV, Tsuglenok NV, Krieger OV, Kashirskih EV. Pulsed infrared radiation for drying raw materials of plant and animal origin. Foods and Raw Materials. 2019;7(1):151–160. https://doi.org/10.21603/2308-4057-2019-1-151-160
20. Santos D, Maurício AC, Sencadas V, Santos JD, Fernandes MH, Gomes PS. Spray drying: An overview. In: Pignatello R, editor. Biomaterials. Physics and chemistry. New edition. InTech; 2018. pp. 9–35. https://doi.org/10.5772/intechopen.72247
21. Haque MA, Adhikari B. Drying and denaturation of proteins in spray drying process. In: Mujumdar AS, editor. Handbook of industrial drying. Boca Raton: CRC Press; 2014. pp. 971–984.
22. Liu L, Dai X, Kang H, Xu Y, Hao W. Structural and functional properties of hydrolyzed/glycosylated ovalbumin under spray drying and microwave freeze drying. Food Science and Human Wellness. 2020;9(1):80–87. https://doi.org/10.1016/j.fshw.2020.01.003
23. Cao J, Zhao X, Wang J, Dou H, Liu C, Yan X, *et al.* Processing micrometer-sized particles in crumpled graphene network for freestanding membrane enabled by freeze casting. Chinese Chemical Letters. 2020;31(1):265–268. https://doi.org/10.1016/j.cclet.2019.03.041
24. Sosnin MD, Shorstkii IA. Microplasma pretreatment of mango fruits during freeze drying with thermoelectric emission. Food Processing: Techniques and Technology. 2020;50(4):681–689. (In Russ.). https://doi.org/10.21603/2074-9414-2020-4-681-689
25. Kanwate BW, Ballari RV, Kudre TG. Influence of spray-drying, freeze-drying and vacuum-drying on physicochemical and functional properties of gelatin from *Labeo rohita* swim bladder. International Journal of Biological Macromolecules. 2019;121:135–141. https://doi.org/10.1016/j.ijbiomac.2018.10.015
26. Salem A, Fakhfakh N, Jridi M, Abdelhedi O, Nasri M, Debeaufort F, *et al.* Microstructure and characteristic properties of dogfish skin gelatin gels prepared by freeze/spray-drying methods. International Journal of Biological Macromolecules. 2020;162:1–10. https://doi.org/10.1016/j.ijbiomac.2020.06.033
27. Feng X, Dai H, Ma L, Fu Y, Yu Y, Zhu H, *et al.* Effect of microwave extraction temperature on the chemical structure and oil-water interface properties of fish skin gelatin. Innovative Food Science and Emerging Technologies. 2021;74. https://doi.org/10.1016/j.ifset.2021.102835
28. Haug IJ, Draget KI. Gelatin. In: Phillips GO, Williams PA, editors. Handbook of food proteins. A volume in woodhead publishing series in food science, technology and nutrition. Woodhead Publishing; 2011. pp. 92–115. https://doi.org/10.1533/9780857093639.92
29. Aslanova MA, Semenova AA, Derevitskaya OK. Formulating a functional drink with antiosteoporosis effects. Foods and Raw Materials. 2021;9(2):354–363. https://doi.org/10.21603/2308-4057-2021-2-354-363
30. Nikoo M, Benjakul S, Ocen D, Yang N, Xu B, Zhang L, *et al.* Physical and chemical properties of gelatin from the skin of cultured Amur sturgeon (Acipenser schrenckii). Journal of Applied Ichthyology. 2013;29(5):943–950. https://doi.org/10.1111/jai.12238

31. Herger A, Dünser K, Kleine-Vehn J, Ringli C. Leucine-rich repeat extensin proteins and their role in cell wall sensing. Current Biology. 2019;29(17):R851–R858. https://doi.org/10.1016/j.cub.2019.07.039
32. Lee HW, Lu Y, Zhang Y, Fu C, Huang D. Physicochemical and functional properties of red lentil protein isolates from three origins at different pH. Food Chemistry. 2021;358. https://doi.org/10.1016/j.foodchem.2021.129749
33. Watford M. Amino Acids. Glutamine. In: Jez J, editor. Encyclopedia of biological chemistry III. Third Edition. Elsevier; 2021. pp. 56–70. https://doi.org/10.1016/B978-0-12-819460-7.00028-1
34. Barrera EE, Zonta F, Pantano S. Dissecting the role of glutamine in seeding peptide aggregation. Computational and Structural Biotechnology Journal. 2021;19:1595–1602. https://doi.org/10.1016/j.csbj.2021.02.014
35. Soriano-Correa C, Barrientos-Salcedo C, Campos-Fernández L, Alvarado-Salazar A, Esquivel RO. Importance of asparagine on the conformational stability and chemical reactivity of selected anti-inflammatory peptides. Chemical Physics. 2015;457:180–187. https://doi.org/10.1016/j.chemphys.2015.06.005
36. Bennett V. Peptide histidine isoleucine. In: Enna SJ, Bylund DB, editors. xPharm: The comprehensive pharmacology reference. Elsevier; 2007. pp. 1–2. https://doi.org/10.1016/B978-008055232-3.62390-6
37. Ahmady A, Abu Samah NH. A review: Gelatine as a bioadhesive material for medical and pharmaceutical applications. International Journal of Pharmaceutics. 2021;608. https://doi.org/10.1016/j.ijpharm.2021.121037
38. Mirzapour-Kouhdasht A, Moosavi-Nasaba M, Yousefi R, Eun J-B. Bio/multi-functional peptides derived from fish gelatin hydrolysates: Technological and functional properties. Biocatalysis and Agricultural Biotechnology. 2021;36. https://doi.org/10.1016/j.bcab.2021.102152

ORCID IDs
Roman A. Voroshilin https://orcid.org/0000-0001-7259-3085
Marina G. Kurbanova https://orcid.org/0000-0003-0563-1007
Elena V. Ostapova https://orcid.org/0000-0002-4704-484X
Eduard M. Makhambetov https://orcid.org/0000-0001-8877-4884
Andrey N. Petrov https://orcid.org/0000-0001-9879-482X
Mohammed El Amine Khelef https://orcid.org/0000-0002-9371-7670

Foods and Raw Materials. 2022;10(2)

ISSN 2310-9599 (Print)
ISSN 2308-4057 (Online)

Research Article
Open Access

Available online at http://jfrm.ru/en
https://doi.org/10.21603/2308-4057-2022-2-535
https://elibrary.ru/WRBAKE

Jelly formulated with different carbohydrate profiles: Quality evaluation

Inessa V. Plotnikova*, Gazibeg O. Magomedov, Irina M. Zharkova, Elena N. Miroshnichenko, Viktor E. Plotnikov

Voronezh State University of Engineering Technologies, Voronezh, Russia

* e-mail: plotnikova_2506@mail.ru

Received 17.11.2021; Revised 02.02.2022; Accepted 23.06.2022; Published online 23.09.2022

Abstract:
Jelly is a popular confectionery product but it has a high content of easily digestible sugars, namely 70–85%. Therefore, modern confectioners are trying to develop new formulations of jelly with reduced sweetness and sugar content. One of the ways to achieve that is to use starch syrup instead of white sugar. Another benefit of starch syrup is that it can slow down the drying and staling of jelly.

We studied three types of starch syrup (low-conversion, confectionery, high-conversion), glucose-fructose syrup, and sugar-free jelly samples based on them. Jelly based on sugar and confectionery syrup was used as the control sample. The main quality indicators were analyzed against standard values; the sensory parameters were determined by the descriptor-profile analysis; and water activity was measured by using a HygroPalm Rotronic hygrometer. The microbiological safety of the experimental jelly samples was assessed after 12 weeks of their storage in plastic containers.

The sample based on confectionery syrup had the most optimal profile, with moderate sweetness and taste richness, good jelly-like texture, viscoelasticity, plasticity, a color similar to that of the control, and no effect of wetting or stickiness. The samples based on starch syrup had a 1.4–2.4-fold decrease in easily digestible sugars and a 1.9–3.4-fold increase in polysaccharides, compared to the control. During storage, the samples based on high-conversion starch syrup and glucose-fructose syrup were less likely to dry out than the others, with their water activity decreasing to a greater extent. The microbiological analysis after storage showed the absence of pathogenic microorganisms and coliform bacteria in three out of the four jelly samples.

Using various types of starch syrup and glucose-fructose syrup instead of white sugar allows for a greater range of jelly types with different carbohydrate profiles and a longer shelf life.

Keywords: Jelly, starch syrup, carbohydrate composition, water activity, quality indicators, storage

Funding: The study was conducted at Voronezh State University of Engineering Technologies (VSUET).

Please cite this article in press as: Plotnikova IV, Magomedov GO, Zharkova IM, Miroshnichenko EN, Plotnikov VE. Jelly formulated with different carbohydrate profiles: Quality evaluation. Foods and Raw Materials. 2022;10(2):262–273. https://doi.org/10.21603/2308-4057-2022-2-535

INTRODUCTION

Modern confectioners prioritize new formulations with a reduced sugar content, lower energy value, extended shelf life, and improved quality. The quality of confectionery products is determined by physicochemical and microbiological processes that take place throughout their shelf life. These processes depend on the product's chemical composition, ingredient ratios, storage conditions, moisture content, pH, water activity, and moisture transfer. The main indicators of jelly quality are moisture content, water activity, and pH. They depend on the formulation, the content and properties of carbohydrate-containing components, as well as storage conditions [1, 2].

Confectionery products vary in moisture that binds nutrients and regulates the product's texture and structure. Products with high moisture contain larger amounts of free and chemically unbound water that intensifies biological processes and causes damage to products [3]. Free water is responsible for molds, yeasts, and bacteria, as well as toxins. It is involved in chemical and biochemical reactions that can affect the product's

texture, aroma, color, taste, nutritional value, stability, and shelf life [4].

Regulatory requirements for confectionery products include an indicator of water content (*W*, %). However, this indicator cannot assess how well water is bound to food substances and how this may affect the quality of the product during storage [5].

What is vital for microorganisms is not the absolute content of water in the product but its availability, or water activity (A_w). This indicator is defined as $A_w = P/P_0$, i.e., the ratio of water vapor pressure over the surface of the product (P) and vapor pressure over pure water (P_0) [6].

The relative equilibrium moisture is based on the partial pressure of water vapor over the product and depends on the product's chemical composition, moisture content, storage conditions (temperature and relative air humidity), type of packaging, etc. [7].

The A_w limits for microorganisms in food products are 0.83–0.98 for bacteria, 0.81–0.88 for yeasts, and for 0.70–0.88 molds. However, some types of mold fungi and osmophilic yeasts can grow even at $A_w = 0.62$. That is why fungi and yeast contents are included in those microbiological indicators that determine the product's stability during storage. All types of microorganisms are capable of reproduction at $A_w > 0.95$ and none can reproduce at $A_w < 0.6$.

The pH and redox potential values have a significant effect on the growth of microorganisms. Products with pH < 3.7 are safe from spoilage, with only lactic acid bacteria and certain yeasts and molds able to develop in them, while products with pH of 5.0 to 7.0 are exposed to risks associated with pathogenic microorganisms [8].

Based on water activity (A_w), products can be divided into high moisture ($A_w > 0.9$), intermediate moisture ($0.6 < A_w < 0.9$), and low moisture ($A_w < 0.6$) products. Low moisture prevents microbiological processes in the product, contributing to a long shelf life. Intermediate moisture creates favorable conditions for predominantly microbiological and enzymatic processes with a growth of yeasts, molds, and some types of bacteria, thus causing the products to dry out and become stale during storage. High moisture products are vulnerable to all types of microorganisms and therefore have a short shelf life [9].

Reducing the water activity index can effectively prevent microbiological spoilage and some chemical reactions in food products that reduce their quality during storage. For this, a number of methods are applied including concentration, dehydration, drying, freezing, increasing osmotic pressure over the product, and using microorganism growth inhibitors. There are also active ingredients that bind water and thereby prevent or significantly slow down its evaporation. These are specific enzymes, emulsifiers, carbohydrate-containing hygroscopic substances, salts, and water-retaining agents. The strength of water binding depends on the origin and chemical composition of the ingredients used, as well as pH and temperature of the medium [10, 11].

The carbohydrate composition of fruit jelly has a significant impact on its consumer properties during storage. Jelly is a sugary confectionery product. Despite its popularity, it has a number of disadvantages: high sugar content (70–85% of easily digestible sugars), high energy value (300–360 kcal/100 g), sweetness, high glycemic index, and an unbalanced composition. According to its chemical composition and structure, jelly belongs to complex colloidal systems. Its osmotically retained moisture has a limited energy of binding with the product's components. Jelly is an intermediate moisture (15–30%) product [12, 13].

During storage, even with all requirements met, jelly gradually becomes exposed to moisture exchange (shrinkage) and sucrose crystallization, with its appearance and structure deteriorating as well [13]. However, when stored at elevated temperatures and relative humidity over 70%, jelly is vulnerable to mold due to the sorption of moisture on its surface. This results in its wetting, with an increase in the A_w index to 0.9 and a growth in *Aspergillus* and *Penicillium* fungi, yeast, and, to a lesser extent, bacteria [15]. The lower limit of jelly moisture for mold fungi is 15%, but under improper storage conditions, spoilage can occur even with a higher dry matter content. With a sugar concentration up to 60–65% and increased moisture, some races of yeast can cause fermentation, especially alcoholic, which gives the product an unpleasant pungent odor [16].

Jelly drying can be prevented and water activity reduced by introducing sugar-containing substances with a high content of reducing agents and water-retaining components (polysaccharides, glycerol, polyhydric alcohols, some sweeteners, starch, proteins, amino acids, lactic acid, etc.) [17].

Fruit jelly is made with natural gel-forming agents such as agar-agar, pectin, gelatin, carrageenans, gum arabic, xanthan gums, etc. These are hydrocolloidal polysaccharides that bind water in jelly, like sugar, making it less available for microorganisms to develop [18–20].

Pectin is the best water-retaining gelling component for jelly. It is a natural polysaccharide with water-soluble fiber properties. Pectin is widely used in therapeutic and preventative nutrition due to its normalizing effect on many vital processes without disturbing the bacteriological balance of the body. In particular, it improves digestion, lowers blood cholesterol, normalizes blood sugar, and removes ions of toxic metals, pesticides, radionuclides, xenobiotics, anabolics, metabolic products, and excess urea from the body. It is recommended to people with disturbed carbohydrate and lipid metabolism, immune and bacterial diseases, obesity, and atherosclerosis [21].

Carbohydrates not only determine sensory, functional, and technological properties of a product,

but they also regulate its acidity and have a preservative antimicrobial effect. Adding sugars increases the binding energy of water in the material and decreases the rate of chemical reactions, reducing water activity and microbial growth [22]. However, not only the quantity of sugars is important but also their qualitative composition. For example, apple jam with 32.6% moisture has a lower A_w index (0.825) than butter cream with 15.2% moisture (0.851) due to a significant content of sugar and reducing sugars [23].

Monosaccharides have the greatest ability to bind water and reduce water activity, followed by disaccharides and polysaccharides. Sugar-containing substances can be arranged in the following order based on their ability to reduce the A_w index in products [24]:

Amylopectin → Maltohexaose → Maltotriose → Sucrose → Maltose → Lactulose → Glucose → Fructose → Xylose → Glycerin

Replacing white sugar with alternative starch products is one of the ways to reduce sweetness and easily digestible sugars, slow down drying and staling, and keep jelly fresh during storage. These alternative materials, e.g., starch syrup and glucose-fructose syrup, vary in carbohydrate composition and are technologically advantageous, inexpensive, and domestically produced in large quantities.

We aimed to study the quality of starch syrup (low-conversion, confectionery, and high-conversion) and glucose-fructose syrup, as well as their effect on the sensory, physicochemical, and microbiological parameters of jelly with different carbohydrate profiles after manufacture and during storage.

STUDY OBJECTS AND METHODS

Samples of starch syrup and glucose-fructose syrup (Kargill Company, Russia) were analyzed according to State Standard 33917-2016 and Specifications 10.62.13-001-00343579-2016 for the following parameters by using the following methods:

– the dry matter content: by the refractometric method;
– the content of reducing substances: by the Lane-Eynon method;
– the content of carbohydrates: by high performance liquid chromatography on a Shimadzu LC-2010 chromatograph with a RID-10A refractometric detector;
– pH value: by measuring the activity of hydrogen ions on a Testo 206 pH meter;
– acidity: by titration; and
– nutritional value: by calculation.

The jelly samples were based on apple pectin. The control sample was based on sugar and confectionery syrup in a ratio of 1:0.5. The experimental samples were free of white sugar and based on starch syrup (low-conversion, confectionery, and high-conversion) and glucose-fructose syrup.

The sensory quality of the jelly samples was evaluated on a 5-point scale by the descriptor-profile analysis according to State Standard ISO 13299-2015 [25]. It involved the following parameters and methods of their determination:

– the water content: by the refractometric method (State Standard 5900);
– the content of reducing substances: by the ferricyanide method (State Standard 5903);
– titratable acidity: by titration; and
– active acidity (pH): by the potentiometric method (State Standard 5898).

Water activity was measured by using a HygroPalm hygrometer (Rotronic, Switzerland) on a scale from 0 to 1, with an absolute error of ± 0.008 (± 0.1°C for temperature). The microbiological indicators were evaluated against State Standard 6442-2014 and Technical Regulations of the Customs Union 021/2011. In particular, we applied microbiological research methods to determine the total aerobic mesophilic count (State Standard 10444.15-94), coliform bacteria (State Standard 50474-93), and spoilage microorganisms (State Standard 10444.12- 88).

The jelly samples were stored in food-grade polyethylene terephthalate containers for 12 weeks at 21.0 ± 1.5°C and relative humidity of 82 ± 2%.

To prepare the control sample, apple pectin was mixed with white sugar in a ratio of 1:3. The resulting dry mixture was gradually added to hot water (70–75°C) and vigorously stirred until a homogeneous water-pectin mixture was obtained with a dry matter content of 25 ± 1%. Then, we added the remaining amount of white sugar, starch syrup heated to 50–55°C, and buffer salt (sodium lactate), stirred the mixture, and boiled it to obtain a jelly mass with a 27–29% water content. The mass was then cooled to 85–90°C, with citric acid and a food flavoring agent introduced into it. The jelly mass was poured into rigid molds to mature, dry, and cool.

The experimental samples were prepared according to the same method as the control, with erythritol used instead of white sugar (Fig. 1). Their ingredients, carbohydrate composition, and energy value are presented in Table 1.

RESULTS AND DISCUSSION

First, we studied the quality indicators of three types of starch syrup (low-conversion, confectionery, and high-conversion) and glucose-fructose syrup in comparison with those of sugar syrup used to prepare the control sample. The starch syrups differed significantly in their carbohydrate composition. They contained easily digestible reducing sugars (glucose and maltose) and polysaccharides (dextries and trisaccharides), with the latter responsible for dietetic properties (Table 2). In addition, the syrups contained minerals (0.10–0.37%) such as potassium, phosphorus, sodium, calcium, magnesium, and iron [26]. Unlike sugar syrup, starch syrup is free of sucrose and fructose,

Table 1 Ingredients, carbohydrate composition, and energy value of jelly samples with different carbohydrate profiles

Ingredients	Control (sugar and confectionery syrup)	Experimental sugar-free samples based on:			
		Low-conversion syrup	Confectionery syrup	High-conversion syrup	Glucose-fructose syrup
White sugar	+	–	–	–	–
Low-conversion syrup	–	+	–	–	–
Confectionery syrup	+	–	+	–	–
High-conversion syrup	–	–	–	+	–
Glucose-fructose syrup	–	–	–	–	+
Erythritol	–	+	+	+	+
Apple pectin	+	+	+	+	+
Sodium lactate (40%)	+	+	+	+	+
Citric acid (50%)	+	+	+	+	+
Food flavoring agent	+	+	+	+	+
Carbohydrates, g/100 g:					
total	79.1	74.6	74.4	72.2	79.0
reducing sugars	14.9 (glucose, maltose, fructose)	27.8 (glucose, maltose)	33.2 (glucose, maltose)	45.8 (glucose, maltose)	77.3 (glucose, maltose)
polysaccharides	13.7	46.9	41.4	26.2	–
Energy value, kcal	301	311	309	302	311

"+" – present, "–" – absent

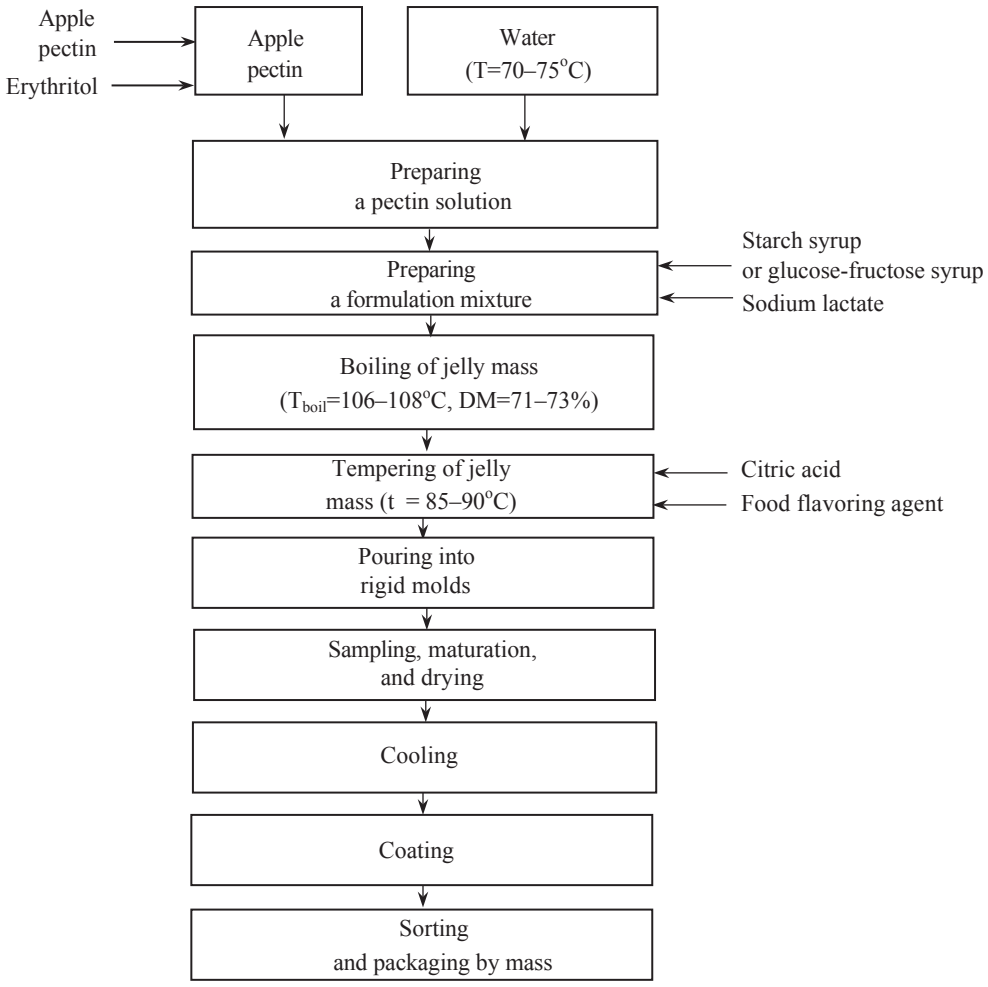

Figure 1 Process chart for jelly samples based on sugar-free starch syrup or glucose-fructose syrup

Table 2 Quality indicators and carbohydrate composition of starch syrup, glucose-fructose syrup, and sugar syrup

Quality indicators and carbohydrates	Sugar syrup (1:0.5)	Starch syrup			Glucose-fructose syrup
		Low-conversion	Confectionery	High-conversion	
Dry matter content, %	80.2	79.3	78.9	83.0	70.6
Content of reducing substances (or dextrose equivalent), %	14.5	32.3 (26–35*)	40.4 (36–44*)	62.6 (45 and over*)	70.5
Content of carbohydrates, %:	80.1	79.1	78.7Ц	82.5	70.5
– sucrose	50.6	–	–	–	–
– glucose	6.3	14.5	20.8	31.8	38.8
– fructose	2.5	–	–	–	28.6
– maltose	5.7	17.8	19.6	30.8	3.1
– polysaccharides (dextrins)	15.0	46.8	38.3	19.9	–
Active acidity, pH units	6.4	5.1	5.0	4.7	3.6
Sweetness coefficient, units	0.8	0.3	0.4	0.6	1.2

* according to State Standard 33917-2016

a highly hygroscopic reducing carbohydrate that significantly increases jelly's wettability during storage.

All the types of starch syrup had a lower sweetness coefficient (by 0.2–0.5 units), lower values of active acidity (by 1.3–1.7 pH units), and a higher ash content (2.0–7.4 times) than the sugar syrup. The high-conversion syrup contained the largest amount of reducing sugars (62.6%, including 31.8% glucose and 30.8% maltose) and the smallest amount of polysaccharides (19.9%). The low-conversion syrup, on the contrary, had the highest content of polysaccharides (46.8%) and the lowest content of reducing sugars (32.3%, including 14.5% glucose and 17.8% maltose). The confectionery syrup contained 40.4% of reducing sugars (20.8% glucose, 19.6% maltose) and 38.3% of polysaccharides. The glucose-fructose syrup had a lower value of active acidity (by 3.6 pH units) and a higher sweetness coefficient (by 1.2) than the sugar syrup. This was due to its significant content of easily digestible reducing sugars (70.5%, including 28.6% fructose, 38.8% glucose, and 3.1% maltose) and the absence of sucrose and polysaccharides.

Replacing sugar with starch syrup or glucose-fructose syrup significantly changed the carbohydrate composition of the jelly samples (Table 1). This not only depended on the chemical composition of the raw materials but also the chemical processes in the jelly mass during boiling. Unlike the control, the experimental samples contained no sucrose.

The control sample had 65.4% of easily digestible carbohydrates, including 50.5% of sucrose and 14.9% of reducing sugars (fructose, glucose, and maltose), as well as 13.7% of polysaccharides. The samples based on low-conversion syrup had a lower content of reducing sugars (glucose and maltose) and more polysaccharides (27.8 and 46.9%, respectively) than the other experimental samples. The samples based on confectionery syrup contained 33.2% of reducing sugars and 41.4% of polysaccharides. The samples based on high-conversion syrup contained more reducing sugars and fewer polysaccharides (45.8 and 26.2%, respectively) than the other experimental samples. The glucose-fructose syrup sample contained more reducing sugars (77.3%) than the other samples but no sucrose or polysaccharides.

Thus, all the samples based on starch syrup contained 1.9–3.4 times more polysaccharides and 1.4–2.4 times fewer reducing sugars than the control. However, the sample based on glucose-fructose syrup had a 1.2 times higher content of reducing sugars.

The sensory evaluation of the jelly samples was based on the quantitative descriptor-profile analysis. In this analysis, each of the main sensory indicators (taste, color, smell, texture) is presented as a set of components

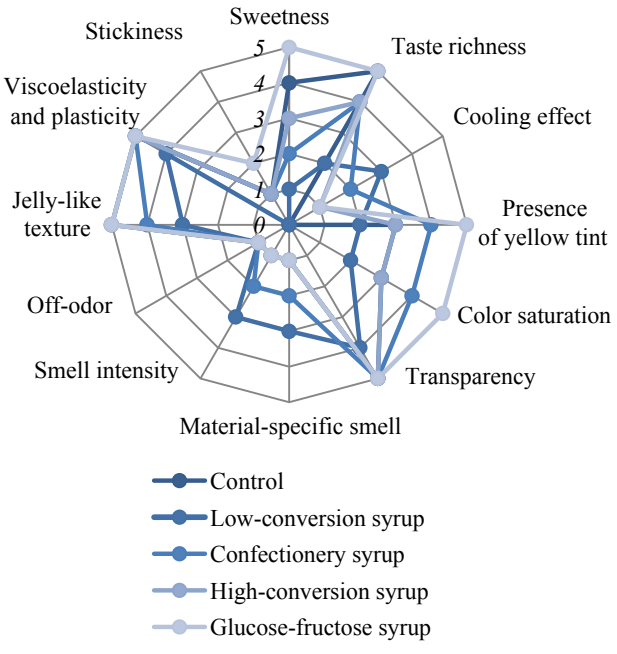

Figure 2 Sensory evaluation of jelly samples with various carbohydrate profiles

Table 3 Water content changes in the jelly samples with various carbohydrate profiles during storage

Storage time, weeks	Water content in the jelly samples based on				
	Sugar and confectionery syrup (control)	Low-conversion starch syrup	Confectionery starch syrup	High-conversion starch syrup	Glucose-fructose syrup
0 (after drying)	20.8 ± 0.2	19.5 ± 0.1	19.1 ± 0.2	20.0 ± 0.1	20.6 ± 0.1
1	19.4 ± 0.1	18.1 ± 0.1	18.7 ± 0.3	19.6 ± 0.1	20.1 ± 0.1
2	18.8 ± 0.1	17.8 ± 0.2	18.4 ± 0.3	19.1 ± 0.1	19.8 ± 0.2
3	17.3 ± 0.1	17.6 ± 0.3	17.9 ± 0.2	18.9 ± 0.2	19.5 ± 0.1
4	16.8 ± 0.2	17.3 ± 0.2	17.5 ± 0.2	18.6 ± 0.1	19.1 ± 0.2
5	16.3 ± 0.3	17.1 ± 0.1	17.2 ± 0.2	18.2 ± 0.2	18.9 ± 0.1
6	15.9 ± 0.2	mold appeared on the surface water content not determined	16.8 ± 0.1	17.8 ± 0.1	18.7 ± 0.1
7	15.4 ± 0.2		16.2 ± 0.2	17.4 ± 0.2	18.5 ± 0.3
8	15.0 ± 0.1		15.6 ± 0.2	16.8 ± 0.2	18.2 ± 0.2
9	14.6 ± 0.2		15.0 ± 0.2	16.4 ± 0.3	17.9 ± 0.1
10	14.1 ± 0.1		14.7 ± 0.1	15.9 ± 0.2	17.7 ± 0.2
11	13.5 ± 0.3		14.1 ± 0.2	15.6 ± 0.2	17.4 ± 0.2
12	12.7 ± 0.1		13.7 ± 0.2	15.1 ± 0.1	17.1 ± 0.1
Changes in water content after 3 months of storage, % of the initial value:					
ΔW, %	–38.9	–	–28.3	–24.5	–17.0

(or descriptors) that are scored by the panelists according to their presence and intensity. The results are graphically depicted in the form of a profile diagram.

In our study, 20 panelists aged 19–23 evaluated the following sensory indicators of the jelly samples (descriptors listed in brackets): taste (sweetness, richness, cooling effect); color (yellow tint, saturation, transparency); smell (material-specific smell, intensity, off-odor); and texture (jelly-like, viscoelasticity and plasticity, stickiness).

Figure 2 shows the profile diagram of the jelly quality evaluated on a 5-point scale of intensity with weight coefficients representing the significance of each indicator.

The descriptor-profile analysis showed that the samples based on high-conversion syrup and glucose-fructose syrup had the greatest sweetness, taste richness, color saturation, and transparency. Also, the sample with glucose-fructose syrup had a slight effect of stickiness on its surface. This was because it had the highest content of reducing sugars (mostly fructose) which turn into coloring, humic substances and aldehydes during boiling and intensify the product's color, aroma, and hygroscopicity.

The jelly based on low-conversion syrup had the lowest sweetness, taste richness, and color brightness, as well as low texture density and elasticity. These values can be explained by its highest content of polysaccharides which bind less water and therefore make the product less viscous and strong. The sample based on confectionery syrup had the most optimal profile, with moderate sweetness and taste richness, good jelly-like texture, viscoelasticity, and plasticity, no effect of wetting or stickiness, and a color similar to that of the control.

The jelly samples with various carbohydrate compositions were packed in plastic containers and stored for 12 weeks to study changes in their water content (W), water activity (A_w), and pH (Table 3). The initial (after preparation) water contents in the control sample, the starch syrup-based samples, and the jelly based on glucose-fructose syrup were 20.8 ± 0.2, 19.1 ± 0.2–20.0 ± 0.1, and 20.6 ± 0.1, respectively. Their pH values were 3.4, 3.0–3.3, and 2.8, respectively.

All the jelly samples showed a gradual decrease in the water content and changes in water activity during storage. After 12 weeks of storage, the control sample had the highest loss of water (38.9%), compared to the experimental samples (17.0–28.3%). This was because it contained a significant amount of sucrose (50.6%) and a small amount of reducing substances (14.9%). In the process of moisture transfer during storage, sucrose crystallization centers gradually began to develop on the sample's surface. They subsequently grew in size forming a thin crystalline sugar crust and gradually sugaring the whole product. During this process, free moisture quickly left the intercrystalline space, causing the product to dry out and stale.

The jelly based on low-conversion syrup was losing water more slowly than the control but faster than the other experimental samples at the beginning of storage. This was due to its significant content of polysaccharides (46.9%), which bind and retain water to a lesser extent than reducing substances. Since mold appeared on its surface after 5 weeks of storage, the studied parameters were no longer determined. The jellies based on confectionery syrup and high-conversion syrup had lower water losses (28.3 and 24.5%, respectively), compared to the control. The lowest water loss (17.0%) was registered in the sample based on glucose-fructose

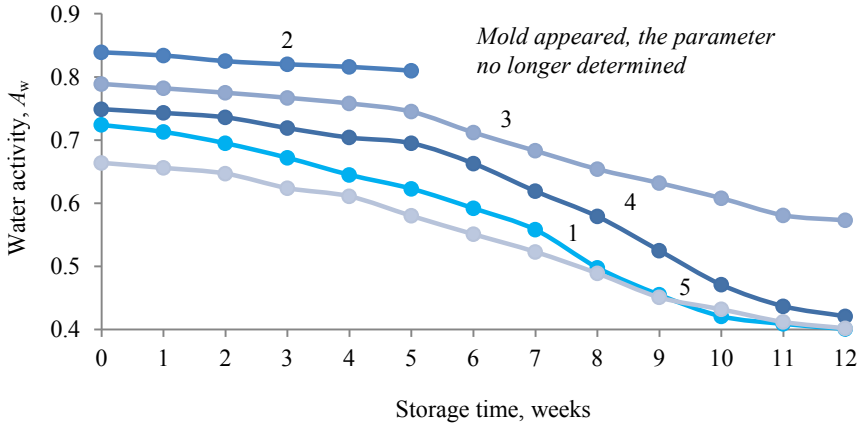

Figure 3 Water activity in jellies with various carbohydrate compositions during storage: 1 – control (based on sugar and confectionery syrup); sugar-free samples: 2 – based on low-conversion syrup; 3 – based on confectionery syrup; 4 – based on high-conversion syrup; 5 – based on glucose-fructose syrup

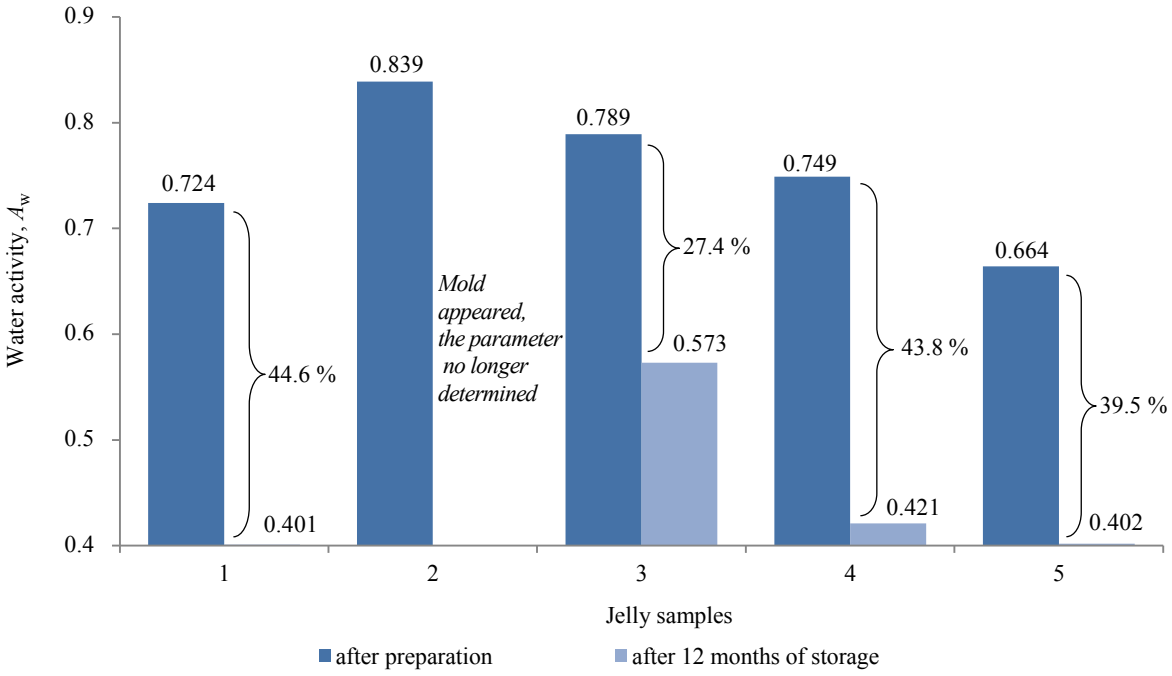

Figure 4 Water activity in jellies with various carbohydrate compositions after preparation and after 12 months of storage: 1 – control (based on sugar and confectionery syrup); sugar-free samples: 2 – based on low-conversion syrup; 3 – based on confectionery syrup; 4 – based on high-conversion syrup; 5 – based on glucose-fructose syrup

syrup. It contained the largest amount of reducing substances (fructose and glucose), which contributed to slower drying and greater freshness preservation.

Thus, the jelly's carbohydrate composition (the ratio of mono-, di-, and polysaccharides) significantly affected the process of moisture exchange during storage and therefore the product's drying and staling. Using various types of starch syrup and glucose-fructose syrup with a high content of reducing sugars (especially glucose and fructose with higher solubility than maltose or dextrins) significantly slowed down the drying of jelly and increased its shelf life.

Figure 3 shows the changes in water activity in the packaged jelly samples during 12 weeks of storage. As we can see, the longer was the storage time, the lower was water activity in all the samples. We also found that the lower was the water loss, the more changes in water activity it caused (Fig. 4).

The decrease in water activity was associated with two processes – water loss during storage and the use of starch products with a different ratio of mono-, di-, and polysaccharides. Monosaccharides reduce water activity to a greater extent than disaccharides due to their solubility and hygroscopicity. The solubility of mono-

and disaccharides varies greatly, amounting (at 100 °C) to 98.4, 87.7, 86.1, and 82.9% for fructose, glucose, maltose, and sucrose, respectively [27, 28]. Fructose contributes to the greatest decrease in water activity, followed by glucose, maltose, and sucrose. The tendency of sugar molecules to hydration is associated with the presence of hydroxyl and aldehyde groups capable of forming hydrogen bonds with water molecules. The more reducing sugars the product contains, the more they bind water molecules and slow down its staling [29].

According to the sorption isotherm (Fig. 5), the initial water activity values in all the jelly samples ranged from 0.664 ± 0.012 to 0.839 ± 0.011. Therefore, we can classify them as intermediate moisture products.

Figure 5 shows a certain correlation between the water content and the water activity index that is determined by both the content of carbohydrates and their ratio in the sample. The control sample had the greatest decrease in water activity, namely 44.6% (Fig. 4). The sample based on low-conversion syrup had the highest initial value of water activity (0.839). This was due to its low content of reducing sugars with a preservative effect and high water-binding capacity, which led to gradual molding after 5 weeks of storage. The water activity values of the samples based on high-conversion syrup and glucose-fructose syrup were initially lower than in the other samples (0.749 and 0.664, respectively). After 12 weeks of storage, they decreased more than in the other samples (by 43.8 and 39.5%, respectively) due to significant amounts of reducing sugars in their composition (45.8 and 77.3%, respectively). The sample based on confectionery syrup had the lowest decrease in water activity, namely 27.4% (Fig. 4). During storage, this sample dried more slowly than the control. It did not get wet and retained its viscoelasticity and plasticity, with no crystalline crust forming on its surface.

The sensory indicators of the jelly samples after 12 weeks of storage are presented in Table 4.

The antimicrobial effect of carbohydrates is primarily based on decreasing water activity, which slows down most chemical reactions responsible for the product's deterioration, increases the binding energy of water, and reduces the ability of microorganisms to use it for metabolism. High water content (21–15%) and water activity (0.6–0.8) in jelly are among the causes of its microbiological spoilage, leading to the development of molds and yeasts [30, 31].

In our samples, the water content was 19.1–20.8% and water activity varied from 0.664 ± 0.012 to 0.839 ± 0.011, which might indicate possible development of microorganisms and mold. Therefore, we decided to study changes in the microbiological indicators throughout the entire shelf life of the jelly samples.

Based on the Technical Regulations of the Customs Union 021/2011, we determined the total number of pathogenic microorganisms, aerobic mesophilic bacteria, molds and yeasts, spore-forming bacteria, and coliform bacteria in the jelly samples. We analyzed their microbiological stability after storage and found that the indicators under study did not exceed the tolerance levels in the control and the experimental samples based on confectionery syrup, high-conversion syrup, and glucose-fructose syrup. Also, we detected no pathogenic microorganisms or coliform bacteria in the samples (Table 5).

Table 4 Sensory indicators of jelly samples with various carbohydrate profiles during storage*

Indicator	Jelly samples based on				
	Sugar and confectionery syrup (control)	Low-conversion starch syrup	Confectionery starch syrup	High-conversion starch syrup	Glucose-fructose syrup
Taste, color, smell	Sickeningly sweet, bright yellow, no off-odor	Slightly sweet, yellow-beige, a subtle smell of syrup	Moderately sweet, yellow with a golden tint, a subtle smell of syrup	Sweet, yellow, no off-odor	Sweet, bright yellow with an orange tint, no off-odor
Texture	Homogeneous, jelly-like, viscoelastic, plastic,				
	Quite dense	Slightly dense	Quite dense	Quite dense	Quite dense
Shape	Regular, with an indistinct contour due to sucrose crystallization on the surface	Regular, with a clear contour, no deformation	Regular, with a clear contour, no deformation	Regular, with a clear contour, no deformation	Regular, with an indistinct contour due to sagging of wet areas of the surface
Surface	Not sticky, covered with a fine crystalline sugar crust, transparent	Not sticky, without a crystalline crust, transparent	Not sticky, without a crystalline crust, transparent	Not sticky, a fine crystalline crust beginning to form due to glucose crystallization, transparent	Slightly wet and sticky, transparent

*The control and the experimental samples based on confectionery syrup, high-conversion syrup, and glucose-fructose syrup were evaluated after 12 weeks of storage; the sample based on low-conversion syrup was evaluated after 5 weeks of storage

Table 5 Microbiological indicators of jelly samples with various carbohydrate profiles during storage*

Indicator	Technical Regulations of the Customs Union 021/2011 (tolerance)	Jelly samples based on				
		Sugar and confectionery syrup (control)	Low-conversion starch syrup	Confectionery starch syrup	High-conversion starch syrup	Glucose-fructose syrup
Pathogenic microorganisms, incl. salmonella (not allowed), g	25			Not detected		
Aerobic mesophilic bacteria, CFU/g	max 1×10^3	1.5×10^2	2.3×10^3	0.8×10^3	2.8×10^2	1.4×10^2
Coliform bacteria (not allowed), g (cm^3)	0.1			Not detected		
Molds, CFU/g	max 100	24	105	64	43	16
Yeast, CFU/g	max 50	18	54	36	24	14

*The control sample and the experimental samples based on confectionery syrup, high-conversion syrup, and glucose-fructose syrup were evaluated after 12 weeks of storage; the sample based on low-conversion syrup was evaluated after 5 weeks of storage

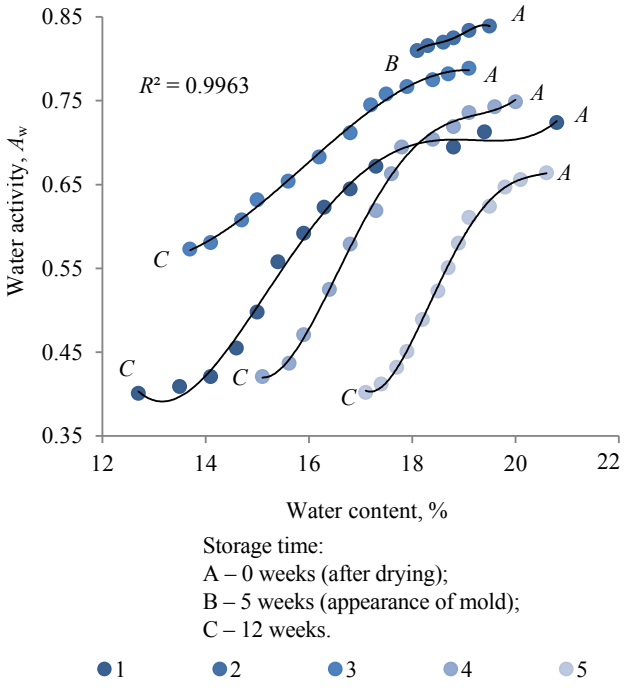

Figure 5 The sorption isotherm of the jelly samples with various carbohydrate compositions: 1 – control (based on sugar and confectionery syrup); sugar-free samples: 2 – based on low-conversion syrup; 3 – based on confectionery syrup; 4 – based on high-conversion syrup; 5 – based on glucose-fructose syrup

The jelly based on low-conversion syrup had its counts of aerobic mesophilic bacteria, molds, and yeasts exceeding the tolerance levels 2.3, 1.9, and 1.8 times, respectively. This can be explained by a low content of reducing sugars with a preservative effect and a high water activity index in this sample. To improve its microbiological indicators and reduce water activity, a larger amount of a preservative agent should be added to its formulation. For example, it could be a sweetener with low sugar and calorie contents and a high water-binding capacity (erythritol, sorbitol, xylitol, etc.). Alternatively, some food acid or concentrated juice with high acidity could be used to increase the carbohydrate content and acidity in the product.

Thus, changing the concentration of carbohydrates with different water-retaining properties can have an additional preservative effect on jelly in combination with other technological factors. The risk of microbiological spoilage can be reduced not only by adjusting the formulation (lowering water activity and pH), but also by ensuring low levels of initial microbiological contamination of the product.

CONCLUSION

Our study showed that jelly can be produced with various types of starch syrup (low-conversion, confectionery, and high-conversion) or glucose-fructose syrup used instead of white sugar. This can expand the range of jellies with different carbohydrate profiles and prolong their shelf life.

We found that using starch or glucose-fructose syrups significantly changed the carbohydrate composition of the jelly. Unlike the control, the experimental samples did not contain any sucrose. The starch syrup-based samples had more polysaccharides (1.9–3.4 times) and fewer easily digestible reducing sugars (1.4–2.4 times), while the sample with glucose-fructose syrup had a higher content of reducing sugars (1.2 times) than the control. The sample based on confectionery syrup had the most optimal profile, with moderate sweetness and taste richness, good jelly-like texture, viscoelasticity and plasticity, no effect of wetting or stickiness, and the color similar to that of the control sample.

Different amounts and ratios of mono-, di-, and polysaccharides significantly affected the moisture transfer and the preservation of jelly freshness after 12 weeks of storage. The control sample had the greatest water loss (38.9 %), compared to the experimental samples. The samples based on high-conversion syrup and glucose-fructose syrup were least subjected to drying due to high contents of reducing sugars, especially fructose and glucose, highly hygroscopic sugars that can bind water and slow down the process

of staling. The water activity index of the jelly samples after preparation ranged from 0.664 ± 0.012 to 0.839 ± ± 0.011, so they were classified as intermediate moisture products. After storage, this index decreased most in the samples based on high-conversion and glucose-fructose syrups and least in the sample based on confectionery syrup.

The microbiological indicators of all the samples, except for the jelly based on low-conversion syrup, did not exceed the standard tolerance levels. Neither did we detect any pathogenic microorganisms or coliform bacteria in them. The jelly based on low-conversion syrup had its counts of aerobic mesophilic bacteria, molds, and yeasts exceeding the tolerance levels 2.3, 1.9, and 1.8 times, respectively. To improve its microbiological indicators and reduce water activity, a larger amount of a preservative should be added to its formulation, such as a sweetener (erythritol, sorbitol, xylitol, etc.), a food acid, or a concentrated juice with high acidity that can increase the carbohydrate content and acidity in the product.

CONTRIBUTION

I.V. Plotnikova reviewed the literature on the study problem, proposed a methodology for the experiment, conducted the experiment, processed experimental data, performed calculations, and edited the manuscript. G.O. Magomedov developed the study concept and supervised the experiment. I.M. Zharkova reviewed the literature on the study problem and edited the manuscript. E.N. Miroshnichenko edited the manuscript for submission. V.E. Plotnikov conducted the experiment, processed experimental data, and performed calculations.

CONFLICT OF INTEREST

All the authors were equally involved in writing the manuscript and are responsible for plagiarism.

ACKNOWLEDGEMENTS

We thank Raisa I. Ivanova, General Director of the Confectionery Factory (Vologda), for providing raw materials and an opportunity to test the samples in industrial conditions.

REFERENCES

1. Kondratev NB, Osipov MV, Rudenko OS, Kazantsev EV, Kalinkina ES. The main factors of marmalade molecular structure formation. Food Systems. 2021;4(3):172–179. (In Russ.). https://doi.org/10.21323/2618-9771-2021-4-3-172-179
2. Pesterev MA, Rudenko OS, Kondrat'ev NB, Bazhenova AE, Usachev IS. Effect of biodegradable and polypropylene film packaging on the safety profile of jelly marmalade. Food Processing: Techniques and Technology. 2020;50(3):536–548. (In Russ.). https://doi.org/10.21603/2074-9414-2020-3-536-548
3. Arslaner A, Salik A, Bakirci I. The effects of adding *Hibiscus sabdariffa* L. flowers marmalade on some quality properties, mineral content and antioxidant activities of yogurt. Journal of Food Science and Technology. 2021;58(1):223–233. https://doi.org/10.1007/s13197-020-04533-z
4. Afi L, Roufegarinejad L, Mitra S. Investigating the effect of sugar replacement with sorbitol as low-caloric sweetener on the physicochemical and sensory characteristics of strawberry marmalade. Food Science and Technology. 2019;16(88):161–172.
5. Kazantsev EV, Kondratyev NB, Osipov MV, Rudenko OS, Linovskaya NV. Management of moisture transfer processes during the storage of confectionery with a jelly-like consistency. Proceedings of the Voronezh State University of Engineering Technologies. 2020;82(4):47–53. (In Russ.). https://doi.org/10.20914/2310-1202-2020-4-47-53
6. Figueroa LE, Genovese DB. Fruit jellies enriched with dietary fibre: Development and characterization of a novel functional food product. LWT. 2019;111:423–428. https://doi.org/10.1016/j.lwt.2019.05.031
7. Gribova NA, Eliseeva LG. Study of structure-forming agents and development of jelly marmalade based on a spent osmotic agent. Proceedings of the Voronezh State University of Engineering Technologies. 2021;83(3):98–105. (In Russ.).
8. Kodatsky YuA, Klyukina ON, Nepovinnykh NV, Ptichkina NM, Shmakov SL, Eganekhzad S, *et al.* Study of the viscoelastic properties and water activity in the marshmallow, based on polysaccharides of plant and microbial origin. Food Industry. 2016;(4):30–33. (In Russ.).
9. Soldatova EA, Misteneva SYu, Savenkova TV. Conditions and criteria for ensuring the storage ability of confectionery. Food Industry. 2019;(5):82–85. (In Russ.). https://doi.org/10.24411/0235-2486-2019-10078
10. Nistor O-V, Bolea CA, Andronoiu D-G, Cotârlet M, Stanciuc N. Attempts for developing novel sugar-based and sugar-free sea buckthorn marmalades. Molecules. 2021;26(11). https://doi.org/10.3390/molecules26113073

11. Belokurova ES, Pankina IA, Sevastianova AD, Asfondiarova IV, Katkova NM. The effect of functional additives on the indicator “water activity” of biscuit semi-finished products. IOP Conference Series: Earth and Environmental Science. 2021;640(2). https://doi.org/10.1088/1755-1315/640/2/022022

12. Iorgachova KG, Avetisian KV. Quality adjustment for jelly marmalade of a modified carbohydrate structure. Eastern-European Journal of Enterprise Technologies. 2016;2(11):48–56. (In Russ.). https://doi.org/10.15587/1729-4061.2016.65768

13. Tabatorovich AN, Reznichenko IYu. Formulation and quality assessment of diabetic jelly marmalade “Karkade” fortified with succinic acid. Food Processing: Techniques and Technology. 2019;49(2):320–329. (In Russ.). https://doi.org/10.21603/2074-9414-2019-2-320-329

14. Kondratyev NB, Kazantsev EV, Osipov MV, Bazhenova AE, Linovskaya NV. The influence of the amount of caramel syrup on the processes of moisture transfer during the storage of marmalade. Proceedings of the Voronezh State University of Engineering Technologies. 2020;82(4):24–29. (In Russ.). https://doi.org/10.20914/2310-1202-2020-4-24-29

15. Bolotov VM, Savvin PN, Komarova EV, Koshevarova IB. Effect of natural carotenoids and anthocyanins on properties of healthy food products. IOP Conference Series: Earth and Environmental Science. 2021;640(5). https://doi.org/10.1088/1755-1315/640/5/052001

16. Teixeira-Lemos E, Almeida AR, Vouga B, Morais C, Correia I, Pereira P, *et al.* Development and characterization of healthy gummy jellies containing natural fruits. Open Agriculture. 2021;6(1):466–478. https://doi.org/10.1515/opag-2021-0029

17. Di Monaco R, Miele NA, Cabisidan EK, Cavella S. Strategies to reduce sugars in food. Current Opinion in Food Science. 2018;19:92–97. https://doi.org/10.1016/j.cofs.2018.03.008

18. Belkacem A, Ellouze I, Debbabi H. Partial substitution of sucrose by non-nutritive sweeteners in sour orange marmalades: effects on quality characteristics and acute postprandial glycemic response in healthy volunteers. The North African Journal of Food and Nutrition Research. 2021;5(11):1–9. https://doi.org/10.51745/najfnr.5.11.1-9

19. Nepovinnykh NV, Klyukina ON, Kodatskiy YuA, Ptichkina NM, Yeganehzad S. Study of the stability of foam and viscoelastic properties of marshmallow without gelatin. Foods and Raw Materials. 2018;6(1):90–98. https://doi.org/10.21603/2308-4057-2018-1-90-98

20. Milani J, Maleki G. Hydrocolloids in food industry. In: Valdez B, editor. Food Industrial processes – methods and equipment. Croatia: InTech; 2012. pp. 17–38. https://doi.org/10.5772/32358

21. Piskunenko KR, Popov VG. Trends in production of functional marmalade. Proceedings of the Voronezh State University of Engineering Technologies. 2020;82(2):72–76. (In Russ.). https://doi.org/10.20914/2310-1202-2020-2-72-76

22. Barbosa-Cánovas GV, Fontana AJ, Schmidt SJ, Labuza TP. Water activity in foods: Fundamentals and applications. Oxford: Blackwell Publishing; 2007. 440 p.

23. Nikitin IA, Nikitina MA, Allilueva NM, Krivosheev AYu. Comprehensive assessment of fruit jelly with an improved carbohydrate profile based on unconventional plant raw materials. Foods and Raw Materials. 2019;7(1):26–34. https://doi.org/10.21603/2308-4057-2019-1-26-34

24. Caballero-Ceron C, Guerrero-Beltran JA, Mujica-Paz H, Torres JA, Welti-Chanes J. Moisture sorption isotherms of foods: Experimental methodology, mathematical analysis, and practical applications. In: Gutiérrez-López GF, Alamilla-Beltrán L, Buera MP, Welti-Chanes J, Parada-Arias E, Barbosa-Cánovas GV, editors. Water stress in biological, chemical, pharmaceutical and food systems. New York: Springer; 2015. pp. 187–214. https://doi.org/10.1007/978-1-4939-2578-0_15

25. Ben Rejeb I, Dhen N, Kassebi S, Gargouri M. Quality evaluation and functional properties of reduced sugar jellies formulated from citrus fruits. Journal of Chemistry. 2020;2020. https://doi.org/10.1155/2020/5476872

26. Kavaya RI, Omwamba MN, Chikamai BN, Mahungu SM. Sensory evaluation of syneresis reduced jam and marmalade containing gum Arabic from *Acacia senegal* var. *kerensis*. Food and Nutrition Sciences. 2019;10(11). https://doi.org/10.4236/fns.2019.1011096
27. Rubio-Arraez S, Capella JV, Castelló ML, Ortolá MD. Physicochemical characteristics of citrus jelly with non cariogenic and functional sweeteners. Journal of Food Science and Technology. 2016;53(10):3642–3650. https://doi.org/10.1007/s13197-016-2319-4
28. Goshchansakaya MN, Fetisov EA, Petrov AN, Radaeva IA, Turovskaya SN, Galstyan AG. Water activity in fructose solutions. Food Processing: Techniques and Technology. 2010;18(3):100–106. (In Russ.).
29. Yazdani F, Raftani Amiri Z, Shahiri Tabarestani H. Preparation of low calorie sour tea jelly using stevia and gelatin of chicken skin-evaluation of the product. Journal of Food Technology and Nutrition. 2021;18(3):55–68.
30. Rubio-Arraez S, Benavent C, Ortolá MD, Castelló ML. Influence of low glycaemic index sweeteners on antioxidant, sensory, mechanical, and physicochemical properties of a watermelon jelly. Journal of Food Quality. 2018;2018. https://doi.org/10.1155/2018/8412017
31. Einhorn-Stoll U, Kunzek H. The influence of the storage conditions heat and humidity on conformation, state transitions and degradation behaviour of dried pectins. Food Hydrocolloids. 2009;23(3):856–866. https://doi.org/10.1016/j.foodhyd.2008.05.001.

ORCID IDs
Inessa V. Plotnikova https://orcid.org/0000-0001-5959-6652
Gazibeg O. Magomedov https://orcid.org/0000-0002-7201-8387
Irina M. Zharkova https://orcid.org/0000-0001-8662-4559
Viktor E. Plotnikov https://orcid.org/0000-0001-6707-8337

Foods and Raw Materials. 2022;10(2)

ISSN 2310-9599 (Print)
ISSN 2308-4057 (Online)

Research Article
Open Access

Available online at http://jfrm.ru/en
https://doi.org/10.21603/2308-4057-2022-2-537
https://elibrary.ru/XJUPLS

Development of plant-based yogurt

Nehaa Baskar, Sabitha Varadharajan, Mathushree Rameshbabu, Sudha Ayyasamy*, Sangeetha Velusamy

Kongu Engineering College, Perundurai, India

* e-mail: sudhaseshu@gmail.com

Received 28.12.2021; Revised 19.02.2022; Accepted 01.03.2022; Published online 23.09.2022

Abstract:
Fermented drinks are regarded as healthy food due to their probiotic nature. Vegan consumers who choose sustainable diet and people allergic to dairy products demand alternatives for dairy products. We aimed to develop a non-dairy plant-based yogurt from peanut, oats, and coconut milk.

Yogurt was formulated using peanut milk, oats milk and coconut milk with addition of sugar, corn starch, pectin, and xanthan gum. Simplex-lattice mixture design was applied to optimize the composition of the yogurt and achieve the desired rheological properties, sensory attributes, and syneresis rate.

Our results revealed that the formulation containing 7.13 mL of peanut milk, 10 mL of oats milk, and 7.86 mL of coconut milk showed low syneresis rate, desired viscosity and flow behavior, as well as high overall acceptability. We found that increased amounts of peanut and oats milk improved the product's viscosity due to high protein contents. However, coconut milk enhanced the taste and flavor of the yogurt. Flow behavior depended on viscosity and stabilizers used in accordance with the power law model. Syneresis rate was influenced by the viscosity of the yogurt. The utilization of corn starch, pectin, and xanthan gum not only improved the texture but also helped achieve the desired viscosity and flow behavior.

The nutrient composition, physicochemical properties, and high sensory characteristics of the yogurt based on peanut, oats, and coconut milk allow using it as a cow milk alterative in the diet of people with lactose intolerance.

Keywords: Plant-based yogurt alternative, peanut milk, oats milk, coconut milk, mixture design

Please cite this article in press as: Baskar N, Varadharajan S, Rameshbabu M, Ayyasamy S, Velusamy S. Development of plant-based yogurt. Foods and Raw Materials. 2022;10(2):274–282. https://doi.org/10.21603/2308-4057-2022-2-537

INTRODUCTION

Conventional yogurt is a product made by fermentation of milk. Bacteria ferment milk sugars and produce acid which can act on milk protein and produce textured yogurt [1]. Nowadays, many people have lactose intolerance and are allergic to dairy products. For them, plant-based yogurt is an alternative.

In this work, we used oats, peanut, or coconut milk as an alternative to cow milk. These ingredients increase the nutritive value of yogurt and provides it with an honest flavor. Fermentation of plant materials using mixed cultures was found to be mutually beneficial for the human body. Mutualism was found to exist between proteolytic *Lactobacillus bulgaricus* and non-proteolytic *Streptococcus thermophilus* as the former releases free amino acids and peptides as a nitrogen source, while the latter supplies growth factors such as pyruvic acid, folic acid, formic acid, and carbon dioxide [2]. *L. bulgaricus* and *S. thermophilus* are used in yogurt as starter cultures [3].

The fermentation time determines the acidity level of yogurt. Longer fermentation produces highly acidic yogurt [4]. A low sugar content in plant milk embarrasses acid production by carboxylic acid bacteria, which requires sucrose addition. Stabilizers and gelling agents are used to improve yogurt texture and creaminess, mostly pectin, starch, gelatin, and gums. They turn into a gel when heated in the presence of liquid. They are widely utilized in jams and jellies [5]. Proper heat treatment of plant-based milk is important before fermentation for starch to gelatinize. It increases the viscosity of yogurt and helps prevent phase separation. In addition, it decreases the quantity of endogenous microbes before starter inoculation [1].

Coconut milk has a milky white color. Its nutritional content includes fat, ash, water, carbohydrate, protein, and their derivatives. The effectiveness of extraction and the composition of coconut milk rely on the processing parameters such as temperature of added water and pressing conditions. The fat content also plays an important role in the flow properties of milk [6]. According to the National Centre for Biotechnology Information, lauric acid has antifungal and antiviral properties which fight against many human diseases. Lauric acid also reduces cholesterol and triglycerides, which is helpful in treating cardiovascular diseases [7].

Oat grains are a rich source of beta-glucan, a dietary soluble fiber. They have a 5–9% lipid content and are rich in polyunsaturated fatty acids, including linoleic acid, an essential fatty acid. In addition, oats contain avenanthramide, an antioxidant, as well as tocotrienols and tocopherols, vitamin E-like compounds. Oats have cardiovascular benefits due to their cholesterol-reducing properties. They have a high content of starch (60%), protein (11–15%), and lipids (5–9%). Their essential amino acids include oleic acid (45.60 g/kg), linoleic acid (36.2–40.4%), and linolenic acid (38.4–41.6%). Thus, oats milk plays a key role in competing with numerous substitutes of dairy milk in the continuously expanding market of dairy and non-dairy products [8].

Peanut milk and its products have high dietary benefits for all age groups due to a high content of protein, essential fatty acids (linoleic and oleic acids), and minerals. Peanut milk also contains hexanal, an important component responsible for its undesirable beany flavor which is entirely eliminated by fermentation or cooking. The stability of peanut milk and its products is highly enhanced by heating at 66–87°C for about 15–20 min and homogenization. This increase in stability is caused by the solubility of proteins [9].

We aimed to formulate a plant-based yogurt, optimize its ingredients and process conditions, as well as analyze its physicochemical, rheological, and nutritive qualities.

STUDY OBJECTS AND METHODS

Raw peanut, coconut, and oats were procured from the local market in Erode, India. We used the Vegan Greek Yogurt Starter Culture (Alla's Posh Flavors, Uttar Pradesh, India) that contained live cultures of *Lactobacillus bulgaricus* and *Streptococcus thermophilus* stored in a freezer at –18°C. Xanthan gum, pectin, and corn starch were of the Urban Platter brands.

Peanut milk was prepared by immersing raw peanuts in potable water for about 8–10 h at room temperature. Then, the soaked peanuts were blended using a food processor with an adequate amount of water and filtered with cheesecloth/muslin or a strainer. The supernatant was collected.

Coconut milk was prepared from fresh and matured coconut endosperm which was cut into pieces and blended using a food processor with an adequate amount of water and filtered with cheesecloth/muslin or a strainer. The supernatant was collected.

Oats milk was prepared by soaking freshly bought oats in water for about 30 min until they absorbed enough moisture for milk extraction. Then, they were blended and filtered using cheesecloth/muslin. The milk was extracted by ensuring enough beta-glucan was present in the supernatant.

To prepare a cow milk yogurt alternative, the milk samples were pasteurized at an optimum temperature of 72°C for 20 min by a double boiling method to avoid gelatinization. This method uses the steam from the simmering water to warm the milk in the bowl gently with indirect heat. Then, the milk was cooled to 45°C. The starter cultures (*L. bulgaricus* and *S. thermophilus*) were added as 0.4% of the milk mixture weight. After inoculation, 10% of sucrose was added to the milk mixture to optimize the growth of lactic acid bacteria. To strengthen the gel network of the yogurt, we added corn starch (5%) at above 60°C, xanthan gum (0.15%) at above 70°C under continuous stirring, and pectin (0.75%) at above 25°C. The milk was incubated at 41°C for 18 h to maintain the humidity and temperature in favorable conditions for the growth of microorganisms. The formed yogurt was cooled to a room temperature of 27°C and stored in a refrigerator at 4°C for 1 h.

The physiochemical properties of the yogurt were analyzed using the AOAC method, 1995. They included pH, titratable acidity, moisture content, total solids, fat, ash, protein, and carbohydrates.

Viscosity was measured using a Brookfield DV-III Ultra rheometer, with a CPE 40 spindle. The samples were measured at different RPM at different shear rates. Particularly, we measured the shear rate, shear stress, viscosity, and torque. The shear rate was kept constant for all the trials to measure changes in viscosity.

The flow behavior was determined by plotting the shear rate versus viscosity and the *n*-value was determined from the power equation. The power equation was generated by a power line in a trendline model graph. The *n*-value was determined from the negative power value in the equation. The *n*-value was estimated to be less than 1 to determine the flow behavior of the yogurt [10].

The centrifugal acceleration test was performed to determine the syneresis rate of the yogurt. In a test tube, 5 g of a yogurt sample was placed and centrifuged at 1.200×g for 0, 3, 6, 9, 12, and 15 min at room temperature. To estimate the initial syneresis rate, the volume of the serum separated from the samples was measured at each time interval, which was expressed as milliliters of serum released per gram of sample per unit of time. To evaluate the syneresis rate for that day, the average of 5 tests (except 0) was calculated [11].

The cups containing 100 mL of a yogurt sample at 10°C were provided for sensory analysis. Each sample was assessed in three repetitions for flavor, texture, appearance, color, and overall acceptability on a nine-point hedonic scale, where 1 = the least/lowest; 9 = the most/

Table 1 Yogurt formulations based on oats milk, peanut milk, and coconut milk in a three-component mixture constrained simplex-lattice design

Run	Ingredients, mL		
	X_1 (oats milk)	X_2 (peanut milk)	X_3 (coconut milk)
1	10.000	5.000	10.000
2	7.500	7.500	10.000
3	5.000	10.000	10.000
4	10.000	10.000	5.000
5	7.500	10.000	7.500
6	9.167	6.667	9.167
7	9.167	9.167	6.667
8	7.500	7.500	10.000
9	10.000	10.000	5.000
10	5.000	10.000	10.000
11	6.667	9.167	9.167
12	8.333	8.333	8.333
13	10.000	5.000	10.000
14	10.000	7.500	7.500

highest. The panelists were trained about the sensory attributes before the sensory analysis.

Design Expert software (version 13.0) was used to optimize the development of a plant-based yogurt. The response surface methodology (RSM) explored the relationship between explanatory variables and one or more response variables. The mixture simplex-lattice design was used to find the optimum combination of constituents in the range between 5 and 10. The values of sugars and stabilizers were taken as constant. Time and temperature of incubation were also taken as constant for improved product quality. The mixture consisted of peanut milk, coconut milk, and oats milk in 14 combinations (Table 1).

Statistical and data analysis. To represent the fitted response value, the linear, special cubic, and special quartic models (Eqs. (1) – (3)) were used. To make predictions about the response for given levels of each factor, the equations could be used in terms of coded factors. The statistical significance of each equation was determined by variance analysis (ANOVA).

$$Y = b_1X_1+b_2X_2+b_3X_3 \quad (1)$$

$$Y = b_1X_1 + b_2X_2 + b_3X_3 + b_1b_2X_1X_2 + b_1b_3X_1X_3 + + b_2b_3X_2X_3 + b_1b_2b_3X_1X_2X_3 \quad (2)$$

$$Y = b_0 + b_1X_1 + b_2X_2 + b_3X_3 + b_{12}X_1X_2 + b_{13}X_1X_3 + + b_{23}X_2X_3 + b_{1123}X_{1\hat{}2}X_2X_3 + b_{1223}X_1X_{2\hat{}2}X_3 + + b_{1233}X_1X_2X_{3\hat{}2}+e \quad (3)$$

where Y is the predictive dependent variable (sensory analysis, viscosity, flow behavior, syneresis rate); b is the equation coefficient; X is the proportion of pseudo-components [12].

For Simple Quartic, X_1, X_2 and X_3 are the proportions of each number grade; b_0 is the constant, b_1, b_2 and b_3 are the coefficients of linear terms; b_{12}, b_{13} and b_{23} are the coefficients of two-term interactions; b_{1123}, b_{1223} and b_{1233} are the coefficients of special three-term interactions.

Table 2 Experimental design for viscosity, sensory analysis, flow behavior, and syneresis rate for each plant-based yogurt formulation

Run	Response 1 Viscosity, P	Response 2 Sensory analysis	Response 3 Flow behavior (n-value)	Response 4 Syneresis rate, mL/min
1	49.050	8.0	0.139	0.0324
2	53.810	7.0	0.058	0.0210
3	49.467	6.5	0.134	0.0314
4	56.960	6.0	0.034	0.0125
5	55.685	6.0	0.020	0.0128
6	49.051	8.0	0.140	0.0335
7	55.680	6.5	0.020	0.0170
8	53.760	7.0	0.068	0.0220
9	56.961	6.0	0.034	0.0160
10	49.460	6.0	0.133	0.0356
11	49.000	6.5	0.134	0.0354
12	53.960	6.6	0.078	0.0240
13	49.010	8.0	0.130	0.0312
14	55.980	7.0	0.060	0.0110

RESULTS AND DISCUSSION

Fitting for the best model. Table 2 shows the results of mixture design studies. The independent and dependent variables were fitted to linear, cubic, and special quartic models and the residuals plots were formulated to check the goodness of model fit. Low standard deviation, low predicted sum of squares, and high predicted R-squared were the parameters for the best model [13]. The linear model was found to be best fitted for sensory analysis and viscosity. The special cubic model was best fitted for the response flow behavior. The special quartic model was found to be best fitted for syneresis.

The linear and the quadratic models were used to relate the response to the operating factors of the experiment design. The fit of the polynomial models was analyzed using the coefficient of determination R^2 and the adjusted R^2, with statistical significance tested by the F-test. A large value specified that variations in the response could be revealed by the regression equation. To point out the statistical significance, the desired larger F-value was tested by the P-value. The model that showed a confidence interval greater than 95% (prob > [t] < 0.05) by the probability test was regarded as statistically significant. The Prob > F-value for the linear model was less than 0.0032 R^2 and the adjusted R^2 was found to have a maximum of 0.6474 and 0.5833, respectively. Although the cubic model was found to be aliased, the linear model was selected for further analysis of viscosity.

Table 3 ANOVA for the linear model of plant-based yogurt viscosity

Source	Sum of squares	df	Mean square	*F*-value	*P*-value
Model	93.03	2	46.51	10.10	0.0032
Linear mixture	93.03	2	46.51	10.10	0.0032
Residual	50.66	11	4.61		
Lack of fit	50.66	7	7.24	13950.78	< 0.0001
Pure error	0.0021	4	0.0005		
Cor total	143.69	13			

The ANOVA results for the model fitted for viscosity are shown in Table 3. As we can see, the linear effects of coconut (X_3), oats (X_1), and peanut (X_2) milk on the yogurt viscosity were found to be significant. Considering the significant factors, equation (4) represents the model developed for viscosity.

$$\text{Viscosity} = 65.25X_1 + 65.64X_2 + 28.72X_3 \quad (4)$$

The interaction effect of the process parameters was studied using response surface plots, which helped predict the optimal levels of each parameter to achieve maximum viscosity. Figure 1a shows the influence of three parameters on viscosity. According to Table 2, runs 5, 9, and 14 show greater viscosity. This means that viscosity increased with an increase in peanut and oats milk, but decreased with an increase in coconut milk.

The optimum region was determined by setting the maximum viscosity as the goal. In a study by Ye *et al.*, the increase in viscosity was due to a higher protein content in peanut and oats milk [14]. Brückner-Gühmann *et al.* suggested that due to a high content of protein, oats could be used as a plant-based gelling agent even at temperatures below the temperature of denaturation [15]. The addition of pectin and xanthan gum also influenced the viscosity range. Figure 1b shows that viscosity ranged from 48.000 to 58.000 P.

Our results showed that peanut and oats milk, as well as stabilizers, had a greater effect on the viscosity of the plant-based yogurt than other components, such as coconut milk or sucrose.

The cubic model was used to relate the response to the operating factors of the experiment design. The fit of the polynomial models was analyzed using the coefficient of determination R^2, the adjusted R^2, with statistical significance tested by the *F*-test. A large value specified that response variations could be revealed by the regression equation. To point out the statistical significance, the desired larger *F*-value was tested by the *P*-value. The model that showed a confidence interval greater than 95% (prob > [t] < 0.05) by the probability test was regarded as statistically significant. The Prob > *F*-value for the special cubic model was less than 0.0135 R^2 and the adjusted R^2 was found to have a maximum of 0.8467 and 0.7154, respectively. The cubic model was selected for further analysis of flow behavior.

The ANOVA results for the model fitted for the flow behavior are shown in Table 4. As can be seen, the cubic effects of coconut (X_3), oats (X_1), and peanut (X_2) milk on the flow behavior were found to be significant. Considering the significant factors, equation (5) represents the model developed for the flow behavior.

$$\begin{aligned}\text{Flow behavior} = &-19.43355X_1 - 20.93901X_2 - \\ &- 20.43434X_3 + 85.28998X_4 + 85.42010X_5 + \\ &+ 89.18653X_6 - 229.73535X_7\end{aligned} \quad (5)$$

where X_4 = oats milk + peanut milk, X_5 = oats milk + + coconut milk, X_6 = peanut milk + coconut milk, X_7 = oats milk + peanut milk + coconut milk.

The interaction effect of the process parameters was studied using response surface plots, which helped to predict the optimal levels of each parameter for achieving maximum flow behavior. Figure 2a shows the influence of three parameters on the flow behavior. The flow behavior depends on viscosity and the shear rate. This was determined by the power law model. The power law does not consider yield stress since it is a

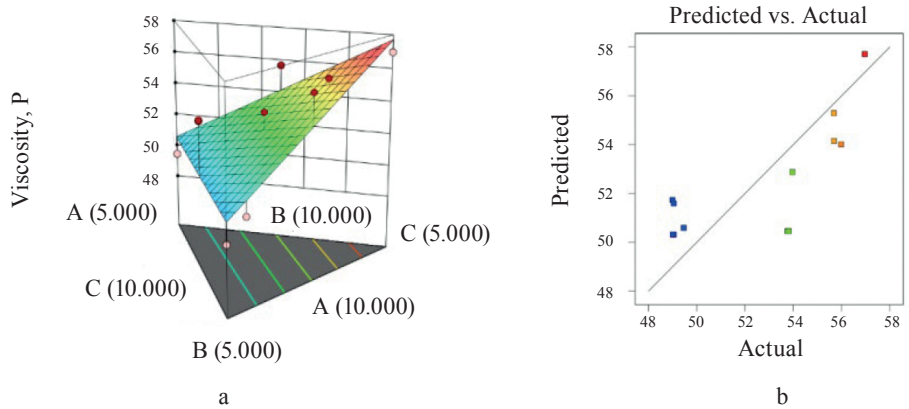

Figure 1 3D surface graph (a) and diagnostic plots (b) of the effect of independent variables on viscosity of the plant-based yogurts with oats milk (A), peanut milk (B), and coconut milk (C)

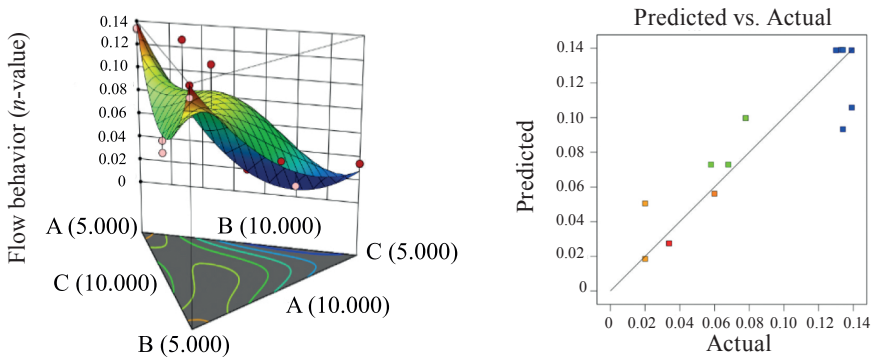

Figure 2 3D surface graph (a) and diagnostic plots (b) of the effect of independent variables on flow behavior of the plant-based yogurts with oats milk (A), peanut milk (B), and coconut milk (C)

Table 4 ANOVA for the special cubic model of yogurt flow behavior

Source	Sum of squares	df	Mean square	*F*-value	*P*-value
Model	0.0257	6	0.0043	6.45	0.0135
Linear mixture	0.0170	2	0.0085	12.81	0.0046
X_4 (oats milk + peanut milk)	0.0059	1	0.0059	8.81	0.0208
X_5 (oats milk + coconut milk)	0.0035	1	0.0035	5.24	0.0558
X_6 (peanut milk + coconut milk)	0.0006	1	0.0006	0.9169	0.3702
X_7 (oats milk + peanut milk + coconut milk)	0.0037	1	0.0037	5.50	0.0514
Residual	0.0047	7	0.0007	–	–
Lack of fit	0.0046	3	0.0015	66.81	0.0007
Pure error	0.0001	4	0.0000	–	–
Cor total	0.0304	13	–	–	–

non-Newtonian fluid model. The relationship between viscosity and the shear rate in the power law model is defined as $\eta = m\gamma^{n-1}$, where η is apparent viscosity, γ is the shear rate, and m and n are the power law constants [16].

Figure 2b shows that the *n*-value of the flow behavior ranged from 0 to 0.14. Yogurt is a thixotropic fluid with $n < 1$, where n is the flow behavior index (dimensionless) indicating the non-Newtonian or Newtonian character. According to Ghica *et al.*, $n < 1$ determines a non-Newtonian pseudo plastic fluid, $n > 1$ determines a non-Newtonian dilatant fluid, and $n = 1$ determines a Newtonian fluid [10]. Table 2 shows changes in the flow behavior with respect to viscosity and the composition of milk. The lesser the viscosity, the greater the flow behavior. This was due to the influence of stabilizers and the composition of milk.

The linear model was used to relate the response to the operating factors of the experiment design. The fit of the polynomial models was analyzed using the coefficient of determination R^2 and the adjusted R^2, with statistical significance tested by the *F*-test. A large value specified that variations in the response could be revealed by the regression equation. To point out the statistical significance, the desired larger *F*-value was tested by the *P*-value. The model with a confidence interval greater than 95% (prob > [t] < 0.05) by the probability test was regarded as statistically significant. The Prob > *F*-value for the linear model was less than 0.0001 R^2 and the adjusted R^2 was found to have a maximum of 0.9222 and 0.9080, respectively. Although the cubic model was found to be aliased, the linear model was selected for further analysis of sensory evaluation.

The ANOVA results for the model fitted for sensory evaluation are shown in Table 5. As we can see, the linear effects of coconut (X_3), oats (X_1), and peanut (X_2) milk were found to be significant on sensory attributes. Considering the significant factors, equation (6) represents the model developed for sensory evaluation.

$$\text{Sensory evaluation} = 9.64X_1 + 0.14X_2 + 10.50X_3 \quad (6)$$

The interaction effect of the process parameters was studied using response surface plots, which helped predict the optimal levels of each parameter to achieve maximum sensory values. Figure 3a shows the influence of three parameters on sensory evaluation. We found a decrease in sensory values with higher contents of peanut milk. However, higher contents of coconut and oats milk provided maximum sensory values. This was due to the nutty flavor of peanut producing off-flavor.

Table 5 ANOVA for the linear model of yogurt sensory evaluation

Source	Sum of squares	df	Mean square	*F*-value	*P*-value
Model	6.74	2	3.37	65.17	< 0.0001
Linear mixture	6.74	2	3.37	65.17	< 0.0001
Residual	0.5689	11	0.0517	–	–
Lack of fit	0.4439	7	0.0634	2.03	0.2577
Pure error	0.1250	4	0.0313	–	–
Cor total	7.31	13	–	–	–

Ye *et al.* noted that the application of flavoring agents improved the sensory and overall acceptability of peanut milk-based yogurt [14]. This confirmed earlier reports that adding flavoring agents and fruits to yogurt increased the product range, as well as consumers' liking of the product [17].

Figure 3b shows that the overall acceptance ranged from 6 to 8. According to Table 2, runs 1, 6, and 13 showed higher sensory values in the formulations with a lower quantity of peanut milk compared to oats and coconut milk. Therefore, the flavor problem in peanut milk yogurt could be corrected or improved by applying commercial flavoring agents.

The simple cubic and quadratic models were used to relate the response to the operating factors of the experiment design. The fit of the polynomial models was analyzed using the coefficient of determination R^2 and the adjusted R^2, with statistical significance tested by the *F*-test. A large value specified that variations in the response could be revealed by the regression equation. The *P*-value was used to test whether *F*-value was large enough to point out statistical significance. The model with a confidence interval greater than 95% (prob > [t] < 0.05) by the probability test was regarded as statistically significant. The Prob > *F*-value for the special quartic model was less than 0.0300 R^2 and the adjusted R^2 was found to have a maximum of 0.9083 and 0.7616, respectively. Although the cubic model was found to be aliased, the special quartic model was selected for further analysis of syneresis.

The ANOVA results for the model fitted for syneresis are shown in Table 6. As can be seen, the quartic effects of coconut (X_3), oats (X_1), and peanut (X_2) milk were found to be significant on syneresis. Considering the significant factors, equation (7) represents the model developed for syneresis.

$$\begin{aligned}\text{Syneresis} = {} & 0.0338X_1 + 0.0321X_2 + \\ & + 0.0146X_3 - 0.0433X_4 - 0.0403X_5 - 0.0442X_6 + \\ & + 0.8024X_7 + 0.7247X_8 - 0.1370X_9 \end{aligned} \quad (7)$$

where X_4 = oats milk + peanut milk, X_5 = oats milk + coconut milk, X_6 = peanut milk + coconut milk, X_7 = oats milk^2 + peanut milk + coconut milk, X_8 = oats milk + peanut milk^2 + coconut milk, X_9 = oats milk + peanut milk + coconut milk^2.

The interaction effects of the process parameters were studied using response surface plots, which helped predict the optimal levels of each parameter to achieve minimum syneresis rate values. Figure 4a shows the influence of three parameters on syneresis. We found that syneresis was minimum when viscosity was maximum, i.e., syneresis decreased as viscosity increased. Figure 4b represents the syneresis values ranging from 0.01 to 0.04.

According to Table 2, runs 4, 5, 9, and 14 had minimum syneresis with maximum viscosity values. This was due to the binding of molecules in higher viscosity that holds the water during syneresis. In a study by Dönmez *et al.*, the interaction with casein micelles in conventional yogurt influenced the strength of the casein network and the stabilized yogurt structure, increasing the consistency by reducing the syneresis rate

Table 6 ANOVA for the special quartic model of syneresis

Source	Sum of squares	df	Mean square	*F*-value	*P*-value
Model	0.0010	8	0.0001	6.19	0.0300
Linear mixture	0.0006	2	0.0003	15.35	0.0073
X_4 (oats milk + peanut milk)	0.0002	1	0.0002	7.88	0.0377
X_5 (oats milk + coconut milk)	0.0001	1	0.0001	4.12	0.0982
X_6 (peanut milk + coconut milk)	0.0001	1	0.0001	4.97	0.0763
X_7 (oats milk^2 + peanut milk + coconut milk)	0.0001	1	0.0001	3.32	0.1281
X_8 (oats milk + peanut milk^2 + coconut milk)	0.0001	1	0.0001	2.71	0.1608
X_9 (oats milk + peanut milk + coconut milk^2)	1.869E-06	1	1.869E-06	0.0940	0.7715
Residual	0.0001	5	0.0000	–	–
Lack of fit	0.0001	1	0.0001	20.59	0.0105
Pure error	0.0001	4	4.041E-06	–	–
Cor total	0.0011	13	–	–	–

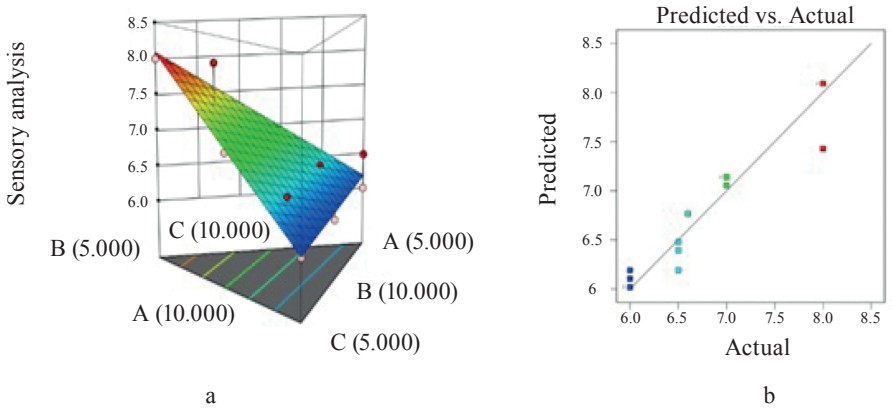

Figure 3 3D surface graph (a) and diagnostic plots (b) of the effect of independent variables on sensory evaluation of the plant-based yogurts with oats milk (A), peanut milk (B), and coconut milk (C)

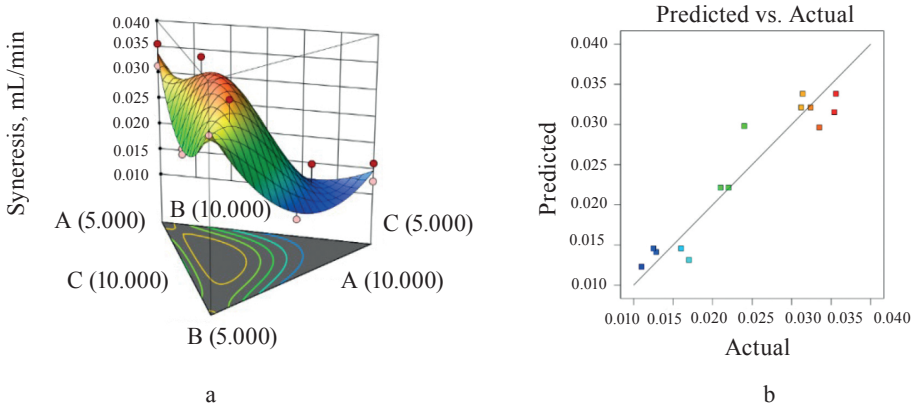

Figure 4 3D surface graph (a) and diagnostic plots (b) of the effect of independent variables on syneresis rate of the plant-based yogurts with oats milk (A), peanut milk (B), and coconut milk (C)

Table 7 Optimum ingredient proportions for plant-based yogurt

Components	Percentage
Oats milk	40
Coconut milk	31.5
Peanut milk	28.5

at certain concentrations [18]. The syneresis value also depends on the composition of the stabilizers used.

Optimization of component proportion. We solved the equations to yield the average values of each independent variable in order to obtain the optimal yogurt. This allowed us to find a desirable combination of oats, coconut, and peanut milk (Table 7). Then, we analyzed the optimized yogurt for viscosity, sensory evaluation, flow behavior, and syneresis rate. The optimized yogurt consisted of 7.134 mL of peanut milk, 10 mL of oats milk, and 7.866 mL of coconut milk. Its predicted values of syneresis, viscosity, flow behavior, and sensory evaluation were 0.0138081, 53.4733, 0.0648189, and 7.20565, respectively, with a desirability value of 0.717.

Physiochemical analysis of raw milk and optimized yogurt. The optimized plant-based yogurt and raw milk were exposed to nutritional analysis to compare the predicted and actual values (Table 8). This ensured adequate nutritional values in the developed yogurt.

CONCLUSION

Our results showed the effectiveness of the mixture simplex-lattice design approach for optimizing yogurt based on plant milk. According to our experimental results and counter plots, an increase in peanut and oats milk improved the viscosity and reduced the flow behavior and syneresis rate. The samples with higher contents of peanut milk received low sensory values. This indicates that peanut milk has to be used in minimum amounts with stabilizers, such as corn starch, pectin, and xanthan gum, to ensure optimum texture properties. The plant-based yogurt with an

Table 8 Physiochemical analysis of raw milk and optimized plant-based yogurt

Responses	Predicted value for optimized yogurt	Actual value for optimized yogurt	Raw materials		
			Oats milk	Peanut milk	Coconut milk
Sensory analysis	7.20	7.30	–	–	–
Viscosity, P	53.47	53.76	43.31	40.69	30.72
Syneresis rate, mL/min	0.013	0.011	–	–	–
Flow behavior	0.064	0.068	–	–	–
Moisture, %	–	46	45	42	39
pH	–	5.500	6.908	6.512	7.412
Titratable acidity	–	3.560	0.966	1.066	1.066
Total solids, %	–	11.49	22.90	11.46	12.10
Fat, %	–	9.45	6.78	4.40	9.40
Protein, %	–	17	16	19	12
Ash, %	–	0.490	0.344	0.394	1.240
Carbohydrates, %	–	27.00	30.80	32.80	34.40

optimized composition was found to have high sensorial acceptance. The physiochemical analysis of raw milk and the optimized yogurt showed adequate amounts of nutrients.

CONTRIBUTION

The authors were equally involved in the writing of the manuscript and are equally responsible for any potential plagiarism.

CONFLICT OF INTEREST

The authors declare no conflict of interest.

ACKNOWLEDGEMENTS

We thank the management of Kongu Engineering College, Perundurai, Erode, India for their support with our work.

REFERENCES

1. Montemurro M, Pontonio E, Coda R, Rizzello CG. Plant-based alternatives to yogurt: State-of-the-art and perspectives of new biotechnological challenges. Foods. 2021;10(2). https://doi.org/10.3390/foods10020316
2. Tangyu M, Muller J, Bolten CJ, Wittmann C. Fermentation of plant-based milk alternatives for improved flavour and nutritional value. Applied Microbiology and Biotechnology. 2019;103(23–24):9263–9275. https://doi.org/10.1007/s00253-019-10175-9
3. Irkin R, Eren UV. A research about viable *Lactobacillus bulgaricus* and *Streptococcus thermophilus* numbers in the market yoghurts. World Journal of Dairy and Food Sciences. 2008;3(1):25–28.
4. Trachoo N. Yogurt: The fermented milk. Songklanakarin Journal of Science and Technology. 2002;24(4):727–738.
5. Arioui F, Ait Saada D, Cheriguene A. Physicochemical and sensory quality of yogurt incorporated with pectin from peel of *Citrus sinensis*. Food Science and Nutrition. 2017;5(2):358–364. https://doi.org/10.1002/fsn3.400
6. Alyaqoubi S, Abdullah A, Samudi M, Abdullah N, Addai ZR, Musa KH. Study of antioxidant activity and physicochemical properties of coconut milk (Pati santan) in Malaysia. Journal of Chemical and Pharmaceutical Research. 2015;7(4):967–973.
7. Patil U, Benjakul S. Coconut milk and coconut oil: Their manufacture associated with protein functionality. Journal of Food Science. 2018;83(8):2019–2027. https://doi.org/10.1111/1750-3841.14223
8. Paul AA, Kumar S, Kumar V, Sharma R. Milk analog: Plant based alternatives to conventional milk, production, potential and health concerns. Critical Reviews in Food Science and Nutrition. 2020;60(18):3005–3023. https://doi.org/10.1080/10408398.2019.1674243
9. Diarra K, Nong ZG, Jie C. Peanut milk and peanut milk based products production: A review. Critical Reviews in Food Science and Nutrition. 2005;45(5):405–423. https://doi.org/10.1080/10408390590967685
10. Ghica MV, Hîrjău M, Lupuleasa D, Dinu-Pîrvu C-E. Flow and thixotropic parameters for rheological characterization of hydrogels. Molecules. 2016;21(6). https://doi.org/10.3390/molecules21060786
11. Dönmez Ö, Mogol BA, Gökmen V. Syneresis and rheological behaviors of set yogurt containing green tea and green coffee powders. Journal of Dairy Science. 2017;100(2):901–907. https://doi.org/10.3168/jds.2016-11262

12. Nikzade V, Tehrani MM, Saadatmand-Tarzjan M. Optimization of low-cholesterol–low-fat mayonnaise formulation: Effect of using soy milk and some stabilizer by a mixture design approach. Food Hydrocolloids. 2012;28(2):344–352. https://doi.org/10.1016/j.foodhyd.2011.12.023
13. Cornell JA. Experiments with mixtures: Designs, models, and the analysis of mixture data. John Wiley & Sons; 2011. 680 p.
14. Ye M, Ren L, Wu Y, Wang Y, Liu Y. Quality characteristics and antioxidant activity of hickory-black soybean yogurt. LWT – Food Science and Technology. 2013;51(1):314–318. https://doi.org/10.1016/j.lwt.2012.09.027
15. Brückner-Gühmann M, Kratzsch A, Sozer N, Drusch S. Oat protein as plant-derived gelling agent: Properties and potential of modification. Future Foods. 2021;4. https://doi.org/10.1016/j.fufo.2021.100053
16. Pratumwal Y, Limtrakarn W, Muengtaweepongsa S, Phakdeesan P, Duangburong S, Eiamaram P, *et al.* Whole blood viscosity modeling using power law, Casson, and Carreau Yasuda models integrated with image scanning U-tube viscometer technique. Songklanakarin Journal of Science and Technology. 2017;39(5):625–631. https://doi.org/10.14456/sjst-psu.2017.77
17. Mohameed HA, Abu-Jdayil B, Al-Shawabkeh A. Effect of solids concentration on the rheology of labneh (concentrated yogurt) produced from sheep milk. Journal of Food Engineering. 2004;61(3):347–352. https://doi.org/10.1016/S0260-8774(03)00139-0
18. Dönmez Ö, Mogol BA, Gökmen V. Syneresis and rheological behaviors of set yogurt containing green tea and green coffee powders. Journal of Dairy Science. 2017;100(2):901–907. https://doi.org/10.3168/jds.2016-11262

ORCID IDs
Sudha Ayyasamy https://orcid.org/0000-0001-8859-0073
Sangeetha Velusamy https://orcid.org/0000-0002-3777-1891

Foods and Raw Materials. 2022;10(2)

ISSN 2310-9599 (Online)
ISSN 2308-4057 (Print)

Research Article
Open Access

Available online at http://jfrm.ru/en
https://doi.org/10.21603/2308-4057-2022-2-539
https://elibrary.ru/ZEPWPQ

A comparative study of phytochemical, antioxidant, anticarcinogenic, and antidiabetic potential of coriander (*Coriandrum sativum* L.): Microgreen and mature plant

G. M. Dhakshayani, S. Janaki Alias Priya*

Women's Christian College, University of Madras, Chennai, India

* e-mail: drjanagipriya@gmail.com

Received 14.02.2022; Revised 23.03.2022; Accepted 05.04.2022; Published online 23.09.2022

Abstract:
Microgreens are immature edible leafy greens with a higher concentration of phytonutrients than in mature leaves, which makes them a novel functional food. This research featured antioxidant, anticarcinogenic, and antidiabetic properties of coriander microgreens.

Aqueous and ethanolic extractions of coriander microgreens and mature leaves underwent a phytochemical analysis of antioxidant potential using the DPPH (2,2-diphenyl-1-picryl-hydrazyl-hydrate) free radical method and the ferric reducing antioxidant power (FRAP) assay. The analysis of antidiabetic and anticarcinogenic properties included the method of α-amylase enzyme inhibition and the MTT colorimetric assay.

The screening test inferred the presence of alkaloids, terpenoids, glycosides, steroids, tannins, flavonoids, phenols, carbohydrates, and proteins in both microgreens and mature leaves. The quantitative analysis showed that the ethanolic extract of the microgreen sample exhibited higher total phenols. Total flavonoids, steroids, carbohydrates, and proteins were higher both in microgreen extracts, if compared with those of mature leaves. Ascorbic acid, chlorophyll-a, chlorophyll-b, and carotenoids demonstrated a more substantial presence in mature leaves. The gas chromatography-mass spectrometry (GC/MS) analysis of coriander microgreens revealed such bioactive compounds as thienopyrimidines, phenolic amide, imidazo pyridazine, phenolic constituents, and essential oil. Mature leaves were rich in phenolic compounds, steroids, terpenoids, essential oils, and fatty acid esters. All these substances are known for their therapeutic antioxidant, antidiabetic, and anticarcinogenic properties. The microgreen samples exhibited greater ferric reducing antioxidant power, α-amylase enzyme inhibition, and cytotoxicity activity at a lower concentration of extract than mature leaves.

Coriander microgreens proved to have a promising antioxidant, anticarcinogenic, and antidiabetic potential and can be used in daily food additives.

Keywords: Coriander, microgreens, coriander mature leaves, phytochemical, antioxidant, anticarcinogenic, antidiabetic properties

Please cite this article in press as: Dhakshayani GM, Priya SJA. A comparative study of phytochemical, antioxidant, anticarcinogenic, and antidiabetic potential of coriander (*Coriandrum sativum* L.): Microgreen and mature plant. Foods and Raw Materials. 2022;10(2):283–294. https://doi.org/10.21603/2308-4057-2022-2-539

INTRODUCTION

According to the International Diabetes Federation report of 2017, approximately 425 million adults between 20 and 79 years old suffered from diabetes worldwide. By 2045, this number will escalate to 629 million. In 2017, India reported 72 946 400 cases of diabetes [1]. Type II diabetes patients showed higher cancer risks, especially in the colorectal area. Association between these two diseases may result from shared cellular and molecular pathways. Genome-wide association studies also linked diabetes-associated genes (e.g., *TCF7L2*) to colorectal cancer [2, 3]. Globally, colorectal cancer is the fourth most commonly diagnosed type of cancer. The past five years have seen 3.2 million prevalence rates. It means that 1.3 million new colorectal cancer cases are registered every year [4].

According to Ayurvedic studies, food (*Ahara* in Hindi) is the sustainer of life, which helps maintain good health and protects human body from diseases [5].

Herbs and spices are indispensable parts of human diet. Since ancient times, herbs and spices have played a vital role in the lifestyle of people. Not only do they add flavor to food, but they also possess valuable preservative and medicinal properties because the bio-molecules in some plants maintain and promote human health.

In the past few decades, natural products have become more popular as an alternative therapy against various diseases because conventional medicine often cause unwanted side effects. As a result, modern science also started exploring the medicinal properties of spices [6, 7].

Coriander (*Coriandrum sativum* L.), sometimes called the herb of happiness, is the most well-known culinary spice worldwide and an age-old traditional medicine. *C. sativum* contains a wide range of phytochemical elements, which makes it a promising functional food that protects from all kinds of lifestyle-related diseases. Indeed, coriander is known for its antioxidant, anticancer, neuroprotective, anticonvulsant, migraine-relieving, hypolipidemic, hypoglycemic, hypotensive, antimicrobial, anxiolytic, analgesic, and anti-inflammatory activities [8].

Mature coriander leaves have medicinal properties, but new scientific data demonstrate that coriander microgreens contain higher amounts of such phytonutrients as β-carotene, ascorbic acid, α-tocopherol, and phylloquinone, as well as minerals, e.g., Ca, Mg, Fe, Mn, Zn, Se, and Mo. They also have lower nitrate content than mature leaves [9, 10].

As a novel functional food, microgreens are tender and immature leafy greens with developed cotyledons and with or without partially emerged pair of the first true leaves [10]. They are harvested for consumption within 10 to 20 days of seedling emergence and are larger than sprouts but younger than baby greens [11]. They give vivid color, soft texture, and multifarious quality to the main dish, thus enhancing its aesthetic appeal [12, 13]. Microgreens are a highly perishable food with a very short shelf life of three to five days at ambient temperature [14]. Microgreens can be easily grown at home, in containers on a terrace, or in kitchen gardens with minimal sunlight. In the present study, the microgreens were evaluated *in vitro* for antioxidant, antidiabetic, and anticancer properties, which were compared with those of mature leaves.

STUDY OBJECTS AND METHODS

Sample growth and preparation. Coriander (*Coriandrum sativum* L.) microgreens were grown under ambient conditions using vermicompost enriched soil. A 50-g sample of coriander seeds (Chennai, India) was sown at an even depth of one inch (2.5 cm) in soil-filled plastic pots. After germination, the pots were hydrated thrice a day and exposed to ambient light. Coriander microgreens were harvested after seven or eight days when they were three inches (7.5 cm) tall. The cotyledon stems were cut with sterile scissors as close to the soil surface as possible. Coriander mature leaves were grown under the same conditions as microgreens and harvested after 60 days. The roots and defected parts were removed, and the edible stems and leaves were cleaned from soil particles.

Species identification. The species were identified with the help of the faculty of Plant Biology and Plant Biotechnology, Women's Christian College, Chennai.

Preparation of extract. Mature leaves and microgreens were washed three or four times with tap water and then rinsed twice with de-ionized water. After that, they were shade-dried at room temperature under constant observation to avoid any contamination. After drying, the leafy samples were crushed in an electric grinder. The powdered samples were stored for further use. Extraction was done by aqueous and ethanolic methods.

Aqueous extraction. Powdered mature leaves (10 g) and powdered microgreens (10 g) were put in separate conical flasks with 100 mL of de-ionized water. The samples were kept in a water bath at 90°C for 1 h and cooled at room temperature. Then, the extract was filtered with Whatman filter paper. The filtrate was condensed in a hot plate at 50°C and stored at 4°C.

Ethanolic extraction. Powdered mature leaves (10 g) and powdered microgreens (10 g) were soaked separately in 100 mL of ethanol for 72 h. The supernatant was filtered with Whatman filter paper. The filtrate was condensed in a hot plate at 50°C.

Phytochemical analysis.

Qualitative phytochemical screening. The crude ethanolic and aqueous extracts of *C. sativum* microgreens and mature leaves were subjected to a qualitative phytochemical analysis. They were tested using standard procedures for various classes of active phytoconstituents, such as alkaloids, terpenoids, glycosides, steroids, saponins, tannins, flavonoids, phenols, carbohydrates, and proteins [15–21].

Quantitative phytochemical analysis. *Estimation of total phenols.* Total phenolic compounds in the coriander samples were quantified by using a slightly modified the Folin-Ciocalteu reagent method [22]. During the procedure, 100 µL of extracts were mixed with 900 µL of methanol and 1 mL of the Folin-Ciocalteu reagent (diluted with distilled water as 1:10). After 5 min, 1 mL of 20% (w/v) Na_2CO_3 solution was added. The reaction was incubated in the dark for 30 min. A UV-Vis spectrophotometer measured the optical density at 765 nm. The total phenolic content was expressed as (mg/g of sample) gallic acid equivalent.

Estimation of total flavonoids. The aluminum chloride reagent method with slight modifications was used to define the total flavonoid content in the *C. sativum* samples [23]. Each extract (500 µL) was mixed with 500 µL of methanol and 500 µL of 5% (w/v) sodium nitrite solution followed by adding 500 µL of 10% (w/v) aluminum chloride solution. After a 5-min incubation, 1 mL of 1M NaOH solution was added. By adding distilled water, the total volume was brought up

Table 1 Formulas for chlorophyll-a, chlorophyll-b, total chlorophyll, and carotenoid estimation [28–30]

Chlorophyll-a, mg/g tissue	$\left(\frac{12.7(A_{663})-2.69(A_{645})\times V\times W}{1000}\right)$
Chlorophyll-b, mg/g tissue	$\left(\frac{22.9(A_{645})-4.68(A_{663})\times V\times W}{1000}\right)$
Total chlorophyll (TC), mg/g tissue	$\left(\frac{20.2(A_{645})-8.02(A_{663})\times V\times W}{1000}\right)$
Carotenoid, mg/g tissue	$\left(\frac{7.6(A_{480})-1.49(A_{510})\times V\times W}{1000}\right)$

where A is the absorbance at a specific wavelength (480, 510, 645, and 663 nm); V is the final volume of chlorophyll extract; and W is the fresh weight of tissue extracted

to 5 mL. Absorbances were measured at 510 nm, and the results were expressed as (mg/g of sample) quercetin equivalent.

Estimation of steroids. According to the procedure described in [24], 1 mL of each extract was put in a 10-mL volumetric flask. 4 N sulphuric acid (2 mL) and 0.5% iron (III) chloride (2 mL) were added, followed by a 0.5% potassium hexacyanoferrate (III) solution (0.5 mL). The mix was heated at 70 ± 20°C in a water bath for 30 min with occasional shaking. The total volume was diluted to the mark with distilled water. The optical density was measured at 780 nm against the reagent blank. The results were expressed as (mg/g of sample) cholesterol equivalent.

Estimation of total carbohydrates. The total carbohydrate content was measured by the Hedge and Hofreiter method [25]. According to the procedure, 0.5 mL of each extract was put in a separate test tube. The volume was brought up to 1 mL with distilled water. After that, 4 mL of anthrone reagent was added in each tube and mixed thoroughly. D-glucose was used as standard. Blank was taken as distilled H_2O and anthrone. The reaction mix was heated in a boiling water bath for 8 min and cooled. The absorbance of the green color solution was tested at 630 nm using a UV-Vis spectrophotometer. The carbohydrate content of the plant extract was calculated from the calibration curve of glucose, and the results were expressed as (mg/g of sample) glucose equivalent.

Estimation of proteins (Bradford colorimetric assay). The Bradford protein assay described in [26] quantified the total protein content in the *C. sativum* samples. According to the procedure, 0.5 mL of each extract was put in a test tube and brought up to 1 mL with distilled water. After that, 2 mL of Bradford's reagent was added in each tube and mixed thoroughly. Bovine serum albumin served as standard. Blank was taken as distilled water and Bradford's reagent. The absorbance of the pale blue color solution was tested at 595 nm. The unknown concentration of amino acids/protein in the coriander samples was illustrated as a graph.

Estimation of ascorbic acid. The ascorbic acid content in the fresh samples were estimated using the 2, 6-dichlorophenol indophenol (DCPIP) titration method according to the procedure previously described by Rao and Deshpande [27]. According to the procedure, 5 mL of the ascorbic acid working standard was pipetted into a 100 mL conical flask together with 5 mL of 0.625% oxalic acid and titrated against the dye solution (V_1). The endpoint was the appearance of a transient pink color that persisted for a few minutes. After that, 5 mL of each test sample was similarly titrated against the dye solution. The ascorbic acid content, mg/100 g, was determined using the following formula:

$$\text{Amount of ascorbic content} = \frac{500\times V_2\times 25\times 100}{V_1\times 5\times 5} \quad (1)$$

where 500 is the amount of standard ascorbic acid taken for titration, µg; V_1 is the volume of dye consumed by 500 µg of standard ascorbic acid; V_2 is the volume of dye consumed by 5 mL of each test sample; 25 is the total volume of extract; 100 is the ascorbic acid content per 100 g of sample; 5 is the weight of fresh sample taken for extraction; and 5 is the volume of test sample taken for titration.

Estimation of chlorophylls and carotenoids using acetone. During this procedure, 1 g of finely cut fresh leaves was homogenized with 80% acetone. The mass was then centrifuged at 5000 rpm for 5 min. After the supernatant was transferred, the procedure was repeated until the residue contained no trace of green color. The final volume was brought up to 100 mL in the volumetric flask with 80% acetone. The optical density of the extracted solution was measured at 480, 510, 645, and 663 nm. From these readings, concentrations of chlorophylls and carotenoid pigment were determined by using the following formulas given in Table 1.

Gas chromatography–mass spectrometry (GC/MS). The aqueous extracts of *C. sativum* microgreens and mature leaves underwent a GC/MS analysis by using Agilent technologies 6890 N JEOL GC Mate II GC-MS model. The samples were injected into an HP-5 column (30 m×0.25 mm i.d with 0.25 µm film thickness). During the gas chromatography, helium served as the carrier gas, the flow rate was 1 mL/min, and the injector operated at 200°C. The column oven temperature was programmed as 50–250°C at a rate of 10°C/min injection mode. The list of mass spectrometry

conditions included: ionization voltage – 70 eV; ion source temperature – 250°C; interface temperature – 250°C; mass range – 50–600 mass units. The results were compared using the spectrum of the known components stored in the National Institute Standard and Technology (NIST) library database [31].

In vitro* antioxidant assays. *DPPH radical scavenging assay. The antioxidant activity of the extracts was measured based on the stable (2, 2-diphenyl-1-picryl-hydrazyl-hydrate) DPPH free radical scavenging method [32]. Various concentrations (50, 100, 150, 200, 250, and 300 µg/mL) of *C. sativum* extracts (1 mL) were mixed with 0.1 mM of DPPH solution (1 mL) in methanol. The reaction was carried out in triplicate, and the decrease in absorbance was measured at 517 nm after 30 min in the dark using a UV-Vis spectrophotometer. Ascorbic acid served as the standard reference, while methanol (1 mL) with DPPH (1 mL) solution served as control. The percentage of inhibition was calculated as follows:

$$\%\ \text{of DPPH radical inhibition} = \\ = \frac{\text{Control} - \text{Sample}}{\text{Control}} \times 100 \quad (2)$$

The procedure made it possible to determine the sample concentration required to inhibit 50% of the DPPH free radical (IC_{50}).

Ferric (Fe^{3+}) reducing antioxidant power assay (FRAP). The reducing power of the extracts was determined by the Fe^{3+} reduction method with slight modification [33]. In brief, 1 mL of *C. sativum* extracts at different concentrations (50, 100, 150, 200, 250, and 300 µg/mL) were taken in 1 mL of phosphate buffer (0.2 M, pH 6.6) in a test tube. After that, 1 mL of potassium ferricyanide [$K_3Fe(CN)_6$] (1% w/v) was added. After 30 min of incubation at 50°C in a water bath, 1 mL of trichloroacetic acid (10 % w/v) was added to each mix. Then, 1 mL of fresh $FeCl_3$ (0.1% w/v) solution was poured in, and the absorbance was measured at 700 nm in a UV-Vis spectrophotometer. The experiment was replicated in three independent assays. Ascorbic acid was used as the standard reference. The reducing concentration (RC_{50}) of sample required to reduce the free radicals (Fe^{3+}) by 50 % was calculated to interpret the FRAP results.

The percentage of reduction was calculated as follows:

$$\%\ \text{of } Fe^{3+}\text{reduction} = \\ = \frac{\text{Sample} - \text{Control}}{\text{Sample}} \times 100 \quad (3)$$

In vitro* antidiabetic activity. *α-amylase enzyme inhibition assay. The α-amylase enzyme inhibition assay relied on the starch-iodine test [34]. The coriander extracts at various concentrations (50, 100, 150, 200, 250, and 300 µg/mL) were added to α-amylase enzyme (10 µL). The α-amylase enzyme had been prepared in 0.02 M sodium phosphate buffer (pH 6.9 containing 6 mM sodium chloride). The procedure was followed by 10 min of incubation at 37°C. After pre-incubation, 500 µL of 1% soluble starch was added to each reaction and incubated at 37°C for 60 min.

To stop the enzymatic reaction, 1 N HCl (100 µL) was added and followed by 200 µL of iodine reagent (5 mM I_2 and 5 mM KI). The color change was registered, and the optical density was tested at 595 nm. Acarbose was used as the standard reference. The control reaction representing 100% enzyme activity contained no plant extract.

The experiment was carried out in triplicate. A dark-blue color indicated the presence of starch; a yellow color indicated the absence of starch; a brownish color indicated partially degraded starch in the reaction mix. In the presence of inhibitors, the starch added to the enzyme assay mix did not degrade and gave a dark-blue color complex. No color complex developed in the absence of the inhibitor, indicating that starch was completely hydrolyzed by α-amylase. The IC_{50} value was calculated as follows:

$$\%\ \text{of } \alpha\text{-amylase enzyme inhibition} = \\ = \frac{\text{Sample} - \text{Control}}{\text{Sample}} \times 100 \quad (4)$$

Cytotoxicity assay on colon cell lines. The conventional MTT reduction assay was used to measure the cell viability [35]. HT 29 Colon cells were obtained from the National Centre for Cell Science (Pune). The culturing was performed on the medium developed by the Roswell Park Memorial Institute (RPMI). It included 10% fetal bovine serum (FBS), gentamycin (100 µg/mL), penicillin/streptomycin (250 U/mL), and amphotericin B (1 mg/mL). All cell cultures were maintained at 37°C in a humidified atmosphere of 5% CO_2. Cells grew to confluence for 24 h before use.

As described in [36], we plated HT 29 cells (5×10^3/well) in 96-well plates for 24 h in 200 µL of the RPMI medium with 10% fetal bovine serum. After the culture supernatant was removed, the RPMI samples with various concentrations (0.001–100 µg/mL) of aqueous *C. sativum* extracts were added and incubated for 48 h. After the treatment, cells were incubated with MTT (10 µL, 5 mg/mL) at 37°C for 4 h and then with dimethyl sulfoxide at room temperature for 1 h. The plates were tested at 595 nm on a scanning multi-well spectrophotometer. All experiments were performed in duplicates [36].

The effect of the extracts on growth inhibition of HT-29 colon cancer cell line line, %, was calculated using the following formula:

$$\text{Growth inhibition} = \frac{\text{Positive control optical density} - \text{Sample optical density}}{\text{Positive control optical density}} \times 100 \quad (5)$$

Table 2 Phytochemical content of aqueous and ethanol extracts of *Coriandrum sativum* microgreens and mature leaves

Phytochemicals	Aqueous extract		Ethanol extract	
	Microgreens	Mature leaves	Microgreens	Mature leaves
Phenols, mg GAE/g	98.25 ± 0.27*	107.26 ± 0.29*	116.78 ± 0.28*	72.23 ± 0.28*
Flavonoids, mg QE/g	119.43 ± 0.36*	18.58 ± 0.38*	29.15 ± 0.26*	13.61 ± 0.37*
Steroids, mg CE/g	140.34 ± 0.57*	101.77 ± 0.28*	50.41 ± 0.52*	33.58 ± 0.38*
Carbohydrates, mg GE/g)	457.65 ± 1.6*	398.38 ± 2.3*	169.73 ± 1.50*	124.35 ± 1.04*
Proteins, mg/g	156.41 ± 0.38*	117.80 ± 0.31*	101.40 ± 0.37*	75.36 ± 0.35*

Each value is expressed as mean ± standard deviation (n = 3) and statistically significant at *$P < 0.05$

Table 3 Ascorbic acid, chlorophyll, and carotenoid contents in *Coriandrum sativum* microgreens and mature leaves

Samples	Phytonutrients				
	Ascorbic acid, mg/100 g W	Chlorophyll-a, mg/g W	Chlorophyll-b, mg/g W	Total chlorophyll, mg/g W	Carotenoid, mg/g W
Microgreens	18.56 ± 0.45*	0.04 ± 0.01*	0.07 ± 0.01*	0.04 ± 0.01*	0.13 ± 0.01*
Mature leaves	77.68 ± 0.37*	0.27 ± 0.04*	0.33 ± 0.03*	0.33 ± 0.03*	0.31 ± 0.04*

Each value is expressed as mean ± standard deviation (n = 3) and statistically significant at *$P < 0.05$

From the above growth inhibition, (%) percentage of cell viability was derived using the following formula:

$$\% \text{ Cell viability} = 100 - \text{Percent growth inhibition} \quad (6)$$

Statistical analysis. The phytochemical, antioxidant, and antidiabetic assays were carried out in triplicates, while the anticarcinogenic analysis was carried out in duplicates. The results obtained were expressed as mean ± SD. The statistical analysis was calculated by one-way ANOVA and Student's t-test using Microsoft excel. All statistical significance was accepted at $P < 0.05$.

RESULTS AND DISCUSSION

Phytochemical analysis. ***Qualitative phytochemical analysis.*** The qualitative phytochemical analysis of the aqueous and ethanolic extracts of coriander microgreens and mature leaves revealed such phytochemicals as alkaloids, terpenoids, steroids, tannins, flavonoids, phenols, carbohydrates, and proteins. Saponins were absent in both aqueous and ethanol extracts of microgreens and mature leaves. However, glycosides were present in the aqueous extract of microgreens and mature leaves, as well as in the ethanol extract of mature leaves. However, they were absent in the ethanol extract of microgreens.

Quantitative phytochemical analysis. Tables 2 shows the quantitative phytochemical mean values of both aqueous and ethanol extracts of *Coriandrum sativum* microgreens and mature leaves.

According to Table 2, the aqueous extract of microgreens showed a lower total phenol content (98.25 mg GAE/g) than that of mature leaves (107.26 mg GAE/g). However, the ethanol extract of microgreens had significantly ($P < 0.05$) higher total phenol (116.78 mg GAE/g) in comparison to that of mature leaves (72.23 mg GAE/g). In general, both extracts of microgreens had more total flavonoids, steroids, carbohydrates, and proteins than both extracts of mature leaves. Table 3 illustrates the contents of ascorbic acid, chlorophyll, and carotenoid.

Gas chromatography–mass spectrometry (GC/MS). The GC/MS method revealed various bioactive constituents in the aqueous extracts of coriander microgreens and mature leaves. The analysis showed peaks at different locations on the chromatogram. In Figs. 1 and 2, the X-axis represents the retention time, while the Y-axis represents the relative abundance. The GC/MS analysis of a crude extract of microgreens showed nine major peaks. The crude extract of mature leaves eluted seven major peaks. Tables 4 and 5 illustrate a comparative analysis of the mass spectra of the constituents with the NIST library data.

In vitro **antioxidant assays.** ***DPPH radical scavenging assay.*** The scavenging capacity of the aqueous and ethanol extracts of both coriander microgreens and mature leaves on DPPH free radicals was expressed as inhibition (%) (Tables 6 and 7). The IC_{50} was inhibition concentration at 50%: the lowest IC_{50} indicated the strongest ability of the extracts to act as DPPH radical scavengers. The aqueous and ethanol extracts of mature leaves showed the lowest IC_{50}, which were 44.64 and 186.74 µg/mL, respectively. As for the aqueous and ethanol extracts of microgreens, they were 90.09 and 293.54 µg/mL, respectively. Compared to the reference standard ascorbic acid inhibition percentage (Fig. 3), the test samples required higher concentration to inhibit DPPH free radical. Thus, the test samples of microgreens and mature leaves showed dose-dependent scavenging activity.

Ferric (Fe^{3+}) reducing antioxidant power assay. For Fe^{3+} reducing activity, the ascorbic acid was used as

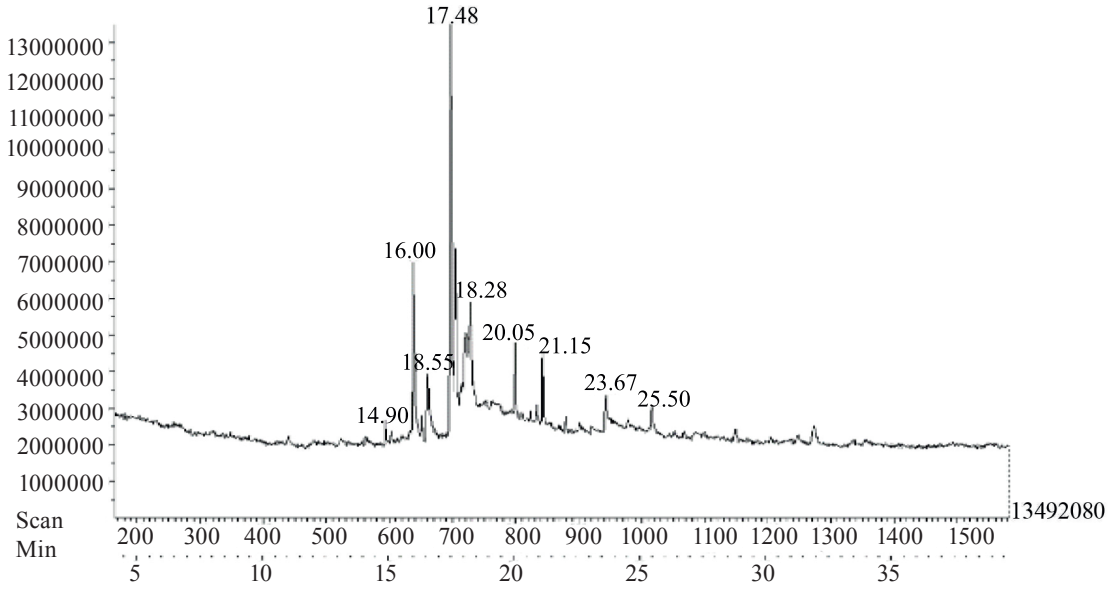

Figure 1 Bioactive constituents identified in *Coriandrum sativum* microgreens

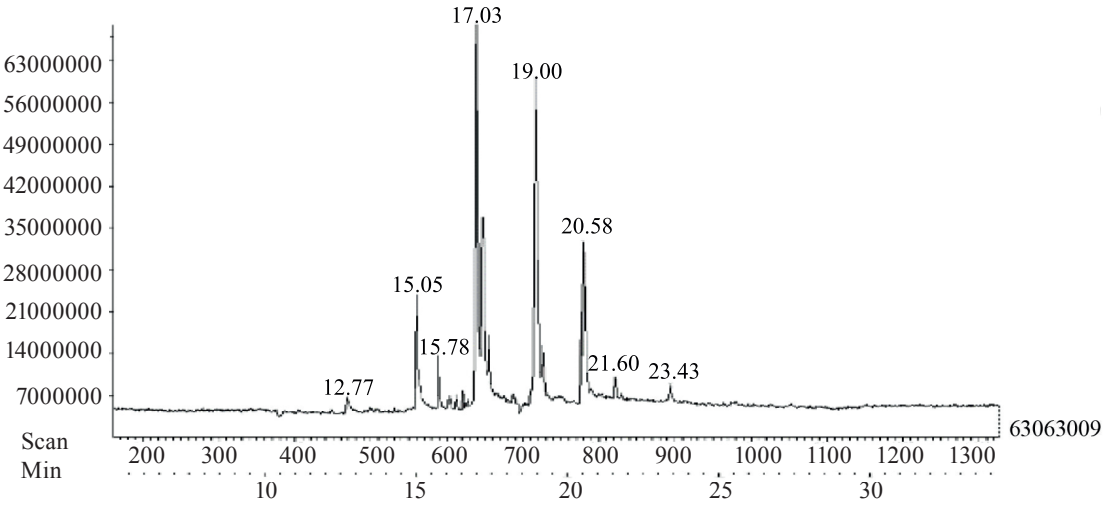

Figure 2 Bioactive constituents identified in coriander mature leaves

standard. Figure 4 illustrates the standard curve; Tables 8 and 9 show the reducing power of test samples.

The aqueous extract of mature leaves showed a slight increase in Fe^{3+} reduction compared to that of microgreens. The RC_{50} (50% reducing concentration) of microgreens and mature leaves in the aqueous extracts were 234.87 and 167.25 µg/mL, respectively. Interestingly, the ethanol extract of microgreens exhibited a greater ferric ion reducing power (31.66% at 300 µg/mL concentration) than that of mature leaves (18.77% at 300 µg/mL concentration). The ethanol extracts were unable to reduce the free radicals by RC_{50}. The causes may be in some other chemical constituents that compete for reduction by Fe^{3+} and do not permit Fe^{3+}

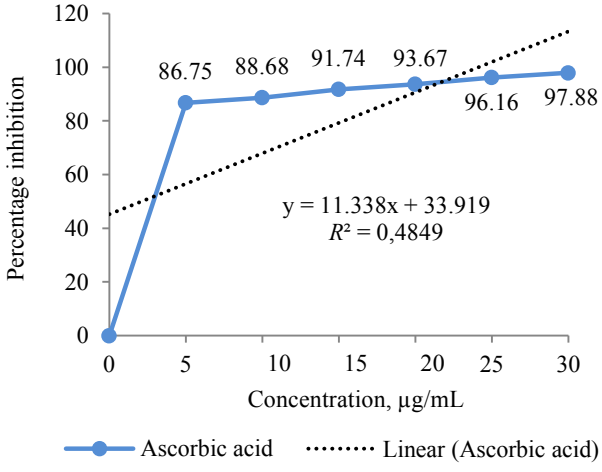

Figure 3 DPPH standard curve of ascorbic acid

Table 4 GC/MS analysis of bioactive compounds in *Coriandrum sativum* microgreens

RT	Name	Structure	Mol.wt g/mol & Mol. formula	Biological activity
14.9	Benzene, (1-methylenebutyl)-		146 $C_{11}H_{14}$	n.d.a.
16	10-Methylundecanoic acid methyl ester		214 $C_{13}H_{26}O_2$	n.d.a.
16.55	(7-Phenyl-1H-imidazo[4,5-d] pyridazin-4-yl)-hydrazine	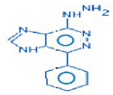	226 $C_{11}H_{10}N_6$	Anticancer, antidiabetic, antiviral, antiosteoporotic, anti-inflammatory, antiparasitic, antihypertensive
17.48	Phenol, 2,6-bis(1,1-dimethylethyl)-4-ethyl-(Phenol)	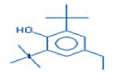	234 $C_{16}H_{26}O$	Antioxidant, cytotoxicity, antidiabetic
18.28	Propenamide,2-acetamido-3-Phenyl-N-(3-hydroxypropyl)-(amide)		262 $C_{14}H_{18}N_2O_3$	Antioxidant
20.05	8-carbetoxy-1-methyl-1,4,5,6,7,8-hexahydropyrrolo[2,3-b]azepin-4-one-3-carboxylic acid	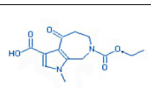	280 $C_{13}H_{16}N_2O_5$	n.d.a.
21.15	5-Phenyl-5,6,7,8-tetrahydro-[1] benzothieno[2,3-d]pyrimidine-2,4-diamine	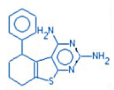	296 $C_{16}H_{16}N_4S$	Antioxidant, antitumor, anticancer, antidiabetic, antimicrobial, antiviral, anti-inflammatory
23.67	Z-13-Octadecen-1-yl acetate (Essential oil)		310 $C_{20}H_{38}O_2$	Antioxidant, anti-inflammatory
25.5	But-2-endiamide,N,N'-bis[4-methoxyphenyl]-	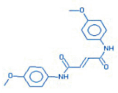	326 $C_{18}H_{18}N_2O_4$	n.d.a.

n.d.a. – no data available

Table 5 GC/MS analysis of bioactive compounds in *Coriandrum sativum* mature leaves

RT	Name	Structure	Mol.wt g/mol & Mol. formula	Biological activity
12.77	2,4-bis[1,1-dimethylethyl]-phenol (Phenolic compound)		206.00 $C_{14}H_{22}O$	Antioxidant, antibacterial, anti-inflammatory
15.05	1-Cyclopentenylphenylmethane	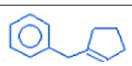	158.00 $C_{12}H_{14}$	n.d.a.
15.78	7-Dodecen-6-one (Terpenoid)	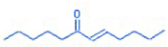	182.00 $C_{12}H_{22}O$	Antioxidant, antibacterial, anti-fungal, anti-malarial
17.03	E, E-6,8-Tridecadien-2-ol, acetate (Essential oil)		238.00 $C_{15}H_{26}O_2$	Antimicrobial
19	2-Hexadecenoic acid, 2,3-dimethyl-, methyl ester, (E)- (Unsaturated fatty acid ester)		296 $C_{19}H_{36}O_2$	Antioxidant, antidiabetic, antitumor, antibacterial, anti-inflammatory, anthelmintic, immunostimulant, lipoxygenase inhibitor
20.58	3-Hydroxypregn-5-en20-one (Steroid)	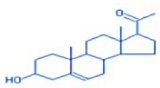	316 $C_{21}H_{32}O_2$	Anti-proliferative
23.43	Methoxyaceticacid, octadecyl ester		342 $C_{12}H_{42}O_3$	n.d.a.

n.d.a. – no data available

Table 6 DPPH radical scavenging activity of *Coriandrum sativum* microgreens and mature leaves (aqueous extract)

Extract concentration, µg/mL	Inhibition, %		Test samples (IC_{50} µg/mL)		Standard ascorbic acid (IC_{50} µg/mL)
	Microgreens	Mature leaves	Microgreens	Mature leaves	
50	49.51 ± 0.49*	56.22 ± 0.47*	90.09 ± 0.45	44.64 ± 0.46	2.88 ± 0.37
100	55.41 ± 0.45*	66.66 ± 0.48*			
150	59.17 ± 0.30 *	70.00 ± 0.50*			
200	65.44 ± 0.47*	75.55 ± 0.45*			
250	76.44 ± 0.47*	77.75 ± 0.46*			
300	81.17 ± 0.30*	84.63 ± 0.41*			

Each value is expressed as mean ± standard deviation (n = 3) and statistically significant at * $P < 0.05$

Table 7 DPPH radical scavenging activity of *Coriandrum sativum* microgreens and mature leaves (ethanol extract)

Extract concentration, µg/mL	Inhibition, %		Test samples (IC_{50} µg/mL)		Standard ascorbic acid (IC_{50} µg/mL)
	Microgreens	Mature leaves	Microgreens	Mature leaves	
50	7.35 ± 0.39*	14.20 ± 0.30*	293.54 ±0.36	186.74 ± 0.43	2.88 ± 0.37
100	22.34 ± 0.41*	31.88 ± 0.34*			
150	37.90 ± 0.36*	39.48 ± 0.45*			
200	42.79 ± 0.26*	53.42 ± 0.36*			
250	45.56 ± 0.32*	65.44 ± 0.39*			
300	51.16 ± 0.30*	75.57 ± 0.32*			

Each value is expressed as mean ± standard deviation (n = 3) and statistically significant at * $P < 0.05$

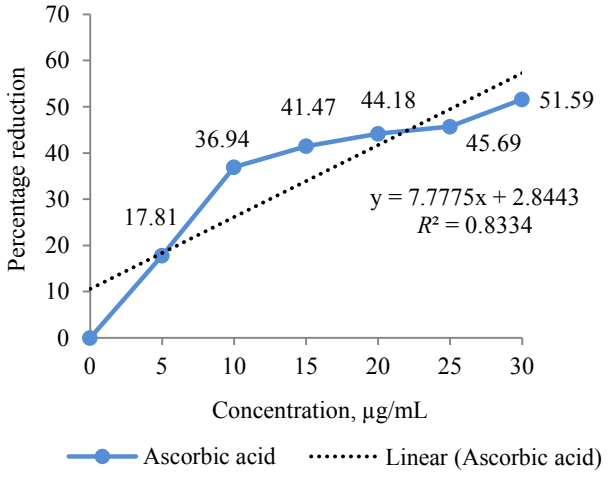

Figure 4 FRAP standard curve of ascorbic acid

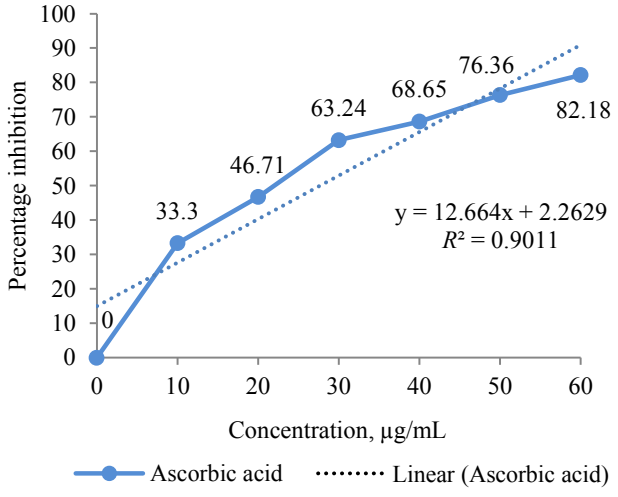

Figure 5 Standard curve of acarbose

to donate an electron. The RC_{50} value for standard ascorbic acid was 29.1 µg/mL.

In vitro* antidiabetic activity. *α-amylase enzyme inhibition assay. Tables 10 and 11 show the inhibitory activity of test samples on the α-amylase enzyme. The aqueous and ethanol extracts of microgreens exhibited 50% of inhibition on α-amylase enzyme at 222.22 and 84.25 µg/mL. The results were lower than those of mature leaves IC_{50} values, which were 228.31 and 206.82 µg/mL, respectively. The standard reference drug acarbose (Fig. 5) showed α-amylase inhibitory activity with an IC_{50} valueof 23.71 µg/mL.

Cytotoxicity assay on colon cell lines. In the present study, the antioxidant activities of the aqueous extracts were compared to those of the ethanolic extracts. The aqueous extract of microgreens and mature leaves were examined for potential anticancer activity against the human colon HT-29 carcinoma cell line by using the MTT assay. The tests were performed in duplicate. The absorbance values were registered in the ELISA reader at 595 nm once purple color developed after 24 h of incubation. The mean was calculated for two trials (Table 12).

Table 8 Ferric reducing antioxidant power activity of *Coriandrum sativum* microgreens and mature leaves (aqueous extract)

Extract concentration, µg/mL	Reduction, %		Test samples (RC_{50} µg/mL)		Standard ascorbic acid (RC_{50} µg/mL)
	Microgreens	Mature leaves	Microgreens	Mature leaves	
50	22.64 ± 0.21*	19.23 ± 0.25*	234.87 ± 0.33	167.25 ± 0.36	29.10 ± 0.36
100	25.50 ± 0.35*	33.79 ± 0.31*			
150	35.36 ± 0.31*	44.36 ± 0.29*			
200	48.42 ± 0.33*	59.79 ± 0.32*			
250	53.22 ± 0.23*	60.60 ± 0.36*			
300	60.31 ± 0.27*	64.64 ± 0.35*			

Each value is expressed as mean ± standard deviation (n = 3) and statistically significant at * $P < 0.05$

Table 9 Ferric reducing antioxidant power activity of *Coriandrum sativum* microgreens and mature leaves (ethanol extract)

Extract concentration, µg/mL	Reduction, %		Test samples (RC_{50} µg/mL)		Standard ascorbic acid (RC_{50} µg/mL)
	Microgreens	Mature leaves	Microgreens	Mature leaves	
50	11.27 ± 0.27*	9.52 ± 0.35*	Nil	Nil	29.10 ± 0.36
100	15.41 ± 0.37*	10.59 ± 0.30*			
150	15.80 ± 0.32*	13.83 ± 0.25*			
200	19.32 ± 0.32*	14.85 ± 0.24*			
250	20.04 ± 0.40*	16.50 ± 0.36*			
300	31.66 ± 0.38*	18.77 ± 0.28*			

Each value is expressed as mean ± standard deviation (n = 3) and statistically significant at * $P < 0.05$

Table 10 *α*-amylase enzyme inhibition activity of *Coriandrum sativum* microgreens and mature leaves (aqueous extract)

Extract concentration, µg/mL	Inhibition, %		Test samples (IC_{50} µg/mL)		Standard ascorbic acid (IC_{50} µg/mL)
	Microgreens	Mature leaves	Microgreens	Mature leaves	
50	15.66 ± 0.42*	9.57 ± 0.30*	222.22 ± 0.37	228.31 ± 0.31	23.70 ± 0.34
100	29.83 ± 0.23*	37.82 ± 0.31*			
150	39.27 ± 0.37*	39.16 ± 0.29*			
200	46.45 ± 0.37*	45.61 ± 0.44*			
250	56.25 ± 0.30*	54.75 ± 0.23*			
300	87.31 ± 0.36*	79.55 ± 0.36*			

Each value is expressed as mean ± standard deviation (n = 3) and statistically significant at * $P < 0.05$

Table 11 *α*-amylase enzyme inhibition activity of *Coriandrum sativum* microgreens and mature leaves (ethanol extract)

Extract concentration, µg/mL	Inhibition, %		Test samples (IC_{50} µg/mL)		Standard ascorbic acid (IC_{50} µg/mL)
	Microgreens	Mature leaves	Microgreens	Mature leaves	
50	45.70 ± 0.35*	11.84 ± 0.24*	84.25 ± 0.25	206.82 ± 0.35	23.70 ± 0.34
100	59.35 ± 0.39*	33.44 ± 0.37*			
150	65.10 ± 0.31*	40.45 ± 0.36*			
200	68.82 ± 0.21*	46.58 ± 0.36*			
250	69.46 ± 0.34*	60.44 ± 0.39*			
300	69.73 ± 0.25*	61.13 ± 0.27*			

Each value is expressed as mean ± standard deviation (n = 3) and statistically significant at * $P < 0.05$

As the concentration of the test samples increased, the corresponding absorbance value decreased ($P < 0.05$). The MTT assay showed that the microgreen sample increased the percentage inhibition and consequently decreased the cell viability to 49.08% with the lowest IC_{50} value of 98.34 µg/mL. Mature leaves showed the least percentage inhibition and reduced viable cells to 59.53% with an IC_{50} value of 123.54 µg/mL (Figs. 6 and 7). Doxorubicin was used as the reference standard. Figure 8 demonstrates the standard curve of percent cell viability, which showed a cytotoxicity activity with an IC_{50} value of 11.75 µg/mL.

Table 12 Absorbance values at different concentrations in ELISA reader at 595 nm

Concentration, µg/mL	Optical density of:	
	Microgreens at 595 nm	Mature leaves at 595 nm
0.001	0.757 ± 0.007*	0.807 ± 0.007*
0.01	0.641 ± 0.008*	0.752 ± 0.004*
0.1	0.555 ± 0.009*	0.709 ± 0.012*
1	0.510 ± 0.001*	0.637 ± 0.008*
10	0.484 ± 0.001*	0.592 ± 0.001*
100	0.439 ± 0.001*	0.533 ± 0.006*
Control optical density at 595 nm	0.895 ± 0.002*	
Negative control optical density at 595 nm	0.847 ± 0.007*	

Each value is expressed as mean ± standard deviation (n = 3) and statistically significant at * $P < 0.05$

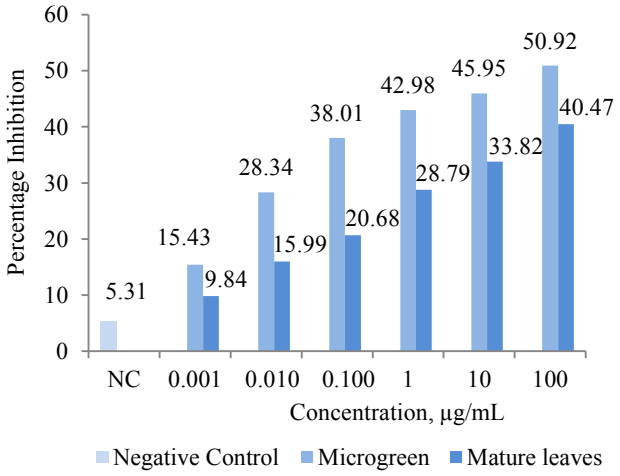

Figure 6 Effect of aqueous extracts of *Coriandrum sativum* microgreens and mature leaves on growth inhibition of HT-29 colon cell line

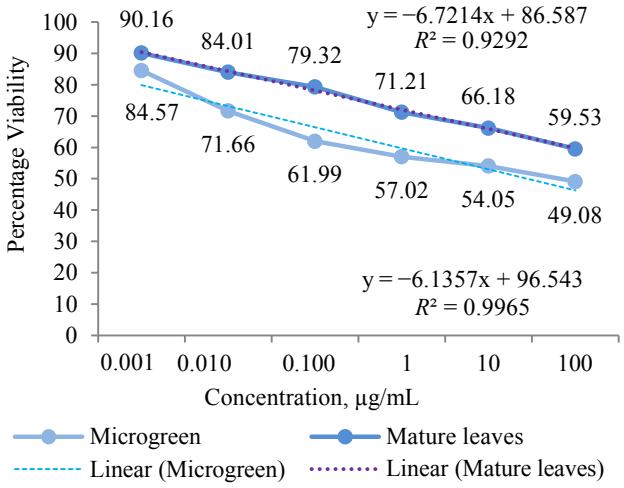

Figure 7 Cytotoxic effect of aqueous extracts of *Coriandrum sativum* microgreens and mature leaves on HT-29 colon cell lines

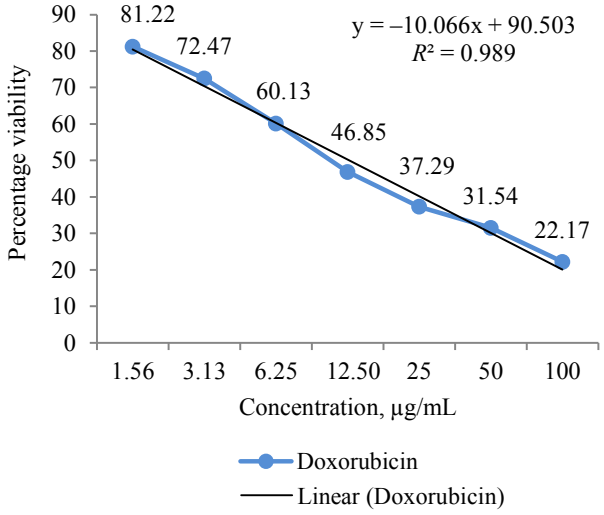

Figure 8 Cytotoxic effect of standard drug doxorubicin on HT-29 colon cell line

CONCLUSION

In the present research, aqueous and ethanol solvents of varying polarity were used to extract phytoconstituent compounds from *Coriandrum sativum* microgreens and mature leaves. The aqueous solvent had higher polarity for bio-extraction. According to the phytochemical analysis, *C. sativum* microgreens proved to be an abundant source of phenol, flavonoids, and steroids, compared to mature leaves. However, *C. sativum* mature leaves had more ascorbic acid, total chlorophylls, and carotenoids. The GC/MS test revealed various phyto-constituents with good therapeutic properties. The microgreens exhibited a much higher correlation with free radical reducing power than with the radical scavenging activity. The microgreens also had a higher α-amylase enzyme inhibitory property and a greater anticarcinogenic effecton colon cancer cell line. Therefore, *C. sativum* microgreens proved to be amore effective antioxidant, antidiabetic, and anticarcinogenic agent than mature leaves. Coriander microgreens can be as good as mature coriander leaves for the daily diet of a disease-free community.

CONTRIBUTION

The authors are equally involved in writing the manuscript and are equally responsible for plagiarism.

CONFLICT OF INTEREST

The authors have declared no conflict of interests regarding the publication of this manuscript.

REFERENCES

1. International Diabetes Federation [Internet]. [cited 2022 Jan 10]. Available from: https://www.idf.org/aboutdiabetes/what-is-diabetes/facts-figures.html
2. González N, Prieto I, del Puerto-Nevado L, Portal-Nuñez, S, Ardura JA, Corton M, *et al.* 2017 update on the relationship between diabetes and colorectal cancer: Epidemiology, potential molecular mechanisms and therapeutic implications. Oncotarget. 2017;8(11):18456–18485. https://doi.org/10.18632/oncotarget.14472
3. Suh S, Kim K-W. Diabetes and cancer: is diabetes causally related to cancer? Diabetes and Metabolism Journal. 2011;35(3)193–198. https://doi.org/10.4093/dmj.2011.35.3.193
4. Meyer B, Are C. Current status and future directions in colorectal cancer. Indian Journal of Surgical Oncology. 2018;9(4):440–441. https://doi.org/10.1007/s13193-017-0711-9
5. Nishteswar K. Ayurvedic concept of food and nutrition. Journal of Nutrition & Food Sciences. 2017;6(4). https://doi.org/10.4172/2155-9600.1000530
6. De Souza EL, Stamford TLM, De Oliveira Lima E, Tarajano VN, Barbosa Filho JM. Antimicrobial effectiveness of spices: An approach for use in food conservation system. Brazilian Archives Biology Technology. 2005;48(4):549–558. https://doi.org/10.1590/s1516-89132005000500007
7. Sachan AKR, Kumar S, Kumari K, Singh D. Medicinal uses of spices used in our traditional culture: World wide. Journal of Medicinal Plants Studies. 2018;6(3):116–122.
8. Prachayasittikul V, Prachayasittikul S, Ruchirawat S, Prachayasittikul V. Coriander (*Coriandrum sativum*): A promising functional food toward the well-being. Food Research International. 2018;105:305–323. https://doi.org/10.1016/j.foodres.2017.11.019
9. Pinto E, Almeida AA, Aguiar AA, Ferreira IMPLVO. Comparison between the mineral profile and nitrate content of microgreens and mature lettuces. Journal of Food Composition and Analysis. 2015;37:38–43. https://doi.org/10.1016/j.jfca.2014.06.018
10. Xiao Z, Lester GE, Luo Y, Wang Q. Assessment of vitamin and carotenoid concentrations of emerging food products: Edible microgreens. Journal of Agricultural and Food Chemistry. 2012;60(31):7644–7651. https://doi.org/10.1021/jf300459b
11. Ebert AW, Wu TH, Yang RY. Amaranth sprouts and microgreens-A homestead vegetable production option to enhance food and nutrition security in the rural-urban continuum. SEAVEG2014: families, farms, food: Proceedings of the regional symposium on sustaining small-scale vegetable production and marketing systems for food and nutrition security; 2014; Bangkok. Taiwan: AVRDC; 2015. p. 233–244.
12. Kou L, Yang T, Luo Y, Liu X, Huang L, Codling E. Pre-harvest calcium application increases biomass and delays senescence of broccoli microgreens. Postharvest Biology and Technology. 2014;87:70–78. https://doi.org/10.1016/j.postharvbio.2013.08.004
13. Mir SA, Shah MA, Mir MM. Microgreens: Production, shelf life and bioactive components. Critical Reviews in Food Science and Nutrition. 2017;57(12):2730–2736. https://doi.org/10.1080/10408398.2016.1144557
14. Chandra D, Kim JG, Kim YP. Changes in microbial population and quality of microgreens treated with different sanitizers and packaging films. Horticulture Environment and Biotechnology. 2012;53(1):32–40. https://doi.org/10.1007/s13580-012-0075-6
15. Banu SK, Cathrine L. General techniques involved in phytochemical analysis. International Journal of Advanced Research in Chemical Science. 2015;2(4):25–32.
16. Finar IL. Stereo chemistry and the chemistry of natural products. Vol. 2. Longman; 1986. 518 p.
17. Hindi NKK, Al-Charrakh AH, Naher HS, Abbas AS. Study of chemical analysis of Iraqi propolis and active component of proplis, Iraq. Journal of Science. 2015;15(11):1095–1103.
18. Kokate CK. Practical pharmacognosy. 4th edition. New Delhi: Vallabh Prakashan; 1994. 186 p.
19. Shrivastava DK. Phytochemical analysis of a miracle herb *Coriander sativum*. Indian Journal of Scientific Research. 2017;13(2):09–14.
20. Singh V, Kumar R. Study of phytochemical analysis and antioxidant activity of *Allium sativum* of Bundelkhand region. International Journal of Life Sciences Scientific Research. 2017;3(6):1451–1458.
21. Wagner H, Bladt S. Plant drug analysis. A thin layer chromatography atlas. Heidelberg: Springer Berlin; 1996. 384 p. https://doi.org/10.1007/978-3-642-00574-9
22. Singleton VL, Orthofer R, Lamuela-Raventós RM. Analysis of total phenols and other oxidation substrates and antioxidants by means of folin-ciocalteu reagent. Methods in Enzymology. 1999;299:152–178. https://doi.org/10.1016/S0076-6879(99)99017-1

23. Ahmed D, Fatima K, Saeed R. Analysis of phenolic and flavonoid contents, and the anti-oxidative potential and lipid peroxidation inhibitory activity of methanolic extract of *Carissa opaca* roots and its fractions in different solvents. Antioxidants. 2014;3(4):671–683. https://doi.org/10.3390/antiox3040671
24. Kharate MS, Pandhure NB. Quantitative estimation of phytochemical and antimicrobial properties of crude leaf extract, *Mimusops elengil* L. International journal for research in applied science & engineering technology. 2017;5(12):2699–2707.
25. Hedge JE, Hofreiter BT. Carbohydrate chemistry. 17th edition. New York: Academic Press; 1962.
26. Mahavi MO, Nilesh PS. Quantitative estimation of amino acids and carbohydrates in the root exudates of *Salvadora persica*. International Journal of Biology Research. 2016;1(3):4–10.
27. Rao BS, Deshpande V. Experimental biochemistry: A student companion. Royal Tunbridge Wells: Anshan; 2006. 302 p.
28. Aron DI. Copper enzymes in isolated chloroplasts phenoloxidase in *Beta vulgaris*. Plant physiology. 1949;24(1):1–15. https://doi.org/10.1104/pp.24.1.1
29. Duxbury AC, Yentach CS. Plankton pigment monograph. Journal of Marine Research. 1956;15:190–191.
30. Maclachalam S, Zalik S. Plastid structure, chlorophyll concentration and free amino acid composition of a chlorophyll mutant of barely. Canadian Science Publishing. 1963;4:1053–1062.
31. Ravisankar N, Sivaraj C, Seeni S, Joseph J, Raaman N. GC-MS Analysis and anticancer activity of methanol extract of leaves of *Hypericum hookerianum* Wight & Arn. International Journal of Pharmacy and Pharmaceutical Sciences. 2014;6(5):515–519.
32. Khalaf NA, Shakya AK, Al-othman A, El-agbar Z, Farah H. Antioxidant activity of some common plant. Turkish Journal of Biology. 2008;32(1):51–55.
33. Oyaizu M. Studies on products of browning reaction: antioxidative activities of products of browning reaction prepared from glucosamine. Japanese Journal of Nutrition. 1986;44(4):307–315. https://doi.org/10.5264/eiyogakuzashi.44.307
34. Gayathri S, Sivaraj C, Sangeetha ST, Arumugam P, Manimaran A. Evaluation of antioxidant, antibacterial, alpha amylase enzyme inhibition activities and GC-MS analysis of leaves extract of *Gymnema sylvestre* L. Journal of Pharmacognosy and Phytochemistry. 2018;7(6):2326–2333.
35. Mosmann T. Rapid colorimetric assay for cellular growth and survival: Application to proliferation and cytotoxicity assays. Journal of Immunological Methods. 1983;65(1–2):55–63. https://doi.org/10.1016/0022-1759(83)90303-4
36. Vardhini SP, Sivaraj C, Arumugam P, Himanshu R, Kumaran T, Baskar M. Antioxidant, anticancer, antibacterial activities and GCMS analysis of aqueous extract of pulps of *Aegle marmelos* (L.) Correa. The Journal of Phytopharmacology. 2018;7(1):72–78. https://doi.org/10.31254/phyto.2018.7115

ORCID IDs
S. Janaki Alias Priya https://orcid.org/0000-0001-7224-6905

Foods and Raw Materials. 2022;10(2)

ISSN 2310-9599 (Print)
ISSN 2308-4057 (Online)

Research Article
Open Access

Available online at http://jfrm.ru/en
https://doi.org/10.21603/2308-4057-2022-2-536
https://elibrary.ru/WVYEGP

Near-infrared spectroscopy as a green technology to monitor coffee roasting

Krzysztof Wójcicki

Poznań University of Economics and Business, Poznań, Poland

e-mail: krzysztof.wojcicki@ue.poznan.pl

Received 17.12.2021; Revised 10.03.2022; Accepted 05.04.2022; Published online 23.09.2022

Abstract:
Wet chemistry methods are traditionally used to evaluate the quality of a coffee beverage and its chemical characteristics. These old methods need to be replaced with more rapid, objective, and simple analytical methods for routine analysis. Near-infrared spectroscopy is an increasingly popular technique for nondestructive quality evaluation called a green technology.

Our study aimed to apply near-infrared spectroscopy to evaluate the quality of coffee samples of different origin (Brazil, Guatemala, Peru, and Congo). Particularly, we analyzed the roasting time and its effect on the quality of coffee. The colorimetric method determined a relation between the coffee color and the time of roasting. Partial least squares regression analysis assessed a possibility of predicting the roasting conditions from the near-infrared spectra.

The regression results confirmed the possibility of applying near-infrared spectra to estimate the roasting conditions. The correlation between the spectra and the roasting time had R^2 values of 0.96 and 0.95 for calibration and validation, respectively. The root mean square errors of prediction were low – 0.92 and 1.05 for calibration and validation, respectively. We also found a linear relation between the spectra and the roasting power. The quality of the models differed depending on the coffee origin and sub-region. All the coffee samples showed a good correlation between the spectra and the brightness (L^* parameter), with R^2 values of 0.96 and 0.95 for the calibration and validation curves, respectively.

According to the results, near-infrared spectroscopy can be used together with the chemometric analysis as a green technology to assess the quality of coffee.

Keywords: Spectroscopy, near-infrared spectroscopy, coffee, roasting, partial least squares analysis

Please cite this article in press as: Wójcicki K. Near-infrared spectroscopy as a green technology to monitor coffee roasting. Foods and Raw Materials. 2022;10(2):295–303. https://doi.org/10.21603/2308-4057-2022-2-536

INTRODUCTION

Near-infrared spectroscopy (NIRS) is an increasingly popular technique used for non-destructive quality evaluation in a variety of industries, including the food, agricultural, pharmaceutical, and wood industries [1–3]. It ensures rapid and easy measurements without the need for multiple chemical reagents. Recent NIRS methods include online measurement, portable measurement, and imaging analysis [4–6]. NIRS is continuously expanding its uses in food analysis and becoming an important tool for food quality control.

The quality of coffee as a beverage is determined by multiple factors such as the production system, geographical origin, chemical composition of roasted beans, and final beverage characteristics. Raw coffee beans contain a wide range of chemical compounds which interact amongst themselves at all stages of coffee roasting, resulting in greatly diverse final products [7–9]. For instance, the caffeine content, which has a significant effect on the final quality of coffee products, needs to be determined fast and reliably by analytical techniques.

Wet chemistry methods are traditionally used to evaluate coffee quality and chemical characteristics, but these methods are destructive and time-consuming. Therefore, it is in scientific interests to find rapid, more objective, and simpler analytical methods for routine coffee analysis to replace the old methods.

Recent research has shown that spectroscopy in near-infrared (NIR) and mid-infrared (MIR) radiation is useful in coffee analysis [10–20]. Infrared spectroscopy (especially NIRS) coupled with chemometrics has been proposed as an analytical method to determine the degree of coffee roasting, adulterants in ground coffee, and sensory attributes [17, 18, 21]. It is also used to distinguish between robusta and arabica varieties,

discriminate coffee based on origin, and predict its chemical composition [15, 20, 22–24].

The growing global demand for specialty coffee increases the need for improved coffee quality assessment. For this reason, Tolessa *et al.* proposed NIR spectroscopy to predict specialty coffee quality [13]. They examined the NIR spectra of 86 green Arabica bean samples of various quality. To create a model that correlates spectral data to cupping score data, they applied the partial least squares (PLS) regression method. The high correlation coefficient between the measured and predicted cupping scores (R^2-values of 90, 90,78, 72 and 72) indicate that NIR spectroscopy coupled with chemometric analysis could be a promising tool for fast and accurate prediction of coffee quality and for classifying green coffee beans into different specialty grades.

The sensory analysis of espresso coffee with the attenuated total reflectance-Fourier transform infrared spectroscopy (ATR-FTIR) was proposed by Belchior *et al.* [10]. The authors evaluated the potential of ATR-FTIR and chemometrics in discriminating espresso coffees with different sensory characteristics reported by a panel of coffee tasters. They performed partial least-squares discriminant analysis (PLS-DA) based on spectroscopic data to classify the coffee samples according to their sensory qualities, demonstrating the potential of FTIR and chemometric analysis in assessing coffee quality.

In another study, Magalhaes *et al.* proposed FT-NIR spectroscopy and PLS regression as a non-destructive and rapid tool to assess the content of three main phenolics (caffeic acid, (+)-catechin, and chlorogenic acid) and methylxanthines (caffeine, theobromine, and theophylline) in spent coffee grounds [11]. The best PLS model was obtained for caffeine content (0.95) followed by caffeic acid (0.92), (+)-catechin (0.88), theophylline (0.84), and chlorogenic acid (0.71), indicating FT-NIR spectroscopy as a suitable technique to screen spent coffee grounds.

Mees *et al.* identified coffee leaves using FT-NIR spectroscopy and soft independent modelling by class analogy (SIMCA) [12]. In particular, they investigated nine taxa of *Coffea* leaves harvested over nine years in a tropical greenhouse of the Meise Botanic Garden (Belgium). The FT-NIR coupled with SIMCA allowed the authors to discriminate the spectral profile by taxon, aging stage, and harvest period with a correct classification rate of 90, 100, and 90%, respectively.

NIRS, PLS, and variable selection were used by Ribeiro *et al.* to predict concentrations of a wide range of compounds in raw coffee beans [15]. The authors proposed NIR spectroscopy coupled with chemometrics as a low-cost, rapid, and eco-friendly method in both off-line and on-line analyses of coffee beans and coffee beverages. The obtained values of root mean square error of prediction (RMSEP) (0.08, 0.07 and 0.27) and r_{cv} (0.98, 0.96, and 0.96) showed linear relations of PLS models for quantifying caffeine, trigonelline, and 5-caffeoylquinic acid, respectively.

Near-infrared spectroscopy was used by Macedo *et al.* to evaluate the chemical properties of intact green coffee beans based on PLS regression models [25]. The highest determination coefficients obtained for the samples in the validation set were 0.810, 0.516, 0.694, and 0.781 for moisture, soluble solids, total sugar, and reducing sugars, respectively. These results indicate that the NIR technology can be applied routinely to predict the chemical properties of green coffee.

In another study, Baqueta *et al.* investigated the use of NIR spectroscopy in conjunction with the PLS approach to identify the sensory properties of coffee [21]. The coffee samples varied in species, production region, variety, drying conditions, transit, postharvest procedure, storage times, coffee blend, coffee composition, and roasting process. The performance of PLS models was verified with the following merit parameters: sensitivity, accuracy, linearity, residual prediction deviation, fit, quantification, and detection limits. Since all the sensory qualities were predicted with acceptable values compatible with the merit criteria, the created models were suitable for quantifying, detecting, differentiating, and predicting the sensory features of coffee samples.

Kyaw *et al.* reported encouraging findings about utilizing NIR spectroscopy to forecast the moisture content of ground unroasted coffee beans [26]. The spectral data processed with second derivative and Kubelka-Munk (K/S) data yielded good accuracy for moisture prediction (r = 0.87 and accuracy = 99%).

In view of the above, we aimed to develop a simple, rapid, and accurate method for evaluating the quality of coffee samples by NIR spectroscopy, especially to investigate changes in the coffee spectra during roasting.

STUDY OBJECTS AND METHODS

Samples. Our study objects were arabica coffee samples roasted by the Cafe Creator in Poznań, Poland. The coffee samples were divided into four groups based on their origin, namely Brazil, Guatemala, Peru, and Congo. Their roasting parameters included the roaster power and roasting time (Table 1).

Color measurements. The color of 41 samples of coffee beans was measured by the *L* a* b** method using a Konica Minolta Chroma Meter CR-310 trichromatic colorimeter. Each sample was measured 10 times. Before the measurements, the device was calibrated against a white standard with the following parameters: Y = 93.00, x = 0.3170, y = 0.3330. The entire analysis was carried out using a D65 light source, i.e. the daylight phase and the CIE *L* a* b** color system.

Near-infrared (NIR) measurements. NIR spectra were performed on a MPA/FT-NIR spectrometer (Bruker). Single beam spectra of the coffee samples were collected and rationed against the background of air. For each sample, the NIR spectra were recorded from 12500 to 400 cm^{-1} by co-adding 16 interferograms at a resolution of 4 cm^{-1}. Each sample was measured five

Table 1 Roasting parameters of coffee samples

Origin	Power of the roaster, %	Roasting time, min
Brazil	Green	–
	75	8, 10, 12, 13
	80	8, 10, 12
	95	8, 10, 12
Guatemala	Green	–
	75	8, 10, 12, 15
	80	8, 10, 12, 14
	95	8, 10, 12, 13
Peru	Green	–
	75	8, 10, 12, 14
	80	8, 10, 12, 14
	95	8, 10, 12, 14
Congo	Green	–
	80	8, 10, 12

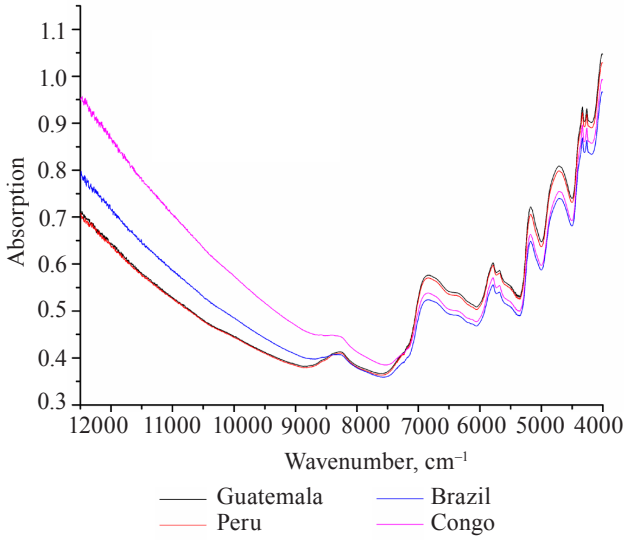

Figure 1 Absorption spectra of ground coffee in near-infrared region (12500–4000 cm^{-1})

times. The coffee was ground in an electric grinder for measurements. Between the measurements, the samples were mixed in order to obtain reliable results. The measurements were registered in the OPUS software (Bruker, USA).

Partial Least Squares (PLS) regression. The PLS regression method was used to determine relations between the spectra and the roasting time. Independent variables (X) were the NIR spectra and dependent variables (Y) were the color parameter or the roasting time. Full cross-validation was applied to the regression model. The regression models were evaluated using the adjusted R^2 and the root mean-square error of cross-validation. The quality models were evaluated by the ratio of the standard deviation of reference data to the root mean-square error of prediction, or the ratio of performance to deviation. The PLS analysis was carried out using the Unscrambler X software (CAMO, Oslo, Norway).

RESULTS AND DISCUSSION

Color measurements. Table 2 shows the color measurements of coffee beans in the L^*, a^*, b^* system.

The L^* parameter is responsible for the brightness of color in the tristimulus model. The higher it is, the greater the brightness of the tested sample. Among the coffees under study, the green coffee beans from Peru had the highest L^* value, i.e., the highest brightness. The Congo coffee, which was roasted at the power of 80% for 12 min, had the lowest L^* parameter, i.e., the lowest brightness. All the samples had positive a^* and b^* values, with their shades varying between red and yellow.

As we can see in Table 2, the green coffee beans showed the greatest brightness, followed by the samples roasted for 8 min. With the increasing degree of roasting, the color of coffee beans became darker, which is consistent with literature [27, 28].

Spectral characteristics of coffee samples. Figure 1 shows the absorption spectra of the coffees from Brazil, Congo, Guatemala, and Peru roasted for 12 min (80% roasting power). The spectral range was recorded throughout the region of 12 500–4000 cm^{-1}. The most intense absorption bands were recorded in the range of 8230–4440 cm^{-1}. The spectra were characterized by seven bands with maximum absorption at 8238, 6819, 5800, 5700, 5100, 4700, and 4440 cm^{-1}. These bands corresponded to the C-H, N-H, and O-H vibrations [29]. The spectral range of 4545–4000 cm^{-1} corresponded to the C-H stretching vibrations. The bands in the region of 5000–4545 cm^{-1} were assigned to the combination of the N-H and O-H stretching vibrations. The range of 6060–5555 cm^{-1} corresponded to the first tone of the C-H stretching vibration. In the 7142–6666 cm^{-1} region, it was associated with the first shade of the N-H and O-H stretching vibrations, while the absorption band in the 7692–7142 cm^{-1} range was derived from the C-H stretching vibrations. The band in the region of 9090–8163 cm^{-1} originated from the second tone of the C-H stretching vibrations [30]. Specific chemical compounds can be described with the following wavenumbers: caffeine (8865, 7704, 5981, 5794, and 5171 cm^{-1}), trigonelline (8865 cm^{-1}), chlorogenic acid (6770, 5794, 5171, and 4699 cm^{-1}), lipids (6770, 5794, 5171, and 4699 cm^{-1}), hydrocarbons (6770, 5171, and 4699 cm^{-1}), sucrose (5794, 5405, and 5171 cm^{-1}), proteins and amino acids (5171 cm^{-1}), and water (5171 cm^{-1}) [9, 14, 31]. Table 3 presents the origin of the bonds occurring at the given wavenumbers for the tested coffee beans.

Coffee roasting. Many physical and chemical changes take place during coffee roasting. The method of roasting depends on the origin of coffee beans and consumer preferences. Heavily roasted coffee has a lower nutritional value than light coffee [32].

Numerous efforts have already been made to use NIR spectroscopy as an alternative technique to determine coffee quality during roasting and analyze its chemical composition. According to Ribeiro *et al.*, NIR spectroscopy can be used to determine the relationship

Table 2 Color measurements of green and roasted coffee beans

Origin	Power of the roaster, %	Roasting time, min	*L** average	*b** average	*a** average
Guatemala (green beans)	–	–	51.670 ± 0.200	0.870 ± 0.120	11.700 ± 0.141
Guatemala (roasted beans)	95	8	45.440 ± 0.163	5.980 ± 0.057	12.650 ± 0.013
		10	42.410 ± 0.233	5.240 ± 0.064	9.810 ± 0.177
		12	38.050 ± 0.099	3.550 ± 0.099	6.250 ± 0.085
		13	36.390 ± 0.318	3.210 ± 0.042	4.760 ± 0.086
	80	8	45.480 ± 0.255	6.060 ± 0.156	12.290 ± 0.383
		10	42.460 ± 0.283	5.300 ± 0.106	9.980 ± 0.163
		12	39.720 ± 0.191	4.150 ± 0.077	7.380 ± 0.205
		14	36.770 ± 0.282	3.230 ± 0.071	4.550 ± 0.085
	75	8	48.120 ± 0.184	6.280 ± 0.163	14.470 ± 0.134
		10	43.210 ± 0.269	5.600 ± 0.106	10.490 ± 0.185
		12	40.620 ± 0.184	4.570 ± 0.099	7.860 ± 0.120
		15	36.460 ± 0.141	3.300 ± 0.064	4.160 ± 0.141
Peru (green beans)	–	–	53.440 ± 0.042	0.880 ± 0.049	12.840 ± 0.078
Peru (roasted beans)	95	8	42.540 ± 0.120	5.560 ± 0.085	10.430 ± 0.148
		10	38.940 ± 0.099	4.330 ± 0.064	7.280 ± 0.057
		12	38.060 ± 0.410	3.710 ± 0.121	6.440 ± 0.234
		14	36.860 ± 0.155	3.390 ± 0.064	5.270 ± 0.049
	80	8	45.010 ± 0.057	6.360 ± 0.064	12.620 ± 0.042
		10	42.240 ± 0.078	5.510 ± 0.092	10.420 ± 0.127
		12	39.910 ± 0.156	4.160 ± 0.020	7.510 ± 0.106
		14	37.350 ± 0.120	3.200 ± 0.049	5.360 ± 0.099
	75	8	45.350 ± 0.092	6.440 ± 0.057	12.930 ± 0.106
		10	40.240 ± 0.157	4.850 ± 0.085	8.290 ± 0.142
		12	39.270 ± 0.099	4.120 ± 0.049	7.130 ± 0.071
		14	37.610 ± 0.134	3.530 ± 0.021	5.440 ± 0.071
Congo (green beans)	–	–	51.440 ± 0.134	0.610 ± 0.085	11.050 ± 0.071
Congo (roasted beans)	80	8	42.150 ± 0.141	4.620 ± 0.041	9.270 ± 0.078
		10	39.240 ± 0.141	3.810 ± 0.078	6.680 ± 0.078
		12	36.120 ± 0.156	2.670 ± 0.085	3.950 ± 0.041
Brazil (green beans)	–	–	52.360 ± 0.205	1.140 ± 0.057	13.080 ± 0.058
Brazil (roasted beans)	95	8	46.240 ± 0.092	6.810 ± 0.064	13.910 ± 0.099
		10	41.650 ± 0.128	5.360 ± 0.640	9.310 ± 0.064
		12	36.980 ± 0.085	3.460 ± 0.085	4.780 ± 0.064
	80	8	45.600 ± 0.071	6.040 ± 0.084	13.110 ± 0.099
		10	42.290 ± 0.134	5.800 ± 0.099	10.290 ± 0.065
		12	37.930 ± 0.092	3.910 ± 0.071	5.860 ± 0.042
	75	8	43.570 ± 0.184	6.190 ± 0.057	11.300 ± 0.064
		10	39.340 ± 0.128	4.600 ± 0.057	7.340 ± 0.014
		12	37.440 ± 0.170	3.710 ± 0.058	5.160 ± 0.085
		13	36.690 ± 0.134	3.080 ± 0.057	4.210 ± 0.071

between the quality of a coffee cup and the chemical composition of roasted coffee beans [9]. In addition, the authors created a model from roasted beans to predict the quality attributes of a coffee cup (e.g. acidity, body, and flavor).

The relationship between some coffee roasting variables (weight loss, density, and moisture) and near-infrared spectra of original green and differently roasted coffee samples was investigated by Alessandrini *et al.* [14]. They developed separate calibration and validation models based on partial least square (PLS) regression, correlating NIR spectral data of 168 representatives and suitable green and roasted coffee samples with each roasting variable. As a result, the authors constructed robust and reliable models to predict roasting variables for unknown roasted coffee samples, considering that measured vs. predicted values showed high correlation coefficients (0.92–0.98).

Pires *et al.* used multivariate calibration and NIR spectroscopy to correctly predict roasting degrees in ground coffee and coffee beans as a substitute for the Agtron method [18]. The mathematical models for predicting Agtron values of new coffee samples using the PLS approach were based on the association between NIR spectra data and Agtron reference results. All Agtron roasting characteristics were investigated in order to create representative models. With RMSEP

Table 3 The origin of bonds occurring at given wavenumbers for tested coffee beans [31]

Bond type	Wavenumber, cm^{-1}
CH_3; second overtone; stretching symmetric	8545–8042
CH	7020–6562
CH_3; first overtone; stretching asymmetric	5841–5751
CH_2; first overtone; stretching asymmetric	5725–5654
OH; stretching	5234–5000
CH; stretching	4954–4509
CH_3; stretching	4358–4302

values of 4.48 and 3.67, respectively, the proposed models showed promising results in predicting roasting characteristics in roasted whole coffee beans and ground coffees.

Yergenson and Aston investigated the use of in situ NIR spectroscopy in the prediction of cracking events (start and end) during coffee roasting in order to develop a more robust method of roasting based on cracks [33]. Two sets of popping sounds (first and second cracks) that occur during coffee roasting are essential indicators for establishing the roasting endpoint. The coffee samples were roasted using various time-temperature profiles. In situ NIR spectroscopy proved to be a reliable tool in forecasting the start and finish times of first and second crack occurrences based on the PLS regression (PLSR) with audio recordings from coffee roasting.

The NIR spectra of coffees (beans and ground) roasted under different conditions are shown in Fig. 2. The obtained spectra were similar to each other, although varying in intensity. Longer roasting time lowered the intensity of the bands in all the ranges. This was due to decreased values of coffee components, as well as their volume and weight [34–36]. We found that the samples with the shortest roasting time (8 min) showed the highest absorbance, while those with the longest roasting time (12 min) showed the lowest absorbance at the same wavelength. We also noticed that the intensity of the spectrum bands decreased with increasing roasting time. The NIR spectra obtained during the roasting assays were similar to the spectra reported in other studies [37, 38]. According to the authors, the main changes in the spectra of the roasting process were an absorbance decrease in the water band region (5200–5000 cm^{-1}), which was due to moisture loss, and an absorbance increase in the combination band region (5000–4000 cm^{-1}). A more detailed discussion of the main wavelength intervals and their relationships to chemical and physical changes in coffee during roasting can be found in the work by Santos *et al.* [37]. Our results were also consistent with those reported by Catelani *et al.* [38]. The roasting process degraded coffee compounds, namely chlorogenic acid, coffee sugar, fat, and water. Literature data shows that the roasting time also affects the caffeine content in coffee [39]. The longer the coffee is roasted, the lower its caffeine content. All the samples showed a lower intensity with an increase in the roasting time. We concluded that regardless of the origin, the roasting time caused a decrease in the coffee components. The most intense bands occurred in the coffees roasted for the shortest time, which means that they lost the least of their components and nutritional value.

The partial least squares (PLS) analysis was performed to determine the time of roasting. The PLS models were obtained for the entire spectral range (12500–4000 cm^{-1}) and sub-regions without mathematical transformations (Table 4).

We found good correlations between the spectra and the roasting time for all the coffee samples. The R^2 values for the calibration and validation curves were 0.94 and 0.78, respectively. The root mean-square errors (RMSE) were low – 0.39 and 0.76 for calibration and validation, respectively. The obtained models were improved when analyzing each type of coffee samples separately. Also, the sub-regions were used to improve the model quality.

There was a weak correlation between the spectra and the roasting power for all the coffee samples. For this reason, we analyzed the samples separately. The most accurate model for Guatemala coffee was obtained in the spectral region of 6813–5332 cm^{-1}. The R^2 was 0.97 for calibration and 0.64 for validation. For Peru coffee, the spectral range of 5374–4954 cm^{-1} gave the best quality model, with R^2 values of 0.97 and 0.84 for calibration and validation, respectively. There was no correlation between the spectra and the roasting power for Brazil coffee. The coffee from Congo was not analyzed (only one power condition – 80%).

The degree of coffee roasting can be assessed by the color: the longer the roasting, the darker the beans. We studied a possibility of estimating the roasting time on the basis of the NIR spectra by using the PLS analysis to correlate the NIR spectra (coffee beans) with the L^* parameter (Table 4). By analyzing the values of the calibration ($R^2 = 0.96$) and validation ($R^2 = 0.95$) curves, as well as the RMSE values (0.92 for calibration and 1.05 for validation), we assumed that the coffee roasting time could be determined based on the PLS regression analysis and the brightness parameter (L^*).

Our study indicates the potentiality of NIR spectroscopy in evaluating coffee quality. Based on the changes of spectra, it is possible to monitor changes during roasting. Chemometric analysis also delivered very promising results. The PLS models (for roasting time and power conditions) hold potential as a rapid and reliable method which could be helpful in coffee manufacturing. Our next step will be to determine the chemical composition of the coffee samples and identify the potential of NIR spectroscopy in correlating roasting

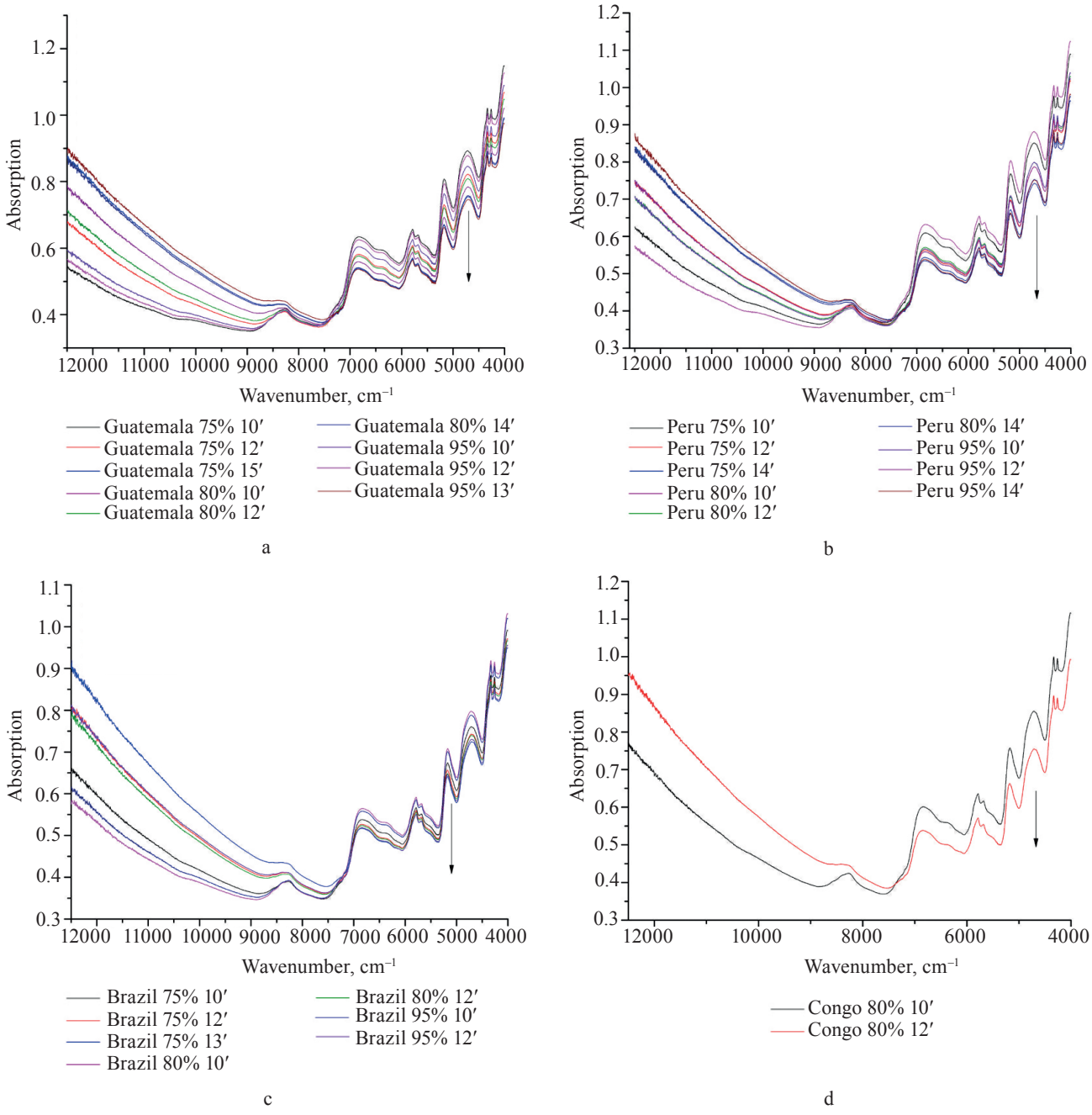

Figure 2 Changes in near-infrared spectra in coffee roasted at different power and time: (a) Guatemala coffee, (b) Peru coffee, (c) Brazil coffee, (d) Congo coffee. Full range spectrum (12500–4000 cm^{-1})

conditions (time and power) with the chemical changes in order to select optimal roasting conditions for the final product.

CONCLUSION

Our study aimed to apply near-infrared spectroscopy to evaluate the quality of the coffee samples from Brazil, Guatemala, Peru, and Congo. We investigated their composition based on the spectral bands and vibrations.

The regression results confirmed the possibility of applying the NIR spectra to predict the roasting conditions. There was a correlation between the spectra and the roasting time, with the R^2 of 0.94 and 0.78 for calibration and validation, respectively. The RMSEs were low – 0.39 and 0.76 for calibration and validation, respectively. We also obtained a linear relation between the spectra and the roasting power. The quality of the models differed based on the coffee's origin and sub-region. All the coffee samples showed a good correlation between the spectra and the brightness (L^* parameter). The R^2 values were 0.96 and 0.95 for the calibration and validation curves, respectively.

The results proved that NIR spectroscopy coupled with chemometrics could be a promising tool to predict

Table 4 Partial least squares (PLS) regression analysis

PLS model	Samples	Spectral region, cm^{-1}	Root mean-square error		R^2	
			Calibration	Validation	Calibration	Validation
Roasting time	All coffee samples	12500–4000	0.39	0.76	0.94	0.78
	Guatemala	12500–4000	0.09	0.79	0.99	0.83
		6813–5332	0.24	0.48	0.98	0.94
	Peru	12500–4000	0.39	0.70	0.94	0.85
		6030–4000	0.18	0.82	0.99	0.80
	Brazil	12500–4000	0.22	0.30	0.96	0.95
	Congo	–	–	–	–	–
Roasting power	All coffee samples	–	–	–	–	–
	Guatemala	12500–4000	1.15	6.23	0.98	0.57
		6314–5295	1.44	5.72	0.97	0.64
	Peru	12500–4000	1.70	6.16	0.96	0.58
		6314–5295	1.26	4.32	0.98	0.79
		6227–4000	0.84	4.54	0.99	0.77
		5374–4954	1.51	3.84	0.97	0.84
		4416–4090	2.29	4.27	0.93	0.80
	Brazil	–	–	–	–	–
	Congo	–	–	–	–	–
Color (L^* parameter)	All coffee samples	12500–4000	0.92	1.05	0.96	0.95

the roasting conditions of coffee samples. However, the models developed in this study need to be further tested on independent data sets from other coffee varieties to assess their stability and accuracy. Because of its characteristics, NIR spectroscopy has been applied in different production stages in the coffee industry: from green coffee beans to the end product. The growing interest in NIR spectroscopy is primarily due to the technique's numerous advantages over other analytical techniques. In addition, this technique is nondestructive and noninvasive, with a minimal or non-sample preparation. NIR spectroscopy is also fast, low-cost, and robust, so it can be used in different environments such as laboratories and industrial plants. In the future, the availability of portable instruments will also allow its use in the field. For these reasons, NIR spectroscopy could be named a "green technology".

CONFLICT OF INTEREST

The author declares that there is no conflict of interest.

REFERENCES

1. Andrés S, Murray I, Navajas EA, Fisher AV, Lambe NR. Bünger L. Prediction of sensory characteristics of lamb meat samples by near infrared reflectance spectroscopy. Meat Science. 2007;76(3):509–516. https://doi.org/10.1016/j.meatsci.2007.01.011
2. Cozzolino D, Murray I, Chree A, Scaife JR. Multivariate determination of free fatty acids and moisture in fish oils by partial least-squares regression and near-infrared spectroscopy. LWT – Food Science and Technology. 2005;38(8):821–828. https://doi.org/10.1016/j.lwt.2004.10.007
3. Woodcock T, Fagan CC, O'Donnell CP, Downey G. Application of near and mid-infrared spectroscopy to determine cheese quality and authenticity. Food and Bioprocess Technology. 2008;1(2):117–129. https://doi.org/10.1007/s11947-007-0033-y
4. Dixit Y, Casado-Gavalda MP, Cama-Moncunill R, Cama-Moncunill X, Markiewicz-Keszycka M, Cullen PJ, *et al.* Developments and challenges in online NIR spectroscopy for meat processing. Comprehensive Reviews in Food Science and Food Safety. 2017;16(6):1172–1187. https://doi.org/10.1111/1541-4337.12295
5. Basri KN, Hussain MN, Bakar J, Sharif Z, Khir MFA, Zoolfakar AS. Classification and quantification of palm oil adulteration via portable NIR spectroscopy. Spectrochimica Acta Part A: Molecular and Biomolecular Spectroscopy. 2017;173:335–342. https://doi.org/10.1016/j.saa.2016.09.028
6. Mahesh S, Jayas DS, Paliwal J, White NDG. Comparison of partial least squares regression (PLSR) and principal components regression (PCR) methods for protein and hardness predictions using the near-infrared (NIR) hyperspectral images of bulk samples of Canadian wheat. Food and Bioprocess Technology. 2014;8(1):31–40. https://doi.org/10.1007/s11947-014-1381-z

7. Baqueta MR, Caporaso N, Coqueiro A, Valderrama P. A review of coffee quality assessment based on sensory evaluation and advanced analytical techniques. In: Kalschne DL, Corso MP, Dias RCE, editors. Innovations in coffee quality. New York: Nova Science Publishers; 2020. pp. 15–31.
8. Ribeiro JS, Augusto F, Salva TJG, Ferreira MMC. Prediction models for Arabica coffee beverage quality based on aroma analyses and chemometrics. Talanta. 2012;101:253–260. https://doi.org/10.1016/j.talanta.2012.09.022
9. Ribeiro JS, Ferreira MMC, Salva TJG. Chemometric models for the quantitative descriptive sensory analysis of Arabica coffee beverages using near infrared spectroscopy. Talanta. 2011;83(5):1352–1358. https://doi.org/10.1016/j.talanta.2010.11.001
10. Belchior V, Botelho BG, Oliveira LS, Franca AS. Attenuated Total Reflectance Fourier Transform Spectroscopy (ATR-FTIR) and chemometrics for discrimination of espresso coffees with different sensory characteristics. Food Chemistry. 2019;273:178–185. https://doi.org/10.1016/j.foodchem.2017.12.026
11. Magalhães LM, Machado S, Segundo MA, Lopes JA, Páscoa RNMJ. Rapid assessment of bioactive phenolics and methylxanthines in spent coffee grounds by FT-NIR spectroscopy. Talanta. 2016;147:460–467. https://doi.org/10.1016/j.talanta.2015.10.022
12. Mees C, Souard F, Delporte C, Deconinck E, Stoffelen P, Stévigny C, *et al.* Identification of coffee leaves using FT-NIR spectroscopy and SIMCA. Talanta. 2018;177:4–11. https://doi.org/10.1016/j.talanta.2017.09.056
13. Tolessa K, Rademaker M, De Baets B, Boeckx P. Prediction of specialty coffee cup quality based on near infrared spectra of green coffee beans. Talanta. 2016;150:367–374. https://doi.org/10.1016/j.talanta.2015.12.039
14. Alessandrini L, Romani S, Pinnavaia G, Rosa MD. Near infrared spectroscopy: An analytical tool to predict coffee roasting degree. Analytica Chimica Acta. 2008;625(1):95–102. https://doi.org/10.1016/j.aca.2008.07.013
15. Ribeiro JS, Salva TJG, Silvarolla MB. Prediction of a wide range of compounds concentration in raw coffee beans using NIRS, PLS and variable selection. Food Control. 2021;125. https://doi.org/10.1016/j.foodcont.2021.107967
16. Fioresi DB, Pereira LL, Catarina da Silva Oliveira E, Moreira TR, Ramos AC. Mid infrared spectroscopy for comparative analysis of fermented arabica and robusta coffee. Food Control. 2021;121. https://doi.org/10.1016/j.foodcont.2020.107625
17. Flores-Valdez M, Meza-Márquez OG, Osorio-Revilla G, Gallardo-Velázquez T. Identification and quantification of adulterants in coffee (*Coffea arabica* L.) using FT-MIR spectroscopy coupled with chemometrics. Foods. 2020;9(7). https://doi.org/10.3390/foods9070851
18. Pires FC, Pereira RGFA, Baqueta MR, Valderrama P, Alves da Rocha R. Near-infrared spectroscopy and multivariate calibration as an alternative to the Agtron to predict roasting degrees in coffee beans and ground coffees. Food Chemistry. 2021;365. https://doi.org/10.1016/j.foodchem.2021.130471
19. Chang Y-T, Hsueh M-C, Hung S-P, Lu J-M, Peng J-H, Chen S-F. Prediction of specialty coffee flavors based on near-infrared spectra using machine- and deep-learning methods. Journal of the Science of Food and Agriculture. 2021;101(11):4705–4714. https://doi.org/10.1002/jsfa.11116
20. Munyendo L, Njoroge D, Hitzmann B. The potential of spectroscopic techniques in coffee analysis – A review. Processes. 2022;10(1). https://doi.org/10.3390/pr10010071
21. Baqueta MR, Coqueiro A, Valderrama P. Brazilian coffee blends: A simple and fast method by near-infrared spectroscopy for the determination of the sensory attributes elicited in professional coffee cupping. Journal of Food Science. 2019;84(6):1247–1255. https://doi.org/10.1111/1750-3841.14617
22. Medina J, Caro Rodríguez D, Arana VA, Bernal A, Esseiva P, Wist J. Comparison of attenuated total reflectance mid-infrared, near infrared, and ^{1}H-nuclear magnetic resonance spectroscopies for the determination of coffee's geographical origin. International Journal of Analytical Chemistry. 2017;2017. https://doi.org/10.1155/2017/7210463
23. Okubo N, Kurata Y. Nondestructive classification analysis of green coffee beans by using near-infrared spectroscopy. Foods. 2019;8(2). https://doi.org/10.3390/foods8020082
24. Zhu M, Long Y, Chen Y, Huang Y, Tang L, Gan B, *et al.* Fast determination of lipid and protein content in green coffee beans from different origins using NIR spectroscopy and chemometrics. Journal of Food Composition and Analysis. 2021;102. https://doi.org/10.1016/j.jfca.2021.104055
25. Levate Macedo L, da Silva Araújo C, Costa Vimercati W, Gherardi Hein PR, Pimenta CJ, Henriques Saraiva S. Evaluation of chemical properties of intact green coffee beans using near-infrared spectroscopy. Journal of the Science of Food and Agriculture. 2021;101(8):3500–3507. https://doi.org/10.1002/jsfa.10981
26. Kyaw EM, Budiastra IW, Sutrisnoa, Samsudin. Estimation of moisture content in Liberica coffee by using near infrared spectroscopy. IOP Conference Series: Earth and Environmental Science. 2020;542(1). https://doi.org/10.1088/1755-1315/542/1/012013

27. Bicho NC, Leitão AE, Ramalho JC, de Alvarenga NB, Lidon FC. Impact of roasting time on the sensory profile of arabica and robusta coffee. Ecology of Food and Nutrition. 2013;52(2):163–177. https://doi.org/10.1080/03670244.2012.706061
28. Hernández JA, Heyd B, Irles C, Valdovinos B, Trystram G. Analysis of the heat and mass transfer during coffee batch roasting. Journal of Food Engineering. 2007;78(4):1141–1148. https://doi.org/10.1016/j.jfoodeng.2005.12.041
29. Buratti S, Sinelli N, Bertone E, Venturello A, Casiraghi E, Geobaldo F. Discrimination between washed *Arabica*, natural *Arabica* and *Robusta* coffees by using near infrared spectroscopy, electronic nose and electronic tongue analysis. Journal of the Science of Food and Agriculture. 2015;95(11):2192–2200. https://doi.org/10.1002/jsfa.6933
30. Cen H, He Y. Theory and application of near infrared reflectance spectroscopy in determination of food quality. Trends in Food Science and Technology. 2007;18(2):72–83. https://doi.org/10.1016/j.tifs.2006.09.003
31. Adnan A, von Hörsten D, Pawelzik E, Mörlein D. Rapid prediction of moisture content in intact green coffee beans using near infrared spectroscopy. Foods. 2017;6(5). https://doi.org/10.3390/foods6050038
32. Chindapan N, Soydok S, Devahastin S. Roasting kinetics and chemical composition changes of robusta coffee beans during hot air and superheated steam roasting. Journal of Food Science. 2019;84(2):292–302. https://doi.org/10.1111/1750-3841.14422
33. Yergenso N, Aston DE. Monitoring coffee roasting cracks and predicting with in situ near-infrared spectroscopy. Journal of Food Process Engineering. 2020;43(2). https://doi.org/10.1111/jfpe.13305
34. Noor Aliah AM, Fareez Edzuan AM, Noor Diana AM. A review of quality coffee roasting degree evaluation. Journal of Applied Science and Agriculture. 2015;10(7):18–23.
35. Dutra ER, Oliveira LS, Franca AS, Ferraz VP, Afonso RJCF. Preliminary study on the feasibility of using the composition of coffee roasting exhaust gas for the determination of the degree of roast. Journal of Food Engineering. 2001;47(3):241–246. https://doi.org/10.1016/S0260-8774(00)00116-3
36. Franca AS, Mendonça JCF, Oliveira SD. Composition of green and roasted coffees of different cup qualities. LWT – Food Science and Technology. 2005;38(7):709–715. https://doi.org/10.1016/j.lwt.2004.08.014
37. Santos JR, Lopo M, Rangel AOSS, Lopes JA. Exploiting near infrared spectroscopy as an analytical tool for on-line monitoring of acidity during coffee roasting. Food Control. 2016;60:408–415. https://doi.org/10.1016/j.foodcont.2015.08.007
38. Catelani TA, Páscoa RNMJ, Santos JR, Pezza L, Pezza HR, Lima JLFC, *et al.* A non-invasive real-time methodology for the quantification of antioxidant properties in coffee during the roasting process based on near-infrared spectroscopy. Food and Bioprocess Technology. 2017;10(4):630–638. https://doi.org/10.1007/s11947-016-1843-6
39. Alqarni MH, Alam P, Salkini MA, Abdel-Kader MS. Roasting effect on the caffeine contents and antioxidant potential of different coffee grades available in the saudi market. Indo American Journal of Pharmaceutical Sciences. 2018;5(12):16738–16745.

ORCID IDs
Krzysztof Wójcicki https://orcid.org/0000-0003-4902-8613

Foods and Raw Materials. 2022;10(2)

ISSN 2310-9599 (Print)
ISSN 2308-4057 (Online)

Research Article
Open Access

Available online at http://jfrm.ru/en
https://doi.org/10.21603/2308-4057-2022-2-542
https://elibrary.ru/ZNYDIT

Thermodynamic factor and vacuum crystallization

Evgeniy V. Semenov, Anatoliy A. Slavyanskiy, Daria P. Mitroshina*, Natalya N. Lebedeva

K.G. Razumovsky Moscow State University of Technologies and Management (the First Cossack University), Moscow, Russia

* e-mail: d.mitroshina@mgutm.ru

Received 22.03.2022; Revised 11.04.2022; Accepted 04.05.2022; Published online 23.09.2022

Abstract:
Sucrose crystallization depends on various thermal phenomena, which makes them an important scientific issue for the sugar industry. However, the rationale and theory of sucrose crystallization still remain understudied. Among the least described problems is the effect of time and temperature on the condensation rate of sucrose molecules on crystallization nuclei in a supersaturated sugar solution. This article introduces a physical and mathematical heat transfer model for this process, as well as its numerical analysis.

The research featured a supersaturated sugar solution during sucrose crystallization and focused on the condensation of sucrose molecules on crystallization nuclei. The study involved the method of physical and mathematical modeling of molecular mass transfer, which was subjected to a numerical analysis.

While crystallizing in a vacuum boiling pan, a metastable solution went through an exothermal reaction. In a supersaturated solution, this reaction triggered a transient crystallization of solid phase molecules and a thermal release from the crystallization nuclei into the liquid phase. This exogenous heat reached 39.24 kJ/kg and affected the mass transfer kinetics. As a result, the temperature rose sharply from 80 to 86°C.

The research revealed the effect of temperature and time on the condensation of solids dissolved during crystalline sugar production. The model involved the endogenous heat factor. The numerical experiment proved that the model reflected the actual process of sucrose crystallization. The obtained correlations can solve a number of problems that the modern sugar industry faces.

Keywords: Vacuum boiling pan, sucrose, phase, metastable solution, heat, dissolution, condensation, crystallization

Please cite this article in press as: Semenov EV, Slavyanskiy AA, Mitroshina DP, Lebedeva NN. Thermodynamic factor and vacuum crystallization. Foods and Raw Materials. 2022;10(2):304–309. https://doi.org/10.21603/2308-4057-2022-2-542

INTRODUCTION

Vacuum boiling pans are an essential component of sugar and starch production. A vacuum pan is a crystallizer filled with a liquid solution of sucrose, salts, or other substances.

A metastable liquid solution behaves like a homogeneous liquid. If it is oversaturated, a thin suspension or a solid phase introduced into the crystallization nuclei can trigger a rapid and powerful thermal reaction. This reaction turns the homogeneous solution into a heterogeneous liquid system called massecuite.

The thermal release during crystal formation is caused by two factors. On the one hand, the force of attraction accelerates the flow of sucrose molecules to the crystallization nuclei. On the other hand, when the molecule clusters stop on the surface of the crystallization nucleus, the accumulated kinetic energy is spent on embedding the molecules into the crystal lattice, as well as on internal energy. As a result, molecules get accumulated on the crystallization nucleus, and this process is known as crystallization of sucrose in a vacuum pan.

In the sugar industry, energy production relies on all physical forms of thermal energy of water, be it liquid or vaporized. Thermal equipment turns water into steam, which acts as the main heat generator to obtain sugar or sugar products. After that, the steam serves as a heater and evaporates moisture from another heterogeneous liquid system, e.g., beet juice. The steam can also go into a new physical state: it settles on the cooled solid walls of the equipment, turns into a liquid, and releases the heat.

This phenomenon illustrates the law of energy conservation. Water molecules move in this gaseous medium and settle down on the equipment walls. As vapor transforms into liquid, it releases thermal energy, which is a powerful and efficient reaction. As a result, the temperature inside the environment rises, which makes steam the main source of thermal energy in sugar production.

The same law of energy conservation is responsible for crystallization, which occurs in a supersaturated sugar solution when the distance between the crystallization nuclei becomes small enough to trigger the forces of attraction between sucrose molecules. Hence, crystallization happens when sucrose molecules concentrate on the surface of the crystallization nuclei.

A lot of studies concentrate on the scientific and technical issues of metastable and supersaturated solutions because these phenomena are crucial for sugar production technology [1–19].

For instance, Saifutdinov *et al.* focused on the effect of various organic solvents on the molar changes in the Gibbs energy, enthalpy, and entropy during adsorption [1]. They established the role of intermolecular interactions in the solution and at the phase boundary.

In another article, Saifutdinov *et al.* reported the adsorption thermodynamics for some 1,3,4-oxadiazoles and 1,2,4,5-tetrazines from water-acetonitrile and water-methanol solutions on the surface of porous graphitized carbon at 313–333 K [2]. The absolute values of the change in the Gibbs energy and enthalpy increased during the adsorption from water-organic solutions as the surface area of adsorbate molecules became larger, the absolute values of the change in entropy decreased, and the Van der Waals volume of molecules increased.

Makhmudov *et al.* calculated the thermodynamic parameters for the phenol and sulfonol sorption from wastewater on activated carbon and anion exchanger [3].

Sagitova *et al.* described the sorption of cobalt ions by native and modified organic pharmacophores of pectins [4]. They determined the effect of acidity, temperature, and solution/sorbent module on the distribution of cobalt ions in the heterophase system of polysaccharide sorbent and aqueous solution. This research also revealed the effect of various biosorbents on the thermodynamics of cobalt ions.

Sharma *et al.* used the method of isothermal microcalorimetry to determine the dilution enthalpy of fluorosiloxane rubber and polychloroprene solutions in various organic liquids [5]. The dissolution processes of polychloroprene were accompanied by exothermic processes, while those of fluorosiloxane rubber – by endothermic ones.

Sayfutdinov and Buryak applied liquid chromatography to study the adsorption of isomeric dipyridyls and their derivatives from aqueous acetonitrile, aqueous methanol, and aqueous isopropanol solutions on a graphite-like carbon [6].

Fedoseeva and Fedoseev proved that size changes the state and physicochemical properties of dispersed systems in small (nano-, pico-, femtoliter) volumes [7]. The scientists used digital optical microscopy to interpret the concepts of chemical thermodynamics. Their experiments established the effect of such geometric parameters as radius and contact angle on the kinetics of phase and chemical transformations. The research featured polydisperse accumulations of droplets in organic and water-organic mixes that interacted with volatile gaseous reagents.

Other publications reported on the kinetics, mechanism, and heat of crystallization processes [8–15]. Some of them [8–10] focused on phase thermal effects in the sugar industry based on the laws of thermodynamics and the Gibbs theory.

Jamali *et al.* studied such independent kinetic factors as thermodynamics and sucrose crystal transfer that occur in an aqueous sugar solution during crystallization [16]. They used high-precision tools and scaling to prove that the experimental results confirmed the precalculated fluid densities, thermodynamic factors, shear viscosity, self-diffusion coefficients, and the Fick diffusion coefficients.

Li *et al.* described a modern view on crystal nucleation [17]. Traditional physical organic chemistry always combined kinetics and thermodynamics to study crystallization. The authors studied sucrose and p-aminobenzoic acid to show how solution chemistry, crystallography, and kinetics complement each other to provide a complete picture of all nucleation processes.

Kumagai proved the effect of the water sorption isotherm on the interaction of water and solids in food products [18]. In thermodynamics, the Gibbs free energy (ΔGs) describes the interaction of a solid substance and water. Therefore, the plasticizing effect of water on food products can be evaluated by applying the Gibbs free energy.

Ebrahimi *et al.* studied a mix of 1-butanol + water with or without sugars and their effect on clouding [19]. This experiment established that 1-butanol + water solution fortified with sucrose or alcohol reduced clouding.

These publications give a thorough account of phase transition of liquid to vapor and back, but they provide a poor quantitative assessment of the heat released or absorbed in each case.

The present paper introduces the thermal problem of heat propagation in the intercrystal solution volume adjacent to crystallization nuclei (instantaneous heat source).

STUDY OBJECTS AND METHODS

The research featured a supersaturated sugar solution in a vacuum boiling pan under the conditions of industrial sugar production.

The methods included physical and mathematical modeling of heat and mass transfer in heterogeneous liquid systems.

Modeling. Heat transfer in a vacuum pan is a difficult task for physical and mathematical modeling,

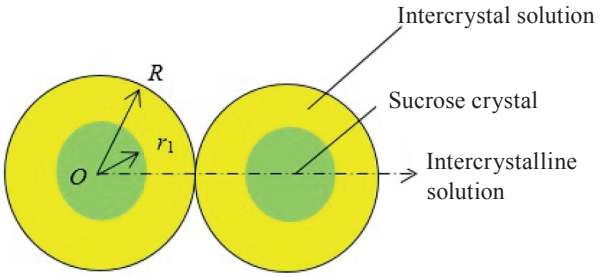

Figure 1 Heat and mass transfer for sucrose crystallization in a vacuum boiling pan

while its numerical calculation provides a scheme that reflects the actual process [13].

The modeling relied on the assumption that crystallization nuclei are uniformly distributed in the vacuum pan. Therefore, the calculations relied on the spherical symmetry of the liquid + solid mix relative to center O in the region of $0 < r < R$, where r is the radius of the model sphere and R is the average radial distance between the spheres (Fig. 1).

The boundary value problem was based on the theory of thermal conductivity for an isolated model particle of sucrose near the crystallization nucleus. A certain volume of intercrystalline solution was represented as a spherical region with radius R and center point O at saturation temperature T_s. The volume included a model sucrose particle represented as a sphere with radius $r = r_1$ and center O. The initial instantaneous heat source distributed over spherical surface $r = r_1$ (Fig. 1) with force Q_l (J). Heat exchange occurred in accordance with the boundary condition of the third kind between sphere surface $r = R$ and its environment. The task was to find the temperature field in the region of $0 < r < R$ and the average temperature of the medium over time.

The heat transfer equation looks as follows:

$$\frac{\partial\,[rT(r,\tau)]}{\partial\tau} = a\,\frac{\partial^2[rT(r,\tau)]}{\partial r^2} \quad (\tau > 0, 0 < r < R) \tag{1}$$

where $T(r,\tau)$ is the temperature, K; τ is the time, s; and a is the thermal diffusion coefficient, m²/s.

The initial data include:

$$T(r,0) = \begin{cases} (T_0 + \delta T)\ \text{at}\ r \le r_1 \\ T_0\ at\ r > r_1 \end{cases} \tag{2}$$

where

$$\delta T = Q_{sp}/c_0 \tag{3}$$

temperature difference between sphere surface $r = r_1$ and the environment, K; Q_{sp} is the specific heat of crystallization, J/kg; and c_0 is the heat capacity of the solution, J/(kg· K).

Boundary conditions:

$$\frac{\partial T(0,\tau)}{\partial r} = 0, T(0,\tau) \neq \infty, \text{at}\ \tau > 0 \tag{4}$$

$$\frac{\partial T(R,\tau)}{\partial r} + H[T(R,\tau) - T_1] = 0 \tag{5}$$

where T_0 and T_1 are the initial temperature (K) of the environment (massecuite) and the temperature on sphere surface $r = R$, m, respectively; $H = \alpha/\lambda$, α is the thermal diffusion coefficient, Vt/(m²·K); and λ is the thermal conduction coefficient, Vt/(m·K).

If we introduce the following substitution

$$t(r,\tau) = T(r,\tau) - T_1 \tag{6}$$

the boundary problem (1)–(5) looks as follows:

$$\frac{\partial[rt(r,\tau)]}{\partial\tau} = a\,\frac{\partial^2[rt(r,\tau)]}{\partial r^2} \quad (\tau > 0, 0 < r < R) \tag{7}$$

$$t(r,0) = n\begin{cases} (\Delta t + \delta T)\text{at}\ r \le r_1 \\ \Delta t\ \text{at}\ r > r_1 \end{cases} \tag{8}$$

$$\frac{\partial t(0,\tau)}{\partial r} = 0, t(0,\tau) \neq \infty, \text{at}\ \tau > 0 \tag{9}$$

$$\frac{\partial t(R,\tau)}{\partial r} + Ht(R,\tau) = 0 \tag{10}$$

where $t(r,\tau)$ is the reduced temperature, $\Delta t = T_0 - T_1$, and δT is defined according to (3).

Boundary problems (7)–(10) are based on the following correlation [20]:

$$(r,\tau) = \frac{b}{4\pi R}\cdot\sum_{n=1}^{\infty}\frac{1}{rr_1}\cdot\frac{\mu_n}{\mu_n - \sin\mu_n\cos\mu_n}\cdot \cdot\sin\frac{\mu_n r_1/R}{r_1}\cdot\sin\frac{\mu_n r/R}{r}\cdot\exp(-\mu_n^2 Fo) \tag{11}$$

$b = V\cdot t(r,0), V = 4\pi r_1^3/3$, sucrose crystal volume, m³; $t(r,0)$ as in (8), K; and μ_1 and μ_2, are the roots of the characteristic equation:

$$tg\mu = -\mu/(Bi - 1) \tag{12}$$

where $Bi = \alpha h/\lambda$ – Biot number (thermal), $Fo = \alpha\tau/R^2$ – Fourier number [20].

According to (11),

$$(r,\tau) = \frac{b}{4\pi R}\cdot\sum_{n=1}^{\infty}\frac{1}{rr_1}\cdot\frac{[(Bi-1)^2 + \mu_n^2]^{1/2}\,A_n}{Bi}\cdot \cdot\sin(\mu_n r_1/R)\cdot\sin(\mu_n r/R)\cdot\exp(-\mu_n^2 Fo) \tag{13}$$

where A_n is the table coefficients [20].

Formula (6) provides the following solution for (7)–(10):

$$T(r,\tau) = T_1 + t(r,\tau) \tag{14}$$

where $t(r,\tau)$ is the calculated according to (13).

Mean temperature $0 < r < R$ is calculated as follows:

$$T_m(\tau) = \frac{3}{R^3}\int_0^R T(r,\tau)r^2 dr \tag{15}$$

where function $T(r,\tau)$ under the integral depends on correlation (14).

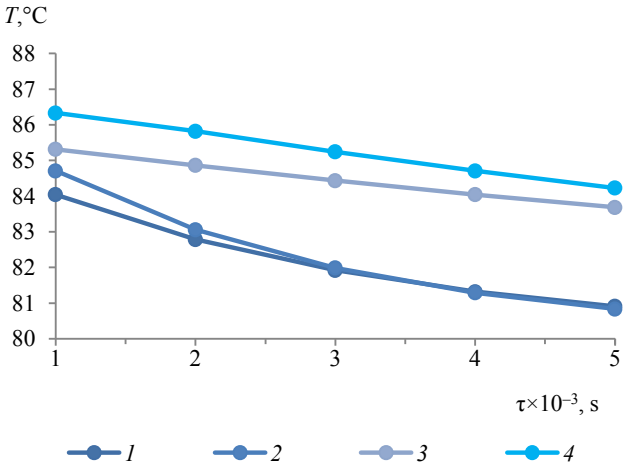

Figure 2 Correlation of temperature T on surface r_1 of the model sucrose particle with volume concentration c of the solid phase in the solution and crystallization time τ ($r_1 = 1\times10^{-5}$ m: *1* – $c = 40\%$, *2* – $c = 50\%$; $r_1 = 2\times10^{-5}$ m: *3* – $c = 40\%$, *4* – $c = 50\%$)

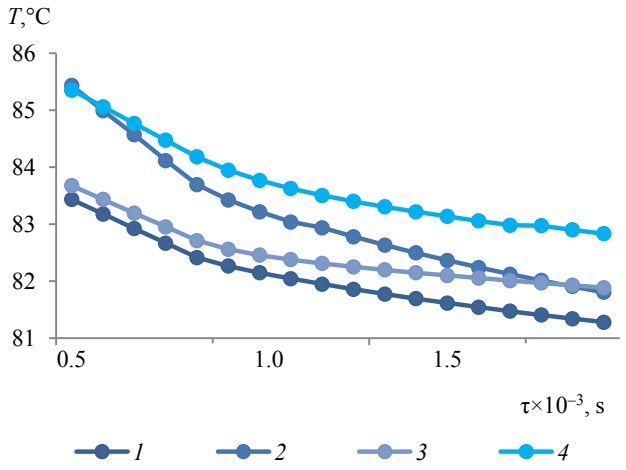

Figure 3 Correlation of mean massecuite temperature T with volume concentration $\boldsymbol{c}$ of the solid phase in the solution and crystallization time τ ($r_1 = 1\times10^{-5}$ m: *1* – $c = 40\%$, *2* – $c = 50\%$; $r_1 = 2\times10^{-5}$ m: *3* – $c = 40\%$, *4* – $c = 50\%$)

The temperature and the mean temperature in the vacuum pan depend on the processing time and are calculated based on correlations (14) and (15). As follows from the assumption about the uniform distribution of the crystallization nuclei, the calculated thermal characteristics for the selected elementary volume with radius R are also valid for the entire volume of the vacuum pan.

RESULTS AND DISCUSSION

The initial data included: crystal radius $r_1 = 1\times10^{-5}$ and 2×10^{-5} m; volume concentration $c = 40$ and 50% ($c = 0.4$, 0.5); density of intercrystalline solution (massecuite) $\rho = 1450$ kg/m^3; thermal conduction and diffusion coefficient (for water at 80°C), respectively, $\lambda = 0.56$ Vt/(m·°C), $c_0 = 1250$ J/(kg·K), heat transfer coefficient $\alpha = 240$ Vt/(m^2·°C) [10, 21].

The resulting thermal diffusion coefficient is $a = \lambda/(c_0\cdot\rho) = 3.09\times10^{-7}$ m^2/s. The equivalent radius of elementary volume was calculated as follows:

$$R = r_1\cdot c^{-1/3} \quad (16)$$

Biot number $Bi = \alpha\cdot r_1/(\lambda\cdot c^{1/3})$.

The specific heat of sucrose crystallization was as in [13]: $Q_{sp} = 13.42$ kJ/mol (39.24 kJ/kg).

The numerical simulation was based on MATHCAD software.

Sum (13) was calculated based on (12)–(16) with the same four additive components, while the parameters of A_n and μ_n in (13) were based on the tables published in [20].

Temperatures T_0 and T_1 were 80°C all the time, which means that ΔT (9) = 0.

Figures 2 and 3 show the calculation results at the accepted values of the thermal process: volume concentration c of the solid phase in the solution, time τ, and temperature T on surface r_1 for model sucrose particle and mean massecuite temperature T.

Figures 2 and 3 show that the heat transfer into the sugar solution during crystallization of the model sucrose particle proceeded very quickly and took some thousandths of a second. That was why the thermal regime in the intercrystalline solution stabilized so quickly.

Figures 2 and 3 also demonstrate the same gradual exponential decrease in temperature, which is typical for heat transfer problems. If particles differed in radius by a factor of two, smaller particles with a larger specific surface area and a greater heat transfer cooled faster than particles with a larger radius. For curves 1 and 2, the temperature rise rate of the particles with radius $r_1 = 1\times10^{-5}$ m exceeded curves 3 and 4 for particles with a radius twice as large. The accumulation and release of heat for crystals with radius $r_1 = 2\times10^{-5}$ m was eight times bigger than those for crystals with a radius two times smaller. Figure 3 clearly demonstrates that curves 3 and 4 are much higher than curves 1 and 2.

CONCLUSION

The equation of non-stationary Fourier diffusion with initial and boundary conditions of the third kind was applied to calculate the endogenous heat released into the solution during the condensation of sucrose molecules on a spherical particle of a sucrose crystal in a supersaturated sugar solution.

The numerical study involved conditions close to the actual sucrose crystallization process in a vacuum boiling pan. It revealed an increase in temperature as a

result of the phase transition from 80 to 86°C in 2×10^{-3} s, which means the process was almost instantaneous. The calculations were confirmed in practice. The results can facilitate calculating the effect of temperature on massecuite viscosity, wash water temperature, and other characteristics of massecuite vacuum processing in the sugar and starch industries.

CONTRIBUTION

E.V. Semenov and A.A. Slavyanskiy supervised the project. D.P. Mitroshina and N.N. Lebedeva performed the experiments.

CONFLICT OF INTEREST

The authors declare that there is no conflict of interests regarding the publication of this article.

REFERENCES

1. Saifutdinov BR, Buryak AK. The influence of water–acetonitrile solvent composition on thermodynamic characteristics of adsorption of aromatic heterocycles on octadecyl-bonded silica gels. Colloid Journal. 2019;81(6):754–761. https://doi.org/10.1134/S1061933X19060176
2. Saifutdinov BR, Buryak AK. Thermodynamics of the adsorption of isomeric dipyridyls and their derivatives from water–organic solutions on HYPERCARB™ porous graphitic carbon. Russian Journal of Physical Chemistry A. 2019;93(9):1796–1803. https://doi.org/10.1134/S0036024419090218
3. Makhmudov FT, Raqimli MA, Aliyeva SA, Ilyasova KA, Jabbarova ZA, Nuriyev AN. Thermodynamics of sorption processes of toxic components of organic nature from solutions on solid sorbents. Sorption and Chromatography Processes. 2018;18(3):338–345. (In Russ.).
4. Sagitova AF, Kukovinets OS, Mudarisova RKh. Study of the sorption activity of pharmacophore-containing pectins with respect to cations of cobalt (II). Sorption and Chromatography Processes. 2018;18(4):527–535. (In Russ.). https://doi.org/10.17308/sorpchrom.2018.18/560
5. Sharma T, Bandral A, Bamezai RK, Kumar A. Interaction behavior of sucrose in aqueous tributylmethylammonium chloride solutions at various temperatures: A volumetric, ultrasonic and viscometric study. Chemical Thermodynamics and Thermal Analysis. 2022;6. https://doi.org/10.1016/j.ctta.2022.100043
6. Saifutdinov BR, Buryak AK. Thermodynamics of the adsorption of isomeric dipyridyls and their derivatives from water-organic solutions on Hypercarb™ porous graphitic carbon. Russian Journal of Physical Chemistry A. 2019;93(9):1392–1400. (In Russ.). https://doi.org/10.1134/S004445371909022X
7. Fedoseeva EN, Fedoseev VB. Possibilities and peculiarities of spray technologies in organic synthesis. Condensed Matter and Interphases. 2020;22(3):397–405. (In Russ.). https://doi.org/10.17308/kcmf.2020.22/3001
8. Slavyansky AA, Nikolaeva NV, Gribkova VA, Lebedeva NN, Mitroshina DP. Improvement of the technology of separation of utfel i crystallization in batch centrifuges. Proceedings of the International Scientific and Practical Conference “Biotechnology, Ecology, Nature Management”; 2021; Moscow. London: European Publisher; 2022. p. 309–318. https://doi.org/10.15405/epls.22011.37
9. Guo W, Zhang Z, Hacking J, Heeres HJ, Yue J. Selective fructose dehydration to 5-hydroxymethylfurfural from a fructose-glucose mixture over a sulfuric acid catalyst in a biphasic system: Experimental study and kinetic modelling. Chemical Engineering Journal. 2021;409. https://doi.org/10.1016/j.cej.2020.128182
10. Verma P, Iyer SR, Shah N, Mahajani S. Insights into the crystallization phenomenon in the production of non-centrifugal sugar. Journal of Food Engineering. 2021;290. https://doi.org/10.1016/j.jfoodeng.2020.110259
11. Wang Y, Zheng Y, Zhou R, Ma M. Kinetic studies on soluble sugar profile in rice during storage: Derivation using the Laplace transform. Innovative Food Science and Emerging Technologies. 2022;76. https://doi.org/10.1016/j.ifset.2021.102915
12. Bharti MK, Bansal L, Chalia S. Catalytic potential of microsized additives in enhancing the linear burn rate of potassium nitrate-sucrose based composite solid propellant strands. International Journal of Energetic Materials and Chemical Propulsion. 2021;20(4):61–77. https://doi.org/10.1615/IntJEnergeticMaterialsChemProp.2021038209
13. Semenov EV, Slavyanskiy AA, Gribkova VA, Mitroshina DP, Lebedeva NN. Assessment of the influence of the thermodynamic factor on the crystallization process in a vacuum apparatus. News of Institutes of Higher Education. Food Technology. 2021;383–384(5–6):42–47. (In Russ.). https://doi.org/10.26297/0579-3009.2021.5-6.8
14. Shtangeev KO, Skorik KD, Shtangeeva NI. Thermotechnical and technological aspects of improving the product department of a beet sugar plant. Sugar. 2021;(12):20–25. (In Russ.). https://doi.org/10.24412/2413-5518-2021-12-20-25
15. Semenov EV, Slavyansky AA, Gribkova VA, Mitroshina DP, Antipov ST. Simulation of the growth of sucrose crystals in a sugar-containing solution. Proceedings of the Voronezh State University of Engineering Technologies. 2021;83(1):62–70. (In Russ.). https://doi.org/10.20914/2310-1202-2021-1-62-70

16. Jamali SH, Westen TV, Moultos OA, Vlugt TJH. Optimizing nonbonded interactions of the OPLS force field for aqueous solutions of carbohydrates: How to capture both thermodynamics and dynamics. Journal of Chemical Theory and Computation. 2018;14(12):6690–6700. https://doi.org/10.1021/acs.jctc.8b00909
17. Li X, Wang J, Wang T, Wang N, Zong S, Huang X, *et al.* Molecular mechanism of crystal nucleation from solution. Science China Chemistry. 2021;64(9):1460–1481. https://doi.org/10.1007/s11426-021-1015-9
18. Kumagai H. Physical properties of foods and the effect of water on them-water activity and glass transition. Japan Journal of Food Engineering. 2020;21(4):161–169. https://doi.org/10.11301/jsfe.20584
19. Ebrahimi N, Sadeghi R, Ameen BAH. Thermodynamics of clouding process in 1-butanol + water mixtures in the presence and absence of sugars. Journal of Molecular Liquids. 2019;278:164–174. https://doi.org/10.1016/j.molliq.2019.01.011
20. Lykov AV. Theory of thermal conductivity. Moscow: Vysshaya Shkola; 1967. 599 p. (In Russ.).
21. Tao Y, Yan B, Zhang N, Wang M, Zhao J, Zhang H, *et al.* Do non-thermal effects exist in microwave heating of glucose aqueous solutions? Evidence from molecular dynamics simulations. Food Chemistry. 2022;375. https://doi.org/10.1016/j.foodchem.2021.131677
22. Slavyanskiy AA, Semenov EV, Babakin BS, Lebedeva NN. Intensification of cooling fluid process. Foods and Raw Materials. 2020;8(1):171–176. https://doi.org/10.21603/2308-4057-2020-1-171-176

ORCID IDs
Evgeniy V. Semenov https://orcid.org/0000-0001-6203-1783
Anatoliy A. Slavyanskiy https://orcid.org/0000-0002-0262-8841
Daria P. Mitroshina https://orcid.org/0000-0002-8724-3368
Natalya N. Lebedeva https://orcid.org/0000-0003-4936-7498

Foods and Raw Materials. 2022;10(2)

ISSN 2310-9599 (Print)
ISSN 2308-4057 (Online)

Research Article
Open Access

Available online at http://jfrm.ru/en
https://doi.org/10.21603/2308-4057-2022-2-541
https://elibrary.ru/ZNISDX

Molecular genetic studies of microbiocenosis and microstructure of jejunum wall in young rams grown on biofortified feed additives

Tatiana M. Giro[1,*], Larisa A. Ilina[2,3], Andrey V. Kulikovsky[1], Irina V. Ziruk[1], Anna V. Giro[1]

[1] N.I. Vavilov Saratov State Agrarian University, Saratov, Russia
[2] LLC BIOTROF, St. Petersburg, Russia
[3] Saint-Petersburg State Agrarian University, Pushkin, Russia

* e-mail: girotm@sgau.ru

Received 02.03.2022; Revised 06.04.2022; Accepted 04.05.2022; Published online 23.09.2022

Abstract:
The research featured the effect of a diet fortified with essential microelements on the ruminal microbiota of young rams. Ruminal microbiota is largely responsible for feed digestibility and body functioning of cattle.
The study involved the contents of the rumens and jejuna of seven-month-old rams of the Edilbaev breed, which were subjected to a biofortified diet. The diet included the Russian feed additives Yoddar-Zn and DAFS-25 represent a protein-carbohydrate complex with plant silicon. The microflora of the digestive tract was tested using the molecular genetic method of terminal restriction fragment length polymorphism (T-RFLP) sequestration. The microstructural studies of the jejunum samples exploited light microscopy.
The feed additives increased the population of cellulolytic and lactate-fermenting bacteria, as well as the *Prevotella* sp. microbiome and bifidobacteria in the rumen samples. The data obtained revealed the effect of essential microelements on the taxonomic pattern of microorganisms and the microflora profile. The research revealed the ratio of normal, opportunistic, pathogenic, nonculturable, and transit microflora. The jejunum wall samples obtained from the experimental group that fed on Yoddar-Zn and DAFS-25 had a more distinct micropicture of mucous membrane. Their rumen microflora balance had fewer pathogenic and opportunistic microorganisms, which was also confirmed by the jejunum morphology.
The feed additives DAFS-25 and Yoddar-Zn proved beneficial for ram diet and inhibited the negative effect of pathogenic treponemas on the rumen. The additives improved digestion, absorption, and assimilation of food nutrients, as well as increased the livestock yield.

Keywords: Young rams, animal diet, feed additives, essential microelements, molecular genetics, jejunum, microbiocenosis, microstructural studies

Funding: The research was financed by the Russian Science Foundation, Project No. 19-76-10013 "Development and implementation of production and storage technology for environmentally friendly mutton fortified with essential microelements".

Please cite this article in press as: Giro TM, Ilina LA, Kulikovsky AV, Ziruk IV, Giro AV. Molecular genetic studies of microbiocenosis and microstructure of jejunum wall in young rams grown on biofortified feed additives. Foods and Raw Materials. 2022;10(2):310–317. https://doi.org/10.21603/2308-4057-2022-2-541

INTRODUCTION

Feed composition has a direct impact on the qualitative and quantitative characteristics of the gastrointestinal microbial community. Minerals and vitamins are essential micronutrients that participate in such vital processes as enzyme formation or the synthesis and metabolism of hormones and vitamins. They affect the nervous, cardiovascular, and endocrine systems, as well as the activity of the endocrine glands and the gastrointestinal tract.

Micronutrient deficiency may trigger various infectious and non-infectious diseases [1, 2]. A poorly-

balanced feed ration often leads to undesirable changes in the microbiota of small ruminants. The resulting digestive disorders cause various diseases and eventually lead to poor livestock yield. Biofortification fortifies animal diet with essential nutrients, thus improving the chemical composition of meat. It renders high-quality mutton that provides consumers with essential microelements [3–9].

Practical microbiology gives scientific data on the composition, role, or function of the microbial community in the rumen content of small ruminants. However, some of these methods have disadvantages or limitations. For instance, researchers cannot choose the optimal environment for microbial cultivation. Fortunately, contemporary molecular genetic methods make it possible to skip the stage of cultivation and study microorganisms without the restrictions that traditional diagnostic microbiology are prone to [10–14].

Small intestine (lat. *intestinum tenue*) of farm animals absorbs nutrients from the chyme. It is in the small intestine that the main digestion takes place, and this is where most digestive enzymes come from. Partially digested food leaves the stomach and enters the duodenum, where it is processed by intestinal and pancreatic juices and bile. The small intestine is where digested food, toxins, poisons, medicinal substances, etc. are absorbed into the bloodstream or lymphatic channel [15–19].

The jejunum is somewhat structurally different from other parts of the small intestine. Membrane digestion is at its utmost in the upper parts of the jejunum. As a result, its wall is thicker; it has more folds in the mucous membrane, denser villi, and a more abundant blood supply [20–22]. Therefore, the small intestine is a vital system of animal body, and its flawless work is essential for sheep farming, which proves the relevance of this research.

Sheep farming needs new fundamental data on the effect of biofortification on the bacterial rumen community. Bacterial profile includes normal, opportunistic, and pathogenic microflora, as well as nonculturable and transit microflora that does not affect the life of the animal. Light microscopy revealed the morphology of the intestine and the main differences between the samples obtained from animals fed with Yoddar-Zn and DAFS-25.

The research objective was to assess the effect of essential microelements on the ruminal microbiocenosis and the microstructure of the jejunum in young rams.

STUDY OBJECTS AND METHODS

The next-generation sequencing (NGS) revealed the digestive microflora of seven-month-old rams of the Edilbaev breed. The experiment made it possible to evaluate the effect of the feed additives Yoddar-Zn (Material Specifications TU 10.91.10-252-10514645-2019) and DAFS-25 (Material Specifications TU 10.91.10-253-10514645-2019). The studies took place in the laboratory of molecular genetic research of the Research and Production Company BIOTROF (St. Petersburg, Russia).

The feed additives were developed at the Volga Region Research Institute for the Production and Processing of Meat and Dairy Products. Both feed additives contain Coretron, an enterosorbent used in Russia in cattle diet, and cold-pressed pumpkin cake, which served as a protein-carbohydrate component (Tables 1 and 2) [6].

A scientific and economic experiment was necessary to assess the effectiveness of various diets fortified with organic microelements, i.e., mono- and di-iodotyrosines and selenomethionine. After weaning from mothers at the age of four months, 100 lambs of the Edilbaev breed were divided into four groups, 25 animals in each. The lambs were fed and fattened in the same way. On day 105, when the animals were seven months old, they were slaughtered by the traditional method according to the Technical Regulations of the Customs Union on the safety of meat and meat products TR TS 034/2013. Prior to slaughter, all experimental animals had received no food for 24 h.

Yoddar-Zn is a source of bioavailable organic iodine and zinc. It also contains iodized milk proteins associated with amino acids and zinc compounds. Yoddar-Zn owes its biological properties to bound iodine, which is necessary for the biosynthesis of such thyroid hormones as thyrotoxin and triiodothyropine. They are important for metabolism and immune system [6].

The control group of young rams received 300 grams of mixed fodder per head per day. The first experimental group received daily the same mixed fodder together with 300 mg of Yoddar-Zn, the second experimental

Table 1 Yoddar-Zn feed additive

Ingredient	Amount
Plant silicon (diotomite Coretron)	1.0
Iodine-containing additive Yoddar-Zn, %	1.0
Pumpkin cake protein-carbohydrate complex, %	98.0, including 20.0 of pumpkin cake
Organic iodine (mono- and di-iodotyrosines), mg/100 g	3.0

Table 2 DAFS-25 feed additive

Ingredient	Amount
Plant silicon (diotomite Coretron), %	1.0
Pumpkin cake protein-carbohydrate complex, %	99.0, including 20.0 of pumpkin cake
Organic selenium (selenomethionine), mg /100 g	0.16

group – 0.5 mg of DAFS-25, and the third experimental group – a mix of these additives (300 and 0.5 mg).

The effect of the organic additives was studied *in vivo* by comparing the microbiocenosis and microstructural parameters of the small intestine in the experimental and control groups of young rams.

The next generation sequencing (NGS) is currently one of the most optimal research methods. NGS technologies provide metagenomic studies of complex microbial communities with a large volume of read nucleotide sequences. This technology is much more accurate than the Sanger sequencing in determining the phylogenetic species of microorganisms [23].

The *in vivo* assessment of the impact on the intestinal microbiocenosis took 105 days. Samples of the rumen contents were put into sterile containers (Pan Eco, Russia) immediately after the slaughter and tested for microbial composition. Next step included histology of jejunum samples. The preparations were stained with hematoxylin and eosin to assess any possible changes in the intestinal mucosa.

The bacterial content of the ram rumen was analyzed by NGS method. Total DNA was isolated by using the Genomic DNA Purification Kit (Fermentas, Inc., Lithuania) according to the manual. The final concentration of total DNA in the solution was measured using a Qubit fluorimeter (Invitrogen, Inc., USA) with Qubit dsDNA BR Assay Kits (Invitrogen, Inc., USA) according to the manual.

The NGS was performed on a second-generation MiSeq sequencing platform (Illumina, Inc., USA) with primers for the V3-V4 region of 16S rRNA; upstream primer – 5′-TCGTCGGCAGCGTCAGATGTGTATAAG AGACAGCCTACGGGNGGCWGCAG-3′; downstream primer – 5′-GTCTCGTGGGCTCGGAGATGTGTATA AGAGACAGGACTA-CHVGGGTATCTAATCC-3′ [24].

Libraries were prepared with Nextera® XT IndexKit reagents (Illumina, Inc., USA); the PCR products were purified with Agencourt AMPure XP (Illumina Inc., USA); the sequencing was performed with MiSeq® ReagentKit v2 (500 cycle) (Illumina, Inc., USA) [25].

The obtained reads underwent overlapping, filtering by Q30 quality, and primer trimming. The processing involved the Illumina bioinformatics platform (Illumina, Inc., USA). The quality control and assessment of the taxonomic composition were carried out using the QIIME2 v.2019.10 software (https://docs.qiime2.org) and the Green-Genes database 13.5 (https://greengenes.secondgenome.com).

Pieces of ram jejunum samples were removed by preparation and fixed in 10% aqueous neutral formalin solution at room temperature for 48 h. The selected samples were removed from the fixing liquid and washed under running water for 48 h. For dehydration, the material was washed in alcohols of increasing concentration from 50 to 96%. After that, the material was embedded in paraffin shaped in paraffin blocks. Sections of 5–8 μm were sliced with a sledge microtome, deparaffinized, and stained by Ehrlich hematoxylin and eosin dyes. Hematoxylin stains basophilic cellular elements bright blue, while eosin alcohol acid dye stains Y-eosinophilic cell elements pink. Basophilic structures most often contain nucleic acids (DNA and RNA), i.e., nucleus, ribosomes, and RNA-containing cytoplasm sections. Eosinophilic elements contain intra- and extracellular proteins. Cytoplasm belongs to the main eosinophilic environment, so its elements stain bright red [1].

Microscopy involved a Levenhuk MED PRO 600 Fluo microscope, which is designed for transmitted light brightfield microscopy or for a luminescent (fluorescent) method (Magnification ×300).

The morphometric analysis of the obtained data traced the thickness of the jejunum layers. The experiment relied on a screw eyepiece micrometer MOV-1-15× and an eyepiece ruler with 60 units of scale division. The quantitative parameters of the histological structures underwent further statistical processing.

Statistical processing of the obtained digital data followed standard methods using the Microsoft Excel 2010 (Microsoft Corp., USA) and the statistical data analysis package StatPlus 2009 Professional 5.8.4 for Windows (StatSoft, Inc., USA). Student's t-test was applied to assess the reliability of data between the experimental and control groups.

RESULTS AND DISCUSSION

This section describes the effect of feed additives Yoddar-Zn and DAFS-25 in the diet of young Edilbaev breed rams on their ruminal microbiocenosis and jejunum microstructure.

The NGS analysis revealed the ruminal bacteria community in the control and experimental groups. The rumen samples contained 31 phyla of bacteria and 1 phylum of archaea (Fig. 1). *Firmicutes* and *Bacteroides* predominated with a total share of 86–94%. The share of *Actinobacteria*, *Spirochaetes*, and *Candidatus Saccharibacteria* was 1–6%. In the control group, *Firmicutes* ranked first: their relative value in the community was 65%, while the proportion of Bacteroides was only 29.4%. This ratio was different in the experimental groups. In the group that received Yoddar-Zn, the proportion of *Firmicutes* and *Bacteroides* was the same (42–43%). In the groups that received DAFS-25 and DAFS-25 + Yoddar-Zn, the ratio of these two phyla was reversed compared to the control group: *Bacteroides* – 50–60%, *Firmicutes* – 30–35%.

At the level of orders, the community was dominated by *Bacteroidales*, *Erysipelotrichales*, and *Clostridiales*. Rams fed with DAFS-25 had a larger proportion of *Bifidobacteriales* (5.8%). The control group had more *Erysipelotrichales* – 28.8%.

Cellulolytic bacteria are important bacterial community members. They break down the fiber of plant foods and convert it to volatile fatty acids. Cellulolytic bacteria in the rumen samples were mainly represented by the bacterial families *Clostridiaceae*, *Prevotellaceae*, *Flavobacteriaceae*,

Eubacteriaceae, *Lachnospiraceae*, *Ruminococcaceae*, and *Thermoanaerobacteraceae*, as well as by the *Bacteroidetes* phylum.

The total proportion of cellulolytic bacteria was different in all samples. The share of beneficial cellulolytic bacteria ranged from 51.3 to 75.4%, depending on the sample. The control group had the smallest proportion of cellulolytic bacteria, while the group that received DAFS-25 had the largest one. In the groups treated with Yoddar-Zn and DAFS-25 + Yoddar-Zn, the proportion of cellulolytic bacteria was 56.6 and 64.1%, respectively.

Lactate-utilizing bacteria are another important group in the ruminal bacterial community. They ferment lactic acid produced by bacteroids and lactic acid bacteria and other organic acids into volatile fatty acids used in metabolic processes.

The NGS analysis showed that the content of *Veillonellaceae* lactate-utilizing bacteria was very large in some samples. In the groups that received Yoddar-Zn and DAFS-25 + Yoddar-Zn, their content was 20.6 and 12.9%, respectively, while the control group and the experimental group fed with DAFS-25 alone, it was 9.1 and 5.1%, respectively. This indicator may demonstrate that these bacteria are especially active in the sheep rumen, depending on their physiological state of the animal.

The share of bacterial pathogens was insignificant in all samples and totaled about 0.5% in all groups. Opportunistic *Enterobacteriaceae* were also represented in a very small amount (≤ 0.1%) in all samples.

Prevotella appeared to be the dominant genus. Its relative abundance in the experimental groups exceeded the control (28.3, 38.9, and 33.4 vs. 22.8%). *Prevotella* sp. often is the most numerous genera in sheep rumen.

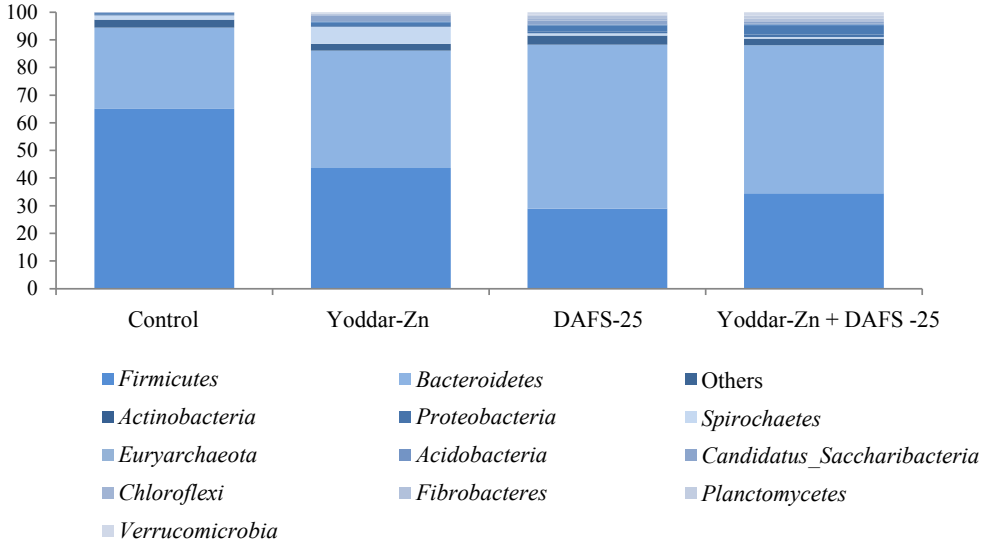

Figure 1 Rumen microbial community at phylum level, %

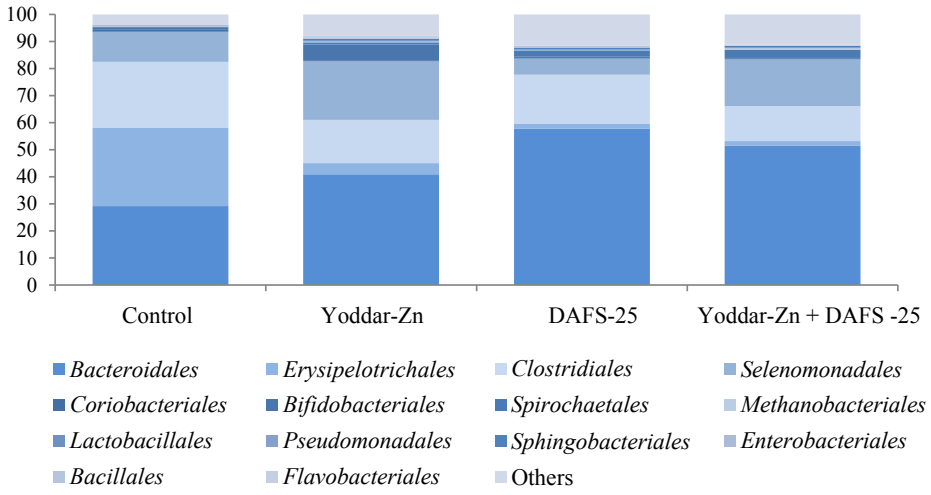

Figure 2 Rumen microbial community at the level of orders, %

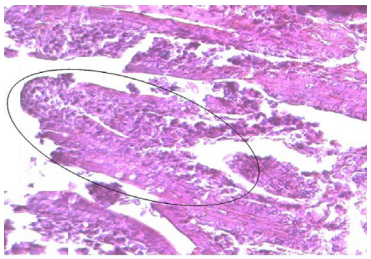

Figure 3 Jejunum samples in the control group. Epitheliocytes of cylindrical villi and gland; stained with Ehrlich hematoxylin and eosin. Magnification ×300

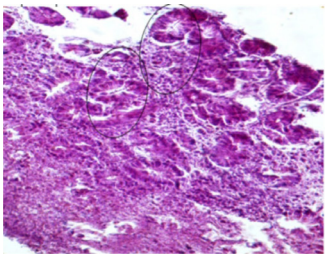

Figure 4 Jejunum samples in the group fed with Yoddar-Zn. Goblet cells of the villi are quite pronounced; stained with Ehrlich hematoxylin and eosin. Magnification ×300

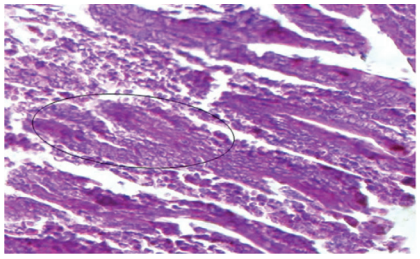

Figure 5 Jejunum sampled in the animals fed with DAFS-25. Epitheliocytes are cylindrical, the villi are distinct and elongated; stained with Ehrlich hematoxylin and eosin. Magnification ×300

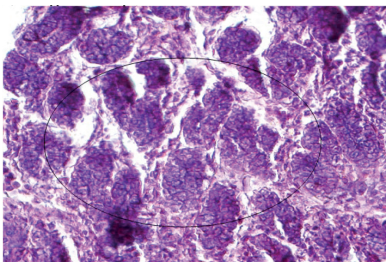

Figure 6 Jejunum samples in the animals fed with DAFS-25 + Yoddar-Zn. The villi are distinct, with cylindrical goblet cells; stained with Ehrlich hematoxylin and eosin. Magnification ×300

For instance, *Prevotella* also dominated in a similar study by Cui *et al.* on the effect of selenium feed additives on the microbial community in sheep [3]. Cui *et al.* also proved the significant effect of selenium on ruminal bacterial populations and microbial fermentation in the rumen in general.

Subdominant microorganisms in the rumen were represented by the *Dysgonomonas*, *Saccharofermentans*, *Tangfeifania*, and *Treponema* genera. Cui *et al.* showed that the abundance of *Saccharofermentans* sp. was in inverse relationship with selenium. Our research, on the contrary, proved that the amount of *Dysgonomonas* sp. and *Prevotella* sp. depended on the presence of selenium in the diet.

To identify and evaluate the changes in the small intestine wall, jejunum wall pieces were subjected to microscopy [1].

This research of the effect of biofortification on the microstructure of sheep jejunum yielded a more accurate assessment of the safety of Yoddar-Zn and DAFS-25 for small rumens [7, 8].

Light microscopy of the jejunum in all samples revealed that the mucous membrane was well-structured, with distinct layers. The mucous membrane of the jejunum consisted of four layers: innermost mucosa outermost, submucosa, muscularis (outer and inner layers), and serosa. The columnar villi (Fig. 3) of the mucosal epithelial layer were distinct and consisted of a single-layer columnar epithelium lining the crypts. The structure of the layer was dominated by goblet cells and limbic epithelial cells, which produce mucus. The lamina propria consisted mostly of cells and fibers of loose fibrous connective tissue. The muscular layer was represented by two distinct alternating layers of myocytes: annular and longitudinal. The submucosa was represented by loose fibrous tissue with clear contoured blood and lymphatic vessels, as well as complex tubular-alveolar glands that produced intestinal juice.

The muscular membrane of the jejunum tissue had two distinct layers of myocytes, which were separated by a minimal layer of connective tissue. The structure was clear; the cells were elongated and spindle-shaped.

On the outside, the jejunum was covered with a serous membrane with layers of loose connective tissue and mesothelium. The integrity of the latter was intact.

Figure 3 shows the mucous membrane of the jejunum samples in the control group. The general histological structure remained the same. We observed a slight accumulation of mucus between the villi produced by goblet cells. Epithelial cells were of an elongated cylindrical shape. The glands of the lamina propria were well expressed. The integrity of the layers was intact.

The jejunum samples in the experimental groups had some histological features that differed from the control group samples.

The jejunum of young rams that received Yoddar-Zn had a single-layer cylindrical border epithelium on the transverse sections of the villi (Fig. 4).

The lumen of the tubular glands looked deserted, and the crypts were separated by a minimal layer of

Table 3 Wall thickness of the jejunum of seven-month-old rams fed with various feed additives

Research subject	Wall thickness, μm		
	Mucus membrane	Muscular membrane	Serous membrane
Control	17.40 ± 1.07	8.30 ± 0.79	0.80 ± 0.51
Yoddar-Zn	19.10 ± 0.52	9.50 ± 0.81	0.90 ± 0.22
DAFS-25	19.40 ± 0.97	9.60 ± 0.79	0.90 ± 0.55
DAFS-25 + Yoddar-Zn	19.80 ± 0.97*	10.30 ± 0.71*	1.00 ± 0.44

*$P \leq 0.005$

connective tissue (Fig. 4). The muscular plate of the mucosa was well expressed; the submucosa consisted of connective tissue layers with elongated tubular glands. The integrity of all membranes was intact.

Figure 5 shows the jejunum samples obtained from animals that received DAFS-25. The cylindrical epitheliocytes and the villi of the lamina propria were distinct, with moderately pronounced glands with empty lumens and numerous goblet cells. The integrity of the membranes was intact: the muscle layers were separated from each other by connective tissue. The serous tissue was hardly developed.

Figure 6 shows the jejunum samples obtained from animals that received DAFS-25 + Yoddar-Zn. The organ wall had a very obvious microstructure. The structure of the mucous membrane of the small intestine was intact, its constituent elements having clear contours. The goblet cells and the single-layered columnar epithelium were quite distinct. The villi were separated from each other by a minimal layer of connective tissue. The submucosa demonstrated contoured blood vessels, some of which were filled with blood. This fact indicates a more intensive metabolism in animals fed with DAFS-25 + Yoddar-Zn.

The myocytes of the muscular membrane are quite clearly separated by loose fibrous connective tissue with a minimal number of blood vessels. Muscle cells corresponded to the state of contraction, i.e., the cells were as if the muscle was contracted, and the morphology of the early autolysis process.

The morphological analysis proved that the structure of the jejunum wall in the control and experimental groups was intact and typical. The layers had an integral structure in all experimental groups. Samples obtained from animals that received DAFS-25 + Yoddar-Zn had the best developed structure.

Table 3 shows that the arithmetic mean value of the thickness of the jejunum mucous layer was 19.40 ± 0.55 μm in the rams of the experimental groups, which exceeded the control by 2.0 μm. The thickness of the muscular membrane in experimental groups also exceeded this indicator in the control group by an average of 0.8–2.0 μm. The experimental rams also had a slightly thicker serous layer.

The minimal thickening of the jejunum membranes was minimal in the experimental groups, the lowest observed in the animals that received DAFS-25 + Yoddar-Zn. This fact may be an indirect indicator of a more active digestion, a better digestibility, and a greater absorption of feeds and nutrients into the bloodstream.

CONCLUSION

Biofortification of young rams' diet with essential microelements had a positive effect on the quality and quantity of the gastrointestinal microbial community, which means a better digestion process and a greater animal yield.

In the rumen samples, cellulosolytic bacteria, which break down the fiber of plant foods into volatile fatty acids, were mainly represented by *Clostridiaceae*, *Prevotellaceae*, *Flavobacteriaceae*, *Eubacteriaceae*, *Lachnospiraceae*, *Ruminococcaceae*, and *Thermoanaerobacteraceae* families, as well as by the *Bacteroidetes* phylum. The content of lactate-utilizing bacteria in the rumen samples reached 40%, which may indicate a high degree of activity of these bacteria, depending on their physiological state of the animal.

The content of bacilli in the rumen samples was ≤ 1%. The total proportion of pathogenic species ranged from 0.2 to 6.3%. The experiment revealed ≥ 50 types of pathogenic microorganisms, which were most abundant in the group fed with Yoddar-Zn + DAFS-25. The pathogenic microorganisms belonged to erysipelothrix, fusobacterial, and streptococci. The content of porphyromonas reached 0.68% of total microorganisms, while the proportion of *Treponema* in the samples ranged from 0.6 to 1%. Lactobacilli were represented mainly by *Lactobacilliales* (0.06–0.45%). This fact may indicate a high degree of activity of these bacteria in the sheep rumen, depending on their physiological state of the animal.

The balance of the microflora in the sheep rumen samples was good, and the amount of beneficial microflora was enough to inhibit the pathogenic and opportunistic bacteria.

The light microscopy revealed no adverse effect of the feed additives DAFS-25 and Yoddar Zn on the microstructural parameters of sheep jejunum. Therefore, they can be recommended for fattening purposes in industrial conditions.

The additives had no negative impact on the rumen microbiocenosis and the jejunum microstructure. The structure of the jejunum corresponded to the morphological characteristics for this type and age of

farm animal in all the groups. A clearer micropicture of the jejunum wall was revealed in the experimental group of rams fed with DAFS-25 + Yoddar Zn.

The complex application of additives DAFS-25 and Yoddar Zn helped optimize the processes of digestion, absorption, and assimilation of feed nutrients, which was partly confirmed by the minimal thickening of the jejunum membranes.

Further research is needed to study the effect of these additives on other important systems of animal organism, e.g., digestive (liver), excretory (kidneys), nervous (cortex and base of brain), and immune (spleen and mesenteric lymph nodes) systems.

CONTRIBUTION

Authors are equally relevant to the writing of the manuscript, and equally responsible for plagiarism.

CONFLICT OF INTEREST

The authors declare no conflict of interest.

REFERENCES

1. Khvylya SI, Giro TM. Assessment of the quality and biological safety of meat and meat products by microstructural methods. Saratov: Bukva; 2015. 240 p. (In Russ.).
2. Ozer N, Birişik C, Sakata R, Yetim H, Ahhmed MA. Meat therapy for hypertension: hybrid hydrolysate as ace inhibitory compounds. Proceeding of the 61st international congress of Meat Science and Technology; 2015. Clermont. Clermont; 2015. p. 108–111.
3. Cui X, Wang Z, Tan Y, Chang S, Zheng H, Wang H, *et al.* Selenium yeast dietary supplement affects rumen bacterial population dynamics and fermentation parameters of Tibetan sheep (*Ovis aries*) in alpine meadow. Frontiers in Microbiology. 2021;12. https://doi.org/10.3389/fmicb.2021.663945
4. Kulikovskii AV, Lisitsyn AB, Chernukha IM, Gorlov IF, Savchuk SA. Determination of iodotyrosines in food. Journal of Analytical Chemistry. 2016;71(12):1215–1219. https://doi.org/10.1134/S1061934816100087
5. Bo Trabi E, Seddik H, Xie F, Wang X, Liu J, Mao S. Effect of pelleted high-grain total mixed ration on rumen morphology, epithelium-associated microbiota and gene expression of proinflammatory cytokines and tight junction proteins in Hu sheep. Animal Feed Science and Technology. 2020;263. https://doi.org/10.1016/j.anifeedsci.2020.114453
6. Giro TM, Kulikovsky AV, Knyazeva AS, Domnitsky IYu, Giro AV. Biochemical and microstructural profile of the thyroid gland from lambs raised on experimental diets. Food Processing: Techniques and Technology. 2020;50(4): 670–680. (In Russ.). https://doi.org/10.21603/2074-9414-2020-4-670-680
7. Giro TM, Kulikovski AV, Giro VV, Mosolov AA. Microstructural studies of muscle tissue of lamb of aboriginal breeds of the Volga region. IOP Conference Series: Earth and Environmental Science. 2020;548(8). https://doi.org/10.1088/1755-1315/548/8/082082
8. Chernukha IM, Mashentseva NG, Vostrikova NL, Kovalev LI, Kovaleva MA, Afanasev DA. Generation of bioactive peptides in meat raw materials exposed to lysates of bacterial starter cultures. Agricultural Biology. 2020;55(6): 1182–1203. (In Russ.). https://doi.org/10.15389/agrobiology.2020.6.1182eng
9. Ben Said M, Belkahia H, Messadi L. *Anaplasma* spp. in North Africa: A review on molecular epidemiology, associated risk factors and genetic characteristics. Ticks and Tick-borne Diseases. 2018;9(3):543–555. https://doi.org/10.1016/j.ttbdis.2018.01.003
10. Zhang J, Li H, Kong L, Su J, Ma J, Feng B. Optimization of processing parameters of straw and particles feed for fattening lamb. Nongye Gongcheng Xuebao/Transactions of the Chinese Society of Agricultural Engineering. 2018;34(5):274–281. https://doi.org/10.11975/j.issn.1002-6819.2018.05.036
11. Traisov BB, Smagulov DB, Yuldashbaev YuA, Esengaliev KG. Meat productivity of crossbred rams after fattening. Journal of Pharmaceutical Sciences and Research. 2017;9(5):574–577.
12. Bhatt RS, Sahoo A, Soni LK, Gadekar YP. Effect of protected fat as ca-soap and formaldehyde-treated full-fat soybean in the finisher diet of lambs on growth performance, carcass traits and fatty acid profile. Agricultural Research. 2017;6(4):427–435. https://doi.org/10.1007/s40003-017-0273-7
13. Al-Suwaiegh SB, Al-Shathri AA. Effect of slaughter age on the fatty acid composition of intramuscular and subcutaneous fat in lamb carcass of Awassi breed. Indian Journal of Animal Research. 2014;48(2):162–170. https://doi.org/10.5958/j.0976-0555.48.2.035
14. Johnson RA, Bhattacharyya GK. Statistics. Principles and methods. 6th ed. John Wiley & Sons; 2010. 706 p.
15. Masatani T, Hayashi K, Andoh M, Tateno M, Endo Y, Asada M, *et al.* Detection and molecular characterization of *Babesia*, *Theileria*, and *Hepatozoon* species in hard ticks collected from Kagoshima, the southern region in Japan. Ticks and Tick-borne Diseases. 2017;8(4):581–587. https://doi.org/10.1016/j.ttbdis.2017.03.007

16. Guang-Xin E, Zhao Y-J, Huang Y-F, Sheep mitochondrial heteroplasmy arises from tandem motifs and unspecific PCR amplification. Mitochondrial DNA Part A: DNA Mapping, Sequencing, and Analysis. 2018;29(1):91–95. https://doi.org/10.1080/24701394.2016.1242582
17. Koseniuk A, Słota E, Mitochondrial control region diversity in Polish sheep breeds. Archives Animal Breeding. 2016;59(2):227–233. https://doi.org/10.5194/aab-59-227-2016
18. Othman OE, Pariset L, Balabel EA, Marioti M, Genetic characterization of Egyptian and Italian sheep breeds using mitochondrial DNA. Journal of Genetic Engineering and Biotechnology. 2015;13(1):79–86. https://doi.org/10.1016/j.jgeb.2014.12.005
19. Boujenane I, Petit D, Between-and within-breed morphological variability in Moroccan sheep breeds. Animal Genetic Resources. 2016;58:91–100. https://doi.org/10.1017/S2078633616000059
20. Gorkhali NA, Han JL, Ma YH. Mitochondrial DNA variation in indigenous sheep (*Ovis aries*) breeds of Nepal. Tropical Agricultural Research. 2015;26(4):632–641. https://doi.org/10.4038/tar.v26i4.8125
21. Xu S-S, Gao L, Xie X-L, Ren Y-L, Shen Z-Q, Wang F, *et al.* Genome-wide association analyses highlight the potential for different genetic mechanisms for litter size among sheep breeds. Frontiers in Genetics. 2018;9. https://doi.org/10.3389/fgene.2018.00118
22. Tam V, Patel N, Turcotte M, Bosse Y, Pare G, Meyre D. Benefits and limitations of genome-wide association studies. Nature Reviews Genetics. 2019;20(8):467–484. https://doi.org/10.1038/s41576-019-0127-1
23. Bo Trabi E, Seddik H, Xie F, Lin L, Mao S. Comparison of the rumen bacterial community, rumen fermentation and growth performance of fattening lambs fed low-grain, pelleted or non-pelleted high grain total mixed ration. Animal Feed Science and Technology. 2019;253:1–12. https://doi.org/10.1016/j.anifeedsci.2019.05.001
24. Bhatt RS, Soni L, Gadekar YP, Sahoo A, Sarkar S, Kumar D. Fatty acid profile and nutrient composition of muscle and adipose tissue from Malpura and fat-tailed Dumba sheep. Indian Journal of Animal Sciences. 2020;90(3).
25. Scheuer R. From the art of tasting to global standardization. The development of analytical chemistry in Flesch research in Kulmbach. Bulletin of the meat research Kulmbach. 2013;52(201):141–146. (In Germ.).

ORCID IDs
Tatiana M. Giro https://orcid.org/0000-0003-3039-1324
Andrey V. Kulikovsky https://orcid.org/0000-0002-9140-5390
Irina V. Ziruk https://orcid.org/0000-0001-7300-3956

FRM
Foods and Raw Materials. 2022;10(2)
ISSN 2310-9599 (Print)
ISSN 2308-4057 (Online)

Research Article
Open Access

Available online at http://jfrm.ru/en
https://doi.org/10.21603/2308-4057-2022-2-538
https://elibrary.ru/YFQHAZ

Developing colloidal structure of beer by grain organic compounds

Irina N. Gribkova[1,*], Mikhail N. Eliseev[2], Maxim A. Zakharov[1], Olga A. Kosareva[3], Varvara A. Zakharova[1]

[1] All-Russian Research Institute of Brewing, Non-Alcoholic and Wine Industry, Moscow, Russia
[2] Plekhanov Russian University of Economics, Moscow, Russia
[3] Moscow University for Industry and Finance "Synergy", Moscow, Russia

* e-mail: beer_institut@mail.ru

Received 01.12.2021; Revised 21.01.2022; Accepted 01.02.2022; Published online 23.09.2022

Abstract:
The present article introduces the problem of determining the general structure of beer as a complex system of related biomolecules. The objective was to establish the correlation of various quantities of organic compounds in beer formulation.
The research featured samples of filtered pasteurized beer obtained from a retail chain shop in Moscow (Russia). The experiment relied on standard research methods, including instrumental methods of analysis, e.g., high-performance liquid chromatography (HPLC). The obtained experimental data underwent a statistical analysis using the Statistica software (StatSoft, 2016).
The research established the correlation between the type of grain (barley or wheat malt) and the content of organic compounds, e.g., *β*-glucan, polyphenols, soluble nitrogen, etc. The research also revealed some patterns in the distribution of proteins, which served as a framework for the system of organic compounds. The distribution of thiol proteins proved to depend on the dissolution degree of the grain and was different in barley light, barley dark, and wheat malt samples. The fraction distribution of *β*-glucan depended on the color of the malt. In light beer samples, it concentrated in high- and medium-molecular fractions of nitrogenous substances, in dark beer – in low-molecular fractions (≤ 63%). Initial wort density and alcohol content affected the amount of catechins and total polyphenols. Nitrogenous compounds depended on the color, initial extract, and alcohol content.
The nitrogenous structure and other organic compounds of beer proved to depend on protein substances. The research also revealed a number of factors that affected the fraction distribution of biomolecules in different beer sorts.

Keywords: Beer, nitrogenous compounds, polyphenols, *β*-glucan, fractioning, structure

Please cite this article in press as: Gribkova IN, Eliseev MN, Zakharov MA, Kosareva OA, Zakharova VA. Developing colloidal structure of beer by grain organic compounds. Foods and Raw Materials. 2022;10(2):318–328. https://doi.org/10.21603/2308-4057-2022-2-538

INTRODUCTION

Alcoholic beverages have a colloidal structure that depends on primary plant raw materials or secondary organic compounds. Secondary organic compounds are a product of the microbial activity. They appear as a result of various biochemical or chemical processes presupposed by the particular production technology. The combination of primary and secondary organic compounds affects the sensory profile of the beverage and, consequently, its demand on the food market.

Similarly, beer is an alcoholic drink with a complex colloidal structure formed by organic biomolecules of various molecular weights, which are interconnected by hydrogen, covalent, disulfide, and other bonds [1, 2]. Nitrogenous compounds, phenols, and carbohydrate biomolecules shape both the sensory profile of beer and its stability as a fermented drink (Fig. 1) [2]. However, flavor profile development is a versatile process. It depends both on the primary biomolecules that get hydrolyzed during wort production and on the secondary biomolecules that appear as a result of biomodification in the Krebs cycle during fermentation [3].

Depending on the size and fraction, some organic compounds develop both the sensory profile and consumer characteristics of beer, while others are responsible for haze.

Foam stability and settling time are important consumer characteristics that are associated with the quality of beer [4]. Foam quality depends on

protein fractions, bitter hop resins, pentosans, gum substances, and other fractions of plant materials that produce carbon dioxide bubbles on beer surface [5]. Protein biomolecules play the key role in foam development during brewing. Some proteins possess foaming properties, while others are responsible for stabilizing [6]. The composition of beer foam is strongly associated with lipid carrier proteins (LTP1). Their molecular weight is 9.7 kDa, and they include 91 amino acids. Other foam-related proteins are protein Z (40 kDa) and various derivatives of hordein (10–30 kDa) [7].

Beer foam has a complex composition, which consists not only of protein fractions but also of ligand compounds. Ligands are formed by bitter isoforms of α-bitter acids found in hop. The carboxyl group of the asparagine residue in the LTP1 protein molecule is linked by covalent bonds with the hydroxy group of resin, flavonoids, phytosterols, etc. [8]. Foam stability always correlates with the degree of malt dissolution and sometimes with another protein Z fraction [9].

Protein Z is part of the fraction of hordein proteins. Good solubility of malt stimulates the release of this protein into the liquid fraction and causes haze [10, 11]. Similarly, the intensity of haze depends on the content of fractions with a molecular weight of 8–14 kDa in barley malt and < 7 kDa in wheat malt [12].

The last 40 years of beer studies have established a partial similarity in the composition of the protein fractions of the foam and the body of beer. It includes three groups of protein molecules of 40, 10, and 8 kDa (proteins and peptides), which are similar to barley nitrogenous compounds [13].

Non-starch polysaccharides also affect the taste of beer [14]. For instance, maltodextrins and β-glucan can enhance flavor profile. The molecular weight of β-glucan in barley is 150–1937 kDa, in malt – 800–1220 kDa, and in beer – 10–10 000 kDa [15]. The content of β-glucan in the initial barley affects that of malt, and the content of β-glucan in malt affects that in wort. The correlation is different for different types of barley. For instance, the correlation coefficient was 0.9717 for barley malt and 0.9998 for barley wort colloids [15].

Phenolics are other important compounds of beer. Catechins, non-condensed phenolic compounds, and monophenolic acids have a positive effect on the flavor profile of beer, while proanthocyanidins spoil both its taste and stability [16]. In fact, proanthocyanidins possess an extraordinary reactivity and condense into large globules, dragging along proteins and other biomolecules [2].

Thus, the effect of grain organic compounds on the finished product is diverse and quantitatively unclear. For instance, the issue of the interrelation between grain biomolecules and other plant materials still remains understudied in the brewing industry. The research objective was to establish the correlation between the biomolecules of beer plant raw materials to cast light upon the general structure of beer as a colloidal system. The research will make it possible to update the methodology for quality control in the brewing industry.

STUDY OBJECTS AND METHODS

Beer samples. Samples of filtered pasteurized beer were purchased from a retail network in Moscow and stored in the dark at temperature 15 ± 20°C and air

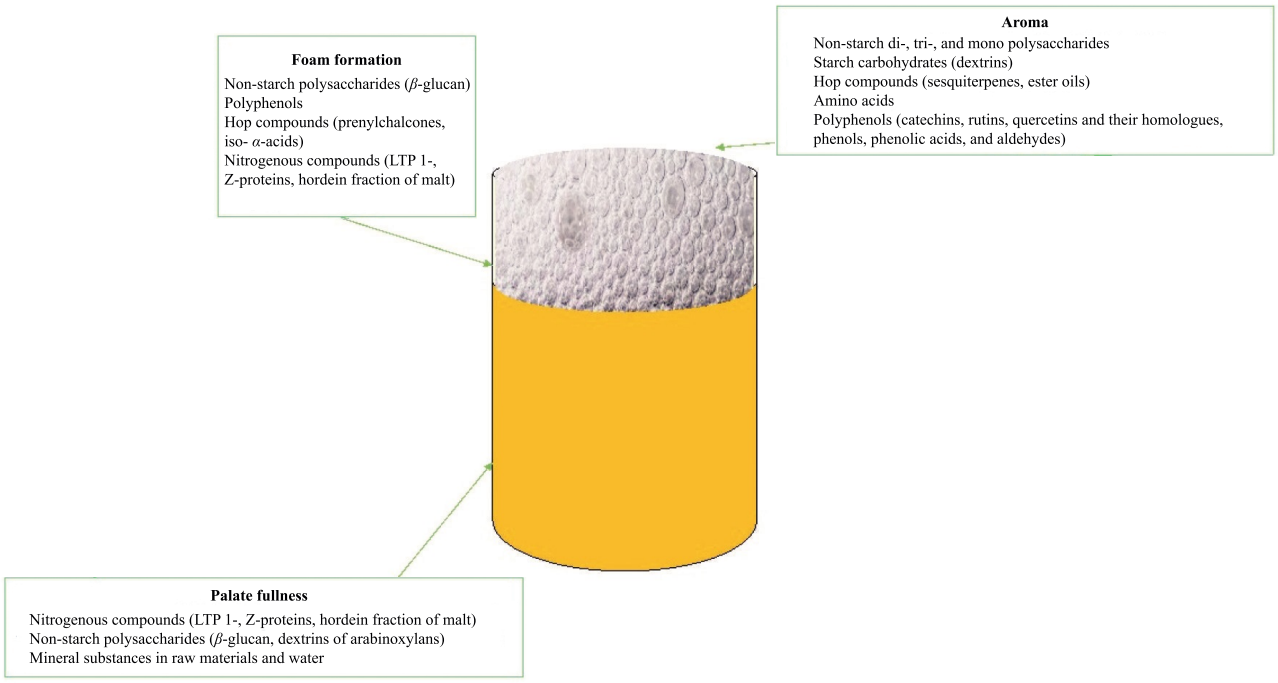

Figure 1 Colloidal structure of beer

humidity W ≤ 75 ± 2%. The list included light beers (45 samples), dark beers (10 samples), wheat beers (10 samples), and non-alcoholic beers (5 samples), five bottles or cans per each sort.

Fractioning the organic compounds of beer. To preserve the spatial structure of the protein fractions of biomolecules, the protein fractioning was carried out by two methods. High-molecular proteins and related organic compounds were precipitated with a 2% tannin aqueous solution. High-molecular and medium-molecular nitrogenous compounds were precipitated using a 50% sodium molybdate (Na_2MoO_4) solution in an acid medium. The fractions of nitrogenous compounds, polyphenols, and *β*-glucans in the filtrate were determined as described below.

An aliquot (62 cm^3) of decarbonated beer was taken into two volumetric flasks of 100 cm^3. Into the first flask, we added 35 cm^3 of distilled water, followed by 2 cm^3 of concentrated sulfuric acid, which made it possible to establish the acidic pH of the medium. The solution was stirred, mixed with a 2% tannin aqueous solution, and filtered. Into the other flask, we added 30 cm^3 of distilled water, followed by 5 cm^3 of 50% Na_2MoO_4 solution. The mix was brought to the mark with distilled water, followed by another 5 cm^3 of concentrated sulfuric acid. The resulting phosphomolybdic acid in the medium made it possible to precipitate protein nitrogen from beer. The initial samples of beer, post-tannin fraction, and post-molybdate fraction were tested for the mass concentrations of soluble nitrogen, nitrogenous compounds with unoxidized disulfide bonds, *β*-glucan, catechins, and polyphenolic compounds.

The content of organic compounds in the high molecular weight fraction was calculated as the difference between the total amount of a particular compound and its content in the post-tannin extract. The low molecular weight fraction was determined in the postmolybdate filtrate. The average molecular fraction was calculated as the difference between the total amount of the substance and the sum of the high and low molecular weight fractions.

Determining the nitrogenous compounds. The Kjeldahl method for determining total soluble nitrogen was used according to the European Brewery Convention method No. 4.9.3 [17].

Determining the total content of polyphenols. The mass concentration of polyphenols was measured according to the European Brewery Convention method No. 9.9 [18].

Determining the mass concentration of catechins. The content of catechins was determined by high-performance liquid chromatography (HPLC). The procedure involved an Agilent Technologies 1200 device (Agilent, USA) with a diode array detector and a Hypersil 5u C18 250×4.6 mm 5 µm column (Thermo, USA) with a wavelength of 280 nm. According to the procedure, 0.001 cm^3 of samples and all standard solutions were injected into a reverse phase column at 30°C. The mobile phase for HPLC was prepared as follows. Solution A included 0.1 mL of phosphoric acid dissolved in 900 cm^3 of HPLC water. The volume was brought up to 1000 cm^3 with water. The solution was filtered through a 0.45-µm membrane filter and degassed in an ultrasonicator for 3 min. Solution B was acetonitrile. The mobile phase used gradient elution: at 0.01 min – 11% B; 30 min – 25% B; 35–39 min – 100% B; 40–50 min – 11% B. The flow rate of the mobile phase was 1.0 cm^3/min, and the injection volume was 0.001 cm^3 [19].

Determining the mass concentration of nitrogenous compounds with disulfide groups. The Ellman method detected nitrogenous compounds that contained unoxidized sulfhydryl (thiol) groups [20]. The procedure was based on the reaction of thiol with dithiobisnitrobenzoic acid, which formed a mixed disulfide and 2-nitro-5-thiobenzoic acid. They were quantified by anion absorption at 412 nm in a spectrophotometer. A number of reagents made it possible to determine the concentration of thiol groups. The list included 0.1 and 0.2 M phosphate buffer and Ellman's reagent that consisted of 37 mg of dithiobisnitrobenzoic acid dissolved in 10 cm^3 of 0.1 M phosphorus buffer with pH = 7.0 and 15 mg of $NaHCO_3$. The experiment was prepared as follows. First, 3 cm^3 of the protein solution was poured into a test tube, followed by 2 cm^3 of a 0.2 M phosphate buffer solution and 5 cm^3 of distilled water. The aliquot (3 cm^3) was poured into another tube, followed by 0.02 cm^3 of Elman's reagent. After 3 min, the optical density was measured at 412 nm against the control solution. The control solution was prepared similarly, but 0.02 cm^3 of distilled water was added to 3 cm^3 in another test tube at the last stage.

The mass concentration of thiol-containing nitrogenous compounds (mol/dm^3) was calculated by the following formula:

$$C_{s\text{-}s} = D \cdot P / 11{,}400 \quad (1)$$

where D is the optical density at 412 nm; P is the dillution.

Determining the mass concentration of *β*-glucan. The mass concentration of *β*-glucan was determined by the enzymatic European Brewery Convention method No. 8.13.1 [21].

Statistical analysis. All experiments were performed in five repetitions. The obtained values were presented as mean ± standard deviation (SD). The Student's t-test was applied to test the homogeneity of the samples. The multivariate models in the correlation-regression analysis were checked using the Fisher test ($P \leq 0.95$). The data were processed using Statistica software (StatSoft, Redmond, WA, USA, 2006).

RESULTS AND DISCUSSION

Relationship between the beer quality and the quantity of organic compounds in grain. The first stage of the research was aimed at finding the quantitative characteristics of the main organic

compounds that shape the colloidal structure of beer. The list included nitrogenous compounds, polyphenols, and a non-starch carbohydrate *β*-glucan. Together with divalent metal ions, hop resins, and melanoidins, these compounds are responsible for both haze and beer quality [22]. The dual behavior of biomolecules can be explained by their grain origin: they originate in malted or unmalted grain and pass into the liquid phase during processing. Table 1 illustrates the quantitative characteristics of the main organic compounds.

Non-alcoholic and light beer had a similar content of solids in the initial wort (Table 1). As a result, they both were poor in *β*-glucan, polyphenols, and soluble nitrogen. Apparently, this fact can be explained by the technology of removing alcohol from beer by thermal or membrane methods.

Thermal de-alcoholization processes include vacuum evaporation, vacuum distillation, and centrifugation. They have a negative effect on the sensory profile of beer, which loses in aroma and palate fullness while acquiring new unwanted aromas [23]. Adsorption extraction is another de-alcoholization method. It involves adsorbents, e.g., zeolites. Their surface has charged sites that have an affinity for polar organic substances, which means they can adsorb them. Zeolites often have an affinity for Ca^{2+} and Mg^{2+} ions [24]. Molecules of nitrogenous substances, polyphenols, and *β*-glucan can be connected to other biomolecules via Ca^{2+} and Mg^{2+} bridges [25]. Nanofiltration can decrease both the level of alcohol and some polyphenolic compounds [23].

Thus, differences between the de-alcoholization methods can reduce the mass concentration of these compounds. This fact can explain the decrease in the level of non-starch polysaccharides, polyphenols, and soluble nitrogen in non-alcoholic beer, compared to light varieties.

In light beer, *β*-glucan, polyphenols, and soluble nitrogen are proportional to the increase in the solids of the initial wort (Table 1).

In dark beer, the content of *β*-glucan was 30%, and the content of soluble nitrogen was two times higher. This effect might have been caused by colored malt, which has higher dissolving properties during germination [26]. Colored malt is also responsible for the lower total amount of polyphenols because they contain lower amounts of such polyphenols as catechin, prodelphinidin B3, procyanidin B3, and ferulic acid [27].

Wheat beer with 12–15% of Brix, °P in the initial malt had twice as much *β*-glucan as light barley beer. The amount of polyphenols in these samples was higher by 30% and that of soluble nitrogen (lower limit) – by 33% (Table 1). In [28], wheat beer also contained a greater amount of non-starch polysaccharides with a structure-dependent difference and a higher degree of polymerization, compared to light barley beer. Barley malt has a *β*-glucan polymerization of 38–48, while wheat malt has a polymerization of 38–83 [28]. In wheat beers with 16÷20% solids, the content of non-starch polysaccharide was 1.5 times higher (upper limit), polyphenols – 1.3–1.6 times higher, protein – by 5.0÷32% higher than in the samples of barley-malt beer, which was probably caused by wheat malt [29].

Distribution of biomolecules of grain raw materials by nitrogenous fractions. The content of soluble nitrogen in beer samples was more significant. Thus, the structure of beer was studied depending on the ratio of different groups of biomolecules with protein substances. The beer samples were tested for nitrogen with thiol groups and catechins. Table 2 shows the averaged data, while Fig. 2 demonstrates the quantitative distribution of biomolecules by fractions of nitrogenous compounds.

The catechin content confirmed the data obtained by Maia *et al.* [30]. No correlations between thiol groups were detected. However, dark beer had more catechins because the malt had better dissolution and antioxidant activities. As a result, catechins did not oxidize until the final stage of beer production [30].

Table 2 shows a high level of nitrogen with thiol groups in dark and light barley-malt beers with a lot of

Table 1 Quantitative profile of beer compounds

Beer	Brix, °P	Content* of organic substances, mg/dm^3					
		β-glucan		Polyphenols		Soluble nitrogen	
		from	to	from	to	from	to
Non-alcoholic, barley-malt, light	7÷8	69.8 ± 4.9	93.0 ± 6.5	32.8 ± 3.0	65.6 ± 5.9	440.0 ± 6.6	864.0 ± 13.0
Light, barley-malt	10÷11	31.0 ± 2.2	93.0 ± 6.5	70.4 ± 6.3	217.0 ± 19.5	560.0 ± 8.4	920.0 ± 13.8
	11÷15	45.0 ± 3.2	125.0 ± 8.8	85.5 ± 7.7	225.0 ± 20.2	580.0 ± 8.7	880.0 ± 13.2
	15÷23	78.0 ± 5.5	180.0 ± 12.6	100.0 ± 9.0	305.0 ± 27.5	850.0 ± 12.8	1350.0 ± 20.3
Dark, barley-malt	10÷11	76.5 ± 5.4	125.0 ± 8.8	102.0 ± 9.2	172.0 ± 15.5	1200.0 ± 18.0	1780.0 ± 26.7
	15÷23	120.0 ± 8.4	180.0 ± 12.6	110.0 ± 9.9	180.0 ± 16.2	1200.0 ± 18.0	1800.0 ± 27.0
Light, wheat-malt	12÷15	95.0 ± 6.7	240.0 ± 16.8	110.0 ± 10.0	290.0 ± 26.0	770.0 ± 11.6	890.0 ± 13.4
	16÷20	125.0 ± 8.8	280.0 ± 19.6	145.0 ± 13.0	290.0 ± 26.0	1150.0 ± 17.3	1380.0 ± 20.7

* Each value is the mean ± standard deviation of five independent experiments

Table 2 Thiol nitrogen-containing compounds and catechins in beer samples

Beer type	Brix, °P	Content in beer	
		Protein with thiol groups, μmoL/dm^3	Catechins, mg/dm^3
Non-alcoholic barley malt	7÷8	5.61 ± 0.56	2.25 ± 0.23
Light, barley malt	10÷11	12.7 ± 1.26	6.33 ± 0.65
	11÷15	16.4 ± 1.55	8.14 ± 0.80
	15÷23	36.7 ± 3.60	14.4 ± 1.40
Dark barley malt	10÷11	28.0 ± 2.80	14.9 ± 1.50
	15÷23	35.5 ± 3.50	18.0 ± 1.80
Light, wheat malt	12÷15	11.4 ± 1.00	1.98 ± 0.20
	16÷20	8.80 ± 0.90	6.90 ± 0.70

Each value is the mean ± standard deviation of five independent experiments

initial wort solids. This fact was probably associated with the antioxidant capacity of these samples, which retained thiol groups in unoxidized form.

Light wheat beers contained a relatively low amount of nitrogen with thiol groups (8.80–11.4 μm) compared to barley-malt light beers (12.7–16.4 μm), as confirmed by other studies [31].

The fraction distribution of organic compounds (Fig. 2a–h) depended on the type of beer.

The high-molecular fraction of soluble nitrogen ranged from 7 to 15% of the total amount. Its minimal amount was in dense light barley-malt beers, where the solids content in the initial wort was 15÷23%. The maximal amount was in light barley-malt beer with the solids content of 11÷15%.

The average molecular fraction correlated with the density. The biggest amount of soluble nitrogen (8÷40 kDa) was registered in the beer samples with initial wort solids content ≥ 23%: it was 20–34% of the total amount of protein compounds. The low molecular fraction of soluble nitrogen was inversely related to the density of beer. For all samples, the higher the content of dry matter in the initial wort, the lower the content of protein compounds with a molecular weight of ≤ 8 kDa.

The distribution of thiol groups of nitrogenous substances was as follows. In light barley-malt beers, the maximal amount was in the medium molecular weight fraction (8÷40 kDa). In dark barley-malt beers, it was in the low molecular weight fraction (≤ 8 kDa). In light wheat-malt beer, it was in the high molecular weight fraction (40÷100 kDa).

The *β*-glucan dextrins differed in distribution. In light barley-malt beer, 58–68% of the total content of non-starch polysaccharide fractions accounted for the protein fraction with a molecular weight of 8÷40 kDa. In dark barley-malt beer, 59–63% of *β*-glucan molecules were concentrated in the fraction of nitrogenous substances of ≤ 8 kDa, and 73–79% of its total content was distributed in nitrogenous substances of 40÷100 kDa.

Catechins did not depend on the type and composition of beer: 45–74% of the total content accumulated in the high molecular weight fraction of soluble nitrogen. However, the total content of polyphenols showed strong correlation with the type of beer.

Table 3 shows the correlation between the total polyphenol content and the catechin content.

Table 3 revealed a strong correlation between the total polyphenols and catechins and the type of beer. According to the determination coefficient, the total polyphenols depended on the content of catechins when the latter was 50–99%. Therefore, some unknown factors affected the total polyphenols in different beer samples. The lowest determination coefficient was registered in light barley-malt beers 15÷23%, dark beers 15÷23%, and wheat-malt beers 16÷20%. When the solids in the initial wort was high, the composition of polyphenolic compounds experienced a stronger impact from anthocyanogens, phenolic acids, aldehydes, hop resins, and prenylflavanoids. Apparently, strong beer requires a greater proportion of hops, which, like grain, is a source of polyphenolic compounds [32]. On the other hand, the stability of phenolic compounds depends on many factors, e.g., temperature, pH, coactivating substances, polar solvents, etc., which makes the amount of alcohol a more significant factor for strong beer sorts [33].

Table 4 illustrates the dependence of the distribution of thiol groups and catechins.

Table 4 shows that the change in *β*-glucan was 50%, while the content of thiol groups and catechins changed by 80%, which depended on the parameters of the plant material, i.e., barley or wheat malt. On the one hand, this fact can be traced back to grain varieties. On the other hand, non-starch polysaccharides can develop colloidal suspensions and links with other beer compounds, which leads to product losses and affects the content of *β*-glucan [15, 34].

Figures 3 and 4 illustrate the analysis of correlations and regressions, which registered the presence and degree of the relationship between the content of soluble nitrogen and other parameters. The analysis established a close and logical relationship between the amount of raw materials (solids in the initial wort) and the content of alcohol and polyphenols, which was confirmed by

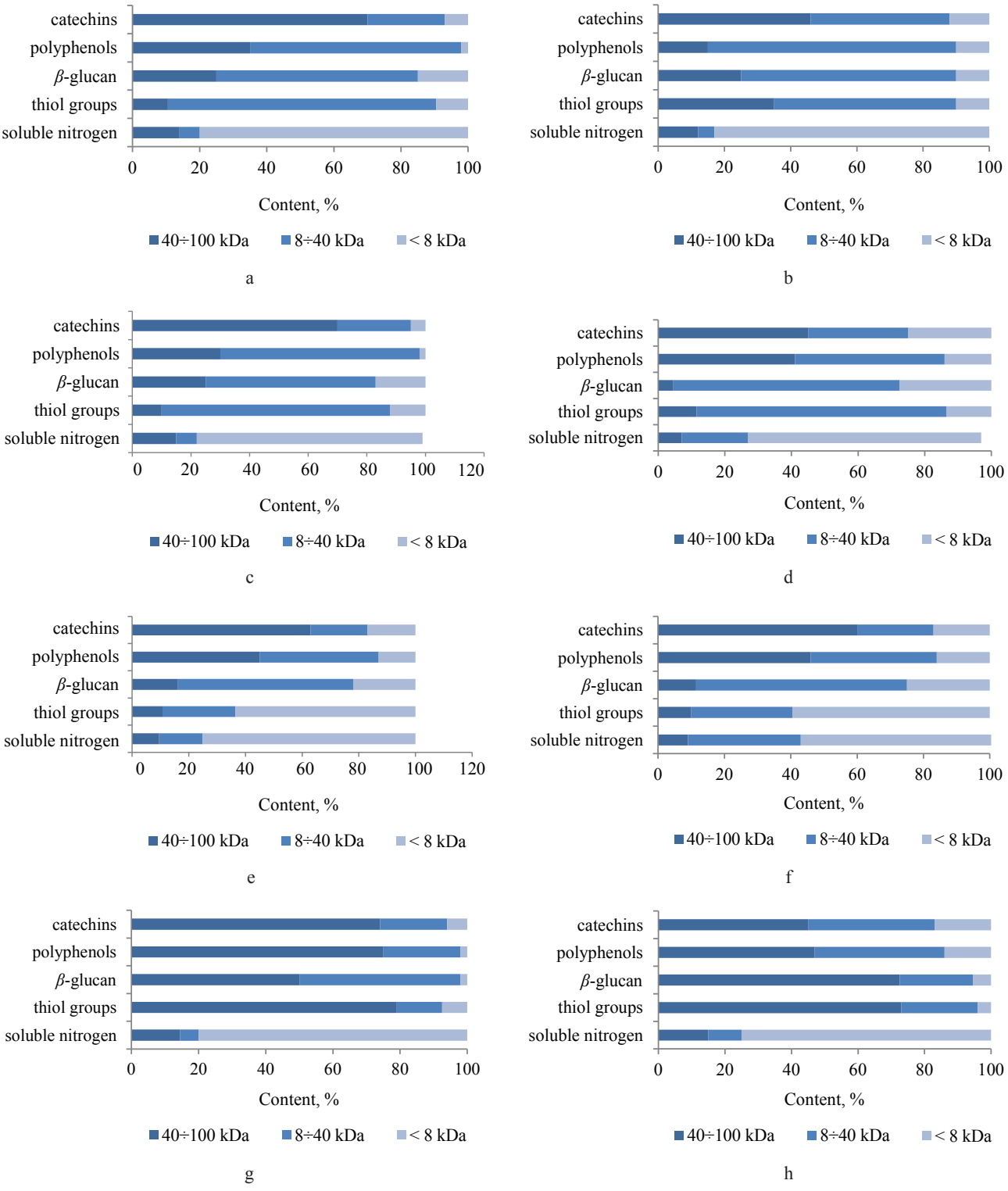

Figure 2 Distribution of compounds by fractions of soluble nitrogen: (a) non-alcoholic barley-malt beer; (b) light barley-malt beer with 11÷12 Brix, °P; (c) light barley-malt beer with 12÷15 Brix, °P; (d) light barley-malt beer with 15÷23 Brix, °P; (e) dark barley-malt beer with 10÷11 Brix, °P; (f) dark barley-malt beer with 15÷23 Brix, °P; (g) light wheat-malt beer with 12÷15 Brix, °P; (h) light wheat-malt beer with 16÷20 Brix, °P

previous studies [32, 33]. Fermentation and the content of polyphenols in the finished product also proved closely interconnected. This fact has been described in different publications [32].

The content of soluble nitrogen proved to depend on the color (type) of beer. This result was quite predictable since a greater degree of dissolution of colored malt means a greater effect of low molecular

Table 3 Analysis of correlation and regression between components and beer parameters

Beer type	Brix, °P	Correlation coefficient (r)	Equation of dependance	Correlation according to Chaddock scale	Determination coefficient
Non-alcoholic barley malt	7÷8	0.744	y = 48.2 – 2.56 x	Direct, high	0.553
Light, barley malt	10÷11	0.713	y = 77.4 + 6.22 x	Direct, high	0.508
	11÷15	0.975	y = 54.9 + 12.2 x	Direct, high	0.952
	15÷23	0.517	y = 81.9 + 15.3 x	Direct, moderate	0.267
Dark barley malt	10÷11	0.999	y = –133 + 19.4 x	Functional	0.999
	15÷23	0.556	y = 294.7 – 8.9 x	Direct, moderate	0.310
Light, wheat malt	12÷15	0.959	y = 19.8 + 38.7 x	Direct, high	0.919
	16÷20	0.557	y = 225.5 – 2.1 x	Direct, moderate	0.310

Significance level ≤ 0.05
x – type of beer; y – total polyphenols and catechins

Table 4 Analysis of correlation and regression between beer parameters and raw material

Component	Correlation coefficient (r)	Equation of dependance	Correlation according to Chaddock scale	Determination coefficient
Thiol-containing Proteins	0.920	y = –9.8 + 1.9 x	Direct, high	0.846
Catechins	0.896	y = –4.0 + 0.8 x	Direct, high	0.803
β-glucan	0.708	y = 19.5 + 9.8 x	Direct, high	0.501

*Significance level ≤ 0.05
x – solids in initial wort; y – component amoun

weight nitrogenous compounds on colored compounds. Similar conclusions were obtained by Castro *et al.* and Filipowska *et al.* [26, 35]. Partial correlation coefficients (Fig. 4) were based on the changes in the pair correlation of the corresponding features (Y and X_i), provided they experienced no effect from other factors (X_j). This aspect demonstrated much deeper dependencies of the analyzed indicators. The change in the content of soluble nitrogen was confirmed by the conclusion about the correlation with the color (type) of beer, as well as correlation coefficients YX_3, YX_5, and X_5. The experiment confirmed the hypothesis about the relationship of nitrogenous fractions of nitrogenous substances with polyphenolic and non-starch compounds. X_2, X_4, and Y also appeared to correlate, which means that polyphenolic compounds affected soluble nitrogen fraction. Polyphenols transformed when the parameters of young beer changed during fermentation while pH became more acidic, oxygen dissolved, carbon dioxide accumulated, etc.

The calculations represented in Figs. 3 and 4 resulted in the following multiple regression equation (2):

$$Y = 117.2991 - 33.1413 \cdot X_1 + 15.1575 \cdot X_2 + \\ + 34.8177 \cdot X_3 + 2.6063 \cdot X_4 + 7.7755 \cdot X_5 \quad (2)$$

Color or type of beer (X_3) was the most significant parameter in the regression equation. This result confirmed our previous conclusion that the fraction distribution of biomolecules depended on the type of beer (Fig. 2). The overall coefficient of multiple correlation R equaled 0.9073, while the multiple determination coefficient R^2 equaled 0.82. The difference indicates that the change in the content of soluble nitrogen depended the abovementioned parameters by 82%.

The study of the protein fractionation could be used to determine the accompanying groups of organic molecules. The acidic extraction regime of biomolecules was quite sparing. Different conditions, e.g., alkaline pH, organic polar solvents, etc., disrupt the equilibrium of nitrogenous substances, polyphenols, and other compounds. As they oxidize, their amount in equilibrium systems cannot be determined [36, 37].

The behavior of organic compounds in the colloidal system of beer revealed a strong correlation between the technological conditions and the low amount of *β*-glucan, polyphenols, and soluble nitrogen. In particular, thermal or adsorption de-alcoholization had a great impact on the abovementioned substances, which is consistent with data obtained Muller *et al.* and Yassue-Cordeiro *et al.* [23, 24].

The distribution of biomolecules by types of beer also revealed an obvious connection between the type of beer and the biochemical composition of the raw materials (barley or wheat malt), production technology, and the amount of mashed grain (Table 1). These results are consistent with other publications [26–30].

	Soluble nitrogen content, mg/L (Y)	Raw materials content, % (X_1)	Alcohol content, % (X_2)	Beer type (color, EBC) (X_3)	Polyphenols content, mg/L (X_4)	β-glucan content, mg/L (X_5)
Y	1	0.33**	0.35	0.74	0.49	0.57
X_1	–	1	0.956***	0.02*	0.79	0.42
X_2	–	–	1	0.13	0.864	0.30
X_3	–	–	–	1	0.42	0.10
X_4	–	–	–	–	1	0.12
X_5	–	–	–	–	–	1

* – weak bond strength; ** – moderate connection; *** – strong bond

Figure 3 Correlation coefficients of beer parameters

	YX_1	YX_2	YX_3	YX_4	YX_5
Y	–	–	–	–	–
X_1	–	0.156*	0.777***	0.395	0.501
X_2	–0.0502	–	0.748	0.381	0.518
X_3	0.462	0.383	–	0.287	0.740
X_4	–0.112	–0.148	0.677**	–	0.587
X_5	0.117	0.239	0.836	0.512	–
	X_1X_2	X_1X_3	X_1X_4	X_1X_5	X_2X_3
Y	0.952	–0.348	0.769	0.302	–0.204
X_1	–	–	–	–	0.395
X_2	–	–0.376	–0.229	0.500	–
X_3	0.963	–	0.865	0.420	–
X_4	0.885	–0.566	–	0.540	–0.500
X_5	0.961	–0.0229	0.825	–	0.111
	X_2X_4	X_2X_5	X_3X_4	X_3X_5	X_4X_5
Y	0.847	0.121	0.102	–0.583	–0.218
X_1	0.594	–0.410	0.663	0.098	–0.390
X_2	–	–	0.609	0.0612	–0.282
X_3	0.898	0.285	–	–	0.085
X_4	–	0.384	–	0.053	–
X_5	0.874	–	0.413	–	–

* – weak bond strength; ** – moderate connection; *** – strong bond

Figure 4 Pair correlation coefficients of beer parameters

The quantitative assessment of organic compounds and their biochemical properties resulted in the hypothesis about the structural character of nitrogenous substances in the colloidal system of beer. This experiment also made it possible to trace the changes in polyphenols, carbohydrates, and other compounds relative to the fraction distribution of nitrogenous compounds [38].

The results of nitrogenous fractionation (Fig. 2) showed its obvious correlation with the beer type. The high molecular weight fraction of soluble nitrogen (40÷100 kDa) varied in the range of 7÷15%, depending on the Brix, °P. The higher was the solids content, the lower was the amount of the high molecular weight fraction of nitrogenous compounds. High-molecular fractions of nitrogenous substances are associated with the palate fullness, which is most typical for light beers with low density [14, 39]. In the samples where the content of extractive substances of the initial wort was 15÷23%, the palate fullness depended not only on the raw materials but also on the secondary products of yeast metabolism, i.e., secondary alcohols, aldehydes, ketones, ethers, and other carbonyl compounds. Our results were quite similar. The medium molecular

fraction (8÷40 kDa), which is responsible for foam structure, correlated with the density of beer or the proportion of grain products in it, which is consistent with some previously obtained data [40]. In all samples, the low molecular weight fraction of soluble nitrogen (≤ 8 kDa) developed inversely to the density of beer, which is consistent with other studies on sensory perception of beer body [14, 39]. In other words, the low molecular weight fraction of protein compounds depended on the yeast metabolism, i.e., the enzyme systems of the strain.

Thiol groups of nitrogenous substances are responsible for foam and palate fullness. Their distribution proved to depend on the grain raw material – barley or wheat malt. Thus, light barley-malt beer contained the maximum of thiol groups in the medium molecular weight fraction, dark barley-malt beer – in the low molecular weight fraction, and wheat-malt beer – in the high molecular weight fraction. This finding indicates a great effect of the type of grain on beer quality.

The fraction distribution of non-starch β-glucan depended on the type of malt. In light beers, this non-starch polyaccharide was mostly represented in high- and medium-molecular fractions of nitrogenous substances (Fig. 2). In dark beers, up to 63% of β-glucan molecules concentrated in low molecular weight fractions of nitrogenous compounds, which means they linked to peptides through hydrogen bonds [12]. Probably, this fact can be explained by the competitive distribution of catechins and their bonding with nitrogenous biomolecules in high and medium molecular weight fractions of dark beer (Fig. 2).

The correlation analysis revealed a close and logical relationship between catechins and total polyphenols (Table 3) in different types of beer. The amount of polyphenols depended on the density of the initial wort, as well as on the increase in the alcohol content, which stabilized polyphenolic compounds [33].

The analysis of correlation and regression (Figs. 3 and 4) showed the strong impact of the raw material factor (light, dark barley, and wheat malt) on the content of alcohol and polyphenols. This finding was consistent with the previously obtained research results (Tables 1 and 2) [32, 33].

The statistical analysis revealed a correlation between the color (type) of beer and the amount of nitrogenous compounds in terms of colloidal structure (Fig. 3). This correlation is associated with the technology of coloring malts and the degree of dissolution of malt endosperm during the hydrolysis that occurs during barley germination [33].

Therefore, the experimental part of the research confirmed the hypothesis that fractionation of nitrogenous compounds can be conducted by the method specified in *Study Objects and Methods*. Fractions of soluble nitrogen and polyphenolic compounds demonstrated a close correlation under various beer production technologies. This relation can be illustrated by a multiple correlation equation (2), in which the color (type) of beer is the most significant parameter.

CONCLUSION

The present research featured the fractionation of organic compounds in various beers. It established the dependences and factors affecting the distribution of nitrogenous compounds in the colloidal system of beer, as well as the relationship between polyphenolic and non-starch biomolecules. The study also revealed the relationship between the fractional composition of beer and such parameters as contents of solids in the initial wort, raw materials, alcohol, color, etc.

CONTRIBUTION

I.N. Gribkova designed the research, collected, analyzed, and interpreted the data. M.N. Eliseev designed the article, developed the concept, and interpreted the data. M.A. Zakharov and V.A. Zakharova collected and analyzed the data. O.A. Kosareva edited and proofread the manuscript.

CONFLICT OF INTEREST

The authors declare that there is no conflict of interests regarding the publication of this article.

REFERENCES

1. Humia BV, Santos KS, Barbosa AM, Sawata M, Mendonça MC, Padilha FF. Beer molecules and its sensory and biological properties: A review. Molecules. 2019;24(8). https://doi.org/10.3390/molecules24081568
2. Wannenmacher J, Gastl M, Becker T. Phenolic substances in beer: Structural diversity, reactive potential and relevance for brewing process and beer quality. Comprehensive Reviews in Food Science and Food Safety. 2018;17(4):953–988. https://doi.org/10.1111/1541-4337.12352
3. Pandin C, Darsonval M, Mayeur C, Le Coq D, Aymerich S, Briandet R. Biofilm formation and synthesis of antimicrobial compounds by the biocontrol agent *Bacillus velezensis* QST713 in an *Agaricus bisporus* compost micromodel. Applied and Environmental Microbiology. 2019;85(12). https://doi.org/10.1128/AEM.00327-19
4. Lukinac J, Mastanjevic K, Mastanjevic K, Nakov G, Jukic M. Computer vision method in beer quality evaluation – a review. Beverages. 2019;5(2). https://doi.org/10.3390/beverages5020038

5. Kemp B, Condé B, Jégou S, Howell K, Vasserot Y, Marchal R. Chemical compounds and mechanisms involved in the formation and stabilization of foam in sparkling wines. Critical Reviews in Food Science and Nutrition. 2018;59(13):2072–2094. https://doi.org/10.1080/10408398.2018.1437535
6. Gonzalez Viejo C, Fuentes S, Torrico D, Howell K, Dunshea FR. Assessment of beer quality based on foamability and chemical composition using computer vision algorithms, near infrared spectroscopy and machine learning algorithms. Journal of the Science of Food and Agriculture. 2018;98(2):618–627. https://doi.org/10.1002/jsfa.8506
7. Nyarko EK, Glavaš H, Habschied K, Mastanjević K. Determination of foam stability in lager beers using digital image analysis of images obtained using RGB and 3D cameras. Fermentation. 2021;7(2). https://doi.org/10.3390/fermentation7020046
8. Moraes AH, Asam C, Almeida FCL, Wallner M, Ferreira F, Valente AP. Structural basis for cross-reactivity and conformation fluctuation of the major beech pollen allergen Fag s 1. Scientific Reports. 2018;8(1). https://doi.org/10.1038/s41598-018-28358-1
9. Kerr ED, Caboche CH, Schulz BL. Posttranslational modifications drive protein stability to control the dynamic beer brewing proteome. Molecular and Cellular Proteomics. 2019;18(9):1721–1731. https://doi.org/10.1074/mcp.RA119.001526
10. Liger-Belair G, Cilindre C. How many CO_2 bubbles in a glass of beer. ACS Omega. 2021;6(14):9672–9679. https://doi.org/10.1021/acsomega.1c00256
11. Wang Y, Ye L. Haze in beer: Its formation and alleviating strategies, from a protein-polyphenol complex angle. Foods. 2021;10(12). https://doi.org/10.3390/foods10123114
12. Zheng Y, Du J, Li M. Haze-active protein and turbidity in commercial barley and wheat beers at different storage temperatures. International Food Research Journal. 2020;27(2):295–307.
13. Goldman AR, Beer LA, Tang H-Y, Hembach P, Zayas-Bazan D, Speicher DW. Proteome analysis using gel-LC-MS/MS. Current Protocols in Protein Science. 2019;96(1). https://doi.org/10.1002/cpps.93
14. Krebs G, Müller M, Becker T, Gastl M. Characterization of the macromolecular and sensory profile of non-alcoholic beers produced with various methods. Food Research International. 2019;116:508–517. https://doi.org/10.1016/j.foodres.2018.08.067
15. Loskutov IG, Polonsky VI. Content of β-glucans in oat grain as a perspective direction of breeding for health products and fodder. Agricultural Biology. 2017;52(4):646–657. (In Russ.). https://doi.org/10.15389/agrobiology.2017.4.646eng
16. Habschied K, Lalic A, Horvat D, Mastanjevic K, Lukinac J, Jukic M, *et al.* β-glucan degradation during malting of different purpose barley varieties. Fermentation. 2020;6(1). https://doi.org/10.3390/fermentation6010021
17. Goiris K, Jaskula-Goiris B, Syryn E, Van Opstaele F, De Rouck G, Aerts G, *et al.* The flavoring potential of hop polyphenols in beer. Journal of the American Society of Brewing Chemists. 2014;72(2):135–142. https://doi.org/10.1094/ASBCJ-2014-0327-01
18. Ofoedu CE, Akosim CQ, Iwouno JO, Obi CD, Shorstkii I, Okpala CO. Characteristic changes in malt, wort, and beer produced from different Nigerian rice varieties as influenced by varying malting conditions. PeerJ. 2021;9. https://doi.org/10.7717/peerj.10968
19. Dvorakova M, Hulin P, Karabin M, Dostálek P. Determination of polyphenols in beer by an effective method based on solid-phase extraction and high performance liquid chromatography with diode-array detection. Czech Journal of Food Sciences. 2007;25(4):182–188. https://doi.org/10.17221/690-CJFS
20. Gottumukkala RVSS, Nadimpalli N, Sukala K, Subbaraju GV. Determination of catechin and epicatechin content in chocolates by high-performance liquid chromatography. International Scholarly Research Notices. 2014;2014. https://doi.org/10.1155/2014/628196
21. Wu M, Cao Y, Lei S, Liu Y, Wang J, Hu J, *et al.* Protein structure and sulfhydryl group changes affected by protein gel properties: process of thermal-induced gel formation of myofibrillar protein. International Journal of Food Properties. 2019;22(1):1834–1847. https://doi.org/10.1080/10942912.2019.1656231
22. Huismann M, Gormley F, Dzait D, Speers RA, Maskell DL. Unfilterable beer haze Part I: The investigation of an India pale ale haze. Journal of the American Society of Brewing Chemists. 2021;80(1):17–25. https://doi.org/10.1080/03610470.2021.1937460
23. Muller C, Neves LE, Gomez L, Guimaraes M, Ghesti G. Processes for alcohol-free beer production: A review. Food Science and Technology. 2020;40(2):273–281. https://doi.org/10.1590/fst.32318
24. Yassue-Cordeiro PH, Zandonai CH, Genesi BP, Lopes PS, Sanchez-Lopez E, Garcia ML, *et al.* Development of chitosan/silver sulfadiazine/zeolite composite films for wound dressing. Pharmaceutics. 2019;11(10). https://doi.org/10.3390/pharmaceutics11100535

25. Zambrzycka-Szelewa E, Nalewajko-Sieliwoniuk E, Zaremba M, Bajguz A, Godlewska-Żyłkiewicz B. The mineral profile of Polish beers by fast sequential multielement HR CS FAAS analysis and its correlation with total phenolic content and antioxidant activity by chemometric methods. Molecules. 2020;25(15). https://doi.org/10.3390/molecules25153402
26. Castro LF, Affonso AD, Lehman RM. Impact of specialty malts on wort and beer characteristics. Fermentation. 2021;7(3). https://doi.org/10.3390/fermentation7030137
27. Carvalho DO, Curto AF, Guido LF. Determination of phenolic content in different barley varieties and corresponding malts by liquid chromatography-diode array detection-electrospray ionization tandem mass spectrometry. Antioxidants. 2015;4(3):563–576. https://doi.org/10.3390/antiox4030563
28. Li M, Du J, Zheng Y. Non-starch polysaccharides in wheat beers and barley malt beers: A comparative study. Foods. 2020;9(2). https://doi.org/10.3390/foods9020131
29. Krstanović V, Habschied K, Mastanjević K. Research of malting procedures for winter hard wheat varieties – Part I. Foods. 2021;10(1). https://doi.org/10.3390/foods10010052
30. Maia C, Cunha S, Debyser W, Cook D. Impacts of adjunct incorporation on flavor stability metrics at early stages of beer production. Journal of the American Society of Brewing Chemists. 2021. https://doi.org/10.1080/03610470.2021.1993054
31. Jastrzębska A, Kowalska S, Szłyk E. Determination of free tryptophan in beer samples by capillary isotachophoretic method. Food Analytical Methods. 2020;13(4):850–862. https://doi.org/10.1007/s12161-020-01699-2
32. Boronat A, Soldevila-Domenech N, Rodríguez-Morató J, Martínez-Huélamo M, Lamuela-Raventós RM, de la Torre R. Beer phenolic composition of simple phenols, prenylated flavonoids and alkylresorcinols. Molecules. 2020;25(11). https://doi.org/10.3390/molecules25112582
33. Arczewska M, Kamiński DM, Gieroba B, Gagoś M. Acid-base properties of xanthohumol: A computational and experimental investigation. Journal of Natural Products. 2017;80(12):3194–3202. https://doi.org/10.1021/acs.jnatprod.7b00530
34. Pater A, Zdaniewicz M, Cioch-Skoneczny M, Duliński R. Different methods of mash pH adjustment and its influence on the quality of wort and brewing process performance. Post Techn Przetw Spoż. 2019;1:47–51.
35. Filipowska W, Jaskula-Goiris B, Ditrych M, Bustillo Trueba P, De Rouck G, Aerts G, *et al.* On the contribution of malt quality and the malting process to the formation of beer staling aldehydes: a review. Journal of the Institute of Brewing. 2021;127(2):107–126. https://doi.org/10.1002/jib.644
36. Honda S, Ishida R, Hidaka K, Masuda T. Stability of polyphenols under alkaline conditions and the formation of a xanthine oxidase inhibitor from gallic acid in a solution at pH 7.4. Food Science and Technology Research. 2019;25(1):123–129. https://doi.org/10.3136/fstr.25.123
37. Munir S, Javed M, Hu Y, Liu Y, Xiong Sh. The effect of acidic and alkaline pH on the physico-mechanical properties of surimi-based edible films incorporated with green tea extract. Polymers. 2020;12(10):1–15. https://doi.org/10.3390/polym12102281
38. Feige MJ, Braakman I, Hendershot LM. Disulfide bonds in protein folding and stability. In: Feige MJ, editor. Oxidative folding of proteins: Basic principles, cellular regulation and engineering. Royal Society of Chemistry; 2018. pp. 1–33. https://doi.org/10.1039/9781788013253-00001
39. Gastl M, Kupetz M, Becker T. Determination of cytolytic malt modification – Part II: Impact on wort separation. Journal of the American Society of Brewing Chemists. 2020;79(1):66–74. https://doi.org/10.1080/03610470.2020.1796155
40. Krebs G, Gastl M, Becker T. Chemometric modeling of palate fullness in lager beers. Food Chemistry. 2021;342. https://doi.org/10.1016/j.foodchem.2020.128253

ORCID IDs

Irina N. Gribkova https://orcid.org/0000-0002-4373-5387
Maxim A. Zakharov https://orcid.org/0000-0002-4569-3088
Olga A. Kosareva https://orcid.org/0000-0002-9639-8302
Varvara A. Zakharova https://orcid.org/0000-0003-1862-7410

Foods and Raw Materials. 2022;10(2)

ISSN 2310-9599 (Print)
ISSN 2308-4057 (Online)

Research Article
Open Access

Available online at http://jfrm.ru/en
https://doi.org/10.21603/2308-4057-2022-2-540
https://elibrary.ru/ZNGQOE

Carboxymethyl cellulose and psyllium husk in gluten-free pasta

Siham M.M. Faheid[1], Ibrahim R.S. Rizk[2], Yasser F.M. Kishk[2], Gamal H. Ragab[1], Sayed Mostafa[1,*]

[1] National Research Centre, Giza, Egypt
[2] Ain Shams University, Cairo, Egypt

* e-mail: abnody.sayed@gmail.com

Received 02.01.2022; Revised 18.03.2022; Accepted 05.04.2022; Published online 23.09.2022

Abstract:
Formulating high-quality pasta from wheat-free materials is a technological challenge. We aimed to make gluten-free pasta with carboxymethyl cellulose and psyllium husk and evaluate their effect on the quality of the final product.
Gluten-free pasta was produced from rice flour, white corn flour, potato starch, soy protein isolate, and carboxymethyl cellulose or psyllium husk used as binding agents. Then, we evaluated the effect of these hydrocolloids on the color, texture, cooking quality, and sensory characteristics of the product.
The uncooked gluten-free pasta containing psyllium husk showed significantly higher values of hardness compared to the samples with carboxymethyl cellulose, while the cooked pasta with psyllium husk had a significantly lower nitrogen loss. Also, psyllium husk improved the texture of the cooked gluten-free pasta, providing the highest values of resilience, springiness, and chewiness. Generally, the psyllium husk samples received higher quality values for texture, cooking quality, and sensory parameters, compared to the pasta with carboxymethyl cellulose.
Psyllium husk showed a better ability to bind gluten-free pasta than carboxymethyl cellulose. Consequently, psyllium husk could become a feasible alternative to wheat gluten in producing high-quality gluten-free pasta.

Keywords: Celiac, gluten free pasta, psyllium husk, carboxymethyl cellulose, potato starch, soy protein isolate

Please cite this article in press as: Faheid SMM, Rizk IRS, Kishk YFM, Ragab GH, Mostafa S. Carboxymethyl cellulose and psyllium husk in gluten-free pasta. Foods and Raw Materials. 2022;10(2):329–339. https://doi.org/10.21603/2308-4057-2022-2-540

INTRODUCTION

Functional foods that are consumed as part of a regular diet have the potential to improve health or reduce disease risk. For example, gluten-free foods are particularly useful for celiac patients [1]. Preventive medicine has made significant progress in the previous decade and proved the critical importance of nutrition in avoiding diseases, particularly those related to diet [2].

Celiac disease is a chronic inflammatory autoimmune disease of the small intestine mucosa triggered by the consumption of gluten proteins [3]. It is characterized by a lifelong intolerance to gluten, specifically the prolamin portion of wheat (gliadin), rye (secalin), and barley (hordein) [4].

Today, 1% of the world's population has celiac disease [5]. A life-long rigorous gluten-free diet is currently the only treatment available for celiac patients. It improves the quality of life, prevents refractory celiac disease, and alleviates symptoms [6]. In the long run, this diet also benefits patients with previously unexplained persistent watery diarrhea or dominating bloating symptoms who satisfy the criteria for functional bowel disorders [7]. Thus, gluten-free food production must be prioritized to meet the needs of people with celiac disease [8].

Gluten-free pasta is one of the options for people with celiac disease caused by their inability to digest gluten adequately [9]. Gluten-intolerant people, who are becoming more common in society, will prefer this product to gluten-containing pasta [10].

Pasta is generally regarded as a classic food product that is frequently consumed due to its sensory qualities, as well as convenience and ease of transportation, cooking, handling, and storage. In addition, pasta has grown popular due to its nutritional qualities that

are linked to a low glycemic index. In short-term human intervention studies, low-glycemic-index foods reduced appetite and increased fullness [11]. However, people with celiac disease prefer gluten-free pasta for health reasons [12].

Rice flour has been included in gluten-free product formulations to give the batter structure and nutritional value [13]. It is a primary ingredient in pasta production [14]. Furthermore, the use of rice flour is appealing because of its low salt content and high digestibility [15].

Hydrocolloids are commonly used as thickening agents that increase dough viscosity and bind water to improve texture, volume, and final quality. In addition to their advantages for the technological properties of gluten-free products, hydrocolloids may impact the final product's glycemic index [16]. Particularly, fiber increases satiety after eating and reduces the glycemic index of food [17]. As a result, hydrocolloids such as psyllium husk are particularly crucial materials for gluten-free flour [18].

In addition, using psyllium in cooking may help celiacs live longer by allowing them to eat fiber with regular meals rather than separately as a supplement, which may not be as tasty [19]. On the other hand, the consumption of soybean food or fortified foods has recently increased due to its benefits for human nutrition and health [20].

Gluten-free pasta is more expensive and it is often brittle and pale compared to wheat flour pasta [21]. Therefore, we aimed to produce high-quality gluten-free pasta from various formulas fortified with soy protein isolate and two types of hydrocolloids (psyllium husk or carboxymethyl cellulose), as well as to evaluate the physicochemical and sensory characteristics of the final product.

STUDY OBJECTS AND METHODS

Our study involved the production and evaluation of gluten-free pasta made from white corn flour, rice flour, soy protein isolate, psyllium husk, and carboxymethyl cellulose.

Materials. Wheat flour with 72% extraction (11.31% protein, 0.95% protein, 0.57% ash, 0.66% fiber, and 86.51% nitrogen-free extract) was obtained from Amoun Milling Company (Giza, Egypt). Rice flour (7.16% protein, 1.50% protein, 0.57% ash, 1.21% fiber, and 89.56% nitrogen-free extract) and white corn flour (9.76% protein, 4.24% protein, 1.27% ash, 2.94% fiber, and 81.79% nitrogen-free extract) were obtained from the local market (Giza, Egypt). Soy protein isolate (87.74% protein, 0.43% protein, 2.87% ash, 0.29% fiber, and 8.67% nitrogen-free extract) was obtained from American Food Chemicals. Potato starch (0.16% protein, 0.17% protein, 0.03% ash, 0.01% fiber, and 99.63% nitrogen-free extract) was obtained from Emsland Group, Germany. Carboxymethyl cellulose was obtained from Sigma Company. Psyllium husk powder (*Plantago psyllium* L.) was obtained from Now Foods, USA. All the chemicals used in the estimation and analysis were of analytical grade.

Methods.

Technological methods.

Preparation of composite flour. Wheat flour (72% ext.) pasta was used as a control sample. The experimental samples, in addition to gluten-free flours, contained soy protein isolate and psyllium husk or carboxymethyl cellulose, with varying levels of white corn flour, rice flour, and potato starch (Table 1). Individual flour combinations were homogenized, sealed in polyethylene bags, and stored at –18°C until needed.

Pasta dough preparation. Pasta was produced according to Collins and Pangloli with some modifications [22]. All dry ingredients were sieved through a 100-mesh sieve, combined, and mixed to produce a homogenized mixture. Then, the mixture was placed in a mixing bowl and mixed until the dough formed (31 ± 1% of tap water). The dough was shaped into a ball, covered with a plastic wrap, and allowed to rest for 30 min. Then, it was hand-kneaded for 1 min, divided into 100-g portions, and shaped in a cylindrical

Table 1 Pasta formulas

Samples	Raw materials, g						
	Wheat flour	White corn flour	Rice flour	Potato starch	Soy protein isolate	Psyllium husk	Carboxymethyl cellulose
Control	100.00	–	–	–	–	–	–
A	–	45.0	45.0	–	10	2.5	–
B	–	37.5	37.5	15.0	10	2.5	–
C	–	30.0	30.0	30.0	10	2.5	–
D	–	22.5	22.5	45.0	10	2.5	–
E	–	15.0	15.0	60.0	10	2.5	–
F	–	45.0	45.0	–	10	–	2.5
G	–	37.5	37.5	15.0	10	–	2.5
H	–	30.0	30.0	30.0	10	–	2.5
I	–	22.5	22.5	45.0	10	–	2.5
J	–	15.0	15.0	60.0	10	–	2.5

form by using a pasta machine without vacuum (Philips Pasta Maker HR 2357/05, Italy).

Pasta drying process. In line with Kishk *et al*., the pasta samples were air-dried at 23–25°C for 4 h in a room equipped with a fan [23]. After drying in the open air, the samples were placed in a cabinet dehydrator and dried at 70°C to a moisture level of about 12%. After cooling to room temperature (25 ± 2°C), the samples were placed in plastic bags, sealed, and stored at 12–14°C until analysis.

Analytical methods.

Color determination. The color of the samples was measured according to Humter by using a Hunter Lab colorimeter [24]. *L**, *a**, and *b** parameters were measured by a spectro-colorimeter (Tristimulus Color Machine) with a CIELAB color scale (Hunter Lab Scan XE-Reston VA, USA) and the reflection mode. The instrument was standardized with white tiles (Hunter Lab Color Standard (LX No.16379), X = 72.26, Y = 81.94, and Z = 88.14 (L^* = 92.46, a^* = –0.86; b^* = –0.16)). The instrument (65°/0° geometry; D25 optical sensor; 10° observer) was calibrated by using black and white reference tiles. The color values were expressed as lightness to darkness for *L**, redness to greenness for *a**, and yellowness to blueness for *b**.

Physical properties of pasta. Pasta cooking quality was determined according to the method approved by the American Association of Cereal Chemists [25]. Optimum cooking time was the time required for the opaque core of the pasta to disappear when squeezed gently between two glass plates after cooking. Pasta pieces of 25 g were cooked for optimum time in a beaker with 300 mL of tap water, rinsed in cold water, drained for 15 min, and weighed. The percentage of increased weight was calculated as a cooking yield.

The content of solids in the cooking water was determined by drying at 105°C overnight. The cooking loss was expressed as a percentage between the solid weight and the initial dry matter. To calculate the swelling index, we divided the difference between the weight of cooked and uncooked pasta by the weight of uncooked pasta. The nitrogen loss was determined according to the Kjeldahl method approved by the American Association of Cereal Chemists by using conversion factor of 5.7 [25].

Texture profile analysis of pasta. The texture of the pasta samples (hardness, springiness, cohesiveness, chewiness, gumminess, and resilience) was determined by Texture Profiles Analysis (TPA) using a CT3™ Texture Analyzer (Brookfield) according to Boume [26]. The Test Works software was installed and an appropriate test was selected for the TPA analysis: a 2.50 mm/s test speed, a 10 000 g load cell, two cycles for cooked pasta, one cycle for uncooked pasta, and a 10 mm depth. The parameters, such as length, diameter, speed, compression percentage, and the number of cycles, were entered as input data before starting the compression. Then the load cell started to slowly move downwards, compressing the sample, with a 5-s wait between the first and the second compression cycles. After two cycles, the compression stopped automatically.

Sensory evaluation of pasta. The sensory attributes of the gluten-free pasta were evaluated by ten panelists from the Department of Food Technology, National Research Centre, according to the method reported by Inglett *et al.* [27]. Color, texture, flavor, and overall acceptability were evaluated on the 9-point hedonic scale. The scale was verbally anchored with nine categories, namely: like extremely, like very much, like moderately, like slightly, neither like nor dislike, dislike slightly, dislike moderately, dislike very much, and dislike extremely. The quality attributes of the experimental samples were compared with those of the control sample (100% wheat flour).

Statistical analysis. The results were analyzed statistically by performing analysis of variance (ANOVA) and Duncan's multiple range test in the SPSS statistical package (Version 9.05). The least significant difference was chosen to determine significant differences among various formulations. Differences were considered significant at $P \leq 0.05$.

RESULTS AND DISCUSSION

We studied effects of psyllium husk (2.5%) and carboxymethyl cellulose (2.5%) on gluten-free pasta with different proportions of white corn flour, rice flour, potato starch, and a fixed amount of soy protein isolate (10%).

Color parameters of gluten-free uncooked pasta. The color parameters (*L**, *a**, *b**, and color intensity) of the uncooked pasta samples are presented in Table 2. As we can see, the samples containing potato starch (60%) and carboxymethyl cellulose or psyllium husk (samples J and E, respectively) recorded the highest values of *L** color (more lightness) with significant differences between them or in comparison with the other samples ($P \leq 0.05$).

We also found that lightness was affected by the amount of potato starch in the samples: the more potato starch, the lighter the samples. The control sample had the lowest value of lightness. The highest values of redness (*a** value) were observed in the control sample (3.22) and the sample with carboxymethyl cellulose and without potato starch (2.52). However, there were no significant differences in redness among the rest of the samples.

As for yellowness (*b** values), the lowest value (13.20) was recorded in the control sample, while the highest values (16.70 and 15.93) were observed in the samples without potato statrch (samples A and F). There were no significant differences in yellowness among the gluten-free samples with soy protein isolate. However, the highest value of color intensity was found in the sample containing 60% potato starch + carboxymethyl cellulose, in contrast to the control sample with the lowest value. These results were consistent with those of Bolarinwa and Oyesiji who reported that gluten-free

Table 2 Color parameters of uncooked wheat flour pasta and gluten-free pasta with psyllium husk or carboxymethyl cellulose

Samples	Color parameters			
	*L** (lightens)	*a** (redness)	*b** (yellowness)	Color intensity
Control	61.73^{i}	3.22^{a}	13.20^{d}	1.510^{d}
Gluten-free pasta with psyllium husk:				
A (0% of potato starch)	68.86^{h}	1.77^{c}	15.93^{ab}	1.530^{c}
B (15%)	70.36^{g}	1.67^{cd}	15.30^{bc}	1.530^{c}
C (30%)	71.90^{f}	1.57^{cd}	14.73^{bc}	1.540^{b}
D (45%)	73.96^{d}	1.49^{cd}	14.33^{c}	1.540^{b}
E (60%)	75.70^{b}	1.46^{cd}	14.26^{c}	1.540^{b}
Gluten-free pasta with carboxymethyl cellulose:				
F (0% of potato starch)	69.50^{h}	2.52^{b}	16.70^{a}	1.530^{c}
G (15%)	70.86^{g}	1.71^{cd}	15.60^{ab}	1.536^{b}
H (30%)	72.80^{e}	1.68^{cd}	15.23^{bc}	1.540^{b}
I (45%)	74.86^{c}	1.36^{cd}	15.16^{bc}	1.540^{b}
J (60%)	77.50^{a}	1.29^{d}	15.06^{bc}	1.550^{a}

Means in the same column with different letters are significantly different ($P \leq 0.05$)

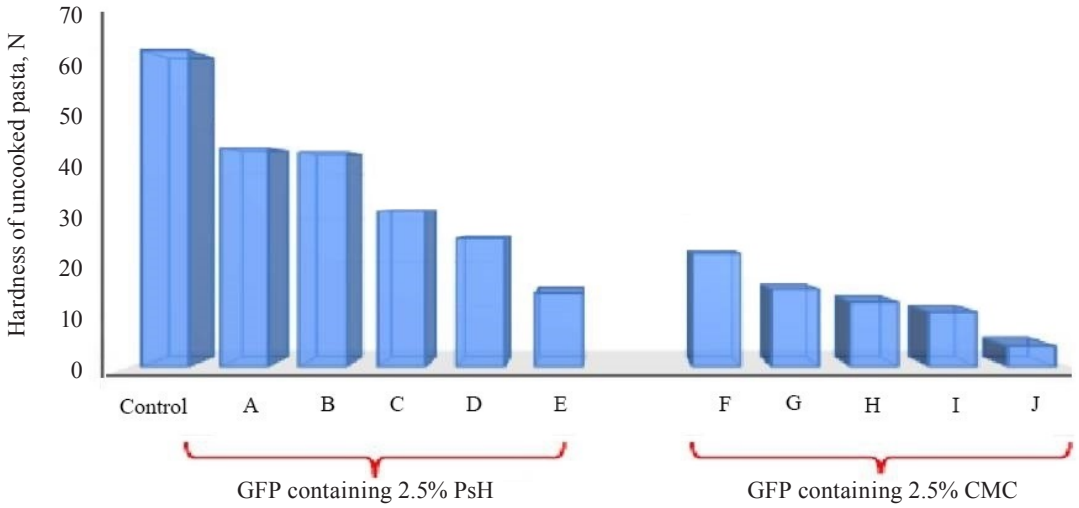

Figure 1 Texture profile analysis of uncooked pasta: Control – 100 % wheat flour pasta; A, F – no potato starch; B, G – 15% of potato starch; C, H – 30% of potato starch; D, I – 45% of potato starch; E, J – 60% of potato starch

pasta with rice and corn flour had higher lightness and lower redness compared to wheat flour pasta [28].

The hardness of gluten-free uncooked pasta. Hardness (N) is related to the strength of structure under compression during the first compression cycle. It is a force required to attain a given deformation. The hardness of uncooked pasta was determined by the texture profile analyzer (Fig. 1).

As can be seen, the control pasta showed the highest value of hardness (65.13) compared to the gluten-free samples, which reflected the strength of structure provided by the gluten network.

However, there was a clear difference in hardness between the samples with psyllium husk and those with carboxymethyl cellulose. Particularly, the highest hardness (44.97) was recorded in the psyllium husk sample without potato starch (sample A) compared to the carboxymethyl cellulose samples without starch (sample F) (23.30).

In general, the psyllium husk pasta had hardness values in the range of 44.97 to 15.16, whereas the carboxymethyl cellulose samples had this parameter ranging from 23.30 to 4.26. Thus, potato starch played an important role in the hardness of uncooked pasta: higher contents of potato starch led to lower hardness. These results were confirmed by Kang *et al.* who found that the hardness of gluten-free pasta containing potato starch was lower than that of wheat flour pasta [29].

Color parameters of gluten-free cooked pasta. The color parameters of the cooked pasta samples are presented in Table 3 and Fig. 2. As we can see, the samples containing 60% potato starch and

Table 3 Color parameters of cooked wheat flour pasta and gluten-free pasta with psyllium husk or carboxymethyl cellulose

Samples	Color parameters			
	*L** (lightens)	*a** (redness)	*b** (yellowness)	Color intensity
Control	52.70^{c}	2.80^{ab}	19.20^{b}	1.50^{b}
Gluten-free pasta with psyllium husk:				
A (0% of potato starch)	57.84^{b}	3.03^{a}	21.23^{a}	1.51^{a}
B (15%)	57.94^{b}	2.90^{ab}	20.40^{ab}	1.51^{a}
C (30%)	58.57^{b}	2.83^{ab}	20.20^{ab}	1.51^{a}
D (45%)	58.80^{b}	2.73^{b}	19.46^{b}	1.51^{a}
E (60%)	60.70^{a}	2.33^{c}	16.40^{c}	1.51^{a}
Gluten-free pasta with carboxymethyl cellulose:				
F (0% of potato starch)	57.90^{b}	3.03^{a}	21.23^{a}	1.51^{a}
G (15%)	58.50^{b}	2.90^{ab}	20.33^{ab}	1.51^{a}
H (30%)	58.80^{b}	2.76^{b}	19.53^{b}	1.51^{a}
I (45%)	58.90^{b}	2.73^{b}	19.40^{b}	1.51^{a}
J (60%)	61.66^{a}	2.10^{d}	14.76^{d}	1.51^{a}

Means in the same column with different letters are significantly different ($P \leq 0.05$)

carboxymethyl cellulose or psyllium husk (samples J and E) recorded the highest values of *L** (more lightness), with no significant difference between them. However, they showed significant differences when compared to the other samples ($P \leq 0.05$). Consequently, lightness was affected by the content of potato starch in the samples, with higher contents leading to lighter color. The control sample had the lowest value of lightness.

The highest redness (*a**) values were recorded in the samples containing 45% white corn flour, 45% rice flour, 10% soy protein isolate, and 2.5% carboxymethyl cellulose or 2.5% psyllium husk, with no significant differences. The lowest redness was observed in the samples containing 60% potato starch with 2.5% carboxymethyl cellulose or 2.5% psyllium husk. However, the lowest value of color intensity was significantly recorded in the control sample, with no significant differences between the gluten-free samples.

Our results were in agreement with those of Yaseen and Shouk [30]. The authors found that pasta with corn starch had higher lightness and lower redness values compared to the control (100% wheat flour). Similarly, Mohammadi *et al.* reported that increased amounts of rice flour in gluten-free products led to higher lightness of the final product [31].

The quality of gluten-free cooked pasta. The cooking time and quality parameters of the pasta samples prepared with hydrocolloids (carboxymethyl cellulose and psyllium husk) are presented in Table 4. As can be seen, the optimum cooking time was highest (13.16 min) for the control sample ($P \leq 0.05$) compared to the other samples except for the samples without potato starch (A and F). However, the optimum cooking time gradually decreased with higher contents of potato starch. Also, potato starch had a positive effect on the cooking yield, whether the samples contained carboxymethyl cellulose or psyllium husk as binding agents.

The swelling index of pasta is an indicator of how much water is absorbed by starch and proteins during cooking. It is utilized for the gelatinization of starch and hydration of proteins [32]. According to Table 4, the swelling index was the lowest (142.82) for the control sample and highest (190.60) for the psyllium husk sample with 60% of potato starch (sample E), with significant difference. The swelling index was also high (186.66) for the carboxymethyl cellulose with 60% of starch (sample J).

Cooking loss is defined as the quantity of solids going into water during cooking. It determines the quality of pasta, with compact-textured pasta having a lower cooking loss [33]. According to our results (Table 4), the control sample significantly recorded the lowest value of cooking loss (6.16%). We also found that potato starch had a negative effect on the quality of the gluten-free pasta, i.e., higher contents of potato starch gradually increased cooking loss. However, this negative effect was reduced by adding psyllium husk.

The results also showed a significantly high value of nitrogen loss in the gluten-free samples with carboxymethyl cellulose, compared to the control and the samples with psyllium husk. Moreover, potato starch significantly increased nitrogen loss in the carboxymethyl cellulose samples. In general, nitrogen loss ranged from 12.10 to 40.55% in the samples with carboxymethyl cellulose and from 6.50 to 10.20% in the samples with psyllium husk.

In the study by De Arcangelis *et al.*, such hydro-thermal treatments inhibited granule swelling, retarded gelatinization, and increased starch paste stability, having thus enhanced the texture properties and cooking

Table 4 Cooking time and quality parameters of cooked wheat flour pasta and gluten-free pasta with psyllium husk or carboxymethyl cellulose

Samples	Optimum cooking time	Cooking yield	Swelling index	Cooking loss	Nitrogen loss
Control	13.16^{a}	136.93^{g}	142.83^{h}	6.16^{j}	4.00^{h}
Gluten-free pasta with psyllium husk:					
A (0% of potato starch)	12.83^{ab}	144.80^{f}	159.43^{f}	6.83^{i}	6.50^{gh}
B (15%)	12.50^{b}	152.60^{e}	171.46^{e}	7.36^{h}	6.80^{g}
C (30%)	12.00^{c}	160.40^{d}	178.43^{d}	8.30^{g}	7.30^{g}
D (45%)	11.33^{d}	175.40^{b}	182.80^{c}	8.90^{f}	9.00^{fg}
E (60%)	10.16^{e}	183.80^{a}	190.60^{a}	9.80^{e}	10.20^{ef}
Gluten-free pasta with carboxymethyl cellulose:					
F (0% of potato starch)	13.00^{a}	120.80^{h}	150.00^{g}	9.70^{e}	12.10^{e}
G (15%)	12.00^{c}	132.80^{g}	157.53^{f}	11.43^{d}	17.30d
H (30%)	11.33^{d}	142.40^{f}	169.33^{e}	13.30^{c}	21.60^{c}
I (45%)	10.33^{e}	154.40^{e}	182.93^{c}	15.40^{b}	34.50^{b}
J (60%)	10.00^{e}	166.40^{c}	186.66^{bc}	18.76^{a}	40.55^{a}

Means in the same column with different letters are significantly different ($P \leq 0.05$)

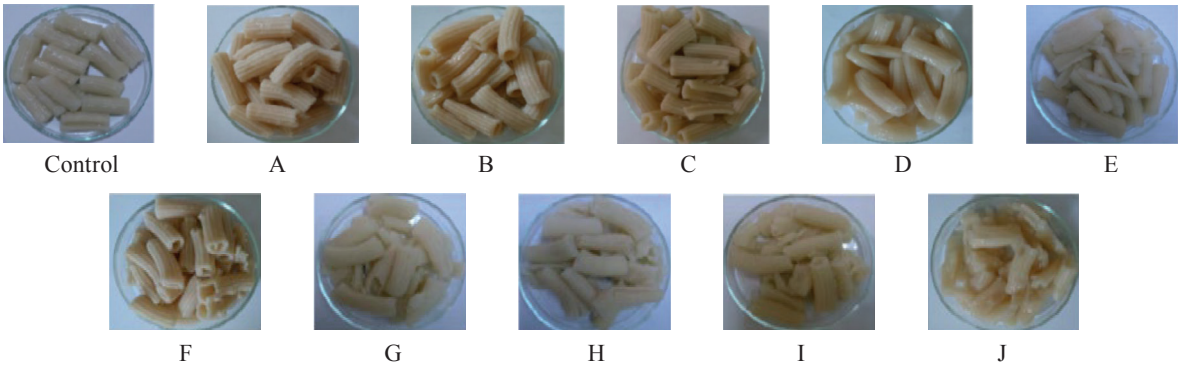

Figure 2 Gluten-free pasta samples: Control – 100% wheat flour; A – psyllium husk without potato starch ; B – psyllium husk + 15% of potato starch; C – psyllium husk + 30% of potato starch; D – psyllium husk + 45% of potato starch; E – psyllium husk + 60% of potato starch; F – carboxymethyl cellulose without potato starch; G – carboxymethyl cellulose + 15% of potato starch; H – carboxymethyl cellulose + 30% of potato starch; I – carboxymethyl cellulose + 45% of potato starch; J – carboxymethyl cellulose + 60% of potato starch

behavior of rice noodles [32]. Further, Khosla *et al.* reported that higher contents of rice flour in gluten-free pasta might increase the optimum cooking time [34].

The texture profile of gluten-free cooked pasta. The textural properties of cooked pasta are an important parameter that determines the overall acceptability by consumers [35]. The results of texture profile analysis of our gluten-free cooked pasta against the control (100% wheat flour) are shown in Table 5.

During the first bite, we obtained hardness, adhesiveness, and resilience values.

Hardness is defined as the maximum load applied to the samples during a compression cycle, corresponding to the peak force [36]. According to Table 5, the control pasta recorded the highest value of cycle 1 hardness (3.96 N) compared to the gluten-free samples. This result was in agreement with Larrosa *et al.* who stated that wheat control pasta showed higher hardness values than all gluten-free tagliatelles, demonstrating the impact of the gluten matrix on tagliatelle texture [37].

In our study, the gluten-free samples with psyllium husk had higher hardness values than those with carboxymethyl cellulose, ranging from 3.31 to 1.76 N and from 1.73 to 0.69 N, respectively. We also found that higher contents of potato starch decreased the hardness values in all gluten-free samples. Similarly, Detchewa *et al.* reported an increase in the hardness of gluten-free spaghetti when hydrocolloids were incorporated [38].

Adhesiveness measures the extent to which the product gets attached to teeth and is considered the most undesirable characteristic of pasta [39]. According to Table 5, the control pasta recorded the lowest value of adhesiveness (0.1 mJ). As for the gluten-free pasta, the samples with psyllium husk had lower

Table 5 Texture profile analysis of cooked pasta under study

Samples	First bite			Second bite				
	Hardness cycle 1, N	Adhesiveness, mJ	Resilience	Hardness cycle 2, N	Cohesiveness	Springiness, mm	Gumminess	Chewiness, mJ
Control	3.96	0.1	0.61	3.74	0.90	4.95	3.56	17.64
Gluten-free pasta with psyllium husk:								
A (0% of potato starch)	3.31	0.2	0.57	3.16	0.75	4.58	2.48	11.37
B (15%)	3.11	0.2	0.53	2.94	0.66	4.33	2.05	8.89
C (30%)	2.33	0.2	0.45	1.93	0.45	4.24	1.05	4.45
D (45%)	1.84	0.3	0.36	1.26	0.42	3.67	0.77	2.84
E (60%)	1.76	0.3	0.32	0.84	0.38	3.34	0.67	2.23
Gluten-free pasta with carboxymethyl cellulose:								
F (0% of potato starch)	1.73	0.3	0.55	1.64	0.83	4.30	1.09	4.69
G (15%)	1.46	0.4	0.36	0.87	0.43	4.04	0.63	2.54
H (30%)	1.44	0.5	0.14	0.72	0.32	3.79	0.46	1.75
I (45%)	1.22	0.6	0.12	0.64	0.05	2.19	0.06	0.13
J (60%)	0.69	0.7	0.10	0.56	0.04	1.80	0.03	0.05

values of adhesiveness (0.2–0.3 mJ) than those with carboxymethyl cellulose (0.3–0.7 mJ).

These results reflect the good quality of the control wheat pasta compared to the gluten-free pasta. They also show that psyllium husk improved the quality of gluten-free pasta compared to the samples with carboxymethyl cellulose. Piwinska *et al.* reported such special qualities of durum wheat pasta as high hardness, low adhesiveness, low cooking loss, and tolerance to overcooking [40].

During the second bite, we obtained hardness, cohesiveness, springiness, gumminess, and chewiness values (Table 5). As we can see, the control had a lower value of hardness (3.74 N) compared to the same sample in cycle 1 (3.96 N), with a decreasing rate of 5.55%. In the gluten-free pasta, the decreasing rate of hardness from cycle 1 to cycle 2 ranged from 4.53 to 52.27% in the samples with psyllium husk and from 5.20 to 47.54% in those with carboxymethyl cellulose. The maximum decrease was recorded in the carboxymethyl cellulose sample with 45% potato starch.

Cohesiveness quantifies the internal resistance of food structure and can be briefly defined as an ability of a material to stick to itself [41]. According to our results, the highest value of cohesiveness (0.90) was recorded in the control sample. Also, quite high (0.75) cohesiveness was in the psyllium husk sample without potato starch (sample A). We also found that cohesiveness values gradually decreased with the increasing contents of potato starch.

Springiness measures elasticity by determining the extent of recovery between the first and the second compression. According to our results, the control sample recorded the highest value of springiness (4.95 mm). In the gluten-free samples with psyllium husk, springiness ranged from 4.58 to 3.34 mm, whilst in those with carboxymethyl cellulose, from 4.30 to 1.80 mm. Also, the control sample recorded the highest values of gumminess and chewiness.

Among the gluten-free samples, those with psyllium husk had higher values of gumminess and chewiness than those with carboxymethyl cellulose. We found that higher contents of potato starch in the gluten-free samples decreased their gumminess and chewiness. These results showed a more positive effect of psyllium husk than carboxymethyl cellulose.

As reported by Udachan and Sahoo, the primary parameters of pasta quality are hardness, springiness, and cohesiveness (they should be higher), whereas the secondary parameters are chewiness and resilience [9]. Generally, our results were in agreement with Anisa *et al.* who stated that gluten-free pasta was characterized by lower hardness, gumminess, chewiness, and springiness, and it had higher adhesiveness than wheat pasta [42].

Sensory evaluation of gluten-free cooked pasta. Sensory evaluation is a unique tool that uses human senses to determine organoleptic characteristics of a food product and the consumer's attitude to it. Therefore, it is a reliable comprehensive test of the final product's quality. Additionally, sensory evaluation provides important reference information to be compared with the results of instrumental or chemical methods [43].

In our study, the cooked gluten-free pasta samples were evaluated on a hedonic scale, with a wheat sample (72% ext.) used as a control (Table 6). We found no significant differences ($P \leq 0.05$) in color between the control sample and those containing 15, 30, 45, and 60% of potato starch and 2.5% psyllium husk or 30, 45, and 60% of carboxymethyl cellulose. There were no significant differences in texture between the control sample and sample B containing 15% potato starch and 2.5% psyllium husk. Sample B had the most optimal

Table 6 Sensory characteristics of cooked wheat flour and gluten-free pasta

Samples	Color	Texture	Flavor	Taste	Appearance	OAA
Control	5.0^{a}	5.0^{a}	5.0^{a}	5.0^{a}	5.0^{a}	5.0^{a}
Gluten-free pasta with psyllium husk:						
A (0% of potato starch)	4.1^{bc}	3.4^{bc}	4.9^{ab}	3.0^{d}	3.8^{c}	4.0^{b}
B (15%)	4.5^{ab}	4.6^{a}	4.9^{ab}	4.0^{b}	4.5^{b}	4.8^{a}
C (30%)	5.1^{a}	3.9^{b}	4.8^{ab}	3.8^{bc}	4.0^{c}	3.7^{bc}
D (45%)	5.0^{a}	3.3^{cd}	4.7^{ab}	3.3^{cd}	3.3^{d}	3.2^{c}
E (60%)	5.0^{a}	3.0^{d}	4.7^{ab}	2.4^{e}	2.6^{ef}	1.9^{e}
Gluten-free pasta with carboxymethyl cellulose:						
F (0% of potato starch)	3.7^{c}	3.7^{bc}	4.8^{ab}	3.3^{cd}	3.3^{d}	3.5^{bc}
G (15%)	4.3^{bc}	3.9^{b}	4.7^{ab}	3.7^{bc}	3.9^{c}	3.6^{bc}
H (30%)	5.0^{a}	3.0^{d}	4.7^{ab}	2.9^{de}	2.7^{e}	2.4^{d}
I (45%)	5.0^{a}	2.4^{e}	4.5^{b}	2.4^{e}	2.2^{f}	1.3^{f}
J (60%)	5.0^{a}	1.4^{f}	4.0^{c}	1.3^{f}	1.2^{g}	1.0^{f}

Means in the same column with different letters are significantly different ($P \leq 0.05$)

content of potato starch among those containing psyllium husk as a binding agent, since increased levels of potato starch (30, 45, and 60%) significantly lowered the scores for texture. Also, psyllium husk had a more positive effect on texture than carboxymethyl cellulose, with the texture scores of 3.00–4.60 and 1.40–3.70, respectively.

As for flavor, there were no significant differences between the control and the gluten-free samples except for two carboxymethyl cellulose samples with 45 and 60% potato starch, respectively. Taste received the highest score (5.0) for the control sample ($P \leq 0.05$) followed by sample B (4.0) containing 15% potato starch and psyllium husk. While the best score for taste among the carboxymethyl cellulose samples was 3.7 for the sample with 15% potato starch, it was significantly different from the control sample but not from sample B.

The best scores for appearance were obtained by the control sample and the gluten-free sample containing psyllium husk and 15% of potato starch and (sample B), with significant differences. However, there were no significant differences between the sample containing psyllium husk and 30% of potato starch (sample C), and the one with carboxymethyl cellulose and 15% of potato starch and (sample G).

Overall acceptability showed no significant differences between the control and the gluten-free sample containing 15% potato starch and psyllium husk. In general, 15% was the most optimal content of potato starch in the samples with both psyllium and carboxymethyl cellulose. On the other hand, the samples with psyllium husk had a better effect on overall acceptability than those with carboxymethyl cellulose, with the scores of 1.90–4.80 and 1.0–3.50, respectively. Our results were consistent with a study by Bolarinwa and Oyesiji, where the acceptability of gluten-free rice-soy pasta was highly ranked for sensory attributes [28]. Additionally, Ribeiro *et al.* stated that incorporating legume flour in rice pasta resulted in acceptable scores for color, taste, flavor, and appearance [44]. Also, Peressini *et al.* reported that psyllium husk had a positive effect on sensory evaluation, improving overall acceptability [45].

CONCLUSION

Based on the overall results, we can conclude that hydrocolloids have an important effect on the physical and sensory characteristics of gluten-free pasta. The experimental samples with psyllium husk used as a binding agent had better texture properties due to an increased hardness of uncooked pasta, compared to the samples with carboxymethyl cellulose. Therefore, the cooked samples with psyllium husk showed better quality parameters such as swelling index, cooking loss, cooking yield, and nitrogen loss, compared to those with carboxymethyl cellulose.

CONTRIBUTION

S.M.M. Faheid was involved in the conceptualization, methodology, investigation, and visualization. I.R.S. Rizk was responsible for visualization, drafting of the manuscript, and supervision. G.H. Ragab took part in the investigation and drafting of the manuscript. Y.F.M. Kishk contributed to the conceptualization and data analysis. S.M. Mostafa was involved in the conceptualization, methodology, and writing the manuscript.

CONFLICT OF INTEREST

The authors declare no conflict of interest.

ACKNOWLEDGMENTS

The authors are grateful to the Food Technology Department, Food Industries and Nutrition Institute, National Research Centre, Egypt for their assistance with the research and for providing the equipment required for measurements.

REFERENCES

1. Butnariu M, Sarac I. Functional food. International Journal of Nutrition. 2019;3(3):7–16. https://doi.org/10.14302/issn.2379-7835.ijn-19-2615
2. Moghadam FH, Khalghani J, Moharramipour S, Gharali B, Mohasses MM. Investigation of the induced antibiosis resistance by zinc element in different cultivars of sugar beet to long snout weevil, *Lixus incanescens* (Col: Curculionidae). Banat's Journal of Biotechnology. 2018;9(17):5–12 https://doi.org/10.7904/2068-4738-IX(17)-5
3. Lebwohl B, Sanders DS, Green, PHR. Coeliac disease. The Lancet. 2018;391(10115):70–81. https://doi.org/10.1016/S0140-6736(17)31796-8
4. Lexhaller B, Colgrave ML, Scherf KA. Characterization and relative quantitation of wheat, rye, and barley gluten protein types by liquid chromatography–tandem mass spectrometry. Frontiers in Plant Science. 2019;10. https://doi.org/10.3389/fpls.2019.01530
5. Weisbrod VM, Silvester JA, Raber C, McMahon J, Coburn SS, Kerzner B. Preparation of gluten-free foods alongside gluten-containing food may not always be as risky for celiac patients as diet guides suggest. Gastroenterology. 2020;158(1):273–275. https://doi.org/10.1053/j.gastro.2019.09.007
6. Caio G, Volta U, Sapone A, Leffler DA, De Giorgio R, Catassi, C, *et al.* Celiac disease: a comprehensive current review. BMC Medicine. 2019;17(1). https://doi.org/10.1186/s12916-019-1380-z
7. Fernández-Bañares F, Arau B, Raga A, Aceituno M, Tristán E, Carrasco A, *et al.* Long-term effect of a gluten-free diet on diarrhea or bloating-predominant functional bowel disease: Role of the "low-grade coeliac score" and the "coeliac lymphogram" in the response rate to the diet. Nutrients. 2021;13(6). https://doi.org/10.3390/nu13061812
8. Remes-Troche JM, Uscanga-Domínguez LF, Aceves-Tavares RG, Calderón de la Barca AM, Carmona-Sánchez RI, Cerda-Contreras E, *et al.* Clinical guidelines on the diagnosis and treatment of celiac disease in Mexico. Revista de Gastroenterología de México. 2018;83(4):434–450. https://doi.org/10.1016/j.rgmx.2018.05.005
9. Udachan IS, Sahoo AK. Effect of hydrocolloids in the development of gluten free brown rice pasta. International Journal of ChemTech Research. 2017;10(6):407–415.
10. Sissons M. Development of novel pasta products with evidence based impacts on health – A review. Foods. 2022;11(1). https://doi.org/10.3390/foods11010123
11. Atkinson FS, Brand-Miller JC, Foster-Powell K, Buyken AE, Goletzke J. International tables of glycemic index and glycemic load values 2021: a systematic review. The American Journal of Clinical Nutrition. 2021;114(5):1625–1632. https://doi.org/10.1093/ajcn/nqab233
12. Levinta A, Mukovozov I, Tsoutsoulas C. Use of a gluten-free diet in schizophrenia: A systematic review. Advances in Nutrition. 2018;9(6):824–832. https://doi.org/10.1093/advances/nmy056
13. Bouasla A, Wojtowicz A, Zidoune MN. Gluten-free precooked rice pasta enriched with legumes flours: Physical properties, texture, sensory attributes and microstructure. LWT – Food Science and Technology. 2017;75:569–577. https://doi.org/10.1016/j.lwt.2016.10.005
14. Bouasla A, Wojtowicz A. Rice-buckwheat gluten-free pasta: Effect of processing parameters on quality characteristics and optimization of extrusion-cooking process. Foods. 2019;8(10). https://doi.org/10.3390/foods8100496
15. Phongthai S, D'Amico S, Schoenlechner R, Homthawornchoo W, Rawdkuen S. Fractionation and antioxidant properties of rice bran protein hydrolysates stimulated by *in vitro* gastrointestinal digestion. Food Chemistry. 2018;240:156–164. https://doi.org/10.1016/j.foodchem.2017.07.080
16. Culetu A, Duta DE, Papageorgiou M, Varzakas T. The role of hydrocolloids in gluten-free bread and pasta; Rheology, characteristics, staling and glycemic index. Foods. 2021;10(12). https://doi.org/10.3390/foods10123121
17. Zhu R, Larsen TM, Fogelholm M, Poppitt SD, Vestentoft PS, Silvestre MP, *et al.* Dose-dependent associations of dietary glycemic index, glycemic load, and fiber with 3-year weight loss maintenance and glycemic status in a high-risk population: a secondary analysis of the diabetes prevention study. PREVIEW. Diabetes Care. 2021;44(7):1672–1681. https://doi.org/10.2337/dc20-3092
18. Herawati H. Hydrocolloids to the effects of gluten free bakery products. Journal of Physics: Conference Series. 2019;1295(1). https://doi.org/10.1088/1742-6596/1295/1/012052
19. Fradinho P, Soares R, Niccolai A, Sousa I, Raymundo A. *Psyllium* husk gel to reinforce structure of gluten-free pasta? LWT. 2020;131. https://doi.org/10.1016/j.lwt.2020.109787

20. Mishra P, Bhatt DK. Development of quality characteristics of dried pasta enriched with soya protein isolate powder. IOSR Journal of Environmental Science, Toxicology and Food Technology. 2017;11(10):1–6.

21. Scarton M, Ribeiro T, Godoy HT, Behrens JH, Campelo PH, Clerici MTPS. Gluten free pasta with natural ingredient of color and carotene source. Research, Society and Development. 2021;10(4). https://doi.org/10.33448/rsd-v10i4.13959

22. Collins JL, Pangloli P. Chemical, physical and sensory attributes of noodles with added sweetpotato and soy flour. Journal of Food Science. 19976;62(3):622–625. https://doi.org/10.1111/j.1365-2621.1997.tb04446.x

23. Kishk YF, Elsheshetawy HE, Mahmoud EAM. Influence of isolated flaxseed mucilage as a non-starch polysaccharide on noodle quality. International Journal of Food Science and Technology. 2011;46(3):661–668. https://doi.org/10.1111/j.1365-2621.2010.02547.x

24. Hunter RS. Photoelectric color difference meter. Journal of the Optical Society of America. 1958;48(12):985–995. https://doi.org/10.1364/JOSA.48.000985

25. Approved method of the American Association of Cereal Chemists. 10th ed. Minnesota: AACC; 2000.

26. Boume M. Food texture and viscosity. Concept and measurement. 2nd. ed. London: Academic press; 2002. pp.257–290.

27. Inglett GE, Peterson SC, Carriere CJ, Maneepun S. Rheological, textural, and sensory properties of Asian noodles containing an oat cereal hydrocolloid. Food Chemistry. 2005;90(1–2):1–8. https://doi.org/10.1016/j.foodchem.2003.08.023

28. Bolarinwa IF, Oyesiji OO. Gluten free rice-soy pasta: proximate composition properties and sensory attributes. Heliyon. 2021;7(1). https://doi.org/10.1016/j.heliyon.2021.e06052

29. Kang J, Lee J, Choi M, Jin Y, Chang D, Chang YH, *et al.* Physicochemical and textural properties of noodles prepared from different potato varieties. Preventive Nutrition and Food Science. 2017;22(3):246–250. https://doi.org/10.3746/pnf.2017.22.3.246

30. Yaseen A, Shouk AE. Low phenylalanine pasta. International Journal of Nutrition and Metabolism. 2011;3(10):128–135.

31. Mohammadi M, Khorshidian N, Yousefi M, Khaneghah AM. Physicochemical, rheological, and sensory properties of gluten-free cookie produced by flour of chestnut, date seed, and modified starch. Journal of Food Quality. 2022;2022. https://doi.org/10.1155/2022/5159084

32. De Arcangelis E, Cuomo F, Trivisonno MC, Marconi E, Messia MC. Gelatinization and pasta making conditions for buckwheat gluten-free pasta. Journal of Cereal Science. 2020;95. https://doi.org/10.1016/j.jcs.2020.103073

33. Espinosa-Solis V, Zamudio-Flores PB, Tirado-Gallegos JM, Ramírez-Mancinas S, Olivas-Orozco GI, Espino-Díaz M, *et al.* Evaluation of cooking quality, nutritional and texture characteristics of pasta added with oat bran and apple flour. Foods. 2019;8(8). https://doi.org/10.3390/foods8080299

34. Khosla R, Rathi N, Gururani P, Upadhyay S, Singh M. Development and physichochemical analysis of gluten free pasta using rice, corn and flaxseeds. International Journal of Recent Scientific Research. 2019;10(05):32300–32305.

35. Ainsa A, Roldan S, Marquina PL, Roncalés P, Beltrán JA, Calanche Morales JB. Quality parameters and technological properties of pasta enriched with a fish by-product: A healthy novel food. Journal of Food Processing and Preservation. 2022;46(2). https://doi.org/10.1111/jfpp.16261

36. Peleg M. The instrumental texture profile analysis revisited. Journal of Texture Studies. 2019;50(5):362–368. https://doi.org/10.1111/jtxs.12392

37. Larrosa V, Lorenzo G, Zaritzky N, Califano, A. Improvement of the texture and quality of cooked gluten-free pasta. LWT. 2016;70:96–103. https://doi.org/10.1016/j.lwt.2016.02.039

38. Detchewa P, Prasajak P, Phungamngoen C, Sriwichai W, Naivikul O, Moongngarm A. Substitution of rice flour with rice protein improved quality of gluten-free rice spaghetti processed using single screw extrusion. LWT. 2021;153. https://doi.org/10.1016/j.lwt.2021.112512

39. Chauhan A, Saxena DC, Singh S. Effect of hydrocolloids on microstructure, texture and quality characteristics of gluten-free pasta. Journal of Food Measurement and Characterization. 2017;11(3):1188–1195. https://doi.org/10.1007/s11694-017-9495-4

40. Piwinska M, Wyrwisz J, Kurek MA, Wierzbicka A. Effect of drying methods on the physical properties of durum wheat pasta. CYTA – Journal of Food 2016;14(4):523–528. https://doi.org/10.1080/19476337.2016.1149226
41. Hosseini Ghaboos SH, Seyedain Ardabili SM, Kashaninejad M. Physico-chemical, textural and sensory evaluation of sponge cake supplemented with pumpkin flour. International Food Research Journal. 2018;25(2):854–860.
42. Ainsa A, Vega A, Honrado A, Marquina P, Roncales P, Gracia JAB, *et al.* Gluten-free pasta enriched with fish by-product for special dietary uses: Technological quality and sensory properties. Foods. 2021;10(12). https://doi.org/10.3390/foods10123049
43. Tóth M, Kaszab T, Meretei A. Texture profile analysis and sensory evaluation of commercially available glutenfree bread samples. European Food Research and Technology. 2022;248(6):1447–1455. https://doi.org/10.1007/s00217-021-03944-2
44. Ribeiro THS, Bolanho BC, Montanuci FD, Ruiz SP. Physicochemical and sensory characterization of gluten-free fresh pasta with addition of passion fruit peel flour. Ciência Rural. 2018;48(12). https://doi.org/10.1590/0103-8478cr20180508
45. Peressini D, Cavarape A, Brennan MA, Gao J, Brennan CS. Viscoelastic properties of durum wheat doughs enriched with soluble dietary fibres in relation to pasta-making performance and glycaemic response of spaghetti. Food Hydrocolloids. 2020;102. https://doi.org/10.1016/j.foodhyd.2019.105613

ORCID IDs
Siham M.M. Faheid https://orcid.org/0000-0002-1692-4174
Yasser F.M. Kishk https://orcid.org/0000-0003-3745-2775
Gamal H. Ragab https://orcid.org/0000-0002-5180-168X
Sayed M. Mostafa https://orcid.org/0000-0002-3770-8024

Foods and Raw Materials. 2022;10(2)

ISSN 2310-9599 (Print)
ISSN 2308-4057 (Online)

Research Article
Open Access

Available online at http://jfrm.ru/en
https://doi.org/10.21603/2308-4057-2022-2-544
https://elibrary.ru/ZVCUUW

Effects of bioactive substances isolated from Siberian medicinal plants on the lifespan of *Caenorhabditis elegans*

Elizaveta R. Faskhutdinova[1,*], Andrey S. Sukhikh[1], Violeta M. Le[1], Varvara I. Minina[1], Mohammed El Amine Khelef[2], Anna I. Loseva[1]

[1] Kemerovo State University, Kemerovo, Russia
[2] Moscow State University of Food Production, Moscow, Russia

* e-mail: faskhutdinovae.98@mail.ru

Received 10.02.2022; Revised 10.03.2022; Accepted 05.04.2022; Published online 23.09.2022

Abstract:
Medicinal plants are sources of natural antioxidants. Acting as reducing agents, these substances protect the human body against oxidative stress and slow down the aging process. We aimed to study the effects of bioactive substances isolated from medicinal plants on the lifespan of *Caenorhabditis elegans* L. used as a model organism.

High-performance liquid chromatography was applied to isolate bioactive substances from the extracts of callus, suspension, and root cultures of meadowsweet (*Filipendula ulmaria* L.), ginkgo (*Ginkgo biloba* L.), Baikal skullcap (*Scutellaria baicalensis* L.), red clover (*Trifolium pretense* L.), alfalfa (*Medicágo sativa* L.), and thyme (*Thymus vulgaris* L.). Their effect on the lifespan of *C. elegans* nematodes was determined by counting live nematodes treated with their concentrations of 10, 50, 100, and 200 µmol/L after 61 days of the experiment. The results were recorded using IR spectrometry.

The isolated bioactive substances were at least 95% pure. We found that the studied concentrations of trans-cinnamic acid, baicalin, rutin, ursolic acid, and magniferin did not significantly increase the lifespan of the nematodes. Naringenin increased their lifespan by an average of 27.3% during days 8–26. Chlorogenic acid at a concentration of 100 µmol/L increased the lifespan of *C. elegans* by 27.7%. Ginkgo-based kaempferol and quercetin, as well as red clover-based biochanin A at the concentrations of 200, 10, and 100 µmol/L, respectively, increased the lifespan of the nematodes by 30.6, 41.9, and 45.2%, respectively.

The bioactive substances produced from callus, root, and suspension cultures of the above medicinal plants had a positive effect on the lifespan of *C. elegans* nematodes. This confirms their geroprotective properties and allows them to be used as anti-aging agents.

Keywords: Plants, antioxidants, callus culture, suspension culture, root culture, nematodes, aging

Funding: The study was financed by the Ministry of Science and Higher Education of the Russian Federation (Minobrnauka) (project FZSR-2020-0006 “Screening bioactive plant-based substances with geroprotective properties and developing technology for producing anti-aging nutraceuticals”).

Please cite this article in press as: Faskhutdinova ER, Sukhikh AS, Le VM, Minina VI, Khelef MEA, Loseva AI. Effects of bioactive substances isolated from Siberian medicinal plants on the lifespan of *Caenorhabditis elegans*. Foods and Raw Materials. 2022;10(2):340–352. https://doi.org/10.21603/2308-4057-2022-2-544

INTRODUCTION

According to the WHO, average life expectancy is steadily increasing worldwide [1]. Over the last 20 years, it has grown by 6 years as a result of advances in science and medicine. However, behind these advances is an increase in diseases associated with aging, which has become a serious problem of public health in the 21st century. Aging is a process that affects the entire human body, in particular its cardiovascular, nervous, digestive, and immune systems.

The aging process is directly related to oxidative stress. Age-related diseases cause structural changes in mitochondria, as well as changes in the functions of the electron transport chain, which ultimately leads to oxidative stress. The cardiovascular system is particularly susceptible to this effect, which explains the increase in cardiovascular diseases in the elderly [2–5].

The problem of aging is widely covered by the free-radical theory of aging developed by Denham Harman in the 1950s [6]. According to this theory, the body's defense mechanisms stop responding to damage caused by reactive oxygen species, resulting in the deterioration of cellular homeostasis, energy imbalance, and mitochondrial insufficiency [7].

The molecules of reactive oxygen species include nitric oxide, hydrogen peroxide, monoxide radicals, superoxide anions, tocopherols, ascorbic acid, and polyphenols [8]. Reactive oxygen species alter cellular activities such as cell survival, stress responses, and inflammation. They are also involved in muscle contractions, regulate vascular tone, as well as determine bactericidal and bacteriostatic activity [9]. However, their increase leads to oxidative stress, disrupting the balance of antioxidants and pro-oxidants [10]. This causes damage to macromolecules (lipids, DNA, and proteins) and subsequently to whole cells, tissues, and organs [4]. Higher concentrations of reactive oxygen species in the body promote inflammation, which, in turn, can accelerate the formation of their molecules [11]. Therefore, it is very important to maintain a balance between antioxidants and pro-oxidants.

Antioxidants can react with free radicals and neutralize them by causing them to decay. The human body has three lines of defense against oxidative stress. The first line consists of body enzymes such as superoxide dismutase, catalase, glutathione peroxidase, glutathione S-transferase, and glutathione reductase [12]. They prevent cell damage by scavenging free radicals that cause premature aging and age-related disorders. The first line also includes non-enzymatic molecules in the blood plasma such as transferrin, ferritin, ceruloplasmin, and albumin [13]. These preventative antioxidants inhibit the formation of new reactive oxygen species by binding transition metal ions (for example, copper and iron). The second line of defense is represented by non-enzymatic antioxidants that provide intermediate protection against oxidative radicals. The third line of defense serves to regenerate biomolecules damaged by oxidative stress [14].

However, protection against oxidative stress should not be limited to the protective function of the biological system itself. Noteworthily, one antioxidant molecule is capable of reacting with only one oxidizing radical. Therefore, there is a need to replenish antioxidant molecules, including the use of supplements.

There are three groups of exogenous antioxidants: mineral elements, nutritional antioxidants (carotenoids, vitamins E and C), and natural antioxidants derived from natural sources commonly known as phytochemicals or phytonutrients [15].

Synthetic antioxidants have been widely used until recently, but there is some doubt as to their usefulness and safety. According to some studies, synthetic antioxidants are ineffective against oxidative stress. Moreover, their long-term use can lead to diseases such as skin allergies, gastrointestinal and cardiovascular diseases, and even increase the risk of cancer [16]. Therefore, there is a need for thorough research into the safety of synthetic antioxidants.

The main sources of exogenous antioxidants are fruits, vegetables, cereals, etc. However, modern research is focused on traditional medicinal plants as a source of natural antioxidants [17, 18].

Since ancient times, plants have been a source of many useful substances, including exogenous antioxidants. These substances act as reducing agents that scavenge free radicals, protect the body against oxidative stress, and, as a result, maintain a balance between oxidants and antioxidants [19]. This is achieved due to the presence of polyphenols, tocopherols, carotenoids, ascorbic acid, and macromolecules (including polysaccharides and peptides), as well as essential oils [20].

Polyphenols are substances that contain a multiple number of structural units of phenol [21]. Their number affects the chemical, biological, and physical properties of polyphenolic compounds. Polyphenols are represented by flavonoids, phenolic acids, and nonflavonoids [22, 23]. Depending on the chemical structure, flavonoids are classified into flavonols, flavanones, isoflavones, anthocyanins, and flavan-3-ols. They are the most abundant class of polyphenols, with about 8000 compounds identified to date [24]. A couple of decades ago, researchers significantly increased their interest in polyphenols due to their beneficial properties for humans [25]. In particular, polyphenols curb oxidative stress and related conditions through their reductive ability to protect cellular components from oxidative damage caused by free radicals [26].

Model organisms have become an indispensable part of biological studies that would be impossible to conduct on humans for ethical or economic reasons [27]. Studies of aging and age-related diseases require an organism with a relatively short lifespan and clearly identified genetic factors to ensure reproducibility and reliability [28]. Nematodes (*Caenorhabditis elegans* L.), drosophila (*Drosophila melanogaster* L.), and yeasts (*Saccharomyces cerevisiae* L.) are used to test the effect of bioactive substances on lifespan [29, 30].

C. elegans is a non-parasitic, free-living nematode that feeds on various bacteria, primarily *Escherichia coli* [31]. This simple multicellular organism up to 1 mm long is a hermaphrodite capable of self-fertilization [32]. Its hermaphroditic structure contributes to low genetic variability [33]. *C. elegans* has a short life cycle (2–4 days) and remains viable for 20–25 days at 20°C as an adult [34]. The nematode can be stored in liquid nitrogen for an almost unlimited amount of time [35].

C. elegans was first used as a model organism for biological research by Sydney Brenner in the 1965s [36]. Since then, it has been widely used to study aging and associated oxidative stress, as well as neurodegeneration and inflammation processes [37].

C. elegans has a number of advantages that explain its common uses as a model organism. Firstly, the nematode is easily cultivated and has a transparent body, which makes it easy to track the changes microscopically [33, 38–40]. Secondly, *C. elegans* has four organ systems that are the same as in vertebrates (nervous, digestive, immune, and reproductive), which allows for reliable and valuable conclusions [41]. Thirdly, its short lifespan (20–25 days) enables scientists to conduct rapid experiments aimed to study the effect of various substances on the lifespan [42]. Finally, the nematode's genome is completely deciphered and easily modified, which facilitates studies of the aging process [43–46].

Plants of the Siberian Federal Okrug (Russia) are potential sources of geroprotectors – substances that can slow down the aging process [47].

Meadowsweet (*Filipendula ulmaria* L.) is a herbaceous perennial plant common in Russia and many European countries [48]. Extracts of this plant have anticancerous, antioxidant, and anti-inflammatory activity [49]. This activity is associated with tannins, phenolic compounds, phenolcarboxylic acids, catechins, flavonoids, essential oils, and other bioactive substances contained in the roots and flowers of the plant [50]. Many previous studies confirm its medicinal properties [51, 52]. Rutin, one of its phytochemicals, belongs to the class of natural flavonoids and is known as quercetin-3-O-rutinoside or vitamin P [53]. It has antitumorous, anticarcinogenic, and antimicrobial properties [54, 55].

Ginkgo (*Ginkgo biloba* L.) is a special medicinal plant that contains a variety of compounds with a unique structure due to its phylogenetic divergence from other plants. Its extract obtained by drying the leaves is used to treat many neurodegenerative diseases (memory impairment, dementia, Alzheimer's disease) [56]. It is also widely applied as an anti-inflammatory, cardioprotective, and antioxidant agent [57]. The plant's active components are flavonoids, terpenoids, polyphenols, and organic acids [58]. Quercetin and kaempferol are two of these beneficial compounds. Quercetin is a flavonoid that has a positive effect on cardiovascular diseases, breast cancer, and ischemia [59–62]. Kaempferol is a valuable component with anticancerous, antitumorous, and anti-inflammatory properties [62].

Baikal skullcap (*Scutellaria baicalensis* L.) belongs to the genus *Lamiaceae* and is still widely used in Chinese traditional medicine [63]. This plant grows in China, Russia, Mongolia, Japan, and North Korea. To date, scientists have identified 126 low-molecular weight compounds in it, mostly in its root. These compounds include flavonoids, flavonoid glycosides, and phenylethanoid glycosides [64]. The most widespread and studied of them is baicalin, which is used for various medical purposes [66].

Red clover (*Trifolium pretense* L.) is one of the most important representatives of the *Leguminosae* family, numbering over 240 species [66]. It has numerous medicinal properties and therapeutic effects on respiratory diseases, bacterial and fungal infections, tumors, and diabetes [67]. The plant is rich in isoflavones (biochanin A, genistein, trifoside), flavonoids (quercetin, kaempferol), as well as cinnamic, caffeic, and chlorogenic acids [68].

Alfalfa (*Medicágo sativa* L.) is a flowering plant in the *Fabaceae* family, which is the largest and most widespread family in the world. The genus *Medicágo* includes 83 species rich in alkaloids, flavonoids, naphthoquinones, and saponins [69]. Naringenin, one of its components, is a water-soluble flavonoid of great value due to its anticancerous, antioxidant, and anti-inflammatory effects [70, 71].

Thyme (*Thymus vulgaris* L.) is an aromatic perennial flowering plant belonging to the *Lamiaceae* family. Its therapeutic properties are mainly associated with its essential oil that has antitussive, expectorant, antiseptic, antimicrobial, and anthelmintic effects [72]. The plant is traditionally used to treat oral, gastrointestinal, and urinary tract infections, as well as respiratory diseases (cough, bronchitis, asthma) [73]. Ursolic acid, one of its bioactive substances, is a promising agent against cancer, cardiovascular disease, brain and liver diseases, obesity, and diabetes [74, 75].

We aimed to study the effect of individual bioactive substances on the lifespan of the model organism *C. elegans*.

STUDY OBJECTS AND METHODS

We used individual bioactive substances isolated from the extracts of suspension, callus, and root cultures of Siberian medicinal plants. The extraction parameters are presented in Table 1.

Table 1 Parameters for obtaining extracts from Siberian medicinal plants

Sample	Extraction time, h	Temperature, °C	Ethanol, %
Callus cultures of meadowsweet (*Filipendula ulmaria* L.)	5	35	70
Suspension cultures of ginkgo (*Ginkgo biloba* L.)	6	55	70
Root cultures of Baikal skullcap (*Scutellaria baicalensis* L.)	5	35	70
Callus cultures of red clover (*Trifolium pretense* L.)	5	70	60
Callus cultures of alfalfa (*Medicágo sativa* L.)	3	50	70
Callus cultures of thyme (*Thymus vulgaris* L.)	4	50	70
Root cultures of sweetvetch (*Hedysarum neglectum* L.)	6	30	70

High-performance liquid chromatography (HPLC) was applied (Shimadzu LC-20 Prominence liquid chromatograph, Japan) to isolate the following bioactive substances from the extracts of the above cultures:

1. Rutin from the callus culture extract of meadowsweet (*Filipendula ulmaria*) [76];
2. Quercetin from the suspension culture extract of ginkgo (*Ginkgo biloba*) [77];
3. Kaempferol from the suspension culture extract of ginkgo (*G. biloba*) [77];
4. Baicalin from the root culture extract of Baikal skullcap (*Scutellaria baicalensis*) [78];
5. Trans-cinnamic acid from the root culture extract of Baikal skullcap (*S. baicalensis*) [79];
6. Chlorogenic acid from the callus culture extract of red clover (*Trifolium pratense*) [80];
7. Biochanin A from the callus culture extract of red clover (*T. pratense*) [80];
8. Naringenin from the callus culture extract of alfalfa (*Medicágo satíva*) [81];
9. Ursolic acid from the callus culture extract of thyme (*Thymus vulgaris*) [82]; and
10. Magniferin from the root culture extract of sweetvetch (*Hedysarum neglectum*) [83].

To isolate rutin from the callus culture extract of meadowsweet, the plant's ethanol extract was evaporated under vacuum at a temperature under 40°C on an IKA RV 8 rotary evaporator (IKA, Germany). After adding deionized water to 1/4 of the concentrate's initial volume, evaporation continued until a thick precipitate was formed. The precipitate was treated with a chloroform:ethylacetate mixture for 5 min with vigorous stirring in triplicate. The extracts were combined and mixed with anhydrous sodium sulfate (2.0 g per 100 mL of extract). The mixture was kept for 3 h at +4°C and then filtered. The residue containing a flavonoid fraction was dissolved in 50% ethanol. Then, 50.0 g of activated carbon was added to the mixture and evaporated until a dry residue was formed. The adsorbent with the extract residue was transferred to a shot filter and successively eluted with methanol, water, 7% aqueous phenol, and 15% phenol in methyl alcohol. The fraction extracted with 7% aqueous phenol was treated with 100 mL of diethyl ether in triplicate. The resulting extract was evaporated under vacuum to a thick precipitate, which was then mixed with 40.0 g of silica gel (column chromatography grade, Sigma), dried completely, and transferred to a column (5×6 cm BioRad) as a suspension in chloroform. The substances were eluted with a mixture of chloroform:ethanol (80:20) and evaporated to isolate rutin.

To isolate quercetin and kaempferol from the suspension culture extract of ginkgo, the extract was filtered through cellulose filters, diluted with water, and kept at +4°C for 48 h to filter lipid precipitates. The extract was then concentrated in a vacuum evaporator in the presence of sodium chloride (up to 10% by salt content in solution). Resinous substances were removed by decantation. Lipophilic substances were purified by liquid-liquid extraction with n-heptane to isolate terpenolactones. The aqueous phase was extracted with n-butanol in triplicate.

The three phases were combined and concentrated under vacuum until a dry precipitate was formed. The precipitate was dissolved in a water-alcohol solution and purified by liquid-liquid extraction with ethyl acetate. The resulting phase was washed with a sodium chloride solution and evaporated. The dry residue was dissolved in acetone containing 40 wt.% of water, cooled to 10°C, and filtered. Flavonogicosides were chromatographed on polyamide (Sigma) packed in a 5.3×250 mm chromatographic column on a BioLogic low-pressure chromatograph (BioRad) using gradient elution mixtures: chloroform-methanol (100:0 → 60:40) and then water-ethanol (100:0 → 0:100). The components were separated and purified by silica gel rechromatography (Lachema) using an eluent mixture of chloroform:petroleum ether (30:70), followed by recrystallization to isolate quercetin and kaempferol.

Baicalin and trans-cinnamic acid were isolated from the root culture extract of Baikal skullcap by evaporating the extract under vacuum at a temperature under 50°C. The evaporated residue was treated with diethyl ether in triplicate. The resulting ether fraction was chromatographed on silica gel (mobile phase) in a n-hexane-acetone gradient (1:0 → 0:1) to isolate flavonoids and hydroxycinnamic acids. Baicalin and trans-cinnamic acid were isolated by subsequent rechromatography on silica gel (mobile phase) with n-hexane-chloroform (1:0 → 0:1).

To isolate biochanin A from the callus culture extract of red clover, the ethanol extract was vacuum-evaporated on a rotary evaporator at under 50°C. Deionized water was added to the precipitate up to 1/4 of the concentrate's initial volume to continue evaporation to a thick precipitate. The precipitate was treated with n-hexane for 5 min in triplicate and the suspension was treated ultrasonically. The extracts were filtered through filter paper and combined. Then, they were evaporated under vacuum to a thick precipitate. The precipitate was mixed with 50.0 g of silica gel, dried, and transferred to a column (5×6 cm BioRad). Then, it was eluted with a petroleum ether-ethanol mixture (99:1, 98:2, 97:3, 95:5, 93:7, 80:20). Biochanin A was isolated from the evaporated eluates.

To isolate chlorogenic acid from the callus culture extract of red clover, the thick precipitate obtained as described above was treated with diethyl ether to isolate hydroxycinnamic and coumaric acids. The mixture was then evaporated to a dry residue and separated on silica gel (column chromatography grade, Sigma) on a column (0.65×10 cm BioRad). Then, it was eluted with isopropyl alcohol:acetic acid:hexane (65:12:23) to isolate chlorogenic acid.

Naringenin was isolated from the alfalfa extract as follows. The ethanol extract was evaporated under vacuum at under 55°C on a rotary evaporator. The residue was mixed with deionized water added to 1/4 of

the concentrate's initial volume to continue vacuum evaporation to a thick precipitate. The precipitate was placed on a 5×6 cm BioRad chromatographic column and eluted with n-hexane to collect 1-mL fractions. The resulting extracts were evaporated to a thick precipitate, which was then dissolved in ethanol and fractionated on LH-20 Sephadex (Aldrich) in toluene. Silica gel was eluted with isopropyl alcohol:water (40:60) and then evaporated under vacuum to thick residue. The residue was dissolved in ethanol and fractionated on LH-20 Sephadex (Aldrich) in a methanol gradient of 10 → 90% to isolate naringenin.

Ursolic acid was isolated from the callus culture extract of thyme. For this, the ethanolic extract was evaporated under vacuum at under 40°C on a rotary evaporator. The residue was mixed with deionized water added to 1/4 of the concentrate's initial volume to continue vacuum evaporation to a thick precipitate. The resulting precipitate was treated three times with dichloromethane for 5 min with vigorous stirring. The extracts were combined and mixed with anhydrous sodium sulfate (20.0 g per liter of extract). The mixture was kept for 3 h and filtered through a paper filter. The filtered precipitate was dissolved in ethanol. The ethanol fraction was passed through an AN-1 anion exchanger (State Standard 20301-74) and washed with water-ethanol eluents (up to 50% of ethanol). Then, it was desorbed with 0.1 M hydrochloric acid to isolate ursolic acid.

Magniferin was isolated from the root culture extract of sweetvetch. The ethanol extract was evaporated in a vacuum evaporator at 45°C. The residue was fractionated on a BioLogic low-pressure chromatograph (BioRad) using silica gel (column chromatography grade, Sigma). Petroleum ether-ethyl acetate was used as an eluent (100:0; 50:1; 20:1; 10:1; 5:1; 2:1; 1:1; and 0:1). Methanol was fed to the column to desorb gallic acid, resulting in nine 300-mL fractions collected. A crude crystal of magniferin was obtained from fraction 3. Then, it was recrystallized from a mixture of petroleum ether:acetone (20:1) and purified by rechromatography on CL6B Sepharose (Sigma – Aldrich) using a BioLogic low-pressure chromatograph (BioRad) to isolate pure mangiferin.

All the isolated bioactive substances were at least 95% pure. Their IR spectra were registered on an SF-2000 instrument (OKB Spektr, Russia).

Further, we analyzed the effect of bioactive substance concentrations on the lifespan of wild-type *Caenorhabditis elegans* nematodes (strain N2 Bristol, www.wormbook.org). Our study consisted of five stages described below.

Cultivation of nematodes on solid agar.

Obtaining an Escherichia coli bacterial culture. *E. coli* OP50 was seeded on Petri dishes with a Lysogeny broth (L-broth) solid medium (HiMedia Laboratories, India). Then, under sterile conditions, one bacterial colony was selected and placed in 5–10 mL of L-broth (HiMedia Laboratories, India) to incubate at 37°C overnight with vigorous stirring. After that, the culture was transferred to a refrigerator and stored at +4°C.

Inoculating E. coli OP50 on NGM agar plates. 50 µL of the *E. coli* OP50 overnight culture was placed in the center of a 100-mm Petri dish. Using a sterile glass rod, the drop was distributed over the center of the dish in the shape of a square, without touching the walls, and incubated at 37°C for a day. After incubation, the dishes were wrapped in parafilm and stored in the refrigerator for several weeks.

Preparing NGM agar plates. After autoclaving, the sterile NGM agar was cooled to 55°C in a water bath. Then, the cooled nutrient medium was mixed with 1 mL of 1 M $CaCl_2$, 1 mL of 5 mg/mL cholesterol in alcohol, 1 mL of 1 M $MgSO_4$, and 25 mL of 1 M K_3PO_4 buffer. After thorough mixing, it was poured into sterile Petri dishes, 20 mL each. To ensure the absence of bacterial contamination, the dishes were left for 2–3 days at room temperature.

Transferring nematodes to new NGM agar dishes. The nematodes were transferred in two ways: with a loop and with a piece of agar. The first method involved hooking a nematode with a calcined and cooled bacteriological loop and planting it on a bacterial lawn in the center of a new NGM Petri dish with agar. The second method involved cutting a 0.5×0.5 cm piece of agar containing a nematode with a sterile scalpel and transferring it to the center of the dish surface down. The dishes were incubated at 20°C.

Nematode synchronization. 5–10 mL of sterile water was pipetted on the surface of the dish containing a nematode until its eggs were completely attached to the agar. The liquid from the Petri dish was placed in a 50 mL tube and centrifuged for 2 min (1200 rpm). Then, the supernatant was removed and the precipitate was washed with 10 mL of distilled water to repeat centrifugation under the above conditions.

After repeated centrifugation, the supernatant was removed and the precipitate was mixed with 5 mL of a freshly prepared mixture of 1 mL of 10 N NaOH, 2.5 mL of household bleach, and 6.5 mL of H_2O. The mixture was thoroughly vortexed (Biosan, Latvia) for 10 min with 2 min intervals to observe the hydrolysis of nematodes under an Axio Observer Z1 microscope (Karl Zeiss, Germany). At the end of the process, 5 mL of M9 medium was added to neutralize the reaction. The resulting mixture was centrifuged for 2 min (2500 rpm). After that, the supernatant was removed and the precipitate was mixed with 10 mL of sterile water to repeat the washing and centrifugation three times. Then, the precipitate was washed with 10 mL of S-medium and the supernatant was removed. Finally, 10 mL of S-medium was added and the test tube with nematode eggs was placed on a slow shaker for a day at room temperature for the complete transfer of the nematodes to the L1 stage.

Cultivation of nematodes in a liquid medium. After the nematodes passed to the L1 stage, an overnight bacterial culture of *E. coli* OP50 was added to the S-medium. The culture had previously been washed and resuspended in the S-medium to a bacterial concentration of 0.5 mg/mL. Then, 120 µL amounts of the suspension containing the bacteria and nematodes were poured into each well of a 96-well plate (TPP, Switzerland). The plate was sealed with a film and left for 48 h at 20°C.

After that, 15 µL of 1.2 mM 5-fluoro-2-deoxyuredin was poured into each well of the plate to prevent the nematodes from reproduction and left for a day at 20°C. At the end of incubation, the nematodes entered the L4 stage. Then, 15-µL amounts of the bioactive substances under study were added to the wells in accordance with the experiment plan.

Preparation of bioactive substances. Stock solutions of bioactive substances were prepared in dimethyl sulfoxide at a concentration of 10 mmol/L. The substances were tested by diluting stock solutions in sterile distilled water to concentrations of 2000, 1000, 500, and 100 µM. Each well was filled with 15 µL of freshly prepared stock solutions so that working concentrations of each bioactive substance reached 2000, 1000, 500, and 100 µmol/L, respectively. The stocks were stored at 4°C.

Effects of bioactive substances on nematode lifespan. The effect of bioactive substances at concentrations of 0, 10, 50, 100, and 200 µmol/L on the lifespan of *C. elegans* was determined by the number of nematodes surviving in the presence of the tested substances. The experiment was carried out in 6-fold repetitions using 96-well plates and a liquid S-medium for nematode cultivation. The numbers of live and dead nematodes were counted every 4–7 days during the 61-day experiment. The experiment was considered completed when there were no live nematodes left in the control group.

Each concentration of bioactive substances was studied in 6-fold repetitions. Statistical data were analyzed in the Microsoft Office Excel 2007. Statistical analysis was performed using a paired Student's t-test for each pair of interests. Differences were considered statistically significant at $P < 0.05$.

RESULTS AND DISCUSSION

The effects of the bioactive substances obtained from the extracts of suspension, callus, and root cultures of Siberian medicinal plants on the lifespan of *Caenorhabditis elegans* L. nematodes are graphically presented in Fig. 1.

As can be seen in Fig. 1a, rutin, which was isolated from the extract of meadowsweet callus culture, did not significantly increase the lifespan of *C. elegans* nematodes. At concentrations of 50 and 100 µmol/L, it had a positive effect from day 8 to day 34, but then the number of surviving nematodes approached the control. Its greatest effect was observed at a concentration of 50 µmol/L on day 13, with the survival rate of 32.3% (15.3% higher than in the control group).

Quercetin, which was obtained from the suspension culture extract of ginkgo, had a significant effect on the lifespan of *C. elegans* nematodes at concentrations of 10 and 100 µmol/L (Fig. 1b). The proportion of surviving nematodes was 32.6–4.6% from day 8 to day 45 of the experiment. On day 8, all the concentrations of quercetin had a positive effect on the lifespan. The proportions of surviving nematodes treated with 10, 50, 100 and 200 µmol/L of this bioactive substance were 72.9, 74.0, 67.5, and 63.6%, respectively (higher than in the control nematodes by 41.9, 43.0, 36.5, and 32.6%, respectively).

Of special interest was kaempferol obtained from the suspension culture extract of ginkgo (Fig. 1c). At a concentration of 50 µmol/l, this substance increased the lifespan of nematodes throughout the experiment (except for 3 days), compared to the control. The nematode population was active, reaching 10.3% on day 61. We also observed kaempferol's positive effect at a concentration of 10 µmol/L in the period of 8 to 61 days. The maximum proportion of surviving nematodes treated with this concentration was registered on day 8 at 48.6%, which was 17.6% higher than in the control group. However, the greatest increase in the nematode lifespan was provided by a concentration of 200 µmol/L on day 8, with the survival rate of 61.6% (by 30.6% higher than in the control nematodes).

Baicalin was produced from the root culture of Baikal skullcap (Fig. 1d). At concentrations of 10, 100, and 200 µmol/L, it increased the lifespan of nematodes from day 8 to day 13. After that period, the number of surviving nematodes exposed to 200 µmol/L baicalin became lower than in the control group. During days 13–17, their lifespan increased only at baicalin's concentrations of 10 and 100 µmol/L. From day 17 until the end of the experiment, the number of surviving nematodes treated with 10, 50, and 200 µmol/L baicalin was greater than in the control group. Noteworthily, the end of the experiment saw greater proportions of surviving nematodes treated with baicalin at all concentrations (10, 50, 100, and 200 µmol/L) than that of the control (by 4.3, 6.7, 2.3, and 2.1%, respectively).

Trans-cinnamic acid was isolated from the root culture extract of Baikal skullcap (Fig. 1e). As we can see, on day 8, its concentrations of 10, 50, 100, and 200 µmol/L increased the lifespan of nematodes by 18.1, 26.3, 24.1, and 36.6%, respectively. During days 13–34, the concentration of 200 µmol/L had no positive effect on the lifespan of nematodes, unlike the other concentrations. However, from day 34 to the end of the experiment, trans-cinnamic acid at all concentrations increased the percentage of surviving nematodes. The greatest increase in the lifespan was observed in the nematodes treated with 50 µmol/L of this bioactive substance (9.8%).

Chlorogenic acid obtained from the callus culture extract of red clover showed a generally positive effect

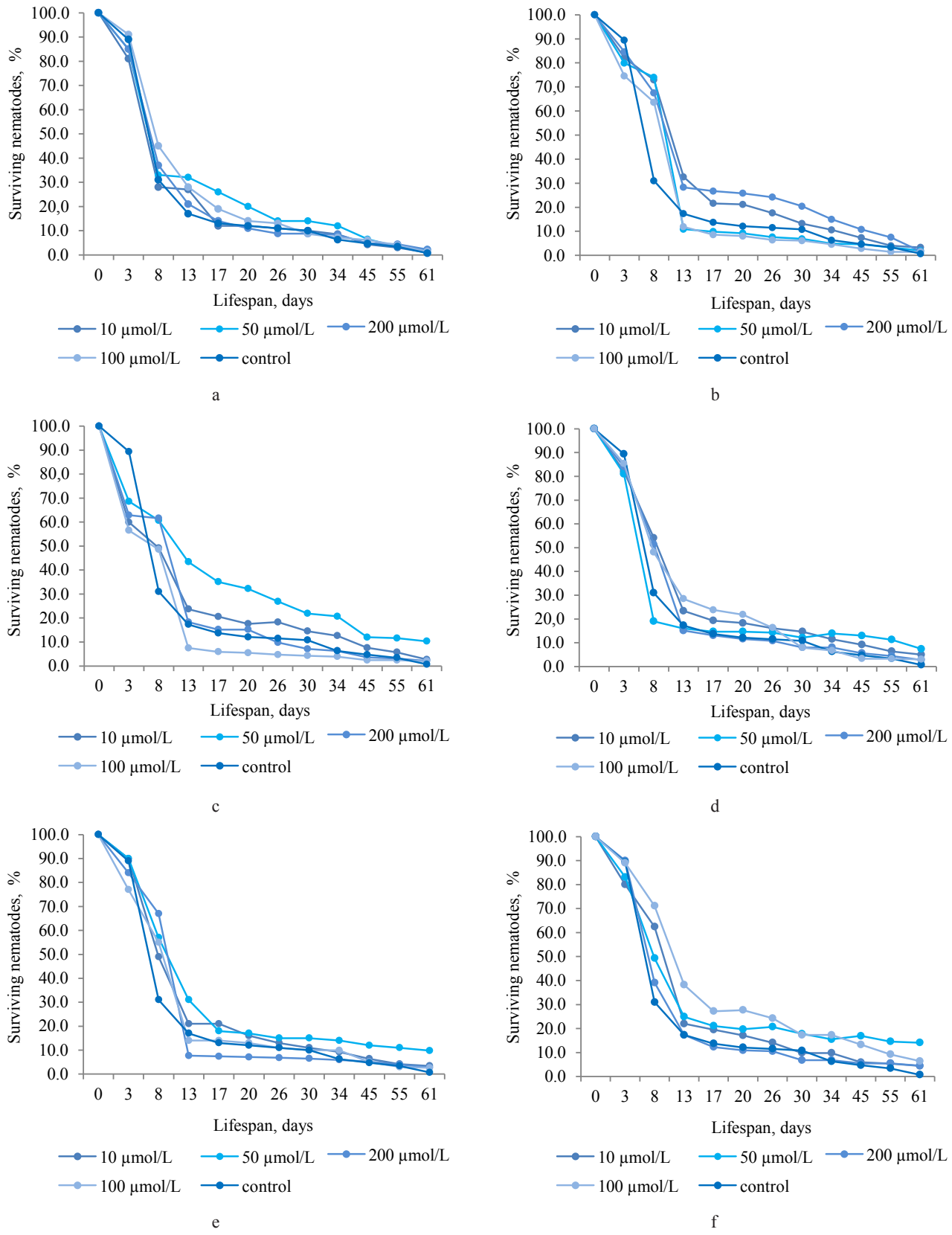

Figure 1 *Beginning.* Effects of bioactive substances isolated from the extracts of suspension, callus, and root cultures of medicinal plants on the lifespan of *Caenorhabditis elegans* nematodes: (a) rutin from the suspension culture extract of meadowsweet; (b) quercetin from the suspension culture extract of ginkgo; (c) kaempferol from the suspension culture extract of ginkgo; (d) baicalin from the root culture extract of Baikal skullcap; (e) trans-cinnamic acid from the root culture extract of Baikal skullcap; (f) chlorogenic acid from the callus culture extract of red clover; (g) biochanin A from the callus culture extract red clover; (h) naringenin from the callus culture extract of alfalfa; (i) ursolic acid from the callus culture extract of thyme; (j) magniferin from the root culture extract of sweetvetch

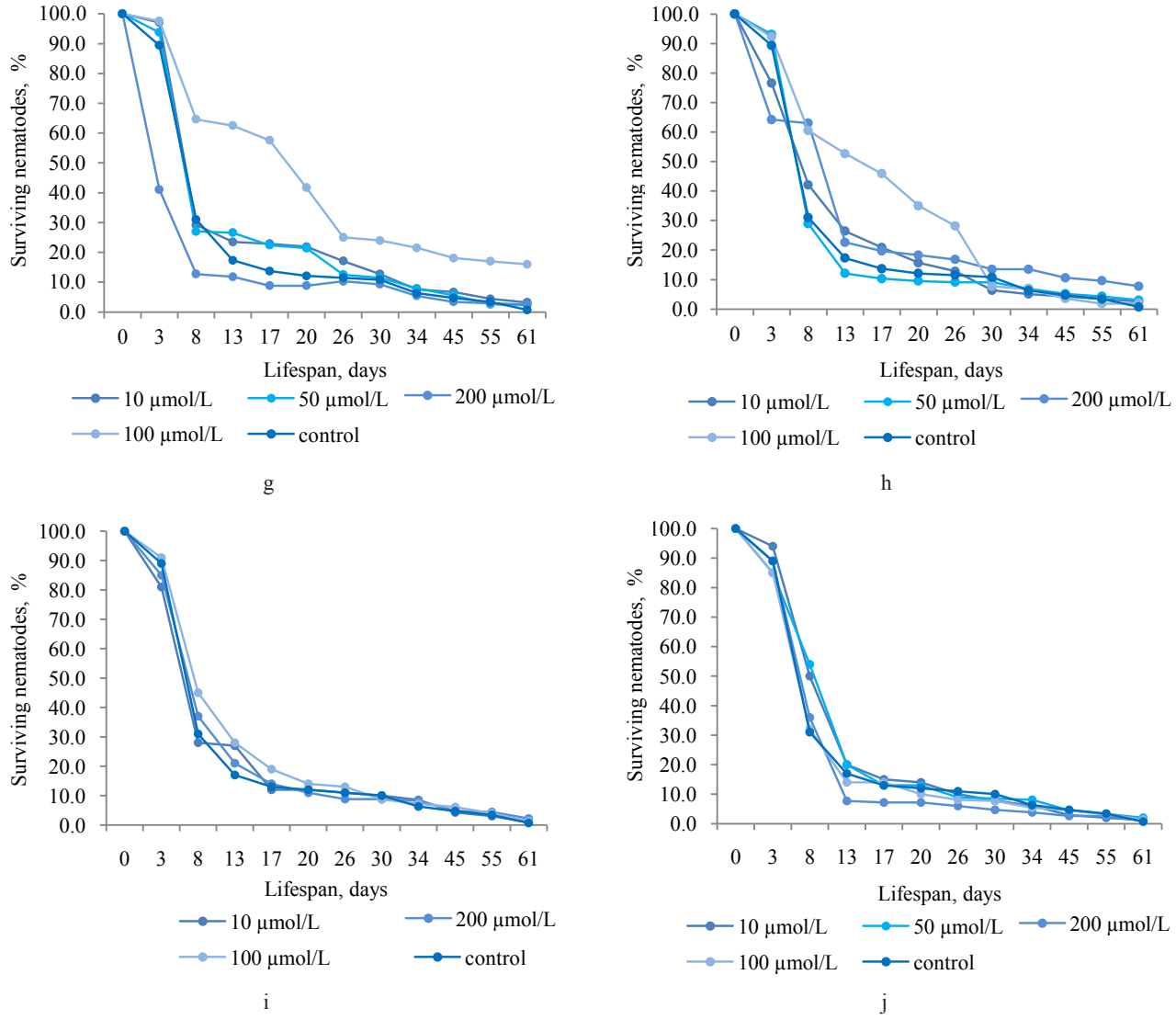

Figure 1 *Ending.* Effects of bioactive substances isolated from the extracts of suspension, callus, and root cultures of medicinal plants on the lifespan of *Caenorhabditis elegans* nematodes: (a) rutin from the suspension culture extract of meadowsweet; (b) quercetin from the suspension culture extract of ginkgo; (c) kaempferol from the suspension culture extract of ginkgo; (d) baicalin from the root culture extract of Baikal skullcap; (e) trans-cinnamic acid from the root culture extract of Baikal skullcap; (f) chlorogenic acid from the callus culture extract of red clover; (g) biochanin A from the callus culture extract red clover; (h) naringenin from the callus culture extract of alfalfa; (i) ursolic acid from the callus culture extract of thyme; (j) magniferin from the root culture extract of sweetvetch

on the lifespan of *C. elegans* (Fig. 1f). As can be seen, 100 µmol/L of this substance increased the survival of nematodes throughout the experiment, with the greatest increase (by 40.1%) on day 8. The other concentrations showed varying survival rates. Days 8–13 saw greater lifespans in the nematodes exposed to chlorogenic acid at all four concentrations. During days 13–26, increased lifespan was provided by the concentrations of 10, 50, and 100 µmol/L. The maximum survival rate was observed on day 20 (27.7%) in the nematodes treated with 100 µmol/L of chlorogenic acid. From day 26 to day 34, the concentration of 200 µmol/L had no effect on the lifespan of *C. elegans*. However, from day 45 to the end of the experiment, chlorogenic acid had a positive effect again at all its concentrations.

Figure 1g shows the effect of biochanin A isolated from red clover callus culture. As we can see, the best survival rate was provided by this substance at 100 µmol/L. Unlike the other concentrations, this concentration had a positive effect on *C. elegans* throughout the entire experiment. Days 8–20 saw the highest survival rates, with the greatest increase in lifespan occurring on day 13 (by 45.2% compared to the control). Noteworthily, 200 µmol/L of biochanin A had a negative effect on the survival and lifespan of *C. elegans* almost throughout the experiment, except for the very end. On day 61, the proportion of surviving nematodes increased by 1.8% and amounted to 2.5% (compared to 0.7% in the control group). The concentrations of 10 and 50 µmol/L increased the

survival of nematodes during days 13–45 by an average of 8.4 and 9.1%, respectively. Both concentrations provided maximum lifespan increases during days 13–20 and had a weaker effect towards the end of the experiment. From day 26 to day 61, biochanin A at 10, 50, and 200 μmol/L had no significant effect on the lifespan of nematodes compared to the control group.

Naringenin was isolated from the extract of alfalfa callus culture. As shown by Fig. 1h, its concentration of 100 μmol/L had the greatest effect on the lifespan of nematodes compared to the other concentrations, especially during days 8–26. During that period, the survival of nematodes increased by an average of 27.3% compared to the control group, with maximum survival on day 13 (by 35.4%). The other concentrations of naringenin (10, 50, and 200 μmol/L) did not have a significant effect on the survival or lifespan of nematodes.

Ursolic acid was isolated from thyme callus culture. According to Fig. 1i, it had no significant effect on the lifespan of nematodes at all its concentrations. The greatest increase in survival (by 14.1%) was observed on day 8 in the nematodes treated with 100 μmol/L of ursolic acid.

Similarly, we found no positive effect in magniferin obtained from the root culture extract of sweetvetch (Fig. 1j). Moreover, its concentrations of 100 and 200 μmol/L reduced the proportion of surviving nematodes from day 13 to day 55 of the experiment. The greatest increases in the lifespan of nematodes were observed at magniferin concentrations of 10 and 50 μmol/L on day 8, amounting to 19.3 and 24.2%, respectively. At the end of the experiment, the longest lifespan was demonstrated by the nematodes exposed to 100 μmol/L of magniferin (1.4%).

CONCLUSION

Having applied HPLC methods, we isolated the following bioactive substances from the extracts of callus, suspension, and root cultures of medicinal plants growing in the Siberian Federal Okrug: rutin – from the callus culture extract of meadowsweet (*Filipendula ulmaria* L.); quercetin – from the suspension culture extract of ginkgo (*Ginkgo biloba* L.); kaempferol – from the suspension culture extract of ginkgo (*G. biloba*); baicalin – from the root culture extract of Baikal skullcap (*Scutellaria baicalensis* L.); trans-cinnamic acid – from the root culture extract of Baikal skullcap (*S. baicalensis*); chlorogenic acid – from the callus culture extract of red clover (*Trifolium pretense* L.); biochanin A – from the callus culture extract of red clover (*T. pratense*); naringenin – from the callus culture extract of alfalfa (*Medicágo sativa* L.); ursolic acid – from the callus culture extract of thyme (*Thymus vulgaris* L.); and magniferin – from the root culture extract of sweetvetch (*Hedysarum neglectum* L.). All the bioactive substances were at least 95% pure and were registered using IR spectroscopy on an SF-2000 instrument (OKB Spektr, Russia).

We determined the effect of the above bioactive substances at concentrations of 10, 50, 100, and 200 μmol/L on the lifespan of *Caenorhabditis elegans* nematodes, which are widely used as model organisms to study the aging process. We used 96-well plates for the experiment that lasted 61 days. Surviving nematodes were counted every 4–7 days and the experiment was considered completed when there were no live nematodes left in the control group. Stock solutions of the following bioactive substances were prepared for the experiment: rutin, quercetin, kaempferol, baicalin, trans-cinnamic acid, chlorogenic acid, biochanin A, naringenin, ursolic acid, and magniferin.

Trans-cinnamic acid, baicalin, rutin, ursolic acid, and magniferin did not significantly increase the lifespan of the nematodes.

Chlorogenic acid and naringenin had a little effect on the lifespan of nematodes, while quercetin, kaempferol, and biochanin A demonstrated their high survival.

Noteworthily, the greatest proportions of surviving nematodes treated with various concentrations of bioactive substances were recorded on days 8 to 13 for all the experimental samples. Then, the lifespan of *C. elegans* decreased and their survival rates approached those of the control group.

Thus, 200 μmol/L of kaempferol, 10 μmol/L of quercetin (both obtained from ginkgo suspension culture extract), and 100 μmol/L of biochanin A (obtained from red clover callus culture extract) increased the lifespan of *C. elegans* nematodes by 30.6, 41.9, and 45.2%, respectively, compared to the control (days 8 and 13). These results suggest that the mentioned bioactive substances can be effectively used as anti-aging agents.

CONTRIBUTION

All the authors are equally responsible for the research results and the manuscript.

CONFLICT OF INTEREST

The authors declare no conflict of interest.

REFERENCES

1. WHO: People living longer and healthier lives but COVID-19 threatens to throw progress off track [Internet]. [cited 2022 Jan 15]. Available from: https://www.who.int/news/item/13-05-2020-people-living-longer-and-healthier-lives-but-covid-19-threatens-to-throw-progress-off-track

2. Bosch-Morell F, Villagrasa V, Ortega T, Acero N, Muñoz-Mingarro D, González-Rosende M, *et al.* Medicinal plants and natural products as neuroprotective agents in age–related macular degeneration. Neural Regeneration Research. 2020;15(12):2207–2216. https://doi.org/10.4103/1673-5374.284978
3. Elfawy HA, Das B. Crosstalk between mitochondrial dysfunction, oxidative stress, and age related neurodegenerative disease: Etiologies and therapeutic strategies. Life Sciences. 2019;218:165–184. https://doi.org/10.1016/j.lfs.2018.12.029
4. Tan BL, Norhaizan ME, Liew W-P-P, Rahman HS. Antioxidant and oxidative stress: A mutual interplay in age–related diseases. Frontiers in Pharmacology. 2018;9. https://doi.org/10.3389/fphar.2018.01162
5. Prosekov AYu, Dyshlyuk LS, Milentyeva IS, Sykhikh SA, Babich OO, Ivanova SA, *et al.* Antioxidant and antimicrobial activity of bacteriocin-producing strains of lactic acid bacteria isolated from the human gastrointestinal tract. Progress in Nutrition. 2017;19(1):67–80. https://doi.org/10.23751/pn.v19i1.5147
6. Harman D. Aging: A theory based on free radical and radiation chemistry. Journal of Gerontology. 1956;11(3):298–300. https://doi.org/10.1093/geronj/11.3.298
7. McGuire PJ. Mitochondrial dysfunction and the aging immune system. Biology. 2019;8(2). https://doi.org/10.3390/biology8020026
8. Dębowska K, Smulik-Izydorczyk R, Pięta J, Adamus J, Michalski R, Sikora A. Oxidation of the selected probes for detection of reactive oxygen species (ROS) and reactive nitrogen species (RNS) in aqueous solutions of nitric oxide donors. Free Radical Biology and Medicine. 2018;120. https://doi.org/10.1016/j.freeradbiomed.2018.04.258
9. Jakubczyk K, Dec K, Kałduńska J, Kawczuga D, Kochman J, Janda, K. Reactive oxygen species – sources, functions, oxidative damage. Polski merkuriusz lekarski: organ Polskiego Towarzystwa Lekarskiego. 2020;48(284):124–127.
10. He L, He T, Farrar S, Ji L, Liu T, Ma X. Antioxidants maintain cellular redox homeostasis by elimination of reactive oxygen species. Cellular Physiology and Biochemistry. 2017;44(2):532–553. https://doi.org/10.1159/000485089
11. van de Lagemaat EE, de Groot LCPGM, van den Heuvel EGHM. Vitamin B_{12} in relation to oxidative stress: A systematic review. Nutrients. 2019;11(2). https://doi.org/10.3390/nu11020482
12. Singh A, Kukreti R, Saso L, Kukreti S. Oxidative stress: A key modulator in neurodegenerative diseases. Molecules. 2019;24(8). https://doi.org/10.3390/molecules24081583
13. Warraich UA, Hussain F, Kayani HUR. Aging – Oxidative stress, antioxidants and computational modeling. Heliyon. 2020;6(5). https://doi.org/10.1016/j.heliyon.2020.e04107
14. Mirończuk-Chodakowska I, Witkowska AM, Zujko ME. Endogenous non-enzymatic antioxidants in the human body. Advances in Medical Sciences. 2018;63(1):68–78. https://doi.org/10.1016/j.advms.2017.05.005
15. Santos AL, Sinha S, Lindner AB. The good, the bad, and the ugly of ROS: New insights on aging and aging–related diseases from eukaryotic and prokaryotic model organisms. Oxidative Medicine and Cellular Longevity. 2018;2018. https://doi.org/10.1155/2018/1941285
16. Liu R, Mabury SA. Synthetic phenolic antioxidants: A review of environmental occurrence, fate, human exposure, and toxicity. Environmental Science and Technology. 2020;54(19):11706–11719. https://doi.org/10.1021/acs.est.0c05077
17. Asyakina LK, Fotina NV, Izgarysheva NV, Slavyanskiy AA, Neverova OA. Geroprotective potential of *in vitro* bioactive compounds isolated from yarrow (*Achilleae millefolii* L.) cell cultures. Foods and Raw Materials. 2021;9(1):126–134. https://doi.org/10.21603/2308-4057-2021-1-126-134
18. Gadouche L, Zidane A, Zerrouki K, Azouni K, Bouinoune S. Cytotoxic effect of *Myrtus communis*, *Aristolochia longa*, and *Calycotome spinosa* on human erythrocyte cells. Foods and Raw Materials. 2021;9(2):379–386. https://doi.org/10.21603/2308-4057-2021-2-379-386
19. Hassan W, Noreen H, Rehman S, Gul S, Amjad Kamal M, Kamdem JP, *et al.* Oxidative stress and antioxidant potential of one hundred medicinal plants. Current Topics in Medicinal Chemistry. 2017;17(12):1336–1370. https://doi.org/10.2174/1568026617666170102125648
20. Song R, Wu Q, Yun Z, Zhao L. Advances in antioxidative bioactive macromolecules. IOP Conference Series: Earth and Environmental Science. 2020;512(1). https://doi.org/10.1088/1755-1315/512/1/012094
21. Nascimento-Souza MA, de Paiva PG, Pérez-Jiménez J, do Carmo Castro Franceschini S, Ribeiro AQ. Estimated dietary intake and major food sources of polyphenols in elderly of Viçosa, Brazil: a population-based study. European Journal of Nutrition. 2018;57(2):617–627. https://doi.org/10.1007/s00394-016-1348-0
22. Fraga CG, Croft KD, Kennedy DO, Tomás-Barberán FA. The effects of polyphenols and other bioactives on human health. Food and Function. 2019;10(2):514–528. https://doi.org/10.1039/C8FO01997E
23. Majidinia M, Bishayee A, Yousefi B. Polyphenols: Major regulators of key components of DNA damage response in cancer. DNA Repair. 2019;82. https://doi.org/10.1016/j.dnarep.2019.102679

24. Abdel-Moneim AME, Shehata AM, Alzahrani SO, Shafi ME, Mesalam NM, Taha AE, *et al.* The role of polyphenols in poultry nutrition. Journal of Animal Physiology and Animal Nutrition. 2020;104(6):1851–1866. https://doi.org/10.1111/jpn.13455
25. Tungmunnithum D, Thongboonyou A, Pholboon A, Yangsabai A. Flavonoids and other phenolic compounds from medicinal plants for pharmaceutical and medical aspects: An overview. Medicines. 2018;5(3). https://doi.org/10.3390/medicines5030093
26. Papaevgeniou N, Chondrogianni N. Anti-aging and anti-aggregation properties of polyphenolic compounds in *C. elegans*. Current Pharmaceutical Design. 2018;24(19):2107–2120. https://doi.org/10.2174/1381612824666180515145652
27. Chaudhary MK, Rizvi SI. Invertebrate and vertebrate models in aging research. Biomedical Papers. 2019;163(2):114–121. https://doi.org/10.5507/bp.2019.003
28. Ye Y, Gu Q, Sun X. Potential of *Caenorhabditis elegans* as an antiaging evaluation model for dietary phytochemicals: A review. Comprehensive Reviews in Food Science and Food Safety. 2020;19(6):3084–3105. https://doi.org/10.1111/1541-4337.12654
29. Reiss AP, Rankin CH. Gaining an understanding of behavioral genetics through studies of foraging in *Drosophila* and learning in *C. elegans*. Journal of Neurogenetics. 2021;35(3):119–131. https://doi.org/10.1080/01677063.2021.1928113
30. Douglas AE. The *Drosophila* model for microbiome research. Lab Animal. 2018;47(6):157–164. https://doi.org/10.1038/s41684-018-0065-0
31. Markaki M, Tavernarakis N. *Caenorhabditis elegans* as a model system for human diseases. Current Opinion in Biotechnology. 2020;63:118–125. https://doi.org/10.1016/j.copbio.2019.12.011
32. Mack HID, Heimbucher T, Murphy CT. The nematode *Caenorhabditis elegans* as a model for aging research. Drug Discovery Today: Disease Models. 2018;27:3–13. https://doi.org/10.1016/j.ddmod.2018.11.001
33. Salzer L, Witting M. Quo vadis *Caenorhabditis elegans* metabolomics – A review of current methods and applications to explore metabolism in the nematode. Metabolites. 2021;11(5). https://doi.org/10.3390/metabo11050284
34. Martel J, Wu C-Y, Peng H-H, Ko Y-F, Yang, H-C, Young, JD, *et al.* Plant and fungal products that extend lifespan in *Caenorhabditis elegans*. Microbial Cell. 2020;7(10):255–269. https://doi.org/10.15698/mic2020.10.731
35. Elkabti AB, Issi L, Rao RP. *Caenorhabditis elegans* as a model host to monitor the *Candida* infection processes. Journal of Fungi. 2018;4(4). https://doi.org/10.3390/jof4040123
36. Ayuda-Durán B, González-Manzano S, González-Paramás AM, Santos-Buelga C. *Caernohabditis elegans* as a model organism to evaluate the antioxidant effects of phytochemicals. Molecules. 2020;25(14). https://doi.org/10.3390/molecules25143194
37. Van Pelt KM, Truttmann MC. *Caenorhabditis elegans* as a model system for studying aging-associated neurodegenerative diseases. Translational Medicine of Aging. 2020;4:60–72. https://doi.org/10.1016/j.tma.2020.05.001
38. Bouyanfif A, Jayarathne S, Koboziev I, Moustaid-Moussa N. The nematode *Caenorhabditis elegans* as a model organism to study metabolic effects of ω-3 polyunsaturated fatty acids in obesity. Advances in Nutrition. 2019;10(1):165–178. https://doi.org/10.1093/advances/nmy059
39. Wang C, Xia C, Zhu Y, Zhang H. Innovative fluorescent probes for in vivo visualization of biomolecules in living *Caenorhabditis elegans*. Cytometry Part A. 2021;99(6):560–574. https://doi.org/10.1002/cyto.a.24325
40. Sandhof CA, Hoppe SO, Tittelmeier J, Nussbaum-Krammer C. *C. elegans* models to study the propagation of prions and prion-like proteins. Biomolecules. 2020;10(8). https://doi.org/10.3390/biom10081188
41. Hunt PR. The *C. elegans* model in toxicity testing. Journal of Applied Toxicology. 2017;37(1):50–59. https://doi.org/10.1002/jat.3357
42. Martel J, Wu C-Y, Peng H-H, Ko Y-F, Yang H-C, Young JD, *et al.* Plant and fungal products that extend lifespan in *Caenorhabditis elegans*. Microbial Cell. 2020;7(10):255–269. https://doi.org/10.15698/mic2020.10.731
43. Backes C, Martinez-Martinez D, Cabreiro F. *C. elegans*: A biosensor for host-microbe interactions. Lab Animal. 2021;50(5):127–135. https://doi.org/10.1038/s41684-021-00724-z
44. Ma L, Zhao Y, Chen Y, Cheng B, Peng A, Huang K. *Caenorhabditis elegans* as a model system for target identification and drug screening against neurodegenerative diseases. European Journal of Pharmacology. 2018;819:169–180. https://doi.org/10.1016/j.ejphar.2017.11.051
45. Liang JJH, McKinnon IA, Rankin CH. The contribution of *C. elegans* neurogenetics to understanding neurodegenerative diseases. Journal of Neurogenetics. 2020;34(3–4):527–548. https://doi.org/10.1080/01677063.2020.1803302
46. Keith Blackwell T, Sewell AK, Wu Z, Han M. TOR signaling in *Caenorhabditis elegans* development, metabolism, and aging. Genetics. 2019;213(2):329–360. https://doi.org/10.1534/genetics.119.302504

47. Fedorova AM, Dmitrieva AI, Dyshlyuk LS. Cultivation of wild medicinal plants of the SFD *in vitro* to accumulate the potential geroprotectors. Scientific Works of the North Caucasus Federal Scientific Center of Horticulture, Viticulture, Winemaking. 2020;30:134–138. (In Russ.). https://doi.org/10.30679/2587-9847-2020-30-134-138

48. Baranenko D, Bespalov V, Nadtochii L, Shestopalova I, Chechetkina A, Lepeshkin A, *et al.* Development of encapsulated extracts on the basis of meadowsweet (*Filipendula ulmaria*) in the composition of functional foods with oncoprotective properties. 2019;17(5):1829–1838. https://doi.org/10.15159/ar.19.155

49. Bespalov VG, Alexandrov VA, Vysochina GI, Kostikova VA, Semenov AL, Baranenko DA. Inhibitory effect of Filipendula ulmaria on mammary carcinogenesis induced by local administration of methylnitrosourea to target organ in rats. Anti-Cancer Agents in Medicinal Chemistry. 2018;18(8):1177–1183. https://doi.org/10.2174/1871520618666180402125913

50. Shaldayeva TM, Vysochina GI, Kostikova VA. Phenolic compounds and antioxidant activity of some species of the genus *Filipendula* Mill. (Rosaceae). Proceedings of Voronezh State University. Series: Chemistry. Biology. Pharmacy. 2018;(1):204–212. (In Russ.).

51. Kurkin VA, Sazanova KN, Zaitseva EN, Sharipova SKh, Pravdivtseva OE, Avdeeva EV, *et al.* Antidepressant activity of flavonoids and thick extract from *Filipendula ulmaria* fruit. Pharmaceutical Chemistry Journal. 2020;54(8): 797–799. https://doi.org/10.1007/s11094-020-02276-x

52. Adamczak A, Ożarowski M, Karpiński TM. Antibacterial activity of some flavonoids and organic acids widely distributed in plants. Journal of Clinical Medicine. 2020;9(1). https://doi.org/10.3390/jcm9010109

53. Satari A, Ghasemi S, Habtemariam S, Asgharian S, Lorigooini Z. Rutin: A flavonoid as an effective sensitizer for anticancer therapy; insights into multifaceted mechanisms and applicability for combination therapy. Evidence-based Complementary and Alternative Medicine. 2021;2021. https://doi.org/10.1155/2021/9913179

54. Wang C, Shang S, Zheng X, Lei P, Han J, Yuan L, *et al.* Fluorescent sensors based on Cu-doped carbon quantum dots for the detection of rutin. Journal of the Brazilian Chemical Society. 2019;30(5):988–996. https://doi.org/10.21577/0103-5053.20180245

55. Negahdari R, Bohlouli S, Sharifi S, Maleki Dizaj S, Rahbar Saadat Y, Khezri K, *et al.* Therapeutic benefits of rutin and its nanoformulations. Phytotherapy Research. 2021;35(4):1719–1738. https://doi.org/10.1002/ptr.6904

56. Singh SK, Srivastav S, Castellani RJ, Plascencia-Villa G, Perry G. Neuroprotective and antioxidant effect of *Ginkgo biloba* extract against AD and other neurological disorders. Neurotherapeutics. 2019;16(3):666–674. https://doi.org/10.1007/s13311-019-00767-8

57. Priyanka A, Sindhu G, Shyni GL, Preetha Rani MR, Nisha VM, Raghu KG. Bilobalide abates inflammation, insulin resistance and secretion of angiogenic factors induced by hypoxia in 3T3-L1 adipocytes by controlling NF-κB and JNK activation. International Immunopharmacology. 2017;42:209–217. https://doi.org/10.1016/j.intimp.2016.11.019

58. Eisvand F, Razavi BM, Hosseinzadeh H. The effects of *Ginkgo biloba* on metabolic syndrome: A review. Phytotherapy Research. 2020;34(8):1798–1811. https://doi.org/10.1002/ptr.6646

59. Patel RV, Mistry BM, Shinde SK, Syed R, Singh V, Shin H-S. Therapeutic potential of quercetin as a cardiovascular agent. European Journal of Medicinal Chemistry. 2018;155:889–904. https://doi.org/10.1016/j.ejmech.2018.06.053

60. Li X, Zhou N, Wang J, Liu Z, Wang X, Zhang Q, *et al.* Quercetin suppresses breast cancer stem cells ($CD44^+/CD24^-$) by inhibiting the PI3K/Akt/mTOR-signaling pathway. Life Sciences. 2018;196:56–62. https://doi.org/10.1016/j.lfs.2018.01.014

61. Bahadır HM, Sarıgöz T, Topuz Ö, Sevim Y, Ertan T, Sarıcı İŞ. Protective effects of quercetin on hepatic ischemia-reperfusion injury. Istanbul Medical Journal. 2018;19(1):47–51. https://doi.org/10.5152/imj.2017.72325

62. Kashyap D, Sharma A, Tuli HS, Sak K, Punia S, Mukherjee TK. Kaempferol – A dietary anticancer molecule with multiple mechanisms of action: Recent trends and advancements. Journal of Functional Foods. 2017;30:203–219. https://doi.org/10.1016/j.jff.2017.01.022

63. Zhao T, Tang H, Xie L, Zheng Y, Ma Z, Sun Q, *et al. Scutellaria baicalensis* Georgi.(Lamiaceae): a review of its traditional uses, botany, phytochemistry, pharmacology and toxicology. Journal of Pharmacy and Pharmacology. 2019;71(9):1353–1369. https://doi.org/10.1111/jphp.13129

64. Wang Z-L, Wang S, Kuang Y, Hu Z-M, Qiao X, Ye M. A comprehensive review on phytochemistry, pharmacology, and flavonoid biosynthesis of *Scutellaria baicalensis*. Pharmaceutical Biology. 2018;56(1):465–484. https://doi.org/10.1080/13880209.2018.1492620

65. Liao H, Ye J, Gao L, Liu Y. The main bioactive compounds of *Scutellaria baicalensis* Georgi. for alleviation of inflammatory cytokines: A comprehensive review. Biomedicine and Pharmacotherapy. 2021;133. https://doi.org/10.1016/j.biopha.2020.110917

66. Antonescu A-I, Miere F, Fritea L, Ganea M, Zdrinca M, Dobjanschi L, *et al.* Perspectives on the combined effects of *Ocimum basilicum* and *Trifolium pratense* extracts in terms of phytochemical profile and pharmacological effects. Plants. 2021;10(7). https://doi.org/10.3390/plants10071390

67. Egan LM, Hofmann RW, Seguin P, Ghamkhar K, Hoyos-Villegas V. Pedigree analysis of pre-breeding efforts in *Trifolium* spp. germplasm in New Zealand. BMC Genet. 2020;21(1). https://doi.org/10.1186/s12863-020-00912-9

68. Kubes J, Skalicky M, Tumova L, Martin J, Hejnak V, Martinkova J. Vanadium elicitation of *Trifolium pretense* L. cell culture and possible pathways of produced isoflavones transport across the plasma membrane. Plant Cell Reports. 2019;38(5):657–671. https://doi.org/10.1007/s00299-019-02397-y

69. Wang G, Wang J, Liu W, Nisar MF, El-Esawi MA, Wan C. Biological activities and chemistry of triterpene saponins from *Medicago* species: An update review. Evidence-based Complementary and Alternative Medicine. 2021;2021. https://doi.org/10.1155/2021/6617916

70. Sharma P, Kumar V, Guleria P. Naringin: Biosynthesis and pharmaceutical applications. Indian Journal of Pharmaceutical Sciences. 2019;81(6): 988–999. https://doi.org/10.36468/pharmaceutical-sciences.596

71. Bhia M, Motallebi M, Abadi B, Zarepour A, Pereira-Silva M, Saremnejad F, *et al.* Naringenin nano-delivery systems and their therapeutic applications. Pharmaceutics. 2021;13(2). https://doi.org/10.3390/pharmaceutics13020291

72. Salehi B, Mishra AP, Shukla I, Sharifi-Rad M, Contreras MDM, Segura-Carretero A, *et al.* Thymol, thyme, and other plant sources: Health and potential uses. Phytotherapy Research. 2018;32(9):1688–1706. https://doi.org/10.1002/ptr.6109

73. Abbaszadeh S, Teimouri H, Farzan B. An ethnobotanical study of medicinal plants with antianxiety and antidepressant effects in Shahrekord. Egyptian Journal of Veterinary Sciences. 2019;50(1):81–87.

74. Seo DY, Lee SR, Heo J-W, No M-H, Rhee BD, Ko KS, *et al.* Ursolic acid in health and disease. Korean Journal of Physiology and Pharmacology. 2018;22(3):235–248. https://doi.org/10.4196/kjpp.2018.22.3.235

75. Mlala S, Oyedeji AO, Gondwe M, Oyedeji OO. Ursolic acid and its derivatives as bioactive agents. Molecules. 2019;24(15). https://doi.org/10.3390/molecules24152751

76. Bijttebier S, Van Der Auwera A, Voorspoels S, Noten B, Hermans N, Pieters L, *et al.* A first step in the quest for the active constituents in *Filipendula ulmaria* (meadowsweet): Comprehensive phytochemical identification by liquid chromatography coupled to quadrupole-orbitrap mass spectrometry. Planta Medica. 2016;82(6):559–572. https://doi.org/10.1055/s-0042-101943

77. Budeč M, Bošnir J, Racz A, Lasić D, Brkić D, Mosović Ćuić A, *et al.* Verification of authenticity of Ginkgo biloba L. Leaf extract and its products present on the Croatian market by analysis of quantity and ratio of ginkgo flavone glycosides (quercetin, kaempferol and isorhamnetin) to terpene trilactones to the effect of unmasking counterfeit drugs endangering patient health. Acta Clinica Croatica. 2019;58(4):672–692. https://doi.org/10.20471/acc.2019.58.04.15

78. Boyko NN, Pisarev DI, Zhilyakova ET, Maljutina AYu, Novikov OO, Bocharnikova MA. Study of baicalin hydrolysis kinetics in the process of its extraction from Scutellaria baicalensis Georgi roots. Pharmacy and Pharmacology. 2019;7(3):129–137. (In Russ.). https://doi.org/10.19163/2307-9266-2019-7-3-129-137

79. Lay H-L, Chen C-C, Chiang S-T. Simultaneous analysis of nine components in "Byi-Liang-Tang" preparation by high performance liquid chromatography. Journal of Food and Drug Analysis. 2004;12(2):115–119. https://doi.org/10.38212/2224-6614.2654

80. Dyshlyuk LS, Fedorova AM, Loseva AI, Eremeeva NI. Callus cultures of *Thymus vulgaris* and *Trifolium pratense* as a source of geroprotectors. Food Processing: Techniques and Technology. 2021;51(2):423–432. https://doi.org/10.21603/2074-9414-2021-2-423-432

81. Chen XM, Wang FF, Wang YQ, Li XL, Wang AR, Wang CL, *et al.* Discrimination of the rare medicinal plant *Dendrobium officinale* based on naringenin, bibenzyl, and polysaccharides. Science China Life Sciences. 2012;55(12):1092–1099. https://doi.org/10.1007/s11427-012-4419-3

82. Shimada A, Ueno H, Inagaki M. Glutaminase inhibitory activities of pentacyclic triterpenes isolated from *Thymus vulgaris* L. Natural Product Research. 2021;36(11):1864–2868. https://doi.org/10.1080/14786419.2021.1921766

83. Fedorova YuS, Sukhikh AS, Suslov NI, Zakhar YuV, Soboleva OM. Chromatography of hedysarum extracts on modified Sepharose CL sorbents. Fundamental and Clinical Medicine. 2019;4(3):61–67. (In Russ.). https://doi.org/10.23946/2500-0764-2019-4-3-61-67

ORCID IDs
Elizaveta R. Faskhutdinova https://orcid.org/0000-0001-9711-2145
Andrey S. Sukhikh https://orcid.org/0000-0001-9300-5334
Violeta M. Le https://orcid.org/0000-0002-9546-6633
Varvara I. Minina https://orcid.org/0000-0003-3485-9123
Mohammed El Amine Khelef https://orcid.org/0000-0002-9371-7670
Anna I. Loseva https://orcid.org/0000-0003-4037-2653

Foods and Raw Materials. 2022;10(2)

ISSN 2310-9599 (Print)
ISSN 2308-4057 (Online)

Research Article
Open Access

Available online at http://jfrm.ru/en
https://doi.org/10.21603/2308-4057-2022-2-545
https://elibrary.ru/WKBLBM

Synergistic effect of *Balanites aegyptiaca* essential oil and storage materials on cowpea seeds

Feyisola F. Ajayi*, Akama F. Ogori, Vivien O. Orede, Emmanuel Peter

A Federal University Gashua, Gashua, Nigeria

* e-mail: Feyisola.ajayi@yahoo.com

Received 23.03.2022; Revised 25.04.2022; Accepted 04.05.2022; Published online 23.09.2022

Abstract:
The cowpea (*Vigna unguiculata* L.) is a legume produced and consumed all over Africa and especially in Nigeria. These beans are a major source of protein in the region. The cowpea weevil (*Callosobruchus maculatus* L.) is a major pest that affects cowpea seeds. Therefore, cowpea farmers need effective non-toxic pesticides to replace synthetic chemicals. The present research tested the effect of *Balanites aegyptiaca* L. essential oil on cowpea weevils.

This research quantified weevil proliferation and cowpea seed qualities. The samples were treated with 5, 10, and 15 mL of *B. aegyptiaca* essential oil diluted in 1 mL of acetone and stored in five storage materials, i.e., jute bags, polythene bags, sacks, plastic containers, and glass bottles. The study featured a completely randomized design with three replications of each treatment: treatment time – 90 days, storage temperature – 30 ± 5°C, check – 0.125 g of aluminum phosphide, control – acetone.

B. aegyptiaca essential oil proved to be an effective insecticide against cowpea weevils. The treatment achieved 100% mortality rate at 10 and 15 mL of *B. aegyptiaca* essential oil after 72 h of exposure in glass bottles, plastic containers, and jute bags. In addition, *B. aegyptiaca* essential oil demonstrated a potent activity against oviposition and survival of immature cowpea weevils. Cowpea seeds packaged in glass bottles, plastics containers, and jute bags showed significantly less damage than those stored in sacks and polythene bags. Glass bottles were the best storage material in terms of safety and shelf stability, followed by plastic containers and jute bags.

B. aegeptica essential oil has potent insecticidal properties and can be used as pest control during grain storage.

Keywords: Essential oil, *Callosobruchus maculatus*, *Vigna unguiculata*, storage, storage material

Funding: This work was supported by the Tertiary Education Trust Fund (TETFUND) through Institutional Based Research (IBR) in Tertiary Institution by Federal Government of Nigeria awarded to the chief researcher Feyisola Ajayi.

Please cite this article in press as: Ajayi FF, Ogori AF, Orede VO, Peter E. Synergistic effect of *Balanites aegyptiaca* essential oil and storage materials on cowpea seeds. Foods and Raw Materials. 2022;10(2):353–364. https://doi.org/10.21603/2308-4057-2022-2-545

INTRODUCTION

The cowpea, *Vigna unguiculata* (L.), is a legume of the *Fabaceae* family. It is one of the most important legume crops in the world. The plant thrives in temperate climate and requires little agricultural inputs for growth [1]. Cowpeas are popular and cheap in many developing countries. In Nigeria, for instance, they are a major staple crop. Small-holder farmers are the major producer of cowpea grains in Nigeria [2].

Cowpeas serve as a rich and affordable source of nutrients, especially protein, in sub-Saharan Africa and some parts of America and Asia [3]. Cowpea beans can be cooked, powdered, germinated, or even used as part of a weaning formula. As a dish, they complement tubers and cereals. Consequently, cowpea grains are present in the diet of many developing countries where population suffers from malnutrition and protein deficiencies.

Cowpeas are mainly cultivated by the local farmers for profits and satisfy the basic nutritional needs of the local population. However, farmers fail to meet the local demand as a result of drastic post-harvest losses caused by insects and other pests. In fact, these losses are considered as one of the underlying causes of food scarcity and poverty [4].

Insects damage cowpea grains by boring holes, thus causing weight loss, poor quality, and low market value Cowpea aphids (*Aphis craccivora* L.), leafhoppers

(*Empoasca* spp.), cowpea weevils (*Callosobruchus maculatus*), and witch-weed (*Striga gesnerioides*) are the main insect species that feed on cowpea seeds [5, 6].

Callosobruchus maculatus is the main pest that causes losses in cowpea grains. *C. maculatus* is a field-to-store pest that typically begins in the field, and the level of prior-harvest infestation determines the extent of damage to stored grains [7]. A range of insect pest control measures have been adopted over decades to reduce the prevalence of cowpea grain loss in the field and during storage.

According to Ogunfowokan *et al.*, Nigerian farmers use Lindane (Gammalin 20EC), Dichlorvos dichlorodiphenyltrichloroethane (DDT), Chlorpyrifos, Endosufan, and Aldrin to prevent pest infestation [8]. Synthetic chemicals are very effective in preserving grains and increasing their production yield. However, they have major drawbacks as improper use often results in environmental pollution, pesticide residue in food, and toxic poisoning of the ecosystem [9]. Hence, several attempts have been made to test pesticides that are environmentally friendly, harmless to people, and inexpensive.

Resourceful African farmers tried to use such natural preservatives as plant powder, ashes, and cow dung. Several authors have documented the insecticidal efficacy of plant products on different types of pests [10]. In fact, plant products with aromatic properties are known to prevent insect infestation of stored cowpeas [11]. Ikbal and Pavela made an extensive research to assess the use of aromatic plants as pesticides during storage [12]. They reported that essential oils of plant origin could serve as botanical insecticides as they contain a lot of bioactive compounds with insecticidal, nematicidal, larvicidal, and anti-feedant properties that inhibit insect oviposition [13, 14]. Essential oils are natural derivatives from aromatic plants which contain volatile and phenolic compounds with unique flavors. Several works have reported the insecticidal effect of essential oils during grain storage [15–19].

Balanites aegyptiaca fruits have quite a number of bioactive compounds with various medicinal properties [20]. The essential oil extracted from *B. aegyptiaca* possesses anticancer, antimicrobial, antioxidant, anticarcinogenic, antidiabetic, antifeedant, and antiviral activities [21, 22]. Natural fumigants developed from plants do not threaten the ecosystem. Insecticides based on essential oils are sold all over the world, but their production does not exceed 5% [23]. In Asia, Europe, and North America, natural extracts have been used as insecticides for more than a century, much longer than any synthetic insecticides.

Previous studies have investigated the insecticidal efficacy of oil extracted from *B. aegyptiaca*. For instance, Mokhtar *et al.* reported a strong effect of *B. aegyptiaca* seed oil on the mortality rate of red flour beetle (*Tribolium castaneum* Herbst) [17]. Similarly, Nwaogu and Yahaya investigated the insecticidal efficacy of oil extracted from *B. aegyptiaca* in stored cowpea seeds [18]. The studies provided evidence that *B. aegyptiaca* seed oil could be used as an insecticide against storage pest. However, very few publications feature the use of *B. aegyptiaca* essential oils in controlling insect infestation of stored grains.

Storage materials are also important for seed treatments and grain quality. Buleti *et al.* conducted an experiment in the Northeast of Nigeria to assess the effect of *B. aegyptiaca* oil on weevil growth in cowpea grains stored in various packing materials [15]. The present research provides some new data on using plant products as storage pesticides.

STUDY OBJECTS AND METHODS

Plant material. Fruits of *Balanites aegyptiaca* L. were acquired from the Gashua market in Yobe State, Nigeria. The fruits were authenticated at the Department of Agronomy, Faculty of Agriculture, Federal University Gashua, Nigeria.

Preparing the seeds. The mesocarp of *B. aegyptiaca* was scraped with a clean sharp knife and dried in an oven at 45°C for 24 h to reduce stickiness. The endocarp was broken down with a hammer to obtain seeds. Then, the seeds were dried to constant weight in an airtight oven (45°C, 72 h). Subsequently, the seeds were milled into fine particles using an electric blender and stored in zip lock bags.

Extracting *B. aegyptiaca* essential oil. The method developed by Nguefack *et al.* was used to extract essential oil from *B. aegyptiaca* seeds [24]. The experiment began by placing 500 g of pulverized seeds of *B. aegyptiaca* in a 5 L flask. After that, distilled water was added to cover the sample. Essential oil was obtained by hydrodistillation using a modified Clevenger-type apparatus at normal atmospheric pressure and 96–97°C for 4 h. The resulting essential oil was collected by drying it out with anhydrous sodium sulfate and kept at 4°C in Eppendorf tubes until the gas chromatography-mass spectrometry (GC/MS) analysis.

Evaluating the effect of *B. aegyptiaca* essential oil against *Callosobruchus maculatus*.

Experimental site. The experiment was carried out in the Agronomy Laboratory of the Department of Agriculture, Federal University, Gashua, after the growing season of 2021.

Experimental design and treatment. The research involved five storage materials (jute bags, polythene bags, sacks, plastic containers, and glass bottles), experimental samples (5, 10, and 15 mL of *B. aegyptiaca* essential oil diluted in 1 mL of acetone), a check sample (with 0.125 g of aluminum phosphide), and control (acetone). The experiment was laid out in a completely randomized design with three replications of each treatment.

Insect culture: source and rearing. *C. maculatus* was first cultured from a cowpea seed infested at the local market in Gashua. Weevils multiplied in fresh and

previously uninfested cowpea varieties in the laboratory at an ambient temperature (27–30°C) and relative humidity (70–75%).

Treatment and maintenance of cowpea seeds. Forty kilograms of pristine cowpea seeds was purchased directly from the local farmers in Gashua, immediately after harvest. To destroy and/or prevent any initial infection, they were placed in a plastic container and maintained in the freezer below 0°C for five days. After that, the seeds were taken out of the freezer and placed on a laboratory bench, covered with a screen, and left to equilibrate for 72 h [25].

Adult mortality of C. maculatus. Mortality contact effect of *B. agyptiaca* essential oil on adult *C. maculatus* was determined using the method developed by Obeng *et al.* [26]. According to the procedure, 200 g of cowpea seeds was held in different storage materials and then thoroughly mixed with: (a) 5, 10, and 15 mL of essential oil diluted in 1 mL of acetone; (b) 0.125 g of aluminum phosphide; and (c) acetone (control). After that, the storage materials were left open for 2 h at room temperature to disperse acetone. Thereafter, 20 unsexed pairs (10 males and 10 females) of three-day-old *C. maculatus* beetles were introduced into the storage materials. They were kept on laboratory benches. Dead insects were counted after 24, 48, and 72 h after infestation using Abbott's equation [27]. To confirm mortality, insects were probed three times with a sharp pin [28]. The data were subjected to Probit analysis [29].

Oviposition. For this part of the experiment, 100 g of cowpea seeds was held in the varying storage materials and thoroughly mixed with 5, 10, and 15 mL of essential oil diluted in 1 mL of acetone, 0.125 g of aluminum phosphide, and control (acetone). After that, 10 males and 10 females of three-day-old newly sexed *C. maculatus* beetles were introduced into the storage materials, where they paired and laid eggs. Following egg deposition, 100 seeds were randomly selected on days 7, 30, 60, and 90, and the number of eggs deposited on the cowpea seeds was counted and recorded in each treatment and replicate [30].

Egg hatchability. At this stage, 100 g of cowpea seeds was infested with 20 (10 males and 10 females) sexed pairs of five-to-seven-day-old *C. maculatus* beetles in a transparent plastic container. The insects paired and laid eggs for six days. After oviposition, 100 seeds (27 g) bearing eggs were chosen and placed in various storage materials that contained pure and uninfested cowpea seeds (73 g). They were thoroughly mixed with 5, 10, and 15 mL of essential oil diluted in 1 mL of acetone, 0.125 g of aluminum phosphide, and control (acetone).

In each treatment and replicate, the cowpea seeds were stored on the laboratory bench until adult beetles emerged. The number of emerged adults was recorded on days 30, 60, and 90 after the exposure. The percentage of adult emergence was calculated conversely from each of the treatments and replicates according to the method developed by Adesina and Ofuya [31], with a slight modification (1):

$$\text{Egg hatching} = \frac{Number\ of\ progeny\ emerged}{Number\ of\ eggs\ in\ treatment} \times 100 \quad (1)$$

Seed perforation. This test included 100 g of cowpea seeds held in the varying storage materials and thoroughly mixed with 5, 10, and 15 mL of essential oil, 0.125 g of aluminum phosphide, and control (acetone). After that, 10 pairs of three-day-old newly sexed *C. maculatus* beetles were introduced into the storage materials and kept in the laboratory for 90 days. Every four weeks for three months, the number of exit holes was assessed by counting in each seed from a random sample of 100 seeds.

The weevil perforation index (WPI), which measured the protective ability of the storage material, was calculated according to standard methods. If the weevil perforation index was ≥ 50%, it indicated an increase in weevil infestation or a low efficacy of the plant material. To obtain the percent protection ability (PPA), the weevil perforation index was subtracted from 100 using the following equation (2):

$$\text{WPI} = \frac{Percent\ of\ infested\ seeds}{Percent\ of\ infested\ seeds + Percent\ of\ infested\ Seeds\ in\ Control} \times 100 \quad (2)$$

where WPI is the weevil perforation index; WPI > 50 is the negative protectant of plant material, i.e., low anti-weevil activity; WPI < 50 is the positive protectant, i.e., high anti-weevil activity.

Seed weight loss. To calculate the seed weight loss, 100 g of cowpea seeds was randomly selected after 30, 60, and 90 days of storage. To obtain the final seed weight for the sample, all dead insects and other debris in the cowpea seeds were removed, and the cowpea seeds were weighed. As described by Sibakwe and Donga [32], the percentage of seed weight loss was calculated using the following equation (3):

$$\text{Weight loss} = \frac{Initial\ seed\ weight\ of\ cowpea\ seeds - Final\ seed\ weight}{Initial\ weight\ of\ cowpea\ seed\ sample} \times 100 \quad (3)$$

Seed damage. After 30, 60, and 90 days of storage, 100 g of cowpea seeds were randomly selected from the lots. We divided seeds into two groups, damaged and undamaged, and counted seeds with exit holes. Adenekan *et al.* [30] described how to quantify the percentage of damaged seed using the following equation (4):

$$\text{Seed damage} = \frac{Number\ of\ seeds\ damaged}{Total\ number\ of\ seeds} \times 100 \quad (4)$$

Seed germinability. After the storage period, 15 seeds were randomly picked from the various storage materials to test the effect of the essential oil concentrations on the germinability of cowpea seeds. A seed from each treatment was placed in 9-cm Petri dishes with moistened Whatman filter paper on laboratory benches at room temperature (27–30°C) and relative humidity (70–75%) [33]. Each treatment was triplicated. To avoid contamination, the seeds were watered (23 mL) twice a day (morning and evening) with distilled water from a wash bottle. According to Olisa *et al.* [34], the germination percentage of cowpea seeds was estimated from germination data on day 7 after sowing according to the following equation (5):

$$\text{Germination percentage} = \frac{Number\ of\ emerged\ seedlings\ at\ the\ final\ count}{Total\ number\ of\ seeds\ planted} \times 100 \quad (5)$$

Data analysis. Natural mortality in the control samples was corrected using Abbott's formula [27]. The acquired numerical data was square root transformed $\sqrt{n+1}$, and the adjusted mortality and other data in percentages was transformed *arc sine* before being subjected to the analysis of variance using JMP 13 Computer Software (2016). The Student Newman-Keuls (SNK) test was used to differentiate significant treatment means at the 5% level of probability. With the SPSS statistical software (version 19), the data were subjected to a two-way analysis of variance (ANOVA) at the 5 % significance level, and Duncan's Multiple Range Test was used to separate the means.

RESULTS AND DISCUSSION

Mortality of *Callosobruchus maculatus* L. exposed to *Balanites aegyptiaca* L. essential oil stored in different storage materials after 24, 48, and 72 h. The treatment under discussion provided appropriate protection to cowpea seeds against *C. maculatus*. Table 1 shows the effect of *B. aegyptiaca* oil extract and such storage materials as jute bags, polythene bags, sacks, plastic containers, and glass bottles on cowpea weevil mortality.

The experiment showed a statistically significant correlation between the effects of *B. aegyptiaca* essential oil and storage materials ($F(16,75) = 41.813$, $P = 0.000$) after 24 h of exposure. A simple main effect analysis showed that *B. aegyptiaca* essential oil had a statistically significant effect on mortality of cowpea weevils at 24, 48, and 72 h, respectively ($P < 0.000$).

Glass bottles, plastic containers, and jute bags proved to be the most effective storage material, while samples stored in polythene bags had the lowest beetle mortality rate at all the *B. aegyptiaca* essential oil concentrations. Our results confirmed those obtained by Buleti *et al.*, who reported a higher weevil mortality rate in grains stored in glass bottles compared to other storage materials [15]. On the other hand, the results can be explained by the techno-functional properties of the storage materials, e.g., water vapor permeability, the interaction between the plant extracts and the material, etc. [35]. Thus, such vapor proof containers as glass bottles, plastic containers, and jars can provide good insulation against weevils, thereby inhibiting their survival: insects suffocate as soon as they run out of oxygen.

In addition, the abrasive effect and contact toxicity of essential oils on the pest cuticle interferes with insect respiratory mechanism, thereby causing a knock down effect. This study is similar to the research conducted by Karimzadeh *et al.*, who reported that the abrasive effects of combined insecticides may cause abrasion of insect cuticle and dehydration of the insect body, thus leading to insect mortality [36].

Evidently, the *B. aegyptiaca* essential oil treatments had a noticeable effect on the population growth rate and mortality of the weevils. Low quantity of the essential oil (5 mL) resulted in a lower mortality rate, while high quantities (15 mL) provided the highest mortality rate, irrespective of the storage material used.

Similarly, the population of the weevils decreased as the treatment intervals progressed from 24 to 72 h. For instance, at the same essential oil dose, plastic containers and glass bottles caused 62.5 and 70% mortality rate, respectively, after 24 h. Likewise, 80 and 90% mortality rate were recorded after 48 h. However, 100% mortality was recorded for glass bottles, plastic containers, and jute bags after 72 h. Most importantly, all the three doses and storage materials showed high mortality rates of *C. maculatu*s after 72 h of exposure, if compared to the control samples.

The insecticidal efficacy of *B. aegyptiaca* essential oil could be attributed to such active compounds as hexadecanoic acid, (9*Z*,12*Z*)-octadeca-9,12-dienoic acid, (*Z*)-octadec-9-enoic acid, ethyl hexadecanoate, 3,3-dihydroxypropyl hexadecanoate, and methyl hexadecanoate. All these compounds have been reported to possess repellent and insecticide activities [17]. This result confirms the findings obtained by Mokhtar *et al.*, who observed 100% mortality of *C. maculatus* after 24 h on cowpeas treated with chloroform extract of *B. aegyptiaca* seeds at 1.131 mg·cm^{-2} [17]. Various studies have also demonstrated the insecticidal effect of *B. aegyptiaca* essential oil against such pests as *C. maculatus*, *Tribolium casteneum*, and khapra beetle [17,18].

In our research, various doses of *B. aegyptiaca* essential oil and storage materials provided an excellent protection against *C. maculatus*, both independently and synergistically. *B. aegyptiaca* essential oil extract had a substantial impact on the longevity and survival of cowpea weevils. In addition, glass bottles, plastic containers, and jute bags caused 100% mortality at the highest dose (15 mL) after 72 h of exposure.

Table 1 Mortality of cowpea weevils exposed to *Balanites aegyptiaca* oil extract in different storage materials after 24, 48, and 72 h

Samples	Storage materials	Mortality ± SE, %		
		24 h	48 h	72 h
Balanites aegyptiaca essential oil (5 mL)	Glass bottle	20.00 ± 0.00	46.50 ± 4.79	90.00 ± 0.00
	Jute bag	12.50 ± 5.00	25.00 ± 4.08	70.00 ± 0.00
	Plastic container	20.00 ± 0.00	60.00 ± 0.00	61.20 ± 2.50
	Polythene bag	10.00 ± 0.00	25.00 ± 0.00	60.00 ± 0.00
	Sack bag	10.00 ± 0.00	30.00 ± 0.00	75.00 ± 0.00
Balanites aegyptiaca essential oil (10 mL)	Glass bottle	40.00 ± 0.00	65.00 ± 5.77	100.00 ± 0.00
	Jute bag	30.00 ± 0.00	60.00 ± 0.00	83.60 ± 2.50
	Plastic container	35.00 ± 0.00	75.00 ± 0.00	90.00 ± 0.00
	Polythene bag	23.70 ± 2.50	42.00 ± 5.00	70.00 ± 0.00
	Sack bag	32.50 ± 2.89	50.00 ± 0.00	90.00 ± 0.00
Balanites aegyptiaca essential oil (15 mL)	Glass bottle	70.00 ± 0.00	80.00 ± 0.00	100.00 ± 0.00
	Jute bag	50.00 ± 0.00	70.00 ± 0.00	100.00 ± 0.00
	Plastic container	62.50 ± 2.89	90.00 ± 0.00	100.00 ± 0.00
	Polythene bag	32.50 ± 2.89	55.00 ± 0.00	80.00 ± 0.00
	Sack bag	55.00 ± 0.00	70.00 ± 0.00	97.50 ± 5.00
Aluminum phosphide	Glass bottle	90.00 ± 0.00	100.00 ± 0.00	100.00 ± 0.00
	Jute bag	81.20 ± 2.50	90.00 ± 0.00	100.00 ± 0.00
	Plastic container	90.00 ± 0.00	100.00 ± 0.00	100.00 ± 0.00
	Polythene bag	85.00 ± 4.08	90.00 ± 0.00	95.00 ± 5.77
	Sack bag	90.00 ± 0.00	100.00 ± 0.00	100.00 ± 0.00
Control (acetone)	Glass bottle	0	0	20.00 ± 0.00
	Jute bag	0	0	0
	Plastic container	0	0	02.50 ± 2.89
	Polythene bag	0	0	0
	Sack bag	0	0	0
A		$P < 0.05$	$P < 0.05$	$P < 0.05$
B		$P < 0.05$	$P < 0.05$	$P < 0.05$
AB		$P < 0.05$	$P < 0.05$	$P < 0.05$

A – essential oil; B – storage material

Oviposition of *C. maculatus* exposed to *B. aegyptiaca* essential oil stored in different storage materials after 7, 30, and 90 days of storage. Figures 1–3 show the mean value of oviposition in both treated and untreated cowpeas. The analysis of variance showed that a statistically significant correlation between the effects of *B. aegyptiaca* oil extracts and storage materials on the oviposition of cowpea weevils ($F(16,75) = 3346.73$, $P = 0.000$). When compared to the control, the treated samples showed a much lower oviposition. At a seven-day interval, all the storage materials showed the same trend in the total oviposition of cowpea weevils as the essential oil doses increased, except polythene bags (Fig. 1).

B. aegyptiaca essential oil significantly reduced the number of eggs laid by weevils. The highest amount of eggs was recorded at 5 mL, and then it significantly decreased at 10 mL. The lowest amount of eggs was registered at 15 mL. The drastic reduction in the number of eggs laid by cowpea weevils might have been caused by the toxicity of the plant material active components to the weevils rather than by the prevention of oviposition.

The previous section that the *B. aegyptiaca* essential oil caused the highest mortality rate in the experimental samples, which was associated with its insecticidal effect. The chemical composition of plant oils and their phytocompounds is known to produce a toxic and repellent effect on insects that live in stored grain [37].

Grains stored in glass bottles had the fewest eggs, while those stored in polythene bags had the maximal number of eggs. Even though polythene bags had the lowest effect on weevil oviposition, they also showed a significant reduction in the number of eggs laid compared to the untreated samples. Buleti *et al.* also reported a reduction in the number of eggs laid in glass bottles [15]. Furthermore, the experimental samples revealed just a few eggs on day 90, with a mean fecundity of 1–4 eggs for glass bottles and 1–14 eggs for plastic containers. A slightly higher value was recorded for polythene and sack bags with a mean of 18–45 and 8–30 eggs, respectively. However, the values recorded

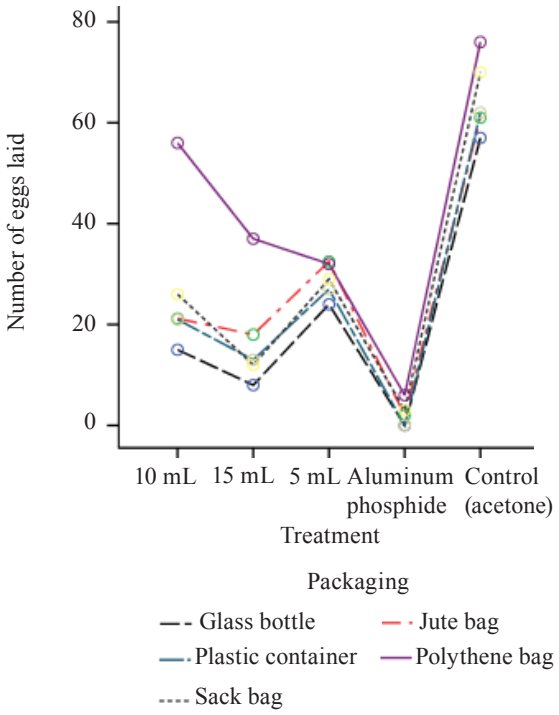

Figure 1 Effect of *Balanites aegyptiaca* on *Callosobruchus maculatus* oviposition at various treatments in different storage materials after 7 days of storage

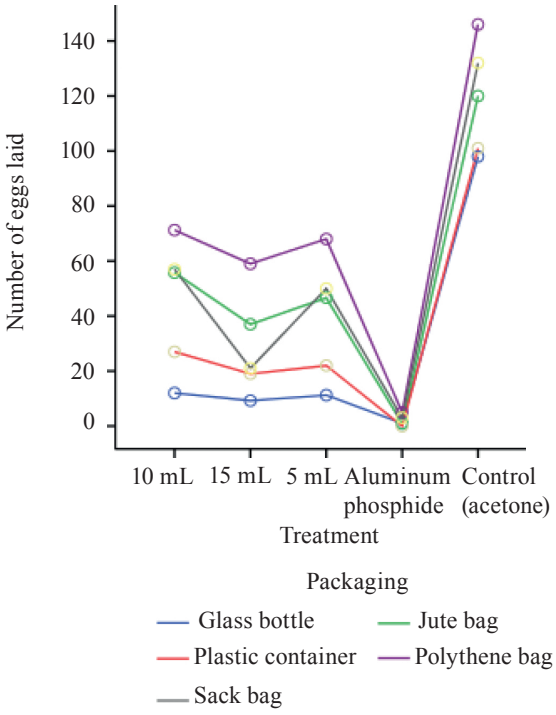

Figure 2. Effect of *Balanites aegyptiaca* on *Callosobruchus maculatus* oviposition at various treatments in different storage materials after 30 days of storage

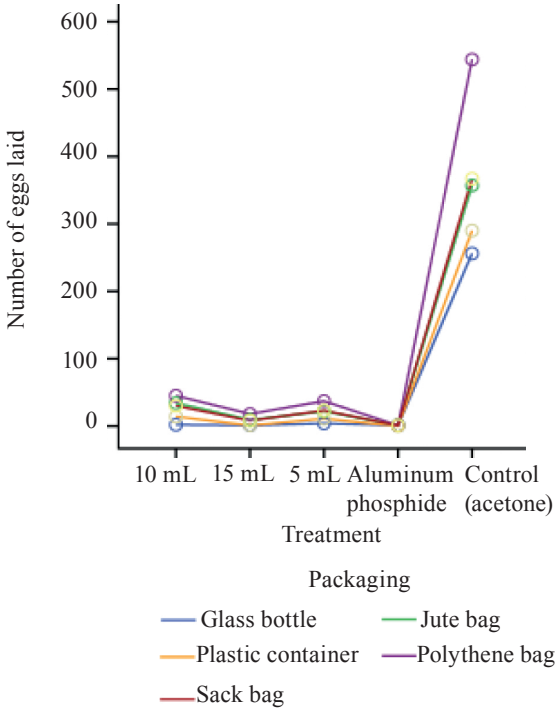

Figure 3. Effect of *Balanites aegyptiaca* on *Callosobruchus maculatus* oviposition at various treatments in different storage materials after 90 days of storage

in polythene and sack bags were lower than in the control samples with a mean fecundity of 256–544 eggs per female after 90 days, which implied a significant difference in the oviposition of treated cowpeas.

The synergic treatment of *B. aegyptiaca* essential oil and storage materials killed more than 50% of the total eggs laid at various stages of development from 7 to 90 days. Likewise, the high numbers of eggs laid in polythene and sack bags could be explained by the porous surface of these materials that allowed moisture and air circulation. Such conditions encouraged weevils present in the seed lot to lay eggs and proliferate continuously.

The lower oviposition rates observed in this study suggested that *B. aegyptiaca* essential oil could be useful as cowpea protectants. This finding confirms that made by Alves *et al.*, who discovered that lemon grass essential oil extract reduced *C. maculatus* oviposition significantly [38]. Previous studies by a Nwaogu and Yahaya and Aous *et al.* reported the effect of essential oil of *Cymbopogon schoenanthus* (L.) on the development of freshly laid eggs and newborn larvae of *C. maculatus* [18, 39]. The extract probably contained a powerful oviposition deterrent. Also, cowpea seeds that are packaged in glass bottles and plastic containers showed a low oviposition, which made them the optimal ovipositional deterrents in this study.

Egg hatchability of *C. maculatus* exposed to *B. aegyptiaca* essential oil stored in different storage materials after 24, 48, and 72 h. Table 2 shows the effect of *B. aegyptiaca* essential oil on *C. maculatus* egg development and hatchability. The main significant effect of *B. aegyptiaca* essential oil and storage materials ($P < 0.05$) was observed after 30, 60, and 90 days. Similarly, the study revealed no significant

Table 2 *Callosobruchus maculatus* egg hatchability treated with *Balanites aegyptiaca* essential oil in different storage materials after 30, 60, and 90 days of storage

Samples	Storage materials	Mean number of hatched eggs ± SE		
		30 days	60 days	90 days
Balanites aegyptiaca essential oil (5 mL)	Glass bottle	4.10 ± 0.17	2.40 ± 0.25	1.00 ± 0.00
	Jute bag	7.00 ± 0.00	4.70 ± 0.14	1.30 ± 0.08
	Plastic container	4.20 ± 0.68	3.10 ± 0.78	1.10 ± 0.03
	Polythene bag	8.60 ± 0.79	7.70 ± 0.17	5.50 ± 0.05
	Sack bag	6.40 ± 0.36	4.60 ± 0.09	1.60 ± 0.00
Balanites aegyptiaca essential oil: (10 mL)	Glass bottle	1.50 ± 0.78	1.00 ± 0.00	1.00 ± 0.00
	Jute bag	5.10 ± 0.15	3.60 ± 0.79	1.20 ± 0.02
	Plastic container	2.20 ± 0.15	1.20 ± 0.96	1.00 ± 0.01
	Polythene bag	5.40 ± 0.34	6.30 ± 0.24	3.30 ± 0.28
	Sack bag	3.20 ± 0.00	2.00 ± 0.02	1.00 ± 0.00
Balanites aegyptiaca essential oil: (15 mL)	Glass bottle	0.80 ± 0.09	1.00 ± 0.00	1.00 ± 0.00
	Jute bag	3.00 ± 0.00	2.20 ± 0.11	1.00 ± 0.00
	Plastic container	1.10 ± 0.05	1.10 ± 0.10	1.00 ± 0.00
	Polythene bag	2.90 ± 0.12	6.10 ± 0.13	1.90 ± 0.01
	Sack bag	2.90 ± 0.17	1.90 ± 0.07	1.00 ± 0.00
Aluminum phosphide	Glass bottle	0.20 ± 0.06	1.00 ± 0.00	1.00 ± 0.00
	Jute bag	1.00 ± 0.13	1.00 ± 0.00	1.00 ± 0.00
	Plastic container	1.00 ± 0.00	1.00 ± 0.00	1.00 ± 0.00
	Polythene bag	1.10 ± 0.00	1.00 ± 0.00	1.00 ± 0.00
	Sack bag	0.50 ± 0.04	1.00 ± 0.00	1.00 ± 0.00
Control (acetone)	Glass bottle	16.60 ± 0.00	20.40 ± 0.67	42.10 ± 1.14
	Jute bag	23.40 ± 0.84	27.30 ± 1.51	52.60 ± 31.1
	Plastic container	18.20 ± 0.56	21.90 ± 0.89	52.00 ± 0.04
	Polythene bag	31.30 ± 0.76	38.90 ± 0.93	72.40 ± 1.47
	Sack bag	26.80 ± 1.30	26.20 ± 0.46	66.40 ± 0.28
A		$P < 0.05$	$P < 0.05$	$P < 0.05$
B		$P < 0.05$	$P < 0.05$	$P < 0.05$
AB		$P > 0.05$	$P > 0.05$	$P > 0.05$

A – essential oil; B – storage material

($P > 0.05$) interactive effect of *B. aegyptiaca* essential oil and storage materials on *C. maculatus* egg hatchability. The results demonstrated that the productivity in the experimental samples was extremely low at all intervals and doses, with the mean values ranging from 1 to 8.6.

Hence, over 65% of the total eggs laid in the experimental samples died at different stages of development in all the trials. *B. aegyptiaca* oil extracts obviously had a strong larvicidal effect on the development of immature weevils. Similarly, the high mortality of *C. maculatus* in the experimental samples implied that the plant had some phytochemical properties, which reduced egg production [40].

Furthermore, the egg hatchability reduced as the storage interval progressed from 30 to 90 days. Among the experimental samples, the highest mean values of egg hatchability were observed in cowpeas stored in polythene bags at all the essential oil concentrations. However, the values observed in polythene bags were lower in comparison to the control samples. Therefore, the low egg hatchability was caused by the effectiveness of *B. aegyptiaca* essential oil with its poisonous component and physical properties, which affected the surface and oxygen tension of eggs.

The essential oils of *Borago officinalis*, *Melissa officinalis*, *Carapichea ipecacuanha*, and *Laurus nobilis* have also been reported to reduce hatchability [41]. Similarly, *Piper gaudichaudianum* essential oil showed a better insecticidal activity against *Lucilia cuprina* third instar larvae under laboratory conditions [42].

Weevil Perforation Index, weight loss, damage, and germinability of cowpea seeds treated with *B. aegyptiaca* essential oil stored in different storage materials after 30, 60, and 90 days. These parameters of cowpea seeds indicate its suitability for consumption and other aesthetic values because damaged seeds with holes and flour dust are not marketable. Figures 4 and 5 show the weevil perforation index for cowpea seeds treated with different concentrations of *B. aegyptiaca* essential oil packaged in different storage materials on days 30, 60, and 90.

After 30 days, the highest weevil perforation index was observed in polythene and sack bags. When compared to the control treatment, the cowpea seed treated with *B. aegyptiaca* essential oil showed a

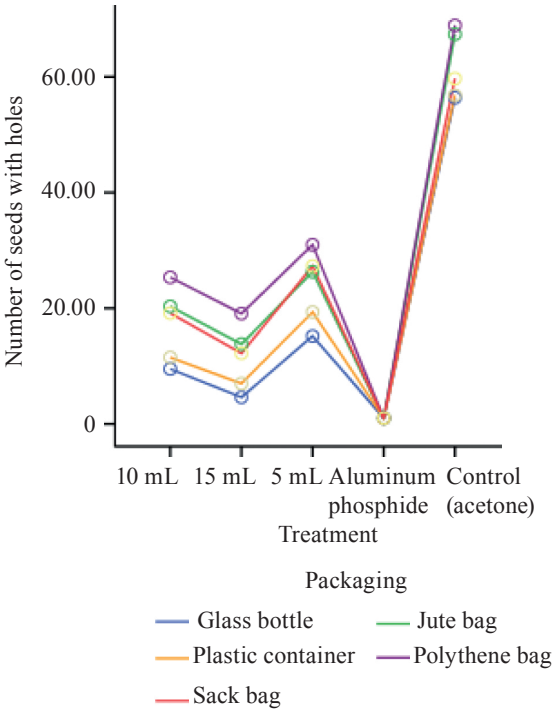

Figure 4 % Weevil perforation index of cowpea seeds treated with *Balanites aegyptiaca* in different storage materials after 30 days of storage

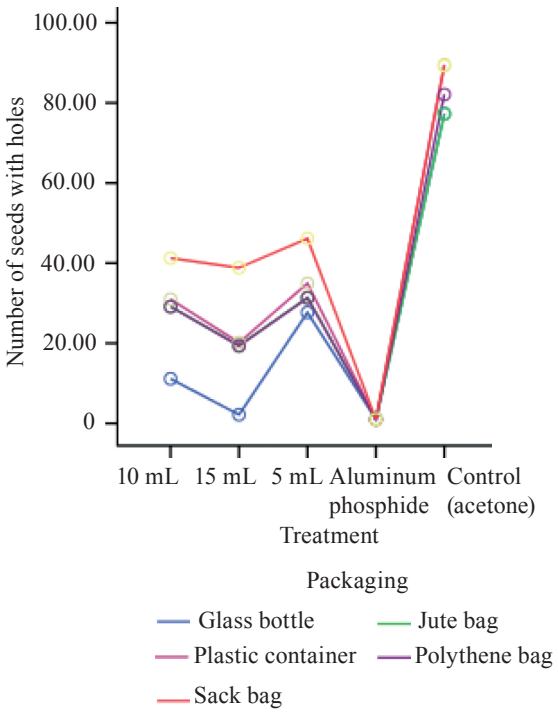

Figure 5 % Weevil perforation index of cowpea seeds treated with *Balanites aegyptiaca* in different storage materials after 90 days of storage

substantial reduction in seed damage. The analysis of variance showed a statistically significant effect of *B. aegyptiaca* oil extracts and storage materials on weevil perforation index ($F(16, 75) = 176.150$, $P = 0.000$). Exposure of weevil-infested cowpea seeds to *B. aegytiaca* essential oil in various storage materials resulted in a significant reduction in seed weight ($F(16,75 = 311.357$, $P = 0.000$).

The weevil perforation index decreased following the increase in *B. aegytiaca* essential oil concentration for all storage materials. The lowest weevil perforation index was observed in the seeds packaged in glass bottles followed by those stored in plastic containers. The highest weevil perforation index was recorded in the seeds stored in polythene bags throughout the storage period (Figs. 4 and 5).

Furthermore, exposure of weevil-infested cowpea seeds to *B. aegytiaca* essential oil in various storage materials resulted in a significant reduction in seed weight ($F(16,75) = 311.357$, $P = 0.000$). After 90 days of exposure, the seeds treated with *B. aegyptiaca* essential oil in all the storage materials showed a significantly low weight loss at all doses (5, 10, and 15 mL), except the cowpea seeds stored in polythene bags (Table 3). For these parameters, interactive treatment of *B. aegyptiaca* essential oil and storage materials had equally significant effects ($P < 0.05$) on cowpea weevils.

Taken together, *B. aegyptiaca* had a more detrimental effect on the weevils in comparison to the control. A similar research by Borzoui *et al.* also registered a significantly low amount of seed damage because the oviposition rate was reduced by the sublethal doses of essential oil [43]. Among all the storage materials, glass bottles and plastic bags showed the lowest weevil perforation index, seed weight loss, and seed damage. The low seed weight loss and damage observed in the seeds stored in these storage materials could be attributed to the significant reduction of weevils that could have caused seed damage.

B. aegyptiaca essential oil and storage materials demonstrated both individual and interactive effects on the germination rate of cowpea seeds. The germination rate of the treated seeds ranged from 46.7 to 93.3%, which was lower than the values reported for cowpea seed germination rate by Gad *et al.* [44].

An increased germination rate of cowpea seeds was observed with increased *B. aegyptiaca* essential oil concentration, which implied a strong relationship between the treatment and germination rate. Similar results were described by Bhavya *et al.* and Harshani and Karunaratne, who indicated that essential oils and their principal components affected seed germination. Storage materials also affected seed germination [45, 46].

In this study, glass bottles proved to be the optimal storage material as indicated by the maximal seed germination rate of 88.3, 91.6, and 93.3% after essential oil treatment of 5, 10, and 15 mL, respectively. Storing seeds in appropriate storage material retained higher germination capacity rate.

Table 3 Effect of *Balanites aegyptiaca* essential oil and storage material on cowpea seed damage, weight loss, and germination rate caused by *Callosobruchus maculatus* infestation

Samples	Storage materials	Seed weight loss			Seed damage			Germination rate
		30 days	60 days	90 days	30 days	60 days	90 days	
Balanites aegyptiaca essential oil (5 mL)	Glass bottle	8.30 ± 0.00	3.50 ± 0.03	1.00 ± 1.63	1.00 ± 0.00	1.00 ± 0.05	3.00 ± 0.00	88.30 ± 3.30
	Jute bag	13.40 ± 0.16	6.00 ± 0.19	1.50 ± 0.25	2.00 ± 1.63	4.50 ± 0.14	7.50 ± 0.21	64.60 ± 4.91
	Plastic container	12.50 ± 0.29	3.90 ± 0.00	1.20 ± 0.19	1.00 ± 0.00	1.90 ± 0.22	3.30 ± 0.23	80.00 ± 0.00
	Polythene bag	15.60 ± 0.17	8.50 ± 0.25	3.00 ± 0.16	5.90 ± 0.25	7.00 ± 0.17	11.40 ± 1.49	46.70 ± 0.00
	Sack bag	13.60 ±0.47	6.80 ± 0.14	1.40 ± 0.25	2.20 ± 0.00	5.00 ± 0.16	7.70 ± 0.81	60.00 ± 0.00
Balanites aegyptiaca essential oil (10 mL)	Glass bottle	7.80 ± 0.09	2.00 ± 0.08	0.80 ± 0.00	0	1.00 ± 0.00	1.90 ± 0.17	91.60 ± 3.30
	Jute bag	11.70 ± 0.04	5.40 ± 0.32	1.50 ± 0.00	2.00 ± 0.00	4.50 ± 0.10	7.00 ± 0.08	60.00 ± 0.00
	Plastic container	10.00 ± 0.13	2.30 ± 0.34	0.90 ± 0.17	0	1.00 ± 0.00	2.00 ± 0.00	80.00 ± 0.00
	Polythene bag	13.00 ± 0.17	11.50 ± 0.57	2.50 ± 0.21	3.90 ± 0.41	7.00 ± 0.00	9.10 ± 0.87	55.00 ± 2.01
	Sack bag	12.00 ± 0.74	5.70 ± 0.19	1.30 ± 0.28	2.00 ± 0.16	5.40 ± 0.18	6.90 ± 0.01	60.00 ± 0.00
Balanites aegyptiaca essential oil (15 mL)	Glass bottle	2.80 ± 0.16	1.60 ± 0.02	0.30 ± 0.23	0	1.00 ± 0.00	1.50 ± 0.00	93.30 ± 0.00
	Jute bag	10.80 ± 0.48	3.10 ± 0.00	0.70 ± 0.19	0	2.00 ± 0.07	5.00 ± 0.16	66.70 ± 0.00
	Plastic container	3.10 ± 0.24	1.90 ± 0.10	0.30 ± 0.19	0	1.00 ± 0.00	2.00 ± 0.71	93.00 ± 0.00
	Polythene bag	11.70 ± 0.84	9.70 ± 0.22	1.40 ± 0.16	2.00 ± 0.16	5.00 ± 0.38	6.00 ± 0.00	65.00 ± 1.88
	Sack bag	10.50 ± 0.38	3.40 ± 0.13	0.80 ± 0.00	0	4.00 ± 0.16	5.00 ± 0.00	60.00 ± 0.00
Aluminum phosphide	Glass bottle	0	0	0.10 ± 0.00	0	0	0	100.00 ± 0.00
	Jute bag	0	0	0.10 ± 0.00	0	0	0	100.00 ± 0.00
	Plastic container	0	0	0.10 ± 0.00	0	0	0	100.00 ± 0.00
	Polythene bag	0	0	0.10 ± 0.00	0	0	0	100.00 ± 0.00
	Sack bag	0	0	0.10 ± 0.00	0	0	0	100.00 ± 0.00
Control (acetone)	Glass bottle	18.60 ± 0.26	37.40 ± 0.13	42.00 ± 0.08	15.70 ± 1.25	28.00 ± 0.16	71.80 ± 0.43	26.70 ± 0.00
	Jute bag	28.60 ± 0.36	42.40 ±1.77	48.50 ± 0.00	20.90 ± 0.68	30.80 ± 1.45	79.70 ± 1.39	20.00 ± 0.00
	Plastic container	20.80 ± 0.16	40.30 ± 1.57	45.70 ± 0.22	16.00 ± 0.16	29.20 ± 0.66	77.80 ± 0.44	26.70 ± 0.00
	Polythene bag	35.60 ± 0.77	56.00 ± 0.00	56.50 ± 0.25	23.70 ± 0.48	38.60 ± 0.41	91.50 ± 1.07	13.30 ± 0.00
	Sack bag	26.40 ± 0.16	44.30 ± 1.80	50.00 ± 1.63	18.90 ± 0.17	34.10 ± 1.57	84.10 ± 1.72	20.00 ± 0.00
A		$P < 0.05$	$P < 0.05$	$P < 0.05$	$P < 0.05$	$P < 0.05$	$P < 0.05$	$P < 0.05$
B		$P < 0.05$	$P < 0.05$	$P < 0.05$	$P < 0.05$	$P < 0.05$	$P < 0.05$	$P < 0.05$
AB		$P < 0.05$	$P < 0.05$	$P < 0.05$	$P < 0.05$	$P < 0.05$	$P < 0.05$	$P < 0.05$

A – *Balanites aegyptiaca* essential oil; B – storage material

Therefore, the *B. aegyptiaca* essential oil could be used to protect cowpea seeds stored in glass bottles because the values observed were related to the international germination threshold of 90% required by seed exportation. This result is similar that obtained by Buleti *et al.*, who also used glass bottles as storage containers [15].

On the contrary, cowpea seeds stored in polythene bags displayed the lowest germination rate, which indicated a strong relationship between weight loss, damage score, and germination rate. However, the germination rates were not as highly related with seed damage traits. The lowest germination rate observed could be explained by weevil damage that occurred due to minimal weevil mortality rate in polythene bags, which, in its turn, led to nutrient exhaustion [15]. Storing seeds in inappropriate storage materials could significantly decline their germination rate and resulted in a rapid loss of seed viability.

Overall, even though *B. aegyptiaca* essential oil had a stronger effect on cowpea weevils, they failed to remove cowpea weevils completely; rather, they only lowered their numbers. Thus, hermetic storage could enhance the quality of cowpea seeds during storage.

CONCLUSION

The combination of essential oil of *Balanites aegyptiaca* L. and storage materials had significant effects on weevil proliferation in cowpea seeds ($P > 0.05$) during storage. *B. aegyptiaca* essential oil proved to possess insecticide properties that can help control *Callosobruchus maculatus* L. in stored cowpea seeds.

After 90 days of storage, mortality, oviposition, and egg hatchability fell down, following the increase in the concentration of *B. aegyptiaca* essential oil. In addition, such storage materials as glass bottles, plastic containers, and jute bags also reduced the population of cowpea weevils in cowpeas during storage. Hermetic storage material – glass bottles – had the greatest effecton weevil infestation and sustained the quality of cowpeas under storage conditions. These findings suggest that *B. aegyptiaca* essential oil could be useful as a botanical insecticide against cowpea pests. A large-scale trial is required to perform a toxicity assay of *B. aegyptiaca* essential oil.

CONTRIBUTION

Feyisola Fisayo Ajayi obtained the funds, designed the experiment, collected the data, and wrote the manuscript original draft, as well as performed the formal laboratory research. Akama Friday Ogori conducted the formal analysis and research, wrote the article, reviewed scientific publications, and edited the manuscript. Vivien O. Orede performed the formal analysis and research, reviewed and editing the manuscript. Emmanuel Peters performed the formal analysis and research, as well as provided the experimental design. All the authors were equally involved in reading and approving of the final manuscript before submission and are equally accountable for any potential cases of plagiarism.

CONFLICT OF INTEREST

The authors declare no conflict of interests regarding the publication of this article.

REFERENCES

1. Aramendiz-Tatis H, Espitia-Camacho M, Cardona-Ayala C. Adaptation and stability of cowpea (*Vigna unguiculata* (L.) Walp) bean cultivars in the tropical dry forest of Colombia. Australian Journal of Crop Science. 2019;13(6): 1009–1016. https://doi.org/10.21475/ajcs.19.13.06.p1965
2. Bolarinwa KA, Ogunkanmi LA, Ogundipe OT, Agboola OO, Amusa OD. An investigation of cowpea production constraints and preferences among small holder farmers in Nigeria. GeoJournal. 2022;87(4):2993–3005. https://doi.org/10.1007/s10708-021-10405-6
3. Affrifah NS, Phillips RD, Saalia FK. Cowpeas: Nutritional profile, processing methods and products – A review. Legume Science. 2021. https://doi.org/10.1002/leg3.131
4. Bechoff A, Shee A, Mvumi BM, Ngwenyama P, Debelo H, Ferruzzi MG, *et al.* Estimation of nutritional postharvest losses along food value chains: A case study of three key food security commodities in sub-Saharan Africa. Food Security. 2022;14(3):571–590. https://doi.org/10.1007/s12571-021-01238-9
5. Stathers TE, Arnold SEJ, Rumney CJ, Hopson C. Measuring the nutritional cost of insect infestation of stored maize and cowpea. Food Security. 2020;12(2):285–308. https://doi.org/10.1007/s12571-019-00997-w
6. Reuben F. Response of improved cowpea genotypes to alectra vogelii strains from selected areas of Tanzania. Sokoine University of Agriculture; 2018. 128 p.
7. Ashaye OA. Post-harvest handling of food crops in a changing climate: an outlook on food research in Iar & T. Ibadan: Moor-Plantation; 2018. 41 p.
8. Ogunfowokan AO, Oyekunle JAO, Torto N, Akanni MS. A study on persistent organochlorine pesticide residues in fish tissues andwater from an agricultural fish pond. Emirates Journal of Food and Agriculture. 2012;24(2):165–184.
9. Li C, Zhu H, Li C, Qian H, Yao W, Guo Y. The present situation of pesticide residues in China and their removal and transformation during food processing. Food Chemistry. 2021;354. https://doi.org/10.1016/j.foodchem.2021.129552
10. Campolo O, Giunti G, Russo A, Palmeri V, Zappalà L. Essential oils in stored product insect pest control. Journal of Food Quality. 2018;2018. https://doi.org/10.1155/2018/6906105
11. Kalpna, Hajam YA, Kumar R. Management of stored grain pest with special reference to *Callosobruchus maculatus*, a major pest of cowpea: A review. Heliyon. 2022;8(1). https://doi.org/10.1016/j.heliyon.2021.e08703
12. Ikbal C, Pavela R. Essential oils as active ingredients of botanical insecticides against aphids. Journal of Pest Science. 2019;92(3):971–986. https://doi.org/10.1007/s10340-019-01089-6
13. Kim S-W, Kang J, Park I-K. Fumigant toxicity of Apiaceae essential oils and their constituents against *Sitophilus oryzae* and their acetylcholinesterase inhibitory activity. Journal of Asia-Pacific Entomology. 2013;16(4):443–448. https://doi.org/10.1016/j.aspen.2013.07.002
14. Afiunizadeh M, Karimzadeh J, Imani S, Moharramipour S. Insecticidal and oviposition deterrent effects of five medicinal plant extracts on the diamondback moth. Journal of Plant Diseases and Protection. 2022;129(4):805–817. https://doi.org/10.1007/s41348-022-00592-w
15. Buleti SI, Mamati EG, Abukutsa-Onyango M. Determination of appropriate packaging materials for cowpea seed storage. Journal of Stored Products and Postharvest Research. 2019;10(4):29–34.

16. Kamara EG, Massaquoi FB, James MS, George A. Effects of packaging material and seed treatment on Weevil (Callosobruchus maculatus (F) Coleoptera: Bruchidae) infestation and quality of cowpea seeds. African Journal of Agricultural Research. 2014;9(45):3313–3318.
17. Mokhtar MM, Li J, Du Z, Cheng F. Insecticidal efficacy and chemical composition of *Balanites aegyptiaca* (L.) Delile seed oils against *Tribolium castaneum* Herbst (Coleoptera: Tenebrionidae). Chilean Journal of Agricultural Research. 2021;81(1):102–108. https://doi.org/10.4067/S0718-58392021000100102
18. Nwaogu J, Yahaya MA, Bandiya HM. Insecticidal efficcay of oil extracts of *Balanites aegyptiaca* seeds and cashew nuts against *Callosobruchus maculatus* Fabr. (Coleoptera: Bruchidae). African Journal of Agricultural Research. 2013;8(25):3285–3288.
19. Owolabi MS, Ogundajo AL, Alafia AO, Ajelara KO, Setzer WN. Composition of the essential oil and insecticidal activity of *Launaea taraxacifolia* (Willd.) Amin ex C. Jeffrey growing in Nigeria. Foods. 2020;9(7). https://doi.org/10.3390/foods9070914
20. Al-Thobaiti SA, Abu Zeid IM. Medicinal properties of desert date plants (*Balanites aegyptiaca*) – An overview. Global Journal of Pharmacology. 2018;12(1):01–12.
21. Ali S, Mohamed A, Mohammed G. Fatty acid composition, anti-inflammatory and analgesic activities of Balanites aegyptiaca seeds in rats. Journal of Agricultural and Veterinary Sciences. 2014;15(1):16–26
22. Hassan LEA, Dahham SS, Saghir SAM, Mohammed AMA, Eltayeb NM, Majid AMSA, *et al.* Chemotherapeutic potentials of the stem bark of *Balanite aegyptiaca* (L.) Delile: An antiangiogenic, antitumor and antioxidant agent. BMC Complementary and Alternative Medicine. 2016;16(1). https://doi.org/10.1186/s12906-016-1369-5
23. Rozman V, Kalinovic I, Korunic Z. Toxicity of naturally occurring compounds of Lamiaceae and Lauraceae to three stored-product insects. Journal of Stored Products Research. 2007;43(4):349–355. https://doi.org/10.1016/j.jspr.2006.09.001
24. Nguefack J, Tamgue O, Dongmo JBL, Dakole CD, Leth V, Vismer HF, *et al.* Synergistic action between fractions of essential oils from *Cymbopogon citratus*, *Ocimum gratissimum* and *Thymus vulgaris* against *Penicillium expansum*. Food Control. 2012;23(2):377–383. https://doi.org/10.1016/j.foodcont.2011.08.002
25. Ileke KD, Bulus DS, Aladegoroye AY. Effects of three medicinal plant products on survival, oviposition and progeny development of cowpea bruchid, *Callosobruchus maculatus* (Fab.) [Coleoptera: Chrysomelidae] infesting cowpea seeds in storage. Jordan Journal of Biological Science. 2013;6(1):61–66.
26. Obeng-Ofori D, Reichmuth C, Bekele J, Hassanali A. Biological activity of 1,8 cineole, a major component of essential oil of *Ocimum kenyense* (Ayobangira) against stored product beetles. Journal of Applied Entomology. 1997;121(4):237–243. https://doi.org/10.1111/j.1439-0418.1997.tb01399.x
27. Abbott WS. A method of computing the effectiveness of an insecticide. Journal of Economic Entomology. 1925;18(2):265–267.
28. Obembe O, Kayode J. Insecticidal activity of the aqueous extracts of four under-utilized tropical plants as protectant of cowpea seeds from *Callosobruchus maculatus* infestation. Pakistan Journal of Biological Sciences. 2013;16(4):175–179. https://doi.org/10.3923/pjbs.2013.175.179
29. Finney D. Statistical logic in the monitoring of reactions to therapeutic drugs. Methods of Information in Medicine. 1971;10(4):237–245.
30. Adenekan MO, Onasanya R, Owolade E. Assessment of the toxicity of *Carica papaya* plant powders against *Sitophilus zeamais* (Mots)(Coleoptera: Curculionidae) on maize seeds during storage. Journal of Bioscience and Biotechnology Discovery. 2019;4(5):108–113.
31. Adesina JM, Ofuya TI. Oviposition deterrent and egg hatchability suppression of *Secamone afzelii* (Schult) K. Schum Leaf extract on *Callosobruchus maculatus* (Fabricius)(Coleoptera: Chrysomelidae). Jordan Journal of Biological Sciences. 2015;8(2):95–100. https://doi.org/10.12816/0027554
32. Sibakwe CB, Donga T. Laboratory assessment of the levels of resistance in some bean varieties infested with bean weevils (*Acanthoscelides obtectus* and *Zabrotes subfasciatus*). International Journal of Plant and Soil Science. 2014;4(2):124–131.
33. Gad HA, Abo Laban GF, Metwaly KH, Al-Anany FS, Abdelgaleil SA. Efficacy of ozone for *Callosobruchus maculatus* and *Callosobruchus chinensis* control in cowpea seeds and its impact on seed quality. Journal of Stored Products Research. 2021;92. https://doi.org/10.1016/j.jspr.2021.101786
34. Olisa BS, Awosanmi FE, Akinropo MS, Ojo PO, Ishiak K, Danlami A, *et al.* Differential response of commercial hybrid and open pollinated maize seeds to mechanical damage during seed processing. Notulae Scientia Biologicae. 2021;13(4). https://doi.org/10.15835/nsb13410738
35. Mir SA, Dar BN, Wani AA, Shah MA. Effect of plant extracts on the techno-functional properties of biodegradable packaging films. Trends in Food Science and Technology. 2018;80:141–154. https://doi.org/10.1016/j.tifs.2018.08.004

36. Karimzadeh R, Javanshir M, Hejazi MJ. Individual and combined effects of insecticides, inert dusts and high temperatures on *Callosobruchus maculatus* (coleoptera: Chrysomelidae). Journal of Stored Products Research. 2020;89. https://doi.org/10.1016/j.jspr.2020.101693
37. Chen H, Singh H, Bhardwaj N, Bhardwaj SK, Khatri M, Kim K-H, *et al.* An exploration on the toxicity mechanisms of phytotoxins and their potential utilities. Critical Reviews in Environmental Science and Technology. 2022;52(3):395–435. https://doi.org/10.1080/10643389.2020.1823172
38. Alves MDS, Campos IM, Brito DMC, Cardoso CM, Pontes EG, Souza MAA. Efficacy of lemongrass essential oil and citral in controlling *Callosobruchus maculatus* (Coleoptera: Chrysomelidae), a post-harvest cowpea insect pest. Crop Protection. 2019;119:191–196. https://doi.org/10.1016/j.cropro.2019.02.007
39. Aous W, Benchabane O, Outaleb T, Hazzit M, Mouhouche F, Yekkour A, *et al.* Essential oils of *Cymbopogon schoenanthus* (L.) Spreng. from Algerian Sahara: chemical variability, antioxidant, antimicrobial and insecticidal properties. Journal of Essential Oil Research. 2019;31(6):562–572. https://doi.org/10.1080/10412905.2019.1612790
40. Ashamo MO, Ileke KD, Ogungbite OC. Entomotoxicity of some agro-wastes against cowpea bruchid, *Callosobruchus maculatus* (Fab.) [Coleoptera: Chrysomelidae] infesting cowpea seeds in storage. Heliyon. 2021;7(6). https://doi.org/10.1016/j.heliyon.2021.e07202
41. Reyad N, Al-Ghamdi H, Abdel-Raheem M, Al-Shaeri M. The effects of botanical oils on the red palm weevil, *Rhynchophorus ferrugineus* Olivier (Coleoptera: Curculionidae). Applied Ecology and Environmental Research. 2020;18(2):2909–2919. https://doi.org/10.15666/aeer/1802_29092919
42. Chaaban A, Santos VMCS, Gomes EN, Martins CEN, do Amaral W, Deschamps C, *et al.* Chemical composition of *Piper gaudichaudianum* essential oil and its bioactivity against *Lucilia cuprina* (Diptera: Calliphoridae). Journal of Essential Oil Research. 2018;30(3):159–166. https://doi.org/10.1080/10412905.2017.1423406
43. Borzoui E, Khaghani R, Nouri-Ganbalani G. Lethal and sublethal effects of *Eucalyptus camaldulensis* and *Mentha piperita* essential oils on the Khapra beetle (Coleoptera: Dermestidae) in terms of feeding inhibition, oviposition, and seed damage. Environmental Entomology. 2021;50(3):692–698. https://doi.org/10.1093/ee/nvab023
44. Gad HA, Abo Laban GF, Metwaly KH, Al-Anany FS, Abdelgaleil SAM. Efficacy of ozone for *Callosobruchus maculatus* and *Callosobruchus chinensis* control in cowpea seeds and its impact on seed quality. Journal of Stored Products Research. 2021;92. https://doi.org/10.1016/j.jspr.2021.101786
45. Bhavya M, Obulaxmi S, Devi SS. Efficacy of *Ocimum tenuiflorum* essential oil as grain protectant against coleopteran beetle, infesting stored pulses. Journal of Food Science and Technology. 2021;58(4):1611–1616. https://doi.org/10.1007/s13197-020-04871-y
46. Harshani HS, Karunaratne S. Chemical composition and insecticidal effect of fruit peel powders of two citrus species against *Callosobruchus maculatus* (F.)(Coleoptera: Bruchidae) in stored cowpea (*Vigna unguiculata*). International Journal of Pest Management. 2021;67(2):131–138. https://doi.org/10.1080/09670874.2019.1698788

ORCID IDs
Feyisola F. Ajayi https://orcid.org/0000-0003-2521-7946
Akama F. Ogori https://orcid.org/0000-0001-8820-5868
Vivien O. Orede https://orcid.org/0000-0002-1345-252X
Emmanuel Peter https://orcid.org/0000-0002-3226-4823

Foods and Raw Materials. 2022;10(2)

ISSN 2310-9599 (Print)
ISSN 2308-4057 (Online)

Research Article
Open Access

Available online at http://jfrm.ru/en
https://doi.org/10.21603/2308-4057-2022-2-543
https://elibrary.ru/ZHEJBR

Antagonistic activity of synbiotics: Response surface modeling of various factors

Svetlana A. Evdokimova, Boris A. Karetkin*, Mikhail O. Zhurikov, Elena V. Guseva, Natalia V. Khabibulina, Irina V. Shakir, Victor I. Panfilov

Dmitry Mendeleev University of Chemical Technology of Russia, Moscow, Russia

* e-mail: karetkin.b.a@muctr.ru

Received 04.04.2022; Revised 16.05.2022; Accepted 07.06.2022; Published online 23.09.2022

Abstract:
Synbiotic compositions have a great potential for curing microbial intestinal infections. Novel targeted synbiotics are a promising field of the modern functional food industry. The present research assessed the effect of various fructan fractions, initial probiotic counts, and test strains on the antagonistic properties of synbiotics.

The research involved powdered roots of *Arctium lappa* L. and strains of *Bifidobacterium bifidum*, *Bacillus cereus*, and *Salmonella enterica*. The exp eriment was based on the central composite rotatable design. A water extract of *A. lappa* roots was purified and concentrated. Fructan fractions were precipitated at various concentrations of ethanol, dried, and subjected to carbon-13 nuclear magnetic resonance (13C-NMR) spectrometry. The bifidobacteria and the test strains were co-cultivated in the same medium that contained one of the fractions. Co-cultivation lasted during 10 h under the same conditions. The acid concentrations were determined by high-performance liquid chromatography to define the synbiotic factor.

The obtained fructans were closer to commercial oligofructose in terms of the number and location of NMR peaks. However, they were between oligofructose and inulin in terms of signal intensity. The response surface analysis for bacilli showed that the minimal synbiotic factor value corresponded to the initial probiotic count of 7.69 log(CFU/mL) and the fructan fraction precipitated by 20% ethanol. The metabolites produced by the bacilli also affected their growth. The synbiotic factor response surface for the experiments with *Salmonella* transformed from parabolic to saddle shape as the initial test strain count increased. The minimal synbiotic factor value corresponded to the lowest precipitant concentration and the highest probiotic count.

The research established a quantitative relationship between the fractional composition of fructans and the antagonistic activity of the synbiotic composition with bifidobacteria. It also revealed how the ratio of probiotic and pathogen counts affects the antagonism. The proposed approach can be extrapolated on other prebiotics and microbial strains *in vivo*.

Keywords: Bifidobacteria, *Bacillus cereus*, *Salmonella enterica*, *Arctium lappa* L. fructans, synbiotics, antagonism, co-culture, rotatable central composite design, response surface methodology

Funding: The research was sponsored by the Russian Science Foundation (RSF) (Project 17-79-20365).

Please cite this article in press as: Evdokimova SA, Karetkin BA, Zhurikov MO, Guseva EV, Khabibulina NV, Shakir IV, *et al.* Antagonistic activity of synbiotics: Response surface modeling of various factors. Foods and Raw Materials. 2022;10(2):365–376. https://doi.org/10.21603/2308-4057-2022-2-543

INTRODUCTION

Intestinal microbiota affects human health and vitality. Microbial community is a powerful and multifunctional metabolic system that modulates immunity, suppresses pathogens, and produces various vitamins [1, 2]. A disturbed qualitative and quantitative microbial composition leads to various alimentary and chronic diseases. For instance, low counts of *Bacteroides* and *Firmicutes*, if accompanied by excessive proteobacteria, fusobacteria, and the mucin-decomposing *Ruminococcus gnavus*, can trigger Crohn's disease, ulcerative colitis, obesity, and diabetes [3].

However, some intestinal microbes inhibit pathogens and food contaminants by producing such antimicrobial substances as organic acids and bacteriocins or competing for nutrients and adhesion sites [4–7]. If it were not for them, unwanted microorganisms would cause constant harm to human health by producing various toxins or enzymes. For instance, *Bacillus cereus* is a common

food contaminant that produces two types of toxins and causes vomiting and diarrhea intoxication [8]. *B. cereus* spores are resistant to heat treatment and chemical preservation [9].

Non-typhoid *Salmonella* is another wide-spread cause of foodborne diseases [10]. *Salmonella enterica* s. *Typhimurium* is often resistant to antibiotics and can develop biofilms, thus causing gastroenteritis, vomiting, and diarrhea [11]. Antibiotic-resistant bacteria are the most dangerous causes of intestinal infections [12]. Therefore, novel non-antibiotic ways to suppress these pathogens and food contaminants for therapy and prevention are one of the most urgent tasks of the modern medicine. Synbiotic compositions offer a potential solution to this problem because they are extremely effective in inhibiting the growth, activity, and pathogenesis of specific undesirable microorganisms.

Probiotics, prebiotics, and synbiotics are parts of functional foods that inhibit unwanted members of intestinal microbiota [13]. These food additives are known to increase α-diversity, combat obesity, improve immunity, and counteract pathogens [13–16]. Synbiotics are the most effective type because they possess synergistically enhanced beneficial properties of probiotics and prebiotics [17].

For synbiotics, the most important criteria are their inhibiting properties, adhesion to intestinal epithelial cells, and pathogen toxicity. Antagonistic research of synbiotic combinations is a promising strategy for developing new synbiotics. Ruiz *et al.* studied the combined antimicrobial activity of a synbiotic based on *Bifidobacterium longum* subsp. *infantis* and galactooligosaccharides against such enteric pathogens as *Escherichia coli*, *Cronobacter sakazakii*, *Listeria monocytogenes*, and *Clostridium difficile*. *C. sakazakii* and *C. difficile* proved to be the most effective pathogen inhibitors [18]. Co-cultivation of *B. longum* or *Bifidobacterium breve* with *C. difficile* in a medium with commercial fructooligosaccharides reduced the pathogen growth, as well as the toxicity of its metabolites [19].

Śliżewska and Chlebicz-Wójcik focused on the effect of various prebiotics co-cultivated with lactobacilli on pathogenic *S. enterica* of various serovars and *L. monocytogenes*. Inulin demonstrated the greatest antagonistic activity, although the effect depended on the test strain [20]. Obviously, the effectiveness of one and the same composition depends on the pathogen. The inhibitory effect can be measured by the inhibitory metabolites produced by probiotics. This effect can be expressed in terms of inhibition constants (K_i) or minimal inhibitory concentrations. The synbiotic factor is another quantitative criterion for evaluating the effectiveness of synbiotic compositions. It shows how many times the specific growth rate of a pathogen or microbial contaminant decreases under the action of acids produced by a probiotic when they are co-cultivated in the same medium with this prebiotic [21].

Plant extracts are common sources of prebiotic substances. In addition to polysaccharides of various molecular weights, they may contain non-carbohydrate substances with a potential beneficial effect, e.g., polyphenols [22, 23]. Precipitation with different concentrations of ethanol can separate plant carbohydrates into fractions with different degrees of polymerization. Polysaccharides with a higher degree of polymerization require a lower concentration of ethanol. As the alcohol concentration increases, the average degree of polymerization of the precipitated fraction decreases [24, 25]. Polysaccharides with a high degree of polymerization are not metabolized by pathogens without extracellular hydrolases. However, they can be metabolized by many types of probiotics, e.g., bifidobacteria and some lactobacilli, which determines their significant prebiotic potential [26]. In our previous research, we evaluated the effectiveness of a synbiotic composition *in vitro* by the degree of its antagonism against staphylococci. It depended on the fractional composition of *Arctium lappa* fructans, as well as on the ratio of the initial probiotic and pathogen counts [27].

The response surface methodology was developed by Box and Wilson [28]. It is a powerful tool for establishing quantitative relationships between various factors and the response function, also by taking into account the mutual effect of factors in multiparameter equations. Shuhaimi *et al.* used this method to optimize the composition of a synbiotic that consisted of *Bifidobacterium pseudocatenulatum* and several prebiotics, while Pandey and Mishra tested this method on a soy drink with lactic acid bacteria and organophosphates [29, 30].

Few researchers venture beyond simple optimization to look for the patterns between various factors and the response function. This approach proved quite effective in studying the change patterns in microbial communities under various environmental factors [31, 32]. Antagonism is a type of relationships in microbial communities. Our research objective was to use the response surface method to evaluate the effect of fructan fractional composition, the initial counts of probiotics and the pathogen test strain on the antagonism of the synbiotic against *B. cereus* and *S. enterica*.

STUDY OBJECTS AND METHODS

Plant raw materials and obtaining fructan fractions. To isolate fructans, we used burdock root powder (*Arctium lappa* L.) in accordance with pharmacopeial monograph 2.5.0025.15 of the Russian Pharmacopoeia. The powder was diluted with distilled water in a ratio of 1:12 (g dry solids per 1 mL extractant) and extracted twice at 75°C and pH 6.5 for 30 min with constant stirring. The pulp was separated by vacuum filtration. To separate high-molecular impurities, the extract was ultrafiltered at 45°C through a hollow fiber module (AR-0.5-20PS, NPO Biotest, Kirishi, Russia) with a retention threshold of 20 kDa. The permeate was stirred with active clarifying carbon at a rate of

15 g/L for 30 min until the extract became colorless. The activated charcoal was separated by vacuum filtration [33].

The extract was evaporated using a rotary film evaporator (model 561-01110-00 with glass set G1, Heidolph, Germany) at 45°C until the carbohydrate concentration reached 170–200 g/L. To separate the carbohydrates into fractions with different degrees of polymerization, the extract was precipitated with varying ethanol concentrations (20.0, 32.2, 50.0, 67.8, and 80.0%) at 4°C for 4 days [24].

The precipitates were separated by centrifugation at 5000 rpm for 15 min and dried in a ScanVac Coolsafe 100-9 freeze-dryer under the following temperature and time conditions: 0°C – 8 h, 5°C – 8 h, 10°C – 6 h, 15°C – 6 h, and 20°C – 6 h. The samples were diluted 1:1 with a 10% solution of trichloroacetic acid and hydrolized for 40 min in a boiling water bath. After that, the content of fructans was determined by the modified Bertrand method.

Microbial objects and cultivation conditions. All the bacterial cultures were obtained from the National Bioresource Center of the All-Russian Collection of Industrial Microorganisms in the National Research Center of Kurchatov Institute (VKPM). *Bifidobacterium bifidum* (AS-1666, ATCC 29521^T) served as a probiotic culture. *Bacillus cereus* (B-8076, ATCC 9634) was used as a model food contaminant. *Salmonella enterica* (B-5300) was a model intestinal pathogen. The medium described in [34] was modified to obtain inoculums and co-cultivate the probiotic and test strains.

The composition of the carbohydrate-free medium was as follows (g/L): casein trypton (Difco Laboratories) – 10; yeast extract (Springer) – 7.6; meat extract (Panreac) – 5; ascorbic acid (AppliChem) – 1; sodium acetate – 1; $(NH_4)_2SO_4$, – 5; urea – 2; $MgSO_4 \cdot 7H_2O$ – 0.2; $FeSO_4 \cdot 7H_2O$ – 0.01; $MnSO_4 \cdot 7H_2O$ – 0.007; NaCl – 0.01; Tween-80 – 1, and L-cysteine – 0.5 (pH 7.0). All the components were dissolved in 80% of the required amount of distilled water and autoclaved at 115°C for 30 min. The fructan precipitates were dissolved in distilled water (20% of the required medium volume) and sterilized separately under the same conditions. Prior to inoculation, carbohydrates were added to the medium aseptically until their concentration was 8 g/L.

Inoculums were cultivated at 37°C and stirred at 180 rpm under anaerobic conditions (2% CO_2, 98% N_2) in a CB-210 CO_2 incubator (Binder, Germany) for 12 h without maintaining a constant pH. After that, the inoculums were centrifuged at 6000 rpm and 4°C for 2 min and washed twice in sterile saline (9 g/L NaCl). Then the precipitate was resuspended in a carbohydrate-free medium to obtain suspensions with an optical density depending on the bacterial count. To achieve the selected initial count of the probiotic and the test strain, 0.5 mL of the obtained solution was added to the media with pre-added fructans. To determine the synbiotic factor, co-cultivation lasted during 10 h under the same conditions. Sampling took place at the beginning and end of fermentation.

Microbial count. Microbial count was conducted in triplicate by seeding tenfold dilutions in Petri dishes with the media. Colonies of *B. cereus* and *S. enterica* were counted after 24 h of aerobic growth at 37°C in MRS medium [35]. *B. bifidum* colonies were counted after 48 h of growth in BFM medium with the following composition (g/L): peptone – 10, NaCl – 5.0, lactulose – 5.0, L-cysteine – 0.5, riboflavin – 0.01, yeast extract – 7, meat extract – 5, starch – 2, thiamine chloride – 0.01, and lithium citrate – 3.3 [36]. The pH was adjusted to 5.5 by adding propionic acid (5 mL/L). The dishes were incubated under anaerobic conditions at 37°C using a BD GasPak™ Anaerobic Container System.

Determining the content of organic acids. The concentration of organic lactic and acetic acids was determined by high-performance liquid chromatography (HPLC) according to a slightly modified standard procedure by the refractometric signal [37]. The experiment involved an Agilent 1220 Infinity chromatograph (Santa Clara, CA, USA) with an Agilent Hi-Plex H column (250×4.6 mm). The supernatant was centrifuged at 12 000 rpm for 15 min, then filtered through 0.45-μm cellulose acetate membranes (HAWP, MF-Millipore, St. Louis, MO, USA). Other parameters included: sample volume – 3 μL, temperature – 50°C, mobile phase flow rate (0.002 M H_2SO_4) – 0.3 mL/min. To prepare calibration solutions, the concentrated organic acids were diluted in their mobile phase to concentrations of 1, 5, and 10 g/L.

Determining the structure of fructans. The structure of the isolated fructans was analyzed using carbon-13 nuclear magnetic resonance (^{13}C-NMR) spectrometry following the procedure described by Mariano *et al.* [38]. One-dimensional spectra were obtained at 298 K on a BRUKER CXP-200 NMR spectrometer (50.3 MHz) (Bruker, Germany) in an aqueous solution of D_2O. Inulin (Orafti ® HSI, BENEO-ORAFTI, Belgium) and oligofructose (Orafti ® P95, BENEO-ORAFTI, Belgium) served as standard.

Calculating the synbiotic factor. The synbiotic factor was calculated in accordance with the previously approach proposed by Karetkin *et al.* and Evdokimiova *et al.* [21, 27]. The microbial count, pH, and the concentration of organic acids were determined at the initial and final stages of co-cultivation. Based on the data obtained, the synbiotic factor was calculated as follows:

$$SF = \frac{pH - pH_{min}}{pH_{opt} - pH_{min}} \times \left[1 - \left(\frac{[LA]}{MIC_{LA}}\right)^{\alpha}\right] \times \left[1 - \left(\frac{[AA]}{MIC_{AA}}\right)^{\beta}\right] \quad (1)$$

where SF is the synbiotic factor; pH_{opt} is pH optimal for test strain growth; pH_{min} is pH the minimal for test strain growth; [LA] is the concentration of undissociated lactic acid, (mg/mL); [AA] is the concentration of undissociated acetic acid, mg/mL; MIC_{LA} is the minimal inhibiting concentration of lactic acid, mg/mL; MIC_{AA} is the minimal inhibiting concentration of acetic acid,

Table 1 Minimal inhibitory concentrations, constants, and optimal and minimal pH during the process of *Bacillus cereus* or *Salmonella enterica* inhibition by lactic and acetic acids

Test strain	pH_{opt}	pH_{min}	MIC_{LA}, mg/mL	MIC_{AA}, mg/mL	α	β
Bacillus cereus	7.0	4.9	3.48	3.20	0.25	0.40
Salmonella enterica	7.0	5.0	2.25	1.77	1.70	0.90

mg/mL; α and β are constants for *B. cereus* or *S. enterica*, which we defined in [39] (Table 1).

Design of experiment and statistical analysis. The central composition rotatable design was applied to study the effect of the following parameters on the co-cultivation: the precipitant concentration x_1, the fractional composition of *A. lappa* fructans, the initial count (decimal logarithm) of bifidobacteria (x_2), and test strain cells (x_3). Synbiotic factor (Y_1) and final test strain count (Y_2) were chosen as response functions. The variation levels were determined based on data obtained from [21, 27] (Tables 3 and 4). The response function was presented as follows:

$$Y_k(x_1, x_2, x_3) = b_0 + b_1x_1 + b_2x_2 + b_3x_3 + b_{12}x_1x_2 + \quad (2)$$
$$+ b_{23}x_2x_3 + b_{13}x_1x_3 + b_{123}x_1x_2x_3 + b_{11}x_1^2 + b_{22}x_2^2 + b_{33}x_3^2$$

The significance test of the coefficients for Eq. (2) was based on the t-test. The adequacy of the equation was assessed by the Fisher criterion at P = 0.05. Response surfaces were calculated and constructed using the MathLab software. The scanning method with a variable step as in [40] was applied to determine the extreme values of the factors. The method consists in a sequential search for points in the parametric space using the GeoGebra Classic software 6.0.694.0 (University of Salzburg, Salzburg, Salzburg state, Austria).

RESULTS AND DISCUSSION

^{13}C-NMR specters of *Arctium lappa* L. root fructan fractions. Figure 1 illustrates ^{13}C-NMR specters of standard inulin and oligofructose, purified from *A. lappa* L. fructan fractions and precipitated by different concentrations of ethanol.

The analysis was based on the difference between the chemical shifts of the carbon atoms of the monomers located inside the chain of oligo- and polysaccharides and the atoms of the terminal monomers [24]. The chemical shifts of carbon atoms in the standard and test samples are typical of inulin-type fructans (Table 2). The obtained spectra of fructan fractions were closer to those of commercial oligofructose in terms of the number and location of peaks. In terms of signal intensity, they were between standard oligofructose and highly purified inulin. None of the test samples demonstrated peaks at the terminal C-2 atom of D-fructofuranose. However, the test samples showed an increase in the relative areas of the peaks, as well as an increase in the precipitant concentration for all carbon atoms of the D-fructofuranose residues within the chain (forming a 2→1 bond).

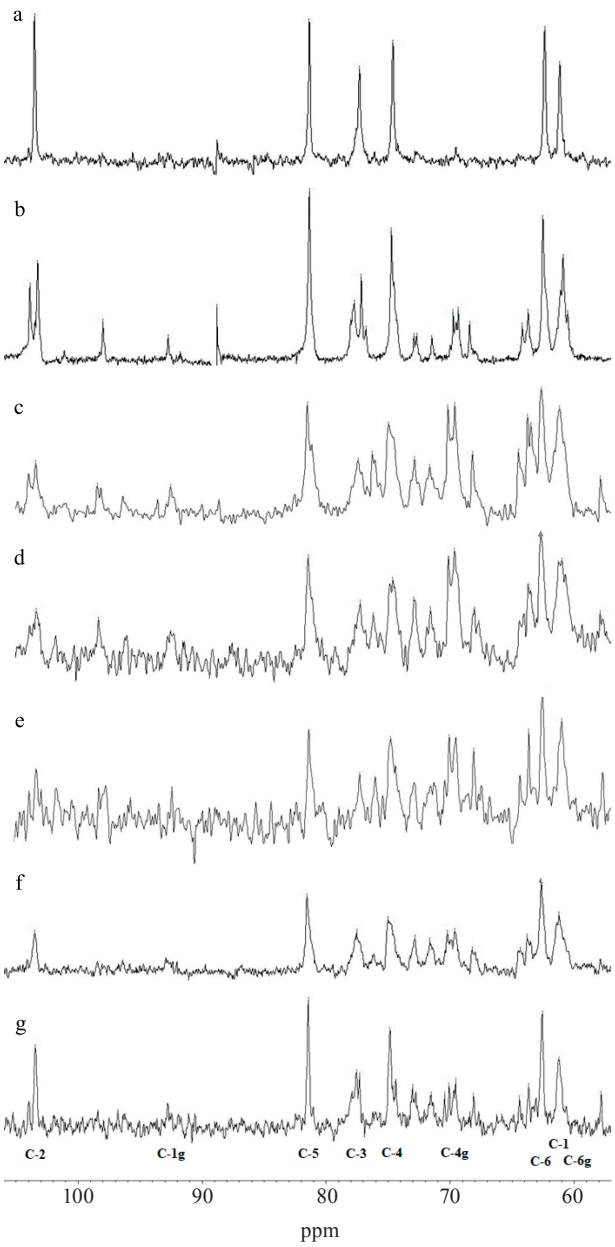

Figure 1 ^{13}C-NMR specters in distilled water with D_2O and (a) HSI inulin, (b) oligofructose and *Arctium lappa* L. fructan fractions precipitated by ethanol with concentrations, (c) 20.0% (Burd-20), (d) 32.2% (Burd-32), (e) 50.0% (Burd-50), (f) 67.8% (Burd-68), and (g) 80.0% (Burd-80)

All the peak areas for the corresponding carbon atoms were smaller than for inulin, and the values obtained for Burd-50 and Burd-68 were closest to

Table 2 ^{13}C-NMR chemical shifts of *β*-D-fructofuranose and *α*-D-glucopyranose of HSI inulin standard samples, oligofructose, and experimental samples of *Arctium lappa* L. root fructan fractions precipitated with various concentrations of ethanol: 20% (Burd-20), 32.2% (Burd-32), 50% (Burd-50), 67.8% (Burd-68), and 80% (Burd-80)

Carbon atom	Chemical shift, ppm						
	Inulin	Oligofuctose	Burd-20	Burd-32	Burd-50	Burd-68	Burd-80
C-2 f (terminal)	–	103.88	–	–	–	–	–
C-2 f (2→1 bond)	103.4262	103.2645	104.26	104.29	103.40	103.43	103.43
	–	97.98	99.31	99.25	–	–	–
C-1 g (terminal)	–	92.7261	93.41	–	–	–	–
	–	88.76	–	–	–	–	–
C-5 f (terminal)	–	–	–	–	–	–	–
C-5 f (2→1 bond)	81.3253	81.3253	82.40	82.30	81.44	81.50	81.44
	–	77.71	–	–	–	–	–
C-3 f (2→1 bond)	77.2824	77.1477	78.31	78.06	77.32	77.48	77.54
C-3 f (terminal)	–	76.77	77.16	77.00	76.07	–	77.32
	–	–	–	–	–	–	–
C-4 f (2→1 bond)	74.5872	74.70	75.85	75.76	74.83	74.96	74.86
C-4 f (terminal)	–	–	–	75.44	–	–	–
C-3 g (terminal)	–	72.8892	73.75	73.75	–	72.79	73.04
C-5 g (terminal)	–	72.6736	–	–	–	–	–
C-2 g (terminal)	–	71.4337	72.53	72.41	–	71.58	71.54
C-4 g (terminal)	69.4	69.3045	71.06	70.94	70.11	70.17	70.46
	–	68.39	69.09	68.83	68.13	68.19	68.13
C-6 f (2→1 bond)	–	64.1566	65.38	64.49	64.30	64.30	64.43
C-6 f (terminal)	–	63.67	64.65	63.47	63.69	63.79	63.69
	–	–	64.36	–	–	–	–
C-1 f (2→1 bond)	62.3777	62.4858	63.53	62.06	62.61	62.61	62.57
C-1 f (terminal)	61.16	60.84	62.06	61.78	61.04	61.20	61.27
C-6 g (terminal)	–	60.49	58.78	58.71	57.88	–	57.85

oligofructose. The differences in the relative proportions of peak areas for Burd-20 and Burd-32 were small and manifested as unidentified peaks in the Burd-20. Probably, carbohydrates of similar molecular weight were precipitated at these ethanol concentrations. No correlation was observed between the relative proportions of the peak areas for the terminal atoms of glucopyranose and fructofuranose.

Synbiotic antagonism to *Bacillus cereus* and response surface analysis. To assess the effect of various factors on the anti-*B. cereus* activity of the synbiotic composition, the experiment was carried out according to a central composition rotatable design. The limiting values of ethanol concentration were chosen as 20 and 80% as in [27]. The average polymerization degree of the precipitated carbohydrate fraction was at its highest at 20% of ethanol.

Zeaiter *et al.* used 33% ethanol to obtain a fraction of inulin-type artichoke fructans with an average degree of 32–42 [26]. Table 3 demonstrates the planning matrix, as well as the experimental and calculated values of response functions, i.e., the synbiotic factor and the final test strain cell count.

The coefficients of the response function equation were determined from the values of the synbiotic factor and the final bacterial count. The response surface was constructed according to Eq. (2) (Fig. 2). The adequacy of the equations was confirmed by Fisher's criterion $F = 1.681$ and 1.66: it was below the tabulated $F = 4.704$ at $P = 0.05$.

$$Y_1 = 0.0211 + 0.008x_1 - 0.0074x_2 + 0.0032x_2^2 \quad (3)$$

$$Y_2 = 4.9 \times 10^7 - 1.6 \times 10^7 x_2 - 1.2 \times 10^7 x_3 - \\ - 7.1 \times 10^6 x_2 x_3 - 7.4 \times 10^6 x_3^2 \quad (4)$$

The synbiotic factor reduced of the specific growth rate of the test strain. It showed how many times the specific growth rate decreased relative to the optimal value under the effect of inhibitors produced by the probiotic and the prebiotic. The maximal inhibition corresponded to the lowest value of the synbiotic factor [21]. The synbiotic factor of the composition of *Bifidobacterium bifidum* and *A. lappa* root fructans had a positive linear dependence on the precipitant concentration (x_1). Therefore, the composition with fructans precipitated by the lowest alcohol concentration had the greatest inhibitory effect on *B. cereus* because it had the highest average degree of polymerization. This result confirms the data obtained by us before [27]. The dependence of the synbiotic factor on the initial probiotic count (x_2) was parabolic and reached its minimum at +1.156, which corresponded

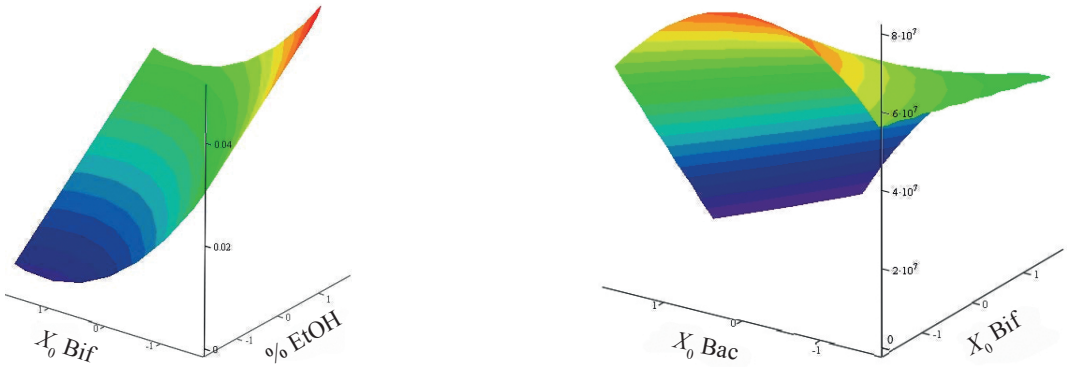

a b

Figure 2 Synbiotic factor response surface (a) and final bacterial count (b), CFU/mL

Table 3 Range of variation and encoding of variables: experimental and calculated values of response functions for *Bacillus cereus*

Test No.	Factors						Synbiotic factor		Final bacterial count, lg(CFU/mL)*	
	Precipitant concentration (EtOH), %		Initial prebiotic count, lg(CFU/mL)		Initial bacterial count, lg(CFU/mL)					
	z_1	x_1	z_2	x_2	z_3	x_3	SF_{obs}	SF_{pred}	$X_{bac\ obs}$	$X_{bac\ pred}$
1	67.8	+1	7.6	+1	6.4	+1	0.0267	0.0249	5.72	6.77
2	67.8	+1	7.6	+1	4.6	–1	0.0310	0.0249	7.48	7.65
3	67.8	+1	6.4	–1	6.4	+1	0.0420	0.0397	7.80	7.72
4	67.8	+1	6.4	–1	4.6	–1	0.0433	0.0397	7.77	7.80
5	32.2	–1	7.6	+1	6.4	+1	0.0136	0.0089	5.43	6.77
6	32.2	–1	7.6	+1	4.6	–1	0.0092	0.0089	7.58	7.65
7	32.2	–1	6.4	–1	6.4	+1	0.0224	0.0236	7.66	7.72
8	32.2	–1	6.4	–1	4.6	–1	0.0244	0.0236	7.79	7.80
9	20.0	–1.682	7.0	0	5.5	0	0.0188	0.0076	7.77	7.69
10	80.0	+1.682	7.0	0	5.5	0	0.0404	0.0346	7.63	7.69
11	50.0	0	6.0	–1.682	5.5	0	0.0471	0.0425	7.82	7.88
12	50.0	0	8.0	+1.682	5.5	0	0.0179	0.0177	7.51	7.34
13	50.0	0	7.0	0	4.0	–1.682	0.0268	0.0211	7.77	7.69
14	50.0	0	7.0	0	7.0	+1.682	0.0301	0.0211	6.63	6.84
15	50.0	0	7.0	0	5.5	0	0.0213	0.0211	7.74	7.69
16	50.0	0	7.0	0	5.5	0	0.0122	0.0211	7.68	7.69
17	50.0	0	7.0	0	5.5	0	0.0239	0.0211	7.76	7.69
18	50.0	0	7.0	0	5.5	0	0.0241	0.0211	7.70	7.69
19	50.0	0	7.0	0	5.5	0	0.0205	0.0211	7.56	7.69
20	50.0	0	7.0	0	5.5	0	0.0237	0.0211	7.66	7.69

* the response function was calculated as CFU/mL; the results are given on a logarithmic scale

to 7.69 lg(CFU/mL). As x_2 rose (> +1.156), the synbiotic factor also increased.

All experimental values appeared to be much higher than those obtained by calculation, both at the minimal point and at high values of x_2. Apparently, the observed decrease in the antagonistic activity could be ignored. All the coefficients at x_3 proved insignificant, and the initial test strain count did not affect the synbiotic factor. Within the range of the variables, the minimal value of the synbiotic factor (maximal suppression of the test strain) was 0.0033 and lied at the point with coordinates –1.682 and 1.156, which corresponded to the initial probiotic count of 7.69 lg(CFU/ml) and the *A. lappa* fructan fraction precipitated with 20% ethanol.

As the initial bifidobacterial count (x_2) increased, the final bacterial count decreased (Fig. 2b). The dependence of the final test strain count (Y_2) on the initial one (x_3) was parabolic. The maximal value of the response function was reached when the bifidobacterial count was minimal, i.e., 6.0 lg(CFU/mL), and the initial test strain count in the design center was 5.5 lg(CFU/mL). At these values, the inhibition was least effective. The minimal final test strain count was around the highest seed doses of both the probiotic and

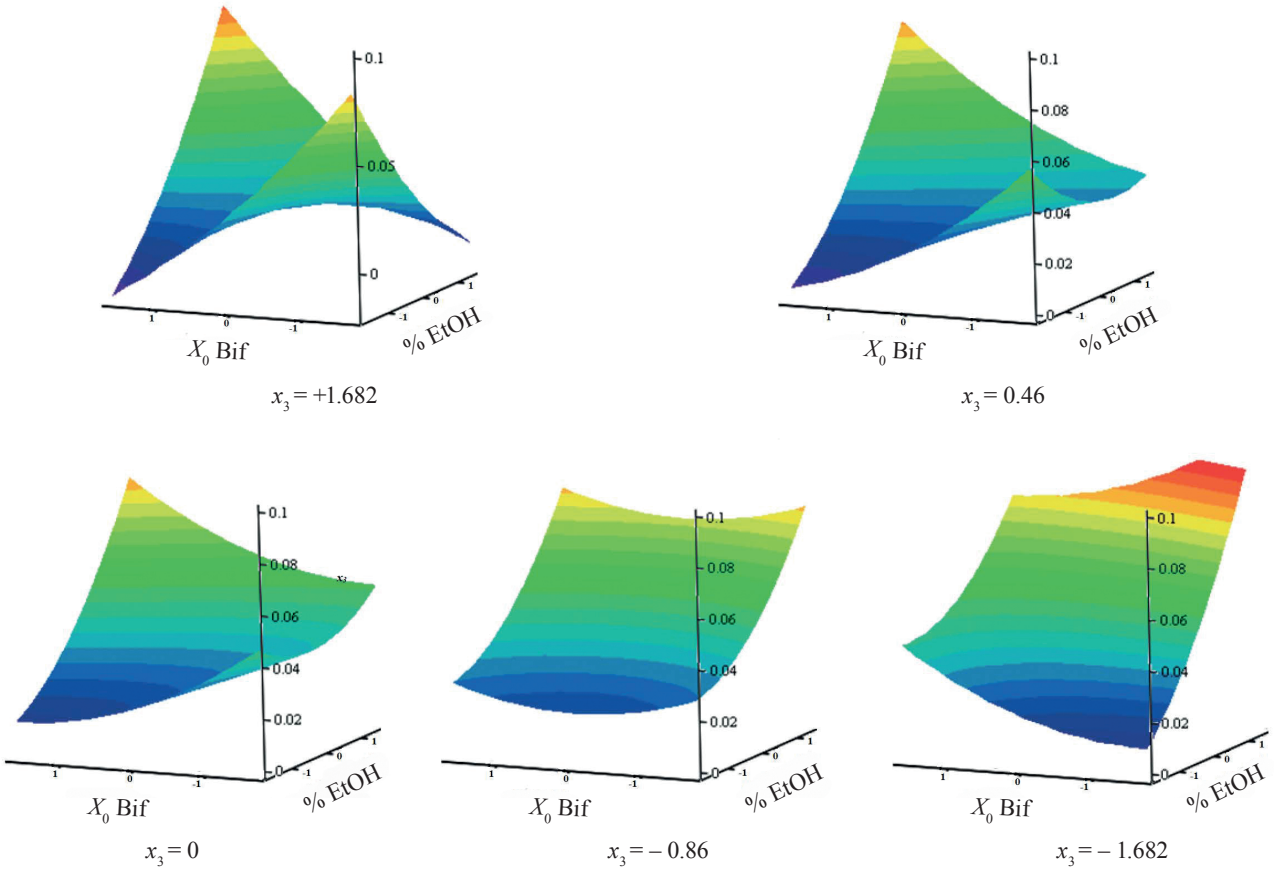

Figure 3 Synbiotic factor response surface as a function of ethanol concentration (x_1) and initial probiotic count (x_2) at fixed initial *Salmonella* count (x_3)

the test strain. As the initial probiotic and test strain concentrations increased, the final bacterial count plummeted. Probably, bacilli inhibited their own growth by their own metabolites, i.e., lactic acid.

Antagonism of synbiotic compositions against *Salmonella enterica* and response surface analysis. Table 4 shows the design matrix with experimental and calculated values of the response functions for *S. enterica*. The variation range of variables in natural coordinates did not differ from that of bacilli, except for the shift in the initial test strain count by +1 lg(CFU/mL).

The response surface analysis for synbiotic factor (Y_1) was represented as the following equation confirmed by Fisher's criterion ($F = 3.99 < 4.87$, $P = 0.05$):

$$Y_1 = 0.029 + 0.012x_1 - 0.007x_3 + 0.006x_1x_2 - 0.006x_1x_3 + \\ + 0.007x_1x_2x_3 + 0.004x_1^2 + 0.003x_2^2 \quad (5)$$

The coefficients for all factors and their pairwise interactions turned out to be significant. The response surfaces were calculated for fixed (Fig. 3). For all the surfaces obtained, the smallest value of the response function within the variation range was obtained when the precipitant concentration was minimal. When was below 0.46, which corresponded to the initial *Salmonella* count (6.91 lg(CFU/mL)), the response surface was parabolic, and its analytical minimum was outside the variation range. These surfaces demonstrated an increase in the initial bifidobacterial count, which followed the increase in the initial *Salmonella* count.

The larger bifidobacterial count resulted in the greatest suppression, which varied from $x_3 = -1.682$ to $x_3 = 0$. Thus, the response surface method made it possible to define the critical value of the *Salmonella* count (6.5 lg(CFU/mL)). When this value was exceeded, only the maximal count of viable bifidobacterial cells could inhibit the pathogen. If the initial pathogen count exceeded 6.91 lg(CFU/mL), the response surfaces had a saddle shape.

The global minimum of the response function within the variation range was determined by the variable step scanning method. Initially, all variables for each coordinate had an interval with two equal subintervals. The values of the function were calculated at the nodes of the resulting grid to select the optimal point with the lowest synbiotic factor. Subsequently, the interval was cut in two. The calculation cycles continued until the interval along one of the coordinates fell below 0.001. The minimum was determined at the border of the region in coordinates –1.682, +1.682, and +1.682. Therefore, the greatest antagonistic effect was expected at the lowest alcohol concentration of 20% and the

Table 4 Range of variation and encoding of variables: experimental and calculated values of response functions for *Salmonella enterica*

Test No.	Factors						Synbiotic factor		Final bacterial count, lg(CFU/mL)*	
	Precipitant concentration (EtOH), %		Initial prebiotic count, lg(CFU/mL)		Initial bacterial count, lg(CFU/mL)					
	z_1	x_1	z_2	x_2	z_3	x_3	SF_{obs}	SF_{pred}	$X_{sal\ obs}$	$X_{sal\ pred}$
1	67.8	+1	7.6	+1	7.4	+1	0.0544	0.0477	8.55	8.58
2	67.8	+1	7.6	+1	5.6	–1	0.0636	0.0596	8.53	8.47
3	67.8	+1	6.4	–1	7.4	+1	0.0233	0.0214	8.71	8.67
4	67.8	+1	6.4	–1	5.6	–1	0.0689	0.0616	8.64	8.59
5	32.2	–1	7.6	+1	7.4	+1	0.0114	0.0088	8.58	8.58
6	32.2	–1	7.6	+1	5.6	–1	0.0265	0.0267	8.41	8.47
7	32.2	–1	6.4	–1	7.4	+1	0.0328	0.0351	8.60	8.67
8	32.2	–1	6.4	–1	5.6	–1	0.0278	0.0247	8.60	8.59
9	20.0	–1.682	7.0	0	6.5	0	0.0225	0.0202	8.51	8.49
10	80.0	+1.682	7.0	0	6.5	0	0.0525	0.0602	8.47	8.49
11	50.0	0	6.0	–1.682	6.5	0	0.0468	0.0371	8.61	8.64
12	50.0	0	8.0	+1.682	6.5	0	0.0221	0.0371	8.46	8.44
13	50.0	0	7.0	0	5.0	–1.682	0.0399	0.0413	8.59	8.63
14	50.0	0	7.0	0	8.0	+1.682	0.0179	0.0162	8.77	8.74
15	50.0	0	7.0	0	6.5	0	0.0328	0.0287	8.61	8.62
16	50.0	0	7.0	0	6.5	0	0.0289	0.0287	8.61	8.62
17	50.0	0	7.0	0	6.5	0	0.0334	0.0287	8.65	8.62
18	50.0	0	7.0	0	6.5	0	0.0244	0.0287	8.63	8.62
19	50.0	0	7.0	0	6.5	0	0.0230	0.0287	8.63	8.62
20	50.0	0	7.0	0	6.5	0	0.0308	0.0287	8.57	8.62

* the response function was calculated as CFU/mL; the results are given on a logarithmic scale

highest initial bifidobacterial count of 8.0 lg(CFU/mL). Unlike the bacilli, the metabolism of the test strain affected the synbiotic factor and reduced its value. Probably, the reduction happened because of extra acid production.

The final *Salmonella* count equation ($F = 2.20 < 4.74$, $P = 0.05$) looked as follows:

$$Y_2 = 4.14\times10^8 - 4.58\times10^7 x_2 + 3.95\times10^7 x_3 - $$
$$- 3.61\times10^7 x_1^2 - 2.08\times10^7 x_2^2 + 2.63\times10^7 x_3^2 \quad (6)$$

As for the synbiotic factor, all factors had a significant impact on target function Y_2. The response surfaces were calculated for fixed x_3 values (Fig. 4). The surface was parabolic in coordinates x_1 and x_2. The maximal value of the final test strain count was 8.68 lg(CFU/mL) in coordinates 0, –1.101, and +1.685. Thus, the synbiotic composition of fructans precipitated by 50% ethanol and bifidobacteria with the initial count of 6.34 lg(CFU/mL) had the lowest antagonistic effect against *Salmonella*. As the initial *Salmonella* count increased, the efficiency weakened.

The effect of the initial test strain count on the response function was not symmetrical to the design center because the minimum of the function for this variable was at the point – 0.749, 5.83 lg(CFU/mL). The dependence had a quadratic nature. As a result, the final *Salmonella* count remained almost the same when the initial count was below 6.5 lg(CFU/mL). When the values were large, the value of the response function rose sharply. Therefore, the initial *Salmonella* count of 6.5 lg(CFU/mL) was critical from the standpoint of microbiology.

The response paraboloid was symmetrical to the design center of variable. Thus, both fructan fractions precipitated by the highest and the lowest alcohol concentrations possessed the same inhibition effects. However, as the initial probiotic count exceeded 6.34 lg(CFU/mL), the inhibition of the pathogen increased. The lowest values of the final *S. enterica* count (and the greatest antagonistic effect) within the variation range were achieved at the maximal initial bifidobacterial count of 8.0 lg(CFU/mL) in the medium with *A. lappa* root fructan fractions precipitated with 20 or 80% ethanol.

Previously, we considered *Staphylococcus aureus* as the test strain and also found out that the effect of *A. lappa* fructans precipitated with 40 and 60% ethanol was weaker than those precipitated with 20 or 80% ethanol [27]. Apparently, the highest average degree of polymerization was effective because the carbohydrate substrate was less available. The lowest degree of polymerization was effective because the bifidobacteria consumed the substrate faster and thus produced more metabolites. This issue, however, requires further research.

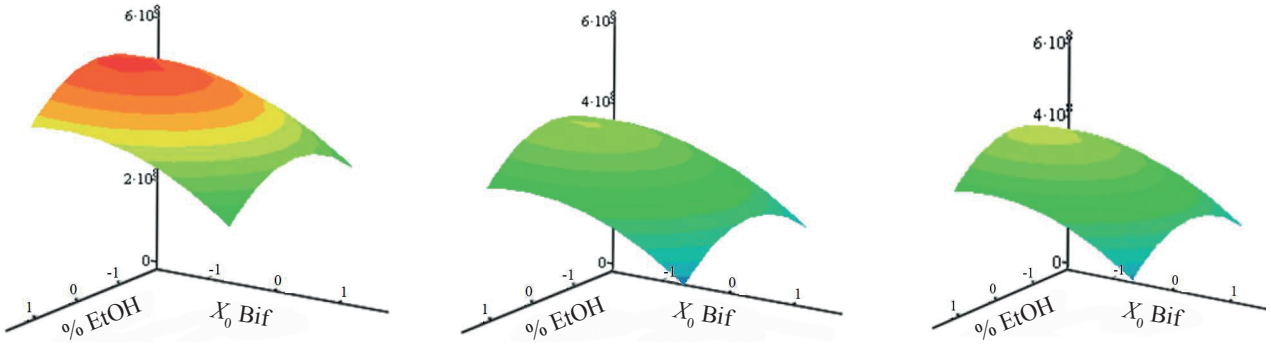

$x_3 = +1.682$ $x_3 = 0$ $x_3 = -1.682$

Figure 4 Final *Salmonella* count response surface as a function of ethanol concentration (x_1) and initial probiotic count (x_2) at fixed initial *Salmonella* count (x_3)

In this study, we considered lactic and acetic acids as inhibitors. As proved by Prosekov *et al.*, many bifidobacteria can produce antimicrobial peptides (bacteriocins), and some representatives of *B. bifidum* are among them [41]. However, their synthesis usually becomes active at the stationary phase, and by that time the bifidobacterial count in the co-culture of bacilli and *Salmonella* stop growing. Therefore, the synbiotic factor calculations did not take into account the effect of bacteriocins. Further research is required to study these inhibitors under conditions close to real, e.g., intestinal simulators with a continuous slow medium flow.

The approach proposed in this paper can also be applied to non-plant prebiotics. Lactulose is one of the best prebiotics [42]. It is often combined with other prebiotics, such as fructooligosaccharides, to make up functional foods. Scientists also turn to oligosaccharides of goat's milk, which are a mix of tri- and tetrasaccharides that consist of glucose, fructose, galactose, and their acylated derivatives [43]. Obviously, the qualitative and quantitative composition affects the action of the prebiotic both separately and as part of a synbiotic composition. Our approach can be applied to similar studies *in vitro*.

CONCLUSION

In this research, the highest synbiotic efficiency belonged to the fraction of fructans with a higher degree of polymerization precipitated by the lowest ethanol concentration and the highest bifidobacterial count. The study established a quantitative relationship between the bifidobacteria and the parameters of fructan production and the antagonistic activity of their synbiotic composition. We also determined the effect of the ratio of probiotic and pathogen counts on antagonism. The proposed approach can substantiate the composition of new synbiotics. In the future, we plan to study other compositions of probiotics and prebiotics *in vivo* to find their optimal ratio.

CONTRIBUTION

S. Evdokimova and B. Karetkin developed the research concept. E. Guseva and I. Shakir were responsible for data curation and formal analysis. B. Karetkin acquired the funding. S. Evdokimova and N. Khabibulina performed the experiments. B. Karetkin and E. Guseva developed the methodology. B. Karetkin supervised the project. E. Guseva and M. Zhurikov worked with the Software. I. Shakir validated the obtained data. S. Evdokimova and M. Zhurikov developed the infographics. S. Evdokimova wrote the original draft. B. Karetkin and V. Panfilov edited the manuscript. All the authors discussed the results and contributed to the final manuscript. All the authors have read and agreed to the published version of the manuscript.

CONFLICT OF INTEREST

The authors declare that there is no conflict of interests regarding the publication of this article.

ACKNOWLEDGEMENTS

NMR spectrometry was performed on the equipment of the Mendeleev Center for Collective Use. The authors would like to express their gratitude to Andrey B. Polyakov.

REFERENCES

1. Heintz-Buschart A, Wilmes P. Human gut microbiome: Function matters. Trends in Microbiology. 2018;26(7): 563–574. https://doi.org/10.1016/j.tim.2017.11.002
2. Martín MÁ, Ramos S. Impact of dietary flavanols on microbiota, immunity and inflammation in metabolic diseases. Nutrients. 2021;13(3). https://doi.org/10.3390/nu13030850

3. von Martels JZH, Sadaghian Sadabad M, Bourgonje AR, Blokzijl T, Dijkstra G, Faber KN, *et al.* The role of gut microbiota in health and disease: *In vitro* modeling of host-microbe interactions at the aerobe-anaerobe interphase of the human gut. Anaerobe. 2017;44:3–12. https://doi.org/10.1016/j.anaerobe.2017.01.001
4. Kamada N, Kim Y-G, Sham HP, Vallance BA, Puente JL, Martens EC, *et al.* Regulated virulence controls the ability of a pathogen to compete with the gut microbiota. Science. 2012;336(6086):1325–1329. https://doi.org/10.1126/science.1222195
5. Rolhion N, Chassaing B. When pathogenic bacteria meet the intestinal microbiota. Philosophical Transactions of the Royal Society B: Biological Sciences. 2016;371(1707). https://doi.org/10.1098/rstb.2015.0504
6. Peluzio MCG, Martinez JA, Milagro FI. Postbiotics: Metabolites and mechanisms involved in microbiota-host interactions. Trends in Food Science and Technology. 2020;108:11–26. https://doi.org/10.1016/j.tifs.2020.12.004
7. Markowiak-Kopeć P, Śliżewska K. The effect of probiotics on the production of short-chain fatty acids by human intestinal microbiome. Nutrients. 2020;12(4). https://doi.org/10.3390/nu12041107
8. Ramarao N, Tran S-L, Marin M, Vidic J. Advanced methods for detection of *Bacillus cereus* and its pathogenic factors. Sensors. 2020;20(9). https://doi.org/10.3390/s20092667
9. Jessberger N, Dietrich R, Granum PE, Märtlbauer E. The *Bacillus cereus* food infection as multifactorial process. Toxins. 2020;12(11). https://doi.org/10.3390/toxins12110701
10. Eastwood LC, Taylor TM, Savell JW, Gehring KB, Arnold AN. Efficacy of antimicrobial interventions in reducing *Salmonella enterica*, Shiga toxin-producing *Escherichia coli*, *Campylobacter*, and *Escherichia coli* biotype I surrogates on non-chilled and chilled, skin-on and skinless pork. Meat Science. 2021;172. https://doi.org/10.1016/j.meatsci.2020.108309
11. Castro VS, Mutz YS, Rosario DKA, Cunha-Neto A, Figueiredo EES, Conte-Junior CA. Inactivation of multi-drug resistant non-typhoidal *Salmonella* and wild-type *Escherichia coli* STEC using organic acids: A potential alternative to the food industry. Pathogens. 2020;9(10). https://doi.org/10.3390/pathogens9100849
12. Beloborodova NV. Integration of metabolism in man and his microbiome in critical conditions. General Reanimatology. 2012;8(4):42–54. (In Russ.). https://doi.org/10.15360/1813-9779-2012-4-42
13. Green M, Arora K, Prakash S. Microbial medicine: Prebiotic and probiotic functional foods to target obesity and metabolic syndrome. International Journal of Molecular Sciences. 2020;21(8). https://doi.org/10.3390/ijms21082890
14. Medina-Vera I, Sanchez-Tapia M, Noriega-López L, Granados-Portillo O, Guevara-Cruz M, Flores-López A, *et al.* A dietary intervention with functional foods reduces metabolic endotoxaemia and attenuates biochemical abnormalities by modifying faecal microbiota in people with type 2 diabetes. Diabetes and Metabolism. 2019;45(2):122–131. https://doi.org/10.1016/j.diabet.2018.09.004
15. Ashaolu TJ. Immune boosting functional foods and their mechanisms: A critical evaluation of probiotics and prebiotics. Biomedicine and Pharmacotherapy. 2020;130. https://doi.org/10.1016/j.biopha.2020.110625
16. Alkhatib A. Antiviral functional foods and exercise lifestyle prevention of coronavirus. Nutrients. 2020;12(9). https://doi.org/10.3390/nu12092633
17. Swanson KS, Gibson GR, Hutkins R, Reimer RA, Reid G, Verbeke K, *et al.* The International Scientific Association for Probiotics and Prebiotics (ISAPP) consensus statement on the definition and scope of synbiotics. Nature Reviews Gastroenterology and Hepatology. 2020;17(11):687–701. https://doi.org/10.1038/s41575-020-0344-2
18. Ruiz L, Flórez AB, Sánchez B, Moreno-Muñoz JA, Rodriguez-Palmero M, Jiménez J, *et al. Bifidobacterium longum* subsp. *infantis* CECT7210 (*B. infantis* IM-1®) displays in vitro activity against some intestinal pathogens. Nutrients. 2020;12(11). https://doi.org/10.3390/nu12113259
19. Valdés-Varela L, Hernández-Barranco AM, Ruas-Madiedo P, Gueimonde M. Effect of *Bifidobacterium* upon *Clostridium difficile* growth and toxicity when co-cultured in different prebiotic substrates. Frontiers in Microbiology. 2016;7. https://doi.org/10.3389/fmicb.2016.00738
20. Śliżewska K, Chlebicz-Wójcik A. The in vitro analysis of prebiotics to be used as a component of a synbiotic preparation. Nutrients. 2020;12(5). https://doi.org/10.3390/nu12051272
21. Karetkin BA, Guseva EV, Evdokimova SA, Mishchenko AS, Khabibulina NV, Grosheva VD, *et al.* A quantitative model of *Bacillus cereus* ATCC 9634 growth inhibition by bifidobacteria for synbiotic effect evaluation. World Journal Microbiology and Biotechnology. 2019;35(6). https://doi.org/10.1007/s11274-019-2665-2

22. Rashmi HB, Negi PS. Phenolic acids from vegetables: A review on processing stability and health benefits. Food Research International. 2020;136. https://doi.org/10.1016/j.foodres.2020.109298

23. Babich O, Sukhikh S, Prosekov A, Asyakina L, Ivanova S. Medicinal plants to strengthen immunity during a pandemic. Pharmaceuticals. 2020;13(10). https://doi.org/10.3390/ph13100313

24. Wack M, Blaschek W. Determination of the structure and degree of polymerisation of fructans from *Echinacea purpurea* roots. Carbohydrate Research. 2006;341(9):1147–1153. https://doi.org/10.1016/j.carres.2006.03.034

25. Li J, Du J. Molecular characterization of arabinoxylan from wheat beer, beer foam and defoamed beer. Molecules. 2019;24(7). https://doi.org/10.3390/molecules24071230

26. Zeaiter Z, Regonesi ME, Cavini S, Labra M, Sello G, Di Gennaro P. Extraction and characterization of inulin-type fructans from artichoke wastes and their effect on the growth of intestinal bacteria associated with health. BioMed Research International. 2019;2019. https://doi.org/10.1155/2019/1083952

27. Evdokimova SA, Nokhaeva VS, Karetkin BA, Guseva EV, Khabibulina NV, Kornienko MA, *et al.* A study on the synbiotic composition of *Bifidobacterium bifidum* and fructans from *Arctium lappa* roots and *Helianthus tuberosus* tubers against *Staphylococcus aureus*. Microorganisms. 2021;9(5). https://doi.org/10.3390/microorganisms9050930

28. Box GEP, Wilson KB. On the experimental attainment of optimum conditions. Journal of the Royal Statistical Society. 1951;13(1):1–45.

29. Shuhaimi M, Kabeir BM, Yazid AM, Nazrul Somchit M. Synbiotics growth optimization of *Bifidobacterium pseudocatenulatum* G4 with prebiotics using a statistical methodology. Journal of Applied Microbiology. 2009;106(1):191–198. https://doi.org/10.1111/j.1365-2672.2008.03991.x

30. Mishra Pandey S, Mishra HN. Optimization of the prebiotic & probiotic concentration and incubation temperature for the preparation of synbiotic soy yoghurt using response surface methodology. LWT. 2015;62(1):458–467. https://doi.org/10.1016/j.lwt.2014.12.003

31. Wang C, Wang Z, Wang P, Zhang S. Multiple effects of environmental factors on algal growth and nutrient thresholds for harmful algal blooms: Application of response surface methodology. Environmental Modeling and Assessment. 2016;21(2):247–259. https://doi.org/10.1007/s10666-015-9481-3

32. Shi Y, Fang H, Li Y-Y, Wu H, Liu R, Niu Q. Single and simultaneous effects of naphthalene and salinity on anaerobic digestion: Response surface methodology, microbial community analysis and potential functions prediction. Environmental Pollution. 2021;291. https://doi.org/10.1016/j.envpol.2021.118188

33. Karetkin BA, Panfilov VI, Baurin DV, Shakir IV. Ultrasonic extraction of fructans from the tubers of jerusalem artichoke: Optimization of conditions, purification methods, C-13 NMR spectroscopy of the product. International Multidisciplinary Scientific GeoConference Surveying Geology and Mining Ecology Management. 2015;1(6): 641–648.

34. Rossi M, Corradini C, Amaretti A, Nicolini M, Pompei A, Zanoni S, *et al.* Fermentation of fructooligosaccharides and inulin by bifidobacteria: A comparative study of pure and fecal cultures. Applied and Environmental Microbiology. 2005;71(10):6150–6158. https://doi.org/10.1128/AEM.71.10.6150-6158.2005

35. De Man JC, Rogosa M, Sharpe ME. A medium for the cultivation of Lactobacilli. Journal of Applied Bacteriology. 1960;23(1):130–135. https://doi.org/10.1111/j.1365-2672.1960.tb00188.x

36. Nebra Y, Blanch A. A new selective medium for *Bifidobacterium* spp. Applied and Environmental Microbiology. 1999;65(11):5173–5176. https://doi.org/10.1128/AEM.65.11.5173-5176.1999

37. Scherer R, Rybka ACP, Ballus CA, Meinhart AD, Filho JT, Godoy HT. Validation of a HPLC method for simultaneous determination of main organic acids in fruits and juices. Food Chemistry. 2012;135(1):150–154. https://doi.org/10.1016/j.foodchem.2012.03.111

38. Mariano TB, Higashi B, Sanches Lopes SM, Pedroza Carneiro JW, de Almeida RTR, Pilau EJ, *et al.* Prebiotic fructooligosaccharides obtained from escarole (*Cichorium endivia* L.) roots. Bioactive Carbohydrates and Dietary Fibre. 2020;24. https://doi.org/10.1016/j.bcdf.2020.100233

39. Evdokimova S, Karetkin B, Nokhaeva V, Guseva E, Shakir I. Minimum inhibitory concentrations of organic acids against foodborne opportunistic microbial pathogens. SGEM International Multidisciplinary Scientific GeoConference. 2021;21(92):193–200. https://doi.org/10.5593/sgem2021/6.1/s25.25

40. Pachkin SG, Kotlyarov RV. Implementation of the methods of identification of static control objects. Science Evolution. 2017;2(2):72–78. https://doi.org/10.21603/2500-1418-2017-2-2-72-78
41. Prosekov AYu, Dyshlyuk LS, Milentieva IS, Sykhikh SA, Babich OO, Ivanova SA, *et al.* Antioxidant and antimicrobial activity of bacteriocin-producing strains of lactic acid bacteria isolated from the human gastrointestinal tract. Progress in Nutrition. 2017;19(1):67–80.
42. Khramtsov AG. New technological paradigm of the Russian dairy industry: formation principles under globalisation. Foods and Raw Materials. 2019;7(2):291–300. https://doi.org/10.21603/2308-4057-2019-2-291-300
43. van Leeuwen SS, Te Poele EM, Chatziioannou AC, Benjamins E, Haandrikman A, Dijkhuizen L. Goat milk oligosaccharides: Their diversity, quantity, and functional properties in comparison to human milk oligosaccharides. Journal of Agricultural and Food Chemistry. 2020;68(47):13469–13485. https://doi.org/10.1021/acs.jafc.0c03766

ORCID IDs
Svetlana A. Evdokimova https://orcid.org/0000-0002-4808-5002
Boris A. Karetkin https://orcid.org/0000-0002-0976-9700
Mikhail O. Zhurikov https://orcid.org/0000-0001-8584-7400
Elena V. Guseva https://orcid.org/0000-0002-6835-4513
Natalia V. Khabibulina https://orcid.org/0000-0001-7056-6921
Irina V. Shakir https://orcid.org/0000-0002-1787-5773
Victor I. Panfilov https://orcid.org/0000-0002-8158-7012

Foods and Raw Materials. 2022;10(2)

ISSN 2310-9599 (Print)
ISSN 2308-4057 (Online)

Research Article
Open Access

Available online at http://jfrm.ru/en
https://doi.org/10.21603/2308-4057-2022-2-546
https://elibrary.ru/UKMATU

Yogurt-like product from lupine (*Lupinus albus* L.) milk as an alternative to dairy products

Nazan Kavas

Ege University, Izmir, Turkey

* e-mail: nazan.kavas@ege.edu.tr

Received 14.04.2022; Revised 16.06.2022; Accepted 02.08.2022; Published online 23.09.2022

Abstract:
Recently, the number of people suffering from allergy to caw's milk has increased. Lupine, a plant rich in protein, can be a good alternative product for non-dairy products production. We aimed to obtain a yogurt-like product based on lupine milk and evaluate its properties.

Lupine milk was obtained from lupine seeds, egg white protein powder, disaccharides, and starter cultures were added to the milk to obtain yogurt-like products: samples with maltose, samples with lactose, and samples without sugars. Physico-chemical and microbiological characteristics of the products were determined by the standard techniques. Sensory attributes were evaluated by trained panelists.

In the study, the effects of egg white protein powder and disaccharides on the activities of starter cultures and the properties of the yogurt-like products obtained were investigated. The relationship between the addition of sugar and the growth of starter cultures was found to be significant ($P < 0.05$). In terms of physico-chemical, rheological, and microbiological properties, the yogurt-like products obtained from lupine milk with disaccharides demonstrated good results, especially the sample with maltose. Sensory analysis revealed high sensory properties of the yogurt-like products.

Yogurt-like products from lupine milk can be used as an alternative to cow's milk fermented products, but more detailed studies should be conducted on their formulations.

Keywords: Lupine milk, maltose, lactose, fermentation, non-dairy yogurt-like product, starter cultures

Please cite this article in press as: Kavas N. Yogurt-like product from lupine (*Lupinus albus* L.) milk as an alternative to dairy products. Foods and Raw Materials. 2022;10(2):377–385. https://doi.org/10.21603/2308-4057-2022-2-546

INTRODUCTION

The increasing prevalence of protein allergenicity to cow's milk has driven the food industry towards the design, supply, and production of new plant-based milk alternatives. Studies on the creating of formulations with sensory acceptability that are suitable for vegetarian diets have rapidly increased in recent years. In addition, fermented products made from plant-derived milk instead of fermented products from animals' milk have become of interest [1].

One of the plant-based alternatives to cow's milk is lupine milk. Lupine (*Lupinus albus* L.) is a plant belonging to the *Lupinus* species of the *Papilioneceae* (*Legumineceae*; butterfly-flowered) family. Lupine is used as a soy alternative in such products as bread, biscuits, cakes, pasta, confectionery, and soy sauce. Besides, due to its antioxidant content, lupine is also used in high-quality vegetable oil, gluten-free flour, emulsifying agents, and alternative fermented products [2, 3].

Today, lupine attracts attention as functional food because it is rich in protein, minerals, vitamins, oleic acid, fiber and other valuable components, as well as because its antioxidant capacity. Lupine seeds contain significant amounts of polyphenols, carotenoids, phytosterols, tocopherols, and alkaloids, as well as peptides with antioxidant, antimicrobial, anti-carcinogenic, and anti-inflammatory activities [4].

Lupine milk is obtained from lupine grains. The protein value of lupine milk is 4.90 g/100 g, the fat content is 5.00 g/100 g, the total dry matter ratio is 11.20 g/100 g, and the pH is 6.30 [1, 2, 5]. Lupine milk characteristics make it suitable to produce dairy products such as set yogurt, probiotic yogurt, and cheese [6].

Clean lupine seeds (1 kg)
↓
Boiling 1:3 seeds/water (30 min)
↓
Dehulling
↓
Removing bitterness from the seeds
↓
Shredding (5 min)
↓
Adding water (10 g/100 mL) so that the lupine dry matter is 10% and pH adjustment (6.5–7.0)
↓
Homogenization
↓
Filtration
↓
Heat treatment (20 min at 30°C)
↓
Cooling to room temperature
↓
Storage at +4°C

Figure 1 Preparation of lupin milk from the seeds of *Lupinus albus* L.

In addition to the use of lupine milk itself, there are studies on the use of its components in the production of dairy products. For example, lupine proteins were used in ice-cream production and yielded ice cream with high sensory properties [7].

Some studies, have reported that fermented products can be produced from lupine milk, but since yogurt starter cultures cannot use carbohydrates in the composition of lupine milk, it is necessary to enrich this milk by adding disaccharides, increasing thereby the activity of starter cultures [6].

The growth of lactic acid bacteria in artificial environments (other than milk) is difficult, but they can easily grow in most plant-based media/substrates. Additionally, lactic acid bacteria have been found to rapidly increase acidity (decrease in pH) in plant-derived environments to a point where other competitive organisms cannot thrive.

Krunglevičiūtė *et al.* have reported that acidity (hence the growth of lactic acid bacteria) in a fermented product made using lupine milk depends on the lupine variety and amino acid levels [8]. However, it has been stated that lupine milk has a unique nutritional composition and may support the increase in the number and survival of lactic acid bacteria in fermented products.

Egg white protein powder is obtained as a result of drying the egg white protein by the traditional drying method. Pasteurized egg white protein powder is produced by drying egg white protein by the conventional spraying method [9]. In our research, egg white protein powder was used to increase dry matter level.

The aim of this study was to obtain a yogurt-like product based on lupine milk as an alternative to cow's milk and evaluate its microbiological, physico-chemical, and sensory attributes.

STUDY OBJECTS AND METHODS

Raw lupine (*Lupinus albus* L.), pasteurized egg white protein powder (Alfasol®), JOINTEC VB530 lyophilized culture, lactose, and maltose were obtained from Ödemiş (Turkey-İzmir), Kimbiotek Chemical Substances Inc. (Istanbul-Turkey), CSL laboratory (Strade per Merlino, 3,26839, Italy), and Sigma-Aldrich, respectively.

Production of lupine milk. Lupine milk was extracted from seeds by the method illustrated in Fig. 1.

Production of non-dairy yogurt-like product. In the study, plant-based yogurt-like products were obtained by from lupine milk with functional properties, egg white protein powder, and disaccharides (lactose and maltose) with the following fermentation with *Lactobacillus bulgaricus* + *Streptecoccus thermophiles* (Table 1).

Lupine milk was aliquoted into three equal batches to obtain three samples, namely milk without saccharides (control), milk with lactose (0.5%, w/v), and milk with maltose (0.5%, w/v). Lactose and maltose were added into the milk, the batches were pasteurized separately at 85°C for 20 min, and cooled to 50–55°C.

Table 1. Experimental design

	Lactobacillus bulgaricus + *Streptecoccus thermophilus*	Egg white protein powder	Lactose	Maltose
Lupine milk (control)	3%	3%		
Lupine milk with lactose	3%	3%	0.5%	
Lupine milk with maltose	3%	3%		0.5%

After adding egg white protein powder (3%, w/v) to each batch, they were homogenized for 3–5 min with an Ultra Turrax Blender at 1200 rpm. Then, the samples were cooled to 42–43°C and the starter culture (3%, w/v) was added. Thus, we prepared three yogurt-like samples based on the lupine milk samples. The samples were incubated at 42–43°C and pH 4.60 for three days. On days 1, 7, 14, and 28 of storage at 4°C, we performed physico-chemical, rheological, microbiological, and sensory analyses.

Physico-chemical analyses. Dry matter was determined by the gravimetric method. The ash content was determined using AOAC methods. The fat content was determined by Gerber's method. pH value was detected using an SS-3 Zeromatic (Beckman Instruments Inc., California, USA) pH meter, and titration acidity (% lactic acid) was determined according to the alkali titration method. The protein value was determined by the Kjeldahl method according to AOAC in milk and yogurt-like product samples [10]. Viscosity was determined with a digital visco-meter (V100003/FungiLabAlpha), and syneresis was determined as described by Kieserling *et al*. [11, 12]. The texture properties were determined with a texture analyzer (HDPL2/CEL5/TA-XT Plus), and the carbohydrate content was determined with an Atago Polax×2L polarimeter (Japanese).

Determination of fatty acid composition. Each homogenized sample was extracted according to the Gerber method to obtain oil as described in [14], fatty acid methyl esters were prepared according to AOCS and investigated using gas chromatography [15]. We used a Supelco SP-2380 (Supelco Inc., Bellefonte, USA) fused a silica capillary column (60×0.25 mm i.d., 0.2 mm film thickness) and a Hewlett-Packard gas chromatographer (model 6890) with a flame ionizing detector. Injection volume: 1 µL; oven temperature: 4°C/min 100°C to 220°C; injector and detector temperature: 300°C; carrier gas: helium; and flow rate: 1 mL/min. Fatty acid methyl esters were detected in the lupine milk and yogurt-like samples on day 1 of storage.

Microbiological analysis. MRS-agar (Merck, Germany) was used to count *L. bulgaricus*. All the samples under study were subjected to anaerobic incubation at 42°C for 3 days on MRS-agar. *L. bulgaricus* count was determined as CFU/g [16]. An M_{17} agar medium containing lactose was used for *S. thermophiles* counting. The incubation of the planted Petri dishes was carried out under aerobic conditions at 37°C for 72 h. The typical colonies formed at the end of the incubation were counted [17].

Sensory tests. Sensory analysis was performed by 10 trained panelists on days 1, 7, 10, 14, and 21 according to Jovanović *et al*. [18].

Statistics. The samples were examined in three repetitions and two replications. SPSS version 15 (IBM SPSS Statistics) statistical analysis package program was used. The data considered significant according to the analysis of variance (ANOVA) was tested at the $P < 0.05$ level using the Duncan multiple comparison test.

RESULTS AND DISCUSSION

Physico-chemical properties. In the study, dry matter in lupine milk was determined as 10.02%, fat 3.58%, protein 5.05%, carbohydrates 2.59 g/100 g, titration acidity (°SH) 0.131, pH value 6.38, ash 1.3%, and viscosity 3.52 cP (20°C). The physico-chemical properties of the yogurt-like samples based on lupine milk are given in Table 2.

The acidity in the samples with lactose and maltose was higher than that in the samples without sugars during storage, which was associated with maltose and lactose added to the lupine milk. The acidity increase in the samples with maltose during storage was higher than that in the products with lactose. The relationship between the increase in acidity and the sugar addition/type added to the samples was significant ($P < 0.05$).

Bintsis has reported that lactic acid bacteria develop better especially in the presence of glucose and some other sugars (sucrose, maltose), which cause higher acidity increase [19]. Our research results were found to be compatible with the literature, and depending on the glucose ratio, the highest acidity increase was determined in the yogurt-like product with maltose. Additionally, the results regarding the increase in acidity were found to be compatible with studies by Ozcan *et al*. who stated that the viability of lactic acid bacteria in plant-based yogurt-like products increased, thus increasing the acidity of the product [20].

Dry matter in all the samples decreased by the end of storage. The highest decrease was determined in the samples without sugars, while the decrease in the samples with lactose and maltose was found to be close to each other. However, the dry matter decrease in the products with maltose was found to be lower than that in the samples with lactose. The relationship between the type of sugar used in the production of non-dairy

Table 2 Physicochemical properties in yogurt-like samples based on lupine milk (n = 3)

	Storage, days	Milk without sugars	Milk with lactose	Milk with maltose
Dry matter, %	1	12.82 ± 1.44^{aA}	13.00 ± 1.14^{aB}	13.00 ± 1.13^{aB}
	7	12.25 ± 1.26^{aA}	12.75 ± 1.06^{aB}	12.85 ± 1.69^{aC}
	14	10.69 ± 1.33^{aA}	11.36 ± 1.46^{aB}	11.65 ± 1.47^{aC}
	28	10.44 ± 1.67^{aA}	11.03 ± 1.57^{aB}	11.26 ± 1.33^{aC}
Viscosity, cP	1	899.00 ± 5.11^{aA}	941.00 ± 8.21^{aB}	1021.00 ± 9.25^{aC}
	7	1056.00 ± 8.23^{bA}	1154.00 ± 8.36^{bB}	1163.00 ± 8.73^{aC}
	14	1274.00 ± 9.63^{bA}	1566.00 ± 9.45^{bB}	1621.00 ± 8.91^{bC}
	28	1663.00 ± 9.74^{bA}	1841.00 ± 9.98^{bB}	2047.00 ± 9.95^{bC}
Syneresis, g	1	9.52 ± 1.01^{aA}	8.67 ± 1.06^{aB}	8.55 ± 1.02^{aC}
	7	12.25 ± 2.06^{aA}	11.36 ± 1.03^{AB}	11.22 ± 1.11^{aC}
	14	13.49 ± 1.12^{aA}	12.41 ± 1.07^{aB}	12.10 ± 1.53^{aC}
	28	15.95 ± 2.07^{aA}	14.65 ± 2.06^{aB}	14.24 ± 2.54^{aC}
pH	1	4.60 ± 1.22^{aA}	4.58 ± 1.29^{aB}	4.56 ± 1.11^{aC}
	7	4.57 ± 0.81^{aA}	4.42 ± 1.06^{aB}	4.39 ± 1.46^{bC}
	14	4.45 ± 0.63^{aA}	4.29 ± 1.21^{aB}	4.25 ± 1.89^{bC}
	28	4.41 ± 0.78^{bA}	4.19 ± 1.63^{bB}	4.16 ± 1.42^{bC}
Acidity (%LA), °SH	1	0.912 ± 0.120^{aA}	0.938 ± 0.100^{aB}	0.944 ± 0.550^{aC}
	7	0.988 ± 0.220^{aA}	1.045 ± 0.650^{aB}	1.095 ± 0.630^{bC}
	14	1.039 ± 0.350^{bA}	1.121 ± 0.750^{bB}	1.133 ± 0.710^{bC}
	28	1.044 ± 0.630^{bA}	1.128 ± 0.430^{bB}	1.139 ± 0.390^{bC}
Fat, %	1	3.55 ± 0.41^{aA}	3.57 ± 0.66^{aB}	3.57 ± 0.51^{aB}
	7	3.12 ± 0.96^{aA}	3.36 ± 0.60^{aB}	3.38 ± 0.62^{aB}
	14	2.75 ± 0.25^{aA}	3.19 ± 0.82^{aB}	3.22 ± 0.84^{aB}
	28	2.35 ± 0.57^{aA}	2.88 ± 0.74^{aB}	2.93 ± 0.78^{aB}
Protein, %	1	5.03 ± 0.91^{aA}	5.00 ± 0.82^{aA}	4.98 ± 0.52^{aB}
	7	4.62 ± 0.93^{aA}	4.45 ± 0.67^{aA}	4.33 ± 0.87^{aB}
	14	4.22 ± 0.67^{bA}	4.16 ± 0.88^{aA}	4.02 ± 0.74^{aB}
	28	4.06 ± 0.76^{bA}	3.86 ± 0.50^{bA}	3.75 ± 0.46^{bB}
Carbohydrates, %	1	2.57 ± 0.92^{aA}	3.51 ± 0.80^{aB}	3.48 ± 0.91^{aB}
	7	2.54 ± 0.82^{aA}	2.85 ± 0.85^{aB}	2.44 ± 0.72^{aC}
	14	2.12 ± 0.49^{aA}	1.57 ± 0.63^{aB}	1.25 ± 0.56^{aC}
	28	1.95 ± 0.57^{aA}	0.92 ± 0.22^{aB}	0.84 ± 0.21^{aC}
Ash, %	1	0.55 ± 0.09^{aA}	0.57 ± 0.09^{aA}	0.57 ± 0.03^{aA}
	7	0.31 ± 0.08^{aA}	0.41 ± 0.07^{aA}	0.43 ± 0.07^{aA}
	14	0.21 ± 0.08^{aA}	0.33 ± 0.09^{aA}	0.34 ± 0.06^{aA}
	28	0.16 ± 0.07^{aA}	0.29 ± 0.02^{aA}	0.30 ± 0.02^{aA}

^{a,b,c} different letters on the same column are statistically significant ($P < 0.05$)

^{A,B,C} different letters on the same line are statistically significant ($P < 0.05$)

yogurt-like products from lupine milk and dry matter was significant ($P < 0.05$).

The fat content decreased in all the samples by the end of storage, but this decrease was not significant ($P > 0.05$). We revealed that during storage fat amounts in the samples with maltose and lactose were higher than in the samples without sugars. This situation is associated with a more pronounced syneresis in the yogurt-like products without sugars compared to the other samples. In this study, the relationship between the fat content and the type of sugar added to the samples and the amount of egg white protein powder was found to be significant ($P < 0.05$).

Protein values decreased in all the samples during storage, and the highest protein hydrolysis had the samples with maltose, followed by the samples with lactose and the samples without sugars. Among the samples, protein hydrolysis is associated with egg white protein powder added to lupine milk to increase the protein content and dry matter in lupine milk. The relationship between the sugar type added to milk and the addition of egg white protein powder and protein hydrolysis was significant ($P < 0.05$). In the study, the relationship between the type of sugar added to lupine milk and viscosity and syneresis was found to be significant ($P < 0.05$).

Al-Saedi *et al*. stated that yogurt-like products can be produced from lupine milk, with shortened fermentation time and the increased amount of the starter culture (especially probiotic microorganisms) [6]. In this respect, our research results are compatible with the literature.

Table 3 Fatty acid composition in yogurt-like products based on lupine milk

Fatty acid, g/100 g	Milk without sugars	Milk with maltose	Milk with lactose
Oleic Acid (C18:1)	49.00 ± 1.13	49.10 ± 1.05	49.10 ± 1.05
Linoleic Acid (C18:2)	23.41 ± 1.21	23.40 ± 1.07	23.40 ± 1.05
Palmitic Acid (C16:0)	7.33 ± 1.03	7.35 ± 1.13	7.34 ± 1.05
Gadoleic Acid (C20:1)	3.46 ± 1.12	3.47 ± 1.15	3.46 ± 1.05
Stearic Acid (C18:0)	1.62 ± 0.26	1.62 ± 0.04	1.62 ± 0.13
Arachidic Acid (C20:0)	2.85 ± 0.65	2.86 ± 0.70	2.85 ± 0.55
Miristic Acid (C14:0)	0.49 ± 0.01	0.48 ± 0.03	0.48 ± 0.06
Pentadecanoic Acid (C15:0)	0.21 ± 0.02	0.20 ± 0.01	0.21 ± 0.02
Lauric Acid (C12:0)	0.050 ± 0.001	0.050 ± 0.004	0.050 ± 0.003

Table 4 Texture changes in yogurt-like products based on lupine milk during storage

Indicator	Storage, days	Milk without sugars	Milk with lactose	Milk with maltose
Hardness, N	1	0.32 ± 0.01^{aA}	0.33 ± 0.02^{aB}	0.34 ± 0.05^{aC}
	7	0.36 ± 0.09^{aA}	0.37 ± 0.07^{bB}	0.40 ± 0.03^{bC}
	14	0.37 ± 0.01^{bA}	0.40 ± 0.06^{bB}	0.43 ± 0.08^{cC}
	28	0.38 ± 0.02^{cA}	0.42 ± 0.01^{cB}	0.48 ± 0.05^{cC}
Adhesiveness	1	0.04 ± 0.02^{aA}	0.05 ± 0.03^{aA}	0.05 ± 0.01^{aA}
	7	0.03 ± 0.01^{aA}	0.03 ± 0.01^{aA}	0.04 ± 0.02^{aA}
	14	0.02 ± 0.01^{aA}	0.03 ± 0.01^{aA}	0.03 ± 0.01^{aA}
	28	0.01 ± 0.01^{aA}	0.02 ± 0.01^{aA}	0.02 ± 0.01^{aA}
Springiness, mm	1	4.00 ± 0.52^{aA}	4.20 ± 0.94^{aB}	4.63 ± 0.99^{aC}
	7	4.11 ± 0.83^{aA}	4.29 ± 0.63^{aA}	5.16 ± 0.66^{aB}
	14	4.36 ± 0.64^{aA}	4.62 ± 0.80^{bB}	5.55 ± 0.83^{bC}
	28	4.58 ± 0.84^{bA}	4.81 ± 0.91^{bA}	5.87 ± 0.80^{bB}
Gumminess, g	1	41.05 ± 1.12^{aA}	72.56 ± 1.27^{aB}	79.47 ± 1.22^{aC}
	7	45.63 ± 1.23^{aA}	78.56 ± 2.24^{aB}	83.47 ± 2.88^{aC}
	14	49.22 ± 1.66^{aA}	82.10 ± 1.96^{bB}	85.33 ± 2.10^{bC}
	28	52.11 ± 1.35^{bA}	85.45 ± 2.67^{cB}	87.22 ± 2.66^{cC}
Chewiness, mJ	1	0.14 ± 0.05^{aA}	0.86 ± 0.11^{aA}	0.92 ± 0.30^{aA}
	7	0.16 ± 0.04^{aA}	1.12 ± 0.26^{aA}	1.21 ± 0.14^{aA}
	14	0.21 ± 0.03^{aA}	1.82 ± 0.49^{aA}	1.88 ± 0.47^{aA}
	28	0.35 ± 0.13^{aA}	2.02 ± 0.28^{aA}	2.09 ± 0.66^{aA}

^{a,b,c} different letters on the same column are statistically significant ($P < 0.05$)

^{A,B,C} different letters on the same line are statistically significant ($P < 0.05$)

In this study, the carbohydrate content decreased in all the samples during storage. The highest decrease was detected in the yogurt-like products with maltose, following by the samples with lactose. The relationship between the acidity increase and sugar addition/type and carbohydrate content was found to be significant ($P < 0.05$).

The ash values of all the samples decreased during storage, with the highest decrease in the sample without sugars, while the values for the products with lactose and maltose did not differ significantly. There was no significant difference between the samples in terms of the ash level ($P > 0.05$).

Fatty acid composition. Saturated fatty acids, monounsaturated fatty acids, and polyunsaturated fatty acids in the yogurt-like products made from lupine milk were detected as 14.17, 52.3, and 9.86 g/100 g, respectively (Table 3).

Rheological properties. Syneresis and viscosity values are given in Table 2, and the texture characteristic are given in Table 4. Consistency values of the samples were found to be significant in terms of sugar type and storage time interaction ($P < 0.05$). During storage, the stability (hardness) of the curd increased and the effect of storage was significant ($P < 0.05$). Hardness, flexibility, gumminess, and chewiness increased, while stickiness decreased in all the samples. The hardness determined in the sample with maltose was higher than that in the other samples. This situation is associated with lower syneresis, higher viscosity increase, lower dry matter decrease compared to the other samples, and higher increase in acidity (decrease in pH value) during storage. The hardness of the samples with lactose was higher than that in the samples without sugars. The difference between the samples in terms of syneresis

and the relationship between syneresis and sugar addition/type was significant ($P < 0.05$).

During storage, syneresis and dry matter decrease in the yogurt-like products with maltose were lower than in the samples without sugars, while those in the samples with lactose were lower than in the samples without sugars. The relationship between increased acidity and syneresis was found to be significant ($P < 0.05$).

The relationships between the viscosity, sugar ratio, egg white protein powder, and acidity increase in the samples under study were significant ($P < 0.05$). We revealed that the viscosity increased in all the samples during storage, with the highest increase in the product with maltose, while the lowest increase was in the samples without sugars. Egg white protein powder in the amount of 3% increased the viscosity of all the samples during storage.

The highest acidity and viscosity increase was determined in the samples with maltose, followed by the samples with lactose and the samples without sugars. The acidity (4.56 pH) and viscosity (1021 cP) values determined in the product with maltose on day 1 of storage were higher than those in the other samples. In the following days of storage, the increase in acidity was higher than in the other samples (Table 2). Accordingly, hardness and viscosity also increased.

The texture properties of the samples showed similar changes during storage. We determined that the rheological properties determined in the samples with maltose and lactose during storage were similar to those for the product without sugars but more acceptable. It was observed that the yogurt-like products without sugars were similar to the yogurt gel but had a more watery (yogurt-like beverage) consistency compared to the other samples. During storage, the increase in acidity was lower, the syneresis was higher, and viscosity was lower in the samples without sugars.

The rheological properties of curd in fermented milk products develop depending on the composition of milk, applied temperature, pH, soluble Ca^{++} ratio, and other factors (such as casein micelle size, various interactions, etc.). The increase in acidity decreases syneresis and increases protein hydrolysis, hardness, more soluble calcium, and in turn, viscosity [21].

In this study, we detected good physico-chemical and rheological properties of the fermented products produced with the addition of maltose and lactose. It was associated with high protein content and saccharide derivatives in the composition of lupine milk. Krunglevičiūtė *et al.* reported that the acidity of the fermented product made using lupine milk and the development of lactic acid bacteria are related to the lupine variety and amino acid level [8].

Sensory evaluation. Sensory evaluation revealed good sensory properties of the yogurt-like products with maltose and lactose (Fig. 2.) During storage, the samples with the disaccharides got close scores in terms of structure and consistency. This situation was associated with the scantiness in syneresis and an increase in

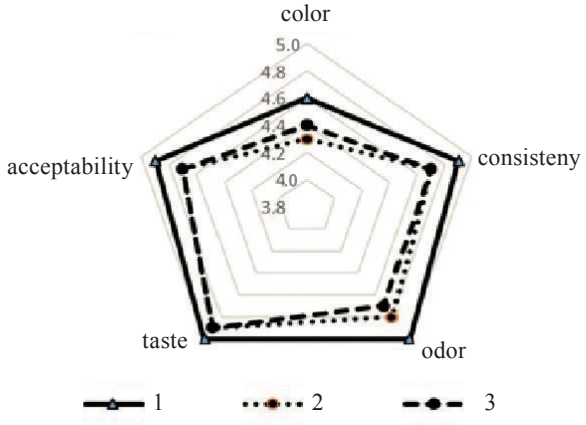

Figure 2 Sensory properties of yogurt-like products based on lupine milk (1), lupine milk with maltose (2), and lupine milk with lactose (3)

acidity, viscosity, and hardness during storage. The relationship between the increase of storage time and structure and consistency was found to be significant ($P < 0.05$).

In the study, the samples with maltose and lactose were found to be close to yogurt with a prolonged storage time, which is a classical fermented product, in terms of structural properties. Additionally, the structure and consistency of these samples were more similar to the classical fermented product (yogurt) with no lupine flavor or with weak one during storage. The texture and consistency in the samples without sugars were found to be less viscous and the panelists concluded that they could be considered as yogurt. Apparently, the level of fat in the samples with disaccharides during storage also influenced the taste of the product.

Microbiological analysis. Changes in *L. bulgaricus* and *S. thermophilus* amounts in the yogurt-like products obtained from lupine milk are given in Fig. 3. The samples with maltose and lactose demonstrated the increased growth and activity of starter cultures.

In the production of non-dairy yogurt-like products from lupine milk, the relationship between the addition of sugar and the growth of starter cultures was found to be significant ($P < 0.05$). In the samples with maltose and lactose, syneresis decreased during storage which had a positive effect on the development of starter cultures.

In the products without sugars, the *L. bulgaricus* and *S. thermophilus* growth was weaker compared to those with sugars. However, this situation did not appear as a problem in the production of yogurt-like products in the study. On the contrary, it strengthened the opinion that the composition of lupine milk is a suitable raw material to produce non-dairy yogurt-like products. Different studies have reported that lupine proteins effectively maintain the viability of starter cultures in different

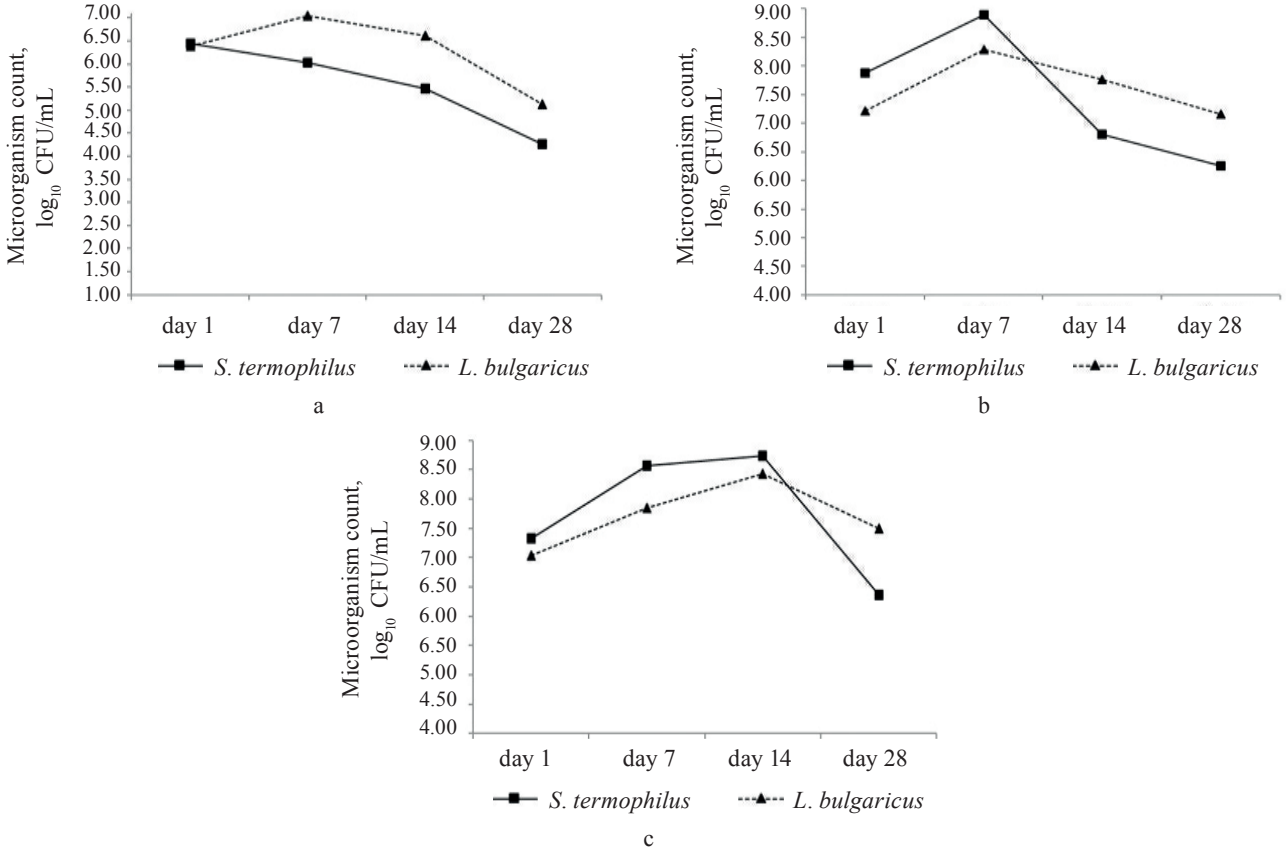

Figure 3 Number of microorganisms in yogurt-like products based on: lupine milk during storage (a), lupine milk with lactose during storage (b), and lupine milk with maltose during storage (c)

products based on lupine milk and can protect the starter cultures by wrapping them like a capsule [22].

Our research results were found to be compatible with studies that stated that starter cultures show better growth in the presence of some sugars (such as glucose and maltose) [19]. It has been reported that lupine milk contains carbohydrates at the level of 2.83 g/100 g, including different types of carbohydrates (galactose and arabinose) [23, 24]. In this work, the maximum growth of *L. bulgaricus* and *S. thermophilus* (8 $\log_{10}$ CFU/mL) in the starter cultures on day 14 in the samples with maltose was associated with the adaptation (prolongation of the lag$^+$ phase) and growth phase of starter cultures in the presence of maltose.

However, this effect could not be detected in the samples with lactose added. On the contrary, the development of starter cultures in the samples with lactose was particularly high (7–8 $\log_{10}$ CFU/mL) until day 7 of storage, and decreased to 6–7 $\log_{10}$ CFU/mL after day 14 of storage.

L. bulgaricus levels in the products with maltose were found to be lower than those in the samples with lactose between days 1 and 7 of storage. However, at days 14 and 28 of storage, *L. bulgaricus* levels in the samples with maltose were found to be higher than those in the samples with lactose. *S. thermophilus* levels, on the other hand, were found to be lower in the yogurt-like product with maltose until day 7 of storage (including day 7) and higher after day 7 than those in the products with lactose.

These results show that *S. thermophilus* was effective, also it is associated with an increased glucose concentration in the medium as a result of reaching a higher level of *S. thermophilus* than of *L. bulgaricus*. We determined relationships between the glucose ratio and bacterial growth, between the bacterial growth and acidity increase, and between acidity increase and hardness, viscosity, and syneresis. These results were found to be compatible with Bintsis [19]. *L. bulgaricus* and *S. thermophilus* were determined in the samples without sugars during storage, as well as the slower growth of acidity on the same storage days was attributed to the increase in syneresis observed in those samples. With the increase in syneresis in the yogurt-like products, the symbiotic relationship between microorganisms was disrupted, pH development slowed down or stopped [25].

Elsamani determined that the levels of *Bifidobacterium bifidum* and *Lactobacillus acidophilus* were preserved and increased in probiotic ice creams produced from lupine milk on day 30 of storage [26]. The author associated it with the protection of the proteins found in high levels in the composition of lupine milk that wrap the probiotics like a capsule.

CONCLUSION

In our study, lupine milk was obtained from lupine with functional properties and egg white protein powder. Different concentrations of lactose and maltose were added to lupine milk to obtain a non-dairy yogurt-like product.

The growth of *Lactobacillus bulgaricus* and *Streptecoccus thermophiles* was weaker in the disaccharide-free products compared to the samples with maltose and lactose. The increase in acidity in the samples with disaccharides during storage (28 days) was higher than that in the samples without sugars, and this was associated with maltose and lactose added to lupine milk.

It has been concluded that yogurt-like samples produced from lupine milk can be produced due to their similarity to fermented products (especially yogurt) of animal origin in terms of physico-chemical and rheological properties. However, with time, the samples with maltose and lactose were found to be closer to classical yogurt in terms of all properties. Sensory evaluation revealed that the smell and aroma of lupine were not pronounced. Thus, lupine yogurt-like products had high sensory properties.

Consequently, yogurt-like products based on lupine milk can be used as an alternative to fermented products produced from cow's milk, and more detailed studies should be conducted to formulate and optimize lupine fermented milk products.

CONFLICT OF INTEREST

The authors declare that there is no conflict of interest.

REFERENCES

1. Pontonio E, Rizzello CG. Milk alternatives and non-dairy fermented products: Trends and challenges. Foods. 2021;10(2). https://doi.org/10.3390/foods10020222
2. Lopes M, Pierrepont C, Duarte CM, Filipe A, Medronho B, Sousa I. Legume beverages from chickpea and lupin, as new milk alternatives. Foods. 2020;9(10). https://doi.org/10.3390/foods9101458
3. Prusinski J. White lupin (*Lupinus albus* L.) – ntritional and health values in human nutrition – A review. Czech Journal of Food Science. 2017;35(2):95–105. https://doi.org/10.17221/114/2016-CJFS
4. Yorgancılar M, Başarı D, Atalay E, Tanur Erkoyuncu M. A functional food: Lupin. Journal of Bahri Dagdas Crop Research. 2020;9(1):89–101.
5. Vogelsang-O'Dwyer M, Sahin AW, Zannini E, Arendt EK. Physicochemical and nutritional properties of high protein emulsion-type lupin-based model milk alternatives: effect of protein source and homogenization pressure. Journal of the Science of Food and Agriculture. 2021;102(12):5086–5097. https://doi.org/10.1002/jsfa.11230
6. Al-Saedi N, Agarwal M, Islam S, Ren Y-L. Study on the correlation between the protein profile of lupin milk and its cheese production compared with cow's milk. Molecules. 2021;26(8). https://doi.org/10.3390/molecules26082395
7. Asres AM, Woldemariam HW, Gemechu FG. Physicochemical and sensory properties of ice cream prepared using sweet lupin and soymilk as alternatives to cow milk. International Journal of Food Properties. 2022;25(1):278–287. https://doi.org/10.1080/10942912.2022.2032733
8. Krunglevičiūtė V, StarkutėV, Bartkienė E, Bartkevics V, Juodeikienė G, Vidmantien D, *et al.* Design of lupin seeds lactıc acıd fermentatıon – changes of dıgestıbılıty, amıno acıd profile and antıoxıdant actıvıty. Veterinarija ir Zootechnika. 2016;73(95):47–53.
9. Sze WK, Huda N, Dewi M, Hashim H. Physicochemical properties of egg white powder from eggs of different types of bird. International Journal on Advanced Science, Engineering and Information Technology. 2018;8(2):384–398. https://doi.org/10.18517/ijaseit.8.2.4087
10. Official Methods of Analysis of AOAC International, 21st Edition. AOAC International; 2019.
11. Mårtensson O, Andersson C, Andersson K, Öste R, Holst O. Formulation of an oat-based fermented product and its comparison with yoghurt. Journal of the Science of Food and Agriculture. 2001;81(14):1314–1321. https://doi.org/10.1002/jsfa.947
12. Kieserling K, Vu TM, Drusch S, Schalow S. Impact of pectin-rich orange fibre on gel characteristics and sensory properties in lactic acid fermented yoghurt. Food Hydrocolloids. 2019;94:152–163. https://doi.org/10.1016/j.foodhyd.2019.02.051
13. Kavas N. Functional probiotic yoghurt production with royal jelly fortification and determination of some properties. International Journal of Gastronomy and Food Science. 2022;28. https://doi.org/10.1016/j.ijgfs.2022.100519
14. Kavas N, Kavas G. Production of yogurt-like product from almond milk enriched with egg white protein powder and different disaccharides. Journal of Agriculture Faculty of Ege University. 2022;59(2):335–346. https://doi.org/10.20289/zfdergi.1000476
15. Official Methods and Recommended Practices of the AOCS. Champaign: AOCS Press; 2009.

16. Wang Y, Song KY, Kim Y. Effects of thermally treated mulberry leaves on the quality, properties, and antioxidant activities of yogurt. Journal of Food Processing and preservation. 2022;46(1). https://doi.org/10.1111/jfpp.16139
17. Silva LF, Sunakozawa TN, Amaral DM, Casella T, Nogueira MCL, De Dea Lindner J, *et al.* Safety and technological application of autochthonous *Streptococcus thermophilus* cultures in the buffalo Mozzarella cheese. Food Microbiology. 2020;87. https://doi.org/10.1016/j.fm.2019.103383
18. Jovanović M, Petrović M, Miočinović J, Zlatanović S, Petronijević JL, Mitić-Ćulafić D, *et al.* Bioactivity and sensory properties of probiotic yogurt fortified with apple pomace flour. Foods. 2021;9(6). https://doi.org/10.3390/foods9060763
19. Bintsis T. Lactic acid bacteria as starter cultures: An update in their metabolism and genetics. AIMS Microbiology. 2018;4(4):665–684. https://doi.org/10.3934/microbiol.2018.4.665
20. Ozcan Ö, Ozcan T, Yilmaz-Ersan L, Akpinar-Bayizit A, Delikanli B. The use of prebiotics of plant origin in functional milk products. Food Science and Technology. 2016;4(2):15–22. https://doi.org/10.13189/fst.2016.040201
21. Matela KS, Pillai MK, Thamae T. Evaluation of pH, titratable acidity, syneresis and sensory profiles of some yoghurt samples from the kingdom of Lesotho. Food Research. 2019;3(6):693–697.
22. Canon F, Mariadassou M, Maillard M-B, Falentin H, Parayre S, Madec M-N, *et al.* Function-driven design of lactic acid bacteria co-cultures to produce new fermented food associating milk and lupin. Frontiers in Microbiology. 2020;11. https://doi.org/10.3389/fmicb.2020.584163
23. Martinez-Villaluenga C, Sirtori E, Vidal-Valverde C, Duranti M. Effect of oligosaccharides removing procedure on the protein profiles of lupin seeds. European Food Research and Technology. 2006;223(5):691–696. https://doi.org/10.1007/s00217-006-0254-8
24. Tangyu M, Muller J, Bolten CJ, Wittmann C. Fermentation of plant-based milk alternatives for improved flavour and nutritional value. Applied Microbiology and Biotechnology. 2019;103(23–24):9263–9275. https://doi.org/10.1007/s00253-019-10175-9
25. Jrad Z, Oussaief O, Zaidi S, Khorchani T, El-Hatmi H. Co-fermentation process strongly affect the nutritional, texture, syneresis, fatty acids and aromatic compounds of dromedary UF-yogurt. Journal of Food Science and Technology. 2021;58(5):1727–1739. https://doi.org/10.1007/s13197-020-04682-1
26. Elsamani MO, Habbani SS, Babiker EE, Mohamed Ahmed IA. Biochemical, microbial and sensory evaluation of white soft cheese made from cow and lupin milk. LWT. 2014;59(1):553–559. https://doi.org/10.1016/j.lwt.2014.04.027
27. Khrundin DV, Ponomarev VYa, Yunusov ESh. Fermented oat milk as a base for lactose-free sauce. Foods and Raw Materials. 2022;10(1):155–162. https://doi.org/10.21603/2308-4057-2022-1-155-162

ORCID IDs
Nazan Kavas https://orcid.org/0000-0002-3141-4973

GUIDE FOR AUTHORS FORMATTING REQUIREMENTS FOR ARTICLES

We publish original, previously unpublished English language articles that possess scientific novelty in the field of food industry and related branches of science. The Journal publishes scientific papers, reports, peer reviews, brief scientific communications, letters to the editor, and related news items.

The main requirements for submitted articles are: validity of factual material, clarity and brevity, reproducibility of experimental data. The manuscript should meet the specified formatting standards. Please make sure that the section "Results and discussion" of your article states the novelty of your research.

All manuscripts submitted to the Foods and Raw Materials should be written in US English. The manuscript should contain no less than 10 pages in Microsoft Word text editor, abstract, tables, figures, and references included.

Format instructions

– 20 mm margins;
– single line spacing without automatic hyphenation;
– no extra interspaces between words or gaps between paragraphs;
– Times New Roman, size 10.

Structure

(1) **The type of your manuscript** should be clarified in the upper left corner (scientific article, review article, short message, note or letter, etc).

(2) **Title** (< 10 words) should be informative and reflect the main results of the research. The title of the article should be in lowercase letters, with the exception of the first letter and proper names. Please avoid abbreviations.

(3) **First and last names of the authors** are separated by commas. Paternal and middle names should be contracted to the first letter. Spelling should coincide with your ORCID id. Please mark the name of the author responsible for correspondence with an asterisk*.

(4) **Affiliation** is a formal name of the institution, city, postal address with postal code. The names and locations of institutions or companies should be given for all authors. If several institutions are listed, match the institution and the corresponding author with superscript numbers. Please include the e-mail address of the author responsible for correspondence.

(5) **Abstract** (200–250 words) cannot exceed 2000 characters with spaces. The abstract should be original and completely reflect the main results and novelty of the article. The best way to structure your abstract is to let it follow the structure of the article itself: relevance, tasks and objectives, methods, results, and conclusions. Please avoid meaningless introductory phrases and vague, general statements.

(6) **Keywords** provide < 10 keywords identifying the subject and the result of the research. Remember that it is key words that enable your potential readers to find your article on the Internet.

(7) **Introduction** gives a brief review of the publications related to the matter and proves its relevance. Referenced sources should be indexed in international scientific databases. In-text references should be given in square brackets and numbered [beginning with №1] in order of their appearance in the text. If several sources are quoted, they are given in chronological order. Make sure your introduction reflects the objectives of your research.

(8) **Study objects and methods:**

– Experimental research papers should contain a full description of the subject of the study, consecutive stages of the experiment, equipment, and reagents. Do not forget to specify the original company names of equipment and reagents manufacturers in brackets. If the method you use is not widely known or has been considerably modified, please provide a brief description.

– Theoretical research papers should specify objectives, approximations and assumptions, conclusions and equations. Please do not overload your text with intermediate data and description of well-known methods (such as numerical methods of solving equations) unless you have introduced some novelty into them.

(9) **Results and discussion** should provide a concise description of experimental data. Rather than repeating the data given in tables and graphs, the text should seek to reveal the principles detected. While describing your research results, it is recommended to use the Past Indefinite verb tense. The discussion should not reiterate the results. The discussion should contain an interpretation of the obtained research results (compliance of the results with the research hypothesis, generalisation of the research results, suggestions for practical application and future research).

Each **table** should be made in MS Word (Table – Add Table) or MS Excel and contain no less than three columns. Provide a number and a title for each table.

The Journal publishes color photographs and diagrams.

Mathematical equations should start with a separate line and be typed in the MathType frame as a whole. Mind that it is not allowed to compile formulae from composite elements (e.g. one part of the formula is a table, another part is a text, and some other part is an embedded frame). Please maintain the common settings for fonts, the size of characters and their placement in MathType formulas. Please avoid manual change for individual symbols or formula elements.

(10) **Conclusion** briefly summarises the main results of your research. Naturally, the conclusion should contain the answer to the question posed by the introduction.

(11) **Contribution** should indicate the actual contribution of each author in the research process. *Foods and Raw Materials* observes the CRediT taxonomy of the authors' contributions.

(12) **Conflict of interest** should indicate a real or potential conflict of interest. If there is no conflict of interests, you should write that "the author declares that there is no conflict of interest".

(13) **Acknowledgements** contains expression of gratitude to those who contributed to the research.

(14) **Funding** indicates how the research and the publication of this article were funded. If the study was performed with the support of a grant, specify the number of the grant and its name. State the name of your employer if the study was performed as part of your routine work and did not receive additional funding.

(15) **References** should be formatted according to the standard defined by the editors. The references are given in the order of their appearance in the text. Make sure you have included the DOI, if available.

Please avoid references to publications that are not readily available, e.g. institutional regulations, state standards, technical requirements, unpublished works, proceedings of conferences, extended abstracts of dissertation, and dissertations. Make sure you do not cite unpublished articles. It is not recommended to use more than three references to web resources. Please avoid citing publications that are more than 10 years old.

Self-citation should be well-justified and cannot exceed 10% of the references. Please make sure that at least 50% of the works you cite are less than 5 years old and published in periodicals registered in such data bases as Scopus, Web of Science, etc.

If you mention no references to fresh, 2–3-year-old papers, it might reduce your chances for publication. The references should reflect the actual impact of representatives of the international scientific community on the issue.

The manuscript should be carefully checked and signed by all authors on the first page of the main text. The article will not be published if it fails to meet the requirements. All articles are subject to general editing.

Correspondence and submission of all documents is done by e-mail: fjournal@mail.ru or www.jfrm.ru/en

The editors expect to receive **the following documents**, in Russian or English:

(1) an e-version of your article in MS Word named by the first author's last name (e.g. SmithJ.doc).

(2) a scanned PDF version of your article, the first page signed by all the authors (SmithJ.pdf);

(3) a form with personal information about the author(s). Please do not forget to mark the name of the author responsible for correspondence with an asterisk*. Name the file by the first author's name, e.g., SmithJ_Form.doc;

(4) a scanned PDF version of a cover letter to the editor-in-chief from the responsible organisation with the conclusion about the relevance of the research and recommendations for its publishing. The document should contain the date, reference number, and the signature of the head of the organisation;

(5) a standard copyright agreement.

Please mind that all the files should contain a single document.

For submission instructions, subscription and all other information visit this journals online at jfrm.ru/en/

FRM
Foods and Raw Materials. 2022;10(2)
ISSN 2310-9599 (Print)
ISSN 2308-4057 (Online)
Available online at https://jfrm.ru/en/
DOI: https://doi.org/10.21603/2308-4057-2022-2

CONTENTS

Editor's column 195

Gadouche Leila, Zerrouki Khayra, Zidane Azdinia, Ababou Adda, Bachir Elazaar Ibtissem, Merabet Dounya, Henniche Wissam, Ikhlef Samah Genoprotective, antimutagenic, and antioxidant effects of methanolic leaf extract of *Rhamnus alaternus* L. from the Bissa mountains in Algeria 196

Rada Artem O., Kuznetsov Aleksandr D. Digital inventory of agricultural land plots in the Kemerovo Region 206

Jafarpour Dornoush, Hashemi Seyed Mohammad Bagher Ohmic heating application in food processing: Recent achievements and perspectives 216

Debnath Bikash, Manna Kuntal Formulating anti-diabetic nutraceutical tablets based on edible plants from Tripura, India 227

Pui Liew Phing, Saleena Lejaniya Abdul Kalam Effects of spray-drying parameters on physicochemical properties of powdered fruits 235

Voroshilin Roman A., Kurbanova Marina G., Ostapova Elena V., Makhambetov Eduard M., Petrov Andrey N., Khelef Mohammed El Amine Effect of gelatin drying methods on its amphiphilicity 252

Plotnikova Inessa V., Magomedov Gazibeg O., Zharkova Irina M., Miroshnichenko Elena N., Plotnikov Viktor E. Jelly formulated with different carbohydrate profiles: Quality evaluation 262

Baskar Nehaa, Varadharajan Sabitha, Rameshbabu Mathushree, Ayyasamy Sudha, Velusamy Sangeetha Development of plant based yogurt 274

Dhakshayani G. M., Priya S. Janaki Alias A comparative study of phytochemical, antioxidant, anticarcinogenic, and antidiabetic potential of coriander (*Coriandrum sativum* L.): Microgreen and mature plant 283

Wójcicki Krzysztof Near-infrared spectroscopy as a green technology to monitor coffee roasting 295

Semenov Evgeniy V., Slavyanskiy Anatoliy A., Mitroshina Daria P., Lebedeva Natalya N. Thermodynamic factor and vacuum crystallization 304

Giro Tatiana M., Ilina Larisa A., Kulikovsky Andrey V., Ziruk Irina V., Giro Anna V. Molecular genetic studies of microbiocenosis and microstructure of jejunum wall in young rams grown on biofortified feed additives 310

Gribkova Irina N., Eliseev Mikhail N., Zakharov Maxim A., Kosareva Olga A., Zakharova Varvara A. Developing colloidal structure of beer by grain organic compounds 318

Faheid Siham M.M., Rizk Ibrahim R.S., Kishk Yasser F.M., Ragab Gamal H., Mostafa Sayed Carboxymethyl cellulose and psyllium husk in gluten-free pasta 329

Faskhutdinova Elizaveta R., Sukhikh Andrey S., Le Violeta M., Minina Varvara I., Khelef Mohammed El Amine, Loseva Anna I. Effects of bioactive substances isolated from Siberian medicinal plants on the lifespan of *Caenorhabditis elegans* 340

Ajayi Feyisola F., Ogori Akama F., Orede Vivien O., Peter Emmanuel Synergistic effect of *Balanites aegyptiaca* essential oil and storage materials on cowpea seeds 353

Evdokimova Svetlana A., Karetkin Boris A., Zhurikov Mikhail O., Guseva Elena V., Khabibulina Natalia V., Shakir Irina V., Panfilov Victor I. Antagonistic activity of synbiotics: Response surface modeling of various factors 365

Kavas Nazan Yogurt-like product from lupine (*Lupinus albus* L.) milk as an alternative to dairy products 377